

LOAN DOCUMENT

		PHOTOGRAPH THIS SHEET		0																				
DTIC ACCESSION NUMBER		LEVEL	INVENTORY																					
	<u>AFRL-ML-TY-TR-2000-4546</u>																							
	DOCUMENT IDENTIFICATION MAR 2000																							
	SEE DOC																							
	DISTRIBUTION STATEMENT																							
<table border="1"><tr><td colspan="2">ACCESSION FOR</td></tr><tr><td>NTIS</td><td>GRAM</td></tr><tr><td>DTIC</td><td>TRAC</td></tr><tr><td>UNANNOUNCED</td><td></td></tr><tr><td>JUSTIFICATION</td><td></td></tr><tr><td colspan="2">BY</td></tr><tr><td colspan="2">DISTRIBUTION/</td></tr><tr><td colspan="2">AVAILABILITY CODES</td></tr><tr><td>DISTRIBUTION</td><td>AVAILABILITY AND/OR SPECIAL</td></tr><tr><td>A-1</td><td></td></tr></table>		ACCESSION FOR		NTIS	GRAM	DTIC	TRAC	UNANNOUNCED		JUSTIFICATION		BY		DISTRIBUTION/		AVAILABILITY CODES		DISTRIBUTION	AVAILABILITY AND/OR SPECIAL	A-1		DATE RECEIVED IN DTIC		
ACCESSION FOR																								
NTIS	GRAM																							
DTIC	TRAC																							
UNANNOUNCED																								
JUSTIFICATION																								
BY																								
DISTRIBUTION/																								
AVAILABILITY CODES																								
DISTRIBUTION	AVAILABILITY AND/OR SPECIAL																							
A-1																								
DISTRIBUTION STAMP		DATE RETURNED																						
20000727 176		REGISTERED OR CERTIFIED NUMBER																						
PHOTOGRAPH THIS SHEET AND RETURN TO DTIC-FDAC																								

H
A
N
D
L
E

W
I
T
H

C
A
R
E

AFRL-ML-TY-TR-2000-4546



**DESIGN, CONSTRUCTION, AND MONITORING
OF THE PERMEABLE REACTIVE BARRIER IN
AREA 5 AT DOVER AIR FORCE BASE**

**ARUN GAVASKAR
NEERAJ GUPTA
BRUCE SASS
WOONG-SANG YOON
ROBERT JANOSY
ERIC DRESCHER
JAMES HICKS**

**BATTELLE
505 KING AVENUE
COLUMBUS OH 43201**

Approved for Public Release; Distribution Unlimited

**AIR FORCE RESEARCH LABORATORY
MATERIALS & MANUFACTURING DIRECTORATE
AIR EXPEDITIONARY FORCES TECHNOLOGIES DIVISION
139 BARNES DRIVE, STE 2
TYNDALL AFB FL 32403-5323**

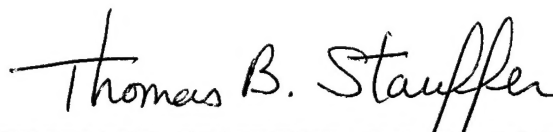
NOTICES

USING GOVERNMENT DRAWINGS, SPECIFICATIONS, OR OTHER DATA INCLUDED IN THIS DOCUMENT FOR ANY PURPOSE OTHER THAN GOVERNMENT PROCUREMENT DOES NOT IN ANY WAY OBLIGATE THE US GOVERNMENT. THE FACT THAT THE GOVERNMENT FORMULATED OR SUPPLIED THE DRAWINGS, SPECIFICATIONS, OR OTHER DATA DOES NOT LICENSE THE HOLDER OR ANY OTHER PERSON OR CORPORATION; OR CONVEY ANY RIGHTS OR PERMISSION TO MANUFACTURE, USE, OR SELL ANY PATENTED INVENTION THAT MAY RELATE TO THEM.

THIS TECHNICAL REPORT HAS BEEN REVIEWED AND IS APPROVED FOR PUBLICATION.



TIMOTHY G. WILEY, Lt Col, USAF, BSC
Program Manager



THOMAS B. STAUFFER, PhD, DR-IV, DAF
Chief, Weapons Systems Logistics Branch



RANDY L. GROSS, Col, USAF, BSC
Chief, Air Expeditionary Forces Technologies Division

REPORT DOCUMENTATION PAGE*Form Approved*
OMB No. 0704-0188

Public reporting burden for this collection of information is estimated to average 1 hour per response, including the time for reviewing instructions, searching existing data sources, gathering and maintaining the data needed, and completing and reviewing the collection of information. Send comments regarding this burden estimate or any other aspect of this collection of information, including suggestions for reducing this burden, to Washington Headquarters Services, Directorate for Information Operations and Reports, 1215 Jefferson Davis Highway, Suite 1204, Arlington, VA 22202-4302, and to the Office of Management and Budget, Paperwork Reduction Project (0704-0188), Washington, DC 20503.

1. AGENCY USE ONLY (Leave blank)		2. REPORT DATE March 2000	3. REPORT TYPE AND DATES COVERED Final, April 1997 through March 2000	
4. TITLE AND SUBTITLE Design, Construction, and Monitoring of the Permeable Reactive Barrier in Area 5 at Dover Air Force Base			5. FUNDING NUMBER F08637-95-C-6004 DO 5503	
6. AUTHORS Arun Gavaskar, Neeraj Gupta, Bruce Sass, Woong-Sang Yoon, Robert Janosy, Eric Drescher, and James Hicks				
7. PERFORMING ORGANIZATION NAME(S) AND ADDRESS(ES) Battelle 505 King Avenue Columbus OH 43201			8. PERFORMING ORGANIZATION REPORT NUMBER	
8. SPONSORING/MONITORING AGENCY NAME(S) AND ADDRESS(ES) AFRL/MLQL 139 Barnes Drive, Ste 2 Tyndall AFB FL 32403-5323			10. SPONSORING/MONITORING AGENCY REPORT NUMBER AFRL-ML-TY-TR-2000-4546	
11. SUPPLEMENTARY NOTES Task was performed by Battelle under contract to AFRL, U.S. Air Force				
12a. DISTRIBUTION/AVAILABILITY STATEMENT Approved for Public Release; Distribution Unlimited PA Case #00-057			12b. DISTRIBUTION CODE A	
13. ABSTRACT (Maximum 200 words) The primary objective of this project was to test the performance of two different reactive media in the same aquifer. To satisfy this objective, Battelle designed, constructed, and monitored a pilot-scale permeable reactive barrier (PRB) in Area 5 at Dover Air Force Base, DE. The PRB was installed in December 1997 to treat a perchloroethylene plume and was monitored over 18 months of operation. The PRB is a funnel-and-gate system with two gates. Both gates contain granular iron as the reactive medium and were installed with the use of caissons. Gate 1 had a pretreatment zone (PTZ) consisting of 10% iron and sand, and Gate 2 had a PTZ consisting of 10% pyrite and sand. The PTZs were designed to remove dissolved oxygen before it entered the 100% iron reactive cell. The pyrite PTZ had the proposed benefit of pH control. However, monitoring showed that the reduced pH in the pyrite PTZ could not be sustained in the 100% iron reactive cell. The PRB is functioning as designed in terms of chlorinated solvent reduction, hydraulic performance, and geochemistry. The use of caissons was found to be a viable method for installing a PRB in the midst of several utility lines and in a relatively deep aquifer.				
14. SUBJECT TERMS permeable barrier, groundwater, reactive medium, funnel-and-gate, chlorinated solvent			15. NUMBER OF PAGES 150 + Appendices	
			16. PRICE CODE	
17. SECURITY CLASSIFICATION OF REPORT UNCLASSIFIED	18. SECURITY CLASSIFICATION OF THIS PAGE UNCLASSIFIED	19. SECURITY CLASSIFICATION OF ABSTRACT UNCLASSIFIED	20. LIMITATION OF ABSTRACT UL	

Preface

The permeable reactive barrier (PRB) demonstration project described in this report was conducted by Battelle for the Air Force Research Laboratory (AFRL). This project was supported by the United States Department of Defense, through the Strategic Environmental Research and Development Program (SERDP). The field demonstration was partially supported by the Dover National Test Site (DNST), which is one of four National Environmental Technology Test Site (NETTS) locations established and managed by the United States Department of Defense SERDP. The support of the NETTS facilities and of the test location manager and staff is gratefully acknowledged. For further information on NETTS locations or SERDP, contact Catherine Vogel at (703) 696-2118 or Matt Chambers at (703) 478-5186, or visit the SERDP Web site at www.serdp.org. Alison Lightner was the AFRL project officer for this effort.

We also would like to acknowledge the efforts of the previous AFRL project officers, namely Maj. Mark Smith, Cpt. Jeff Stinson, 1st Lt. Dennis O'Sullivan, and Cpt. Gus Fadel for keeping the project moving forward.

Battelle and AFRL would like to acknowledge the advisory and review support provided to this project by John Vogan and Robert Focht of EnviroMetal Technologies, Inc., and Timothy Sivavec of the General Electric Co. The Remedial Technologies Development Forum's (RTDF's) Permeable Barriers Subgroup and the Interstate Technologies Regulatory Cooperation Working Group's (ITRC's) Permeable Barriers Group provided document review support for this project. Steve McCutcheon and John Kenneke from the United States Environmental Protection Agency conducted the on-site column tests and reactive media selection in a parallel effort. We appreciate the support of Dover Air Force Base personnel, specifically Greg Jackson and Bob Wickso from the Civil Engineering Group. Minh Le from C³ Environmental provided construction support during installation of the permeable barrier.

This report is a work prepared for the United States Government by Battelle. In no event shall either the United States Government or Battelle have any responsibility or liability for any consequences of any use, misuse, inability to use, or reliance on the information contained herein, nor does either warrant or otherwise represent in any way the accuracy, adequacy, efficacy, or applicability of the contents hereof.

Executive Summary

A. OBJECTIVE

The primary objective of this demonstration was to test the performance of two different permeable reactive barrier (PRB) media in the same aquifer, under uncontrolled field conditions. A secondary objective of the demonstration was to facilitate technology transfer by carefully documenting and disseminating the lessons learned about PRB design, construction, and monitoring.

B. BACKGROUND

The Air Force Research Laboratory (AFRL), Tyndall Air Force Base (AFB), FL contracted Battelle in Columbus, OH, in April 1997 to conduct a demonstration of a field pilot-scale PRB in Area 5 at Dover AFB, DE. The Area 5 aquifer is contaminated with dissolved chlorinated solvents, primarily perchloroethylene (PCE). The Strategic Environmental Research and Development Program (SERDP) provided funding for this project. The United States Environmental Protection Agency's (U.S. EPA's) National Exposure Research Laboratory (NERL) was funded separately by SERDP to conduct long-term aboveground column tests using Area 5 groundwater to evaluate and select suitable reactive media for the field demonstration. The Remediation Technologies Development Forum's (RTDF's) Permeable Barriers Group and the Interstate Technology and Regulatory Cooperation Working Group's (ITRC's) Permeable Barriers Subgroup provided independent document review support for this demonstration.

C. SCOPE

Based on column tests conducted on several alternative reactive media and using site groundwater, U.S. EPA-NERL reported that a pyrite-and-iron combination ranked the best. Because of its potential for scrubbing oxygen and controlling pH in the iron-groundwater system, pyrite was expected to provide the benefits of enhanced kinetics of chlorinated volatile organic compound (CVOC) degradation and reduced precipitation of inorganic constituents. Based on this recommendation, Battelle designed and installed a funnel-and-gate PRB with two gates. Both gates have a reactive cell consisting of 100% granular iron. In addition, Gate 1 incorporates a pre-treatment zone (PTZ) consisting of 10% iron and sand, and Gate 2 incorporates a PTZ consisting of 10% pyrite and sand. The exit zone in both gates consists of 100% coarse sand. The construction of the PRB was completed in January 1998.

The location and design of the barrier were determined by detailed site characterization and modeling conducted in June 1997 to support the PRB and monitoring system design. The groundwater treatment targets for this project were 5 µg/L of PCE and trichloroethylene (TCE), 70 µg/L of *cis*-1,2-dichloroethylene (*cis*-1,2-DCE), and 2 µg/L of vinyl chloride (VC); these targets correspond to the U.S. EPA-recommended maximum contaminant levels (MCLs) for the respective CVOCs. An innovative construction technique involving caissons was used to install

the two gates down to about 40 ft below ground surface (bgs), which is beyond the reach of conventional backhoe installation. This innovative construction technique also facilitated the installation of the PRB in the midst of several underground utility lines.

Following installation, Battelle evaluated the reactive and hydraulic performance of the PRB primarily through two comprehensive monitoring events conducted in July 1998 and June 1999. Limited monitoring events were conducted periodically throughout the demonstration to monitor specific operating parameters. At the end of 18 months of operation, core samples of the gate and surrounding aquifer media were collected and analyzed for precipitate formation. This report describes the detailed methodology and results of the demonstration, and discusses the implications for the technology.

D. CONCLUSIONS

In summary, monitoring results show that, to date, the PRB is functioning at an acceptable level in terms of capturing groundwater, creating strongly reducing conditions, and achieving treatment targets. The PTZs in both gates succeeded in removing dissolved oxygen from the groundwater before it entered the reactive cell. In addition, the use of pyrite did result in some degree of pH control while the groundwater was in the PTZ of Gate 2. However, once the groundwater entered the reactive cell, the tendency of the iron to raise the pH of the system overwhelmed any pH control effect achieved by the pyrite. Magnesium, nitrate, and silica were the main inorganic species precipitating out of the low-alkalinity groundwater as it flowed through the gates.

The innovative use of caissons in this project for installing the reactive media in the midst of underground utility lines and in a relatively deep aquifer offers a viable method for PRB construction at similarly challenging sites. Assessing hydraulic flow and long-term geochemical performance of a RPB remain the most important challenges for the design and monitoring of this technology. Conducting adequate site characterization, simulating multiple hydraulic flow and longevity scenarios, and incorporating adequate safety factors during the design of a PRB are the best ways of addressing these challenges.

Table of Contents

MAIN REPORT (THIS VOLUME)	Page
Preface.....	iii
Executive Summary.....	v
List of Figures	ix
List of Tables	xi
List of Abbreviations and Acronyms.....	xiii
1. Project Description.....	1
1.1 Project Background.....	1
1.2 Technology Background.....	1
1.2.1 CVOC Degradation Mechanism.....	2
1.2.2 PRB Configurations.....	6
1.3 Project Description.....	6
2. PRB Design.....	9
2.1 Preliminary Site Assessment.....	9
2.2 Additional Site Characterization.....	12
2.3 Column Tests for Alternative Media Selection and Kinetics Determination	17
2.4 PRB Design.....	18
3. PRB Construction	25
3.1 Preconstruction/Site Preparation Issues.....	25
3.2 Gates Construction.....	27
3.3 Funnel Construction.....	30
4. Monitoring Plan	33
4.1 Monitoring Strategy	33
4.2 Groundwater Sampling Methods	37
4.3 Hydraulic Measurements	38
4.4 Groundwater Analysis Methods	39
4.5 Core Sample Collection Methods.....	41
4.5.1 Core Sample Locations.....	42
4.5.2 Core Analysis Methods.....	42
5. Reactivity Assessment	47
5.1 CVOC Distribution at Area 5	47
5.2 Degradation of CVOCs by the PRB	51
5.3 Assessment of CVOC Degradation Rates.....	56
5.4 Reactivity Assessment Summary.....	58

Table of Contents (Continued)

	Page
6. Hydraulic Performance Assessment	61
6.1 Groundwater Velocity Estimation	61
6.1.1 Hydraulic Conductivity (K) and Porosity (n)	61
6.1.2 Hydraulic Gradient	66
6.1.3 Summary of Groundwater Modeling for PRB Design	75
6.1.4 Groundwater Velocity Calculation Based on Darcy's Law.....	80
6.1.5 Groundwater Velocity Measurements from the HydroTechnics Probes	84
6.2 Hydraulic Capture Zone Evaluation	89
6.3 Summary of Results and Conclusions	96
7. Geochemical Performance Assessment	99
7.1 Results of Field Parameter Measurements.....	99
7.1.1 pH Measurements	100
7.1.2 Oxidation-Reduction Potential	105
7.1.3 Dissolved Oxygen Measurements	106
7.2 Results of Other Inorganic Chemical Measurements	107
7.3 Trends in Analyte Concentrations	110
7.3.1 Iron.....	110
7.3.2 Sodium and Chloride	111
7.3.3 Alkalinity, Calcium, and Sulfate.....	112
7.3.4 Magnesium, Nitrate, and Dissolved Silica.....	112
7.4 Geochemical Modeling.....	113
7.4.1 Mineral Saturation Indices.....	113
7.4.2 Geochemical Simulations	115
7.5 Evaluation of Core Samples.....	117
7.5.1 X-Ray Diffraction.....	117
7.5.2 Scanning Electron Microscopy.....	119
7.5.3 Raman Spectroscopy.....	119
7.5.4 Infrared Spectroscopy	123
7.5.5 Carbon Analysis.....	123
7.6 Microbiological Evaluation	123
7.7 Summary of Geochemical Evaluation Results and Conclusions.....	125
8. Cost Evaluation.....	129
8.1 Capital Investment	129
8.2 Scaleup.....	131
8.3 Projected Operating and Maintenance Costs	134
8.4 Present Value Analysis of PRB and P&T Options	135

Table of Contents (Continued)

	Page
9. Results and Conclusions	141
9.1 Reactive Performance of the Area 5 PRB.....	141
9.2 Hydraulic Performance of the Area 5 PRB.....	141
9.3 Geochemical Performance of the Area 5 PRB	143
9.4 Economics of PRB Application at Area 5	144
9.5 Recommendations.....	144
10. References.....	147

Appendix A: Points of Contact

APPENDICES B TO H

- Appendix B: Supporting Information for Site Characterization and PRB Design
- Appendix C: Supporting Information for PRB Construction
- Appendix D: Supporting Information for Reactive Performance Evaluation
- Appendix E: Supporting Information for Hydraulic Performance Evaluation
- Appendix F: Supporting Information for Geochemical Performance Evaluation
- Appendix G: Quality Assurance Data
- Appendix H: Supporting Information for Cost Evaluation

LIST OF FIGURES

Figure 1-1. Schematic Illustrations of Some PRB Configurations.....	3
Figure 1-2. Schematic of the PRB in Area 5 at Dover AFB.....	7
Figure 2-1. Steps in the Design of a Permeable Barrier System	10
Figure 2-2. Location of the PRB Demonstration in Area 5 at Dover AFB	11
Figure 2-3. Northwest-Southeast Cross Section near the PRB.....	14
Figure 2-4. Typical Water-Level Map Showing Regional Groundwater Flow in Area 5 at Dover AFB	15
Figure 2-5. Temporary Wells (T-Wells), CVOC Plume, and PRB Locations in Area 5 based on the June 1997 Site Characterization.....	16
Figure 2-6. Simulated Water Levels (Based on December 1993 Conditions) at Area 5 for K_{aq} Values of (a) 10 ft/day and (b) 50 ft/day.....	19
Figure 2-7. Plan View of Complete PRB System.....	21
Figure 2-8. Detailed Plan View of PRB Gate.....	22
Figure 3-1. Elevation View of PRB Gate 1 and Funnel	26

Table of Contents (Continued)

	Page
Figure 3-2. Caisson Driving Equipment.....	28
Figure 3-3. Caisson Drilling Equipment.....	28
Figure 3-4. Gate Frame.....	29
Figure 3-5. Placement of Reactive Media	29
Figure 3-6. Pile-Driving Equipment.....	31
Figure 3-7. Sealable-Joint Sheet Pile Barrier	31
Figure 4-1. Monitoring Point Network Within Gates 1 and 2.....	34
Figure 4-2. Monitoring Well Cluster Profile for (a) Gate and (b) Aquifer Wells	35
Figure 4-3. Monitoring Well Network in Aquifer	36
Figure 4-4. Photograph of Core Sampler Positioned Over Gate 1	41
Figure 4-5. Map of PRB Showing Coring Locations	43
Figure 4-6. Photograph of Core Sleeves Being Placed into Tedlar™ Bags that Contained Packets of Oxygen Scavenging Material.....	44
Figure 4-7. Tedlar™ Bags Flushed with Nitrogen Gas Before Sealing	44
Figure 5-1. Temporary Groundwater Sampling and Permanent Monitoring Well Locations in the Upgradient Vicinity of the PRB.....	49
Figure 5-2. PCE Distribution in the Upgradient Vicinity of the PRB (Based on June 1999 Monitoring Event).....	50
Figure 5-3. PCE Distribution in Gates 1 and 2 and the Surrounding Aquifer (Vertical Cross Section).....	53
Figure 5-4. TCE Distribution in Gates 1 and 2 and the Surrounding Aquifer (Vertical Cross Section).....	54
Figure 5-5. <i>cis</i> -1,2-DCE Distribution in Gates 1 and 2 and the Surrounding Aquifer (Vertical Cross Section).....	55
Figure 6-1. Example Slug Test Recovery Graph for Area 5 Aquifer.....	63
Figure 6-2. Hydraulic Conductivity Distribution in Shallow Wells.....	64
Figure 6-3. Hydraulic Conductivity Distribution in Deep Wells	65
Figure 6-4. Representative Map of Water Levels from Shallow Wells at Site 5	70
Figure 6-5. Representative Map of Water Levels from Deep Wells at Site 5	71
Figure 6-6. Map of Water Levels in Shallow Wells near the PRB (February 1998)	72
Figure 6-7. Map of Water Levels in Shallow Wells near the PRB (July 1998)	73
Figure 6-8. Map of Water Levels in Shallow Wells near the PRB (June 1999).....	74
Figure 6-9. 1998/1999 Water-Level and Precipitation Data for Gate 1 of the PRB	76
Figure 6-10. 1998/1999 Water-Level and Precipitation Data for Gate 2 of the PRB	77
Figure 6-11. Continuous Water-Level Elevations in Gate 2 of the PRB (June and July 1998)	79
Figure 6-12. Simulated Water Levels and Flowpaths for Final PRB Design.....	81
Figure 6-13. Groundwater Flow Velocity in PRB—HydroTechnics Probe 1	85
Figure 6-14. Groundwater Flow Velocity in PRB—HydroTechnics Probe 2.....	86

Table of Contents (Continued)

	Page
Figure 6-15. Groundwater Flow Velocity in PRB—HydroTechnics Probe 3	87
Figure 6-16. Groundwater Flow Velocity in PRB—HydroTechnics Probe 4	88
Figure 6-17. Groundwater Levels (ft amsl) near the PRB	91
Figure 6-18. Groundwater Flow Direction in PRB—HydroTechnics Probe 1	92
Figure 6-19. Groundwater Flow Direction in PRB—HydroTechnics Probe 2	93
Figure 6-20. Groundwater Flow Direction in PRB—HydroTechnics Probe 3	94
Figure 6-21. Groundwater Flow Direction in PRB—HydroTechnics Probe 4	95
Figure 7-1. pH of Selected Upgradient Aquifer Wells at Different Sampling Events	102
Figure 7-2. pH of Selected Gate 1 Wells at Different Sampling Events	103
Figure 7-3. pH of Selected Gate 2 Wells at Different Sampling Events	103
Figure 7-4. Eh in Selected PTZ Wells at Different Sampling Events	105
Figure 7-5. DO in Selected Upgradient Aquifer Wells at Different Sampling Events.....	107
Figure 7-6. Ionic Charge Balance for Selected Wells (June 1999)	111
Figure 7-7. Simulated pH and Eh Reactions with Zero-Valent Iron	116
Figure 7-8. Simulated DO, Dissolved Nitrogen, and Nitrate Reactions with Zero-Valent Iron	116
Figure 7-9. Simulated pH and Eh Reactions with Pyrite	117
Figure 7-10. Simulated DO, Dissolved Nitrogen, and Nitrate Reactions with Pyrite	118
Figure 8-1. Schematic of the Scaleup of the PRB	132

LIST OF TABLES (THIS VOLUME)

Table 1-1. Demonstration Project Schedule.....	2
Table 2-1. Maximum CVOC Concentrations Recorded in Wells Likely to Be Within the Capture Zone of Each Gate	17
Table 2-2. Residence Time Requirements	22
Table 4-1. Analytical Requirements for Groundwater Samples	40
Table 4-2. Characterization Techniques for Coring Samples	45
Table 5-1. Maximum CVOC Concentrations Recorded in Wells Likely to Be Within the Capture Zone of Each Gate	48
Table 5-2. CVOC Degradation Along the Flow Direction in Gate 1	51
Table 5-3. CVOC Degradation Along the Flow Direction in Gate 2	52
Table 5-4. Estimates of Field Degradation Rates Based on June 1999 Data	58
Table 6-1. Summary of Geotechnical Laboratory Testing for Aquifer and Reactive Barrier Media	62
Table 6-2. Summary of Slug Test Results.....	66
Table 6-3. Summary of Average Gradients in Various Zones near the Permeable Barrier	68

Table of Contents (Continued)

	Page
Table 6-4. Summary of Average Water-Level Changes over Time near the Permeable Barriers.....	78
Table 6-5. Power Supply for In Situ Velocity Sensors	39
Table 6-6. Simulated Flow Velocities, Capture Zones and Travel Time through Reactive Cell (from Battelle, 1997)	80
Table 6-7. Groundwater Flow Velocity and Residence Time Based on Observed Gradients and Conductivity	83
Table 6-8. HydroTechnics Probe Measurements in June 1999	89
Table 6-9. Flow Directions Based on HydroTechnics Probe Measurements (June 1999)	96
Table 7-1. Results of Field Parameter Measurements from the June 1999 Sampling Event for Wells Along the Flowpath Through the Gates	100
Table 7-2. pH Measurements in Selected Wells at Several Sampling Intervals	102
Table 7-3. Results of DO Measurements (mg/L) in Wells Along the Flowpath Through the Gates During Different Sampling Events.....	106
Table 7-4. Selected Results of Inorganic Chemical Analysis	108
Table 7-5. Geochemical Modeling Results: Saturation Indices	114
Table 7-6. Results of X-Ray Diffraction Analysis of Core Samples	119
Table 7-7. Results of EDS Analysis of Core Samples	120
Table 7-8. Raman Shifts in Core Samples	121
Table 7-9. Results of Raman Spectroscopic Analysis of Core Samples	122
Table 7-10. Results of FTIR Analysis of Core Samples	124
Table 7-11. Results of Carbon Analysis of Core Samples	124
Table 7-12. Total Heterotrophic Plate Count Results (CFU/g)	125
Table 8-1. Capital Investment Incurred in Installing the Field Pilot-Scale PRB in Area 5.....	130
Table 8-2. Capital Investment Projected for Installing a Full-Scale PRB in Area 5.....	133
Table 8-3. O&M Costs Projected for Operating a Full-Scale PRB in Area 5.....	134
Table 8-4. Capital Investment Projected for Installing a P&T System in Area 5	136
Table 8-5. O&M Costs Projected for Operating a P&T System in Area 5	136
Table 8-6. Present Value Analysis of PRB and P&T Systems in Area 5 Assuming 20-Year Life of PRB	138
Table 8-7. Break-Even Point and Savings by Using a PRB Instead of a P&T System at Area 5	139

List of Acronyms and Abbreviations

AFB	Air Force Base
AFRL	Air Force Research Laboratory
amsl	above mean sea level
ARA	Applied Research Associates, Inc.
ATR	attenuated total internal reflection
bgs	below ground surface
CCD	charged coupled device
CFU/g	colony-forming units per gram
CPT	cone penetrometer test
CQC	construction quality control
CVOC	chlorinated volatile organic compound
D	deep
DCE	dichloroethylene
DNTS	Dover National Test Site
DO	dissolved oxygen
DoD	(United States) Department of Defense
DOE	(United States) Department of Energy
EDS	energy-dispersive spectroscopy
Eh	redox potential
ESTCP	Environmental Security Technology Certification Program
FTIR	Fourier transform infrared spectroscopy
GC	gas chromatography
GE	General Electric Co.
gpm	gallons per minute
HDPE	high-density polyethylene
IAP	ion activity product
ID	identification
I.D.	inside diameter
ITRC	Interstate Technology and Regulatory Cooperation (Working Group)
K	hydraulic conductivity
M	middle
MCL	maximum contaminant level

meq	milliequivalents
mV	millivolts
NA	not applicable
N/A	not available
NAS	Naval Air Station
NC	not calculated
ND	not detected
NERL	National Exposure Research Laboratory
O.D.	outside diameter
O&M	operating and maintenance
ORP	oxidation-reduction potential
PCE	perchloroethylene
PLFA	phospholipid fatty acid
PPE	personal protective equipment
PRB	permeable reactive barrier
P&T	pump and treat
PTZ	pretreatment zone
PV	pore volumes
PVC	polyvinyl chloride
QA	quality assurance
RPM	Remedial Program Manager
RTDF	Remediation Technologies Development Forum
S	shallow
SEI	secondary electron images
SEM	scanning electron microscopy
SERDP	Strategic Environmental Research and Development Program
SI	saturation index
TCA	trichloroethane
TCE	trichloroethylene
TDS	total dissolved solids
TSA	trypticase-soy agar
U.S. EPA	United States Environmental Protection Agency
VC	vinyl chloride
VOA	volatile organic analysis
VOC	volatile organic compound
XRD	x-ray diffraction

1. Project Description

1.1 Project Background

The Air Force Research Laboratory (AFRL), Tyndall Air Force Base (AFB), FL contracted Battelle in Columbus, OH in April 1997 to conduct a demonstration of a field pilot-scale permeable reactive barrier (PRB) in Area 5 at Dover AFB, DE. The Area 5 aquifer is contaminated with dissolved chlorinated solvents, primarily perchloroethylene (PCE). The Strategic Environmental Research and Development Program (SERDP) provided funding for this project. Appendix A lists the points of contact for this project. The primary objective of this demonstration was to test the performance of two different reactive media in the same aquifer, under uncontrolled field conditions. A secondary objective of the demonstration was to facilitate technology transfer by carefully documenting and disseminating the lessons learned about PRB design, construction, and monitoring.

The United States Environmental Protection Agency's (U.S. EPA's) National Exposure Research Laboratory (NERL) was funded separately by SERDP to conduct long-term aboveground column tests using Area 5 groundwater to evaluate and select suitable reactive media for the field demonstration. The Remediation Technologies Development Forum's (RTDF's) Permeable Barriers Group and the Interstate Technology and Regulatory Cooperation Working Group's (ITRC's) Permeable Barriers Subgroup provided independent document review support for this demonstration. Table 1-1 shows the schedule and milestones for this project.

1.2 Technology Background

A PRB is an innovative technology that has become one of the more promising alternatives for remediation of groundwater contaminated with chlorinated volatile organic compounds (CVOCs), such as PCE, trichloroethylene (TCE), dichloroethylene (DCE), and vinyl chloride (VC). Metals (such as chromium) and radionuclides are other contaminants that have been addressed with PRBs. PRBs generally are applied as a long-term passive alternative to conventional pump-and-treat (P&T) systems for groundwater remediation.

Figure 1-1 is an illustration of different PRB configurations. In its simplest form, a PRB consists of a reactive medium that is placed in the path of a dissolved contaminant plume. As the contaminated groundwater flows through the permeable barrier, dissolved contaminants are either destroyed (as in the case of solvents) or precipitated in an insoluble form (as in the case of metals or radionuclides). The most common abiotic reactive medium that has been used so far is zero-valent granular iron, which is a strong reducing agent (Gillham, 1996). Barriers containing adsorptive or biological, rather than reactive, media also have been employed.

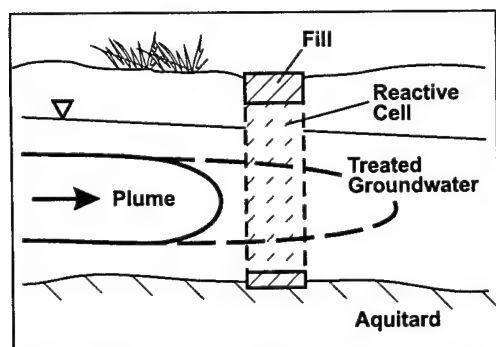
Table 1-1. Demonstration Project Schedule

Milestone	Date
<i>Phase 1</i>	
Project initiation	April 1997
Preliminary site assessment	May 1997
Site characterization	June 1997
Draft design/test plan	September 1997
Preconstruction meeting	October 1997
Final design/test plan	November 1997
<i>Phase 2</i>	
Construction initiated	November 1997
Construction completed	January 1998
First comprehensive monitoring event	July 1998
Limited monitoring events	August 1998 to April 1999
Interim report	February 1999
Second comprehensive monitoring event	June 1999
Limited monitoring events	August 1999
Draft technology demonstration report	November 1999
Review of draft report completed	February 2000
Final technology demonstration report	March 2000

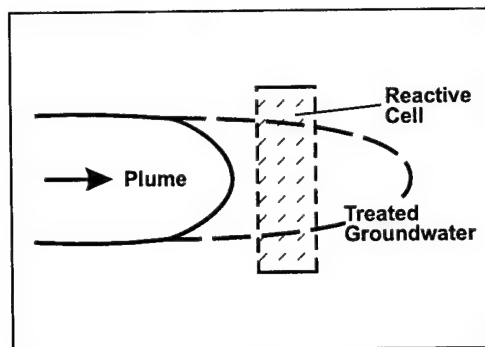
The U.S. EPA has identified more than 5,000 United States Department of Defense (DoD), Department of Energy (DOE), and U.S. EPA Superfund sites contaminated with chlorinated compounds. The U.S. EPA suggests that the PRB technology may be potentially applicable at approximately 10 to 20% of these sites. However, widespread use and acceptance of PRBs is still rather limited, because Remedial Program Managers (RPMs) and regulators do not have a history of field data from multiple applications regarding hydraulic capture efficiency and longevity. Differences in site features, PRB designs, reactive media, and contaminants at existing PRBs add to the complexity of assessing the performance of the technology. The demonstration at Dover AFB is an effort to facilitate technology transfer by documenting and disseminating the results of the assessment of a PRB technology application.

1.2.1 CVOC Degradation Mechanism

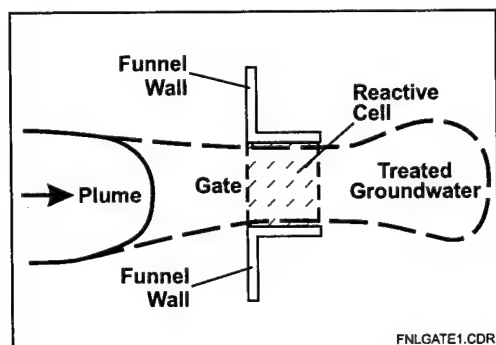
Iron degrades CVOCs by creating strongly reducing conditions in the iron-groundwater environment. The resulting electron activity is believed to reduce chlorinated compounds to potentially nontoxic products. The first reported use of metals to degrade chlorinated organic compounds in the environment was by Sweeny and Fischer (1972), who acquired a patent for the degradation of chlorinated pesticides by metallic zinc under acidic conditions. Other researchers, such as Senzaki and Kumagai (1988a and 1988b) and Senzaki (1988) also suggested the use of iron powder for removal of TCE and trichloroethane (TCA) from wastewater. However, the in situ application of iron was highlighted by researchers at the University of Waterloo (Reynolds et al., 1990; Gillham and O'Hannesin, 1992), who conducted focused efforts in this area. The



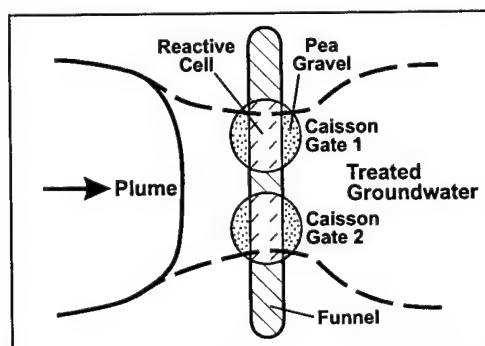
(a) PRB (Elevation View)



(b) Continuous Reactive Barrier (Plan View)



(c) Funnel-and-Gate System (Plan View)

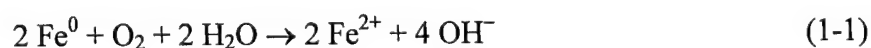


(d) Funnel-and-Gate System with Two Caisson Gates (Plan View)

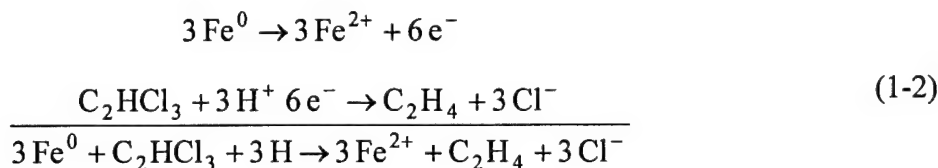
Figure 1-1. Schematic Illustrations of Some PRB Configurations

University of Waterloo currently holds a patent for the use of zero-valent metals for in situ groundwater treatment (Gillham, 1993).

The exact mechanism of degradation of chlorinated compounds by iron or other metals is not fully understood. In all probability, a variety of pathways are involved, although recent research seems to indicate that certain pathways predominate. If some oxygen is present in the groundwater as it enters the reactive iron cell, the iron is oxidized and hydroxyl ions are generated (Equation 1-1). This reaction proceeds quickly, as evidenced by the fact that both the dissolved oxygen (DO) and the oxidation-reduction potential (ORP) drop quickly as the groundwater enters the iron cell. The importance of this reaction is that oxygen can quickly corrode the first few inches of iron in the reactive cell. Under highly oxygenated conditions, the iron may precipitate out as ferric oxyhydroxide (FeOOH) or ferric hydroxide [$\text{Fe}(\text{OH})_3$], in which case the hydraulic conductivity of the reactive cell could potentially become considerably lower in the first few inches at the influent end:



Once oxygen has been depleted, the reducing conditions created lead to a host of other reactions. Chlorinated organic compounds, such as TCE, are in an oxidized state because of the presence of chlorine. Iron, a strong reducing agent, reacts with the chlorinated organic compounds through electron transfers, in which ethene and chloride are the primary products (Equation 1-2).

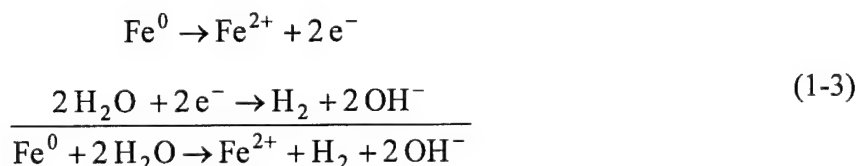


In one study, Orth and Gillham (1996) found that ethene and ethane (in the ratio 2:1) constitute more than 80% of the original equivalent TCE mass. Partially dechlorinated byproducts (such as *cis*-DCE, *trans*-DCE, 1,2-DCE, 1,1-DCE, and VC) of the degradation reaction were found to constitute only 3% of the original TCE mass. Additional byproducts included hydrocarbons (C1 to C4) such as methane, propene, propane, 1-butene, and butane. Virtually all the chlorine in the original TCE mass was accounted for as inorganic chloride in the effluent, or as chlorine remaining on the partially dechlorinated byproducts. Similar results were obtained by Sivavec and Horney (1995), who quantified both liquid and gas phases of the reaction to obtain a carbon balance greater than 90%.

A number of interesting issues are raised by this explanation of the reaction mechanism. For Equation 1-2 to take place in one step, without the generation of larger amounts of partially dechlorinated products (e.g., DCE or VC), six electrons have to be transferred almost instantaneously. Given the low probability of an instantaneous transfer of this magnitude, Orth and Gillham (1996) suggest that the TCE molecule must remain attached to the metal surface long enough for the six-electron transfer to occur. The TCE molecule remains attached to the metal surface either through the inherent hydrophobicity of TCE or, as Sivavec and Horney (1995) suggest, by the formation of a strong chloroethene-iron pi-bond. This bonding prevents desorption until dechlorination is complete, although a few random chloroethene molecules may desorb early, leading to the presence of small amounts of DCE and VC. Taken together, these ideas suggest that degradation of chlorinated organics by metals is a surface phenomenon and that the rate is governed by the specific surface area of the reactive medium.

Equation 1-2 shows the transformation of TCE to ethene, which is the primary product in many studies. It is unclear whether the other significant product, ethane, represents a different degradation pathway for TCE or whether it results from the iron-mediated catalytic transformation of ethene. Also unclear is whether the C1 to C5 hydrocarbons represent an alternative pathway for TCE degradation or some other reaction. One study (Hardy and Gillham, 1996) suggests that aqueous CO₂ is reduced on the iron surface to form these hydrocarbon chains. Another study (Deng et al., 1996) suggests that the source of these hydrocarbons is the acid dissolution of gray cast irons containing both carbide and graphite carbon.

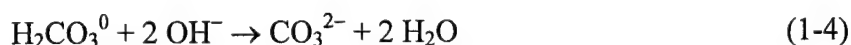
Iron also reacts with water (Equation 1-3) under reducing (anaerobic) conditions, although these reactions are believed to be much slower. Hydrogen gas and OH^- are formed as water is reduced, as shown in Equation 1-3.



Hydrogen generation could be a concern if hydrogen accumulates in the aquifer as it appears to do in some column tests. However, although initial field users were prepared to install hydrogen-gas collection systems, this has not been necessary at any site so far. Hydrogen generated by the slow reaction is believed to degrade through biological transformations (EnviroMetal Technologies, Inc. [ETI], 1996).

Because several of the above reactions produce OH^- , the pH of the water in the reactive iron cell typically increases, often reaching values above 9.0. One effect of increased pH initially was thought to be a slowing down of the TCE degradation rate (O'Hannesin, 1993). The anticipation was that changes in pH might cause changes in the degradation rate through direct involvement of H^+ in Equation 1-2. However, subsequent research is unclear on whether or not pH affects degradation rate (Agrawal and Tratnyek, 1996).

An indirect effect of increasing pH is the potential for formation of precipitates, which could coat the surface of the iron and potentially reduce the reactivity of the iron and the hydraulic conductivity of the reactive cell. The dissolved carbonic acid and bicarbonate (alkalinity) present in many natural groundwaters act as buffers limiting pH increase and precipitate formation (Equations 1-4 and 1-5).



Soluble carbonate ions are formed as the OH^- ions are consumed. If carbonate ions continue to build up, precipitation of carbonate solid species may occur. Depending on the composition of the groundwater, the precipitates formed could be calcite (CaCO_3), siderite (FeCO_3), or magnesium hydrocarbonates (Reardon, 1995). If groundwater carbonate is exhausted through the precipitation of carbonate minerals, the water may become saturated with respect to $\text{Fe}(\text{OH})_2$ as the iron continues to oxidize. $\text{Fe}(\text{OH})_2$ is relatively insoluble and may precipitate out if it builds up.

In summary, most groundwaters contain many different aqueous species that may play some role in affecting the performance of a permeable barrier. In general, the course of chemical reactions taking place in multi-component systems cannot be predicted by considering each species individually, because most of these reactions are interdependent. To some extent, equilibrium and

nonequilibrium behavior in complex systems can be predicted using geochemical modeling codes, which are described in Section 7. Another difficulty is that, even if the type and mass of reaction products could be predicted, it is uncertain as to how many of these products are actually retained in the reactive cell and affect performance. For example, very fine precipitates that may be formed could be carried out of the reactive cell by colloidal transport with the groundwater flow. However, the reaction chemistry discussed above and the geochemical modeling codes described in Section 7 do provide a basis for selecting appropriate reactive media and planning performance monitoring schemes after permeable barrier installation.

Gillham and O'Hannesin (1994) conducted column tests on TCE-contaminated water, with and without an added biocide (azide). Similar degradation rates were observed in both cases, demonstrating that the degradation of TCE was abiotic and could proceed without microbial intervention. Also, microbial analysis (phospholipid fatty acid [PLFA] measurements) of the groundwater conducted during a pilot study at an industrial facility in Sunnyvale, CA indicated no signs that the reactive media encouraged development of a microbial population over that in the surrounding aquifer (ETI, 1995).

However, the potential for microbially mediated processes in the reactive cell may be present under certain conditions. Whether such microbial processes are beneficial or deleterious to the performance of the reactive cell is not clearly understood. No significantly enhanced microbial activity has been noticed in the field installations to date.

1.2.2 PRB Configurations

The two main configurations of PRBs that have been employed are continuous reactive barriers and funnel-and-gate systems (see Figure 1-1). A continuous reactive barrier consists of only a permeable reactive section. A funnel-and-gate system consists of both permeable and impermeable sections, a configuration in which the impermeable section (funnel) generally flanks the permeable section (gate). The "funnel" is expected to channel flow to the "gate" to provide a larger hydraulic capture zone while minimizing the amount of reactive medium used.

1.3 Project Description

Based on column tests conducted on several alternative reactive media and using site groundwater, U.S. EPA-NERL reported that a pyrite-and-iron combination ranked the best (U.S. EPA, 1997). Because of its potential for scrubbing oxygen and controlling pH in the iron-groundwater system, pyrite was expected to provide the benefits of enhanced kinetics of CVOC degradation and reduced precipitation of inorganic constituents. Based on this recommendation, Battelle designed and installed a funnel-and-gate PRB with two gates (Battelle, 1997) at Dover AFB. As shown in Figure 1-2, both gates have a reactive cell consisting of 100% granular iron. In addition, Gate 1 incorporates a pretreatment zone (PTZ) consisting of 10% iron and sand, and Gate 2 incorporates a PTZ consisting of 10% pyrite and sand. The exit zone in both gates consists of 100% coarse sand. The construction of the PRB was completed in January 1998.

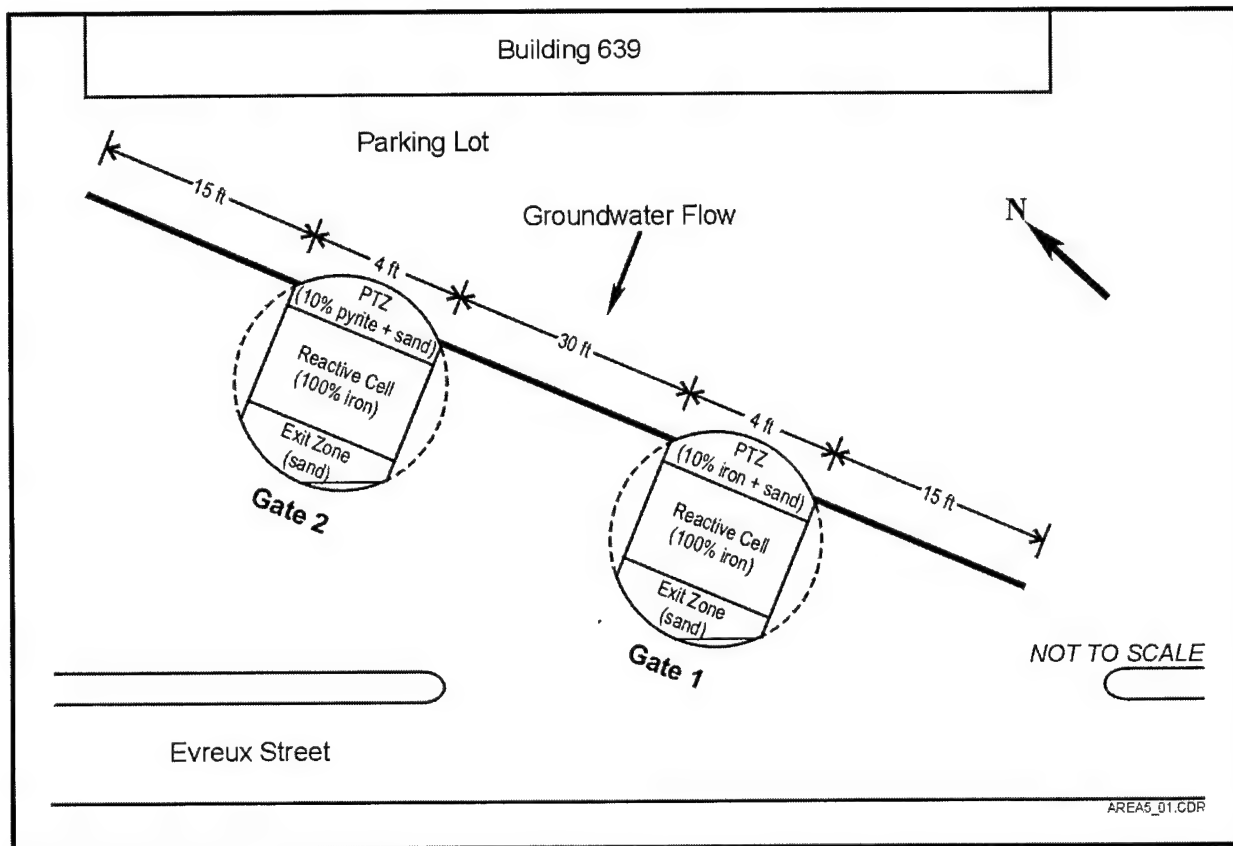


Figure 1-2. Schematic of the PRB in Area 5 at Dover AFB

The location and dimensions of the barrier were determined by detailed site characterization and modeling conducted in June 1997 to support the PRB and monitoring system design (Battelle, 1997). The groundwater treatment targets for this project were 5 $\mu\text{g/L}$ of PCE and TCE, 70 $\mu\text{g/L}$ of *cis*-1,2-DCE, and 2 $\mu\text{g/L}$ of VC; these targets correspond to the U.S. EPA-recommended maximum contaminant levels (MCLs) for the respective CVOCs. An innovative construction technique involving caissons was used to install the two gates down to about 40 ft below ground surface (bgs), which is beyond the reach of conventional backhoe installation. This innovative construction technique also facilitated the installation of the PRB in the midst of several underground utility lines.

Following installation, Battelle evaluated the reactive and hydraulic performance of the PRB primarily through two comprehensive monitoring events conducted in July 1998 and June 1999. Limited monitoring events were conducted periodically throughout the demonstration to monitor specific operating parameters. Core samples of the gate and aquifer media were collected and analyzed after 18 months of PRB operation. Monitoring results show that, to date, the PRB is functioning at an acceptable level in terms of capturing groundwater, creating strongly reducing conditions, and achieving treatment targets.

This report describes the detailed methodology and results of the demonstration, and discusses the implications for the technology. The PRB design methodology and monitoring strategy used in this demonstration follows the *Design Guidance for Application of Permeable Reactive Barriers for Groundwater Remediation* (Gavaskar et al., 2000), the *Regulatory Guidance for Permeable Barrier Walls Designed to Remediate Dissolved Chlorinated Solvents* (ITRC, 1997), and the *Regulatory Guidance for Permeable Reactive Barriers Designed to Remediate Inorganic and Radionuclide Contamination* (ITRC, 1999). The results and conclusions of the demonstration are summarized in Section 9.

2. PRB Design

This section is organized according to the design methodology outlined in Figure 2-1 and describes the preliminary site assessment, additional site characterization, column testing (media screening/selection), hydrogeologic modeling, geochemical evaluation, and evaluation of construction techniques that constituted the design process for the PRB (Gavaskar et al., 2000). More detailed modeling and design of the Dover AFB barrier are described in the *Design/Test Plan: Permeable Barrier Demonstration at Area 5, Dover AFB* (Battelle, 1997). The construction activities also are described in this section.

2.1 Preliminary Site Assessment

Dover AFB is located 2 miles south of the city of Dover, DE and is home to the 436th Airlift Wing and the 512th Airlift Wing. The mission of the Base is to provide strategic global airlift support for either overseas military operations or humanitarian aid using a fleet of C-5 Galaxies as the primary aircraft. Area 5, shown in Figure 2-2, is the site of the PRB demonstration. Area 5 was selected for the demonstration by AFRL in January 1997 after review of historical site geology and contaminant distribution information (Dames and Moore, 1995). The PRB is located in a parking lot on the south side of Building 639, which is the Base Supply Building. The exact locations and activities leading to the solvent releases that caused the Area 5 plume are not known; however, solvents historically have been used at the Base for maintenance. There was no dry cleaning at this site.

Dover AFB lies within the Atlantic Coastal Plain Physiographic Province, which consists of Cretaceous to recent sedimentary deposits. The two uppermost major geologic units are the surficial Pleistocene Columbia Formation on top and the Miocene Calvert Formation of the Chesapeake Group below it. The Columbia Formation, in which the barrier is placed, is a fluvial sedimentary unit predominantly composed of sand with some gravel. The reddish brown to black sand in this formation is poorly sorted and coarse to medium grained in size with interbedded lenses of silt and clay. The thickness of the Columbia Formation ranges from 30 to 70 ft at Dover AFB. The Calvert Formation in the Dover AFB region is 300 ft thick. The upper sediments of the formation are silt to silty clay based on grain size and represent a competent aquitard under the Columbia aquifer.

The Area 5 site was considered suitable for PRB application because:

- The groundwater contaminants, PCE, TCE, and *cis*-1,2-DCE, were known to be degradable by available reactive media.

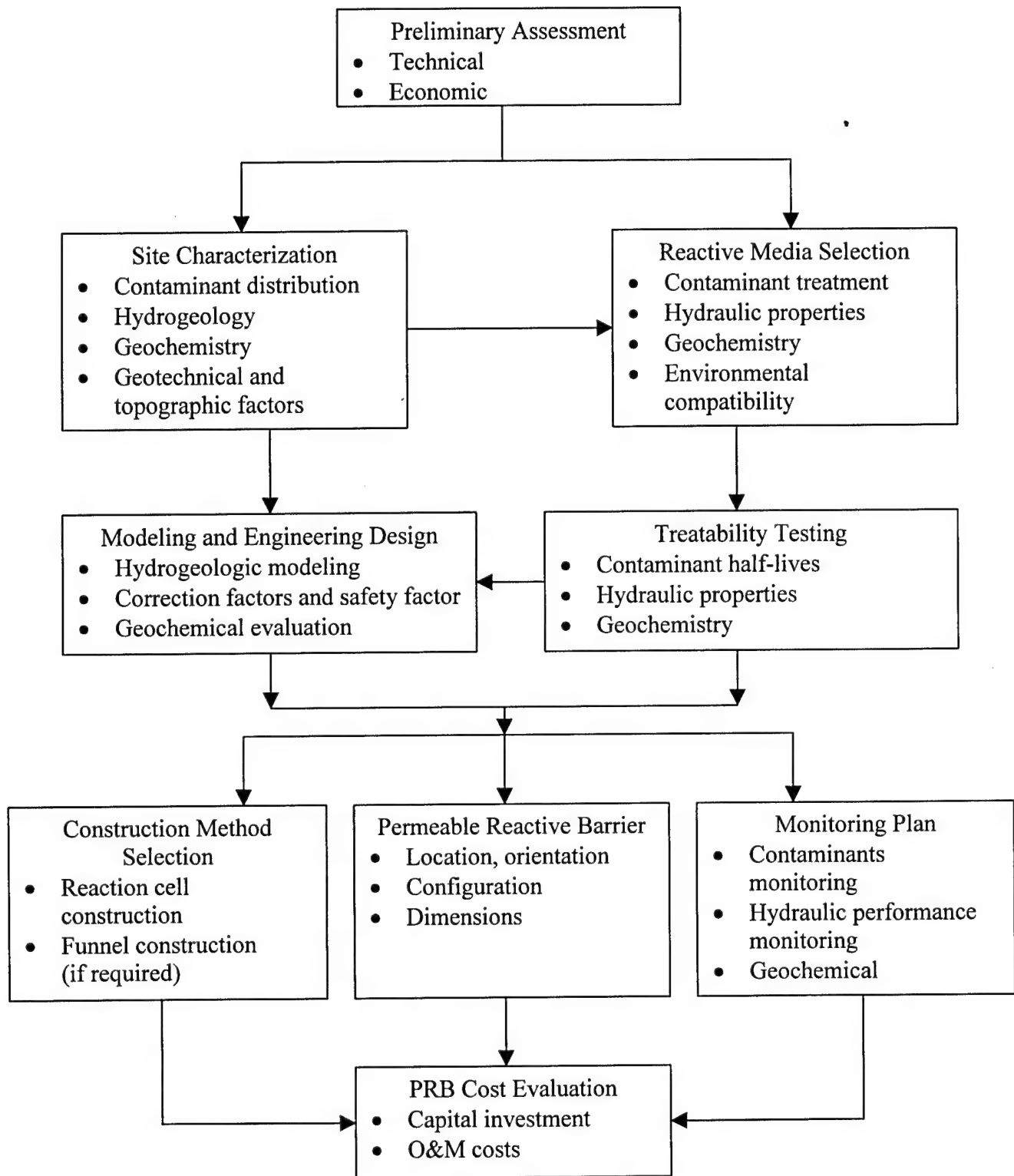


Figure 2-1. Steps in the Design of a Permeable Barrier System

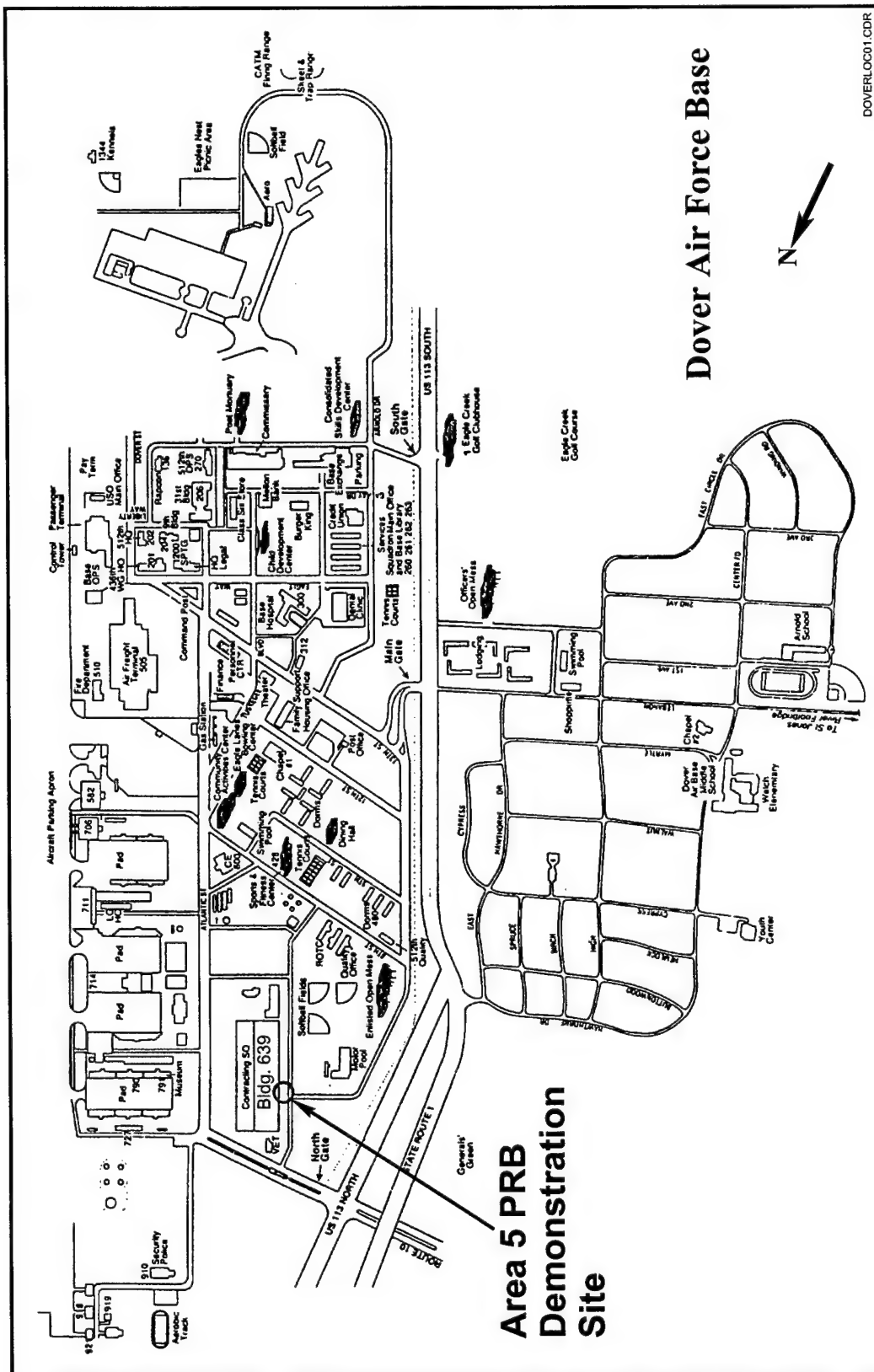


Figure 2-2. Location of the PRB Demonstration in Area 5 at Dover AFB

- ❑ The plume size and distribution were not known at the time of site selection. However, elevated CVOC concentrations had been discovered in two existing wells, one on the north side and one on the south side of Building 639. And, because regional groundwater flow gradient was to the southwest, the parking lot on the south side of the building seemed like a suitable location to intercept the suspected plume.
- ❑ The depth to aquitard at the site was reported to be about 40 ft (Applied Research Associates, Inc. [ARA], 1996). Although this depth was beyond the reach of conventional backhoe excavation, alternative emplacement techniques (such as caisson installation) had the potential to work.
- ❑ A major geotechnical consideration at this site was the presence of underground utilities. Water, gas, storm drainage, and sanitary sewer lines underlay the parking lot. However, construction contractors that were consulted felt that this hurdle could be overcome by choosing a suitable PRB location and by using suitable construction techniques.
- ❑ Historical site-wide data (ARA, 1996) indicated that the underlying aquitard was significantly thick and continuous to establish a key for the barrier.
- ❑ Historical site-wide data indicated a groundwater velocity range of 0.06 to 0.3 ft/day, which seemed relatively low and therefore suitable for PRB application. (Depending on influent concentrations, high groundwater velocities may indicate the need for a very thick reactive cell to provide the required residence time for the plume in the reactive medium. A thicker PRB generally entails higher costs for the reactive medium and construction.)

One key consideration from a demonstration perspective was the high level of DO in the groundwater. DO reacts with the iron medium in a PRB to form corrosion products or precipitates. Because this reaction is very fast, these precipitates tend to deposit in the first few inches of the iron at the influent end. The consideration was that high DO levels at the site might cause excessive deposition in the influent end and adversely affect the reactive and hydraulic properties of the PRB. The Area 5 groundwater contains one of the highest DO levels observed at a site where a PRB has been applied, and one of the objectives of the demonstration was to design the PRB in a way that would scrub out the DO before it reached the reactive cell. Therefore, a PTZ was incorporated in the design for each gate to scrub out the oxygen.

2.2 Additional Site Characterization

Because most of the available site data at the time of site selection were from site-wide investigations (Dames and Moore, 1995; ARA, 1996), more localized characterization in the parking lot on the south side of Building 639 was determined to be necessary for designing the PRB. In June 1997, additional site characterization was conducted, primarily on the south side of Building 639, to better delineate the CVOC plume and to determine the hydrogeology and geochemistry of the aquifer in the vicinity of the tentative PRB location.

Figure 2-3 shows one of several geological cross sections developed at Area 5 from several pushes with a cone penetrometer test (CPT) rig. The water table occurs at approximately 15 ft bgs, although seasonal variations cause the water level to fluctuate between about 13 and 17 ft bgs. The silty clay aquitard occurs at approximately 36 to 38 ft bgs and was found to be competent enough for the barrier to be keyed 2 ft into it. The aquifer consists mostly of sandy soil, and an intermediate thin fine-grained layer occurs at approximately 15 ft bgs near the water table. Although its presence is reported as intermittent on the Base, this fine-grained layer was found to be continuous in the vicinity of the PRB. Depending on seasonal and annual fluctuations in the water table, this intermediate fine-grained layer may or may not be submerged in the groundwater.

The porosity of the aquifer matrix was estimated at 32% based on five soil samples collected in the vicinity of the current PRB. The two aquitard samples collected indicate a porosity of 60% matching their clay content. Historical data from slug tests and pump tests conducted in the aquifer at Dover AFB indicated a hydraulic conductivity (K) ranging from 1.76 to 45.5 ft/day (ARA, 1996). Slug tests conducted during additional site characterization in existing well MW214S, which is positioned close to the current location of the PRB, showed a K ranging from 5.68 to 6.48 ft/day. The K for the aquitard as measured in laboratory tests on two soil samples ranged from 1.29E-3 to 6.83E-3. Based on water-level data, the hydraulic gradient at Area 5 is relatively flat at 0.002. For a likely K value between 10 to 50 ft/day, a relatively low groundwater velocity of 0.06 to 0.3 ft/day was estimated for the Area 5 aquifer, at the time of the PRB design. Subsequent aquifer monitoring showed that the actual velocity is near the lower end of this range. The groundwater flow at Area 5 is generally to the southwest (see Figure 2-4); the actual direction may vary seasonally by as much as 30 degrees.

The results of the site characterization conducted in July 1997 are detailed in the design/test plan (Battelle, 1997). A CPT rig was used to punch temporary wells (T-wells shown in Figure 2-5) at several locations to delineate the geology and CVOC distribution in the parking lot on the south side of Building 639. Based on the results of the site characterization in June 1997, the PCE distribution shown in Figure 2-5 was identified. The CVOC plume contains PCE, TCE, and *cis*-1,2-DCE. No significant nonchlorinated volatile organic compounds (VOCs) were found in the groundwater at Area 5.

CVOC concentrations show sharp variations both horizontally and vertically in the aquifer; however, no clear spatial trends could be identified indicating that the contamination probably originated from multiple sources. Table 2-1 shows the highest concentrations found in the potential capture zone of the PRB during site characterization and subsequent monitoring events. Based on the most recent monitoring event in June 1999, up to 3,900 µg/L of PCE, 160 µg/L of TCE, and 140 µg/L of *cis*-1,2-DCE are present upgradient of the PRB, in the probable capture zone.

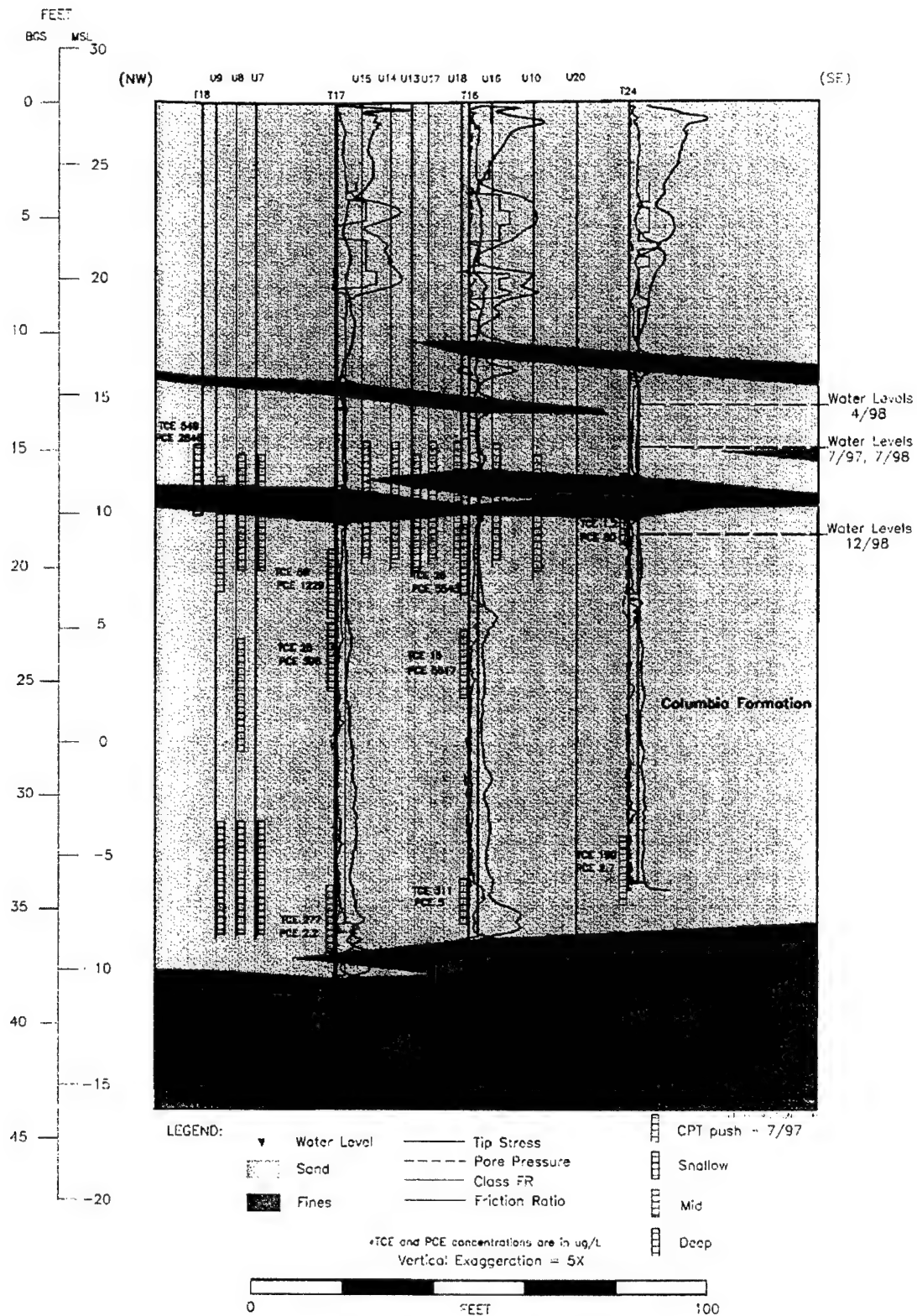


Figure 2-3. Northwest-Southeast Cross Section near the PRB

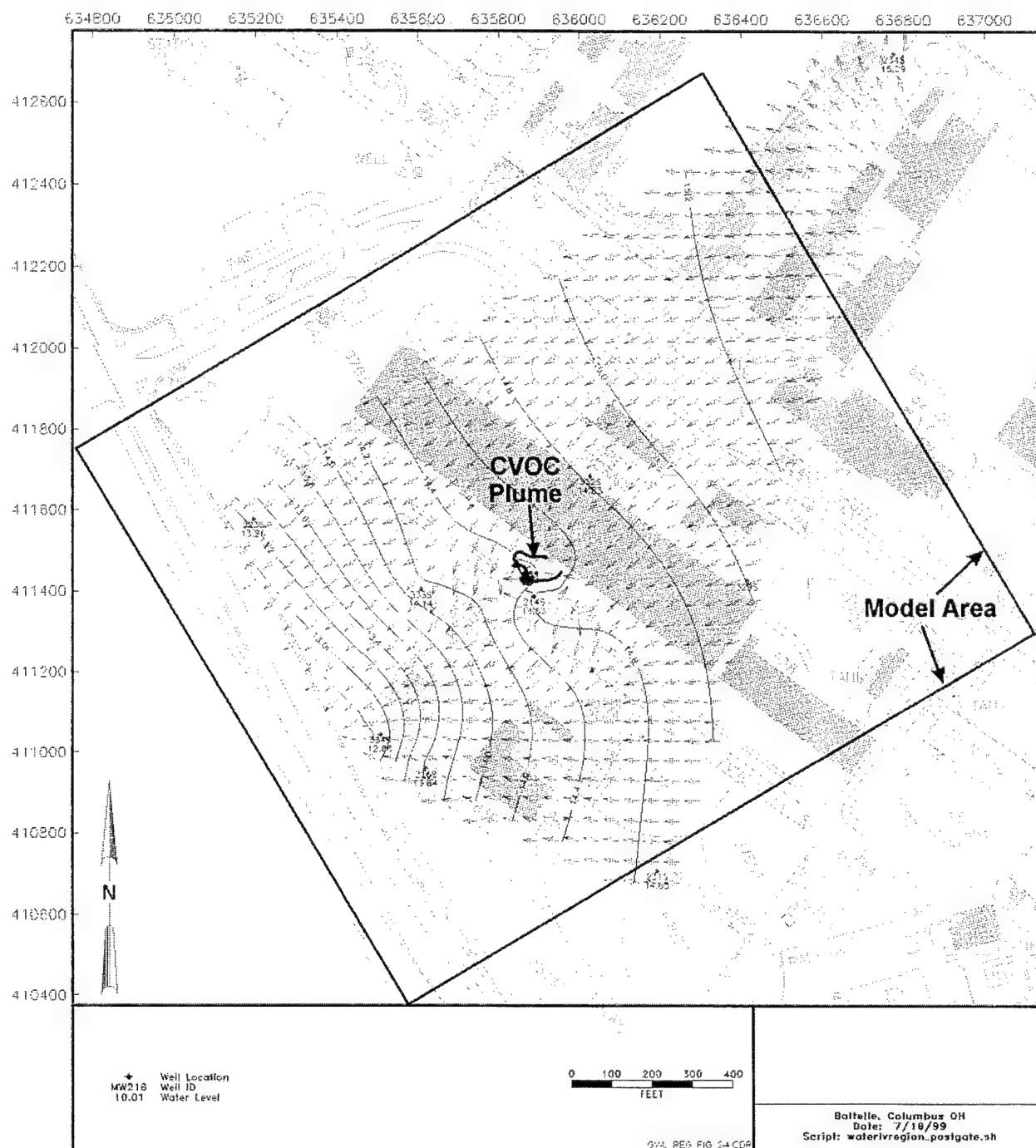


Figure 2-4. Typical Water-Level Map Showing Regional Groundwater Flow in Area 5 at Dover AFB

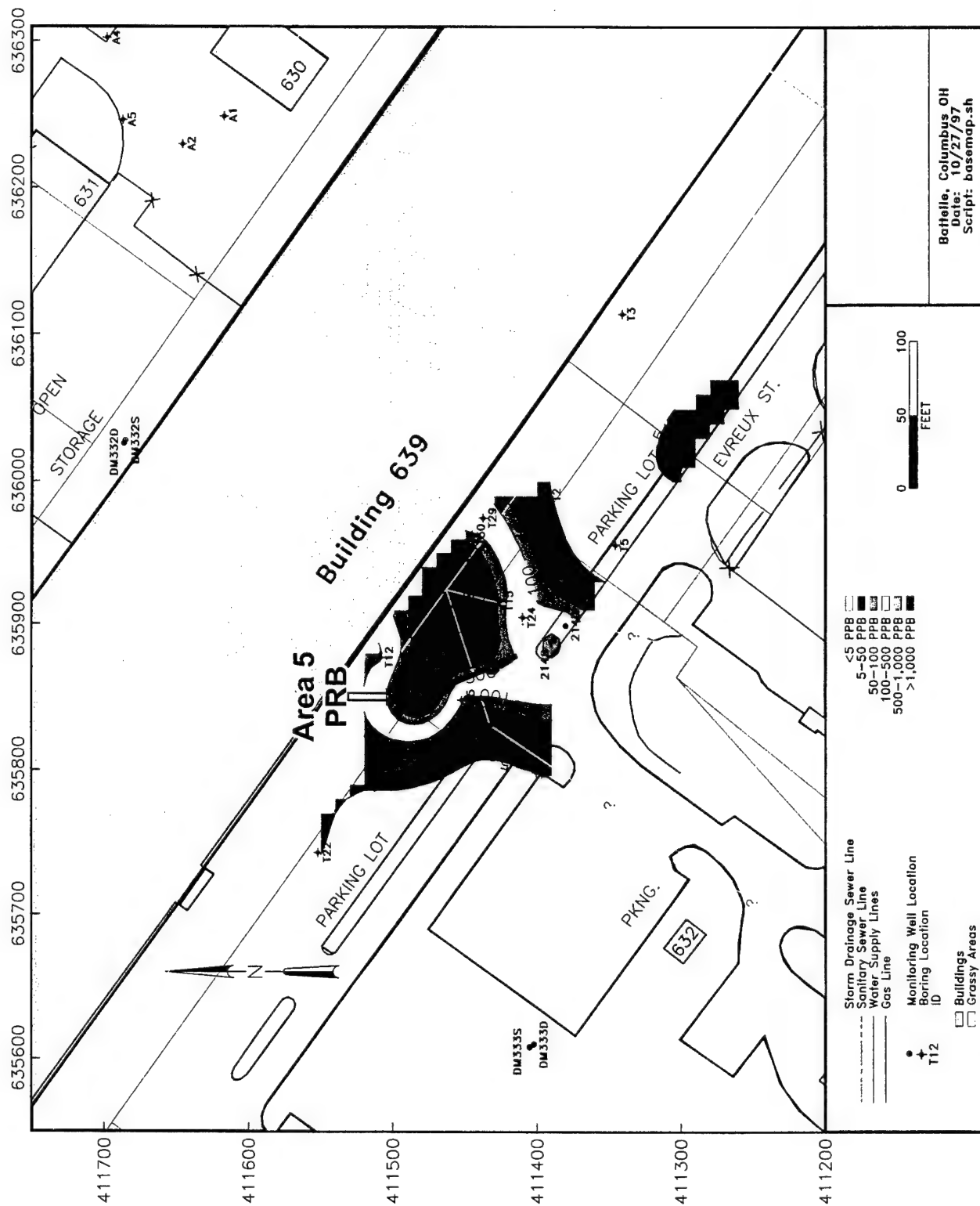


Table 2-1. Maximum CVOC Concentrations Recorded in Wells Likely to Be Within the Capture Zone of Each Gate

Date	Upgradient of Gate #	Monitoring Well(s) ^(a)	Depth of Well Screen (ft bgs)	Maximum PCE Concentration ^(b) (µg/L)	Maximum TCE Concentration ^(b) (µg/L)	Maximum <i>cis</i> -1,2-DCE Concentration ^(b) (µg/L)
June 1997	Gate 1	T16M	23-28	5,617	15	22
		T16D	31-36	ND	311	131
		T15D	31-36	ND	254	176
	Gate 2	T18S	15-20	2,846	549	324
July 1998	Gate 1	U4D	31-36	334	22	69
	Gate 2	U9D	31-36	275	21	52
		U9S	15-20	ND	45	ND
June 1999	Gate 1	T35B ^(c)	21-24	3,900	18	38
		U19 ^(c)	15-25	1,400	ND	120
		U4D	31-36	520	44	130
	Gate 2	U9D	31-36	480	42	140
		T36E	31-34	ND	160	100

(a) Well identifications (IDs) that start with T are temporary wells, and were pushed with a CPT rig.

(b) Bold numbers indicate maximum concentrations recorded for that region.

(c) Well U19 has the highest PCE concentration in the wells closest to Gate 1. Well T35B is further upgradient, but is within the expected capture zone.

ND = Not detected.

2.3 Column Tests for Alternative Media Selection and Kinetics Determination

U.S. EPA-NERL conducted long-term aboveground column tests at Area 5 from February to April 1997 (U.S. EPA, 1997). Four columns containing four different reactive media were installed near an existing well MW214D, which is screened in the lower part of the aquifer. Column tests are useful for determining the degradation rate or half-life for each target contaminant. The half-lives indicated by these tests can be used to design the thickness of the PRB. By using multiple columns containing different reactive media, the effectiveness of the media can be compared.

CVOC concentrations in the column influent for these tests were measured at 90 µg/L of TCE and 10 µg/L of PCE. Installing the columns on site provided access to a continuous supply of site groundwater for the evaluation. The four media evaluated were granular iron from Connelly-GPM, Inc. (Connelly), bimodal iron foam from Cercona™; pyrite (FeS₂), from Ward Scientific, Inc.; and a combination of granular iron (from Connelly) and guar gum. The U.S. EPA (1997) also reported that previous column tests had indicated that higher degradation rates are obtained when a pyrite layer precedes the iron, rather than when the pyrite and iron are mixed together. Therefore, the pyrite was packed in the influent end of the column to serve as a pretreatment area for the 100% granular iron zone that followed.

Pyrite reacts with oxygen as indicated in Equation 2-1. In the process of scrubbing out oxygen from the groundwater, H^+ ions are generated which can act to control pH:

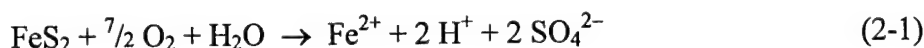


Table B-1 in Appendix B summarizes the reaction rates and half-lives of TCE in the four reactive media reported for the column tests (U.S. EPA, 1997). Based on these results, NERL reported that in terms of effectiveness in achieving cleanup standards and kinetics, the pyrite-iron medium ranked the best. The pH in the pyrite-iron column was reported as showing a slightly smaller increase as compared to the other columns.

2.4 PRB Design

The objective of the design process was to determine the optimum location, orientation, and dimensions of the PRB, and was achieved through the following design steps:

- **Location.** The location of the PRB was determined primarily by the location of the plume and the desire to test the barrier on reasonably high concentrations of CVOCs. Therefore, a decision was made to locate the barrier within the plume rather than at the edge of the plume. Initially, the barrier location was selected approximately 8 ft closer to Building 639 than the actual location shown in Figure 2-5. However, during construction the water line was discovered to be a few feet further away from the building than was shown on historical site maps. To avoid the water line, the barrier eventually was placed 8 ft downgradient from the initially planned location. Due to a low groundwater velocity in the aquifer, barrier placement had considerable bearing on the CVOC concentrations eventually encountered during the period of the demonstration. This PRB placement process shows that underground utilities can play a significant role in determining the location. In fact, in its current location, the barrier still intersects a storm drainage line. This storm drain was cut before installing the barrier and rejoined over the barrier after it was installed.
- **Orientation.** Hydrogeologic modeling with MODFLOW (flow model) (McDonald and Harbaugh, 1988) and Random-Walk (solute transport model) (Naymik et al., 1995) was used to determine the optimum orientation of the barrier. As mentioned in Section 2.2, water-level data for historical high- and low-flow conditions indicate that the groundwater flow direction may change seasonally by as much as 30 degrees. As shown in Figure 2-6, the optimum PRB orientation was chosen to capture the targeted high-CVOC portion of the plume during both flow extremes.
- **Dimensions.** The thickness of the reactive cell was calculated using the CVOC half-lives in the iron determined during column testing (see Section 2.3). The height of the PRB was determined on the basis of historical water levels and depth of the aquitard. The bottom of the reactive cell was designed to obtain a key of 2 ft in the aquitard that was encountered at around 37 ft bgs. The top of the reactive cell was designed to reach a height of 10 ft bgs, which is 3 ft above the water level of 13 ft bgs reached during high-flow conditions in May 1994. The total width of the reactive cell

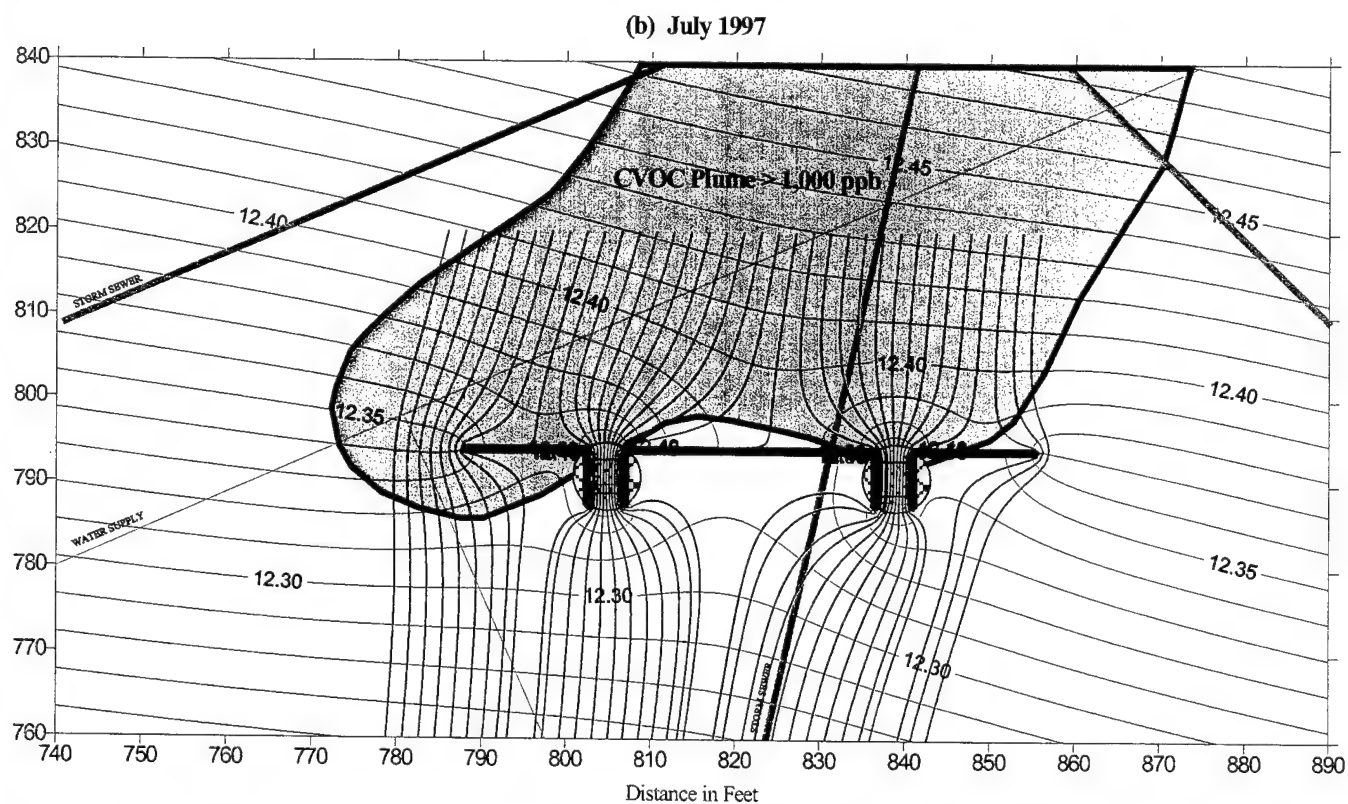
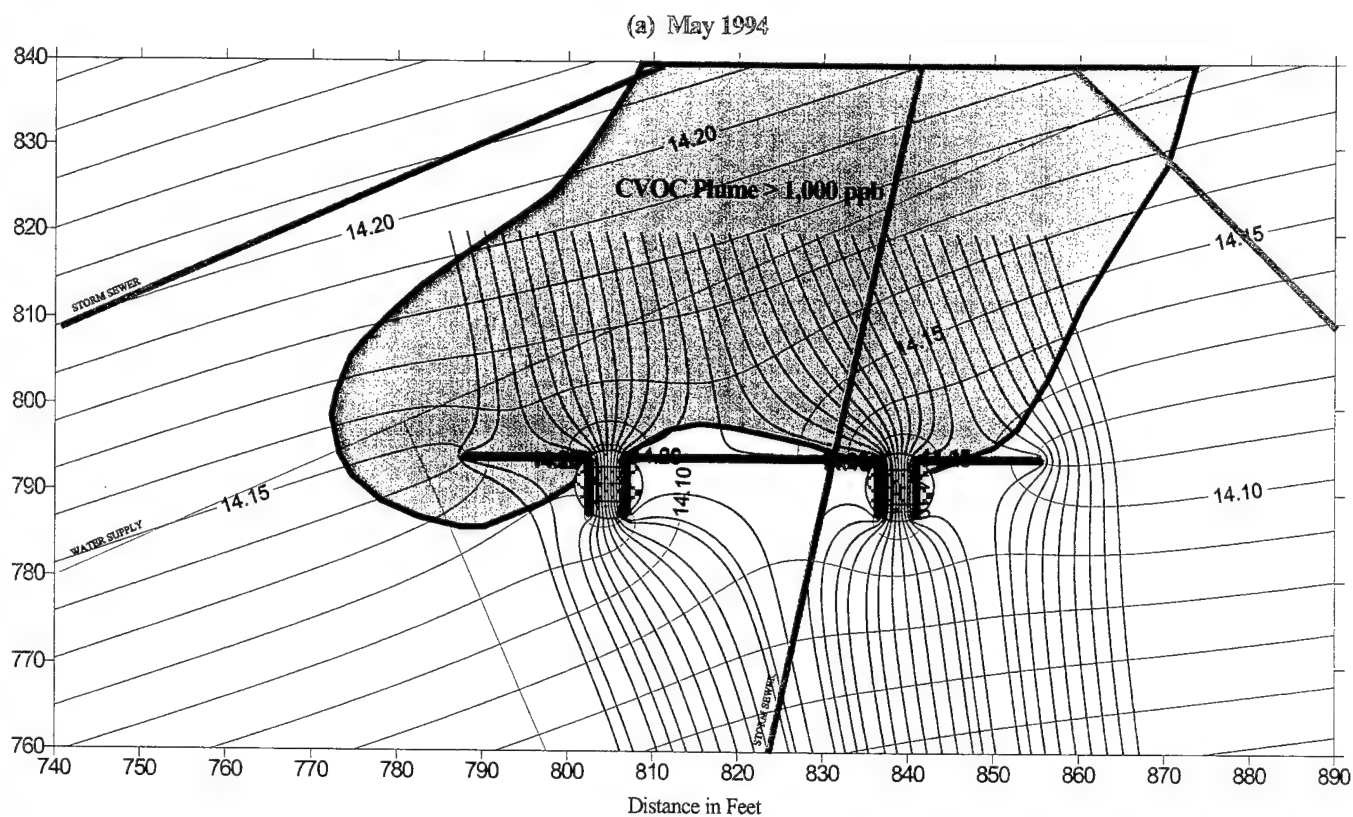


Figure 2-6. Simulated Water Levels (Based on December 1993 Conditions) at Area 5 for K_{aq} Values of (a) 10 ft/day and (b) 50 ft/day

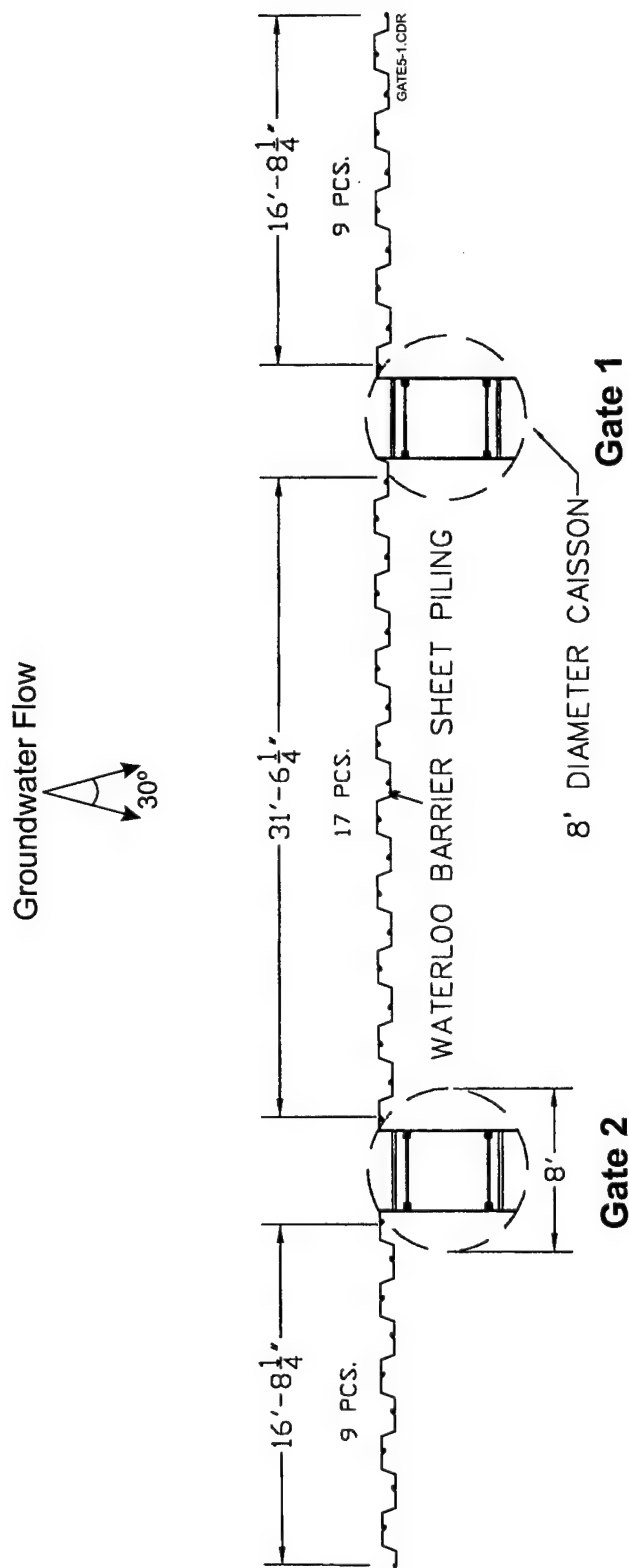
was designed at 8 ft (two 4-ft-wide gates) and the total width of the funnel was designed at 60 ft. As shown in Figure 2-6, these dimensions were based on hydro-geologic modeling which showed that a 40- to 50-ft-wide capture zone that incorporated the more concentrated portions of the plume was likely to be achieved. Detailed modeling description and results are presented in the design/test plan (Battelle, 1997).

Designing two separate gates allowed two different reactive media to be tested in the same plume. Figures 2-7 and 2-8 show a plan view of the complete PRB system and a detailed plan view of a PRB gate, respectively. Both gates consist of a reactive cell containing granular iron, preceded by a PTZ. The PTZ in Gate 1 consists of a 10% iron-sand mixture; the PTZ in Gate 2 consists of a 10% pyrite-sand mixture. The aim of the PTZ is to improve the longevity of the reactive medium by scrubbing out oxygen from the groundwater before it reaches the 100% iron zone. In addition, the pyrite in Gate 2 was aimed at controlling the rise in pH. The presence of DO and high pH are conditions detrimental to the longevity of the reactive medium because these conditions promote the formation of precipitates on the granular iron surfaces, thus potentially altering the reactivity and hydraulic performance of the barrier.

As mentioned in the design steps, the residence time and thickness of the reactive cell (100% iron section) in each gate were based on the on-site column test results reported by U.S. EPA-NERL (U.S. EPA, 1997). Table 2-2 shows the residence time requirements estimated for the CVOC compounds at the maximum expected concentrations. Because the influent to the columns from existing site well MW214D contained primarily TCE (80 µg/L), the TCE half-life was obtained directly from these tests. Proportionately higher half-lives were assumed for PCE, *cis*-1,2-DCE, and VC based on degradation trends reported in other studies. Correction factors of 2 and 1.5 were applied to the maximum residence time to account for temperature and bulk density differences, respectively, between column and field applications. Therefore, the maximum time of 12 hours reported in Table 2-2 was corrected to 36 hours.

The temperature and bulk density corrections are discussed in detail in the design guidance document (Gavaskar et al., 2000). The temperature correction factor accounts for the lower reaction rate that may be expected due to the fact that the temperature in the aquifer (10°C) is lower than the temperature in the columns (18°C). The bulk density correction factor accounts for the fact that the porosity (around 0.65) reported in previous field PRBs tends to be higher than the porosity (0.45) of iron in columns. A higher porosity (or lower bulk density) indicates lower packing density and lower reactive surface area. To account for other uncertainties (e.g., changes in CVOC concentrations over time in the barrier influent, possible persistence of the more recalcitrant byproducts *cis*-1,2-DCE and VC, and/or long-term accumulation of precipitates in the reactive cell) an additional safety factor of 2 was applied to the corrected residence time (36 hours) to obtain a final design residence time requirement of 72 hours or 3 days.

Several funnel-and-gate configuration and dimension scenarios were modeled to determine optimum gate and funnel dimensions that would provide an approximately 50-ft-wide groundwater capture zone, while still providing at least 3 days of residence time (Battelle, 1997). Historical high-flow (May 1994) and low-flow (December 1993) conditions were modeled.



Modified from: C³ Environmental, 1998.

Figure 2-7. Plan View of Complete PRB System

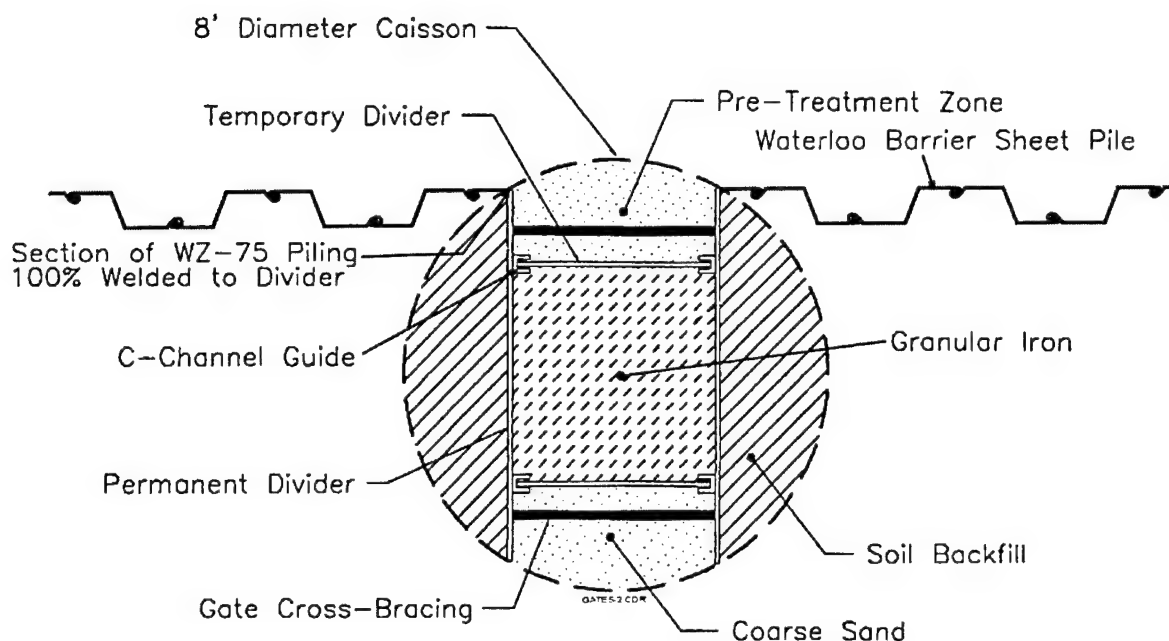


Figure 2-8. Detailed Plan View of PRB Gate

Table 2-2. Residence Time Requirements

Contaminant	Maximum Expected Concentration (µg/L)	MCL (µg/L)	Half-Life (hr) of CVOC in Connelly Iron	Number of Half-Lives to Reach MCL	Residence Time in Iron (hr)
PCE	10,000	5	1 ^(a)	12	12
TCE	1,000	5	0.5 ^(b)	8	4
DCE	1,000 ^(c)	70	1.5 ^(a)	4	6
VC	500 ^(c)	2	1.5 ^(a)	8	12

(a) Based on degradation trends reported in other studies (Gavaskar, 2000) and relative to TCE data.

(b) Based on on-site column tests at Area 5.

(c) Native concentration plus about 5% of PCE and TCE.

With a 4-ft gate width and a 60-ft long funnel (one 30-ft section between the two gates and two 15-ft sections along the wings), the maximum expected groundwater velocity through the gate was expected to be 0.85 ft/day. This scenario assumed that the entire gate would be filled with material similar in size (-8+50 mesh) to the Connelly iron used in the column studies. The funnel-to-gate ratio of 7.5 to 1, although on the high side, seemed reasonable for a low-gradient aquifer.

Two construction-related factors were considered before assigning the final dimensions of the gates. First, preliminary consultations with construction vendors indicated that caisson-based excavation would be the most suitable for this site. Standard circular caissons were available in 4-ft, 6-ft, or 8-ft diameter sizes. It was determined that, with an 8-ft-diameter caisson, a 4-ft thick reactive cell could be incorporated with room for approximately 2-ft thick pretreatment and exit zones on either side, as shown in Figure 2-8. A 4-ft thick reactive cell would provide 4.7 days of residence time under high flow conditions with an expected maximum groundwater velocity through the reactive cell of 0.85 ft/day, thereby meeting the 3-day minimum residence time requirement.

Second, the PTZ and exit zones were incorporated in the design for this demonstration to create transition zones between the reactive cell and the aquifer for measuring influent and effluent concentrations. In a full-scale system, these transition zones could be eliminated to reduce cost. In some PRBs installed at other sites, pea gravel has been used in the transition zones to homogenize flow and facilitate sampling of influent and effluent. Pea gravel has a larger particle size compared to either the aquifer soil or iron, and these size differences results in sharp permeability contrasts that can cause some groundwater accumulation at the transitions from pea gravel to iron and from pea gravel to the aquifer (Battelle, 1998). To reduce such sharp permeability contrasts, coarse sand similar in size to the granular iron was used in the transition zones.

The composition (iron-sand ratio) of the 2-ft thick PTZ in Gate 1 was determined on the basis of the half-life of DO in contact with iron, as reported by General Electric Co. (GE) (Sivavec, 1997). Based on column tests with 100% iron, GE reported that DO had a half-life of 0.5 min. To reduce the DO in the Area 5 groundwater by two orders of magnitude (i.e., from approximately 5 mg/L to 0.005 mg/L), 20 half lives or 10 minutes would be required in 100% iron. Given such a fast reaction, a PTZ consisting of 10% iron by volume was designed to obtain a residence time requirement of 100 min. By applying the same temperature and bulk density corrections (2 and 1.5, respectively) that were used in the design of the reactive cell, a corrected residence time requirement of 300 minutes (0.2 day) in the Gate 1 PTZ was obtained. Similar reaction half-lives of DO were unavailable for the pyrite in the Gate 2 PTZ. An assumption was made that a 10% pyrite zone could be expected to require an order-of-magnitude higher residence time, namely 2 days. With a maximum expected groundwater velocity of 0.85 ft/day in the gate, a 2-ft thick PTZ was expected to exceed the required residence time of 2 days. The 10% iron-sand and 10% pyrite-sand mixtures were prepared in the field by volume instead of by mass, because volume is a better measure of particle surface area-driven reaction rates.

3. PRB Construction

Construction of the PRB at Dover AFB started on November 17, 1997 and was completed on January 14, 1998. The barrier was installed according to the design described in Section 2.4. Figures 2-7 and 2-8 (in Section 2) show the as-built plan views for the installation. Figure 3-1 shows an elevation view of the PRB Gate 1 and funnel. C³ Environmental, an operating division of Canadian Construction Controls Limited, was Battelle's construction subcontractor for the installation of the PRB and the associated monitoring system. C³ Environmental subcontracted a local partner, George & Lynch, Inc. of Dover, DE for caisson installation, aquifer well drilling, and other heavy equipment support. This section describes the construction of the PRB in Area 5. Appendix C contains supporting information on the materials used in the construction. Appendix G contains construction quality control (CQC) information associated with installation of the PRB.

3.1 Preconstruction/Site Preparation Issues

In a preconstruction kickoff meeting, the PRB design (Battelle, 1997) and Dover AFB operational requirements were reviewed by representatives from Battelle, Dover AFB, C³ Environmental, and George & Lynch, Inc. The following key decisions were made in this meeting:

- ❑ Evreux Street (see Figure 2-5 in Section 2) adjoining the parking lot on the south side of Building 639 would remain open to traffic. (Earlier, a decision had been made to install the funnel portion of the PRB using sheet piling instead of a slurry wall. At the desired location of the barrier, a slurry wall would have entailed digging a trench that extended out into Evreux Street, a street that had to remain open to traffic at all times. If constructed in the other direction [i.e., away from Evreux Street], a slurry wall would have entailed digging a trench that intersected the water line parallel to Building 639.)
- ❑ Traffic markers would be used to cordon off one of the three driveways to the parking lot where the PRB was to be located.
- ❑ Installing any structure within 5 ft of the water line parallel to Building 639 (see Figure 2-5 in Section 2) would be avoided.
- ❑ A storm drainage line that intersects the funnel location would be temporarily cut and rejoined over the funnel.
- ❑ Level D safety measures and personal protective equipment (PPE) would be used during construction.
- ❑ The gates would be installed in a way that would avoid the hazard of personnel entering the trench.
- ❑ Iron would be tremied into the trench, instead of being dropped from the ground surface, to minimize dust and improve packing.

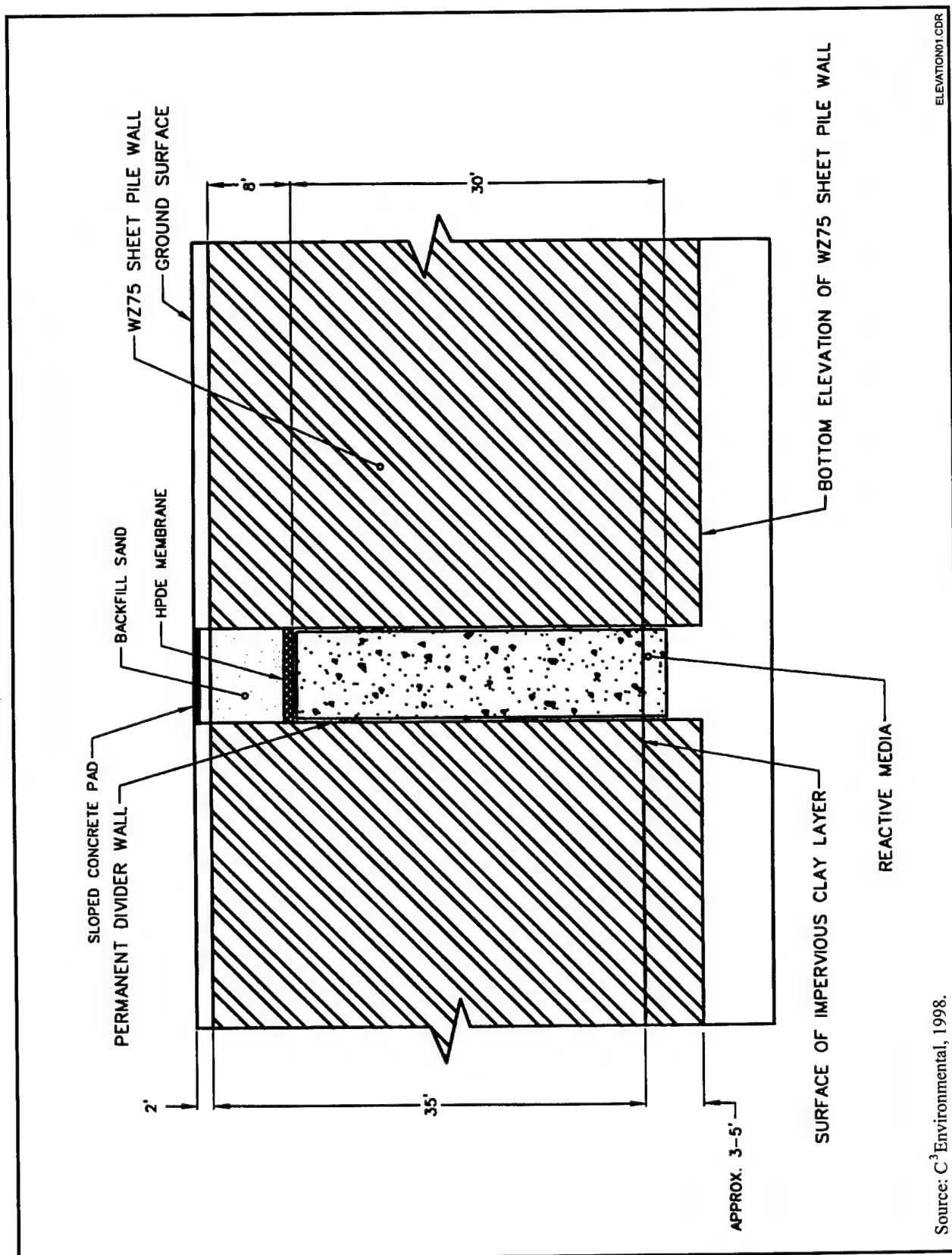


Figure 3-1. Elevation View of PRB Gate 1 and Funnel

Source: C³ Environmental, 1998.

Utilities clearance was obtained from Base personnel after the locations of the barrier and the aquifer monitoring wells were marked on the ground. As an added precaution, a small trench was dug manually to uncover and pinpoint the exact location of the water line. The water line turned out to be about 8 ft south (away from Building 639) of the location shown in the maps and marked on the ground by the Base utilities unit. A field decision was made to move the PRB back (downgradient) approximately 8 ft to avoid hitting the water line, a decision which moved the PRB further away from the more contaminated portion of the plume. In an aquifer with slow-moving groundwater, this decision meant that the desired CVOC concentrations would probably take longer to reach the gates.

3.2 Gates Construction

Figures 3-2 and 3-3 show a caisson gate being installed. Two 8-ft-diameter caissons were driven approximately 40 ft into the ground by a vibratory hammer mounted on a 100-ton mobile crane. The circular caissons were made of 0.5-in.-thick structural steel. The bottoms of the caissons were keyed 2 ft into the clay aquitard. The soil in the interior of the caissons was removed with a 5-ft-diameter auger. The excavated soil was disposed of as construction debris in a sanitary landfill on the Base. The interiors of the caissons were filled with water to create hydrostatic pressure and prevent any caving or heaving at the bottom of the caissons.

As shown in Figure 3-4, a frame, consisting of two parallel steel plates with monitoring wells attached to the cross-bracing between the plates, was lowered into the excavation for each gate. The plates serve as permanent dividers that separate the sides of the reactive cell, PTZ, and exit zone from the surrounding sand and aquifer, as shown in Figure 3-5. A temporary polyvinyl chloride (PVC) pipe was suspended in the excavation by attaching it to the cross-bracing of the frame. One HydroTechnics, Inc. (HydroTechnics) groundwater velocity sensor was installed in each gate through this pipe. The monitoring wells inside the reactive cell were attached to the cross-bracing of the frame.

Granular iron was obtained from Connelly in two-ton Supersacks and tremied into the excavation. An 8-in.-diameter PVC pipe was used as a tremie pipe. Sand and 10% metal (iron or pyrite) by volume were mixed in a concrete mixer and tremied into the PTZs. Sand was tremied into the exit zones and in the annular space between the reactive cell dividers and the caisson. The first few feet of media at the base of each compartment were tremied under water to maintain pressure on the bottom of the excavation; the remaining media were tremied after the water was pumped out of the caissons. The iron (and other media) was added to the reactive cells until its level was approximately 10 ft bgs (3 ft above the historical high water table). A high-density polyethylene (HDPE) membrane was placed on top of the iron.

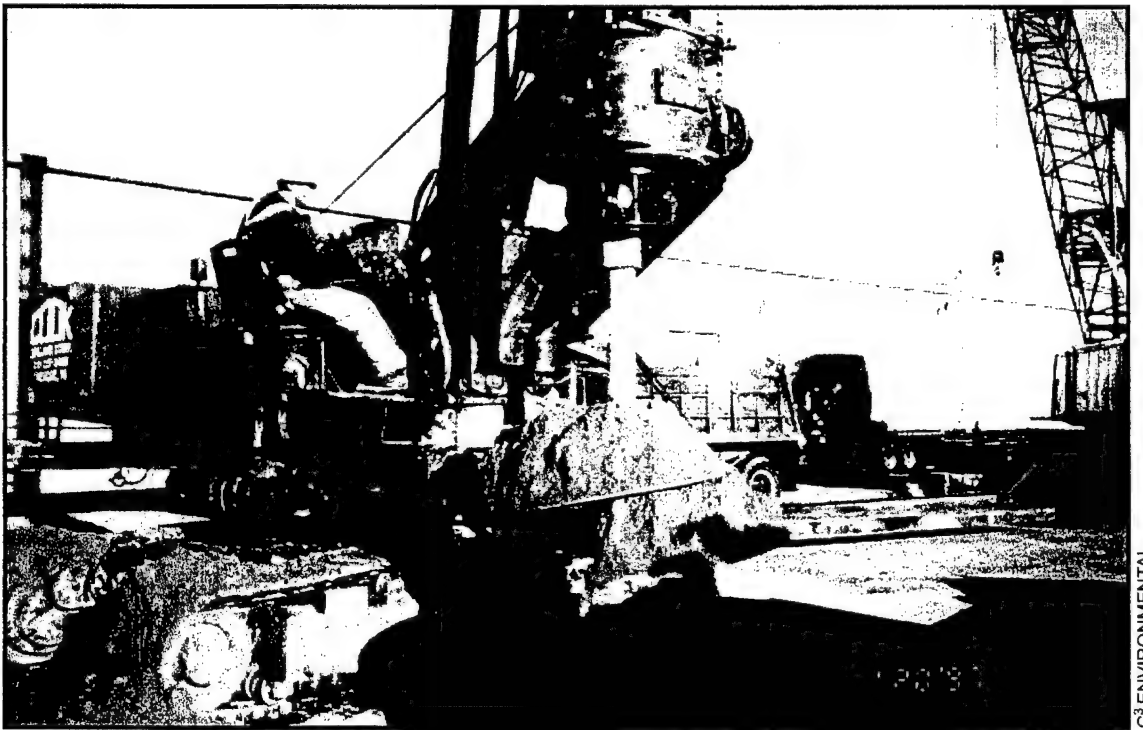
The coarse sand used in the gates was No. 1 Industrial Sand from Ricci Brothers Sand Corporation of Point Norris, NJ. All the media (sand, iron, and pyrite) used in the gates was in the same particle size range as the granular iron (-8+50 mesh). The pyrite was obtained from Top Gem Minerals, Inc. in the state of Arizona, and was crushed and sieved to the required size range by Colorado Minerals Research, Inc. of Golden, CO. Both the sand and pyrite used were analyzed to ensure their compatibility in the aquifer, and the analyses are presented in Appendix C.



PHOTOS 3-2&3-3.CDR

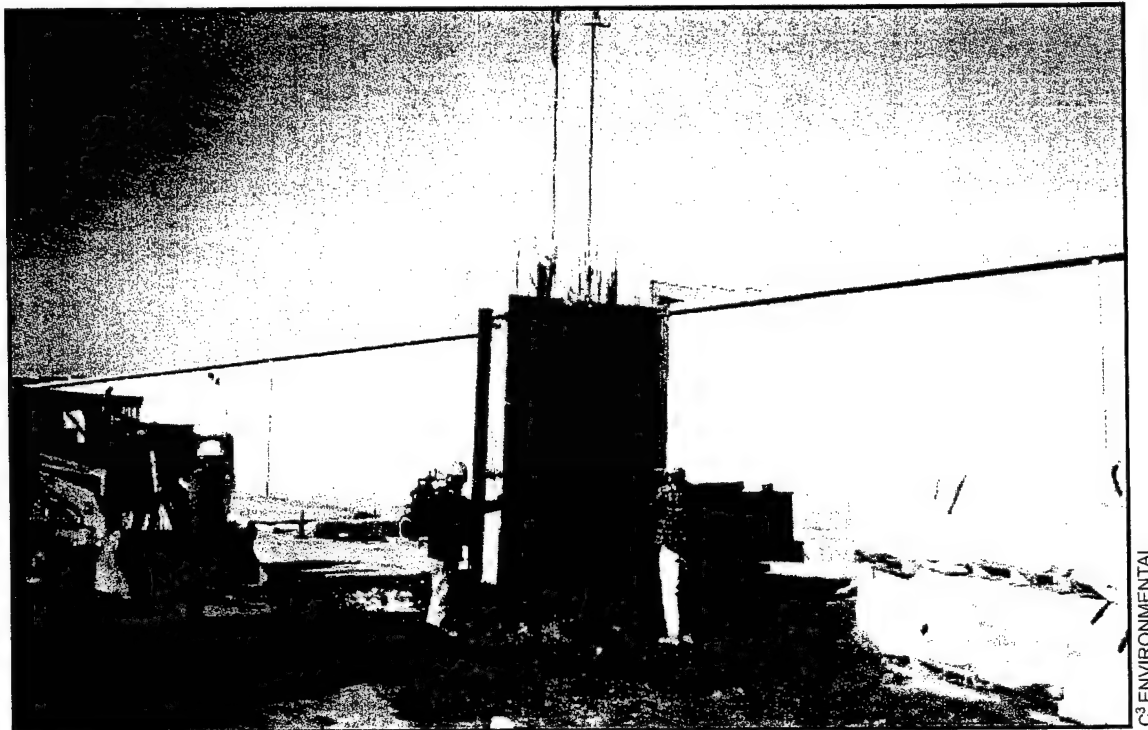
BATTELLE

Figure 3-2. Caisson Driving Equipment



C³ ENVIRONMENTAL

Figure 3-3. Caisson Drilling Equipment



PHOTOS 3-4&3-5.CDR

C³ ENVIRONMENTAL

Figure 3-4. Gate Frame



BATTELLE

Figure 3-5. Placement of Reactive Media

Pulling the caissons out of the ground proved to be somewhat more difficult than driving them in. The top edge of the first caisson removed from the ground kept tearing near the grip of the vibratory hammer. Initially, the location of the grip was changed a few times. When the caisson continued to tear, a 1-in.-thick collar was welded to the top edge of the caisson and the hammer grip was attached to this collar. After that, no more difficulties were encountered and the caissons came out easily. The iron subsided by about 2 ft in the reactive cells while the caissons were being pulled out. The vibrations from the caissons probably caused additional consolidation of the iron in the gates.

The bulk density of the iron in the field PRB was estimated by tracking the mass of the iron filled into the 448-ft³-volume reactive cell (with dimensions 4 ft × 4 ft × 28 ft). The approximately 3.6 ft³ of space taken up by the monitoring wells and the HydroTechnics sensor in the reactive cell was subtracted to arrive at a net volume of 444.4 ft³. Each reactive cell was filled with eighteen 3,000-lb bags of iron for a total of 54,000 lb of granular iron. These measurements imply a field bulk density of 122 lb/ft³ and a porosity of 0.7 (based on a 6.93 specific gravity of Connelly iron measured by the geotechnical laboratory). This field bulk density is lower than the 147 lb/ft³ average bulk density reported in tests conducted by an off-site geotechnical laboratory (see Section 6.1.1), indicating that the iron does not pack as well in the field as it does in a controlled laboratory setting. Filling the reactive cell with a tremie tube probably helped to pack the iron better than it would have by just dropping it from the top of the excavation, as was done at some previous sites.

3.3 Funnel Construction

The same vibratory hammer was used to drive the sheet piles that constituted the funnel. Sealable-joint steel sheet piles (Figure 3-6), patented by the University of Waterloo, were used at Dover AFB. After all the sheet piles were driven in, the final alignment of each pile was recorded using a digital inclinometer. A high-pressure water pump and a rigid hose was used to probe each cavity in the joints to ensure their integrity and to flush out any obstructions. A sealant, consisting of a prepackaged silica fume-modified cementitious grout, was poured into the joints to create the seal. Figure 3-7 shows the special joint that was welded to the steel dividers on either side of each reactive cell. This joint was aligned with the joint from the first sheet pile on each side of the gate and was grouted to obtain a good seal between the gate and the funnel. The volume of grout poured into each joint was inventoried to verify the integrity of the seal.

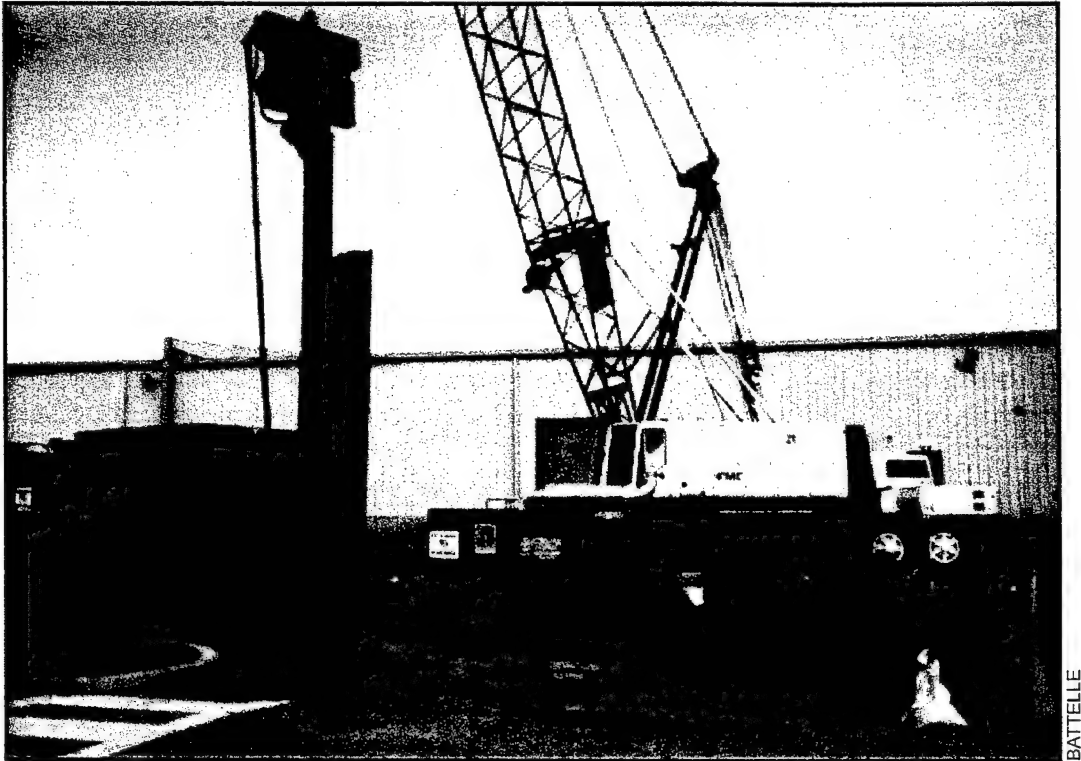


Figure 3-6. Pile-Driving Equipment

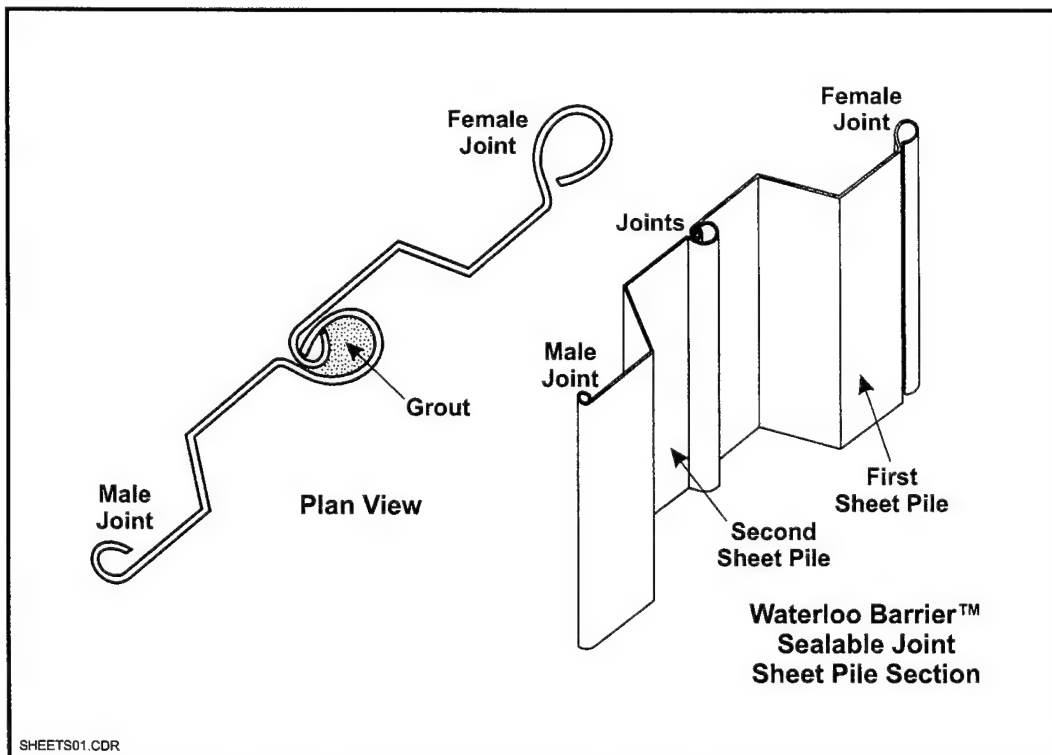


Figure 3-7. Sealable-Joint Sheet Pile Barrier

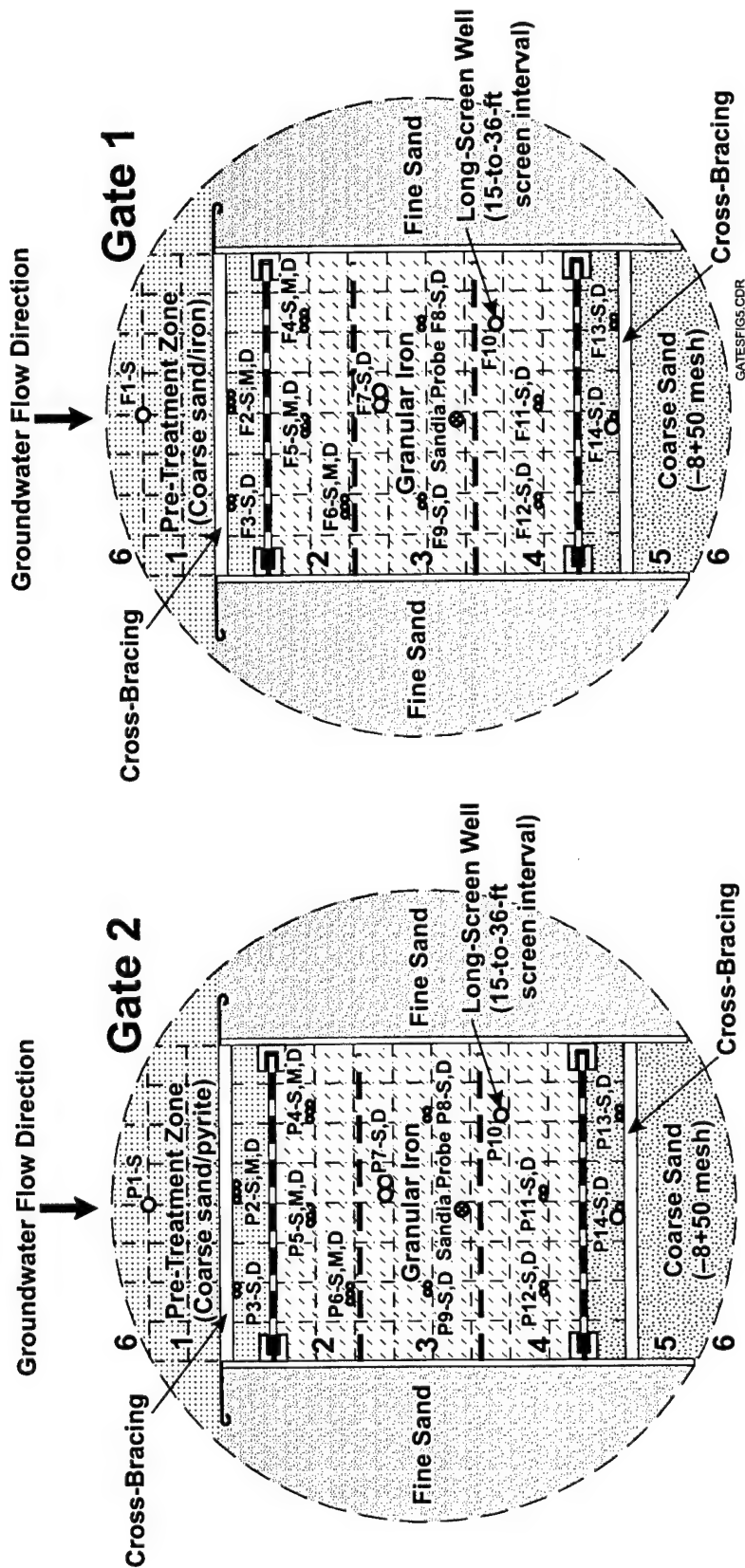
4. Monitoring Plan

The design/test plan (Battelle, 1997) outlined the monitoring strategy for the PRB in Area 5. The PRB performance was monitored during the 18 months following its construction in January 1998. This section summarizes the monitoring strategy and methods used to track the performance of the PRB.

4.1 Monitoring Strategy

Two comprehensive monitoring events were conducted in July 1998 and June 1999, approximately 6 and 18 months after construction, respectively. During the two comprehensive events, groundwater sampling was conducted in all the monitoring wells inside and around the PRB. In addition to CVOC analysis, measurements made during these two events included hydraulic parameters in the aquifer and gates and inorganic analysis of groundwater. Periodically, during the 18 months of PRB operation, limited monitoring events were conducted to track specific parameters of interest. At the end of the 18-month period, core samples of the gate media were collected and analyzed. The following are the key elements of the monitoring strategy:

- Monitoring wells made from 1-in.- or 2-in.-inside diameter (I.D.) PVC pipe were installed in the two gates during the construction of the PRB. In each gate, wells were installed at multiple locations in the PTZ, reactive cell, and exit zone as shown in Figure 4-1. The objectives of these wells are (a) to track the changes in the groundwater constituents as the water passes through the gates, and (b) to track the hydraulic flow system in the gates. At several locations, a three-well cluster was installed instead of a single long-screen well because of the anticipated CVOC variability by depth in the aquifer. The construction of the well clusters in the gates was similar in screened depth to the well clusters in the aquifer shown in Figure 4-2. Shallow (S), middle (M), and deep (D) designations were used with the well IDs to identify the individual wells.
- Following construction of the PRB, 2-in.-I.D. PVC monitoring wells were installed at multiple locations in the upgradient and downgradient aquifer in the vicinity of the PRB, as shown in Figure 4-3. The objectives of the aquifer wells are (a) to track the constitution of the groundwater influent to and effluent from the PRB, and (b) to track the hydraulic capture performance of the PRB. More wells were installed in the vicinity of the Gate 1 to focus limited resources on an intensive hydraulic evaluation of one of the gates. At select locations close to the gates, three-well clusters with screen intervals similar to those for wells inside the gates were installed to monitor CVOC variability by depth (see Figure 4-2).
- The flow system around the barrier was monitored much more intensively immediately after construction, until flow stabilized around six months later (in June 1998).



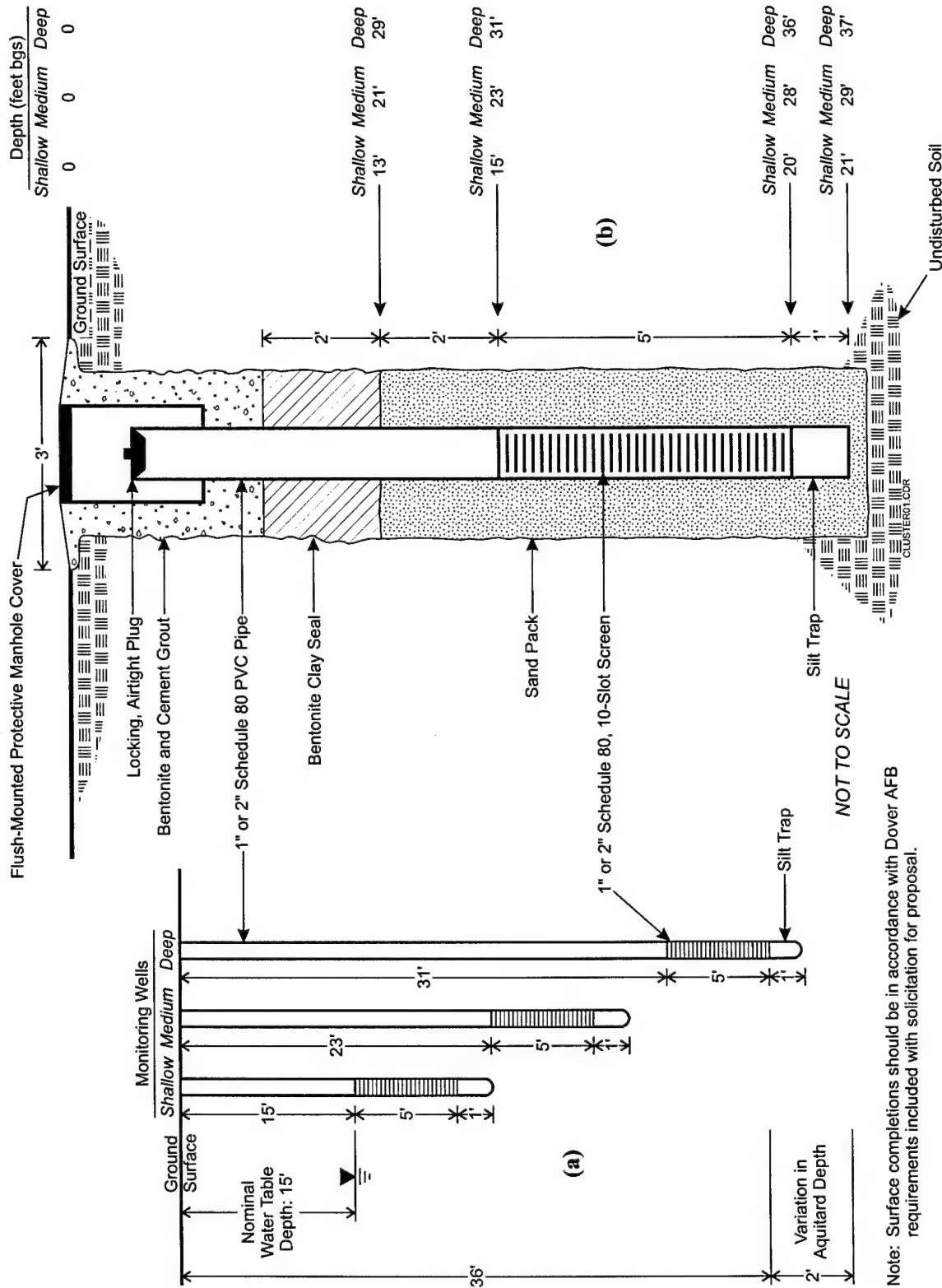
Explanation

- 1-inch-I.D. schedule 80 PVC well
- 2-inch-I.D. schedule 80 PVC well
- Sandia probe

Scale in Feet
0 1 2

Note: Six-inch grid is superimposed on the gate

Figure 4-1. Monitoring Point Network Within Gates 1 and 2



Note: Surface completions should be in accordance with Dover AFB requirements included with solicitation for proposal.

Figure 4-2. Monitoring Well Cluster Profile for (a) Gate and (b) Aquifer Wells

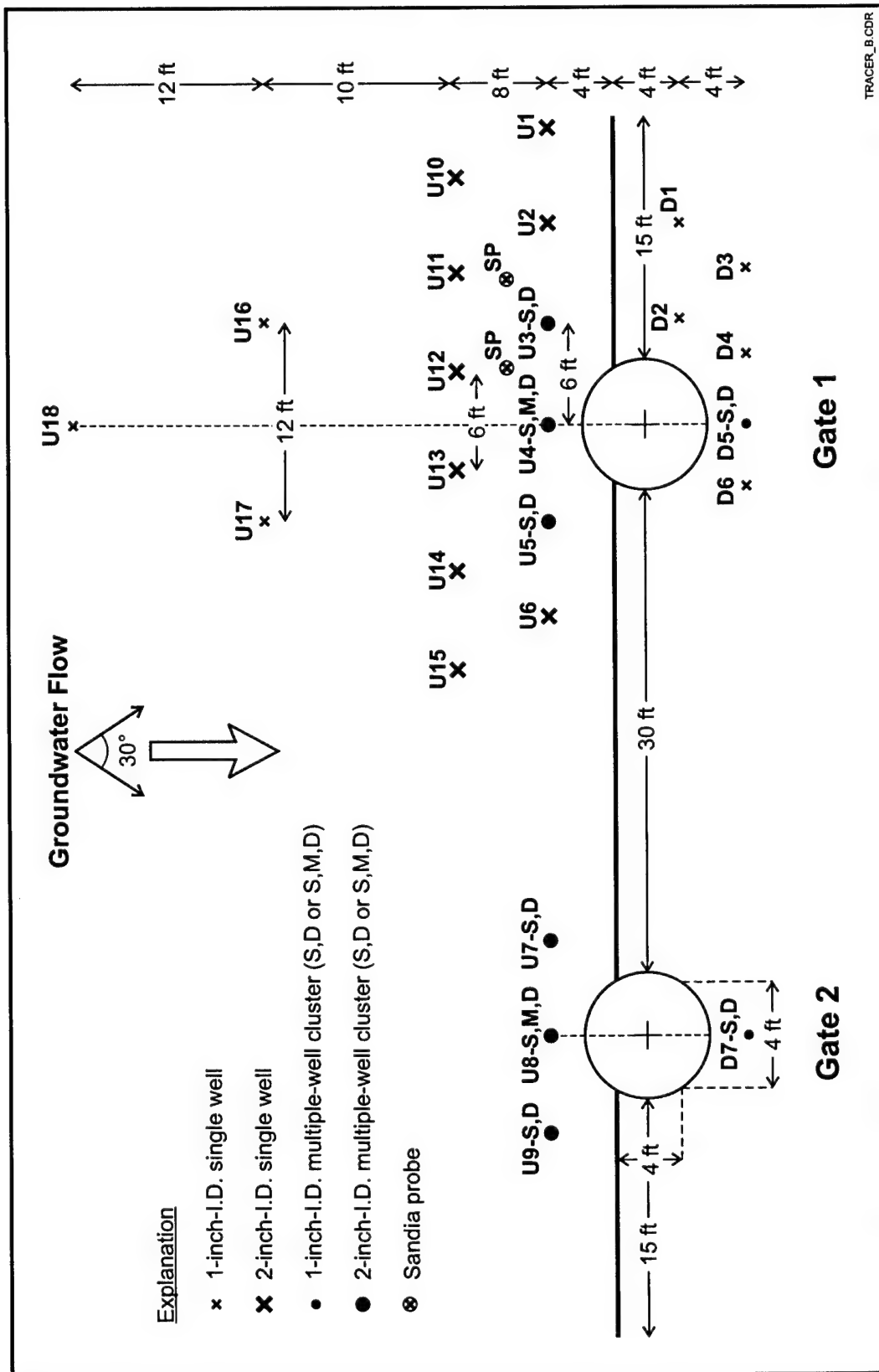


Figure 4-3. Monitoring Well Network in Aquifer

Flow monitoring in the first six months involved a combination of continuous water-level sensor readings in select wells, periodic water-level measurements in all wells, continuous flow velocity measurements in the HydroTechnics sensor installed in each of the two gates, and continuous flow velocity measurements in the two HydroTechnics sensors in the upgradient aquifer near Gate 1.

- The HydroTechnics sensors inside the gates were installed to evaluate flow velocity and direction in the gates. The sensors in the upgradient aquifer were installed to evaluate flow velocity and direction in the aquifer, and to evaluate the extent of the hydraulic capture zone along the funnel wing wall.
- Water levels were measured on a quarterly basis in all wells over the 18 months of monitoring. Slug tests were conducted in the upgradient aquifer wells and in the gates to evaluate hydraulic conductivities.
- Groundwater sampling was conducted in all the wells in the PRB and in its vicinity during the two comprehensive events in July 1998 and June 1999. Groundwater sampling involved the following three components: CVOC analysis to evaluate reductive degradation in the gates, field parameter measurements to evaluate pH and redox conditions in the PRB and vicinity, and geochemical measurements to evaluate precipitation of native inorganic constituents of the groundwater.
- Cores of the iron in the two gates were collected in June 1999 to evaluate precipitate formation in the gates. Cores of the soil from the upgradient and downgradient aquifer were collected to evaluate changes in microbial populations.

4.2 Groundwater Sampling Methods

Groundwater samples were collected in a manner that would minimize the impact of sampling on flow through the permeable barrier. Water withdrawal during sampling can lead to faster flow and reduced residence time of groundwater in the reactive medium. To prevent artificial gradients, water samples were extracted at low flowrates using an aboveground peristaltic pump. Also, to minimize disruption of normal flow through the barrier, successive samples were collected in different parts of the barrier, rather than from neighboring wells.

Semirigid tubing composed of 1/4-in.-outside diameter (O.D.) FEP Teflon™ was used to sample each monitoring well. The Teflon™ tubes were connected to flexible Viton® tubing for use with a peristaltic pump. Groundwater was withdrawn at a rate that caused water-level drawdown at the well to be no greater than 0.05 ft. Water levels within the wells were monitored using a downhole water-level sensor. Typically, a sampling rate of 150 mL/min was used. Purging of wells before sample collection was kept to a minimum in order to restrict the sample to the water immediately surrounding the well. However, to assure that the water samples were representative, at least three volumes of the tubing were purged. For typical 3/16-in.-I.D. 25-ft tubing, three tubing volumes are equivalent to about 400 mL. After sample collection, all tubing was decontaminated as described in the following paragraph. In addition, similar decontamination of any downhole sampling equipment, such as downhole groundwater velocity sensors, was performed prior to reuse.

The possibility of cross-contamination during sampling was minimized by using dedicated sample tubing, consisting of ¼-in.-O.D. FEP-Teflon™. Dedicated tubing was used for each row of wells perpendicular to the flow direction. Five sets of tubing were used in each gate (one for the PTZ, three for the reactive cell, and one for the exit zone) and two sets were used in the aquifer, to avoid cross-contamination between wells with potentially different levels of VOCs. Each set consisted of tubing cut to length for shallow, medium, and deep wells. Each segment of tubing was thoroughly decontaminated by sequential flushing with Liquinox™ detergent, tap water, and deionized water, prior to collecting the next investigative sample.

4.3 Hydraulic Measurements

The two major objectives of hydrogeologic monitoring were to determine the groundwater velocity through the reactive cell and to evaluate the capture zone of the PRB. Groundwater velocity is required to estimate the residence time of the groundwater in the reactive cell to ensure that sufficient contact time is available to degrade the CVOC contaminants. The capture zone width indicates whether or not the targeted portion of the plume is being captured.

Estimation of groundwater velocity (v) in the aquifer and in the gates using Darcy's law requires the estimation of the hydrogeologic parameters of the PRB aquifer system. The required parameters for each medium are hydraulic conductivity (K), effective porosity (n), and hydraulic gradient (i). The porosity and conductivity of the aquifer sediments and the reactive cell media were determined by laboratory testing of the media collected during site characterization in June 1997 and during construction of the PRB. Conductivity also was determined in the field using slug tests performed on 27 wells in and around the PRB two months after the first comprehensive monitoring event in July 1998. Two replicate tests were conducted in 25 wells, and three tests were performed in two wells, for a total of 56 tests. The tests consisted of placing a pressure transducer and 1⅜-in.-diameter × 3-ft-long or 1⅝-in.-diameter × 5-ft-long PVC slug in the well. After the water level reached equilibrium, the slug was rapidly removed. Water levels were monitored for 10 minutes by a pressure transducer and recorded by a Hermit™ datalogger. The data were then downloaded to a notebook computer. The recovery rates of the water levels were analyzed using the Bouwer and Rice method for slug tests (Bouwer and Rice, 1976; Bouwer, 1989). The water levels and hydraulic gradients in and around the PRB were investigated using manual water-level measurements and continuous water-level monitoring probes.

After the PRB was installed, 20 water-level surveys were performed in the wells within and near the PRB to obtain detailed information regarding hydrology in the immediate vicinity of the barrier. Additional wells were included in the site-wide water-level surveys completed in Area 5 during April 1998, May 1998, July 1998, October 1998, February 1999, April 1999, and June 1999. Water levels were measured in approximately 120 wells for each survey. Water levels also were measured with the same probe within a 24-hour period, and the probe was decontaminated between measurements. More frequent measurements were conducted in the first six months after the PRB installation to evaluate any changes in flow. A database of water levels and well details was developed to aid in an analysis of water-level variations over time.

Groundwater velocity also was measured directly using an innovative flow sensor developed by Sandia National Laboratory and marketed by HydroTechnics. Four HydroTechnics in situ groundwater velocity sensors were installed to measure groundwater flow velocity and direction near the permeable barrier. These probes use a thermal perturbation technique to directly measure the three-dimensional groundwater flow velocity vector in unconsolidated, saturated, porous media. The technology allows for long-term and continuous monitoring of the groundwater flow regime in the immediate vicinity of the probe. The probe consists of a cylindrical heater 30 inches long and 2.37 inches in diameter which has an array of 30 calibrated temperature sensors on its surface. The probe is installed directly in contact with the aquifer media at the depth of interest, with only a data transmission wire connecting the sensor to the surface. A heater within the probe heats the surrounding aquifer materials and groundwater to a temperature of about 20 to 30°C above background levels. The temperature distribution at the surface of the probe is affected by the groundwater movement resulting from advective flow of the heated groundwater. The measured temperature distribution is converted to flow velocity and flow direction by a computer program. The technology specifications indicate that a Darcy velocity range of 0.01 to 1.0 ft/day can be measured with the probe with a resolution of 0.001 ft/day and an accuracy of 0.01 ft/day. The lifespan of the probe is 1 to 2 years.

A HydroTechnics probe was installed within each reactive cell (Probe 3 in Gate 1 and Probe 4 in Gate 2) at depths of 29 ft bgs. Special precautions were taken for the probes in the reactive media. It is possible that the relatively high thermal conductivity of the reactive media will induce convection currents in the vicinity of the probes and affect velocity measurements. The probes in the reactive barriers were set at a lower power supply than those in the aquifer to minimize this effect as shown in Table 4-1. Two HydroTechnics probes also were installed upgradient of Gate 1 (Probes 1 and 2) at depths of 29 ft bgs. These probes were located near the flow divide on the eastern side of Gate 1 to establish the capture zone for the PRB.

Table 4-1. Power Supply for In Situ Velocity Sensors

Probe ID	Medium	R (ohms)	V (volts)	I (amps)	P (watts)
1	Aquifer	38.4	50	1.30	65.1
2	Aquifer	40.0	50	1.25	62.5
3	Gate 1 Iron	39.6	30	0.76	22.7
4	Gate 2 Iron	40.5	30	0.74	22.2

4.4 Groundwater Analysis Methods

The primary purpose of taking field parameter measurements is to monitor chemical conditions within the reactive cell that can affect its performance. Therefore, temperature, pH, DO, and ORP were measured at every well location. To obtain accurate readings, the field parameters were measured at the same time the wells were purged prior to sample collection.

The CVOCs of primary interest are the chlorinated hydrocarbons (EPA Method 8260). CVOC analyses were performed to identify the distribution of contaminants in and around the permeable barrier, as well as potential byproducts of degradation. Dissolved gases (EPA Method 3810) also were measured in June 1999, because they can be useful indicators of CVOC degradation. The dissolved gases include methane, ethane, propene, propane, butane, hexane, hexene, and ethene.

Samples were collected from each monitoring well for inorganic analysis as indicated in Table 4-2. Samples for cation analysis were filtered with 0.45 µm-pore size filters. All samples requiring preservation were preserved immediately after collection as indicated in Table 4-2.

Table 4-2. Analytical Requirements for Groundwater Samples

Parameter	Critical	Analysis Method	Minimum Sample Volume	Storage Container	Preservation	Sample Holding Time
Field Parameters						
Water level	Yes	Downhole probe	None	None	None	None
pH	Yes	YSI 6820 probe	None	None	None	None
Water temperature	Yes	YSI 6820 probe	None	None	None	None
ORP	Yes	YSI 6820 probe	None	None	None	None
DO	No	YSI 6820 probe	None	None	None	None
Organic Analytes						
CVOCs	Yes	EPA 8260	2 × 40 mL	VOA vial	4°C, pH<2 (HCl)	14 d
Dissolved gases	No	EPA 3810	2 × 40 mL	VOA vial	4°C, pH<2 (HCl) ^(a)	14 d
Inorganic Analytes						
Cations						
Na, Ca, Mg, Fe, Mn	Yes	EPA 200.7	100 mL	Polyethylene	Filter ^(b) , 4°C, pH<2 (HNO ₃)	180 d
Anions						
NO ₃ , SO ₄ , Cl	Yes	EPA 300.0	100 mL	Polyethylene	4°C	28 d ^(c)
Alkalinity	Yes	EPA 310.1	100 mL	Polyethylene	4°C	14 d ^(d)
Dissolved silica	No	EPA 6010	250 mL	Polyethylene	none	28 d
Neutrals						
TDS	No	EPA 160.1	100 mL	Polyethylene	4°C	7 d
TOC	No	EPA 415.1	40 mL	Glass (amber)	4°C, pH <2 (H ₂ SO ₄)	7 d

(a) Samples for CO₂ and H₂ analysis were not acidified.

(b) The primary filter pore size is 0.45 µm.

(c) Holding time for nitrate is 48 hours when unpreserved; holding time can be extended to 28 days when preserved with sulfuric acid.

(d) Determination of alkalinity in the field using a titration method is preferred whenever there is concern over precipitation in the sample container during storage.

VOA = volatile organic analysis.

Standard analytical methods also are listed in Table 4-2. Individual parameters are grouped according to field measurements, organic analytes, and inorganic analytes.

4.5 Core Sample Collection Methods

Fugro Geosciences, Inc. of Cumming, GA, was contracted to extract the cores. Samples from seven locations in the barrier and aquifer were extracted on June 14-18, 1999. This section describes sampling locations, sample collection methods, and procedures for storing the samples prior to analysis.

Four core samples were collected from within the reactive cell to look for signs of iron encrustation, precipitate formation, and microbial growth. These conditions have the potential to reduce the efficiency of the permeable barrier by restricting flow through the gate and reducing residence time in the reactive cell. They also affect the longevity of the barrier and hence the operating costs. Core samples were taken at several locations within the reactive cell to obtain adequate spatial information about possible changes in the granular iron medium. In addition, soil samples were collected in the upgradient and downgradient aquifer for microbiological analysis.

A push-in sampler was used to extract iron filings, pretreatment sand, and native soil to a depth of approximately 38 ft bgs. The sampler was designed for vertical coring at discrete depth intervals. The core barrel was fitted with three 6-in.-long stainless steel sleeves for collecting samples in 18-in. intervals (see Figure 4-4). After samples were extracted, the sleeves were fitted with tight fitting plastic caps to contain the sample and restrict air. In addition, cores of native soil were collected immediately upgradient and downgradient of Gate 1.

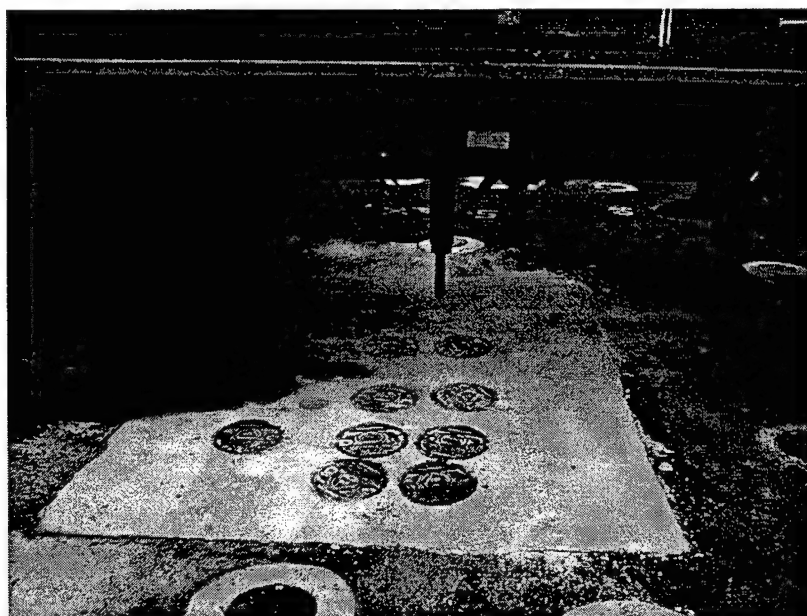


Figure 4-4. Photograph of Core Sampler Positioned Over Gate 1

4.5.1 Core Sample Locations

Coring locations were chosen to provide specimens of the permeable barrier and also to include aquifer samples from upgradient and downgradient of the permeable barrier. Coring locations (seven total) are designated on Figure 4-5. Core numbers PS-1 and PS-6 were located in the PTZs; PS-2 and PS-7 were located in the reactive cells; and PS-4, PS-5, and T-37 were located in the aquifer. PS-3 was abandoned. Sampling equipment was decontaminated by steam spraying between holes to remove any particulate adhering to the sampler.

The sleeves containing the core samples were placed into Tedlar™ bags that contained packets of oxygen scavenging material, as shown in Figure 4-6. The bags were then purged with nitrogen gas, as shown in Figure 4-7, and refrigerated up to 24 hours until they were shipped on blue ice to a Battelle laboratory. Samples for microbiological analysis were shipped in an airtight container to the designated laboratory. The remaining samples were vacuum-dried for inorganic analysis. Vacuum drying was conducted at approximately 40°C, and up to 72 hours was required to achieve complete drying. The core samples then were placed in a nitrogen-filled glove box for preparation for chemical and spectroscopic analysis.

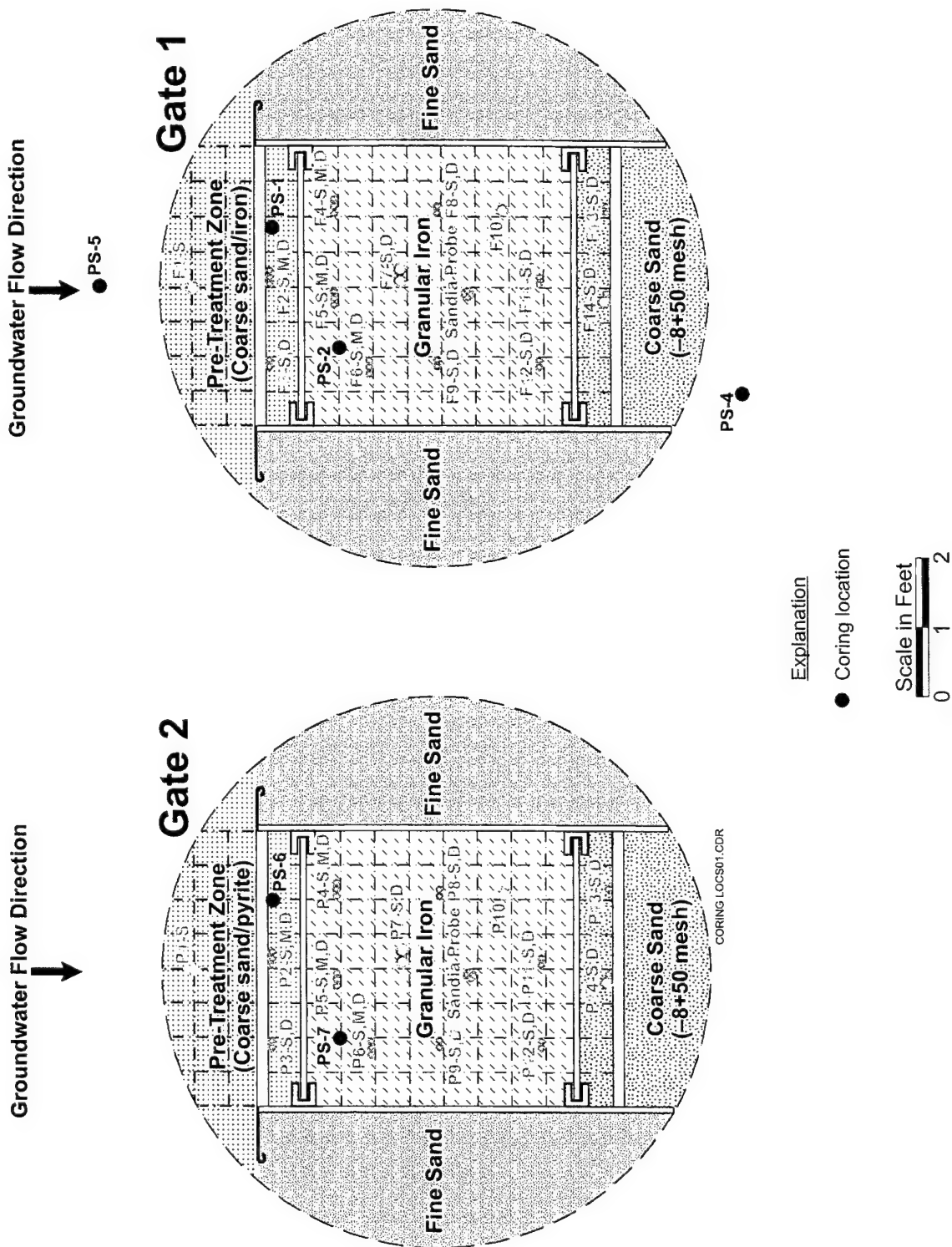
4.5.2 Core Analysis Methods

Samples were analyzed by Battelle and its subcontract laboratories using the methods shown in Table 4-3.

Samples for Raman spectroscopy were sent to Miami University (of Ohio), Molecular Microspectroscopy Laboratory for analysis. Confocal Raman spectra were collected with a Renishaw System 2000 Raman Imaging Microscope. This system employs a 25-milliwatt HeNe laser and Peltier-cooled charged coupled device (CCD) detector for excitation and detection of Raman scattered light, respectively. The system features fast full-range scanning (100 to 4,000 wave-numbers) and direct two-dimensional Raman imaging. Spatial resolutions of 1 μm and axial resolution of 2 μm can be achieved with the use of the confocal feature. Spectra were collected at 4 cm^{-1} resolution using a 300 second per point integration time. Three spectra were collected to obtain an understanding of the heterogeneous nature of the sample.

Infrared spectra were collected with a Perkin Elmer Spectrum 2000 FTIR coupled with an auto-image microscope, also at Miami University. ATR spectra were collected using a germanium internal reflection element. This instrument probes the surface of the sample to a depth of approximately 2 μm . Spectra were collected at 4 cm^{-1} resolution and each spectrum is the result of 32 individual scans. Three spectra were collected to obtain an understanding of the heterogeneous nature of the sample.

Samples for SEM were sent to the Battelle Microscopy Center. A JEOL 840 SEM was used to collect images. The SEM has a resolution of approximately 6 nm and magnifications ranging from 10 to 300,000X. A variety of imaging modes are possible for examination of metallic and nonmetallic samples, including secondary electron and backscattered electron imaging. An EDS permits qualitative analysis of chosen areas for elements with atomic weight equal to or greater



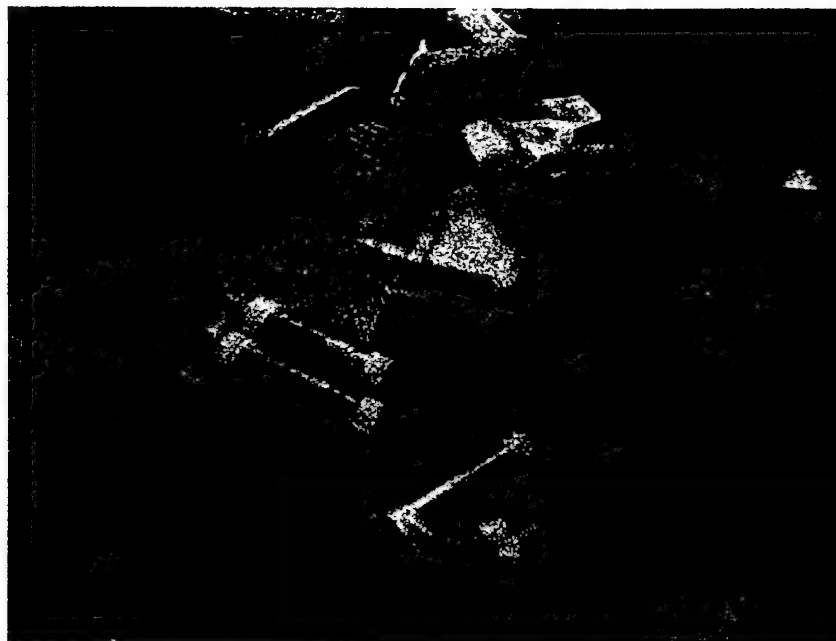


Figure 4-6. Photograph of Core Sleeves Being Placed into Tedlar™ Bags that Contained Packets of Oxygen Scavenging Material

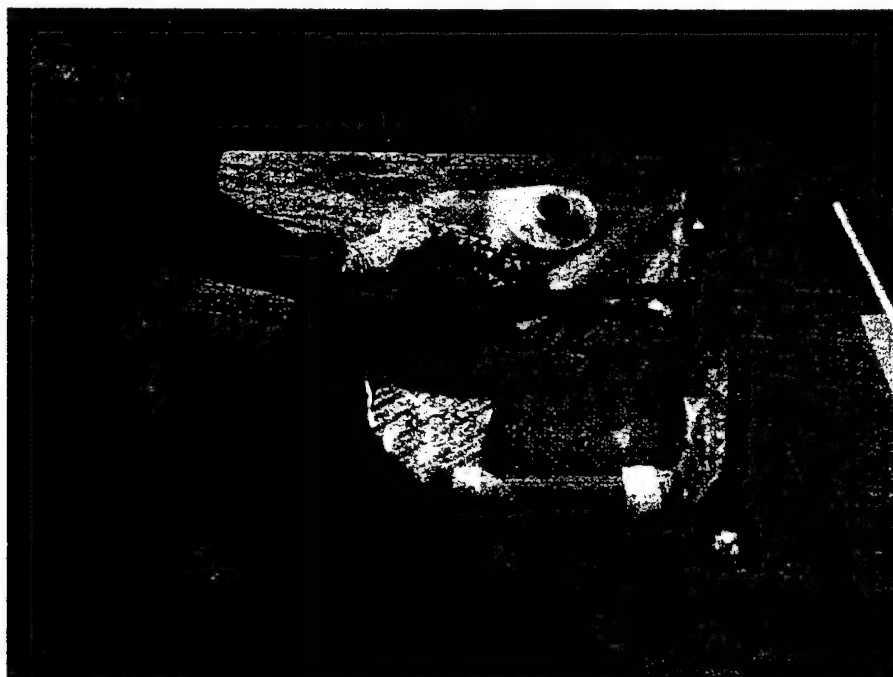


Figure 4-7. Tedlar™ Bags Flushed with Nitrogen Gas Before Sealing

Table 4-3. Characterization Techniques for Coring Samples

Analysis Method	Description
Total Carbon Analysis Combustion furnace used to quantify total organic and inorganic (carbonate) carbon	Quantitative determination of total carbon. Useful for determining fraction of carbonates in core profile.
Raman Spectroscopy Confocal imaging Raman microprobe	Semiquantitative characterization of amorphous and crystalline phases. Suitable for identifying iron oxides and hydroxides, sulfides, and carbonates.
Fourier Transform Infrared Spectroscopy (FTIR) FTIR coupled with auto-image microscopy.	Attenuated total internal reflection (ATR) spectra were collected using a germanium internal reflection element.
Scanning Electron Microscopy (SEM) Secondary electron images (SEI) Energy-dispersive spectroscopy (EDS)	High-resolution visual and elemental characterization of amorphous and crystalline phases. Useful for identifying morphology and composition of precipitates and corrosion materials.
X-Ray Diffraction (XRD) Powder diffraction	Qualitative determination of crystalline phases. Suitable for identifying minerals such as carbonates, magnetite, and goethite.
Microbiological Analysis Heterotrophic plate count Phospholipid fatty acid profile (PLFA)	Identification of microbial population within the cored material. Relates to presence or absence of iron-oxidizing or sulfate-reducing bacteria.

than that of sodium. The SEM 840 is interfaced with a Tracor Northern computer for automatic stage movements and data collection.

Samples for XRD were sent to the Battelle Microscopy Center. The Center's XRD capabilities include preparation of samples; automatic, unattended acquisition of data; and computer-aided interpretation of results. A pretreatment step was performed to concentrate the corrosion compounds so that they would not be masked by the metallic iron peaks. To separate corrosion coatings from the bulk material, the iron filings were placed in a fine sieve and brushed until a sufficient quantity of corrosion coatings was collected. A fully automated Rigaku diffractometer was used to analyze the samples.

Carbon analysis was performed using a UIC Model 5120 Total Carbon Apparatus. A small subsample of vacuum-dried material was placed in a platinum ladle, which then was placed in the combustion area of the carbon analyzer. The combustion temperature was set at 950°C to oxidize both organic and inorganic (carbonate) forms of carbon. The combustion product gases were swept through a barium chromate catalyst/scrubber to ensure that all of the carbon was oxidized to CO₂. Other potentially interfering product gases such as SO₂, SO₃, H₂, and NO_x were removed from the gas stream in a series of chemical scrubbers. The CO₂ then was swept to the coulometer where it was detected by automatic, coulometric titration.

Four samples were sent to Microbe Inotech Laboratories in St. Louis, MO for microbiological analysis. These samples were removed from the core sections before vacuum drying, as required by the procedure. The samples were analyzed for heterotrophic plate counts and PLFA profile of microbial strains. The laboratory procedures involved making liquid dilutions that were plated onto agar with Oxyrase enzyme in anaerobic petri plates. The plates were incubated anaerobically for 48 hours at 28°C. Following isolation, the strains were streaked onto trypticase-soy agar (TSA), then incubated for 24 hours followed by processing by gas chromatography (GC) analysis.

5. Reactivity Assessment

After its construction in January 1998, the reactivity of the PRB was monitored for 18 months of operation. The reactivity of the PRB was assessed in terms of the ability of the two reactive cells to degrade the influent CVOCs (PCE, TCE, and *cis*-1,2-DCE) and their byproducts (*cis*-1,2-DCE and VC) down to the respective MCLs. The MCLs for the target CVOCs are 5 µg/L (PCE and TCE), 70 µg/L (*cis*-1,2-DCE), and 2 µg/L (VC). Some degradation-related issues, such as availability of sufficient residence time in the gates and the geochemical interactions between groundwater and the reactive media, are detailed in Sections 6 and 7, respectively.

The first comprehensive monitoring event was conducted in July 1998, six months after construction of the PRB. During these 6 months, between 20 to 180 pore volumes (PV) of groundwater are estimated to have flowed through each gate. These estimates are based on the estimated residence times in the 4-ft-thick reactive cell of 1 to 9 days in each gate (see Section 6.1). The second comprehensive monitoring event was conducted in June 1999, 18 months after construction of the PRB. During the 18 months of operation, 60 to 540 PV of groundwater are estimated to have flowed through each gate.

Because of the presence of both adsorptive sites and reactive sites on the iron surfaces, several PV of flow are required before a steady state is reached. Steady state is indicated by a steady concentration profile through the thickness of the reactive cell. Previous research by Burris et al. (1995) showed that PCE takes longer (more PV) to reach steady state as compared to TCE. It is difficult to say whether or not the Area 5 PRB had reached steady state during either of these two monitoring events. Given the rapid reduction in CVOC levels to below detection observed during both monitoring events, concentration profiles in a time series could not be generated and compared. During previous column tests (U.S. EPA, 1997), approximately 160 to 200 PV of Area 5 groundwater (from well MW214D containing low levels [90 µg/L] of total CVOCs) was passed through the columns to equilibrate them. Although concentration profiles for this equilibration period are not available, the concentration profiles in the subsequent period were relatively steady. Based on these indicators, it is probable that, by the time of the second comprehensive monitoring event in June 1999, the iron in the field PRB was at steady state.

5.1 CVOC Distribution at Area 5

Table D-1 in Appendix D lists the results of the CVOC analysis of groundwater samples collected in the monitoring wells inside and in the vicinity of the PRB during site characterization (June 1997) and during the two monitoring events (July 1998 and June 1999). Appendix G contains the quality assurance (QA) data associated with these analyses. Table 5-1 summarizes the maximum CVOC concentrations encountered in the wells located in the probable capture zone of the PRB. The "U" wells are the permanent upgradient monitoring wells that were

Table 5-1. Maximum CVOC Concentrations Recorded in Wells Likely to Be Within the Capture Zone of Each Gate

Date	Upgradient of Gate #	Monitoring Well(s) ^(a)	Depth of Well Screen (ft bgs)	Maximum PCE Concentration ^(b)	Maximum TCE Concentration ^(b)	Maximum <i>cis</i> -1,2-DCE Concentration ^(b)
June 1997	Gate 1	T16M	23-28	5,617	15	22
		T16D	31-36	ND	311	131
		T15D	31-36	ND	254	176
	Gate 2	T18S	15-20	2,846	549	324
July 1998	Gate 1	U4D	31-36	334	22	69
	Gate 2	U9D	31-36	275	21	52
		U9S	15-20	ND	45	ND
June 1999	Gate 1	T35B ^(c)	21-24	3,900	18	38
		U19 ^(c)	15-20	1400	ND	120
		U4D	31-36	520	44	130
	Gate 2	U9D	31-36	480	42	140
		T36E	31-34	ND	160	100

(a) Well IDs that start with T are temporary wells pushed with a CPT rig.

(b) Bold numbers indicate maximum concentrations recorded for that region.

(c) U19 has the highest PCE concentration in the wells closest to Gate 1. T35B is further upgradient, but is within the expected capture zone.

installed after the PRB was built. The "T" wells are temporary wells punched with a CPT rig or GeoProbe[®] to obtain better coverage of the CVOC distribution. Figure 5-1 shows the locations of the temporary groundwater sampling and permanent monitoring wells. As described in Sections 2 and 3, it was originally planned to locate the PRB nearer wells T16 and T18, where the maximum concentrations were encountered during site characterization in June 1997. The PRB was eventually constructed 8 ft downgradient of the desired location nearer the building, in order to avoid an underground water utility line. In the aquifer with slow-moving groundwater (groundwater velocity subsequently estimated at 0.026 to 0.16 ft/day), the higher concentrations are slowly approaching the PRB, as seen by the increase in the CVOC concentrations from July 1998 to June 1999 in wells U4D and U9D, which are immediately upgradient of Gates 1 and 2, respectively.

Figure 5-2 shows a three-dimensional view of the PCE plume in the aquifer upgradient of the PRB, as mapped during the June 1999 monitoring event. PCE is the primary contaminant at Area 5. The region described in this figure is the portion of the upgradient aquifer between Building 639 and the PRB. As seen in this figure, regional groundwater flow occurs from the building to the PRB in the westward or southwestward direction. Gate 1 encounters higher CVOC concentrations compared to Gate 2. Along the line where groundwater enters the gates, higher PCE concentrations occur in the middle and deeper sections of the aquifer. More upgradient and closer to Building 639 however, higher PCE concentrations occur at shallow levels as well.

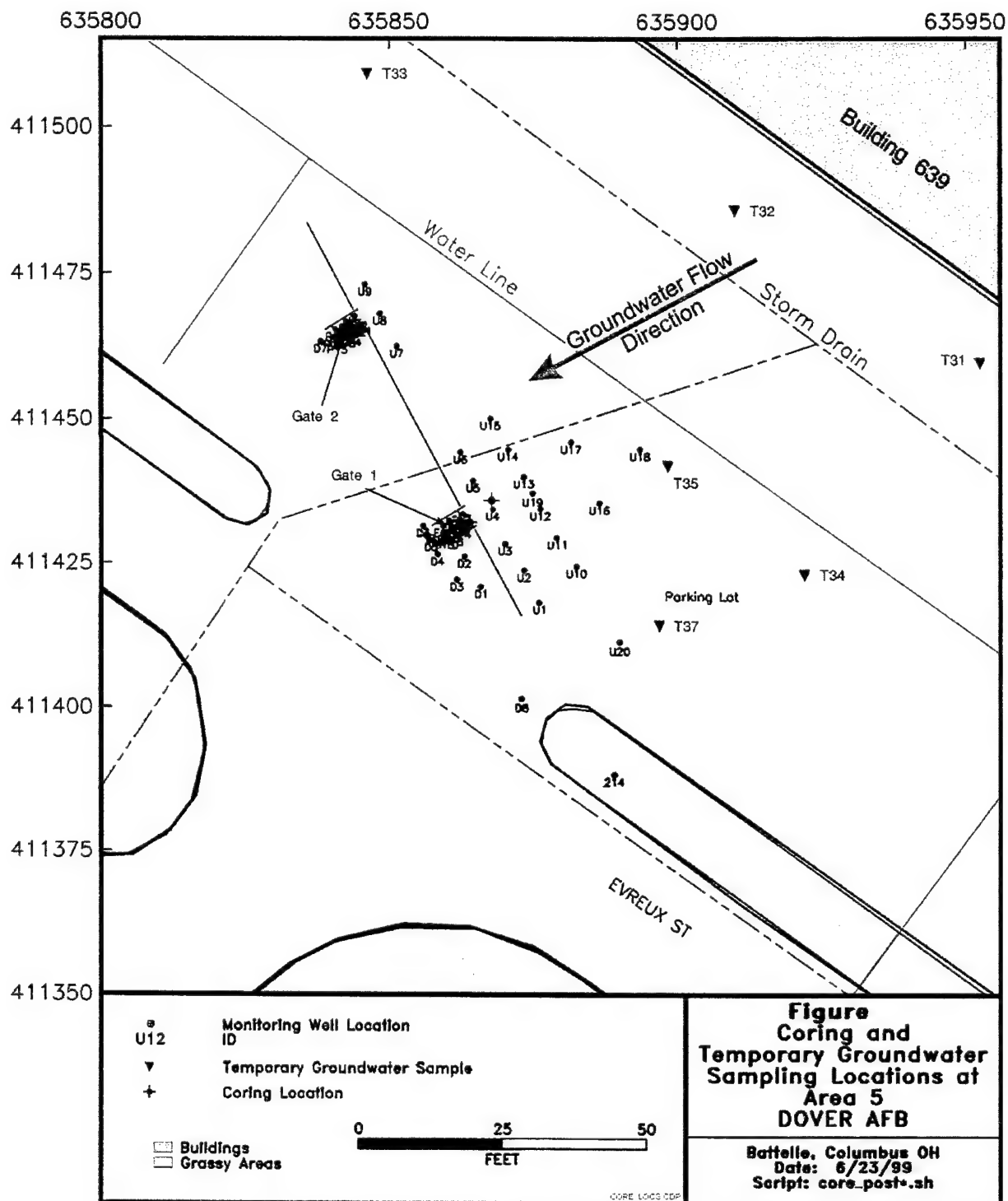


Figure 5-1. Temporary Groundwater Sampling and Permanent Monitoring Well Locations in the Upgradient Vicinity of the PRB

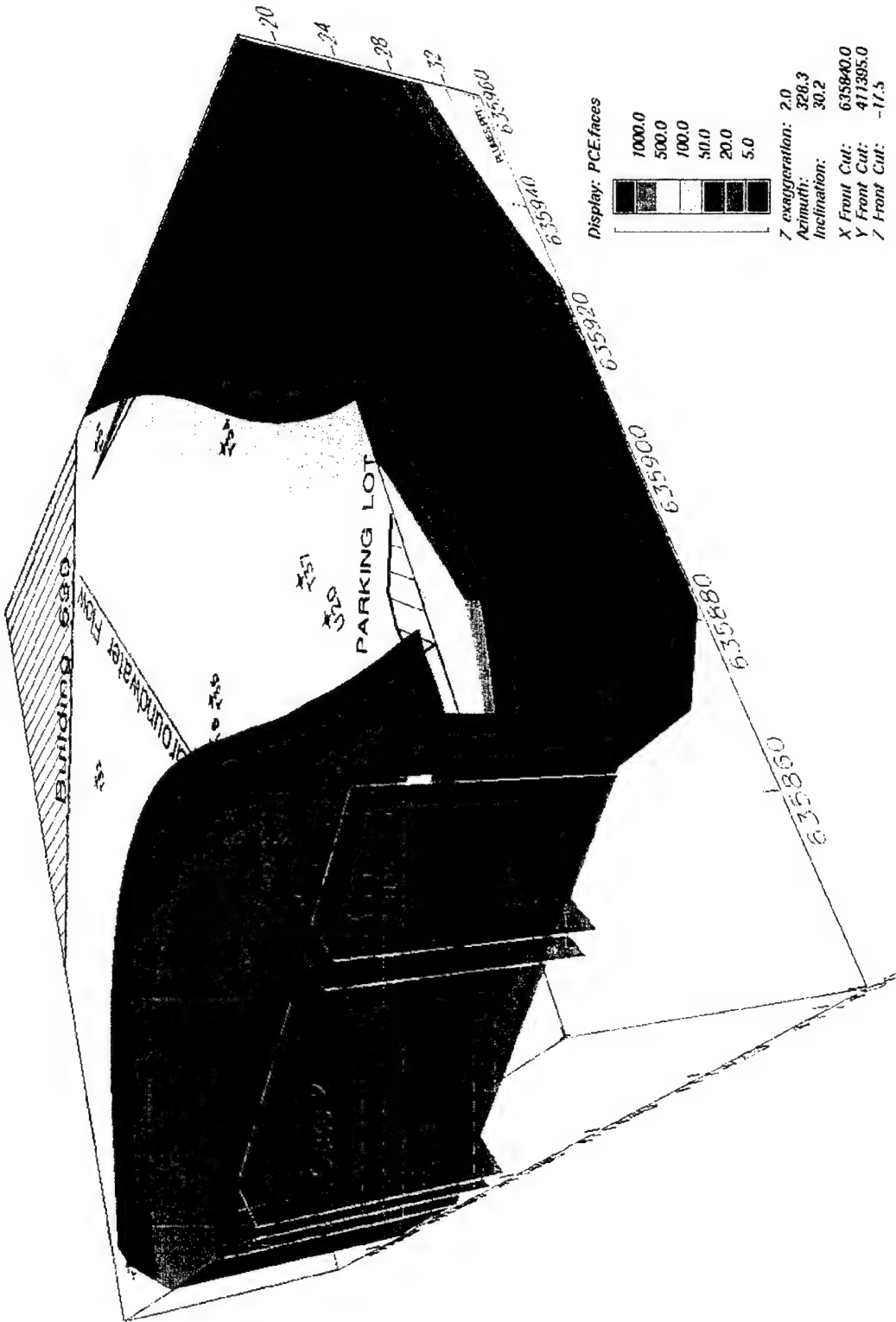


Figure 5-2. PCE Distribution in the Upgradient Vicinity of the PRB
 (Based on June 1999 Monitoring Event)

5.2 Degradation of CVOCs by the PRB

Tables 5-2 and 5-3 show the CVOC concentration distribution along the flow direction through the two gates. PCE is the primary compound detected, followed by TCE and *cis*-1,2-DCE. No VC was detected in any of the wells; any small amount of VC that may have been generated in the system was probably lost by volatilization and/or degradation. In these two tables, monitoring wells are grouped into zones along the groundwater flow direction to facilitate data evaluation. Within each zone, wells are segregated by depth because CVOC concentration tends to vary by depth in the upgradient aquifer (as it also does in the influent groundwater). The data in Tables 5-2 and 5-3 are represented graphically in Figures 5-3, 5-4, and 5-5, which depict PCE, TCE, and *cis*-1,2-DCE degradation, respectively.

Table 5-2. CVOC Degradation Along the Flow Direction in Gate 1

Zone	Wells	PCE (µg/L)		TCE (µg/L)		<i>cis</i> -1,2-DCE (µg/L)	
		July 1998	June 1999	July 1998	June 1999	July 1998	June 1999
Immediately upgradient aquifer	U3S, U4S, U5S	ND	ND	ND	ND	ND	ND
	U4M	300	470	21	34	62	100
	U3D, U4D, U5D	155-334	210-520	11-22	ND-44	20-69	44-130
PTZ upgradient	F1S	ND	8.2	ND	ND	ND	ND
PTZ downgradient	F2S, F3S	ND	ND	ND	ND	ND	ND
	F2M	ND	ND	ND	ND	ND	ND
	F2D, F3D	ND	ND	ND	ND	ND	ND
Reactive cell upgradient	F4S, F5S, F6S	ND	ND	ND	ND	ND	ND
	F4M, F5M, F6M	ND	ND	ND	ND	ND	ND
	F4D, F5D, F6D	ND	ND	ND	ND	ND	ND
Reactive cell middle	F7S, F8S, F9S	ND	ND	ND	ND	ND	ND
	F7D, F8D, F9D	ND-7.0	ND	ND-6.0	ND	ND	ND
Reactive cell downgradient	F11S, F12S	ND	ND	ND	ND	ND	ND
	F10	ND	ND	ND	ND	ND	ND
	F11D, F12D	ND	ND	ND	ND	ND	ND
Exit zone	F13S, F14S	ND	ND	ND	ND	ND	ND
	F13D, F14D	ND	ND	ND	ND	ND	ND
Immediately down- gradient aquifer	D4, D5S, D6	ND-6.0	ND	ND	ND	ND	ND
	D5D	110	73	ND	19	ND	16

The following observations can be made from Tables 5-2 and 5-3:

- No CVOCs were detected in the wells near the downgradient end of the two gates, either in the downgradient portion of the reactive cell or in the exit zone. This result indicates that PCE, TCE, and *cis*-1,2-DCE are degraded by the gates to levels below their respective MCLs, and below detection. Therefore, both gates and both reactive media were meeting the primary design objective.

Table 5-3. CVOC Degradation Along the Flow Direction in Gate 2

Zone	Wells	PCE (µg/L)		TCE (µg/L)		cis-1,2-DCE (µg/L)	
		July 1998	June 1999	July 1998	June 1999	July 1998	June 1999
Immediate upgradient aquifer	U7S, U8S, U9S	ND	5.6-8	ND-45	ND	ND	ND
	U8M	150	58	18	5.9	15	17
	U7D, U8D, U9D	47-275	118-480	9-21	5.9-42	6-52	17-140
PTZ upgradient	P1S	ND	ND	ND	ND	ND	ND
PTZ downgradient	P2S, P3S	ND	ND	ND	ND	ND	ND
	P2M	ND	ND	ND	ND	ND	ND
	P2D, P3D	ND-70	38-71	6-24	35-65	ND-11	23-41
Reactive cell upgradient	P4S, P5S, P6S	ND	ND	ND	ND	ND	ND
	P4M, P5M, P6M	ND	ND	ND	ND	ND	ND
	P4D, P5D, P6D	ND	ND-11	ND	ND-7.6	ND	ND-9.9
Reactive cell middle	P7S, P8S, P9S	ND	ND	ND	ND	ND	ND
	P7D, P8D, P9D	ND	ND	ND	ND	ND	ND
Reactive cell downgradient	P11S, P12S	ND	ND	ND	ND	ND	ND
	P10	ND	ND	ND	ND	ND	ND
	P11D, P12D	ND	ND	ND	ND	ND	ND
Exit zone	P13S, P14S	ND	ND	ND	ND	ND	ND
	P13D, P14D	ND	ND	ND	ND	ND	ND
Immediate down- gradient aquifer	D7S	ND	ND	10	ND	ND	ND
	D7D	ND	ND	ND	ND	9	ND

- Both gates were subject to relatively similar CVOC concentrations, thereby ensuring comparability of their performance. In both gates, groundwater entering through the middle and deep levels of the aquifer is more contaminated compared to the shallow levels.
- Except for one isolated occurrence in well F7D, CVOCs were undetected in the Gate 1 reactive cell. Except for one occurrence of PCE in well F1S in June 1999, CVOCs were also undetected in the Gate 1 PTZ. Given the fact that up to 334 (July 1998) and 520 µg/L (June 1999) of PCE were present in aquifer wells just 2 ft upgradient of Gate 1, it is somewhat surprising that detectable levels of PCE were not present in the PTZ. One possibility is that the groundwater velocity in Gate 1 is at the lower end of the estimated range of 0.46 to 4.1 ft/day (see Section 6.1 for more details), thus allowing a much higher residence time in the PTZ and reactive cell.
- CVOCs persist longer in Gate 2 than in Gate 1. CVOCs were detected in deep wells in the PTZ and in the upgradient portion of the Gate 2 reactive cell. This is because the 10% pyrite in the Gate 2 PTZ is not as strongly reducing as the 10% iron, and therefore does not promote reductive dechlorination to the same extent as iron (see Section 7.1.2 for ORP data).

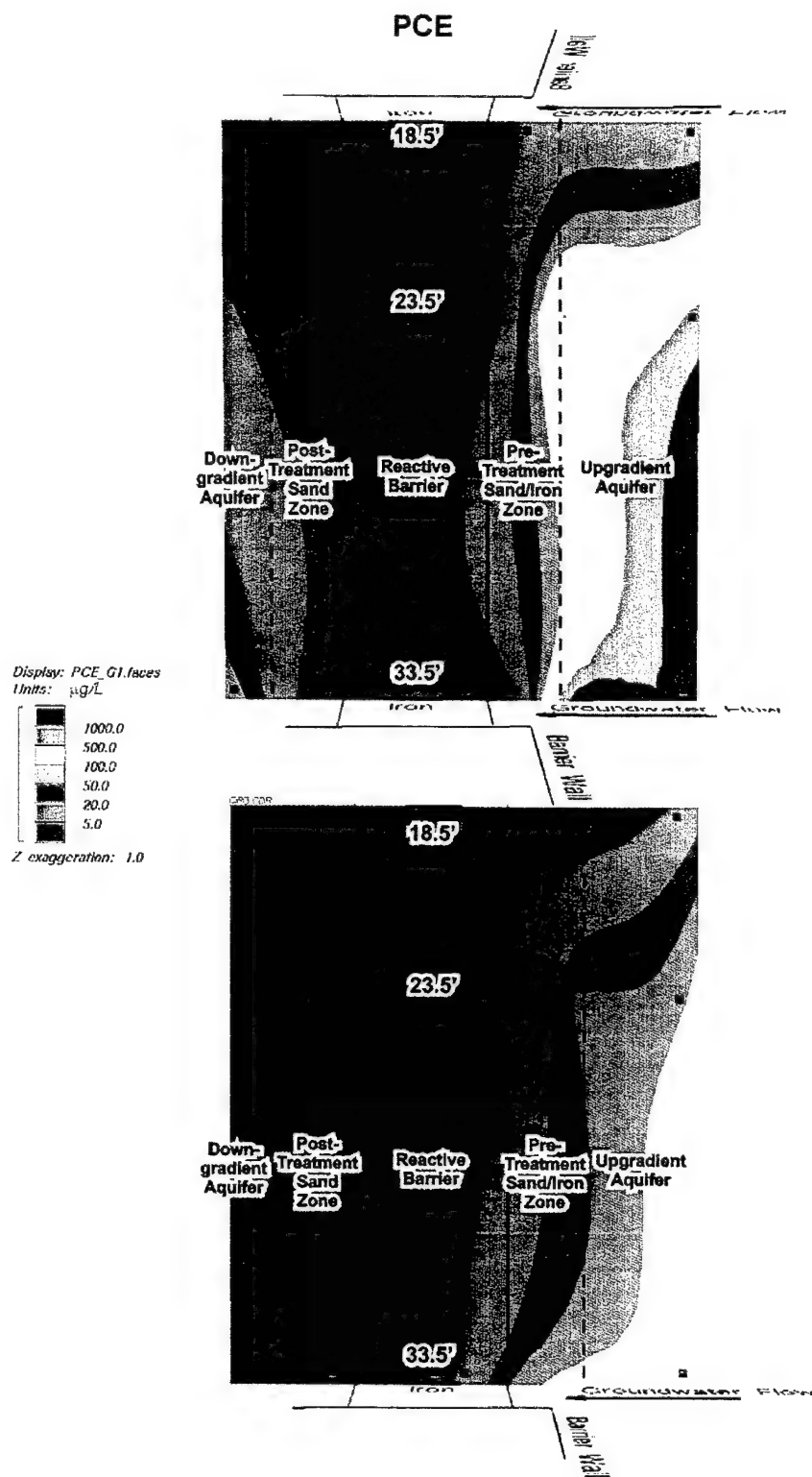


Figure 5-3. PCE Distribution in Gates 1 and 2 and the Surrounding Aquifer (Vertical Cross Section)

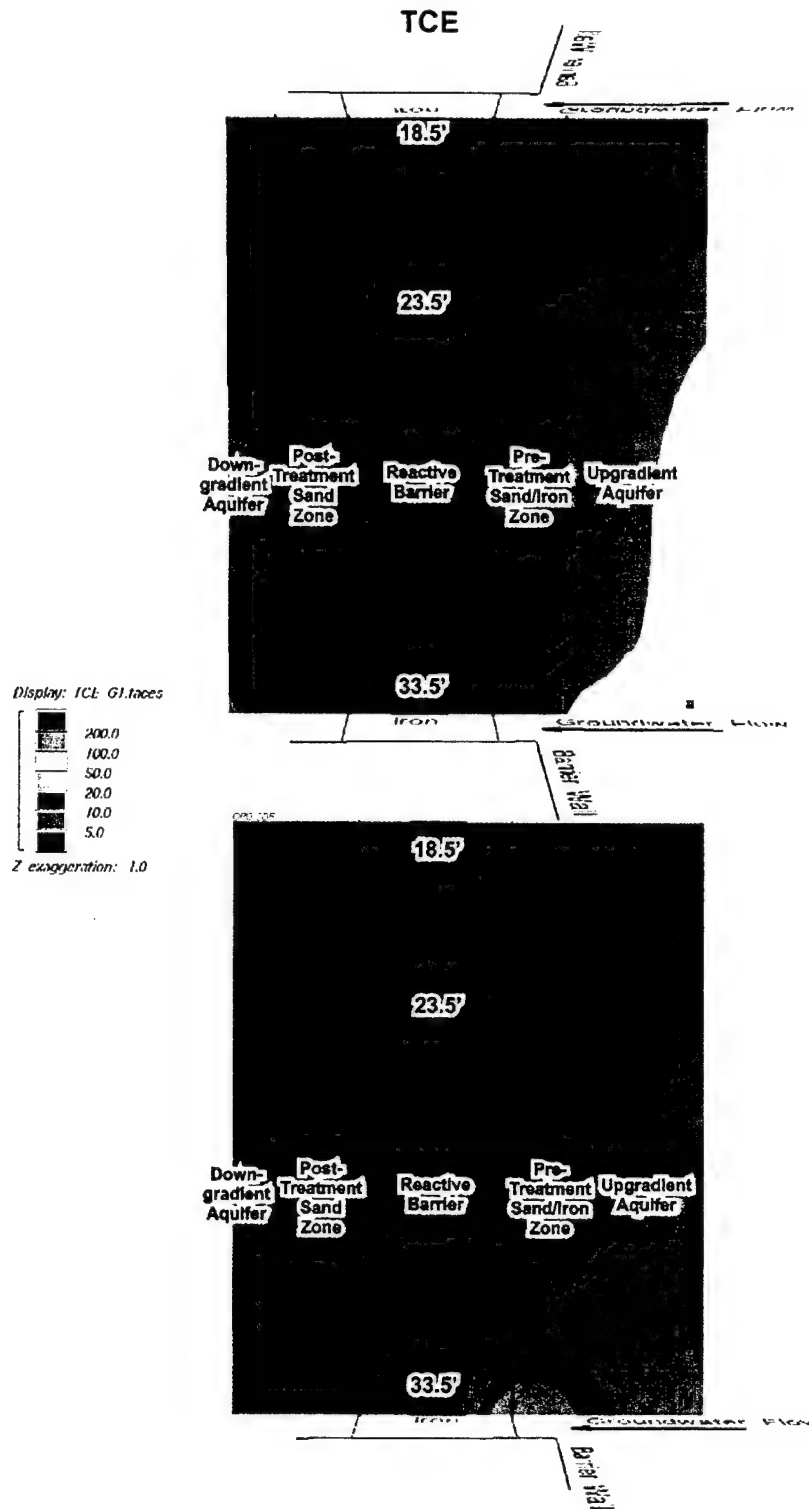


Figure 5-4. TCE Distribution in Gates 1 and 2 and the Surrounding Aquifer (Vertical Cross Section)

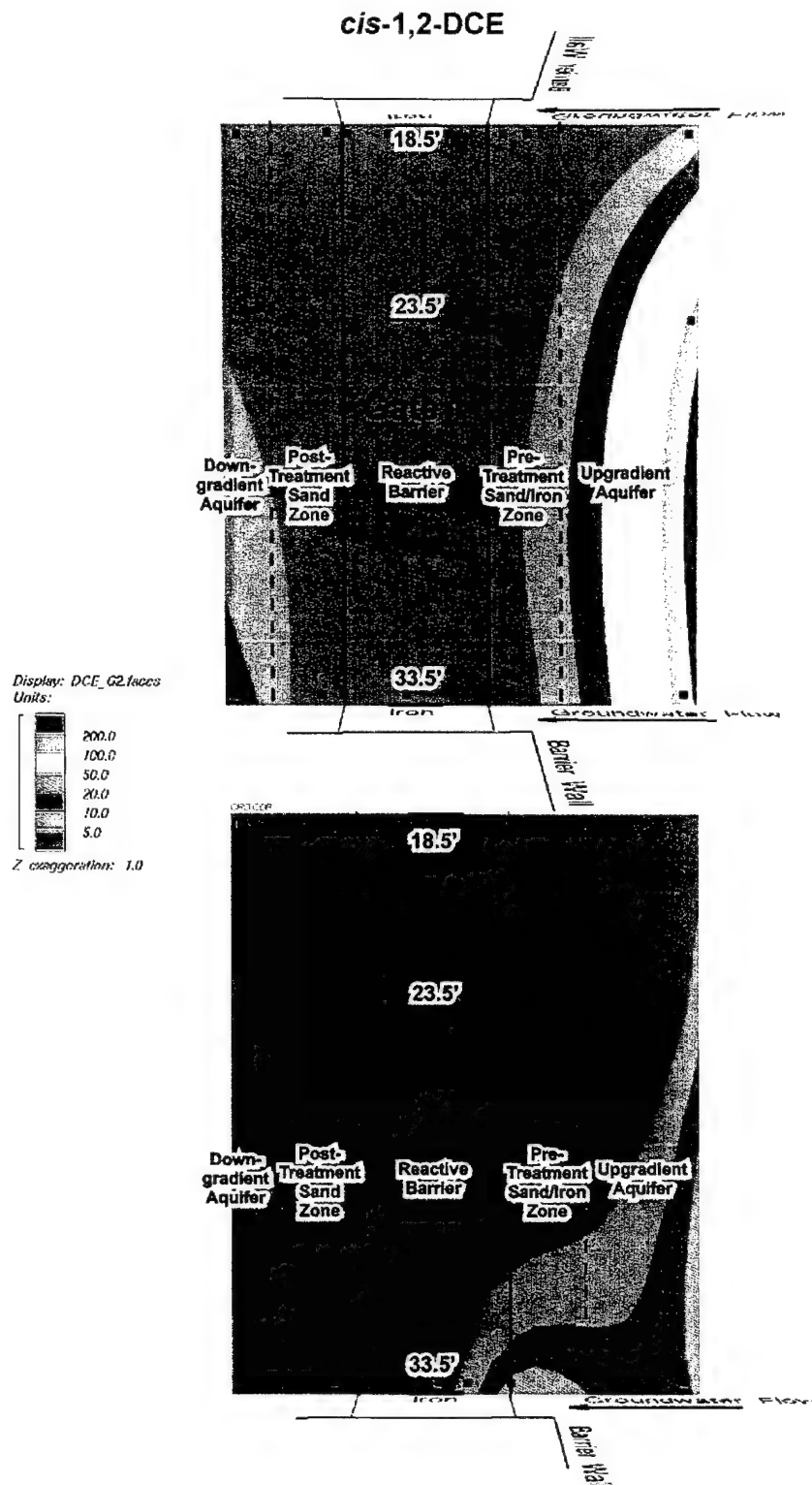


Figure 5-5. *cis*-1,2-DCE Distribution in Gates 1 and 2 and the Surrounding Aquifer (Vertical Cross Section)

- No CVOCs were detected in the exit zones in both gates. In previous barrier studies, where a pea gravel zone was present along the downgradient edge of the iron, CVOC concentrations rebounded in the downgradient pea gravel (Battelle, 1998). Because it is much more permeable than the aquifer, the pea gravel draws in some groundwater and CVOCs from the downgradient aquifer (when the barrier is located inside the plume). Sand was used instead of pea gravel in the exit zones of the Area 5 PRB to minimize sharp permeability contrasts. In the Area 5 PRB, remixing of groundwater flowing through the gates and groundwater flowing around the funnel occurs mostly in the downgradient aquifer, rather than in the exit zone. Although exit zones were installed in the gates to facilitate measurements for the demonstration, many recent PRBs have been installed without upgradient and downgradient pea gravel zones (or entry and exit zones).
- The isolated occurrences of CVOCs in the downgradient aquifer are the result of either preconstruction contamination or remixing of groundwater flowing through and around the barrier.

5.3 Assessment of CVOC Degradation Rates

Estimating CVOC degradation rates in field PRB systems is difficult because of the variability and uncertainties inherent in the parameters involved. Assuming that CVOC degradation by iron (or pyrite) is a pseudo-first order equation, the rate equation is written as:

$$C = C_0 \cdot e^{-kt} \quad (5-1)$$

or,

$$k = \frac{-\ln(C/C_0)}{t} \quad (5-2)$$

In these equations, C_0 and C are the CVOC concentrations at times 0 and t . Time t refers to the residence time of the CVOC (and groundwater) in the reactive cell (or PTZ). The reaction rate constant (k) represents the rate at which the CVOC degrades to other forms. The reaction rate can also be represented by the half-life ($t_{1/2}$) of the reaction, that is, the time it takes to reduce the initial CVOC concentration (C_0) to half its value:

$$t_{1/2} = \frac{\ln 2}{k} \quad (5-3)$$

The difficulty of measuring CVOC half-lives in the field lies with the uncertainties in C_0 , C , and t . The first difficulty involves determining the exact concentration and distribution of CVOCs (C_0) in the influent groundwater. The immediately upgradient aquifer wells, such as U4 and U8, are located at least 2 ft from the edge of the respective PTZs. CVOC concentrations in the slow-moving Area 5 aquifer vary sharply both horizontally and vertically, as described in Section 2. In most wells in the Gate 1 PTZ and reactive cell, CVOCs were undetected ($C = 0$), probably because the groundwater influent contained relatively low CVOC concentrations. Over

time, concentrations are expected to increase as the more contaminated portions of the plume reach the gates. The Gate 2 PTZ and reactive cell had some wells with measurable levels of CVOCs because of the slower reaction with pyrite. From the few wells in the gates that contained detectable levels of CVOCs, it is difficult to know by what flowpath those CVOCs arrived at these wells. Previous studies (Battelle, 1998) have shown that the flow regime in the iron is very complex and the groundwater does not necessarily flow through the gate in straight lines perpendicular to the gate face.

The other difficulty lies in the estimate of residence time (t). This estimate is highly dependent on the groundwater velocity estimate. At most sites, groundwater velocity (v), which is itself dependent on the uncertainties in the estimates of hydraulic conductivity (K), hydraulic gradient (i), and porosity (n), can be estimated at best within an order of magnitude. As discussed in Section 6, seasonal variations and the relatively flat hydraulic gradient in the vicinity of the Area 5 PRB makes groundwater velocity estimation difficult. In a PRB system with higher CVOC influent concentrations and higher local hydraulic gradient, the CVOC distribution in the gate and the groundwater velocity can be better estimated.

Despite these difficulties, an effort was made to estimate the field half-lives for the PRB system at Area 5. The June 1999 concentrations of PCE, TCE, and DCE in Table 5-3 have a measurable distribution in the deep wells of the upgradient aquifer, PTZ, and upgradient end of reactive cell for Gate 2. The data from the deep wells in both gates were the most suitable for calculating degradation rates. Based on these data and Equations 5-2 and 5-3, the rates and half-lives in Table 5-4 were calculated.

The relatively wide range of field half-life estimates in Table 5-4 reflects the relatively wide range of estimated residence times of 1 to 9 days in each reactive cell (see Section 6.1). The best match of field estimates of CVOC half-lives with the design estimates (based on column test results) occurs in the Gate 2 reactive cell (see shaded cells in the table). For example, the field half-life range of PCE (1.5 to 14 hours) includes the design half-life of 3.2 hours. The match is especially good when groundwater velocity through the gate is assumed to be in the lower part of the range (closer to 0.46 ft/day than to 4.1 ft/day). The Gate 2 reactive cell estimates were based on three data points available along the flowpath (see Table 5-3), and the reactive cell influent concentrations are more certain. In Gate 1, CVOC concentrations were reduced to below detection in the PTZ itself, and a degradation rate for the reactive cell was not calculated.

For the PTZs in the two gates, only two data points were available, one in the upgradient aquifer and one in the PTZ. In addition, in both gates, the CVOC concentrations were already below detection in the PTZ. In the Gate 1 PTZ, CVOC half-lives appear to be much shorter than predicted in the design values for 10% iron. For the Gate 2 PTZ, there were no design predictions for CVOC degradation by pyrite; however, half-lives in Gate 2 appear to be longer than in Gate 1, indicating that the less-reducing conditions in Gate 2 PTZ (see Section 7.1.2 for ORP data) lead to slower degradation rates.

Table 5-4. Estimates of Field Degradation Rates Based on June 1999 Data

Reactive Medium	Basis	PCE		TCE		cis-1,2-DCE	
		k (hr ⁻¹)	t _{1/2} (hr)	k (hr ⁻¹)	t _{1/2} (hr)	k (hr ⁻¹)	t _{1/2} (hr)
Design Values Based on Column Test							
100% iron	Column test results ^(a)	0.75	1.0	1.5	0.5	0.50	1.5
100% iron	Adjusted column test results ^(b)	0.23	3.2	0.47	1.6	0.16	4.8
10% iron	Adjusted column test results ^(c)	0.023	32	0.047	16	0.016	48
Values Based on Field Measurements							
10% iron	Gate 1 PTZ ^(d)	0.074-0.69 ^(g)	1.0-9.3 ^(g)	0.053-0.42 ^(g)	1.6-13 ^(g)	0.053-0.54 ^(g)	1.3-13 ^(g)
10% pyrite	Gate 2 PTZ ^(e)	0.0070-0.28 ^(g)	2.5-98 ^(g)	0.0025-0.02 ^(g)	34-274 ^(g)	0.017-0.20 ^(g)	3.5-41 ^(g)
100% iron	Gate 2 reactive cell ^(f)	0.050-0.46	1.5-14	0.048-0.45	1.6-14	0.044-0.41	1.7-16

- (a) Based on k and t_{1/2} measured for groundwater containing primarily TCE, during on-site column tests by U.S. EPA (1997), as described in Section 2.3. A relatively wide groundwater velocity range of 0.46 to 4.1 ft/day or a residence time of 1 to 9 days in the two reactive cells is assumed. The actual groundwater velocity through the PRB probably is in the lower part of this range, as discussed in Section 6.
- (b) Column test results were adjusted to reflect actual field conditions of groundwater temperature (10°C instead of 20°C in the column test) and iron bulk density (122 lb/ft³ instead of 198 lb/ft³ in the column test). A temperature correction factor of 2 and a bulk density correction factor of 1.6 were applied to the column test results from the previous row.
- (c) The k values in the previous row were divided by 10 to reflect the slower reaction rate with 10% iron (in the PTZ) instead of with 100% iron as in the column test.
- (d) Based on CVOC concentrations along a flowpath from upgradient deep wells (U3D, U4D, and U5D) to Gate 1 PTZ deep wells (F2D and F3D), as shown in Table 5-3.
- (e) Based on CVOC concentrations along a flowpath from upgradient deep wells (U7D, U8D, and U9D) to Gate 2 PTZ deep wells (P2D and P3D), as shown in Table 5-3.
- (f) Based on CVOC concentrations along a flowpath from Gate 2 PTZ deep wells (P2D and P3D) to reactive cell upgradient wells (P4D, P5D, and P6D). Half-lives in Gate 1 could not be calculated because of the relatively slow groundwater velocity (and high residence time) compared to the degradation rate (half-life) of TCE in iron.
- (g) k and t_{1/2} calculated from two data points only.

5.4 Reactivity Assessment Summary

At the Area 5 PRB, the following conclusions can be made regarding the reactivity of the media in the two gates:

- Between 180 to 540 PV of groundwater are estimated to have flowed through each gate in the 18 months of PRB operation. Based on previous on-site column tests, the PRB was probably at steady state with respect to CVOC equilibration by the time of

the second comprehensive monitoring event in June 1999. Additional monitoring may be conducted in the future to confirm steady-state conditions.

- CVOC degradation occurs at a faster rate in the Gate 1 PTZ (10% iron) than in the Gate 2 PTZ (10% pyrite). This is due to the stronger reducing conditions created by iron as compared to pyrite (see ORP data in Section 7). However, degrading CVOCs was not the primary design function of the two PTZs. Both PTZs were designed to remove DO before it entered the reactive cells; both PTZs did accomplish DO removal (see DO data in Section 7.1.3).
- Although the PTZ in both gates encountered similar CVOC influent concentrations, CVOC levels entering the reactive cell in Gate 2 were higher because of lower degradation rates in the 10% pyrite PTZ.
- Both gates reduced CVOC levels down to their respective MCLs and to below detection by the time the groundwater reached the end of the PTZ (Gate 1) or the middle of the reactive cell (Gate 2). Extra thickness of iron is available in both gates to accommodate higher CVOC concentrations that may be encountered as the plume progresses.
- To date, the groundwater influent to the PRB has contained up to 520 µg/L and 480 µg/L of PCE, the primary contaminant at Area 5, in Gates 1 and 2, respectively. As much as 3,900 µg/L of PCE is believed to be in the capture zone of the PRB, and will eventually be encountered. Lower levels of TCE and *cis*-1,2-DCE also are present in the influent. The PRB was designed for an influent concentration of up to 10,000 µg/L of PCE, and a safety factor of 2 was incorporated in the reactive cell thickness after accounting for all the known factors. Therefore, the PRB should be able to degrade the expected higher CVOC concentrations to their respective MCLs.
- Variability and uncertainty in hydraulic flow parameters and CVOC distribution in the gates made calculation of CVOC degradation rates in the field PRB system difficult. Therefore, no judgement can be made regarding which gate (or which PTZ media) facilitated greater reactivity or greater degradation efficiency. Column tests under controlled conditions using site groundwater spiked with relatively high levels of CVOCs may be the best way of comparing the reactivity of the two media. The field degradation rates in Gate 2 do indicate that the groundwater velocity through the gates is probably closer to 0.46 ft/day than to 4.1 ft/day; that is, the actual groundwater velocity is in the lower part of the estimated range based on the hydraulic capture zone evaluation (see Section 6).

6. Hydraulic Performance Assessment

This section discusses the hydrogeologic performance of the PRB in terms of two key parameters: groundwater velocity and capture zone width. Groundwater velocity is required to estimate the residence time of the groundwater in the reactive cell in order to ensure that sufficient contact time is available to degrade the CVOC contaminants. The capture zone width indicates whether or not the targeted portion of the plume is being captured. The hydrogeologic characterization and groundwater modeling that was conducted for the design of the PRB is summarized in Section 2 and is detailed in the design/test plan (Battelle, 1997). This section focuses on the results of the characterization and monitoring that was conducted in the PRB and its vicinity after its installation in January 1998.

6.1 Groundwater Velocity Estimation

Estimation of groundwater velocity (v) in the aquifer and in the gates requires the estimation of the hydrogeologic parameters of the PRB aquifer system. The required parameters for each medium are hydraulic conductivity (K), effective porosity (n), and hydraulic gradient (i). Velocity was also measured directly by an innovative flow sensor developed by Sandia National Laboratory and marketed by HydroTechnics.

6.1.1 Hydraulic Conductivity (K) and Porosity (n)

During site characterization in June 1997, aquifer soil samples collected with the CPT rig were visually classified and sent to a certified laboratory for geotechnical testing. Five samples were analyzed for porosity, bulk density, and grain-size distribution (Battelle, 1997). Results of geotechnical laboratory analyses suggest that samples from the surficial aquifer are mostly medium to fine sand. Samples from the confining unit are mostly silt and clay. The visual inspection and grain-size analysis showed a good correlation with CPT log-based sediment classifications. Geotechnical laboratory testing indicated that aquifer porosity averaged 0.31 and specific gravity averaged 2.67. In the confining unit (aquitard), porosity averaged 0.60 and specific gravity averaged 2.85.

Geotechnical laboratory tests also were conducted on samples of the media used in the PRB gates. Table 6-1 summarizes the results of the geotechnical laboratory testing. Results of the constant head conductivity tests on the samples were 778 ft/day for the iron (Gate 1 and 2 reactive cells), 1,426 ft/day for the 10% iron-sand (Gate 1 PTZ), 1,192 ft/day for 10% pyrite-sand (Gate 2 PTZ), and 1,737 ft/day for the sand (exit zones in Gates 1 and 2). These numbers indicate that the conductivity of the gate media may be greater than the 283 ft/day used in design modeling for the Dover AFB and other PRB sites. Porosity and bulk density of the gate media, as measured in the laboratory, are as shown in Table 6-1. The laboratory reported an average bulk density of 147 lb/ft³ and a porosity of 0.66 for the granular iron versus a field bulk density of 122 lb/ft³ and porosity of 0.70 estimated in the field PRB (See Section 3.2). This difference in

Table 6-1. Summary of Geotechnical Laboratory Testing for Aquifer and Reactive Barrier Media

Media	Specific Gravity	Bulk Density (lb/ft ³)	Porosity	K (ft/day)
Surficial Aquifer (Columbia Formation)	2.69	N/A	0.323	N/A
	2.70	N/A	0.341	N/A
	2.66	N/A	0.328	N/A
	2.65	N/A	0.237	N/A
	2.66	N/A	0.329	N/A
Lower Confining Layer (Calvert Formation)	2.80	N/A	0.602	N/A
	2.81	N/A	0.593	N/A
Sand	2.67	89.2	0.46	1,737
		105.0	0.37	
Iron	6.93	127.9	0.70	778
		165.2	0.62	
Sand and 10% Iron	2.86	93.2	0.48	1,426
		114.8	0.36	
Sand and 10% Pyrite	2.82	99.4	0.43	1,192
		119.7	0.32	

N/A = not available.

bulk density indicates that the extent of packing and compaction during construction may be a significant factor.

Slug tests were performed on 27 wells in and around the permeable barrier two months after the first comprehensive monitoring event in July 1998. Two replicate tests were conducted in each of 25 wells and three tests were performed in each of 2 wells for a total of 56 tests. The tests consisted of placing a pressure transducer and 1 $\frac{3}{8}$ -in.-diameter by 3-ft-long or 1 $\frac{5}{8}$ -in.-diameter by 5-ft-long PVC slug within the well. After the water level reached equilibrium, the slug was rapidly removed. Water levels were monitored for 10 minutes by a pressure transducer and recorded by a Hermit™ datalogger. The data then were downloaded to a notebook computer. The recovery rates of the water levels were analyzed with the Bouwer and Rice (Bouwer and Rice, 1976; Bouwer, 1989) method for slug tests. Graphs were made of the change in water level versus time and manually curve fitted on a semi-logarithmic graph. The slope of the fitted line was then used in conjunction with the well parameters to provide a value of the conductivity of the materials surrounding the well. Figure 6-1 shows a sample slug test recovery graph. All slug test graphs and parameters are presented in Appendix E-1. Figure 6-2 shows hydraulic conductivity from the slug tests in shallow wells. Figure 6-3 shows hydraulic conductivity values from the slug tests in deep wells. Table 6-2 summarizes the slug test results. As seen in the Appendix E table, results show a good agreement between the replicate tests.

The conductivity from all aquifer slug tests varied between 1.8 and 101 ft/day with a geometric mean of 7.4 ft/day and standard deviation of 25.0 ft/day. Shallow wells had a geometric mean

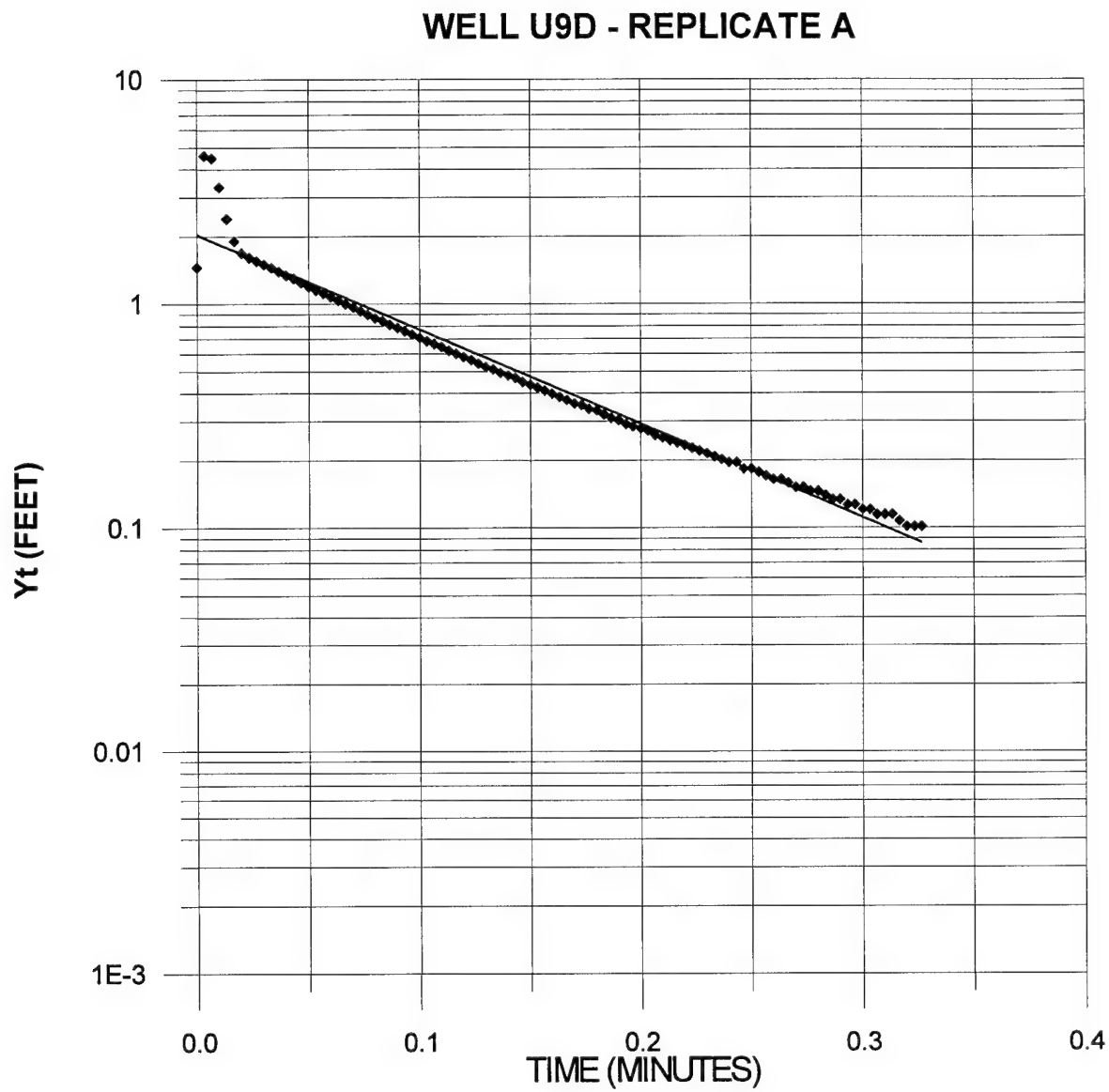


Figure 6-1. Example Slug Test Recovery Graph for Area 5 Aquifer

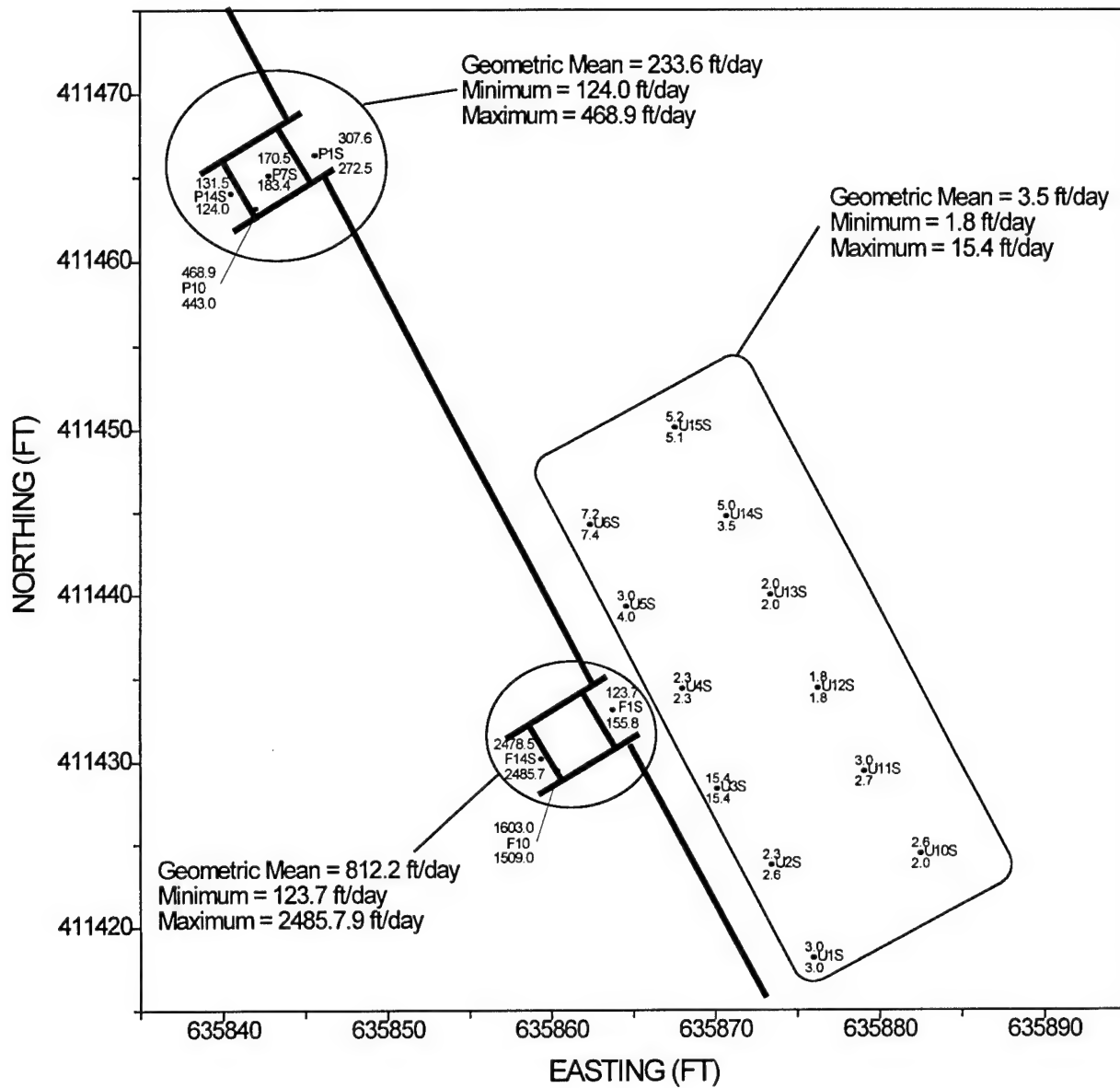


Figure 6-2. Hydraulic Conductivity Distribution in Shallow Wells

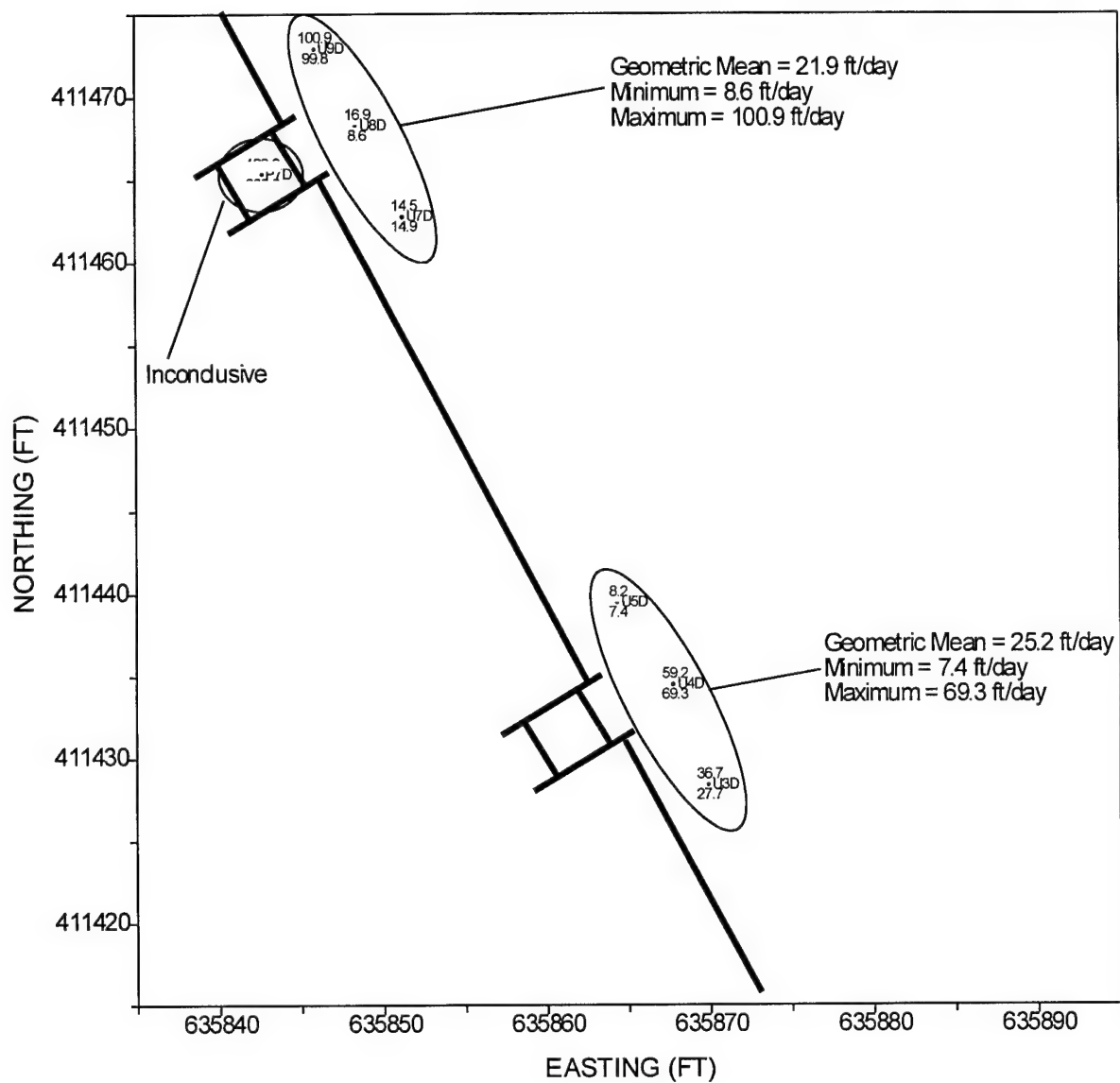


Figure 6-3. Hydraulic Conductivity Distribution in Deep Wells

Table 6-2. Summary of Slug Test Results

Location	Number of Tests	Geometric Mean K (ft/day)	Standard Deviation
All Aquifer Wells	40	7.4	25.0
Gate 1 Upgradient Wells	32	5.7	16.3
Gate 1 Wells	6	812	1,056
Gate 2 Upgradient Wells	8	21.9	40.3
Gate 2 Wells	10	234	135

conductivity of 4.2 ft/day. The wells screened at deep and medium depths together had a geometric mean conductivity of 14.2 ft/day. Gate 1 upgradient aquifer wells had a geometric mean conductivity of 5.7 ft/day. Gate 2 upgradient aquifer wells (deep only) had a geometric mean conductivity of 21.9 ft/day. These tests agree very well with other slug tests that were conducted near permeable barriers (Battelle, 1997) and with the observed lithologic patterns at the site. A conductivity range of 10 to 50 ft/day was used for the design modeling of the PRB in Area 5. The slug tests indicate the actual overall K at the site is probably closer to 10 ft/day.

Overall, slug tests in the reactive cells had a geometric mean conductivity of 399 ft/day. Tests inside Gate 1 ranged in conductivity from 124 ft/day to 2,486 ft/day, with a geometric mean conductivity of 812 ft/day. Tests inside Gate 2 ranged in conductivity from 124 ft/day to 469 ft/day, with a geometric mean conductivity of 233.7 ft/day. Within the reactive cells, water levels recovered within 10-60 seconds and the response curves were not well defined. Therefore, these conductivity values are subject to greater method uncertainty than those for the aquifer wells. Although the overall K values for the reactive media were comparable to the assumed value of 283 ft/day, there is a very large standard deviation even in similar media. For example, the K for exit zone sand in Gate 1 is about 20 times greater than for the same sand in Gate 2. This variability in the conductivity values suggests that heterogeneities may have been introduced in the reactive media due to variable settling and compaction during installation, and points to the need for greater quality control during media emplacement.

6.1.2 Hydraulic Gradient

The water levels and hydraulic gradients in and around the PRB were investigated using manual water-level measurements, HydroTechnics probes, and continuous water-level monitoring probes. A site-wide (regional) gradient of 0.002 has been estimated for Area 5 based on historical data and measurements in existing wells during site characterization (see Section 2). After the PRB was installed, 20 water-level surveys were performed in the wells within and near the PRB to obtain detailed information regarding hydrology in the immediate vicinity of the barrier. Additional wells were included in the site-wide water-level surveys completed in Area 5 during April 1998, May 1998, July 1998, October 1998, February 1999, and June 1999. The objective of the water-level measurements was to obtain information on hydraulic gradients and flow patterns that may affect the performance of the barrier. Water levels were measured in approximately 120 wells for each survey, and the same probe was used for each measurement taken

within a 24-hour period. The probe was decontaminated between measurements. More frequent measurements were conducted in the first six months after PRB installation to evaluate any changes in flow.

A database of water levels and well details was developed to aid in analysis of water-level variations over time. Because gradients at Area 5 were fairly low, it often was difficult to discern water-level differences near and within the permeable barriers. Additionally, the close proximity of the wells to each other resulted in almost negligible differences in water levels in neighboring wells. Consequently, groups of wells present in various zones were lumped together and water-level trends were compared statistically to discern meaningful patterns and to verify that gradients were resulting in flow through the permeable barrier. Appendix E-2 presents results of water-level monitoring and average water levels (Table E-2a) and changes in water levels over successive monitoring events (Table E-2b). A summarized set of information from Appendix E-2 is presented in Table 6-3.

Table 6-3 can be used to evaluate relative hydraulic gradients at the site. A positive gradient indicates that flow took place in the direction indicated. Several observations can be made from Table 6-3:

- For every water-level survey event in Gate 1, the hydraulic gradient between the immediately upgradient wells and downgradient aquifer wells was positive, indicating that flow was taking place through this gate. The average gradient across the entire gate (from immediately upgradient to downgradient aquifer wells) is 0.0052. The average gradient from the upgradient aquifer to the reactive cell is 0.0067. The gradient in the upgradient aquifer wells is much smaller, generally less than 0.0016. The increase in gradient in the immediate vicinity of the Gate 1 indicates that preferential flow is occurring through the gate due to the higher conductivity of sand and iron.
- In all survey events, the measured gradient between the aquifer wells immediately upgradient and downgradient of Gate 1 was positive. However, in some of the events, the gradient between upgradient aquifer and the Gate 1 PTZ was negative, indicating that there may have been transient periods of stagnant groundwater. The negative gradient was observed more often in the first three months after PRB construction. The overall average gradient of 0.0023 from the PTZ to exit zone indicates that, in general, flow occurred through the gate as expected. The lower gradients within the cell are due to the high conductivity of the iron and sand.
- The average gradient from immediately upgradient to immediately downgradient wells for Gate 1 (0.0052) was higher than the average gradient for similar wells through Gate 2 (0.0020). The differences in gradients in the two gates may be the result of conductivity or flow-pattern variations due to differential packing of the gate media. However, the gradients from upgradient aquifer to reactive cell were very similar in both gates (0.0067 for Gate 1 and 0.0064 for Gate 2). Overall, it appears

Table 6-3. Summary of Average Gradients in Various Zones near the Permeable Barrier

	2/3/98	2/9/98	2/16/98	2/26/98	3/7/98	3/13/98	3/20/98	3/27/98	4/3/98	4/10/98	4/18/98	5/6/98	10/7/98	12/16/98	2/1/99	4/8/99	4/26/99	6/1/99	Average Gradients
Gate 1 Average Water Levels																			
Far Upgradient Aquifer ^(a)	12.03	12.36	12.54	13.00	13.42	13.88	14.17	14.61	14.69	14.53	14.32	13.85	10.82	9.73	9.89	10.77	10.98	10.60	NA
Vicinity Upgradient Aquifer ^(b)	12.03	12.38	12.49	12.94	13.37	13.84	14.11	14.55	14.70	14.55	14.35	13.86	10.82	9.73	9.89	10.76	10.98	10.59	NA
Upgradient Aquifer ^(c)	11.99	12.33	12.53	12.97	13.41	13.87	14.16	14.60	14.74	14.51	14.33	13.88	10.84	9.74	9.88	10.75	10.95	10.60	NA
PTZ ^(d)	12.00	12.34	12.52	12.99	13.43	13.89	14.21	14.56	14.65	14.49	14.28	13.82	10.80	9.67	9.83	10.72	10.93	10.57	NA
Reactive Cell ^(e)	11.97	12.31	12.49	12.96	13.38	13.83	14.17	14.53	14.62	14.47	14.25	13.78	10.74	9.65	9.76	10.70	10.73	10.53	NA
Exit Zone ^(f)	12.00	12.30	12.51	13.00	13.40	13.87	14.20	14.55	14.64	14.50	14.26	13.78	10.78	9.67	9.79	10.72	10.89	10.55	NA
Downgradient Aquifer ^(g)	11.94	12.30	12.46	12.94	13.39	13.82	14.13	14.53	14.64	14.47	14.27	13.81	10.70	9.65	9.81	10.70	10.87	10.52	NA
Gate 2 and Vicinity Gradients																			
Far Upgradient to Downgradient Aquifer	0.0021	0.0014	0.0019	0.0014	0.0007	0.0014	0.0010	0.0019	0.0012	0.0014	0.0012	0.0010	0.0029	0.0019	0.0019	0.0017	0.0026	0.0019	0.0016
Far Upgradient to Vicinity Aquifer	0.0000	-0.0017	0.0042	0.0050	0.0042	0.0033	0.0050	0.0050	-0.0008	-0.0017	-0.0025	-0.0008	0.0000	0.0000	0.0000	0.0008	0.0000	0.0008	0.0012
Far Upgradient to Upgradient Aquifer	0.0013	0.0010	0.0003	0.0010	0.0003	0.0003	0.0003	0.0003	-0.0017	0.0007	-0.0003	-0.0010	-0.0007	-0.0003	0.0003	0.0007	0.0010	0.0000	0.0002
Upgradient Aquifer to PTZ	-0.0025	-0.0025	0.0025	-0.0050	-0.0030	-0.0050	-0.0125	0.0100	0.0225	0.0050	0.0125	0.0150	0.0100	0.0175	0.0125	0.0075	0.0050	0.0075	0.0053
Upgradient Aquifer to Reactive Cell	0.0020	0.0020	0.0040	0.0010	0.0030	0.0040	-0.0010	0.0070	0.0120	0.0040	0.0080	0.0100	0.0100	0.0090	0.0120	0.0050	0.0220	0.0070	0.0067
Upgradient to Downgradient Aquifer	0.0042	0.0025	0.0058	0.0025	0.0017	0.0042	0.0025	0.0058	0.0083	0.0033	0.0050	0.0058	0.0117	0.0075	0.0058	0.0042	0.0067	0.0067	0.0052
PTZ to Exit Zone	0.0000	0.0057	0.0014	-0.0014	0.0043	0.0029	0.0014	0.0014	0.0014	-0.0014	0.0029	0.0057	0.0029	0.0000	0.0057	0.0000	0.0057	0.0029	0.0023
Reactive Cell to Downgradient Aquifer	0.0060	0.0020	0.0060	0.0040	-0.0020	0.0020	0.0080	0.0000	-0.0040	0.0000	-0.0040	-0.0060	0.0080	0.0000	-0.0100	0.0000	-0.0280	0.0020	-0.0009
Exit Zone to Downgradient Aquifer	0.0200	0.0000	0.0167	0.0200	0.0033	0.0167	0.0233	0.0067	0.0000	0.0100	-0.0033	-0.0100	0.0267	0.0067	-0.0067	0.0067	0.0067	0.0100	0.0085
Lateral Gradients (U4S-U1S)	-0.0159	-0.0005	0.0007	-0.0039	-0.0022	NA	NA	NA	NA	NA	0.0018	0.0007	0.0018	0.0058	0.0024	NA	0.0013	0.0013	-0.0001
Gate 2 Average Water Levels																			
Upgradient Aquifer ^(h)	12.01	12.33	12.53	12.99	13.43	13.88	14.14	14.58	14.70	14.53	14.33	13.86	10.81	9.72	9.87	10.77	10.96	10.59	NA
PTZ ⁽ⁱ⁾	11.96	12.32	12.51	12.98	13.40	13.87	14.18	14.55	14.66	14.54	14.38	13.83	10.80	9.70	9.85	10.73	10.92	10.57	NA
Reactive Cell ^(j)	11.96	12.31	12.50	12.97	13.40	13.85	14.17	14.55	14.65	14.52	14.38	13.82	10.79	9.70	9.83	10.70	10.91	10.54	NA
Exit Zone ^(k)	11.99	12.33	12.52	12.99	13.41	13.86	14.20	14.57	14.68	14.55	14.42	13.85	10.80	9.71	9.85	10.72	10.93	10.56	NA
Downgradient Aquifer ^(l)	11.96	12.31	12.49	12.96	13.41	13.85	14.18	14.56	14.66	14.53	14.38	13.82	10.79	9.70	9.85	10.75	10.92	10.56	NA
Gate 2 and Vicinity Gradients																			
Upgradient to Downgradient Aquifer	0.0042	0.0017	0.0033	0.0025	0.0017	0.0025	-0.0033	0.0017	0.0033	0.0000	-0.0042	0.0033	0.0017	0.0017	0.0017	0.0017	0.0033	0.0025	0.0020
PTZ to Exit Zone	-0.0043	-0.0014	-0.0014	-0.0014	-0.0014	0.0014	-0.0029	-0.0029	-0.0029	-0.0014	-0.0057	-0.0029	0.0000	-0.0014	0.0000	0.0014	-0.0014	0.0014	-0.0016
Upgradient Aquifer to Reactive Cell	0.0100	0.0040	0.0060	0.0040	0.0060	0.0060	-0.0060	0.0060	0.0060	0.0100	0.0020	-0.0100	0.0080	0.0040	0.0080	0.0140	0.0100	0.0100	0.0064
Reactive Cell to Downgradient Aquifer	0.0000	0.0000	0.0020	0.0020	-0.0020	0.0000	-0.0020	-0.0020	-0.0020	-0.0020	0.0000	0.0000	0.0000	0.0000	-0.0040	-0.0100	-0.0020	-0.0040	-0.0016
Exit Zone to Downgradient Aquifer	0.0060	0.0040	0.0060	0.0060	0.0000	0.0020	0.0040	0.0020	0.0040	0.0040	0.0080	0.0060	0.0020	0.0020	0.0000	-0.0060	0.0020	0.0000	0.0012

(a) U16S, U17S, and U18S.

(b) U10S, U11S, U12S, U13S, U14S, and U15S.

(c) U3S, U3D, U5D, U4S, U4D, and U5S.

(d) F1S, F2S, F2M, F2D, F3S, and F3D.

(e) F4S, F6S, F7S, F8S, F9S, F11S, F12S, F4M, F5M, F6M, F4D, F5D, F6D, F7D, F8D, F9D, F11D, and F12D.

(f) F13S, F14S, F13D, and F14D.

(g) D3S, D4S, D5S, D5D, and D6S.

(h) U7S, U7D, U8S, U8M, U8D, U9S, and U9D.

(i) P1S, P2S, P2M, P2D, P3S, and P3D.

(j) P4S, P5S, P6S, P7S, P8S, P9S, P11S, P12S, P4M, P5M, P6M, P4D, P5D, P6D, P7D, P8D, P9D, P11D, P12D, and P10.

(k) P13S, P14S, and P14D.

(l) D7S and D7D.

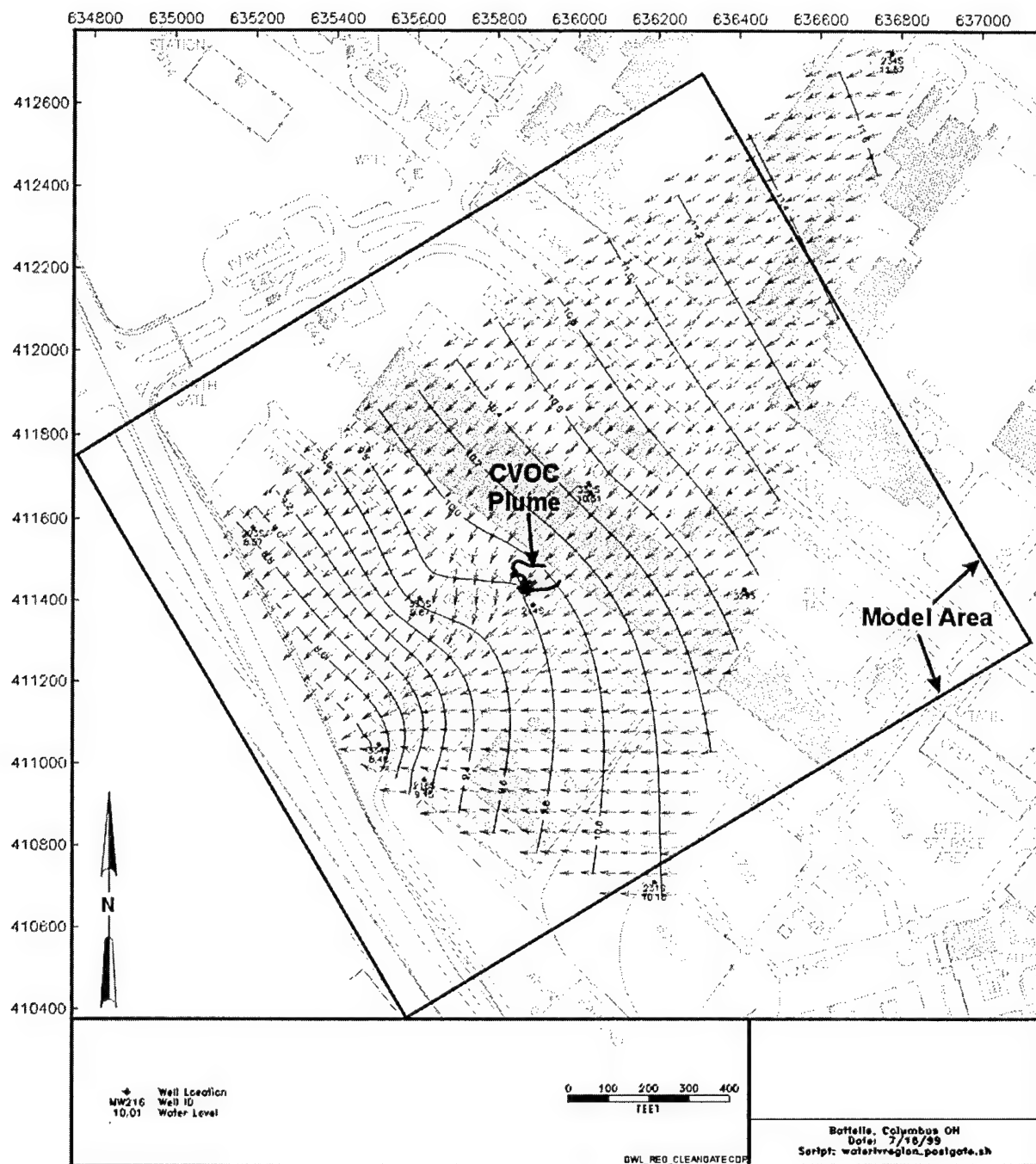
NA = Not applicable

that water flowed more easily and consistently through Gate 1, whereas stagnant conditions prevailed more often in Gate 2.

- For both gates, the gradient from the upgradient aquifer into the reactive cell was positive on average. However, for both gates, the gradient from the reactive cell to the downgradient aquifer was negative on average. In the case of Gate 2, the average gradient from the PTZ to exit zone was marginally negative. This result seems to indicate that groundwater flowed more easily from the upgradient aquifer into the reactive cell, but had to overcome a counter-gradient upon moving out into the downgradient aquifer. This is probably the result of the media in the gates being much more permeable than the aquifer medium (by more than an order of magnitude), as indicated in Table 6-2. This conductivity contrast results in at least a temporary impediment to water flow out of the gate. However, wider available area for flow in the downgradient aquifer eventually leads to wider flow tubes that compensate for lower conductivity. This is shown by steeper gradient between the exit zone and downgradient aquifer (0.0085 for Gate 1 and 0.0012 for Gate 2). Similar resistance to outflow in the exit zone has been observed at other PRBs, such as the one at former Naval Air Station (NAS) Moffett Field (Battelle, 1998).
- The average gradient through Gate 1 (0.0052 between immediately upgradient and downgradient aquifer wells) is positive and much higher than the relatively flat lateral gradient (-0.0001 between U4 and U1) parallel to the funnel wing wall. This result indicates that groundwater immediately upgradient of the gate tends to flow through the gate, rather than flow around the funnel. In other words, groundwater capture does occur in the immediate vicinity of the gates.

The water-level data were contoured to evaluate gradients and flow directions at the site. Area 5 water-level maps for shallow and deep wells are presented in Appendix E-3. Figure 6-4 shows a representative map of water levels from shallow wells at Site 5. Figure 6-5 shows a representative map of water levels from deep wells at Site 5. Site-wide gradients indicate that a positive gradient is maintained through the permeable barrier area. In general, wells indicate that site-wide gradients range from 0.0015 to 0.002 over Area 5. Overall, water-level patterns were similar for each of the surveys, indicating a southwest flow direction. However, the relative elevation of the water table varies seasonally. For example, water levels which occur in the spring are 2-3 ft higher than water levels which occur in the fall.

In the immediate vicinity of the permeable barrier, gradients vary seasonally in both direction and magnitude. Figure 6-6 and Figures 6-7 and 6-8 show maps of water levels near the PRB during the winter (February 1998) and summer (July 1998 and June 1999), respectively. In the immediate upgradient wells for both gates, the contour lines can be drawn so that the flow lines converge towards the reactive cells. These figures indicate that groundwater is being captured by the permeable barrier, an observation previously confirmed by steeper hydraulic gradients in this area. However, beyond the immediate wells, the flow patterns are very difficult to interpret.



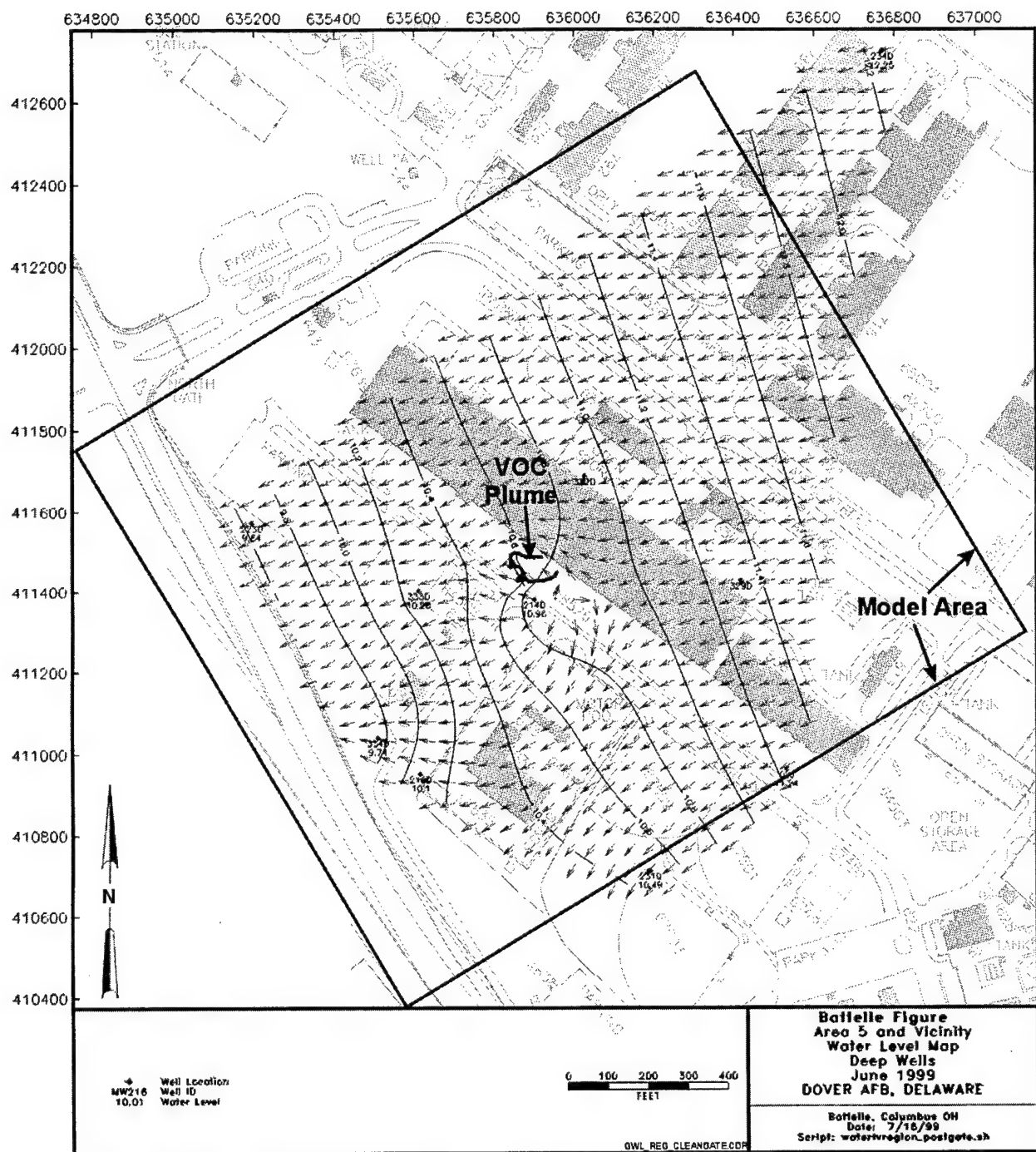


Figure 6-5. Representative Map of Water Levels from Deep Wells at Site 5

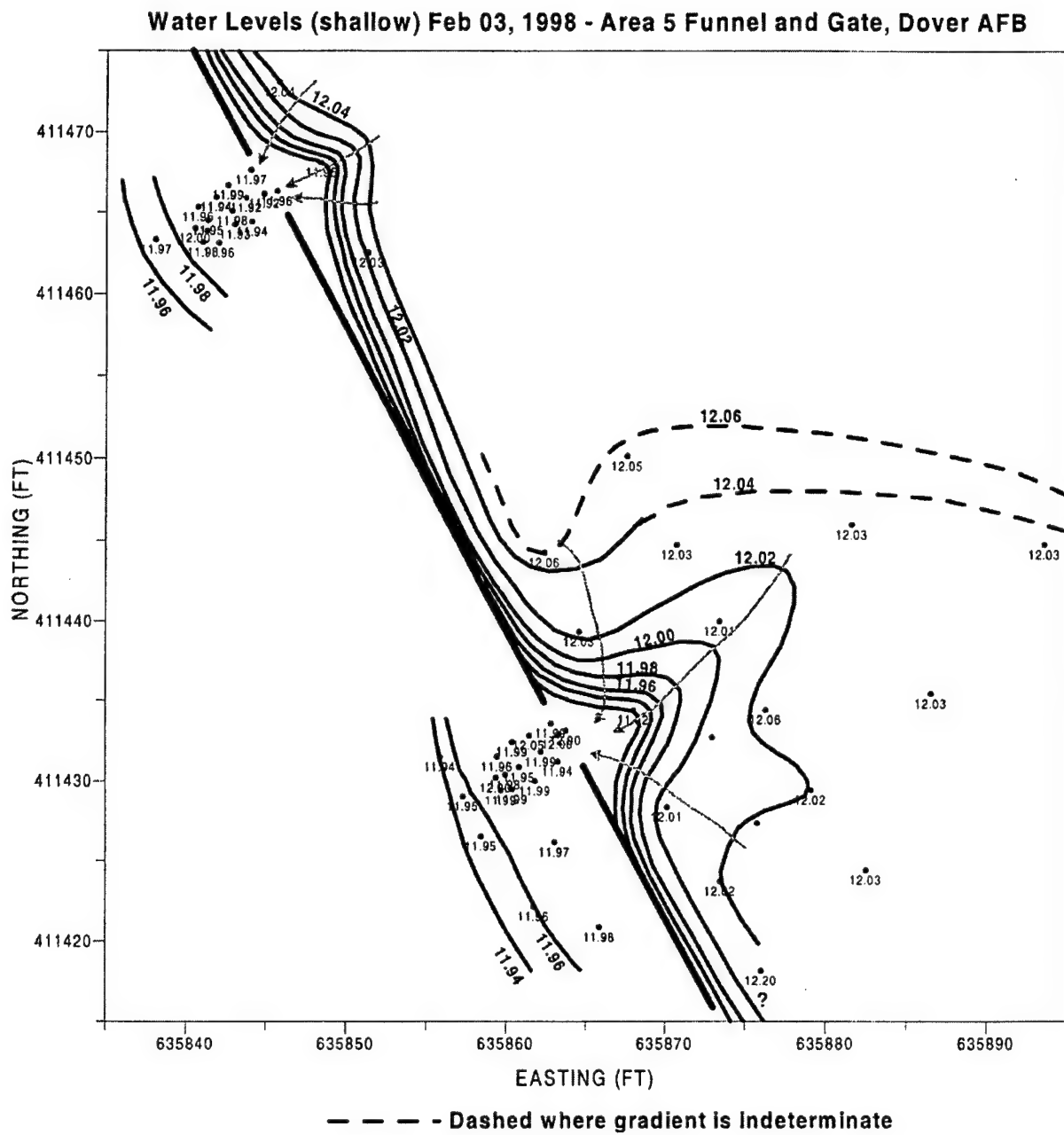


Figure 6-6. Map of Water Levels in Shallow Wells near the PRB (February 1998)

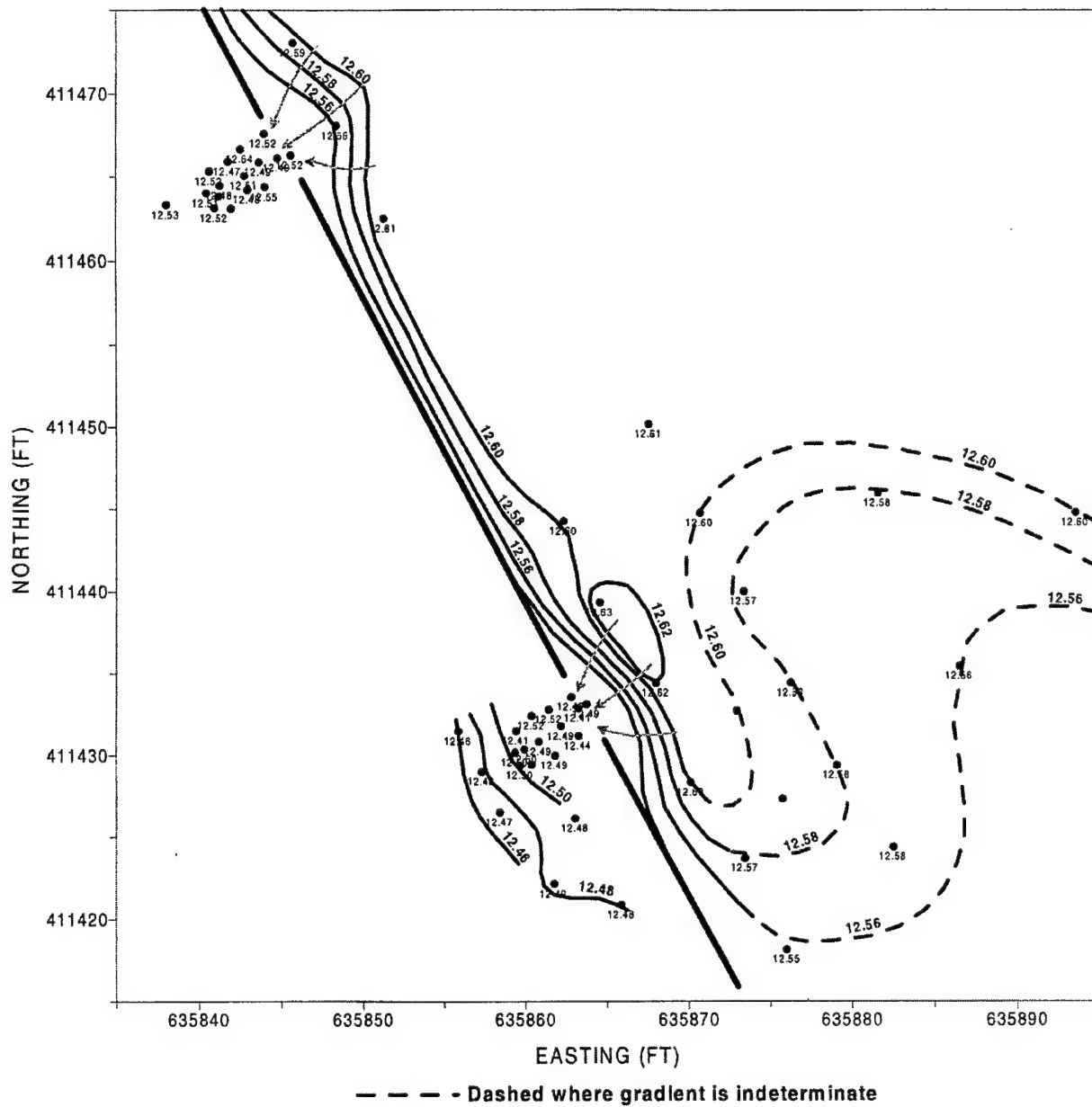


Figure 6-7. Map of Water Levels in Shallow Wells near the PRB (July 1998)

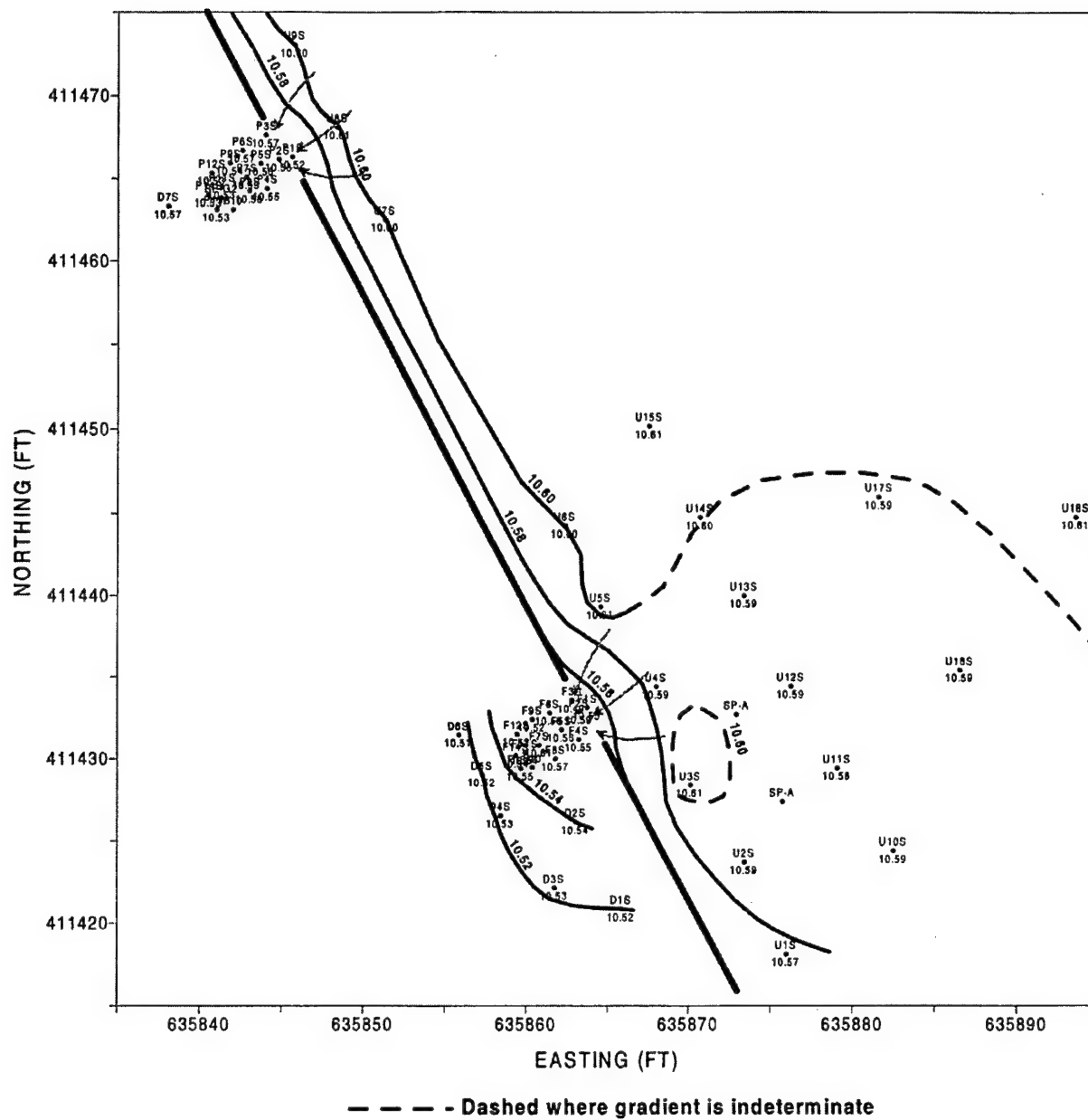


Figure 6-8. Map of Water Levels in Shallow Wells near the PRB (June 1999)

Essentially, the low hydraulic gradients and small area of investigation result in most water-level differences being within margin of error (i.e., the water-level difference in wells U10 through U18 are very similar). Therefore, the exact flow patterns are difficult to determine.

Seasonal variations in water levels also are shown by plotting levels over time. Figures 6-9 and 6-10 show both water-level and precipitation data for selected wells along the midline of Gate 1 and 2, respectively. The yearly high water level occurred in spring and the yearly low water level occurred in late fall, which is a typical seasonal pattern found in the eastern United States. These figures show extremely small differences in water levels in adjacent wells due to their close proximity. These differences are within the measurement uncertainty and therefore no useful observations about stagnant flow can be made from these plots.

Changes in water levels over time were analyzed to reveal trends in water levels. Appendix Table E-2b presents complete results of water-level changes over time. Table 6-4 summarizes water-level changes over successive monitoring intervals in different parts of the study area. As shown in this table, water levels increased from February to March 1998, decreased from March to October, increased from October 1998 to April 1999, and declined from April to June 1999. In general, the amount of water-level change was similar for all wells monitored. Water-level changes were greatest in July-October 1998 when they dropped approximately 1.75 ft. The smallest change occurred from December to February 1999 when water levels increased about 0.15 ft.

During the first half of 1998, water levels were continuously monitored in selected wells near the PRB. Monitoring was performed with in situ Troll™ pressure temperature loggers. Trolls™ are self-contained probes and dataloggers. The probes record data on pressure and temperature at specified intervals. Then data can be downloaded to a laptop computer. Water levels were monitored in four wells at Gate 1 from March 9, 1998, to April 5, 1998. Water levels were monitored at Gate 2 from May 7, 1998, to July 13, 1998. Figure 6-11 shows the results of continuous water-level monitoring in several wells through Gate 2 during June and July 1998. Remaining plots for the continuous water-level data are presented in Appendix E-4. Overall, the water levels over time were similar in pattern. As shown, water levels are consistently higher in the upgradient aquifer than in the downgradient zone, indicating that an overall positive gradient is maintained across the barrier. However, water levels appear to be slightly lower within the iron cell and exit zone than in the immediately downgradient aquifer. This is most likely the result of higher conductivity of the reactive media, which results in flat gradients and lower conductivity of the downgradient aquifer.

6.1.3 Summary of Groundwater Modeling for PRB Design

Preconstruction estimates on residence times and flow velocities were calculated with a flow model (Battelle, 1997). The flow model was designed to evaluate the flux through the reactive cells resulting from different funnel-and-gate designs and from seasonal variations in flow directions. A one-layer model was set up to simulate the Columbia Aquifer following the design guidance document for the application of permeable barriers to remediate dissolved chlorinated

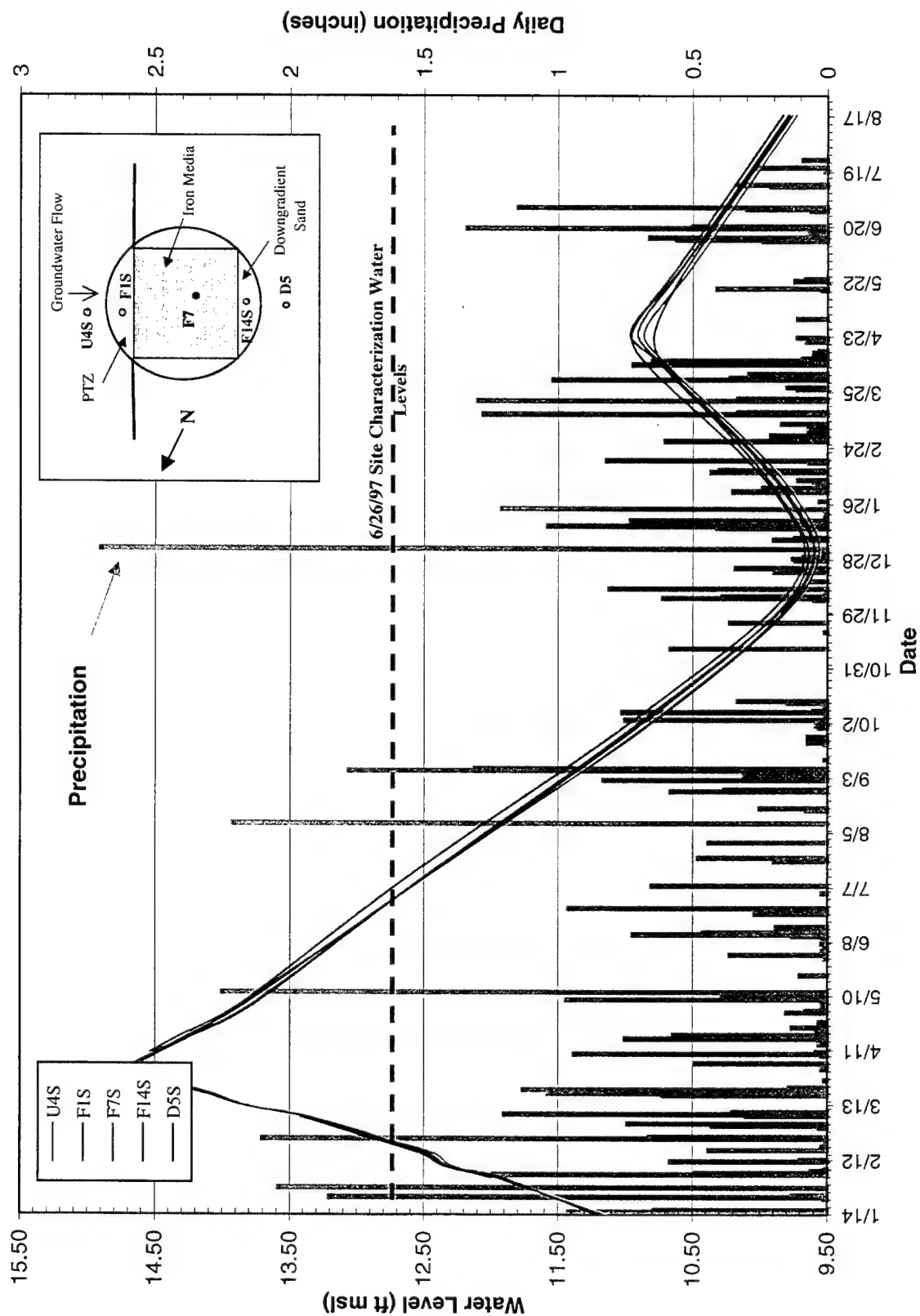


Figure 6-9. 1998/1999 Water-Level and Precipitation Data for Gate 1 of the PRB

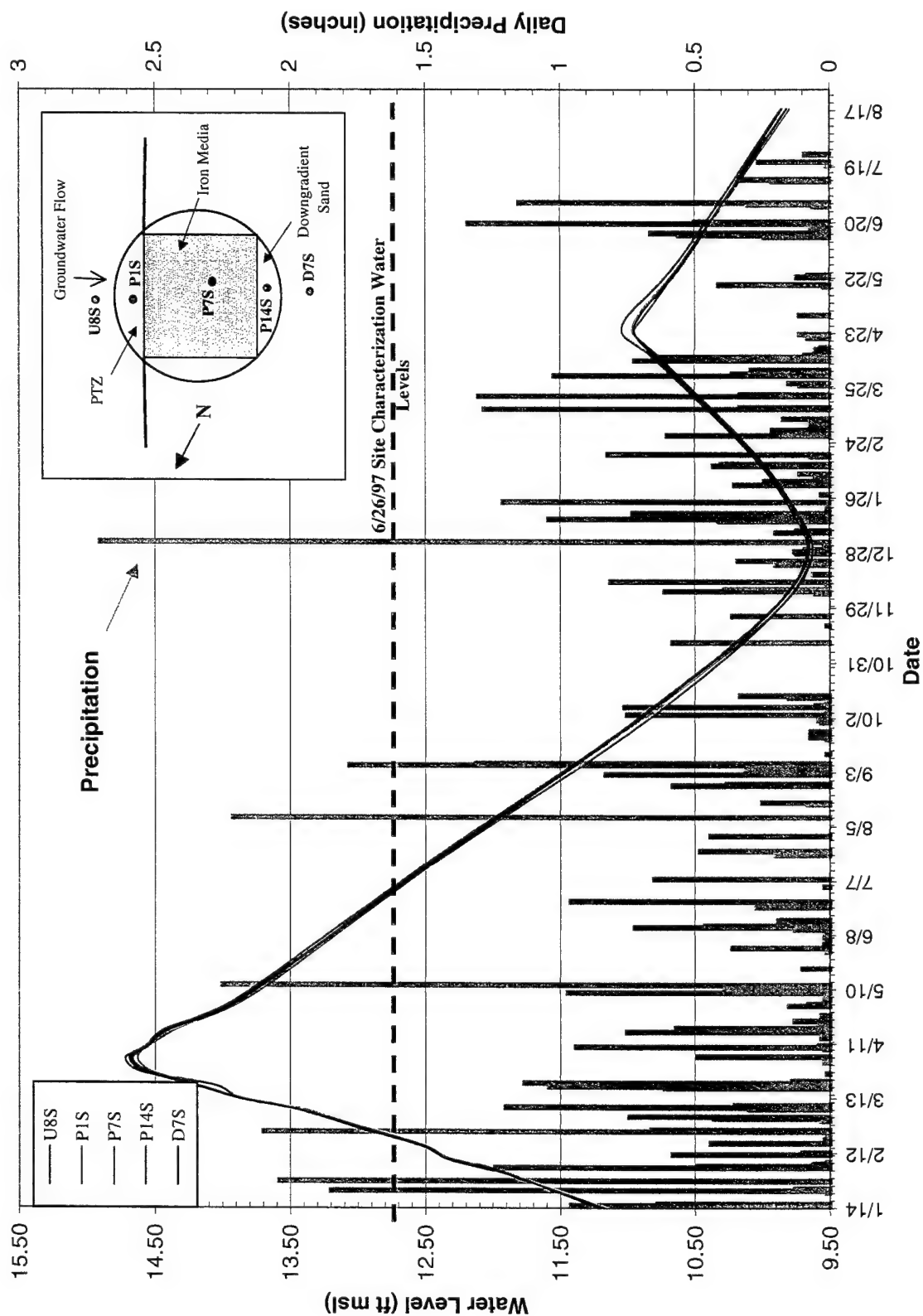


Figure 6-10. 1998/1999 Water-Level and Precipitation Data for Gate 2 of the PRB

Table 6-4. Summary of Average Water-Level Changes over Time near the Permeable Barriers

Well Grouping	Jan 98 - Feb 98	Feb 98 - Mar 98	Mar 98 - Apr 98	Apr 98 - May 98	May 98 - Jul 98	Jul 98 - Oct 98	Oct 98 - Dec 98	Dec 98 - Feb 99	Feb 99 - Apr 99	Apr 99 - Jun 99
Gate 1 Far Upgradient Aquifer Wells	1.31	1.34	0.65	-0.67	-1.27	-1.77	-1.08	0.16	1.09	-0.38
Gate 1 Vicinity Upgradient Aquifer Wells	1.28	1.35	0.71	-0.69	-1.28	-1.77	-1.09	0.15	1.09	-0.39
Gate 1 Upgradient Aquifer Wells	1.33	1.32	0.66	-0.64	-1.29	-1.76	-1.10	0.15	1.07	-0.35
Gate 1 PTZ Wells	N/A	1.37	0.61	-0.67	-1.35	-1.68	-1.12	0.16	1.10	-0.36
Gate 1 Reactive Cell Wells	N/A	1.34	0.64	-0.69	-1.31	-1.73	-1.09	0.11	0.96	-0.20
Gate 1 Exit Zone Wells	N/A	1.36	0.62	-0.72	-1.28	-1.73	-1.11	0.12	1.11	-0.34
Gate 1 Downgradient Aquifer Wells	1.33	1.36	0.65	-0.66	-1.34	-1.79	-1.03	0.16	1.07	-0.36
Gate 2 Upgradient Aquifer Wells	1.33	1.35	0.65	-0.67	-1.27	-1.77	-1.09	0.15	1.09	-0.37
Gate 2 PTZ Wells	N/A	1.36	0.67	-0.71	-1.31	-1.72	-1.10	0.16	1.07	-0.36
Gate 2 Reactive Cell Wells	N/A	1.35	0.67	-0.70	-1.32	-1.72	-1.08	0.13	1.08	-0.37
Gate 2 Exit Zone Wells	N/A	1.34	0.69	-0.70	-1.33	-1.72	-1.09	0.14	1.08	-0.38
Gate 2 Downgradient Aquifer Wells	1.37	1.36	0.68	-0.71	-1.32	-1.72	-1.09	0.15	1.07	-0.37
Existing Wells	N/A	N/A	0.54	-0.64	-1.31	-1.69	-1.05	0.18	1.21	-0.47

Positive water-level changes indicate the groundwater level increased.

Negative water-level changes indicate the groundwater level decreased.

N/A = Not available.

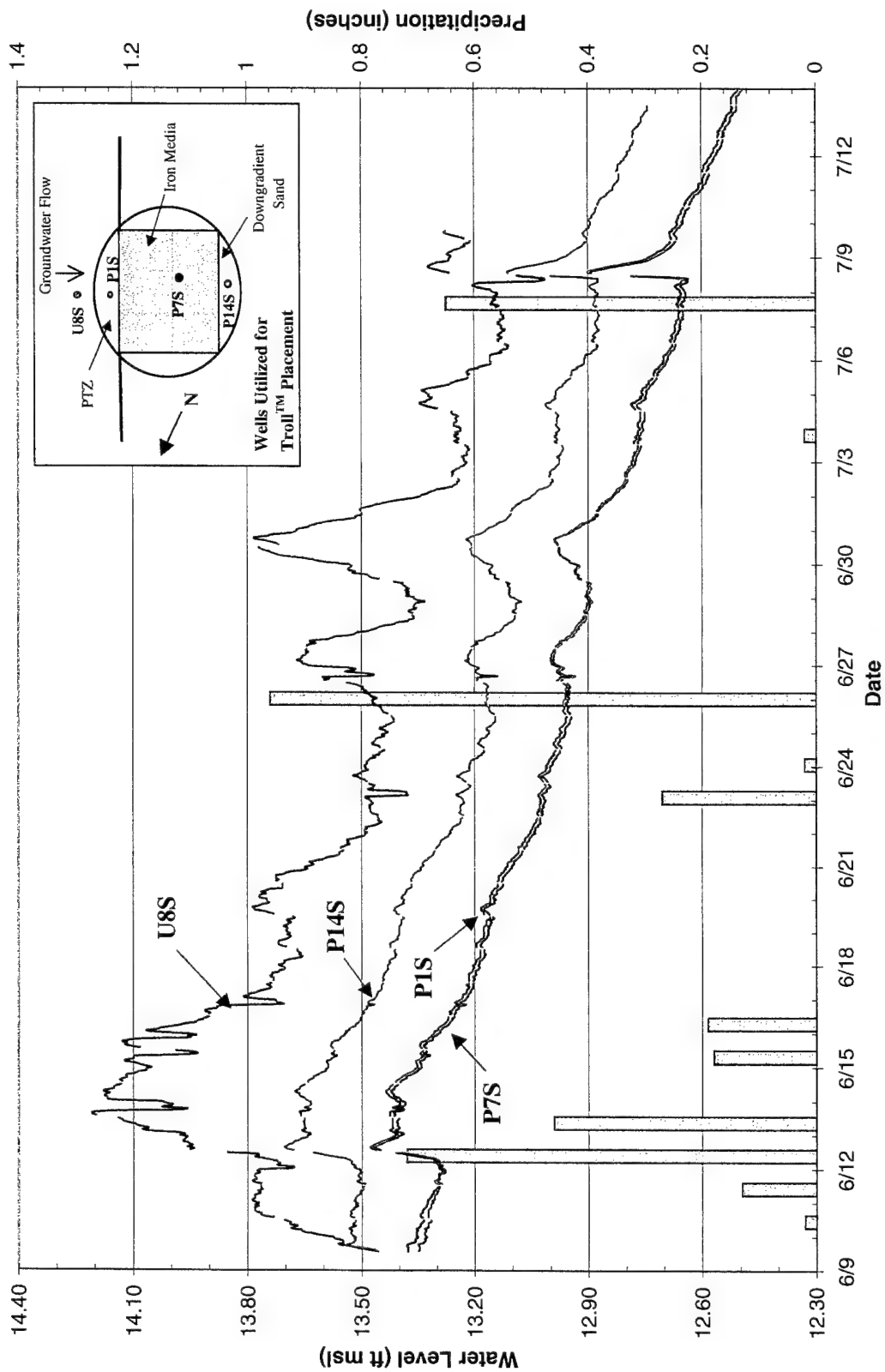


Figure 6-11. Continuous Water-Level Elevations in Gate 2 of the PRB (June and July 1998)

solvents (Battelle, 1997). Groundwater flow simulations were performed using MODFLOW (McDonald and Harbaugh, 1988). Particle tracking for pathway and capture zone analysis was completed using Random-Walk (Naymik et al., 1995). The flow model covers an area of 1,600 ft \times 1,800 ft, and consists of 246 rows and 473 columns for a total of 116,358 nodes. To evaluate the flux and flowpaths through the reactive cells, a variable grid spacing was used. In the vicinity of the funnel-and-gate, model grid cell dimensions were 0.25 \times 0.25 ft to permit more accurate determinations of flux through the reactive cell.

With this model, several scenarios were simulated to predict how the barrier would perform. Scenarios included using different aquifer hydraulic parameters, varying flow directions, and varying dimensions of the gates. The results for the base case (no barrier) and for the approximate final design are shown in Table 6-5. Figure 6-12 shows simulated water levels and flowpaths for the final PRB design layout. In general, the modeling predicted an approximate 5-fold increase in flux and 2.5-fold increase in velocity through the gate.

Table 6-5. Simulated Flow Velocities, Capture Zones and Travel Time through Reactive Cell (from Battelle, 1997)

Scenario	Funnel Lengths (ft-ft-ft)	Aquifer K (ft/day)	Flux Through Each Gate (ft ³ /day)	Gate Velocity (ft/day)	Total Capture Zone Width at Gate (ft)	Travel Time Through Reactive Cell (days)
Base Case	None	10	1.8	0.067	NA	60.0
December 1993	None	50	8.4	0.323	NA	12.4
Base Case	None	10	2.1	0.056	NA	71.0
May 1994	None	50	9.9	0.258	NA	15.5
Base Case	None	10	2.5	0.074	NA	54.2
July 1997	None	50	11.4	0.345	NA	11.6
Final Design	15-30-15	10	9.6	0.179	54.0	22.4
December 1993	15-30-15	50	39.7	0.769	52.0	5.20
Final Design	15-30-15	10	10.0	0.155	53.6	25.8
May 1994	15-30-15	50	40.3	0.645	53.6	6.20
Final Design	15-30-15	10	12.2	0.203	53.8	19.7
July 1997	15-30-15	50	50.5	0.851	52.4	4.70

NA = Not applicable.

6.1.4 Groundwater Velocity Calculation Based on Darcy's Law

Several parameters are required to determine the flowrate through a PRB. The conductivity of the material in the barrier and the surrounding aquifer was determined with slug tests. Gradients in and around the barrier were determined from water-level surveys, HydroTechnics groundwater flowmeters, and continuous water-level monitoring. The porosity of aquifer sediments was obtained from geotechnical testing on sediment samples. Groundwater flow velocities are calculated as a function of these parameters:

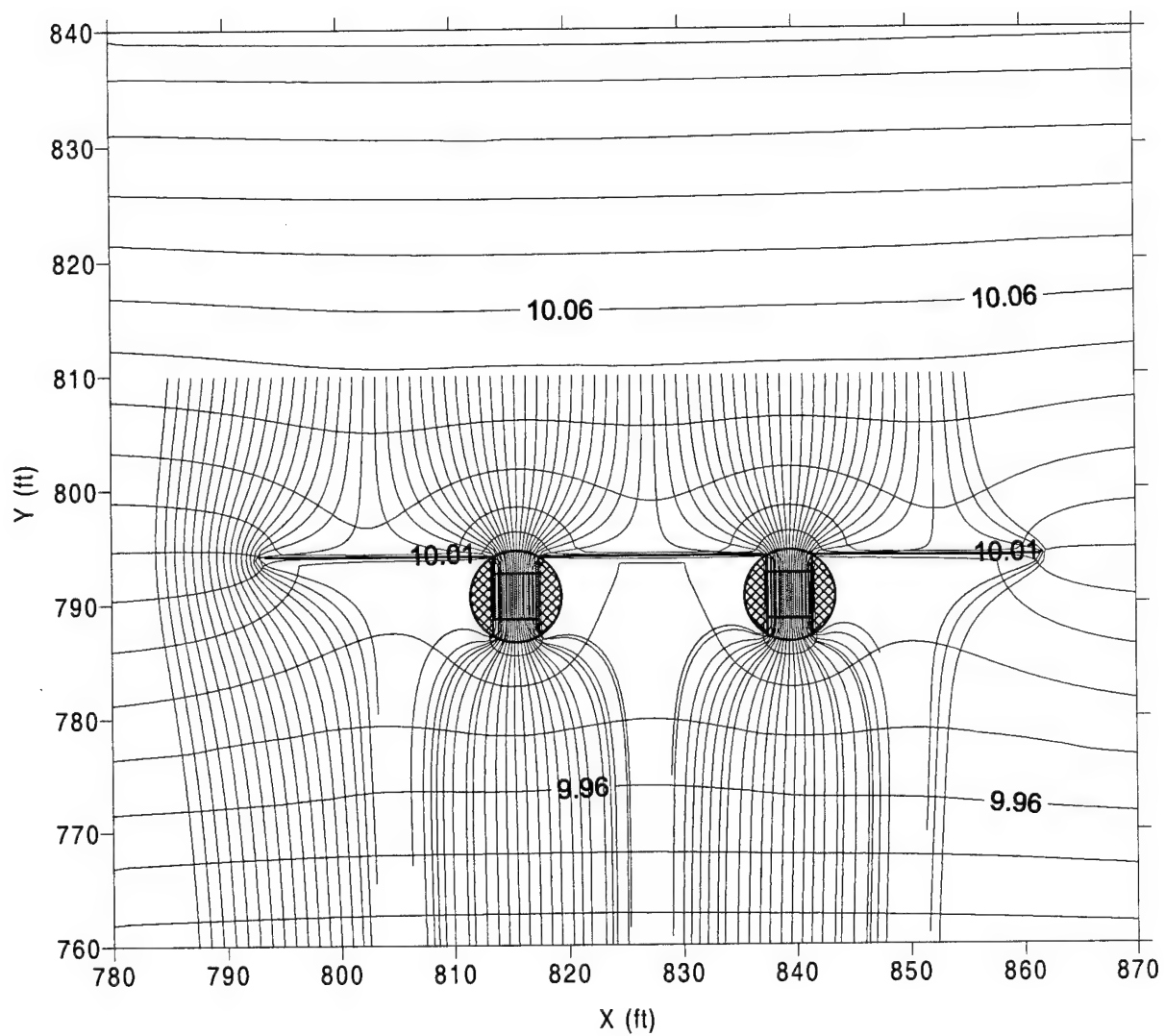


Figure 6-12. Simulated Water Levels and Flowpaths for Final PRB Design

$$v = \frac{Ki}{n} \quad (6-1)$$

where v = linear groundwater flow velocity (ft/day)
 K = hydraulic conductivity (ft/day)
 i = hydraulic gradient (ft/ft)
 n = effective porosity (unitless).

Calculation of flow velocities through the gates requires the use of thickness-weighted geometric mean K values to account for variable conductivity and media thickness along the flowpaths. Residence times are calculated by dividing the length of the barrier (4 ft) by the flow velocity. Flux through the cells may be calculated by multiplying the saturated thickness (approximately 20 ft) and the cell width (4 ft) by the groundwater flow velocity. It should be noted that previous modeling evaluations (Gupta and Fox, 1999; Gavaskar et al., 2000) have shown that the velocity through the reactive gates is largely independent of the gate K , as long as the gate is 5 to 10 times greater than the aquifer K . It appears that any increase in K in such cases is negated by a corresponding decrease in gradient within the gate. However, it is very difficult to measure this gradient with accuracy over the short distances encountered in the PRBs. Therefore, at very high values of reactive media K such as at this site, the Darcy equation (Equation 6-1) should be used with caution.

Table 6-6 summarizes groundwater flow velocities and residence times based on monitoring data including gradients and thickness weighted geometric means. The following velocity estimates are represented in the table:

- Based on the average of all aquifer slug test conductivity and site-wide gradient data, the aquifer flow velocity was estimated at approximately 0.048 ft/day. The aquifer velocity may vary between 0.026 to 0.16 if a conductivity range between 4 and 25 ft/day is considered representative.
- Flow velocities through the gates varied by more than an order of magnitude depending on the K and gradient values used. Velocities through the reactive cells were greater than those calculated for the aquifer. Using a thickness-weighted geometric mean K from slug tests in the aquifer and laboratory tests with the media in the gates, and the average gradient between aquifer wells immediately upgradient and downgradient of the gates, the estimated velocity was 6.0 ft/day for Gate 1 and 2.1 ft/day for Gate 2. For the same gradient, but with only slug test-based K data, the velocity was 4.1 ft/day for Gate 1 and 0.46 ft/day for Gate 2.
- Finally, based on average gradients from the PTZ to the exit zones and slug-test-based conductivities, flow velocity through the reactive cell was 2.7 ft/day for Gate 1. It was not possible to calculate velocity with Gate 2 due to a negative average gradient.

Table 6-6. Groundwater Flow Velocity and Residence Time Based on Observed Gradients and Conductivity

Location	K (ft/day)	Gradient (ft/ft)	Porosity	Groundwater Flow Velocity (ft/day)	Residence Time in Reactive Cell (days)
Upgradient aquifer	7.4 (average aquifer slug tests)	0.002	0.31	0.048	N/A
Upgradient aquifer	4-25 (representative aquifer slug test range)	0.002	0.31	0.026 – 0.16	N/A
Gate 1 (upgradient to downgradient aquifer)	790 ^(a) (laboratory data and slug tests)	0.0053	0.70	6.0	0.7
Gate 2 (upgradient to downgradient aquifer)	750 ^(a) (laboratory data and slug tests)	0.002	0.70	2.1	2.0
Gate 1 (upgradient to downgradient aquifer)	544 ^(b) (slug tests)	0.0053	0.70	4.1	1.0
Gate 2 (upgradient to downgradient aquifer)	160 ^(b) (slug tests)	0.002	0.70	0.46	8.7
Gate 1 (PTZ to exit zone)	812 (slug tests)	0.0023	0.70	2.7	1.5
Gate 2 (PTZ to exit zone)	234 (slug tests)	-0.0016	0.70	N/A	N/A

(a) Thickness-weighted geometric mean of slug test-based aquifer K and laboratory test-based media K.

(b) Thickness-weighted geometric mean of slug test-based aquifer K and media K values.

The velocity estimates based on slug test data and gradients from wells immediately upgradient and downgradient of the gates generally are expected to be the more representative because they are based on a single K estimation method and the gradients are relatively stable along this flow-path. This approach results in a large velocity range, 0.46 to 4.1 ft/day, at the Dover AFB PRB. Based on a reactive cell thickness of 4 ft, the estimated velocity range of 0.46 to 4.1 ft/day indicates a groundwater residence time of approximately 1 to 9 days in the reactive portion of the two gates. This range is inclusive of the variability inherent in the field estimates of K and hydraulic gradient, as well as inclusive of the seasonal fluctuations and aquifer/gate media heterogeneities. Significant variations in velocity also are present within the gates on a localized basis. For example, velocity is extremely slow in the exit zone, where extremely low gradients indicate that the groundwater moves from the high-conductivity sand to the low-conductivity aquifer.

Preconstruction groundwater flow modeling indicated that the flow velocity through the gate would vary from approximately 0.2 to 0.5 ft/day based on aquifer conductivity range of about 10 to 25 ft/day (Table 6-5). As shown in Table 6-6, field-measured velocities ranged from 0.46 to 6 ft/day. The most important reason for this difference is that the field-measured K values were much greater than those used for modeling. As noted above, previous modeling has shown that the increase in velocity is independent of gate K at very high gate K to aquifer K ratios. It is very likely that the actual velocity through the gates is at the low end of this range (or even slower) rather than at the higher end. Modeling did not predict the localized flow variations within the gates or the occurrence of periodic but transient stagnant groundwater conditions during low-flow summer months, even though seasonal variations in flow were included in the modeling. A transient flow model would have been better able to simulate such effects with greater accuracy.

6.1.5 Groundwater Velocity Measurements from the HydroTechnics Probes

The four HydroTechnics probes have monitored flow velocity since the installation of the PRB. The calculated velocity along with the precipitation data for the HydroTechnics Probes 1 through 4 over 18 months is shown in Figures 6-13 through 6-16. A statistical summary of the observed velocities is shown in Table 6-7.

Overall, the probes indicated that flow conditions varied substantially during the first two quarters after PRB construction (January to June 1998), a period followed by relatively stable conditions. All probes showed that changes in flow velocity occurred after precipitation events. For Probe 1, groundwater flow velocity showed a gradual increase from 0.01 ft/day in March 1998 to a relatively stable range of 0.03 to 0.04 ft/day. For Probe 2, flow velocity fluctuated during the first six months after construction and then stabilized at 0.09 ft/day. Both of these probes show velocity ranges that compare very well with the simulated velocity and the hydraulically calculated velocity.

For Probe 3 in Gate 1, groundwater velocities showed large fluctuations in March 1998, but stabilized to between 0.03 to 0.04 ft/day. For Probe 4 in Gate 2, flow velocities varied greatly during the first six months after construction, then stabilized to about 0.03 ft/day. The initial variability in the probes could be attributed to either the stabilization time for the probe after installation or the spring rainfall. The response of velocity to precipitation was faster for probes in the gates, indicating that the reactive gates are more connected with the surface than the aquifer. The residence time for groundwater in the reactive media based on thickness of 4 ft and velocity of 0.03 ft/day is about 133 days.

When compared to the gradient-based flow velocity estimate, the estimate measured using HydroTechnics probes is much lower, a difference that becomes increasingly apparent when residence times are calculated. The HydroTechnics probes indicate a residence time of about 133 days within the reactive cell, whereas the gradient-based residence times are between 0.7 and 9 days. Several reasons may explain this difference in estimates. Perhaps the most important reason is that the probe performance may be adversely affected by the iron in the

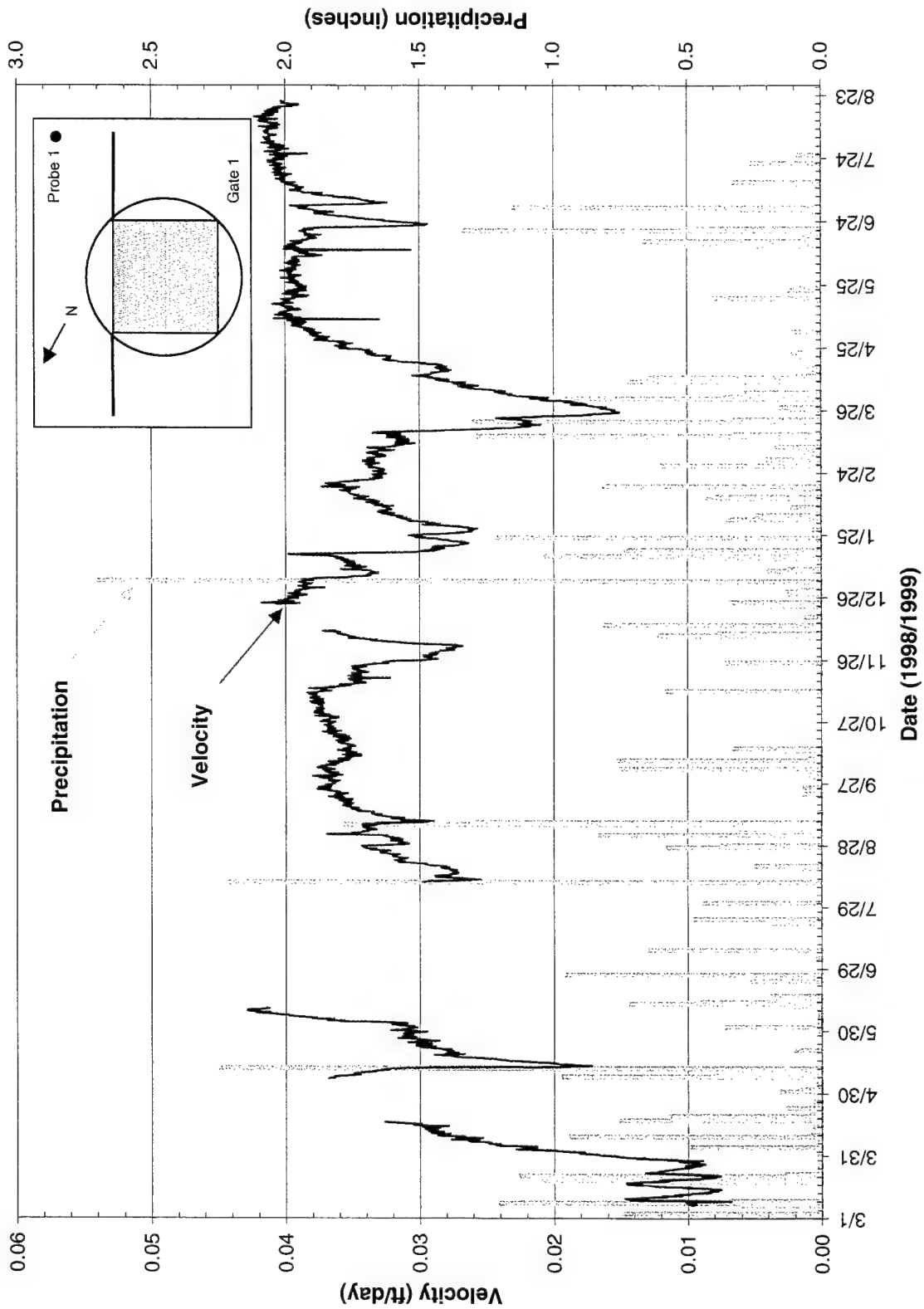


Figure 6-13. Groundwater Flow Velocity in PRB—HydroTechnics Probe 1

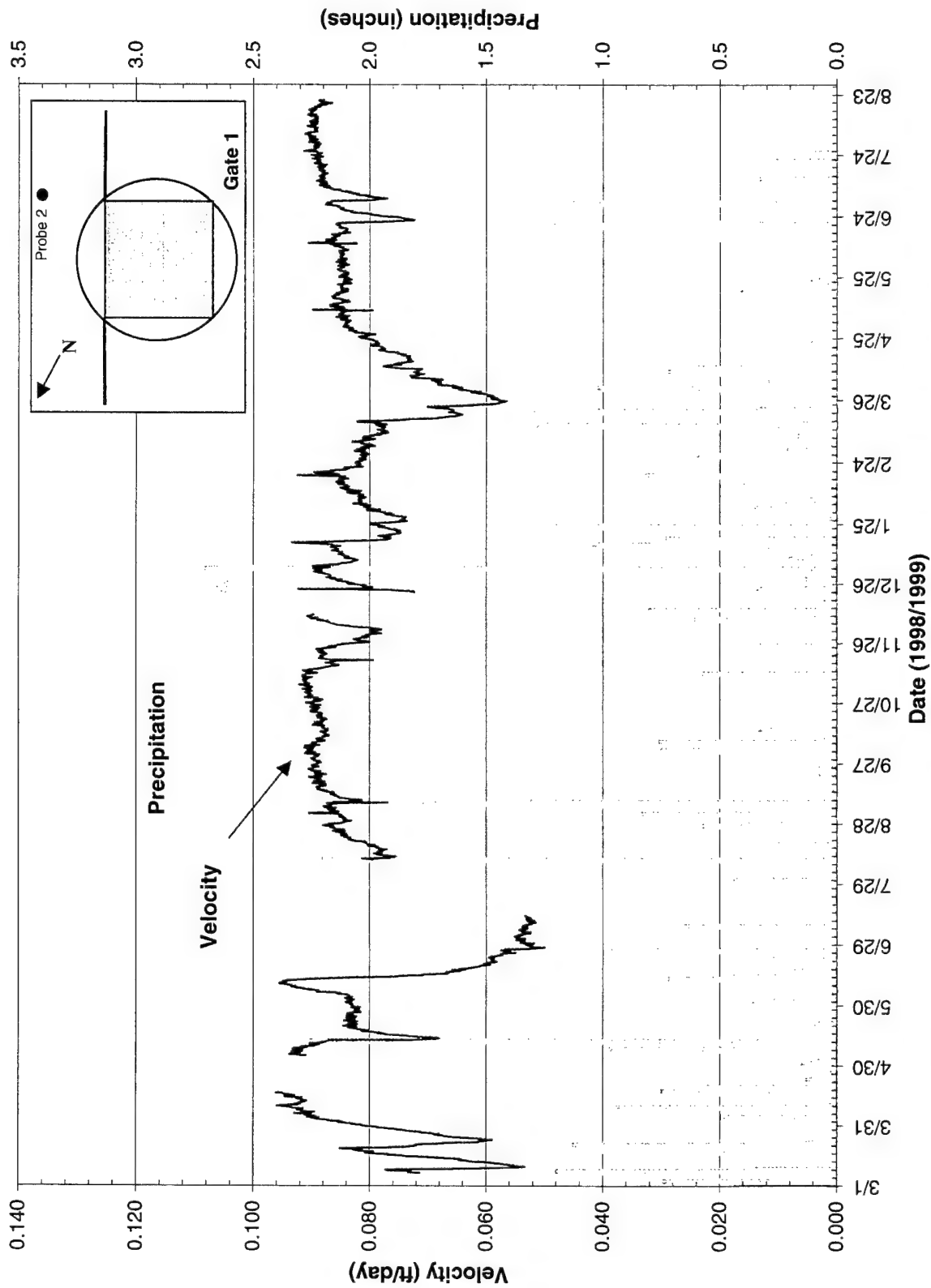


Figure 6-14. Groundwater Flow Velocity in PRB—HydroTechnics Probe 2

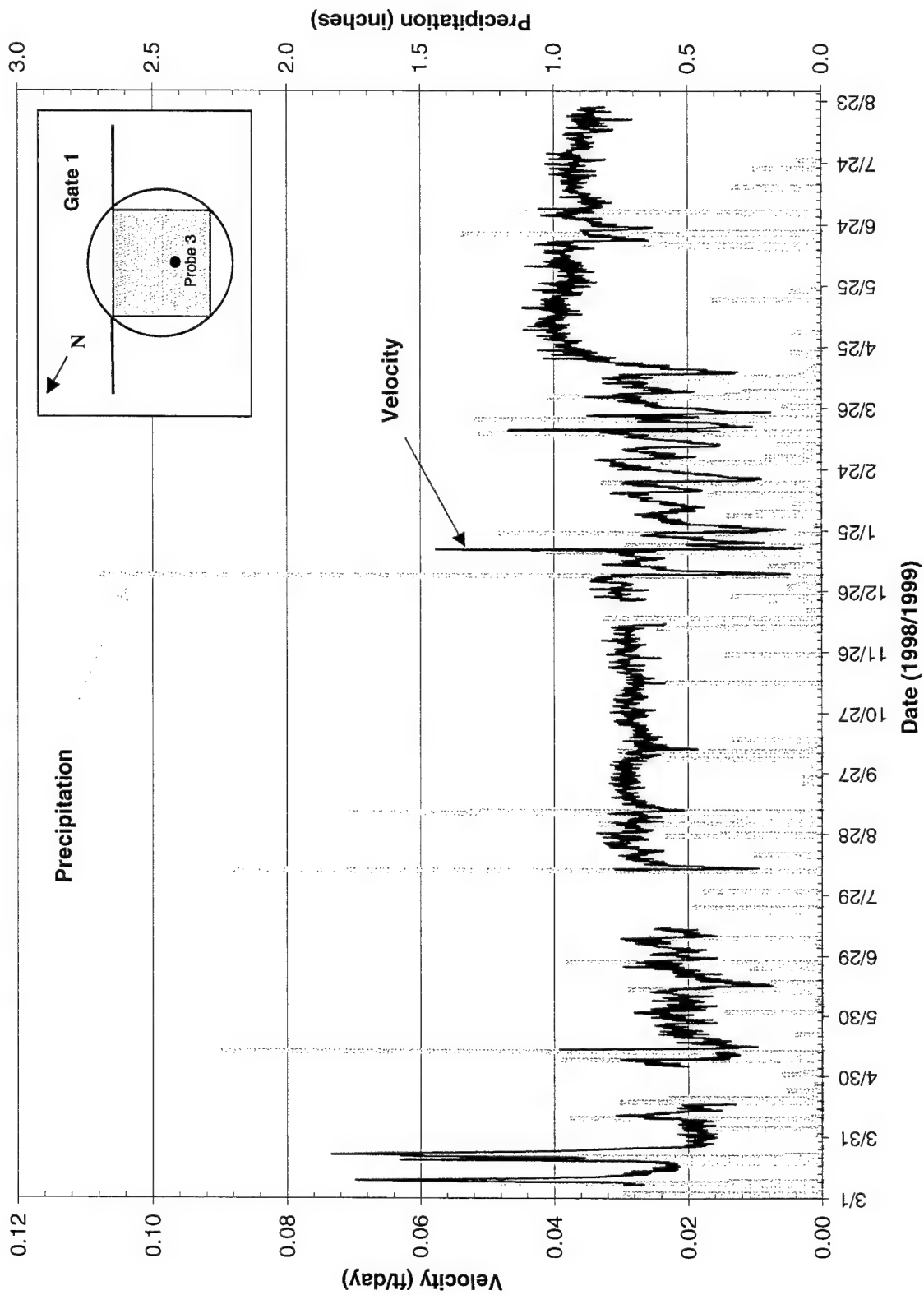


Figure 6-15. Groundwater Flow Velocity in PRB—HydroTechnics Probe 3

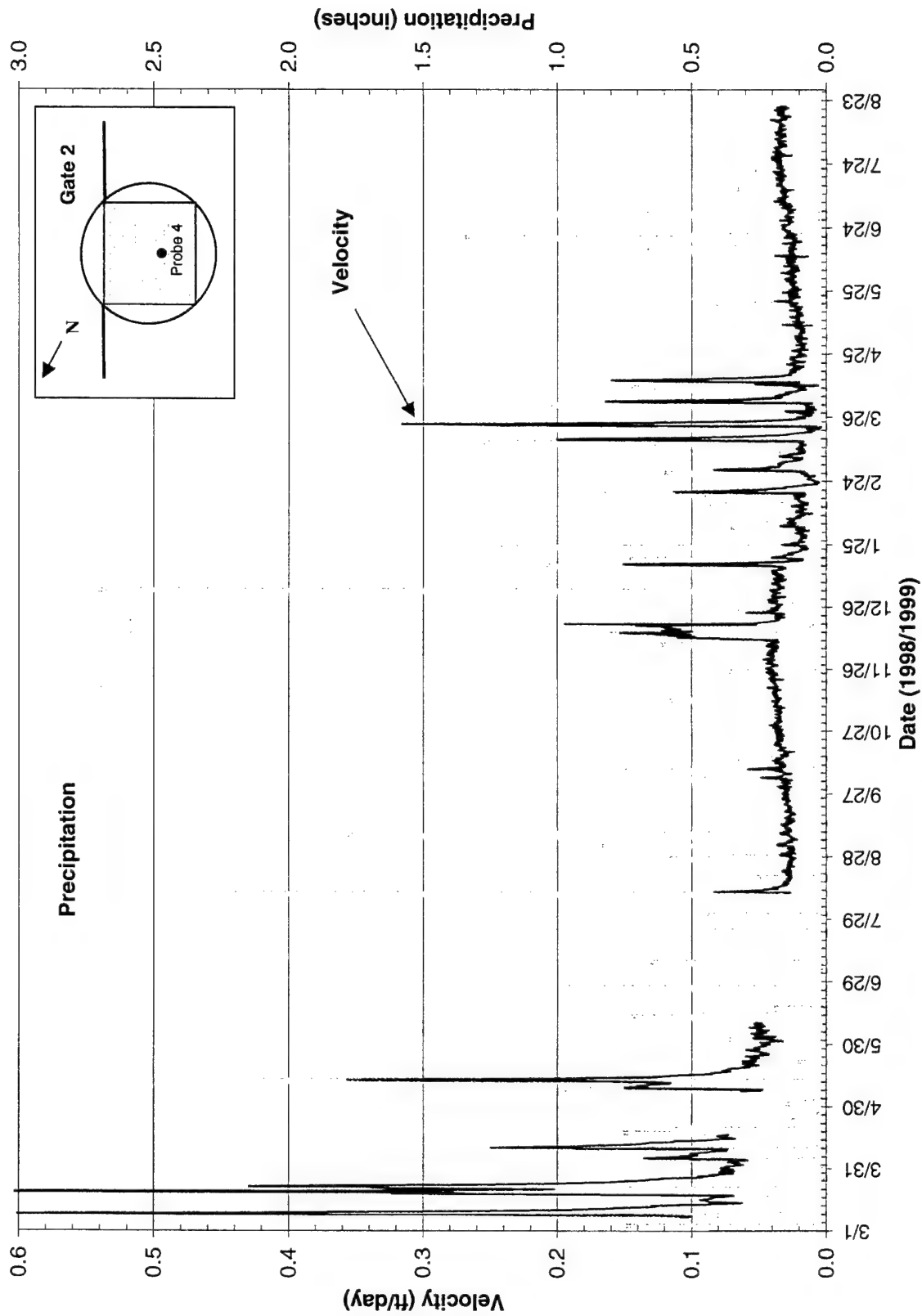


Figure 6-16. Groundwater Flow Velocity in PRB—HydroTechnics Probe 4

Table 6-7. HydroTechnics Probe Measurements in June 1999

Probe	Location	Groundwater Flow Velocity (ft/day)			Residence Time (days)
		Minimum	Maximum	Mode	
1	Upgradient of Gate 1	0.01	0.045	0.04	NA
2	Upgradient of Gate 1	0.05	0.095	0.09	NA
3	Gate 1	0.005	0.075	0.03	133
4	Gate 2	0.01	0.60	0.03	133

surrounding media, because thermal and magnetic effects in iron may interfere with the measurements. This effect can be confirmed by testing the probes under controlled conditions. Additional uncertainty in the probe data may be introduced due to alteration of the surrounding media during installation. The accuracy of the probes also may be affected in low groundwater flow velocity conditions. Finally, the in situ probes represent the velocity in the immediately surrounding media. It is clear that there are zones of very low velocity in the reactive gates, even if the overall velocity through the gate is higher than that represented by the location of the HydroTechnics probes.

6.2 Hydraulic Capture Zone Evaluation

Two major issues are related to capture zone: determining whether or not the reactive barrier is capturing groundwater, and determining the width of the capture zone. Capture zones were evaluated using lithologic characterization, water table maps, continuous groundwater monitoring, and HydroTechnics flow probes in the PRB and in the surrounding aquifer. As shown in Section 6.1, water-level monitoring was the most useful method for demonstrating the capture zone of the PRB, despite the fact that the low aquifer hydraulic gradient and the short distances between wells made the capture zone evaluation more difficult than anticipated.

The evidence for capture and flow into the gates comes from the water-level data presented in Section 6.1.2, as summarized below:

- The gradients become steeper immediately upgradient of the two gates, indicating preferential flow into the two gates. At least at Gate 1, near which more aquifer wells are available for measurement, the gradient through the gate was much steeper than the lateral gradient toward the end of the funnel (Table 6-3).
- The local-scale water-level maps (Figures 6-6, 6-7, and 6-8) clearly show flow lines pointing towards the gates. The flow lines in these figures also show that the capture zones are wider than the gate width. It is expected that the flow lines from the areas upgradient of the funnel wall between the two gates would move towards one or other of the gates, although the flowpaths for water in the center of this zone (at the flow divide) would be longer and slower. The extent of capture upgradient of the two funnel wing walls on either side is more difficult to estimate. The only observation that can be made from the water-level maps is that the capture zone extends several

feet along each wing wall. A reasonable estimate of the total capture zone width based on the water-level maps (Figures 6-6 through 6-8) is probably between 40 to 50 ft (30 ft in front of the middle funnel wall and 5 to 10 ft in front of each wing wall). Furthermore, the capture zone is probably *asymmetric* because the seasonal flow is not always perpendicular to the PRB. The field degradation rates (Section 5) observed at Area 5 support the residence time and groundwater velocity that would result from the volume of water captured in a 40-ft-wide capture zone in the upgradient aquifer.

- The water-level maps (Figures 6-6, 6-7, and 6-8) indicate that flow downgradient of the barrier appears to spread out from the gate, in a direction parallel to the funnel. These observations correlate well with modeling results. The flow lines also indicate that the influence of the PRB on flow directions extends only a few feet (less than 5 to 10 ft) upgradient of the barrier as also indicated by modeling (Figure 6-12). The short distance over which the Area 5 PRB extends its influence on the upgradient flow regime has a bearing on the HydroTechnics flow measurements discussed below.
- Several trends in water levels may be discerned in the gates themselves. Figure 6-17 shows a typical map of water levels within the two gates. As seen on the figure, no clear flowpaths or water-level contours can be drawn, primarily because the small size of the reactive cells makes it difficult to determine trends with any degree of certainty. Additionally, there is likely to be a great deal of mixing in the gates due to sharp conductivity contrasts, making it difficult to find uniform flow lines. An evaluation of water-level data also failed to show any discernible and consistent vertical pattern within the gates.

The four HydroTechnics probes were used to monitor flow directions over an 18-month period. The plots of flow directions over time are shown in Figures 6-18 through 6-21 for Probes 1 through 4, respectively. Probes 1 and 3 show substantial variations over the first few months of monitoring. Then, conditions appear to stabilize in all probes as the flow system reaches steady state. All probes show changes in flow direction after precipitation events. However, the magnitude of fluctuations is greater in the probes located in the reactive cell than those located in the aquifer.

The flow directions in Probes 1 and 2 (Figures 6-18 and 6-19) show an angle of about 200 to 220 degrees relative to north, indicating a south-southwest vector. This direction is similar to the direction of regional groundwater flow as determined from the groundwater measurements. However, the flow vectors do not point toward Gate 1 (which is almost due west). It is possible that the flow direction changes from the regional southwest gradient to the PRB-induced westward gradient only when the water gets very close to the funnel walls. This possibility is also shown in the modeling results (Figure 6-12) where the flow lines seem to bend towards the reactive gates only about 5 ft upgradient of the funnel walls. *From this, it appears that the two aquifer probes are located in a portion of the upgradient aquifer where the flow still follows the regional gradient, rather than the local PRB-induced gradient.* It is therefore difficult to estimate the exact capture zone width from the probe data.

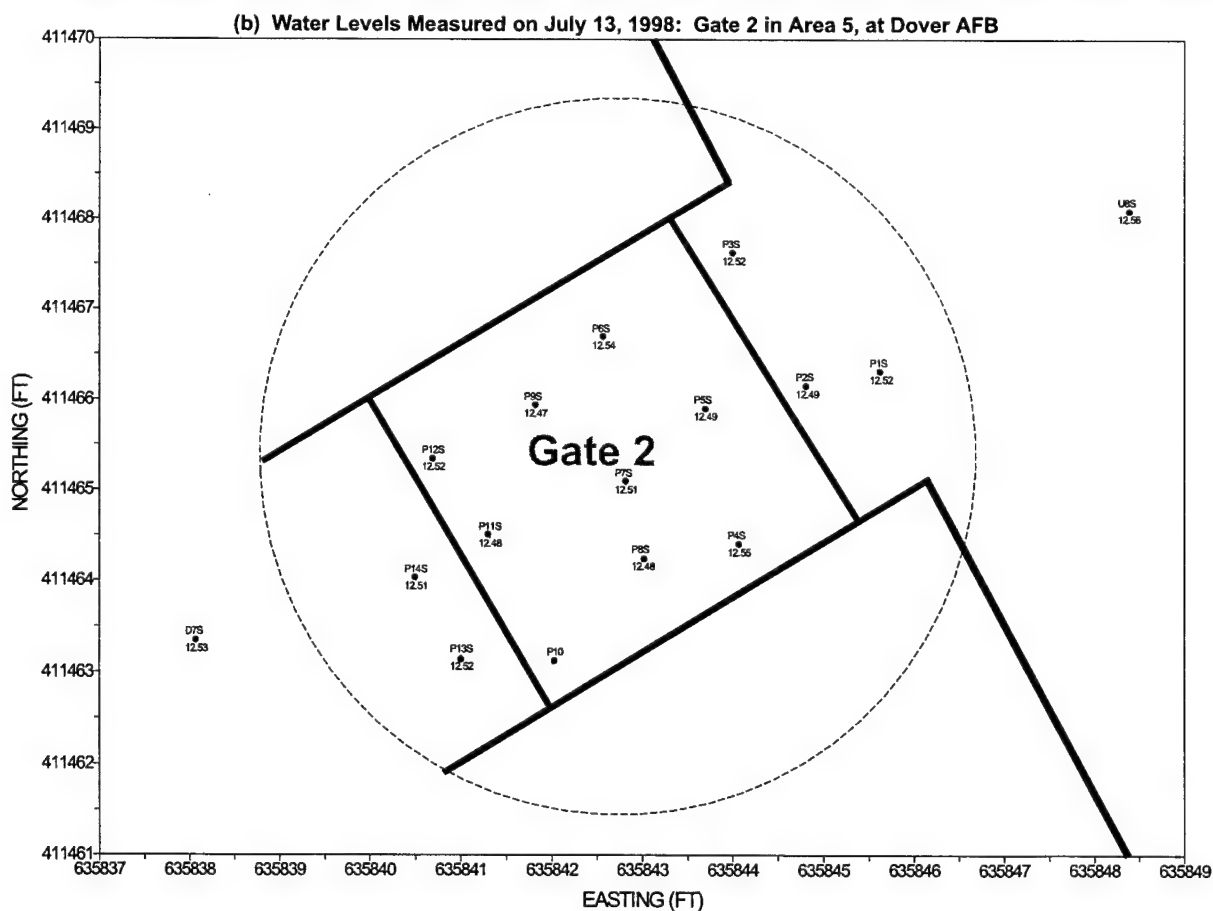
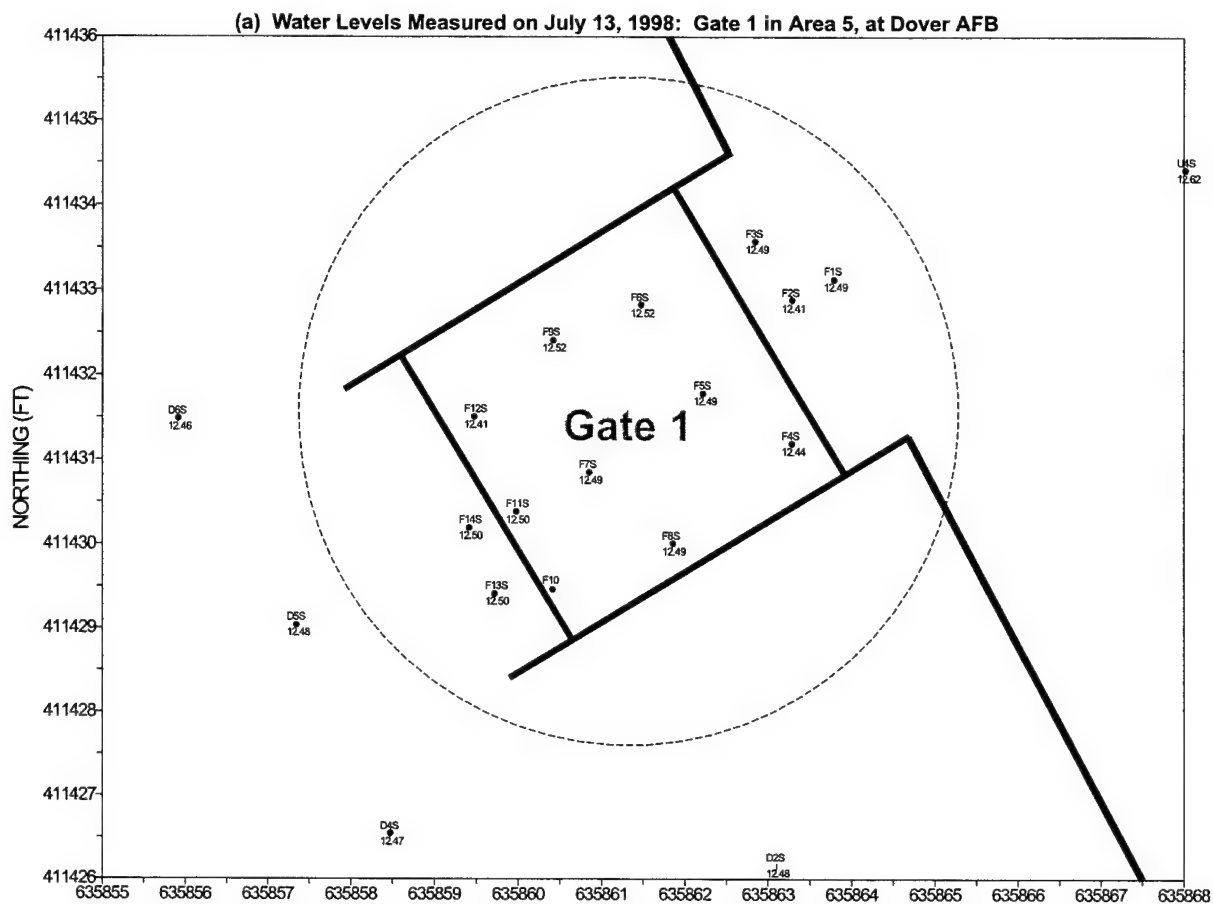


Figure 6-17. Groundwater Levels (ft amsl) near the PRB

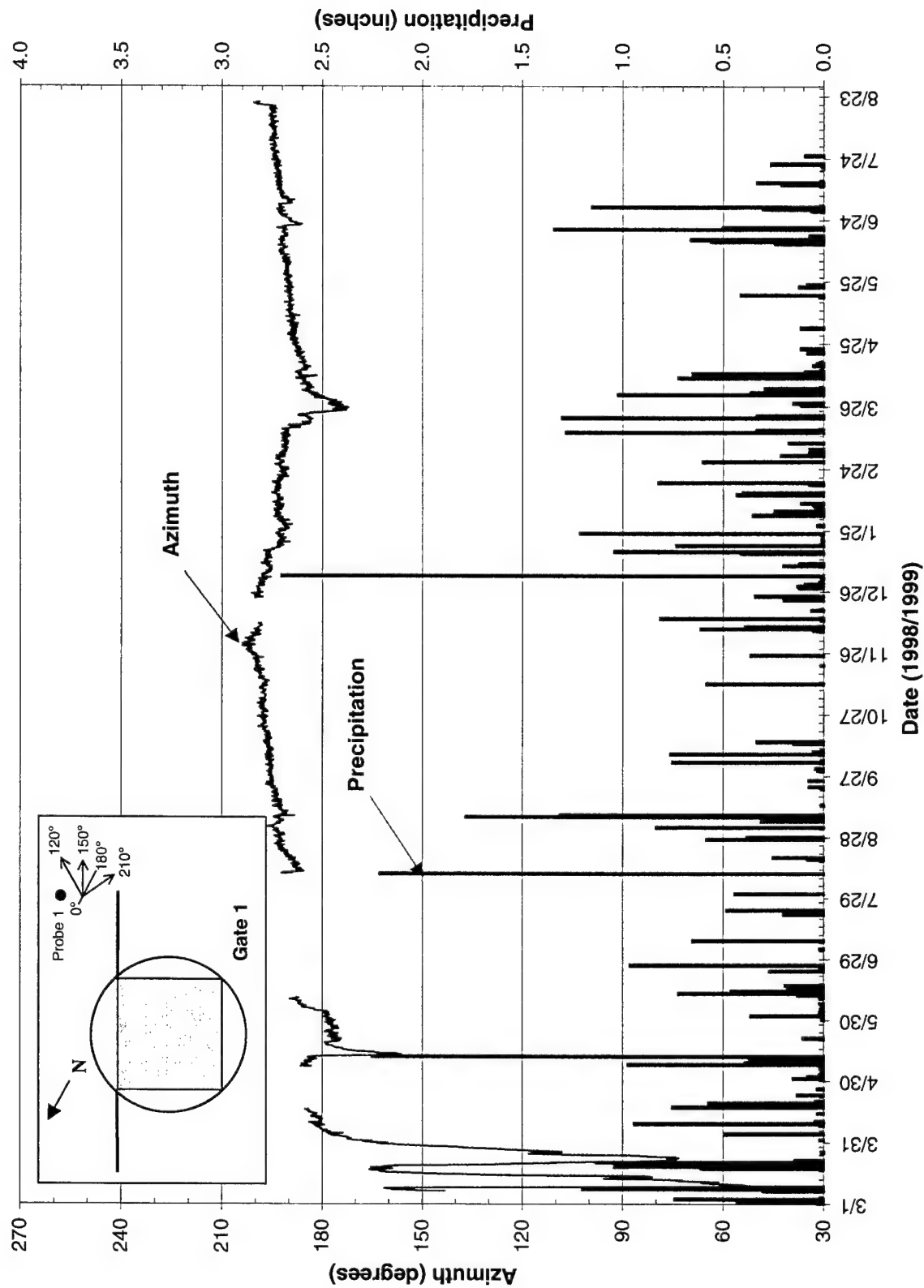


Figure 6-18. Groundwater Flow Direction in PRB—HydroTechnics Probe 1

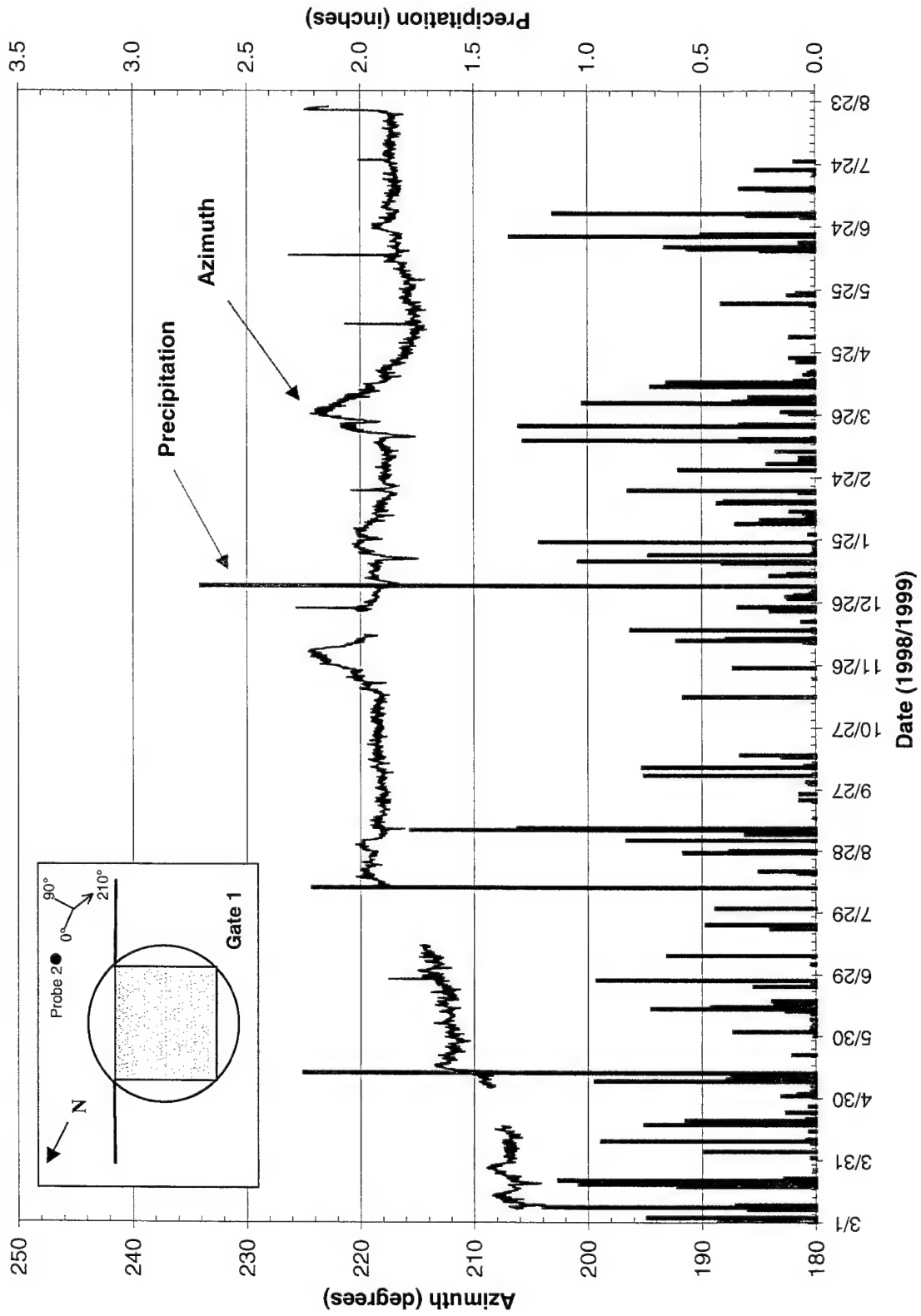


Figure 6-19. Groundwater Flow Direction in PRB—HydroTechnics Probe 2

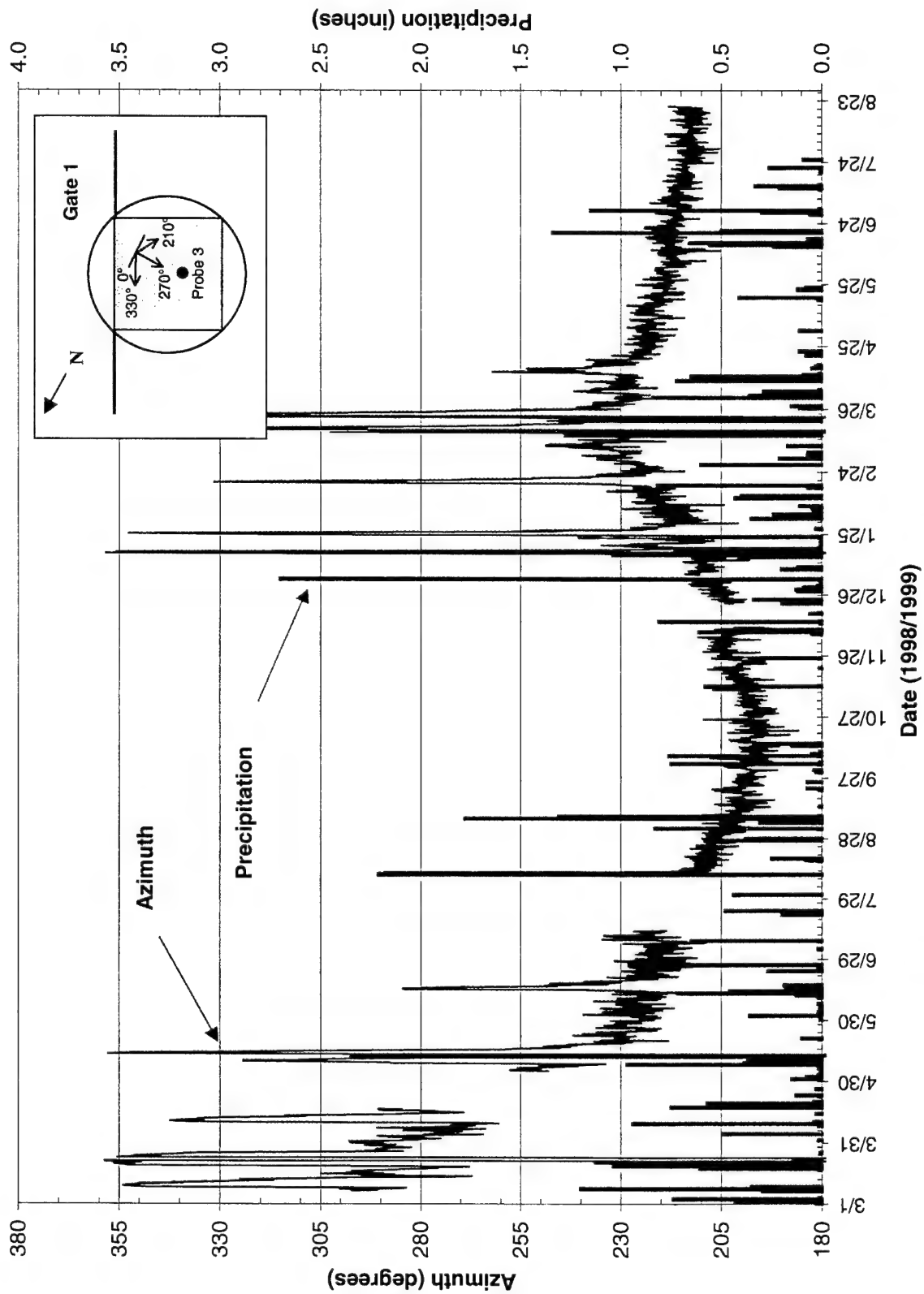


Figure 6-20. Groundwater Flow Direction in PRB—HydroTechnics Probe 3

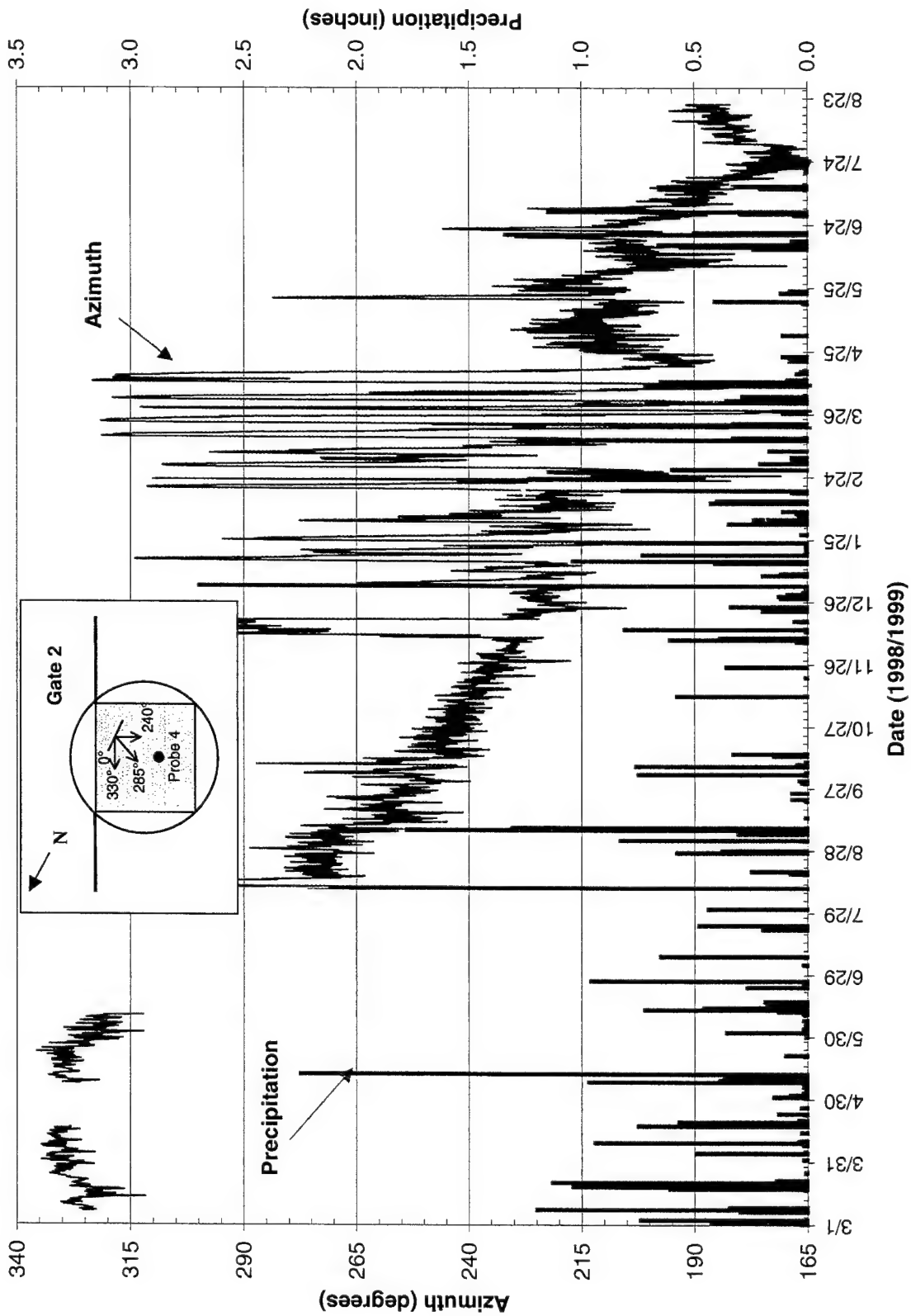


Figure 6-21. Groundwater Flow Direction in PRB—HydroTechnics Probe 4

For Probe 3 in Gate 1, flow directions show large variations in March and April, but gradually stabilize to indicate flow through the barrier (Figure 6-20). For Probe 4 in Gate 2, the directions change from parallel to the barrier to perpendicular to the barrier, indicating flow through the gate once the flow system stabilizes (Figure 6-21). Table 6-8 summarizes flow directions at the end of monitoring as recorded by the HydroTechnics probes.

Table 6-8. Flow Directions Based on HydroTechnics Probe Measurements (June 1999)

Probe	Location	Flow Direction (Azimuth)
1	Upgradient of Gate 1	~200° (southwest)
2	Upgradient of Gate 1	~215° (southwest)
3	Gate 1	~215° (southwest)
4	Gate 2	~190° (southwest)

6.3 Summary of Results and Conclusions

As a result of limitations inherent in the measurements, several uncertainties remain regarding the hydraulic performance of the PRB. The uncertainties relate to estimates of groundwater flow velocities, residence times, and capture zones. First, the low hydraulic gradient at Area 5 was the main reason that made it difficult to determine the hydraulic gradients induced by the PRB. Aquifer heterogeneity and seasonal fluctuations in water levels also led to a degree of variability in flow conditions that made it difficult to isolate consistent trends. However, monitoring information was sufficient to conclude that flow *does* take place through the two gates.

Water-level monitoring showed that seasonal trends in groundwater elevations exist at the PRB site and that the barrier was installed during a period of historically high water levels. Water levels dropped steadily following the installation of the permeable barrier. Water-level monitoring also showed that hydraulic gradients fluctuated with local precipitation events. However, the direction and magnitude of gradients remained fairly consistent throughout Area 5. Near the gate itself, gradients appeared to stabilize over time. Overall, water levels indicated flow through the gate. However, a few flow reversals were observed. In addition, the shallow fine-grained zone may have influenced water levels as the aquifer exhibited semiconfined behavior when water levels were high than the shallow fine-grained zone. Slug testing suggests that hydraulic conductivity varies spatially near the PRB because of lithologic variations. Because the gate materials are more permeable than the surrounding aquifer material, flow will be induced into the gate on both the upgradient and the downgradient sides. When low gradients are present, the conductivity contrast could inhibit flow out of the gate.

The results for groundwater velocity measurements in aquifer by different methods were generally consistent in the aquifer. However, within each reactive gate, the velocity determined through modeling, hydraulic gradients, and HydroTechnics probes showed significant disagreements. The velocity range expected from modeling is about 0.2 to 0.5 ft/day for aquifer K range

of 10 to 25 ft/day with corresponding residence times of 20 to 8 days. This represents about 2 to 3 times increase over aquifer velocity. The velocity ranges based on slug tests in the gates and hydraulic gradients between upgradient to downgradient aquifer wells is 0.46 to 4.1 ft/day (residence times of 9 to 1 days), which is faster than the model-predicted velocity range. The HydroTechnics sensors in the gates show a velocity of 0.03 ft/day and residence times of about 133 days, which is much slower than the model-predicted velocity. The velocity is outside the range of accuracy for the probes and is lower than the ambient aquifer groundwater velocity. Given the uncertainty in measuring the low hydraulic gradient in the reactive gates, it is possible that the actual velocity in the gates is lower than 0.46 ft/day measured in one of the gates. The groundwater velocity range of about 0.4 ft/day also is required for complete degradation of CVOCs entering the reactive gates, as presented in Section 5. This value also is within the range predicted by modeling. This conclusion (velocity ~0.4 ft/day) requires that the observation of lower velocity in the gates measured by the HydroTechnics probes be considered inaccurate because it was below the instrument range.

Capture zones were outlined by using modeling, water levels, and HydroTechnics probes. Again, the low gradient made it difficult to detect capture zones. However, several water table maps do demonstrate capture zones similar to the modeling predictions. Overall, the PRB capture zone was located upgradient of the barrier and was about 40 to 50 ft wide. The shape of the capture zone is probably asymmetric because the seasonal groundwater flow was not always perpendicular to the PRB during the period of monitoring.

Overall, the following conclusions and recommendations can be made regarding the PRB hydraulics:

- ❑ The groundwater flows through the gates as indicated by the hydraulic gradient and conductivity-based assessment (Darcy's law) and the observation that gradients through the reactive gates are stronger than gradients along the funnel wall. Furthermore, flow through the gates is supported by the inorganic geochemical signature in the downgradient aquifer wells (see Section 7).
- ❑ There is significant uncertainty in the exact flow velocity and capture zone estimates due to heterogeneity and hydraulic gradient uncertainty.
- ❑ There is a significant difference in velocity estimates in the two gates. This difference may be due to differential settling and compaction of the reactive media and sand in the gates. There were also transient periods of slight negative gradient in the exit zone which indicate periods of backflow or stagnation. However, there are no indications of complete backflow because the gradient from upgradient aquifer into the reactive gates is much stronger than the transient negative gradient in the exit zones. The negative gradients may reflect the difficulty in movement of water from high conductivity exit zone sand to lower conductivity aquifer. The negative gradient also may be due to uncertainty in groundwater measurements over short distances.

- HydroTechnics probes showed a good match with the estimated velocity and regional flow directions in the aquifer upgradient of the PRB. Within the gates they showed that the groundwater is flowing through the gates in the expected directions. The magnitude of the velocity in the gates, however, was much smaller than expected. This difference may be real because the probes represent only a localized point velocity rather than the overall velocity from upgradient to downgradient of the gates. The difference could also be due to the thermal or magnetic interference from the iron particles.
- The HydroTechnics probes and the water-level measurements indicate that the effects of capture zone on flow lines do not extend more than a few feet upgradient of the PRBs. Therefore, for future investigations, the monitoring wells and velocity probes should be placed as close as physically possible to the reactive cells and funnel walls.
- The uncertainty in hydraulic assessments may be reduced by evaluating larger full-scale systems or sites with higher hydraulic gradients. Such sites would allow determination of the hydraulic effects beyond the method uncertainty (measurement error) for water-level measurements.
- The uncertainty in the use of HydroTechnics probes and other velocity measurement methods should be tested further by comparing the various direct and indirect velocity measurement methods under controlled conditions.
- Detailed tracer tests may be conducted in the reactive cells or upgradient aquifers to more accurately determine the horizontal and vertical flow patterns. This may be useful, especially because the groundwater can take a rather circuitous path in the cells resulting in longer residence times than those estimated from water-level measurements alone. Conversely, the residence times may be much shorter if preferential pathways are present. These aspects can only be examined through detailed tracer testing with continuous monitoring probes (e.g., the tracer test conducted at the former NAS Moffett Field permeable barrier [Battelle, 1998]).

7. Geochemical Performance Assessment

Geochemical parameters are native groundwater constituents that interact with the reactive medium in a PRB. These interactions are important because they can create conditions that may aid or detract from the reactive and hydraulic performance of the PRB. Parameters of primary concern are DO, alkalinity, sulfate (which can be reduced to sulfide), and polyvalent cations. These species can form precipitates that may occupy pore spaces or deposit on the reactive surfaces of the reactive medium. Over long periods of time, such precipitates have the potential to reduce the reactivity and/or impair the hydraulic performance of a PRB. At the Area 5 site, geochemical information was collected through:

- ❑ On-site field parameter measurements
- ❑ Inorganic chemical analysis of groundwater samples
- ❑ Analysis of iron core samples for evidence of chemical and mineralogical changes
- ❑ Analysis of iron core and aquifer soil samples for signs of any unusual microbial activity.

These data were collected primarily during two comprehensive groundwater monitoring events conducted in July 1998 and June 1999, at the same time that samples were collected for VOC analysis. Core samples of the iron and the aquifer were collected only in June 1999. Between October 1998 to April 1999, field parameter measurements were conducted in select wells to verify that the geochemical profiles in the gates were stabilizing. Geochemical data also were used to evaluate any differences in the interaction of the two different reactive media in the PTZs of the two gates.

Appendix F contains the detailed geochemical data collected during the 18 months of PRB operation and summarized for discussion in this section. Appendix G contains the associated QA analysis, which shows that valid data were obtained from all the samples and measurements collected.

7.1 Results of Field Parameter Measurements

Field parameter measurements include pH, ORP, DO, and temperature. Table F-2 (see Appendix F) contains results of the two comprehensive monitoring events. Field parameter measurements were taken simultaneously using a YSI 6820 meter connected to a flowthrough cell. Field parameters were measured while the monitoring wells were micro-purged; values were recorded either after instrument readings had stabilized in aquifer wells, or after the prescribed micropurge volume of water had been withdrawn from wells within or adjacent to the PRB. With the exception of temperature, these measurements are a good representation of downhole water quality

conditions. The recorded temperature may be different from that of the groundwater, because of the difference in temperature between the aquifer and the ambient air.

Figures F-1 to F-3 in Appendix F show the detailed spatial distributions of pH, redox potential (Eh), and DO, respectively, in the two gates and in their immediate vicinity during the two comprehensive monitoring events. These figures illustrate the impact of the different gate media on groundwater field parameters. Typical results of the field parameter measurements are presented in Table 7-1, which is based on the data from the most recent (June 1999) monitoring event. Trends in field parameters appear to be better established in June 1999 (after 18 months of PRB operation) than in July 1998. To illustrate some important trends, the data presented in Table 7-1 are limited to shallow (S) and deep (D) sampling levels in wells located near the centerline through the two gates. These wells represent the geochemical characteristics in the two gates along the groundwater flow direction.

Table 7-1. Results of Field Parameter Measurements from the June 1999 Sampling Event for Wells Along the Flowpath Through the Gates

Well ID	pH	Eh (mV)	DO (mg/L)
<i>Gate 1 Vicinity Upgradient Wells</i>			
U4S	5.07	595.8	4.15
U4D	4.59	618.4	6.01
<i>Gate 1 Pretreatment Zone Wells</i>			
F1S	10.35	-18.3	< 0.50
F2S	10.44	-85.5	< 0.50
F2D	10.35	-39.8	< 0.50
<i>Gate 1 Reactive Cell Wells</i>			
F5S	10.82	-85.7	< 0.50
F5D	10.79	-90.1	< 0.50
F7S	10.77	-479.9	< 0.50
F7D	10.59	-388.2	< 0.50
F11S	10.88	-453.7	< 0.50
F11D	10.80	-427.6	< 0.50
<i>Gate 1 Exit Zone Wells</i>			
F14S	10.62	-58.3	< 0.50
F14D	10.71	-77.4	< 0.50
<i>Gate 1 Downgradient Aquifer Wells</i>			
D5S	5.20	649.8	2.99
D5D	5.77	402.1	1.15

Well ID	pH	Eh (mV)	DO (mg/L)
<i>Gate 2 Upgradient Aquifer Wells</i>			
U8S	5.67	643.1	5.00
U8D	5.74	508.8	4.02
<i>Gate 2 Pretreatment Zone Wells</i>			
P1S	3.88	553.4	3.27
P2S	11.19	-84.6	< 0.50
P2D	7.59	-206.9	< 0.50
<i>Gate 2 Reactive Cell Wells</i>			
P5S	11.63	-414.3	< 0.50
P5D	9.09	-382.8	< 0.50
P7S	11.38	-72.4	< 0.50
P7D	10.44	-281.6	< 0.50
P11S	10.80	-393.6	< 0.50
P11D	10.93	-367.0	< 0.50
<i>Gate 2 Exit Zone Wells</i>			
P14S	10.63	-44.1	< 0.50
P14D	10.38	91.9	< 0.50
<i>Gate 2 Downgradient Aquifer Wells</i>			
D7S	10.00	-17.8	2.96
D7D	9.48	71.5	2.99

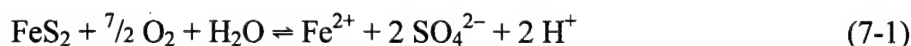
7.1.1 pH Measurements

Groundwater in aquifer wells upgradient of the PRB is generally acidic, with pH values ranging from approximately 4.4 to 5.5 in the vicinity of Gate 1 and approximately 4.6 to 6.3 in the vicinity of Gate 2 (see Table F-1). An absence of buffering minerals in the sandy phreatic aquifer

fer apparently allows the groundwater to maintain its acidity indefinitely. Slightly higher pH values upgradient of Gate 2 could be related to elevated alkalinity, which may have originated from construction activities (see discussion on alkalinity in Section 7.2).

Within the Gate 1 PTZ (10% iron by volume), pH increases abruptly to values similar to those within the reactive cell (100% iron). Average pH values in Gate 1 PTZ wells were 10.34 in July 1998, and 10.33 in June 1999 (six measurements). Similarly, within the Gate 2 PTZ, the average pH value was 10.49 in July 1998 (ten measurements). However, in June 1999, the average pH value in the Gate 2 PTZ decreased to 8.69 (six measurements). The difference between Gate 1 and Gate 2 was especially pronounced in the first PTZ well, where the pH of F1S was 10.35 and P1S was 3.88 in June 1999. During the partial sampling events between October 1998 and April 1999, P1S showed a lower pH in other PTZ or reactive cell wells. In one additional partial sampling event conducted in August 1999, the pH of F1S was 10.35 and P1S was 2.43, the lowest pH value detected during this study.

A decline in pH within the pyrite-filled PTZ was as anticipated, and is due to a reaction between pyrite and DO that produces sulfuric acid. The reaction is the same as one that occurs when oxygenated groundwater flows through sulfidic ore deposits, creating the situation of acid mine drainage. The following chemical equation shows that 2 moles of hydrogen ion are produced for each mole of pyrite that reacts with oxygenated water:



Assuming that the DO level of groundwater entering Gate 2 is 5 mg/L and the pH is 5.7 (see Table 7-1), and that the reaction with pyrite proceeds stoichiometrically until DO is quantitatively removed, the resulting (calculated) pH would be 4.04. If DO were slightly higher, for example 6 mg/L, then the calculated pH would be 3.97. Thus, the pH of 3.88 in well P1S (Table 7-1) is only slightly lower than the pH predicted based on the reaction of pyrite and DO. Of course, more acid would be produced if the groundwater were continually recharged with oxygen, which may well happen in an unconfined aquifer. However, in actual site groundwater, competing reactions could change the net abundance of aqueous species, such that the actual pH could be somewhat different than predicted in this example. Calculations based on real groundwater compositions and which account for the effects of competing reactions are discussed in the section on geochemical modeling (see Section 7.4).

The time trend in pH for select wells in the upgradient aquifer and PTZs is presented in Table 7-2 and illustrated in Figures 7-1 to 7-3. It can be observed that, except for one anomalous value in well U4S in February 1999, pH values were quite consistent in each well in the upgradient aquifer and in Gate 1. Stability in the pH of the aquifer is expected, due to the absence of geochemical mechanisms that would affect pH. In the Gate 1 PTZ, pH is undoubtedly controlled by reaction of the groundwater with iron. In marked contrast, pH in the Gate 2 PTZ decreased steadily over time, with P1S, the first well in the PTZ, declining more than 6 pH units during the 18 months of operation. Wells P2S and P2D, which lie further downgradient in the Gate 2 PTZ, displayed similar trends, but did not become as acidic as P1S.

Table 7-2. pH Measurements in Selected Wells at Several Sampling Intervals

Well ID	Jul-98	Aug-98	Dec-98	Feb-99	Apr-99	Jun-99	Aug-99
<i>Aquifer Wells</i>							
U4S	5.52	NA	5.12	6.37	5.3	5.07	NA
U4D	4.69	NA	4.75	4.83	4.72	4.59	NA
U8S	6.07	NA	5.90	5.86	5.67	5.67	NA
U8D	6.12	NA	6.00	6.04	5.88	5.74	NA
<i>Gate 1 Pretreatment Zone Wells</i>							
F1S	10.33	NA	10.71	NA	NA	10.35	NA
F2S	10.35	NA	NA	NA	NA	10.44	NA
F2D	10.18	NA	NA	NA	NA	10.35	NA
<i>Gate 2 Pretreatment Zone Wells</i>							
P1S	7.98	8.78	9.18	NA	NA	3.88	2.43
P2S	11.39	11.52	NA	NA	NA	11.19	5.17
P2D	10.72	10.60	NA	NA	NA	7.59	7.38

NA = Not available, because a measurement was not taken.

There are two apparent inconsistencies in the pH behavior in the 10% pyrite-filled PTZ that merit explanation. First, the lowest pH values were steadfastly measured at P1S, while higher pH values were measured in the P2 and P3 well clusters, which are approximately 1 ft down-gradient of P1S. According to Equation 7-1, pH should decline as long as DO is present. After

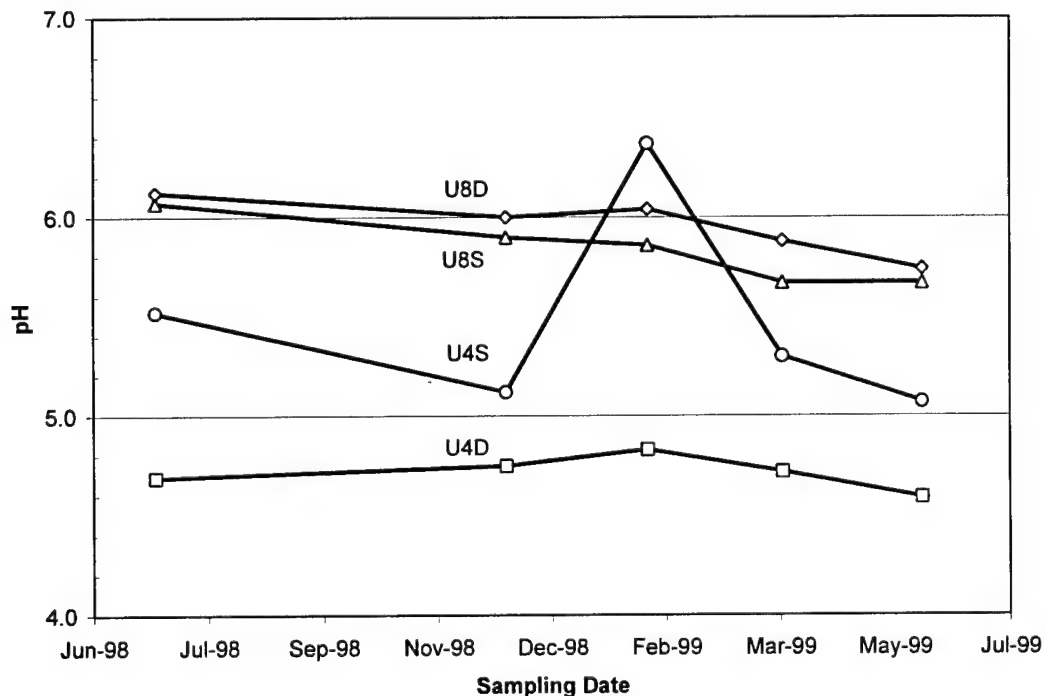


Figure 7-1. pH of Selected Upgradient Aquifer Wells at Different Sampling Events

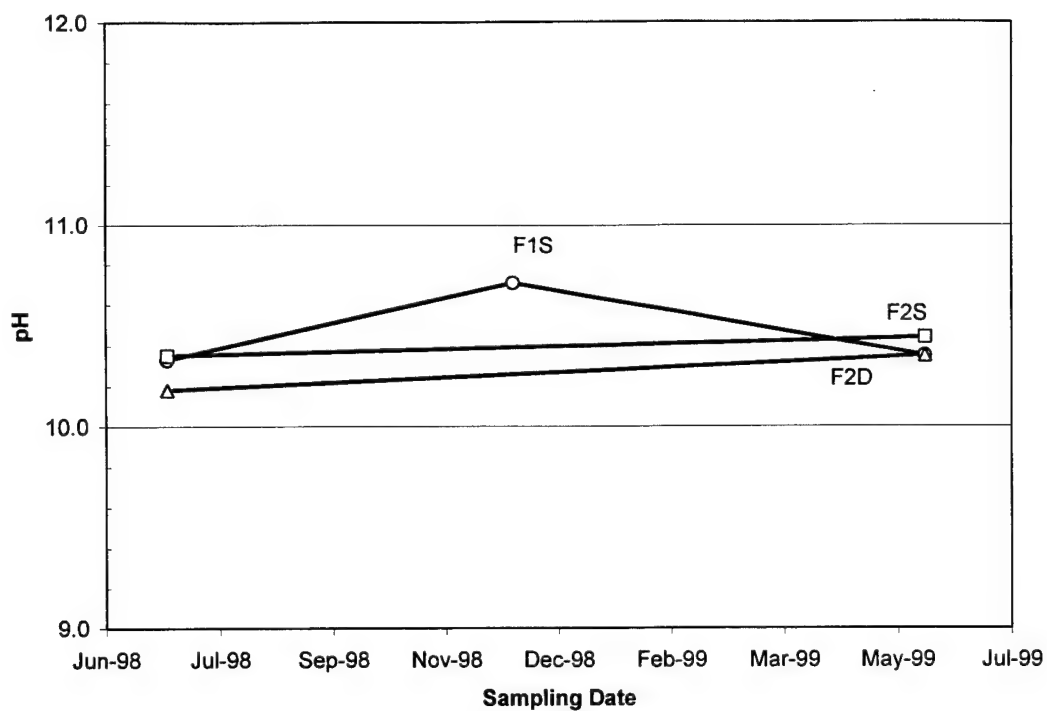


Figure 7-2. pH of Selected Gate 1 Wells at Different Sampling Events

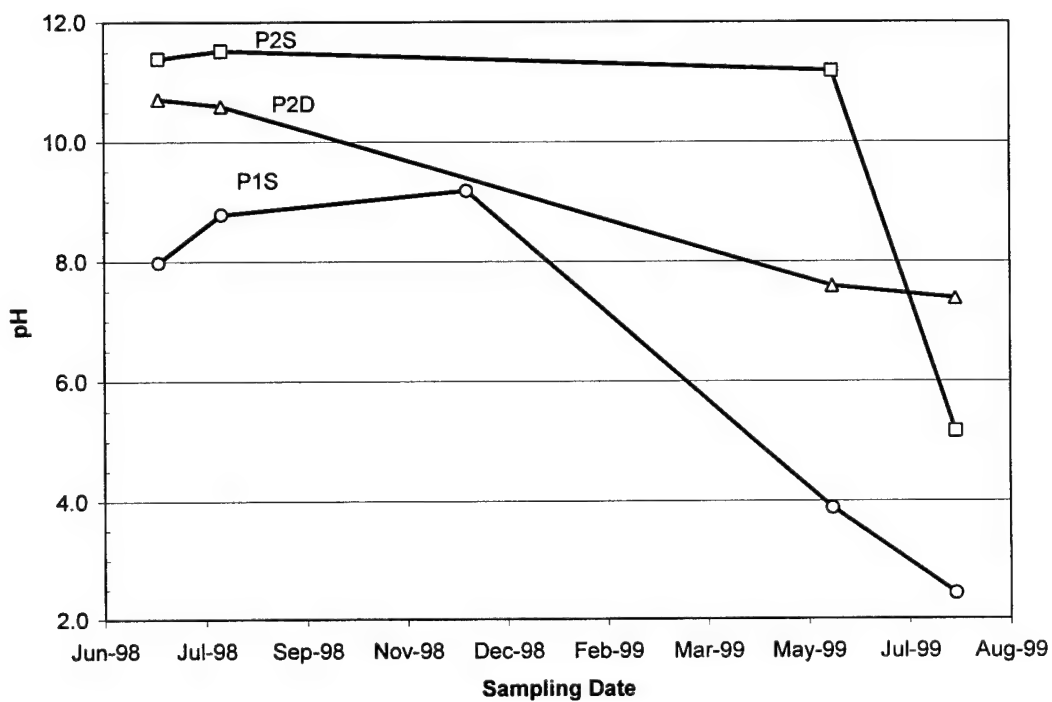


Figure 7-3. pH of Selected Gate 2 Wells at Different Sampling Events

the DO is exhausted, pH should remain constant (in the absence of other reactions). Therefore, pH in the downgradient PTZ wells should be the same or even lower (because some DO still remains in the groundwater) than the upgradient P1S well. (Note that it is not energetically feasible for Equation 7-1 to reverse direction [i.e., pyrite cannot reprecipitate spontaneously]). Second, the groundwater in P2 and P3 well clusters is not quite as acidic as predicted by Equation 7-1; the pH should be at least 4, but could be considerably lower if atmospheric oxygen were able to diffuse into the PTZ. However, the majority of measurements taken in P2 and P3 over the entire study period are actually alkaline, rather than acidic.

Possible explanations for these apparent inconsistencies are that either (1) there has been some mixing of water constituents from the PTZ and reactive cell (which is at a much higher pH) or (2) there was some infiltration of the iron from the reactive cell into the PTZ during construction. The latter explanation is supported by the core sampling and evaluation (see Section 7.5). Granular iron was discovered in the core collected from shallow depths in the Gate 2 PTZ. PTZ wells P2 and P3 lie just 6 inches from the boundary between the PTZ and the reactive cell. Mixing would have the effect of averaging the true pH of the PTZ water (approximately between 2 and 4) with reactive cell water that is typically above a pH of 11 (see Table 7-2). This explanation also shows how the downgradient wells in the PTZ can have higher pH than the upgradient PTZ well. Mixing in the PTZs may be facilitated by periods of relatively low flow velocities, which allow diffusion and possibly density-driven flow to become important mechanisms. Transient backflow of water from the reactive cell could possibly have facilitated mixing. Transient backflow conditions are possible, as discussed in Section 6, particularly after rainfall events, due to uneven aquifer recharging from any cracks in the asphalt ground surface. Similar transient conditions are possible in the Gate 1 PTZ also; however, the 10% iron has already raised the pH in the PTZ to levels similar to those in the reactive cell.

The pH is relatively high in all reactive cell wells in both gates (see Table 7-1 and Figure F-1 in Appendix F). The average pH value for the reactive cell in Gate 1 was 10.62 in July 1998, and 10.71 in June 1999 (20 measurements). The corresponding average pH in the Gate 2 reactive cell was 10.99 and 10.81, respectively (24 measurements). Therefore, the different compositions of the two PTZs (10% iron in Gate 1 vs. 10% pyrite in Gate 2) does not seem to have had a lasting effect on pH within the respective reactive cells (both 100% iron). On the other hand, within the two PTZs, the pH transition from that in the native aquifer to that in the reactive cell exhibits different characteristics.

In the exit zones (100% sand), both gates exhibit pH values that are similar to those inside the reactive cells: values range between pH 10 and 11. The pH values in the aquifer regions immediately downgradient from the two gates differ measurably. Downgradient of Gate 1, wells D5S and D5D vary in pH between 5 and 6, and downgradient of Gate 2, wells D7S and D7D vary in pH between 9.4 and 10. These data suggest better mixing of groundwater flowing through and around the PRB in the downgradient vicinity of Gate 1. Further downgradient from both gates, the aquifer pH is expected to return to native conditions.

7.1.2 Oxidation-Reduction Potential

Table 7-1 shows that Eh is generally positive in the upgradient and downgradient aquifer wells and negative in the reactive cells (see Figure F-2, in Appendix F). In the upgradient aquifer, Eh values are between approximately 200 and 600 millivolts (mV), and indicate moderately oxidizing conditions. A decrease in the oxidation-reduction (redox) potential to much lower Eh values is expected in the reactive cells, due to chemical reactions between the groundwater and highly reducing zero-valent iron. Eh measurements in the reactive cell of both gates ranged between approximately zero and -500 mV. The range of values is similar in both reactive cells. These results indicate that the different reactive media used in the PTZs did not affect redox potential inside the reactive cells.

There is some difference in redox behavior inside the two PTZs. Redox conditions in the Gate 1 PTZ (iron/sand) are similar to conditions in the reactive cell (100% iron). In Gate 2 (pyrite/sand), Eh in the first PTZ well, P1S, increases almost linearly from approximately -100 mV to +750 mV over the study period (see Figure 7-4). The rise in Eh in well P1S may be caused by increased flow of oxygenated groundwater into the PTZ. Note that the DO level in well P1S was 3.27 mg/L in June 1999 (see Table 7-1) vs. <0.5 mg/L in July 1998. Thus, at certain times, Eh (and DO) may become elevated in the upgradient portion of the PTZ. However, reducing conditions were always maintained in the second row of PTZ wells, thus assuring that water entering the reactive cell was free of oxygen. These results indicate that the rate of reaction between 10% pyrite and DO is sufficiently high, and the PTZ is sufficiently thick, to scrub oxygen from the groundwater before it enters the reactive cell.

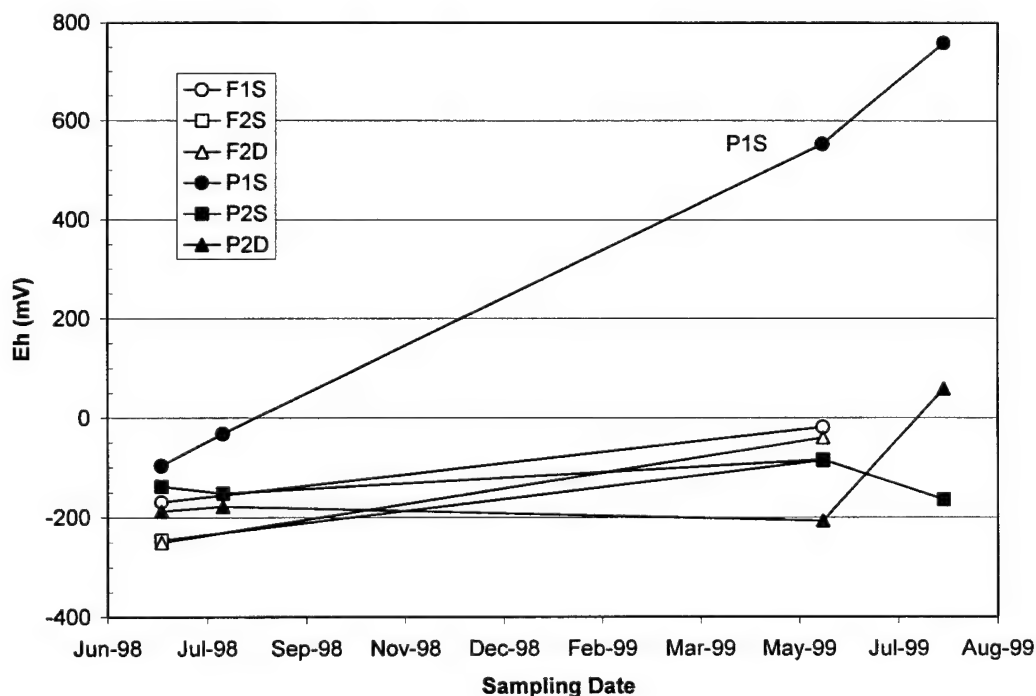


Figure 7-4. Eh in Selected PTZ Wells at Different Sampling Events

7.1.3 Dissolved Oxygen Measurements

Data presented in Table 7-3 show that DO concentrations in the upgradient aquifer tended to be higher near Gate 1 and lower near Gate 2 (see Figure F-3). In July 1998, average DO was 3.90 mg/L in Gate 1 and 1.06 in Gate 2. DO levels increased in all upgradient aquifer wells in June 1999; the average DO was 5.95 mg/L upgradient of Gate 1 and 4.20 mg/L upgradient of Gate 2. Figure 7-5 shows DO levels in aquifer wells that are upgradient of the gates at different sampling events. Higher DO levels over time may be due to aquifer recharge by oxygenated surface water. In general, different DO levels in the aquifer near Gate 1 and Gate 2 imply that either the recharge path is different for the two regions, or that oxygen is consumed at a faster rate by some process within the aquifer (abiotic or biotic) near Gate 2.

Table 7-3. Results of DO Measurements (mg/L) in Wells Along the Flowpath Through the Gates During Different Sampling Events

Well ID	Jul 98	Apr 99	Jun 99
Gate 1 Upgradient Wells			
U4S	2.14	4.92	4.15
U4D	5.32	5.90	6.01
Gate 1 Pretreatment Zone Wells			
F1S	<0.50	NA	<0.50
F2S	<0.50	NA	<0.50
F2D	<0.50	NA	<0.50
Gate 1 Reactive Cell Wells			
F5S	<0.50	NA	<0.50
F5D	<0.50	NA	<0.50
F7S	<0.50	NA	<0.50
F7D	<0.50	NA	<0.50
F11S	<0.50	NA	<0.50
F11D	0.50	NA	<0.50
Gate 1 Exit Zone Wells			
F14S	<0.50	NA	<0.50
F14D	0.89	NA	<0.50
Gate 1 Downgradient Aquifer Wells			
D5S	1.71	NA	2.99
D5D	0.60	NA	1.15

Well ID	Jul 98	Aug 98	Apr 99	Jun 99	Aug 99
Gate 2 Upgradient Aquifer Wells					
U8S	<0.50	NA	0.96	5.00	NA
U8D	0.92	NA	0.50	4.02	NA
Gate 2 Pretreatment Zone Wells					
P1S	<0.50	<0.50	NA	3.27	0.66
P2S	<0.50	<0.50	NA	<0.50	<0.50
P2D	<0.50	0.50	NA	<0.50	<0.50
Gate 2 Reactive Cell Wells					
P5S	<0.50	NA	NA	<0.50	NA
P5D	<0.50	NA	NA	<0.50	NA
P7S	<0.50	NA	NA	<0.50	NA
P7D	<0.50	NA	NA	<0.50	NA
P11S	<0.50	NA	NA	<0.50	NA
P11D	<0.50	NA	NA	0.90	NA
Gate 2 Exit Zone Wells					
P14S	<0.50	NA	NA	<0.50	NA
P14D	<0.50	NA	NA	<0.50	NA
Gate 2 Downgradient Aquifer Wells					
D7S	<0.50	NA	NA	2.96	NA
D7D	<0.50	NA	NA	2.99	NA

Table 7-3 shows that DO is below detection (<0.5 mg/L) in both PTZs. Only well P1S showed detectable levels of DO in June and August 1999. The table also shows that DO is below detection in both reactive cells and exit zones. These results indicate that DO was effectively scrubbed by both pretreatment media, perhaps more efficiently by the 10% iron than the 10% pyrite. The PTZs in both gates succeeded in protecting the reactive cells from the rapid corrosion and precipitation that is observed in the upgradient end of 100% iron reactive cells. This indicates that incorporating a PTZ before the reactive cell may improve the longevity of the iron in the reactive cell. Because the objective of using lower proportions (10%) of the reactive media was to slow down the

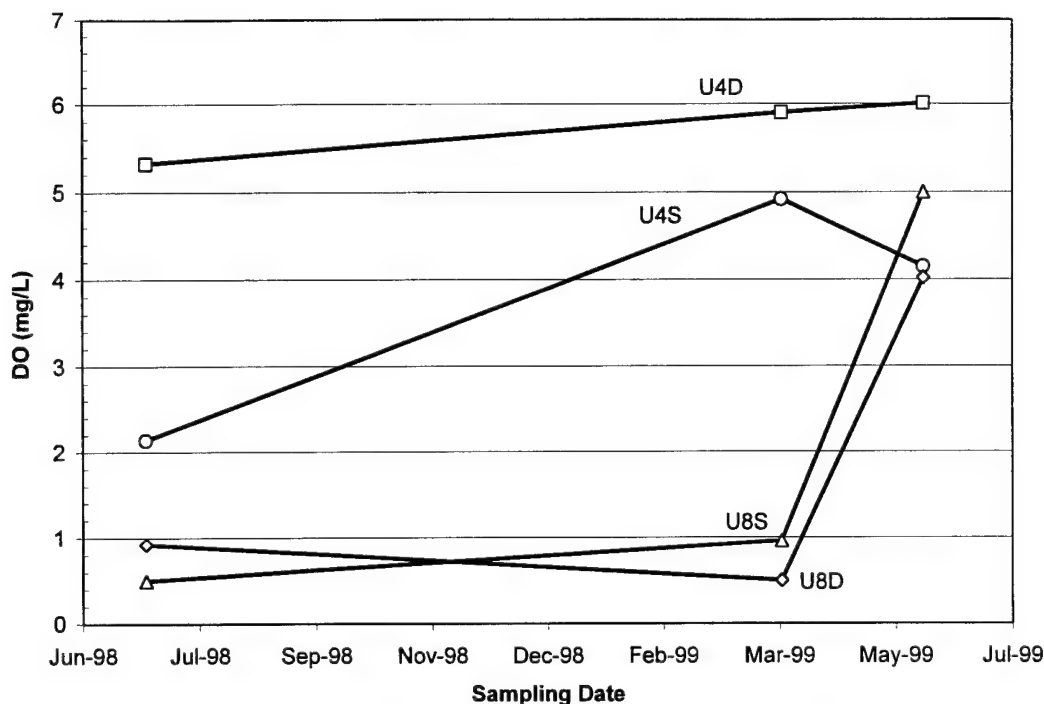


Figure 7-5. DO in Selected Upgradient Aquifer Wells at Different Sampling Events

DO-iron or DO-pyrite reactions so that the precipitates are spread over a larger volume, at least in the Gate 1 PTZ, a still lower proportion (for example, 5%) could have been used.

7.2 Results of Other Inorganic Chemical Measurements

Table F-3 in Appendix F contains a summary of results for inorganic chemical measurements for groundwater samples collected during the two comprehensive monitoring events. For convenience, Table 7-4 lists selected results of inorganic constituents. These results are illustrative of those obtained over a wider sampling region (see Table F-3). Groundwater samples were taken after the monitoring wells were micro-purged and field parameters had stabilized.

Groundwater in the Area 5 aquifer contains a relatively low concentration of dissolved matter. Total dissolved solids (TDS) in the upgradient groundwater range from 100 to 300 mg/L. The predominant constituents in the aquifer groundwater include calcium (Ca), chloride (Cl^-), magnesium (Mg), nitrate (NO_3^-), silica (SiO_2), sodium (Na), and sulfate (SO_4^{2-}). On a molar basis, sodium is the dominant cation, followed by magnesium and calcium. Chloride is the dominant anion, followed by sulfate. As a result of the low groundwater pH, alkalinity is very low and the major species is carbonic acid. Nitrate concentrations are highly variable in the aquifer wells, possibly as a result of fertilizer usage in the grassy strip as well as runoff onto the parking lot. In addition to nitrate, concentrations of most other major species show unusually high variations. It is possible that some of this variability results from salts entering the groundwater through complex pathways provided by the asphalt parking lot.

Table 7-4. Selected Results of Inorganic Chemical Analysis

Well ID	Alkalinity		Calcium		Chloride		Iron		Magnesium	
	Jul 98	Jun 99	Jul 98	Jun 99	Jul 98	Jun 99	Jul 98	Jun 99	Jul 98	Jun 99
<i>Gate 1 Upgradient Aquifer Wells</i>										
U4S	13	6	16.4	5.5	39	37	U	U	14.5	7.1
U4D	4	U	4.9	3.5	20	19	U	U	4.8	4.2
<i>Gate 1 Pretreatment Zone Wells</i>										
F1S	32	26	8.9	3.1	11	4.5	0.04	U	U	U
F2S	34	27	6	3.8	18	2.4	U	U	U	U
F2D	46	33	3.43	3.4	21	16	0.05	0.08	0.48	U
<i>Gate 1 Reactive Cell Wells</i>										
F5S	37	38	12.2	6.6	19	1.6	0.04	U	U	U
F5D	29	34	5.2	4.4	24	19	U	U	U	U
F7S	41	44	12.2	6.9	22	3.1	0.06	U	U	U
F7D	35	36	7.5	4.1	25	18	0.07	U	U	U
F11S	54	52	6	4	28	9.6	0.07	U	U	U
F11D	53	50	10.3	4.4	24	9.2	U	U	U	U
<i>Gate 1 Exit Zone Wells</i>										
F14S	58	41	4.56	6.4	13	8.4	0.11	U	U	U
F14D	36	47	6	5.3	26	9.6	U	U	U	U
<i>Gate 1 Downgradient Aquifer Wells</i>										
D5S	13	8	47.1	0.92	30	8.9	0.04	0.3	20.3	0.71
D5D	28	22	6.2	4.6	43	19	0.22	U	1.16	3.1
<i>Gate 2 Upgradient Aquifer Wells</i>										
U8S	30	8	21.3	21	59	61	0.05	0.08	8.7	15
U8D	54	38	9.2	6.8	26	24	0.04	U	4.99	5.2
<i>Gate 2 Pretreatment Zone Wells</i>										
P1S	59	U	31.1	40	41	6.3	0.49	32	4.61	3.6
P2S	180	96	44.3	48	27	6.9	0.18	U	U	U
P2D	42	32	8.9	40	18	8.9	U	16	U	0.85
<i>Gate 2 Reactive Cell Wells</i>										
P5S	150	140	50	54	24	11	0.04	U	U	U
P5D	79	28	3.37	28	23	11	U	0.34	U	0.78
P7S	133	82	14.8	24	14	13	U	U	1.5	U
P7D	81	26	4.25	42	24	11	U	U	U	U
P11S	73	70	97	3.7	37	12	U	U	U	U
P11D	75	70	45.7	12	29	9.7	U	U	U	U
<i>Gate 2 Exit Zone Wells</i>										
P14S	82	66	5.3	2.5	26	12	U	U	U	U
P14D	92	102	4.65	6.3	22	6.6	0.18	U	U	U
<i>Gate 2 Downgradient Aquifer Wells</i>										
D7S	137	NA	16.3	NA	20	NA	0.11	NA	U	NA
D7D	112	NA	5.3	NA	23	NA	0.11	NA	U	NA
<i>Background Wells</i>										
214S	2	NA	3.18	NA	16	NA	U	NA	3.75	NA
214D	7	NA	3.13	NA	22	NA	U	NA	2.75	NA

Table 7-4. Selected Results of Inorganic Chemical Analysis (Continued)

Well ID	Manganese		Nitrate		Silica		Sodium		Sulfate	
	Jul 98	Jun 99	Jul 98	Jun 99	Jul 98	Jun 99	Jul 98	Jun 99	Jul 98	Jun 99
<i>Gate 1 Upgradient Aquifer Wells</i>										
U4S	0.03	1.7	6.84	8	4.67	10	14.5	20	53	9.3
U4D	0.12	1.1	11	7.1	10.2	15	16.6	13	12	4
<i>Gate 1 Pretreatment Zone Wells</i>										
F1S	U	3.3	0.03	U	U	1.3	23.2	7.1	28	U
F2S	U	NA	U	NA	U	1.7	27	7.4	31	2.4
F2D	U	NA	0.08	NA	U	2.5	23.3	20	U	2.5
<i>Gate 1 Reactive Cell Wells</i>										
F5S	U	NA	U	NA	U	0.25 J	30	5.6	44	2.9
F5D	U	NA	U	NA	U	0.59	24.5	20	15	2.4
F7S	U	4.2	U	U	U	0.55	25.1	8.9	35	U
F7D	U	4.9	U	U	U	1	24	22	24	U
F11S	U	7.4	U	U	U	1.8	38.5	23	22	U
F11D	U	6.5	U	U	U	1.2	35.5	20	19	U
<i>Gate 1 Exit Zone Wells</i>										
F14S	U	NA	U	NA	5.27	5.5	37.5	21	22	15
F14D	U	NA	U	NA	3.01	5.4	31	21	22	5.6
<i>Gate 1 Downgradient Aquifer Wells</i>										
D5S	0.06	1.3	23.1	6.1	4.69	10	13.9	23	94	28
D5D	0.35	1.8	0.16	0.31	9.95	8.8	38.9	21	24	5.1
<i>Gate 2 Upgradient Aquifer Wells</i>										
U8S	0.31	1.5	2.75	2.8	11.7	11	47.9	68	71	140
U8D	0.65	U	2.89	2.3	9.42	13	44.9	29	61	23
<i>Gate 2 Pretreatment Zone Wells</i>										
P1S	0.15	4.5	U	U	8.78	13	40.2	13	84	210
P2S	U	NA	0.05	NA	8.26	5.8	27.5	14	41	60
P2D	U	NA	U	NA	U	4.4	34.6	13	53	98
<i>Gate 2 Reactive Cell Wells</i>										
P5S	U	NA	0.02	NA	3.87	3.7	26.6	24	35	27
P5D	U	NA	0.03	NA	U	1.3	42.3	14	21	81
P7S	U	10	0.06	U	4.74	2.6	47.7	33	46	31
P7D	U	3	U	U	U	0.46 J	40.9	15	29	110
P11S	U	6.4	U	U	U	1.8	48.7	33	71	20
P11D	U	6.2	U	U	U	0.71	39.2	44	37	76
<i>Gate 2 Exit Zone Wells</i>										
P14S	U	NA	U	NA	3.38	3.4	48	33	61	14
P14D	U	NA	U	NA	5.19	5.3	44.8	65	23	67
<i>Gate 2 Downgradient Aquifer Wells</i>										
D7S	U	NA	U	NA	U	NA	29.7	NA	23	NA
D7D	U	NA	U	NA	8	NA	48.3	NA	8	NA
<i>Background Wells</i>										
214S	0.08	NA	4.54	NA	10.8	NA	8.7	NA	U	NA
214D	0.05	NA	3.57	NA	10.8	NA	12.3	NA	U	NA

Concentration units in mg/L.

U = Undetected.

Samples for metals analysis (Na, Mg, Ca, Fe, and Mn) were filtered in the field using 0.45-micron pore-size membranes immediately after collection. This procedure was intended to exclude colloidal material and suspended iron fines from being collected with the water sample, which was subsequently acid-digested and analyzed. Iron and manganese are the most problematic metals to analyze, due to their tendencies to absorb onto colloidal material. Table 7-4 shows that iron concentrations in the filtered samples were generally below 0.1 mg/L. However, there are two important exceptions in the Gate 2 PTZ, which are discussed in Section 7.3.1. Significantly, iron concentrations in the reactive cell tend to be indistinguishable from samples taken elsewhere in the PRB and surrounding aquifer. These results indicate that the permeable barrier does not produce excessive levels of dissolved iron in the downgradient aquifer. Thus, the barrier does not adversely affect water quality with regard to dissolved iron content.

The charge balance was calculated to provide another measure of inorganic data quality. Charge balance is calculated as the percent difference in cation and anion milliequivalents (meq), as shown in the following equation:

$$\text{Charge Balance} = 100 \times \frac{\text{meq cations} - \text{meq anions}}{\text{meq cations} + \text{meq anions}} \quad (7-2)$$

Electrolyte solutions must be electrically neutral, therefore any charge deficiencies to the contrary reflect cumulative errors in analysis of the ionic species. Solutions that are within 10% cation-anion balance are considered adequately balanced for subsequent uses such as geochemical modeling. The majority of data collected in both major sampling rounds are within 10% of charge balance. Figure 7-6 shows charge balance results for June 1999. In this figure, the data are distributed near the charge balance line (heavy line) and most points fall within the $\pm 10\%$ envelope. This figure also illustrates that water in Gate 2 has a higher ionic concentration than water in Gate 1.

7.3 Trends in Analyte Concentrations

Interactions between groundwater and the reactive media, iron and pyrite, give rise to changes in the inorganic composition of the groundwater. In general, formation of precipitates may affect the performance of the reactive media, either by coating the surfaces or taking up void space. A description of chemical changes in groundwater analytes is given below.

7.3.1 Iron

Oxidation of iron by DO, CVOCs, or other reducible species causes a stoichiometric release of dissolved iron. However, dissolved iron concentrations are not particularly high at any location in the two gates. For example, iron concentrations remained low in the Gate 1 PTZ throughout the study. Data in Table F-3 show that in July 1998, iron concentrations were 0.04 $\mu\text{g/L}$ at F1S and 0.05 $\mu\text{g/L}$ at F2D; in June 1999, iron concentrations were <0.05 at F1S and 0.078 $\mu\text{g/L}$ at F2D. Similarly, in Gate 2 in July 1998, iron concentrations were 0.49 $\mu\text{g/L}$ at P1S and <0.03 $\mu\text{g/L}$ at P2D. In contrast, somewhat higher levels of iron were measured in the Gate 2 PTZ in June 1999; analysis of filtered groundwater samples revealed iron concentrations of 32 $\mu\text{g/L}$ in P1S and 16 $\mu\text{g/L}$ at P2D. However, all the measured iron concentrations were below the 0.3 mg/L secondary drinking water standard.

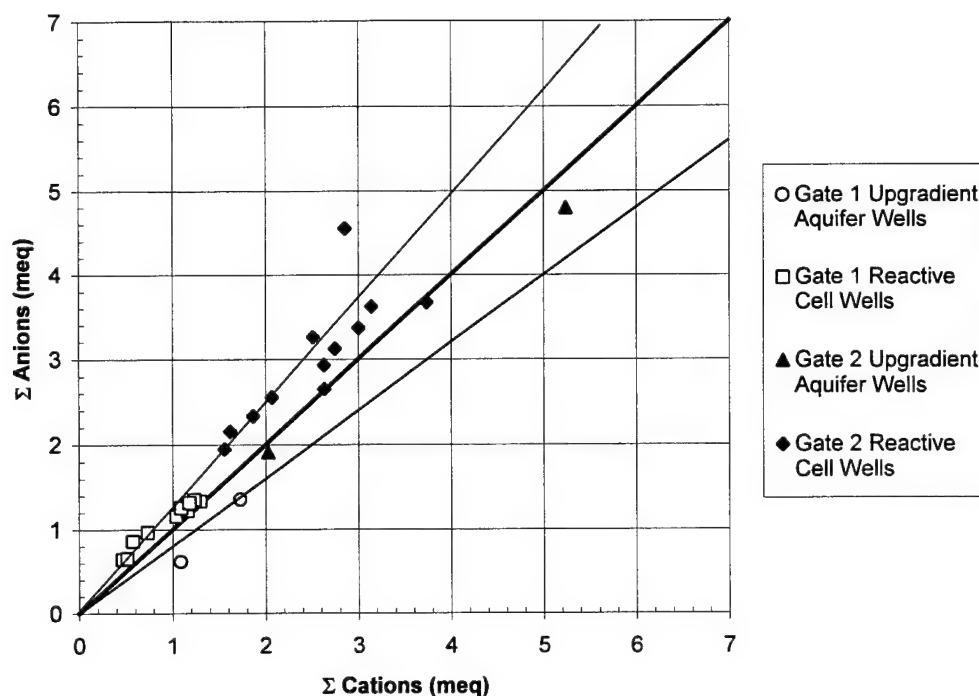
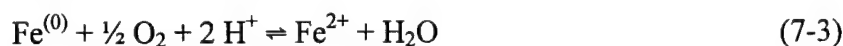


Figure 7-6. Ionic Charge Balance for Selected Wells (June 1999)

According to Equation 7-1, soluble iron (Fe^{2+}) in the Gate 2 PTZ should increase in proportion to the amount of DO consumed by pyrite. Similarly, iron corrosion (see Equation 7-3) in the Gate 1 PTZ should also produce soluble iron species.



Assuming that the typical DO concentration in the aquifer is 5 mg/L, Equation 7-1 (pyrite reaction) indicates that the stoichiometric concentration of Fe^{2+} produced would be approximately 2,500 $\mu\text{g/L}$. Similarly, by Equation 7-3 (iron reaction), the concentration of Fe^{2+} produced would be approximately 17,000 $\mu\text{g/L}$. Based on geochemical modeling, these apparent discrepancies between stoichiometric and actual concentrations appear to be controlled by low-solubility phases that are not necessarily at equilibrium with either zero-valent iron or pyrite. These discrepancies will be discussed in more detail in Section 7.4, on geochemical modeling.

7.3.2 Sodium and Chloride

The distributions of Na and Cl were examined because these species are usually conservative in geologic systems. Although chloride is known to form mixed salts with iron, hydroxide, and sulfate ions, no physical evidence was found to suggest that these so-called "green rust" compounds were formed in the barrier. Figures F-4 and F-5 show concentration profiles of Na and Cl, respectively. Although the concentrations of these ions are distributed rather widely, the data do not suggest systematic changes in concentrations within any of the media. A possible explanation for the variability is due to influx of salts into the groundwater table through the overlying parking lot.

7.3.3 Alkalinity, Calcium, and Sulfate

Concentrations of alkalinity, calcium, and sulfate also vary by several factors in the upgradient aquifer as well as in the gates media (see Figures F-6 to F-8, respectively). Also, it appears that higher levels of these ions exist in the aquifer near Gate 2. Furthermore, concentrations are even higher and seem to be more broadly distributed in the Gate 2 PTZ and its reactive cell. Increased amounts of these species are not readily explained by geochemical reactions resulting from interaction of the native groundwater with the reactive media. In the Gate 2 PTZ, it is expected that there would be an increase in sulfate by approximately 8.6 mg/L, due to dissolution of pyrite (see Equation 7-1). However, sulfate concentrations in Gate 2 are actually about 50 mg/L higher than in Gate 1. A possible explanation is that cement grout used during construction of the funnel or resurfacing of the parking lot caused a release of these ions near Gate 2. This explanation may also be a reason for higher pH in the upgradient vicinity of Gate 2 than Gate 1. It can be seen in Table 7-4 and Figures F-6 and F-7 that alkalinity and calcium were higher in Gate 2 during the July 1998 sampling and lower in the June 1999 sampling, suggesting a trend toward lower concentrations over time. According to geochemical modeling results presented in Section 7.4, water in the reactive cells is oversaturated with respect to calcite, and thus, precipitation of calcium carbonate may be occurring, but is not obvious from the calcium and alkalinity data in Table 7-4. As opposed to calcium and alkalinity, sulfate (Figure F-8) appears to be higher in the June 1999 sampling and was particularly elevated in the Gate 2 PTZ.

7.3.4 Magnesium, Nitrate, and Dissolved Silica

Magnesium, nitrate, and silica species all decrease in concentration as water enters the two gates (see Figures F-9 to F-11, respectively). Reductions in magnesium and nitrate levels appear to take place in both PTZs, while silica concentrations seem to decrease only in the presence of iron. When controlled by carbonate equilibria, magnesium and calcium exhibit concomitant increases or decreases in concentration. However, this does not seem to be the case at the PRB site, because calcium and magnesium there behave quite differently (compare Figures F-7 and F-9). The concentrations of all three species increase in the aquifer downgradient of Gate 1. As noted elsewhere, recovery of dissolved ion concentrations to native conditions does not seem to occur as rapidly downgradient of Gate 2, possibly due to slow mixing.

Nitrate concentrations are reduced to below detection in both PTZs. Nitrate remains absent in the reactive cells and exit zones, but was detected in the aquifer downgradient of Gate 1 (see Figure F-10). Thus, nitrate levels are restored immediately downgradient of Gate 1.

Dissolved silica is present in groundwater, due to the interaction with silicate minerals in aquifers. Monomeric silicic acid, H_4SiO_4 , is known to form polymers that may coat iron grains. As shown in Figure F-11, silica levels decrease abruptly in the Gate 1 PTZ and remain low in both reactive cells. Silica decreases to a lesser extent in Gate 2, suggesting that a slower precipitation rate occurs in the presence of pyrite than iron, or that silica-depleted water in the reactive cell mixes with water in the PTZ. The latter explanation appears to explain behavior of field parameter measurements as well. Note that dissolved silica increases from low concentrations in the

reactive cells to higher concentrations in the exit zones. This is probably caused by equilibration of the reactive cell effluent water with the quartz sand in the exit zones.

7.4 Geochemical Modeling

Geochemical modeling was used to assist in interpreting observed changes in inorganic groundwater chemistry. The U.S. Geological Survey code PHREEQC (Parkhurst, 1995) was used in two different capacities. First, groundwater analysis data were used to calculate species concentrations and mineral saturation indices. Second, simulations were performed to predict the outcome of interactions between groundwater and either zero-valent iron or pyrite.

7.4.1 Mineral Saturation Indices

Mineral saturation indices were calculated using groundwater sampling data from June 1999. Results are presented in Table 7-5. The mineral saturation index (SI) is defined as

$$SI = \log_{10}(IAP/K) \quad (7-4)$$

where IAP is ion activity product and K is the thermodynamic equilibrium constant for a particular mineralogical reaction. When $SI = 0$, the mineral and groundwater are considered to be in equilibrium; negative values imply undersaturation of the mineral phase and positive values imply oversaturation. The positive values in Table 7-5 are bolded, indicating saturation or oversaturation with respect to the mineral phase. In practice, mineral equilibrium may be assumed when SI is within ± 0.20 . The minerals listed in Table 7-5 are those whose composition lies in the groundwater chemical system (H_2O -Na-Mg-Ca-Fe-Cl- SO_4 - SiO_2 - CO_2). Because aluminum was not measured, saturation indices were not calculated for aluminosilicates, which include the majority of clay minerals. Other common mineral groups such as micas and feldspars also cannot be represented in this system.

Based on modeling results (see Table 7-5), groundwater samples from the upgradient and down-gradient aquifer are in equilibrium with quartz (six analyses) and amorphous ferric hydroxide [$Fe(OH)_3$] (two analyses). That the groundwater is in equilibrium with quartz is not surprising, because the aquifer is primarily composed of quartz sand. The magnesium silicate clay mineral, sepiolite, is considerably below saturation in the aquifer. Although metastable with respect to goethite (α - $FeOOH$), amorphous ferric hydroxide appears to be the phase that controls ferric iron concentrations in the aquifer.

Inside the two reactive cells, the modeling results show there is potentially equilibrium with respect to carbonate minerals aragonite and calcite ($CaCO_3$). Typically, aragonite is metastable with respect to calcite in freshwater aquifers, but in column tests with iron, aragonite is generally the form of calcium carbonate that precipitates. Based on the SI calculations, either aragonite or calcite could precipitate inside the reactive cells.

Table 7-5. Geochemical Modeling Results: Saturation Indices

Well ID	Aragonite	Brucite	Calcite	Dolomite	Fe(OH) ₃	Fe ₃ (OH) ₈	Goethite	Magnetite	Quartz	Sepiolite	Siderite
<i>Upgradient Aquifer Wells</i>											
U4S	-4.867	-10.665	-4.720	-9.046	NC	NC	NC	-4.893	0.277	-14.201	NC
U4D	-5.956	-11.831	-5.809	-11.255	NC	NC	NC	-6.013	0.453	-16.005	NC
U8S	-3.711	-9.251	-3.564	-6.993	0.768	-6.773	6.478	-3.996	0.319	-11.247	-6.887
U8D	-3.353	-9.478	-3.205	-6.245	NC	NC	NC	-3.606	0.391	-11.485	NC
<i>Gate 1 Pretreatment Zone Well</i>											
F1S	0.070	NC	0.217	NC	NC	NC	6.382	NC	-1.195	NC	NC
<i>Gate 1 Reactive Cell Wells</i>											
F5S	0.378	NC	0.525	NC	NC	NC	NC	NC	-2.301	NC	NC
F7S	0.555	NC	0.702	NC	NC	NC	NC	NC	-1.915	NC	NC
F7D	0.289	NC	0.436	NC	NC	NC	NC	NC	-1.502	NC	NC
F10	0.488	NC	0.635	NC	NC	NC	NC	NC	-1.819	NC	NC
F11S	0.346	NC	0.493	NC	NC	NC	NC	NC	-1.501	NC	NC
F11D	0.421	NC	0.569	NC	NC	NC	NC	NC	-1.605	NC	NC
<i>Gate 1 Downgradient Aquifer Wells</i>											
D5S	-5.395	-11.404	-5.247	-10.326	0.885	-5.934	6.595	-5.645	0.277	-15.679	-5.777
D5D	-3.694	-9.612	-3.546	-6.981	NC	NC	NC	-4.002	0.221	-12.262	NC
<i>Gate 2 Pretreatment Zone Wells</i>											
P1S	<-5.198	-13.476	<-5.051	<-10.868	-0.365	-6.883	5.345	-6.384	0.392	-19.477	<-2.893
P2S	1.323	NC	1.471	NC	NC	NC	NC	NC	-1.292	NC	NC
<i>Gate 2 Reactive Cell Wells</i>											
P7S	0.605	NC	0.752	NC	NC	NC	NC	NC	-1.827	NC	NC
P7D	0.864	NC	1.012	NC	NC	NC	NC	NC	-1.728	NC	NC
P10	0.812	NC	0.960	NC	NC	NC	NC	NC	-1.699	NC	NC

NC = Not calculated, because critical input parameters were missing (e.g., Mg and Fe concentrations).

Note: Numbers close to zero or positive are bold to indicate saturation (or oversaturation) with respect to the referenced mineral.

The data also show that quartz is quite undersaturated in both reactive cells and in the Gate 1 PTZ. This result suggests that dissolved silica precipitates in the presence of zero-valent iron. It is especially noteworthy that silica depletion takes place in Gate 1 PTZ (F1S). (Note that iron is a minor component in the Gate 1 PTZ, whereas 90% is quartz sand). This behavior implies that the kinetics of silica precipitation are faster than dissolution of quartz sand. The result for the Gate 2 PTZ well P1S is similar to aquifer values and therefore does not indicate that silica precipitation is occurring in the presence of pyrite. However, farther downgradient in well P25, silica is below quartz saturation, which points to the influence of iron at this location in the PTZ.

Knowledge about the presence or absence of many other phases of interest is largely unknown, due to undetectable concentrations of certain key elements, notably Mg and Fe. For example, siderite (FeCO_3), a ferrous carbonate mineral, and magnesite (MgCO_3) are below saturation in the few wells where SI values can be calculated. Even though these results are very limited, they suggest that siderite and magnesite do not precipitate in the reactive cells. Furthermore, groundwater concentration of Mg does not seem to be controlled by brucite [$\text{Mg}(\text{OH})_2$] in the Gate 2 PTZ, based on the result in P1S. Although dolomite saturation is mostly unknown, dolomite does not tend to precipitate in low temperature environments because of slow reaction kinetics.

7.4.2 Geochemical Simulations

Reactions between groundwater and iron or pyrite were simulated by allowing the solid phases to dissolve incrementally to their saturation limits. These simulations were performed to determine whether such predictions can be made accurately, in comparison to actual measurements. If the interaction of site groundwater with reactive media can be simulated within an acceptable level of confidence, then similar models could be run for other groundwater compositions and the practice could become a useful tool for predicting the outcome of such interactions. Another purpose for these simulations is to estimate the extent of these reactions.

Reactions with Zero-Valent Iron. Reactions within Gate 1 were simulated using a groundwater composition obtained from well U4S (June 1999 data). In these simulations iron was allowed to dissolve incrementally in the groundwater, up to saturation (80 $\mu\text{moles Fe}$ per liter of groundwater). Figure 7-7 shows simulated changes in pH and Eh. Initial values are the same as measured in the field (i.e., pH = 5.07 and Eh = 595.8 mV). Constant values of both parameters were obtained after approximately 25 $\mu\text{moles Fe}$ had dissolved. The constant pH of approximately 10.5 is within the range obtained by measurements (see Table D-2 and Figure F-1). The Eh of approximately -475 mV agrees with the lowest measured values (see Table D-2 and Figure F-2). The prediction of redox potential is within acceptable limits, because measurements are often higher than true values.

Figure 7-8 shows results of DO, dissolved nitrogen (N_2), and nitrate simulations. It can be seen that DO and nitrate are quantitatively removed as iron reacts. Dissolved nitrogen and ammonia (not shown) are produced by reduction of N_2 . These results are in good agreement with the rapid disappearance of DO and nitrate in the Gate 1 PTZ and their absence in both reactive cells (see Figures F-3 and F-10).

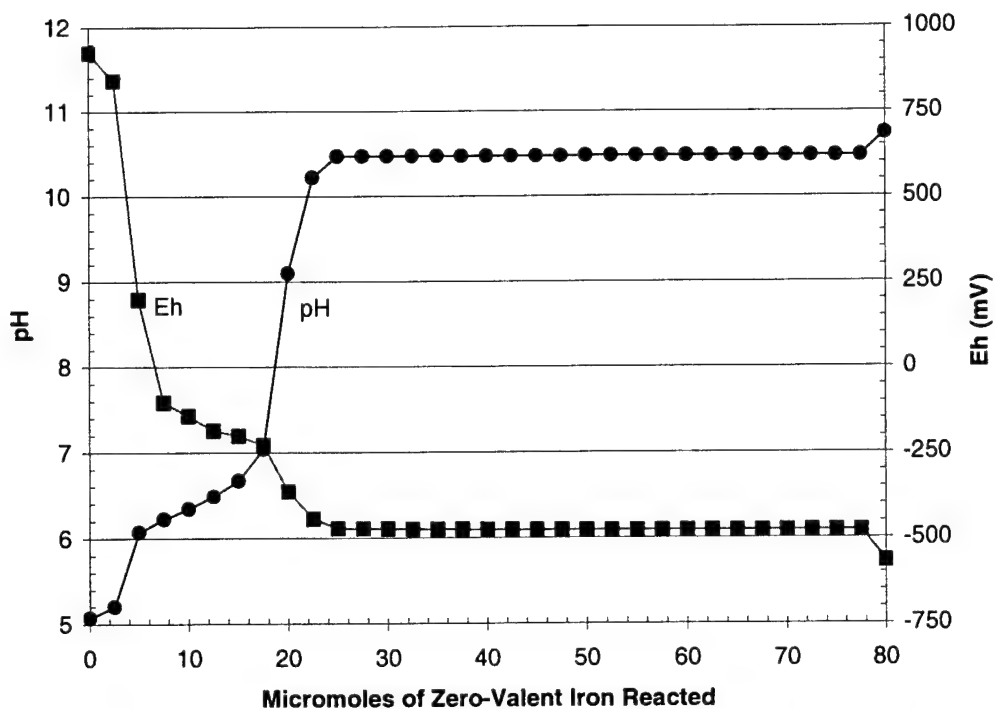


Figure 7-7. Simulated pH and Eh Reactions with Zero-Valent Iron

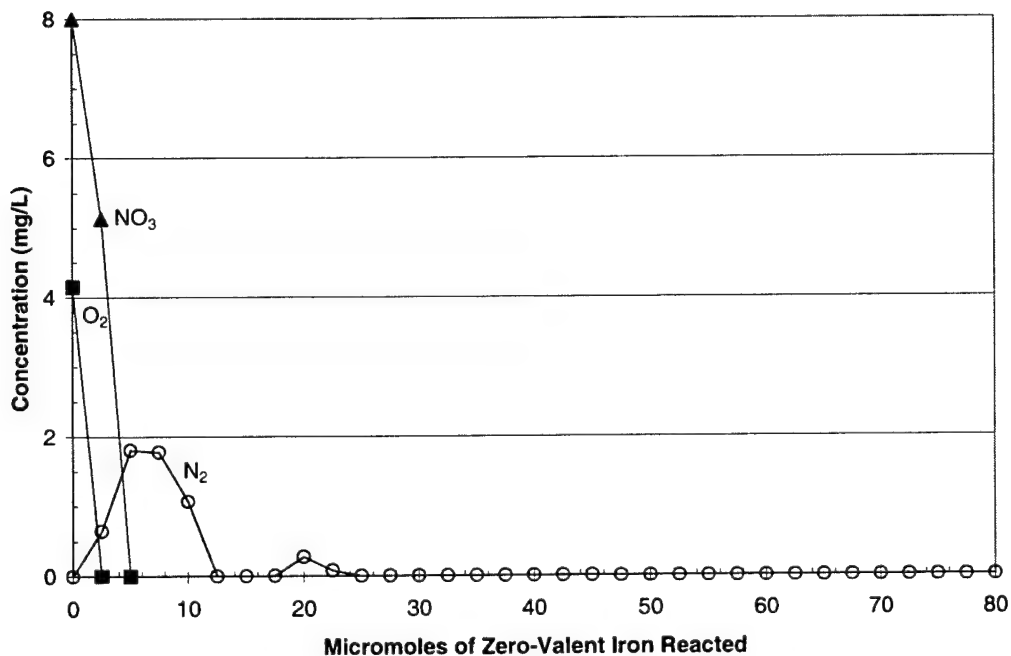


Figure 7-8. Simulated DO, Dissolved Nitrogen, and Nitrate Reactions with Zero-Valent Iron

Reactions with Pyrite. Reactions within the Gate 2 PTZ were simulated using a groundwater composition obtained from well U8S (June 1999 data). In these simulations pyrite was allowed to dissolve incrementally in the groundwater, up to saturation (60.6 μ moles pyrite per liter of groundwater). Results are presented in Figures 7-9 and 7-10. Figure 7-9 shows that pH declines to a low value of 4.7, then increases to about 5.4 at the end of reaction. Eh remains fairly constant throughout most of the reaction, but decreases abruptly toward the end. These results are roughly in agreement with field measurements, which show decrease in pH in the Gate 2 PTZ and Eh values that were generally not as low as in Gate 1.

Figure 7-10 shows that DO decreases incrementally with reaction of pyrite and is complete at 42 μ moles of pyrite. After DO is removed, nitrate reacts and is converted to dissolved nitrogen gas (N_2). These results also agree with the rapid disappearance of DO and nitrate in the Gate 2 PTZ (see Figures F-3 and F-10).

7.5 Evaluation of Core Samples

Cores were collected from the reactive cell so the iron could be examined for signs of the corrosion and precipitation predicted by the groundwater analysis and geochemical modeling.

7.5.1 X-Ray Diffraction

XRD provides a qualitative determination of crystalline phases by comparison of x-ray scattering peaks with those of known compounds. Amorphous materials do not yield precise x-ray

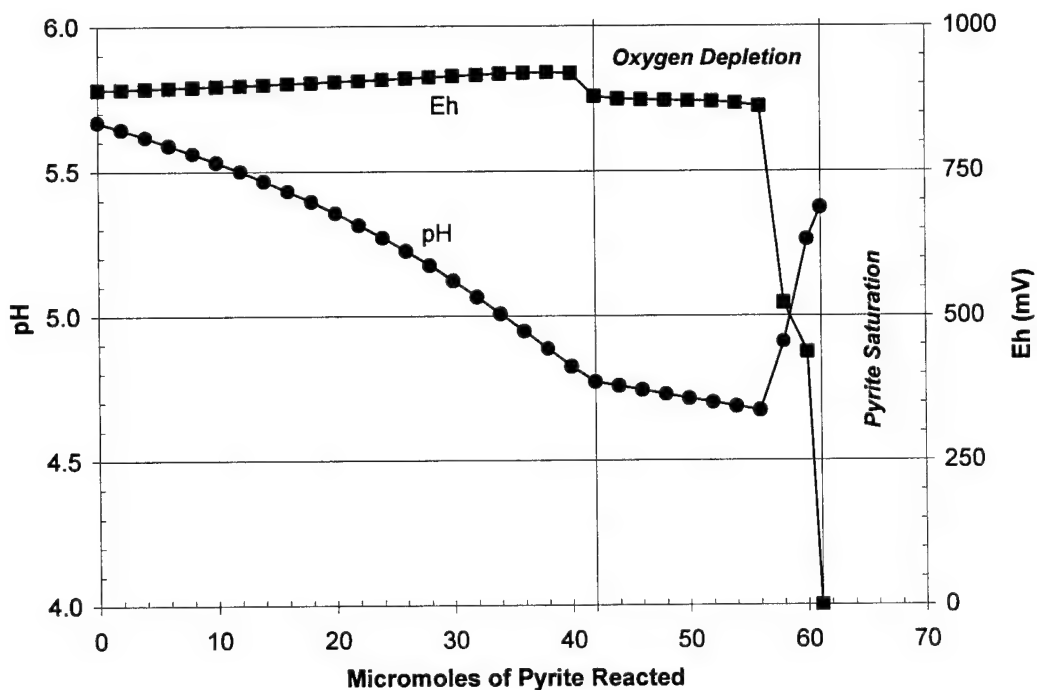


Figure 7-9. Simulated pH and Eh Reactions with Pyrite

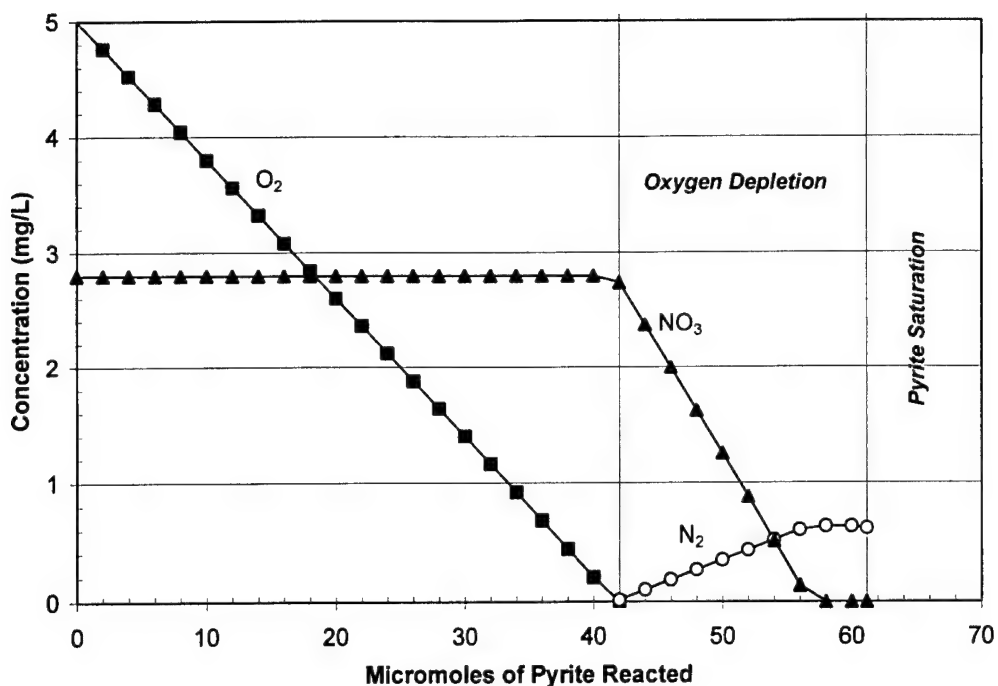


Figure 7-10. Simulated DO, Dissolved Nitrogen, and Nitrate Reactions with Pyrite

scattering peaks. XRD is suitable for identifying metallic iron, metal oxides, sulfides, carbonates, and other crystalline phases of interest to this study.

All of the core samples containing iron were sieved through a 100-mesh screen to remove loose surface coatings, which were then analyzed. This preparation step was performed to enhance the amount of coating material in the XRD sample and thereby minimize the amount of metallic iron. Whole grains of unused iron were analyzed without sieving, because the coating could not be easily removed.

XRD results, presented in Table 7-6, indicate that the crystalline material contained in the iron corrosion coatings is composed principally of magnetite. Although the diffraction pattern for maghemite ($\gamma\text{-Fe}_2\text{O}_3$) is very similar to the pattern for magnetite, the presence of magnetite was confirmed by Raman spectroscopy (see Section 7.4.3), while maghemite was not. No hematite ($\alpha\text{-Fe}_2\text{O}_3$) was detected in any of the samples by XRD.

Quartz was the major mineral component in both gates. As expected, metallic iron and magnetite were identified in Gate 1, while pyrite was detected in Gate 2. The unexpected occurrence of iron in the 15-15.5 ft level (as implied by the presence of iron and magnetite) is probably a result of iron infiltration from the reactive cell into the PTZ, which could have occurred during construction. The presence of iron in the PTZ may explain why high pH readings were obtained (see Section 7.1.1).

No carbonates or sulfides other than pyrite were detected in any of the XRD spectra.

Table 7-6. Results of X-Ray Diffraction Analysis of Core Samples

Sample ID	Depth (ft bgs)	Medium	Major Mineral(s)	Minor Mineral(s)	Trace
Unused iron	N/A	Iron	Iron	Magnetite ^(a)	None
Gate 1 Pretreatment Zone					
PS-1	15-15.5	Iron and sand	Quartz	None	Iron and magnetite ^(a)
PS-1	19-19.5	Iron and sand	Quartz	Iron and magnetite ^(a)	None
PS-1	24-24.5	Iron and sand	Quartz	None	Iron and magnetite ^(a)
Gate 1 Reactive Cell					
PS-2	15.5-16.5 top	Iron	Magnetite ^(a)	Quartz	Iron
PS-2	24-24.5	Iron	Magnetite ^(a)	Iron	None
PS-2	31-31.5	Iron	Magnetite and quartz	None	None
Gate 2 Pretreatment Zone					
PS-6	15-15.5	Pyrite and sand	Quartz	None	Iron, magnetite ^(a) , and pyrite ^(b)
PS-6	24.5-25	Pyrite and sand	Pyrite	None	Quartz
PS-6	27.5-28	Pyrite and sand	Pyrite	None	None
PS-6	No depth	Pyrite and sand	Pyrite	None	None
Gate 2 Reactive Cell					
PS-7	15-15.5	Iron	Magnetite ^(a)	Quartz and iron	None
PS-7	33-33.5	Iron	Quartz and magnetite ^(a)	Iron	None

(a) XRD pattern also corresponds with maghemite.

(b) Analysis indicates the presence of iron in the pyrite PTZ. This could indicate infiltration of granular iron from the reactive cell into the PTZ.

7.5.2 Scanning Electron Microscopy

SEM provides high-resolution visual and elemental characterization of amorphous and crystalline phases. This method is suitable for identifying precipitates. SEM results indicate that the surfaces of the iron particles are coated with iron oxides and that the abundance of these oxides is strong on all samples, including the unused iron.

EDS is helpful in identifying precipitates on the iron. Results of EDS measurements are given in Table 7-7. These data show in weight percent units the concentrations of various elements in the analysis beam. Because the EDS instrument was not calibrated to known standards, the results should be considered relative values, rather than absolute.

7.5.3 Raman Spectroscopy

Raman spectroscopy enables semiquantitative characterization of amorphous and crystalline deposits on the iron. This method is suitable for identifying iron oxides and hydroxides as well

Table 7-7. Results of EDS Analysis of Core Samples

Sample ID	Depth (ft bgs)	Medium	Fe	Mn	Si	O	Al	K	Ca	S	Cu	Na	Total
(% by weight)													
Unused iron	NA	Iron	91.65	0.73	1.78	5.84	0.00	0.00	0.00	0.00	0.00	0.00	100.00
Gate 1 Pretreatment Zone													
PS-1	15-15.5	Iron and sand	60.97	0.63	23.17	12.92	0.47	0.64	0.71	0.50	0.00	0.00	100.01
PS-1	19-19.5	Iron and sand	79.19	0.39	7.53	8.00	0.38	0.08	1.03	0.32	3.09	0.00	100.01
PS-1	27-28.5	Iron and sand	81.20	0.00	10.66	6.15	0.71	0.00	0.86	0.43	0.00	0.00	100.01
Gate 1 Reactive Cell													
PS-2	15.5-16.5 top	Iron	89.41	0.85	2.23	6.71	0.42	0.00	0.38	0.00	0.00	0.00	100.00
PS-2	24-24.5	Iron	82.71	0.60	6.45	8.04	1.30	0.00	0.89	0.00	0.00	0.00	99.99
PS-2	31-31.5	Iron	90.25	1.06	2.14	6.15	0.40	0.00	0.00	0.00	0.00	0.00	100.00
Gate 2 Pretreatment Zone													
PS-6	no depth	Pyrite and sand	54.56	0.00	3.69	0.00	0.43	0.00	0.00	41.33	0.00	0.00	100.01
PS-6	22-22.2	Pyrite and sand	16.17	0.00	48.57	18.69	7.77	5.82	1.35	0.49	0.00	1.14	100.00
PS-6	15-15.5	Pyrite and sand	77.19	0.79	5.88	10.16	1.58	0.37	3.82	0.21	0.00	0.00	100.00
PS-6	24.5-25	Pyrite and sand	55.65	0.00	2.19	0.00	0.40	0.00	0.00	41.76	0.00	0.00	100.00
PS-6	27.5-28	Pyrite and sand	56.67	0.00	1.60	0.00	0.18	0.00	0.00	41.54	0.00	0.00	99.99
Gate 2 Reactive Cell													
PS-7	33-33.5	Iron	86.39	0.42	4.35	7.42	0.51	0.48	0.29	0.15	0.00	0.00	100.01
PS-7	37-37.5	Iron	83.66	1.01	3.68	8.64	1.72	0.22	0.12	0.96	0.00	0.00	100.01
PS-7	24.5-25	Iron	65.10	0.41	15.55	11.21	2.71	1.75	0.43	2.85	0.00	0.00	100.01
PS-7	28-28.5	Iron	84.56	1.12	3.60	8.88	1.16	0.24	0.39	0.05	0.00	0.00	100.00
PS-7	15.15.5	Iron	88.32	0.88	2.75	6.43	0.80	0.21	0.61	0.00	0.00	0.00	100.00

Analysis results in weight percentages.

as other compounds of significance to the reactive barrier. Raman spectra were recorded at three different grain locations for each sample. Multiple locations were chosen because the material was found to be heterogeneous in appearance. For this reason, each spectrum was recorded separately rather than being averaged together. Table 7-8 identifies the Raman shifts detected in the core samples. Raman spectra of the core material are included in Appendix F.

Table 7-8. Raman Shifts in Core Samples

Compound	Raman Shift (cm^{-1})
Magnetite	670
Hematite	227, 297, 412
Goethite	251, 302, 387
Amorphous iron oxide	300 – 500 (diffuse)
Pyrite	345, 381, 433
Quartz	466
Reduced carbon	1350, 1600

Results of Raman spectroscopic analysis are summarized in Table 7-9. In general, iron samples yielded the strongest Raman bands near 670, 1,350 and 1,600 cm^{-1} (wavenumber) shifts. The 670 cm^{-1} shift corresponds to magnetite (Fe_3O_4). The 1,600 cm^{-1} shift is characteristic of graphite-carbon, and the 1,350 cm^{-1} shift corresponds to finely ground graphite. The presence of carbon on the iron grains may be related to cutting oils that were used in machine grinding operations. These oils may have been baked onto the filings during processing. It should be noted that Raman spectroscopy is particularly well suited for identification of carbonate minerals. However, no carbonates were detected in any of the Raman spectra. Quartz was detected in both PTZs, which are each composed of 90% sand.

In addition to magnetite and carbon bands, samples of unused iron showed Raman bands for hematite ($\alpha\text{-Fe}_2\text{O}_3$), which were not evident in any of the core samples. Because the unused iron was not preserved in an inert atmosphere, exposure to air during storage may have caused the iron to oxidize, thus forming hematite. Samples from PS-1 in the Gate 1 PTZ typically show magnetite, carbon, and quartz. Two samples from near the top of the treatment zone (15 to 15.5 and 19 to 19.5 ft bgs) also appear to contain amorphous iron oxide (broad bands between 300 and 500 cm^{-1}). This could have been caused by corrosion of iron with oxygenated water. In the shallower core sample, iron oxide formation also could have occurred due to alternating exposure to water and air during periodic changes in water level. Two samples also contained quartz, which could have originated from the sand grains that comprise the PTZ.

In the Gate 1 reactive cell, Raman spectra of iron samples indicate magnetite and carbon. In addition, amorphous iron hydroxide also was detected in a shallow core sample (15.5 to 16.5). This sample was taken from the top-most portion of the core, where exposure to air during periods of low water level is most likely.

Table 7-9. Results of Raman Spectroscopic Analysis of Core Samples

Sample ID	Depth (ft bgs)	Medium	Sample Composition
Unused iron	NA	Iron	Magnetite, hematite, and carbon
Gate 1 Pretreatment Zone			
PS-1	15-15.5	Iron and sand	Magnetite, iron oxide, quartz, and carbon
PS-1	19-19.5	Iron and sand	Magnetite, iron oxide, and carbon
PS-1	24-24.5	Iron and sand	Magnetite, quartz, and carbon
PS-1	27-28.5	Iron and sand	Magnetite and carbon
Gate 1 Reactive Cell			
PS-2	15.5-16.5 top	Iron	Magnetite, iron oxide, and carbon
PS-2	24-24.5	Iron	Magnetite and carbon
PS-2	31-31.5	Iron	Magnetite and carbon
Gate 2 Pretreatment Zone			
PS-6	15-15.5	Pyrite and sand	Magnetite and carbon ^(a)
PS-6	22-22.2	Pyrite and sand	Magnetite and carbon ^(a) and rutile ^(b)
PS-6	24.5-25	Pyrite and sand	Pyrite and quartz
PS-6	27.5-28	Pyrite and sand	Pyrite and quartz
PS-6	No depth	Pyrite and sand	Pyrite and quartz
Gate 2 Reactive Cell			
PS-7	15.15.5	Iron	Magnetite and carbon
PS-7	24.5-25	Iron	Magnetite, carbon, α -FeOOH, and quartz
PS-7	28-28.5	Iron	Magnetite, carbon, α -FeOOH, and quartz
PS-7	33-33.5	Iron	Magnetite and carbon
PS-7	37-37.5	Iron	Pyrite ^(c)

(a) Analysis indicates the presence of iron in the pyrite PTZ. This could indicate infiltration of granular iron from the reactive cell into the PTZ.

(b) TiO_2 is not an expected component and was not detected by XRD or EDS.

(c) Analysis indicates the presence of pyrite. This could indicate infiltration of pyrite from the PTZ into the reactive cell, or that the core sampler penetrated into the PTZ.

In the Gate 2 PTZ, Raman spectra reveal pyrite and quartz at three sample depths. The unexpected occurrence of iron in the 15 to 15.5 and 22 to 22.5 ft levels (as implied by the presence of magnetite and carbon) is probably a result of iron infiltration from the reactive cell into the PTZ, which could have occurred during construction. The presence of iron in the PTZ may explain why high pH readings were obtained (see Section 7.1.1). In addition, rutile (TiO_2) was detected in the sample at 22 to 22.2 ft bgs. The appearance of rutile is anomalous. However, this sample consisted of a single particle, which could have been a contaminant in the pyrite. Moreover, rutile was not detected by XRD and Ti was not detected by EDS. These results suggest that even if some rutile were present, it may be only a trace mineral. No other compounds were detected that would suggest a possible relationship with pyrite.

In the Gate 2 reactive cell, iron particles show magnetite and carbon. In addition, some samples show evidence of goethite (α -FeOOH), which could have resulted from corrosion of the iron. It

was also unexpected to find pyrite in one core sample, which occurred in the deepest sample from PS-7 (37 to 37.5 ft bgs). This presence of pyrite in the reactive cell could have resulted from infiltration from the PTZ. Alternatively, the core sampler may not have been exactly vertical and penetrated into the PTZ.

7.5.4 Infrared Spectroscopy

Infrared spectroscopy was employed to detect whether silica (SiO_2) coatings were present on the iron grains. ATR spectra were recorded using three different grain assemblages because the material was found to be heterogeneous. Absorbencies at 900, 1,002, and 1,031 cm^{-1} were detected on all of the iron samples from the barrier. These absorbencies are characteristic of a silicate material, but one that is different from quartz. The infrared absorbance of quartz is at approximately 1,062 cm^{-1} . Interestingly, absorbed silica was not found in the unused iron.

FTIR spectra of iron grains also include an absorbance band near 590 cm^{-1} , which is characteristic of most iron oxides. However, this band is not very specific with regard to the polymorph present. Therefore, absorbencies in this region are simply referred to as "iron oxide." In one instance carbonate (1,388 cm^{-1}) was detected in the Gate 1 PTZ (26 to 28.5 ft bgs). Although this is an interesting finding, there were no other observations of carbonates in this sample or in any other by different methods.

FTIR spectra of the core samples are included in Appendix F. Results of the analysis are summarized in Table 7-10.

7.5.5 Carbon Analysis

Samples were analyzed for total carbon using a UIC Model 5120 Total Carbon Analyzer. The combustion temperature was set to 950°C, so that both organic and carbonate carbon could be detected. Results, shown in Table 7-11, indicate that the average carbon content of the unused iron was 2.63 ± 0.10 % by weight. The carbon detected in the unused iron samples may be the graphite-like carbon detected by Raman spectroscopy (see Section 7.5.3). Results of carbon analysis of the core samples were approximately the same as the unused material, indicating that measurable amounts of carbonate precipitates were not detected in the core samples.

7.6 Microbiological Evaluation

Core samples were sent to Microbe Inotech Laboratories in St. Louis, MO for microbiological analysis. After collection, these samples were sent immediately to the laboratory without vacuum drying. The samples were analyzed for heterotrophic plate counts and PLFA analysis. Phospholipids are part of the intact cell membranes and provide a quantitative measure of microbial biomass of microbial strains. The laboratory procedures involved making liquid dilutions that were plated onto agar with Oxyrase[®] enzyme in anaerobic petri plates. The plates were incubated anaerobically for 48 hours at 30°C. Following isolation, the strains were streaked onto TSA, then incubated for 24 hours followed by processing by GC.

Table 7-10. Results of FTIR Analysis of Core Samples

Sample ID	Depth (ft bgs)	Medium	Sample Composition
Unused	NA	Iron	No peaks observed
Gate 1 Pretreatment Zone			
PS-1	15-15.5	10% Iron and sand	Quartz and iron oxide
PS-1	19-19.5	10% Iron and sand	Silicate and iron oxide
PS-1	24-24.5	10% Iron and sand	No peaks observed
PS-1	26-28.5	10% Iron and sand	Quartz, silicate, carbonate, and iron oxide
Gate 1 Reactive Cell			
PS-2	15.5-16.5 top	100% Iron	Silicate and iron oxide
PS-2	24-24.5	100% Iron	Silicate and iron oxide
PS-2	31-31.5	100% Iron	Silicate and iron oxide
Gate 2 Pretreatment Zone			
PS-6	15-15.5	10% Pyrite and sand	No peaks observed
PS-6	22-22.2	10% Pyrite and sand	No peaks observed
PS-6	24.5-25	10% Pyrite and sand	No peaks observed
PS-6	27.5-28	10% Pyrite and sand	No peaks observed
PS-6	No depth	10% Pyrite and sand	No peaks observed
Gate 2 Reactive Cell			
PS-7	15-15.5	100% Iron	Silicate and iron oxide
PS-7	24.5-25	100% Iron	Silicate and iron oxide
PS-7	28-28.5	100% Iron	Silicate and iron oxide
PS-7	33-33.5	100% Iron	Silicate and iron oxide
PS-7	37-37.5	100% Iron	No peaks observed ^(a)

(a) Analysis indicates the presence of pyrite. This could indicate infiltration of pyrite from the PTZ into the reactive cell, or that the core sampler penetrated into the PTZ.

Table 7-11. Results of Carbon Analysis of Core Samples

Sample ID	Depth (ft bgs)	Medium	Location	Average ^(a) (% carbon by weight)	Standard Deviation ^(a)
Unused	NA	Iron	NA	2.63	0.10
PS-1	16-16.5.5	10% Iron and sand	Gate 1 pretreatment zone	2.15	0.51
PS-2	30.5-31	100% Iron	Gate 1 reactive cell	2.67	0.11
PS-2	30-30.5	100% Iron		2.46	0.15
PS-2	31-31.5	100% Iron		2.53	0.15
PS-7	15.5-16	100% Iron	Gate 2 reactive cell	2.40	0.08
PS-7	16-16.5	100% Iron		2.47	0.18
PS-7	22-22.5	100% Iron		2.45	0.27
PS-7	27-27.5	100% Iron		2.60	0.31

(a) Statistics based on three independent measurements.

Plate counting was done after 48 hours at 30°C in an anoxic atmosphere to determine populations of anaerobic microorganisms. After the plates were counted, they were incubated under aerobic conditions for four more days. Plates were counted again after a total of six days. The final results give the populations of facultative anaerobic microorganisms (i.e., microorganisms that can survive under alternating anaerobic and aerobic conditions).

Results of total heterotrophic plate counts are listed in Table 7-12, where values are expressed in colony-forming units per gram (CFU/g). After 48 hours incubation, the largest number of colonies were evident in an aquifer sample from temporary well, T-37. The next largest number of colonies was approximately one order of magnitude lower in an iron/sand sample from core location PS-1 in the Gate 1 PTZ. All other core samples showed negligible microbial growth after the 48-hour incubation period.

Table 7-12. Total Heterotrophic Plate Count Results (CFU/g)

Sample ID	Depth (ft bgs)	Medium	Location	48 Hours	6 Days ^(a)
T-37	33.5-34.0	Soil	Upgradient Aquifer	120,000	120,000
PS-5	34.5-35.0	Soil	Upgradient Aquifer	< 100	200
PS-1	21.5-22.0	Sand/Iron	Gate 1 PTZ	10,600	350,000
PS-6	27.0-27.5	Sand/Pyrite	Gate 2 PTZ	< 100	18,000,000
PS-2	15.0-15.5	Iron	Gate 1 Reactive Cell	< 100	120,000
PS-7	34.0-34.5	Iron	Gate 2 Reactive Cell	200	1,400
PS-4	36.5-37.0	Soil	Downgradient Aquifer	< 100	21,400

(a) Six-day test measures facultative anaerobes.

Most plate counts increased after 6 days incubation (facultative anaerobes). The largest population was measured in a sample extracted from PS-6 in the Gate 2 PTZ. Plate counts in other samples were not exceptionally high after 6 days. It is useful to note that the downgradient aquifer sample, PS-4, did not have particularly high plate counts, suggesting that biomass is not accumulating downgradient of the reactive cell. It is also noteworthy that plate counts for sample T-37, which is soil from a highly contaminated portion of the aquifer, were the same after both 48 hours and 6 days. This result suggests that microorganisms in the contaminated portion of the aquifer are strict anaerobes and are not facultative.

Only two types of microorganisms were evident in any of the samples tested, based on PLFA analysis. These include *Pseudomonas fluorescens* and *Bacillus pumilus*. No information on the significance of these microorganisms is available.

7.7 Summary of Geochemical Evaluation Results and Conclusions

The geochemical evaluation provided a somewhat qualitative indication of the geochemical interactions that may affect the longevity of the PRB. Some degree of quantification, in terms of

the losses of geochemical parameters from the groundwater due to precipitation, was attempted by comparing the levels of these parameters in the influent and effluent from the two gates. However, corroborating these losses with specific types of precipitates in the gate media proved difficult. Given the low alkalinity of the native groundwater, many more pore volumes (and several years of PRB operation) are probably necessary before the precipitation effect becomes significant enough to measure. The data trends and conclusions based on the geochemical evaluation are summarized as follows:

- Both the PTZ media, 10% iron/sand in Gate 1 and 10% pyrite/sand in Gate 2, succeeded in scrubbing DO from the groundwater before it entered the reactive cell. DO removal in Gate 2 validates the column test data and the design assumption that the kinetics of 10% pyrite would be sufficient to remove the DO in the Area 5 aquifer. Removing DO in the less-reducing PTZ reduces the potential for excessive corrosion product build up in the upgradient end of the more-reducing reactive cell.
- The iron/sand medium removed DO more efficiently than pyrite/sand, as indicated by the persistence of low levels of DO in the first well in the Gate 2 PTZ. DO was undetected by the time the water reached the very first well in the Gate 1 PTZ, indicating that a lower percentage of iron (for example, 5%) probably would have been sufficient to remove DO with the current dimensions of the PTZ.
- The pH of the groundwater remained noticeably lower in the Gate 2 PTZ compared to the Gate 1 PTZ. Pyrite reacts with DO to generate hydrogen ions, as opposed to iron, which reacts with DO to form hydroxyl ions. This indicates that pyrite does generate some initial pH control potential.
- The 10% iron in the Gate 1 PTZ created more strongly reducing conditions (lower ORP) than the 10% pyrite in the Gate 2 PTZ. As seen in Section 5, this led to greater degradation of CVOCs in the PTZ itself for Gate 1.
- Groundwater pH in the reactive cell in both gates was similarly high (between 10 and 11). This result indicates that the 100% iron in the reactive cell overwhelms any pH buffering capacity afforded by the pyrite in the PTZ. Adding a higher percentage of pyrite in the PTZ would not have helped because pyrite reacts only to the extent that DO is present. The fact that DO disappeared from the groundwater in the second row of wells in the Gate 2 PTZ indicates that the maximum buffering capacity of the pyrite-groundwater system had been reached and the proportion of 10% pyrite to sand was adequate.
- Under the geochemical conditions present in the two gates, calcium and alkalinity did not show any noticeable decrease as the groundwater flowed through the gates. On the other hand, magnesium, silica, and nitrate did precipitate out of the groundwater in the PTZ and reactive cell of both gates. Magnesium and silica precipitation was faster in the Gate 1 PTZ than in the Gate 2 PTZ. The precipitation of silica, which is

present in a dissolved form in most aquifers, could contribute to long-term loss of reactivity of the iron. Silica losses have not been studied closely at previous PRB installations, but should be investigated in the future.

- ❑ Not much precipitate build up was noticed on the media surfaces in the cores collected in the gates. Qualitatively, the presence of a small amount of iron hydroxide was indicated in the Gate 1 PTZ, while no such precipitate was found in the Gate 2 PTZ. The presence of iron hydroxide is indicated in both reactive cells. All iron samples showed detectable levels of absorbed silicate material, which matches the depletion of dissolved silica in the groundwater. Core collection could be repeated after at least two more years of PRB operation to obtain a better identification.
- ❑ A cursory evaluation of microbial populations in the gates and surrounding aquifer did not reveal any unusual microbial activity.
- ❑ It is difficult to make a judgement regarding the long-term performance of the two reactive media in the two gates. Retention of the precipitates indicated by groundwater losses of inorganic constituents are hard to verify. Relative to Gate 1, the pyrite in Gate 2 did not appear to afford any sustained benefit in terms of pH control, reactivity, or precipitation control.

8. Cost Evaluation

The cost evaluation of the PRB in Area 5 involves the estimation of the capital investment required for both the pilot-scale PRB and for a proposed scaleup. Annual operating and maintenance (O&M) costs are projected for the scaled-up PRB only. Finally, a present value analysis is provided which compares the long-term costs of a PRB and an equivalent P&T system.

8.1 Capital Investment

Table 8-1 lists the capital investment incurred in installing the field pilot-scale PRB in Area 5. This PRB is a funnel-and-gate system with two gates. Each gate is 4 ft wide and is keyed into the aquitard at a depth of 39 ft. Each gate has a 4-ft thickness of iron and incorporates a PTZ and an exit zone as described in Section 2. The funnel is 60 ft wide, giving a total barrier width of 68 ft. The PRB is estimated to capture about 50-ft width of plume in an aquifer that is approximately 25 ft thick. The various items in Table 8-1 include the costs incurred by Battelle and its construction subcontractor C³ Environmental, as well as broad estimates of relevant costs incurred by Dover AFB staff for site arrangements and by U.S. EPA-NERL for the on-site column tests.

Table 8-1 lists the capital investment for the pilot-scale PRB in two categories: preconstruction activities and PRB construction activities. Site characterization is a key cost driver in the preconstruction category. Because the PRB is an in situ structure, it is all the more important that the CVOC distribution and aquifer characteristics be well defined. In a P&T system, site characterization and design deficiencies can be corrected after system installation by adding additional wells or adjusting the aboveground treatment system. However, once a PRB has been installed, making system adjustments or expansions can be relatively expensive. Another factor driving the characterization cost at Area 5 was that the bulk of the plume was not in the area identified by data from regional wells as reported in the existing Remedial Investigation/Feasibility Study documents. Characterization activities were redirected after data from temporary wells pushed during additional site characterization activities (June 1997) became available.

The column test costs in Table 8-1 are illustrative numbers for the type of long-term on-site tests conducted at Dover for reactive media selection and degradation rate estimation for the pilot demonstration. For a full-scale application, much less rigorous column tests are required, with a concomitantly lower cost.

The design, procurement, and regulatory review costs include activities such as site characterization data evaluation, hydrologic and geochemical modeling, draft and final design/test plan preparation, evaluation and procurement of reactive media suppliers and construction subcontractors, and regulatory review. Procurement of a commercial source of pyrite proved to be particularly challenging. Pyrite is no longer the primary source for sulfuric acid production in the chemical

Table 8-1. Capital Investment Incurred in Installing the Field Pilot-Scale PRB in Area 5

Item	Description	Basis	Cost ^(a)
Phase 1: Preconstruction Activities			
Preliminary site assessment	Historical site data evaluation	Remedial Investigation/Feasibility Study, other reports procurement and evaluation; site meeting	\$15,000
Site characterization	Characterization plan, fieldwork, laboratory analysis	CPT pushes for geologic mapping and temporary wells; analysis of water samples for CVOCs; select samples for geotechnical analysis; slug tests; ground-penetrating radar survey ^(a,b)	\$150,000
Column tests	Two columns for two reactive media combinations; Area 5 groundwater	Three-month on-site test and laboratory analysis of water samples ^(b) ; report	\$100,000 ^(b)
Design; procurement; regulatory review	Data evaluation, modeling, engineering design, Design/Test Plan; construction subcontractor procurement; regulatory interactions	Characterization, column test data evaluation; hydrogeologic modeling; geochemical evaluation; engineering design; report; procurement process; regulatory approvals; preconstruction meeting	\$100,000
Subtotal			\$365,000
Phase 2: PRB Construction			
Site preparation	Utilities clearances; arrangement for equipment/media storage and debris disposal	Coordination with Base facilities staff	\$10,000
Reactive media procurement	Connelly iron, shipping; pyrite source identification, procurement; pyrite chunks, crushing, sizing, shipping.	Iron: 54 tons @ \$360/ton Pyrite: 5 tons @ \$1,400/ton Pyrite preparation: \$12,000 Shipping: \$9,000	\$47,000
PRB construction	Mobilization/demobilization; installation of two 8-ft-diameter caisson gates to 40-ft depth; and one 60-ft-long sheet pile funnel; asphalt parking lot restoration	Mob./demob.: \$38,000 Gates: \$133,000 Monitoring wells: \$25,000 Funnel: \$51,000 Surface restoration: \$17,000	\$264,000
Monitoring system construction	Thirty-four PVC aquifer wells installed for monitoring the pilot-scale PRB (fewer wells would be required for a full-scale system); four in situ groundwater velocity sensors	Aquifer wells: \$37,000 Velocity sensors: \$16,000	\$53,000
Subtotal			\$374,000
TOTAL			\$739,000

(a) Includes costs incurred for labor and materials by Battelle and its construction subcontractor C³ Environmental, as well as broad estimates of relevant costs incurred by Dover AFB staff for site arrangements and by U.S. EPA-NERL for the on-site column tests. Some cost items in this table may not be applicable at other sites.

(b) This level of testing was done for demonstration purposes and may be excessive for full-scale application.

industry. With declining use in the United States, pyrite mining currently is conducted mostly in Mexico, South America, and Europe. A U.S. company willing to procure the pyrite from Mexico eventually was located. Procuring a construction subcontractor involved solicitation of bids, arrangement of a site visit for prospective vendors, and selection of the best technical and cost bid. The PRB design was finalized only after discussion of several alternative designs and construction techniques with various bidders and a preconstruction meeting with the winning bidder.

Site preparation involved acquisition of clearances from the Base utilities office, arrangements to receive reactive media and construction equipment shipments, and arrangements to dispose of the construction debris. On a per ton basis, the pyrite was the costlier of the two media, especially after pyrite processing costs were included. It is presumed that if pyrite use for this application grows, less expensive sources of pyrite may become available over time.

Construction costs at this site were driven by the cost of installing the caisson gates. However, this method of installation was found to be less costly compared with other alternatives. Also, caisson gates were easier to install in the midst of multiple utility lines that crisscross Area 5. Note that the mobilization/demobilization costs at this site are probably lower than at other sites, because the construction subcontractor used a local partner in Dover, DE to supply most of the heavy equipment and operators, such as the 100-ton crane, 5-ft-diameter auger, and the pile driver. Having this equipment locally available also significantly minimized the time periods that this equipment had to be retained on site. Most of the heavy equipment and operators were requisitioned only on the days that the equipment was actually used. These advantages may not be available at other sites.

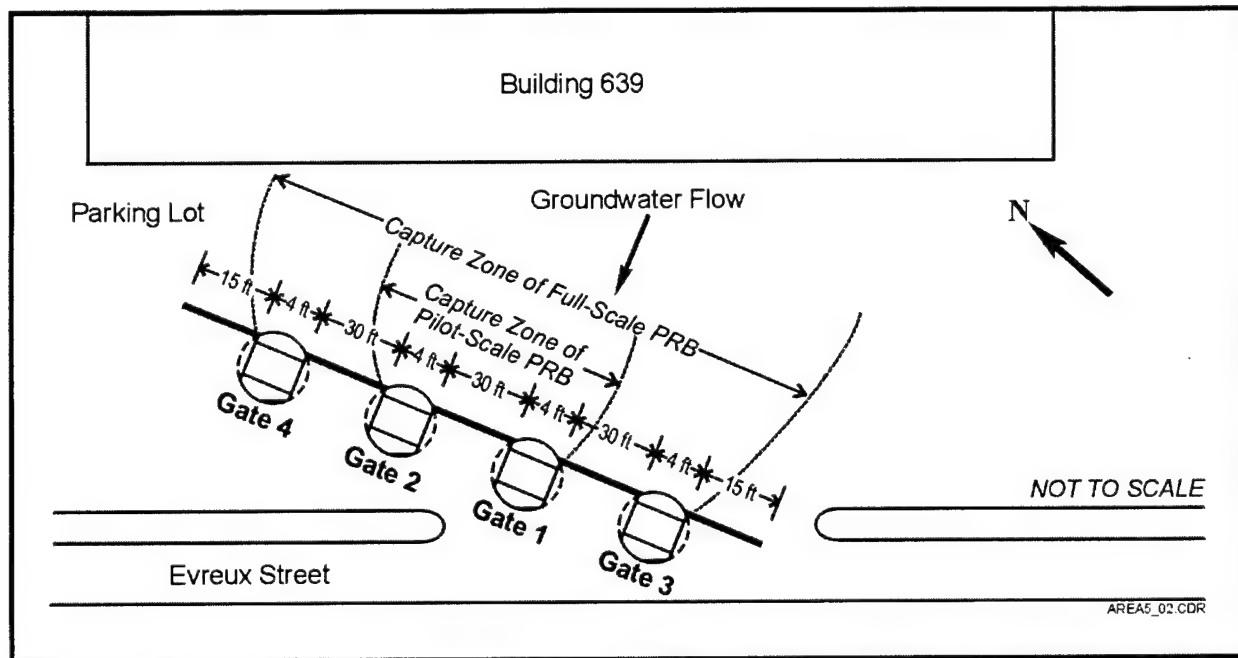
Because of the research needs of the demonstration, more monitoring wells were installed than would be required for full-scale application. The monitoring system also includes the installation of the four velocity sensors.

8.2 Scaleup

Although the PRB in Area 5 is considered pilot-scale, its relatively large size (68 ft wide and 39 ft deep) makes its economics easily scalable to a full-scale PRB. CVOC contamination at Area 5 is fairly widespread, with elevated CVOC concentrations identified in wells on both the north and south sides of Building 639. During additional site characterization in June 1997, an effort was made to identify the most contaminated portion of the plume for this demonstration; however, the boundaries of the entire plume were not mapped. Also, CVOC concentrations at Area 5 tend to vary sharply in both horizontal and vertical planes, indicating the presence of multiple sources of contamination. Lastly, the aquifer region under Building 639 remains unsampled and the CVOC distribution in that region is unknown.

Dover AFB is considering expanding the current pilot-scale PRB to capture more of the plume. In that event, additional site characterization to delineate more of the plume would be required. Based on the CVOC data from monitoring points on the fringes of the demonstration area, it is suspected that the plume may be at least 100 ft wide. The local gradients that drive the

To capture a 100-ft width of the plume with the current configuration, two more gates would have to be added to double the capture zone; the current pilot system captures 40- to 50-ft-width of the plume. The two additional gates could be installed with caissons, and the funnel could be extended using additional sheet piles. The scaled-up system is shown in Figure 8-1. The costs of this extended barrier are listed Table 8-2. The costs have been estimated as if the full-scale barrier had been installed right at the beginning, instead of installing the pilot-scale barrier and then extending it.



In Table 8-2, Phase 1 costs remain mostly the same as in Table 8-1. One difference is that \$50,000 has been added to reflect the cost of additional site characterization to locate the boundaries of the plume and assess the geology along a longer length. Another difference is that the column test costs have been reduced to reflect the less rigorous tests required for the full-scale application. In Phase 2, several of the items change. Assuming that only iron is used in the gates (no pyrite), the reactive media cost does not change significantly because the additional iron required costs much less than the small amounts of pyrite that it replaces.

Table 8-2. Capital Investment Projected for Installing a Full-Scale PRB in Area 5

Item	Description	Basis	Cost
Phase 1: Preconstruction Activities			
Preliminary site assessment	Historical site data evaluation	Remedial Investigation/Feasibility Study, other reports procurement and evaluation; site meeting	\$15,000
Site characterization	Characterization plan, fieldwork, laboratory analysis	CPT pushes for geologic mapping and temporary wells; analysis of water samples for CVOCs; select samples for geotechnical analysis; slug tests; ground-penetrating radar survey	\$200,000
Column tests	Two column tests; Area 5 groundwater	Column tests and laboratory analysis of water samples; report	\$50,000
Design; procurement of subcontractors; regulatory review	Data evaluation, modeling, engineering design, Design Plan; procurement of subcontractors; interactions with regulators	Characterization, column test data evaluation; hydrogeologic modeling; geochemical evaluation; engineering design; report; procurement process; regulatory interactions	\$100,000
Subtotal			\$365,000
Phase 2: PRB Construction			
Site preparation	Utilities clearances; arrangements for equipment/media storage and debris disposal	Coordination with regulators and Base facilities staff	\$10,000
Reactive media procurement	Connelly iron, shipping	Iron: 108 tons @ \$360/ton Shipping: \$9,000	\$48,000
PRB construction	Mobilization/demobilization; installation of four 8-ft-diameter caisson gates to 40-ft depth, and one 120-ft-long sheet pile funnel; asphalt parking lot restoration	Mob./demob.: \$60,000 Gates: \$266,000 Monitoring wells: \$25,000 Funnel: \$102,000 Surface restoration: \$34,000	\$487,000
Monitoring system construction	Thirty-four PVC aquifer wells installed for monitoring the PRB	Aquifer wells: \$37,000	\$37,000
Subtotal			\$582,000
TOTAL			\$947,000

In the category of construction, mobilization/demobilization costs have been increased compared to the pilot system in order to reflect transportation of additional sheet piles and other materials. For a full-scale system, the same number of wells as currently installed for the pilot-scale system could be redistributed over the four gates; a higher number of wells was used for demonstration purposes for the pilot system. The costs for the gates, funnel, and surface restoration have been doubled to reflect the addition of two more gates and another 60 ft of funnel. The aquifer monitoring system cost was kept the same, based on the assumption that the same number of wells could be spread over a larger area. Also, the HydroTechnics velocity meters have been eliminated.

8.3 Projected Operating and Maintenance Costs

The expected O&M costs of the full-scale barrier over the next several years consist of:

- ❑ *Annual monitoring cost.* This item relates to the groundwater sampling and analysis and water-level measurements that would be required to verify acceptable capture and treatment of the plume.
- ❑ *Periodic maintenance cost.* Assuming that the reactivity and/or hydraulic performance of the reactive cell may decline before the plume (or the possible DNAPL source) dissipates, it is probable that some maintenance would be required to regenerate or replace the reactive medium.

It is presumed that groundwater sampling for CVOC analysis would have to be conducted on a quarterly basis, consistent with the regulatory sampling conducted on the rest of the Base. Water levels also could be measured on a quarterly basis to track seasonal flow conditions. Groundwater sampling for inorganic analysis may be required only once a year or once in two years to track the geochemical environment. Other measurements, such as iron core evaluation, may be considered only if required. Table 8-3 provides the projected cost of such a monitoring schedule.

Table 8-3. O&M Costs Projected for Operating a Full-Scale PRB in Area 5

Item	Description	Basis	Cost
<i>Annual Monitoring Activities</i>			
Groundwater sampling	Quarterly, labor, materials, travel	40 wells	\$80,000
CVOC analysis	Quarterly, 40 wells	44 per quarter @ \$120/sample	\$20,000
Inorganic analysis	Annual, 20 wells	22 @ \$150/sample	\$4,000
Water-level survey	Quarterly, labor	40 wells per quarter	\$4,000
Data analysis; report; regulatory review	Quarterly, labor	Four times per year	\$40,000
Annual operating cost			\$148,000
<i>Maintenance Activities (once every 10 years assumed as an illustration)</i>			
Site preparation	Permitting, clearances	Labor	\$10,000
Reactive media procurement	Connelly iron, shipping	Iron: 108 tons @ \$360/ton Shipping: \$9,000	\$48,000
Removal/replacement of gates	Mobilization/demobilization; installation of four 8-ft-diameter caisson gates to 39-ft depth; asphalt parking lot restoration	Mob./demob.: \$38,000 Gates: \$266,000 Monitoring wells: \$25,000 Surface restoration: \$34,000	\$363,000
Periodic maintenance cost (once every 10 years assumed)			\$421,000

Estimating the maintenance cost of the PRB is more difficult. First, the frequency at which such maintenance would be required is unknown. PRBs are a fairly recent development; the longest running PRB has been in the ground for about 5 years. Long-term column tests at accelerated flow rates have been conducted, but extrapolating the results to field conditions has proved difficult. A rule-of-thumb approximation has been proposed and used in the past at some sites to project the cost of long-term maintenance. This approximation suggests a maintenance requirement that 25% of the iron medium would have to be replaced every 5 or 10 years, depending on the level of dissolved solids (or potential for precipitation) in the groundwater. However, there are no data to really drive such projections.

Also, it is unclear as to what physical means would be applied to remove and replace the reactive medium. Presumably, the contents of the gates could be removed with an auger after installing temporary sheet piles along the upgradient and downgradient edges of the reactive cells to retain the sides of the excavation. However, such removal activities may not be easy given that the shape of the reactive cell is square, and that augering probably would be impeded by the presence of monitoring wells. Fresh iron then could be installed in a manner similar to that for the new installation. All the costs in the construction category in Table 8-2 would be incurred, except for the funnel cost. This assumes that all of the reactive medium in the gate is to be replaced; partial removal and replacement would be much more difficult.

Based on these assumptions for monitoring and maintenance, Table 8-3 shows the projected O&M costs for the PRB over the next 30 years. As an illustration, Table 8-3 assumes that periodic maintenance to replace the reactive medium will be required once every 10 years, which is a very conservative assumption. Maintenance is assumed to involve replacement of all the iron in the gates. Maintenance costs are similar to the construction costs of the original gates. The funnel cost and the aquifer monitoring system costs in Table 8-2 have been dropped in Table 8-3. Additional scenarios involving periodic maintenance requirements of every 20 or 30 years are discussed in Section 8.4. Because the longevity of the reactive medium cannot be predicted with certainty, these multiple scenarios show the dependency of the economics of the PRB on the longevity of the reactive medium.

8.4 Present Value Analysis of PRB and P&T Options

The PRB technology is an innovative alternative to conventional P&T systems. As compared with a P&T system, a PRB offers the benefits of passive operation (no external energy input required for operation) and absence of aboveground structures. A long-term comparison of these two technology options for Area 5 is presented in this section. For this comparison, the capital investment and O&M cost of an equivalent P&T system were estimated as shown in Appendix H, and are summarized here in Tables 8-4 and 8-5. The estimated P&T system costs for Area 5 are based on a similar system designed, built, and tested in a CVOC plume in a different area at Dover AFB (Battelle, 1994).

A comparable P&T system for plume migration control would have to capture the same volume of groundwater as the full-scale PRB with four gates. At the maximum flowrate of 4.1 ft/day

Table 8-4. Capital Investment Projected for Installing a P&T System in Area 5

Item	Description	Basis	Cost ^(a)
Phase 1: Preconstruction Activities			
Preliminary site assessment	Historical site data evaluation	Remedial Investigation/Feasibility Study, other reports procurement and evaluation; site meeting	\$15,000
Site characterization	Characterization Plan, fieldwork, laboratory analysis	CPT pushes for geologic mapping and temporary wells; analysis of water samples for CVOCs and inorganics; slug tests in existing wells	\$200,000
Design; procurement; regulatory review	Data evaluation, modeling, engineering design, Design Plan; procurement; regulatory interactions	Characterization data analysis; hydro-geologic modeling; engineering design; report; procurement; regulatory review	\$100,000
Subtotal			\$315,000
Phase 2: P&T System Construction			
Site preparation	Utilities clearances; arrangements for equipment storage	Coordination with regulators and Base facilities staff	\$10,000
P&T system construction	Installation of three 4-inch-diameter extraction wells; pumps; air stripper; catalytic oxidizer; polishing carbon; shed; piping	20-gpm groundwater extraction and treatment system	\$145,000
Monitoring system construction	Thirty PVC aquifer wells installed for monitoring plume movement	Aquifer wells: \$32,000	\$32,000
Subtotal			\$187,000
TOTAL			\$502,000

(a) Based on a similar P&T system designed, built, and tested for a CVOC plume in a different area at Dover AFB (Battelle, 1994). Details are in Appendix H.

Table 8-5. O&M Costs Projected for Operating a P&T System in Area 5

Item	Description	Basis	Cost ^(a)
Annual System O&M (includes routine maintenance)			
System operation	Keeping P&T system operational	Labor, energy consumption, materials replacement, waste handling, routine maintenance, replacement of pumps, etc.	\$66,000
Groundwater monitoring	Quarterly, 40 wells; CVOC, inorganics, water levels	Labor, materials, analytical	\$148,000
Annual operating cost			\$214,000
Periodic Maintenance (once every 10 years)			
Carbon replacement	Polishing carbon for liquid	Used carbon disposal, new carbon installation	\$7,000
Periodic Maintenance (once every 5 years)			
Catalyst replacement	Oxidizer catalysts for effluent air treatment	Used catalyst disposal, new catalyst installation	\$21,000

(a) Based on a similar P&T system designed, built, and tested for a CVOC plume in a different area at Dover AFB (Battelle, 1994). Details are in Appendix H.

through each gate, the PRB is expected to capture the equivalent of approximately 10 gallons per minute (gpm) of flow. Because of possible capture inefficiencies with extraction wells, the P&T system is designed to capture and treat twice as much, or 20 gpm. As described in Table H-1 (in Appendix H) and Table 8-4, the investment in the P&T system includes three extraction wells, pumps, an air stripper to transfer CVOCs to air, a catalytic oxidizer to treat the air effluent from the stripper, and polishing carbon to remove any residual CVOCs down to MCLs.

The O&M cost of the P&T system is described in Table H-2 in Appendix H, and summarized in Table 8-5. The projected cost consists of an annual operating and routine maintenance costs to keep the system running, an annual groundwater monitoring cost, and periodic maintenance costs. The periodic maintenance costs involve replacement of the carbon every 10 years and replacement of the catalyst every 5 years. Tables 8-4 and 8-5 indicate that the P&T system requires a lower initial capital investment as compared to the PRB, but incurs higher O&M costs, primarily because of the labor and energy requirements to operate the P&T system. The P&T system requires more frequent periodic maintenance in the form of carbon and catalyst replacement. Because the PRB and P&T system require maintenance at different points in time and because the CVOC plume is expected to last for several years or decades, a present value analysis is required to consolidate the capital investment and long-term O&M costs into a total (cumulative) application cost in today's dollars.

Table 8-6 shows the discounted cash flow (i.e., present value) analysis of the capital investment and O&M costs over 30 years for both PRB and P&T system options. A real discount rate of 2.9% is used in the analysis, as per the 1999 update to the U.S. EPA Office of Management and Budget's circular (U.S. EPA, 1993). For illustration purposes, it is assumed that the PRB will maintain its reactivity and hydraulic performance over 10 years of operation, after which all four gates will have to be removed and replaced (at an estimated total cost of \$421,000 as shown in Table 8-3). The present values of the capital investment and annual (i.e., O&M) costs are listed in columns 3 and 6, and indicate that the further back in time that the cost occurs, the lower its present value. Columns 4 and 7 list the cumulative present value at the end of each year; the cumulative present value includes the capital investment and the present value of all the O&M costs up to that year. The year in which the cumulative PV cost of the PRB is equal to or below cumulative present value cost of the P&T system is the payback period or break even point for the PRB.

As shown in Table 8-6, there are two break-even times for the PRB in this illustration (indicated by the shaded cells in the table). In Year 8, the cumulative or total present value cost of the PRB becomes lower than the present value cost of the P&T system, indicating the first break-even point. However, in Year 10, the extraordinary maintenance cost of replacing the iron in the four gates is incurred, which makes the total cost of the PRB slightly higher again than the pump-and-treat system. In Year 14, the total present value cost of the PRB again becomes lower, and this is the true break-even point. In other words, over 14 years, the lower annual operating cost (passive operation) of the PRB makes it a worthwhile investment. At the end of the analysis period of 30 years, the present value of the total savings from implementing a PRB versus a P&T system is \$239,000 (that is, the difference between the cumulative costs of \$4,618,291 and \$4,857,476 for the PRB and P&T system at the end of 30 years).

**Table 8-6. Present Value Analysis of PRB and P&T Systems in Area 5 Assuming
10-Year Life of PRB**

Year	PRB			P&T System		
	Annual Cost ^(a)	Present Value of Annual Cost ^(b)	Cumulative Present Value of Annual Cost ^(c)	Annual Cost ^(a)	Present Value of Annual Cost ^(b)	Cumulative Present Value of Annual Cost ^(c)
0	\$947,000 ^(d)	\$947,000	\$947,000	\$502,000 ^(d)	\$502,000	\$502,000
1	\$148,000 ^(e)	\$143,829	\$1,090,829	\$214,000 ^(e)	\$207,969	\$709,969
2	\$148,000	\$139,775	\$1,230,604	\$214,000	\$202,108	\$912,077
3	\$148,000	\$135,836	\$1,366,441	\$214,000	\$196,412	\$1,108,489
4	\$148,000	\$132,008	\$1,498,449	\$214,000	\$190,876	\$1,299,365
5	\$148,000	\$128,288	\$1,626,736	\$235,000	\$203,700	\$1,503,065
6	\$148,000	\$124,672	\$1,751,408	\$214,000	\$180,269	\$1,683,334
7	\$148,000	\$121,159	\$1,872,567	\$214,000	\$175,189	\$1,858,523
8	\$148,000	\$117,744	\$1,990,311	\$214,000	\$170,251	\$2,028,774
9	\$148,000	\$114,426	\$2,104,737	\$214,000	\$165,453	\$2,194,228
10	\$569,000^(f)	\$427,522	\$2,532,259	\$242,000	\$181,828	\$2,376,056
11	\$148,000	\$108,067	\$2,640,326	\$214,000	\$156,259	\$2,532,315
12	\$148,000	\$105,021	\$2,745,347	\$214,000	\$151,855	\$2,684,170
13	\$148,000	\$102,061	\$2,847,408	\$214,000	\$147,575	\$2,831,745
14	\$148,000	\$99,185	\$2,946,593	\$214,000	\$143,416	\$2,975,162
15	\$148,000	\$96,390	\$3,042,983	\$235,000	\$153,051	\$3,128,213
16	\$148,000	\$93,673	\$3,136,656	\$214,000	\$135,446	\$3,263,659
17	\$148,000	\$91,033	\$3,227,690	\$214,000	\$131,629	\$3,395,289
18	\$148,000	\$88,468	\$3,316,158	\$214,000	\$127,920	\$3,523,208
19	\$148,000	\$85,974	\$3,402,132	\$214,000	\$124,314	\$3,647,523
20	\$569,000^(f)	\$321,222	\$3,723,354	\$242,000	\$136,618	\$3,784,141
21	\$148,000	\$81,197	\$3,804,550	\$242,000	\$132,768	\$3,916,908
22	\$148,000	\$78,908	\$3,883,459	\$214,000	\$114,097	\$4,031,006
23	\$148,000	\$76,685	\$3,960,143	\$214,000	\$110,882	\$4,141,887
24	\$148,000	\$74,523	\$4,034,667	\$214,000	\$107,757	\$4,249,644
25	\$148,000	\$72,423	\$4,107,090	\$235,000	\$114,996	\$4,364,641
26	\$148,000	\$70,382	\$4,177,472	\$214,000	\$101,769	\$4,466,409
27	\$148,000	\$68,399	\$4,245,871	\$214,000	\$98,901	\$4,565,310
28	\$148,000	\$66,471	\$4,312,341	\$214,000	\$96,113	\$4,661,423
29	\$148,000	\$64,598	\$4,376,939	\$214,000	\$93,405	\$4,754,827
30	\$569,000^(f)	\$241,352	\$4,618,291	\$242,000	\$102,649	\$4,857,476

- (a) Annual cost is equal to the capital investment in Year 0 and the O&M cost in subsequent years.
(b) Present value cost is the annual cost divided by a discount factor term based on a 2.9% discount rate, as detailed in Appendix H.
(c) Cumulative present value cost is the sum of annual present value costs in each year and previous years.
(d) Initial capital investment.
(e) Annual O&M cost.
(f) Annual monitoring cost of \$148,000, plus maintenance/replacement of gates for \$421,000.

Because the break-even point is sensitive to the assumption on the life of the reactive medium, the present value analysis was repeated assuming that the life of the PRB is 20 or 30 years (see Tables H-3 to H-5 in Appendix H). Because the plume may persist for 50 years or more, an additional scenario for 50 years of operation (and PRB maintenance after the first 30 years) also was evaluated (see Table H-6 in Appendix H). Table 8-7 summarizes the results of running these scenarios.

Table 8-7. Break-Even Point and Savings by Using a PRB Instead of a P&T System at Area 5

Assumed Life of Reactive Medium	Break-Even Point	Present Value of Savings at the End of 30 Years	Time Period of Application^(a) (t)
10 years	14 years	\$239,000	30 years
20 years	8 years	\$734,000	30 years
30 years	8 years	\$793,000	30 years
30 years	8 years	\$1,251,000	50 years

(a) Assumes PRB or P&T system is applied as long as the plume persists.

As seen in Table 8-7, even if the PRB lasts only 10 years, it is less expensive than a P&T system. The longer the PRB lasts, the greater the savings. Assuming that the PRB lasts for 30 years without requiring maintenance and is applied at the site for 50 years or more for plume treatment, the present value of the savings realized is more than \$1 million.

Although considerable savings or cost advantages are realized by using a PRB in Area 5, the savings estimated at some other sites have been higher (Battelle, 1998; Gavaskar et al., 2000). One reason for this is that, in many previous studies, higher discount rates (8 to 15%) have been used to calculate the present value of the two technologies. Because of lower expected inflation, U.S. EPA's recommendations (U.S. EPA, 1993) for discount rates have dropped considerably. This makes the postponement of O&M costs later into the future, as in the case of the PRB, look relatively less attractive than when inflation is higher.

Using a continuous reactive barrier (no funnel) configuration instead of a funnel-and-gate system has been found to result in additional savings at some sites. However, because of the underground utilities at Area 5, a continuous reactive barrier would be more difficult to install. Other innovative PRB construction techniques, such as jetting and hydrofracturing, are being investigated at some sites. These innovative techniques offer the potential for lowering the construction cost at deeper sites. In summary, continuous reactive barrier configurations and/or innovative construction techniques offer the potential for further lowering the PRB construction cost for future applications.

Note that this present value cost analysis only takes into account the more tangible costs of the two options. A significant intangible benefit of using a PRB in Area 5 is that there are no

aboveground structures involved, and the site can still be used as a parking lot. With a P&T system, there would be some loss of space for housing the piping and aboveground treatment equipment. The ability of site owners to use, lease, or sell the space that would have been taken up by a P&T system, and to improve the attractiveness of the property as a whole, is a significant benefit of PRB technology. P&T systems also have a high reported percentage of shutdown time. The degree of operator attention and maintenance time eliminated by installing a PRB instead of a P&T system also is a significant advantage.

9. Results and Conclusions

Monitoring of the PRB in Area 5 at Dover AFB over the 18 months following its installation indicated the performance trends discussed in this section.

9.1 Reactive Performance of the Area 5 PRB

PCE, TCE, and *cis*-1,2-DCE concentrations in the groundwater declined to below their respective MCLs along the flowpath through both gates. This result indicates that, to date, sufficient residence time was available for complete degradation of the target CVOCs at their influent concentrations. Long-term column tests, such as those conducted by the U.S. EPA (1997) were found to be useful for comparing candidate reactive media for a PRB and for determining design parameters, such as reaction rates (half-lives) of contaminants and potential for precipitation.

The maximum influent CVOC concentrations entering the PRB to date were measured at 520 and 480 µg/L of PCE at Gates 1 and 2, respectively. The maximum concentration detected in the expected capture zone of the PRB is 3,900 µg/L of PCE. Lesser concentrations of TCE and *cis*-1,2-DCE also are present in the plume. The field residence time (1 to 9 days) estimated in the reactive cell by the PRB is expected to be sufficient to degrade these higher concentrations to the respective MCLs because of the following reasons:

- ❑ The current CVOC concentrations in the groundwater influent are being degraded to MCLs either in the PTZ or in the first 1 ft of the reactive cell, indicating that the residence time probably is closer to the upper end of the estimated range (i.e., 9 days).
- ❑ The safety factor of 2 incorporated in the design thickness of the reactive cell and the higher CVOC influent concentrations assumed in the design allow for the uncertainties in the field residence time and influent CVOC concentrations.

9.2 Hydraulic Performance of the Area 5 PRB

Evaluation of the residence time in the reactive cells and the capture zone of the PRB were the main objectives of the hydraulic performance evaluation. The results of the demonstration indicated the following:

- ❑ The estimated range of residence times in each reactive cell is 1 to 9 days. This estimate is based on a representative range of gate velocities of 0.46 to 4.1 ft/day measured during the demonstration. Aquifer heterogeneities, differential packing of the media in the two gates, and seasonal fluctuations in groundwater flow volume and direction contribute to this relatively wide range of estimates. However, degradation rates (and half-lives) measured in the field and the expected hydraulic capture zone estimated from water-level maps indicate that the groundwater velocity is much closer to

0.46 ft/day than to 4.1 ft/day. Therefore, the probable residence time is closer to the higher end of the range (i.e., 9 days).

- The higher end of the estimated gate velocity range (near 4.1 ft/day) in the field PRB was higher than the range of model velocities (0.2 to 0.5 ft/day) used in the design. The lower model velocities were based on a hydraulic conductivity (K) of 283 ft/day, which was the prevalent value also used for PRB design at several previous sites (EnviroMetal Technologies, Inc., 1997; Starr and Cherry, 1994). Subsequently, slug tests conducted in the two gates in the Area 5 PRB and geotechnical laboratory analysis of the gate media indicated K values as high as 812 ft/day, which led to the higher field velocity estimates and, consequently, lower residence time estimates based on the use of Darcy's equation. The relatively flat hydraulic gradient across the reactive cell makes velocity and residence time estimation using Darcy's equation difficult.
- Because of the safety factor of 2 incorporated in the design thickness, the PRB should be able to meet MCLs even when higher CVOC concentrations (3,900 µg/L of PCE) are encountered at the gates in the future.
- A relatively strong hydraulic gradient along the flowpath (upgradient aquifer to downgradient aquifer) through both gates indicates that groundwater *is* being captured by the PRB. However, due to the low overall hydraulic gradient in the upgradient aquifer, the size and orientation of the capture zone cannot be determined with certainty. In all probability, the capture zone is about 40 to 50 ft wide, an estimate based on the estimated range of flow velocities in the gates, the measured hydraulic gradients through the gates, and the measured water levels in the upgradient aquifer. Given the seasonal changes in flow, the capture zone may not always be symmetric or oriented perpendicular to the funnel.
- Although the overall hydraulic gradient through both gates was strongly positive in all the surveys done so far, water levels measured at intermediate locations sometimes show a slightly negative local gradient near the exit zones of the two gates. These results may indicate transient stagnant conditions near the exit zone, as the water tries to flow from the high-K gate into the low-K aquifer. However, even in those surveys that showed some stagnation in the exit zone, the overall gradient across the gate remained positive, indicating that groundwater always flowed in the expected direction.
- The two in situ flow velocity sensors from HydroTechnics that were installed in the upgradient aquifer showed a velocity range of 0.03 to 0.09 ft/day, which was a good match with the aquifer velocity range of 0.026 to 0.16 ft/day estimated from water-level surveys and slug tests. There is some uncertainty about the flow direction shown by these sensors. Both sensors tended to point towards the eastern wing wall of the funnel rather than toward Gate 1. At the time of installation, it was expected

that at least the sensor closer to the gate would point towards the gate. However, groundwater modeling indicates that the flow lines approaching the PRB come very close to the funnel before turning toward the gate; that is, the range of influence of the barrier extends less than 5 ft upgradient of the funnel. The sensors, which are located about 6 ft upgradient of the funnel, may be beyond the range of influence of the PRB. In addition, because of seasonal fluctuations, groundwater seldom flows perpendicular to the funnel and the capture zone at most times is probably asymmetric. In the future, if an objective is to use in situ flow sensors to verify groundwater capture, it may be better to place them as close to the funnel as possible.

- The two velocity sensors located inside the reactive cell of each gate both showed a flow direction consistent with flow through the gate. However, the velocity magnitude estimates from the sensors are much lower than either the velocities estimated through water-level measurements and slug tests inside the gates or the velocity predicted by modeling. The sensors in the reactive cells had to be specially calibrated for the iron medium (as opposed to the typical aquifer medium for which they are generally calibrated). It is possible that the much higher heat conductivity of the iron affected the calibration of these instruments. Therefore, there is a great deal of uncertainty in the velocity and direction readings from these two sensors.
- The probable hydraulic capture zone width, based on water-level maps and field degradation rates, is approximately 40 to 50 ft. The capture zone probably is asymmetric at most times due to seasonal variations in flow direction.

9.3 Geochemical Performance of the Area 5 PRB

Evaluating the type and degree of precipitate formation and deposition in the two reactive cells was the main objective of the geochemical performance evaluation. Precipitation in the reactive cell is expected to be the main factor limiting the longevity of the PRB. The following conclusions were based on the results of the demonstration:

- DO and ORP levels in the groundwater decline along the flowpaths, indicating that a strong reducing environment is created in both gates. A strongly reducing environment is essential for the abiotic reductive dechlorination of CVOCs in groundwater.
- The PTZs in both gates succeeded in removing DO from the groundwater before it entered the reactive cells. The PTZ containing iron (Gate 1) was more efficient at removing DO than the PTZ containing pyrite (Gate 2).
- Groundwater pH declined in the PTZ containing pyrite (Gate 2), whereas it increased in the PTZ containing iron (Gate 2). However, this pH reduction by the pyrite was not sustained once the groundwater entered the reactive cell. These results indicate that the 100% iron in the reactive cell overwhelms any pH control effect achieved by the pyrite in the PTZ. The pH of the groundwater increased significantly as the groundwater entered the reactive cells in both gates.

- ❑ The proportion (10%) of pyrite used in the Gate 2 PTZ was adequate for the dimensions of the PTZ because all available DO was consumed in the PTZ. Once DO is removed, the pyrite is not expected to provide any additional pH control.
- ❑ Very little precipitate buildup was observed in cores from both gates after 18 months of PRB operation. Manganese, nitrates, and silica were the predominant species that appeared to be precipitating under the pH, ORP, and alkalinity conditions prevalent in the aquifer and PRB. Available information is insufficient to make any conclusions about the long-term performance (i.e., longevity) of the PRB.

9.4 Economics of PRB Application at Area 5

The economic evaluation was based on the estimated cost of a full-scale PRB at Area 5 for the capture of a 100-ft-wide plume. The long-term cost of this full-scale PRB, an expanded funnel-and-gate system with four gates, was compared to the cost of a conventional P&T system. The evaluation indicated the following:

- ❑ Although the capital investment required for the PRB exceeds the capital investment required for an equivalent P&T system, the P&T system has higher O&M cost requirements.
- ❑ Over a long-term application, the passive operation of the PRB, with the concomitantly lower O&M cost, results in enough savings to make it more economical than an equivalent P&T system.
- ❑ The longer the term of the application (i.e., the longer the DNAPL source and/or the longer the plume persists), the greater the savings.
- ❑ The economics of the PRB are sensitive to the assumed life-span of the reactive medium. The longer the reactive medium lasts without requiring regeneration or replacement, the faster the savings are realized. For example, if the PRB in Area 5 lasts for 30 years, the costs break even with the P&T system after just 8 years. On the other hand, if the reactive medium has to be changed within 10 years, the break-even time is 14 years. In the absence of clear geochemical predictions on the longevity of the Area 5 PRB, these economic scenarios were developed as a way of evaluating the expectations from the PRB technology.

9.5 Recommendations

The lessons learned from the demonstration and the recommendations for future PRB application are as follows:

- ❑ Adequate site characterization is the most important factor governing the successful design and construction of a PRB.

- Understanding and controlling hydraulic flow conditions in a very local setting is difficult, especially at sites with a low hydraulic gradient. Although regional flow conditions on a scale of hundreds of feet are fairly well understood at most sites, local flow on the scale of a few feet or few tens of feet can be difficult to analyze. Uncertainties caused by seasonal flow fluctuations and local aquifer heterogeneities often lead to a wide range of estimates for flow velocity and direction. The resulting design needs to take this uncertainty into account.
- Hydraulic modeling is a useful tool for simulating multiple flow scenarios based on historical flow conditions. These simulations, along with appropriate safety factors, are important for a successful PRB design.
- Although there is general agreement among various studies about the estimate of field bulk density or field porosity (about 0.6 to 0.7) of granular iron medium in the -8+50 mesh size range, there still are differences in the field values of hydraulic conductivity (K). K values of 142 ft/day or 283 ft/day have been used for modeling and design of PRBs at previous sites. However, geotechnical laboratory tests and field slug tests in the reactive cell at Dover AFB have indicated a K as high as 812 ft/day, which leads to higher groundwater velocity estimates and lower residence time estimates in the reactive cell. This discrepancy needs to be resolved with similar tests for the reactive media at other PRB sites. One explanation for the difference could be the iron source. Well-sorted iron with more particles in the higher end of the -8+50 mesh size range may be expected to have a higher K. Poorly sorted iron with a greater proportion of fines may be expected to have a lower K. It is recommended that, for future applications, the source of iron should be determined during the draft design stage, and the final design should incorporate a K determined from geotechnical laboratory tests with a representative sample of iron from the source. Slug tests may be used after PRB construction to verify the field K value, an important determinant of flow volume, flow velocity, and residence time in the reactive medium. The improved measurement of K may still leave significant uncertainty in gate velocity, because it would be very difficult to achieve a corresponding improvement in hydraulic gradient measurement across short distances.
- The HydroTechnics sensor may be a useful device for estimating groundwater velocity in the aquifer during site characterization. However, these sensors should be used at multiple locations in the aquifer to evaluate the spatial variability on the scale of the planned PRB. The use of these sensors for evaluating the capture zone of a PRB is still unclear, because the scale of the sensor measurement relative to the scale of the bulk flow near the barrier is unclear. The applicability of these sensors inside the reactive cell also is uncertain because the effectiveness of their calibration in the iron medium is unclear. The use of downhole or in situ sensors, such as the ones from HydroTechnics, KVA, or the DOE, needs to be studied further under more controlled conditions.

- The ability of granular iron to degrade CVOCs down to target MCLs under laboratory and field conditions has now been proven at this and other sites. CVOC half-life estimates generally are consistent between column and field tests. Rather, the design challenge lies with assuring sufficient residence time for the groundwater in the reactive cell. Given the uncertainties in defining hydraulic flow conditions, the PRB should be designed for the full range of flow conditions anticipated, rather than for average flow conditions. A safety factor between 2 to 4 for the design thickness of the reactive cell may be advisable, depending on the design team's confidence in their understanding of the flow system at a site. A safety factor of around 1.5 to 2 also may be considered for the width of the reactive cell or continuous reactive barrier at any site. These safety factors will increase the dimensions, and hence the cost, of the PRB; however, they will result in a more robust design with respect to residence time and plume capture.

- Judging the longevity of a PRB based on geochemical data evaluation remains a challenge. Evaluation of groundwater geochemistry and iron cores currently appears to be geared more towards assessing past performance rather than predicting future performance. This is because of two reasons: First, it is unclear how much of the precipitates formed, as estimated from the loss of geochemical constituents between PRB influent and effluent groundwater, actually stay in the reactive cell, instead of being removed by colloidal transport. Movement of colloids and deposition of silica in the reactive cell are two areas where further research is required. Second, even if the mass of precipitates retained in the reactive cell could be estimated, the point in time when this mass will adversely affect the reactive and hydraulic performance is unclear. Accelerated long-term column tests, with all their limitations, may still be an important predictive tool. The usefulness of these tests to arrive at conservative predictions of the longevity of the reactive medium merits serious consideration.

- In the absence of clear geochemical predictions on the longevity of a PRB, the economic scenarios developed in this report may be considered as a tool for comparing the relative merits of PRB and P&T applications at a prospective site. These scenarios compare the present value costs of both options under different assumptions about the longevity of the PRB.

- The use of caissons for installing the reactive medium in the ground is a viable option for relatively deep sites or for sites with several underground utilities. Other innovative construction techniques that are being studied, such as jetting and hydrofracturing, may further improve the economics of PRB application at deeper sites.

10. References

Agrawal, A., and P.G. Tratnyek. 1996. "Reduction of Nitro Aromatic Compounds by Zero-Valent Iron Metal." *Environ. Sci. Technol.*, 30(1): 153-160.

Applied Research Associates, Inc. 1996. *Groundwater Remediation Field Laboratory—GRFL: Hydrogeology Characterization and Site Development, Volume I: Site Characterization and Development*. September.

ARA, see Applied Research Associates, Inc.

Battelle. 1994. *Final Report: Crossflow Air Stripping with Catalytic Oxidation*. Prepared by Battelle, Columbus, OH for Environics Directorate, Armstrong Laboratory, Tyndall AFB, FL. September.

Battelle. 1997. *Design/Test Plan: Permeable Barrier Demonstration at Area 5, Dover AFB*. Prepared for Air Force Research Laboratory.

Battelle. 1998. *Performance Evaluation of a Pilot-Scale Permeable Reactive Barrier at Former Naval Air Station Moffett Field, Mountain View, California*. Prepared for NFESC and ESTCP. November 20.

Bouwer, H. 1989. "The Bouwer and Rice Slug Test—an Update." *Ground Water*, 27(3): 304-309.

Bouwer, H., and R.C. Rice. 1976. "A Slug Test for Determining Hydraulic Conductivity of Unconfined Aquifers with Completely or Partially Penetrating Wells." *Water Resources Research*, 12(3): 423-428.

Burris, D.R., T.J. Campbell, and V.S. Manoranjan. 1995. "Sorption of Trichloroethylene and Tetrachloroethylene in a Batch Reactive Metallic Iron-Water System." *Environ. Sci. Technol.*, 29(11): 2850-2855.

C³ Environmental. 1998. *Permeable Barrier Installation Report, Dover Air Force Base, Dover, Delaware*. Prepared for Battelle. March 19.

Dames and Moore. 1995. *Draft Report: West Management Unit Remedial Investigation: Dover Air Force Base, Dover, DE*. April.

Deng, B., T.J. Campbell, and D.R. Burris. 1997. "Hydrocarbon Formation in Metallic Iron/Water Systems." *Environ. Sci. Technol.*, 31(4): 1185-1190.

EnviroMetal Technologies, Inc. 1995. Marketing literature from EnviroMetal Technologies, Inc., Guelph, Ontario.

EnviroMetal Technologies, Inc. 1996. Personal communication from John Vogan, EnviroMetal Technologies, Inc., Guelph, Ontario.

EnviroMetal Technologies, Inc. 1997. Personal communication from John Vogan of EnviroMetal Technologies, Inc., Guelph, Ontario, to Battelle, in form of memo titled "Bench-Scale Evaluation of the EnviroMetal Process (Metal Enhanced Reductive Dehalogenation) at a U.S. Air Force Base."

ETI, see EnviroMetal Technologies, Inc.

Gavaskar, A. G., N. Gupta, B. Sass, T. Fox, R. Janosy, K. Cantrell, and R. Olfenbuttel. 2000. *Design Guidance for Application of Permeable Reactive Barriers for Groundwater Remediation*. Final. Prepared for AFRL, Tyndall AFB, FL. March 31.

Gillham, R.W. 1993. Cleaning Halogenated Contaminants from Groundwater. U.S. Patent No. 5,266,213. Nov. 30.

Gillham, R.W. 1996. "In Situ Treatment of Groundwater: Metal-Enhanced Degradation of Chlorinated Organic Contaminants." In M.M. Aral (Ed.), *Advances in Groundwater Pollution Control and Remediation*, pp. 249-274. Kluwer Academic Publishers: Hingham, MA.

Gillham, R.W., and S.F. O'Hannesin. 1992. "Metal-Catalyzed Abiotic Degradation of Halogenated Organic Compounds." *IAH Conference: Modern Trends in Hydrogeology*. Hamilton, Ontario, May 10-13, pp. 94-103.

Gillham, R.W., and S.F. O'Hannesin. 1994. "Enhanced Degradation of Halogenated Aliphatics by Zero-Valent Iron." *Ground Water*, 32: 958-967.

Gupta, N., and T.C. Fox. 1999. "Hydrogeologic Modeling for Permeable Reactive Barriers." *Journ. Haz. Mat.*, 68: 19-39.

Hardy, L.I., and R.W. Gillham. 1996. "Formation of Hydrocarbons from the Reduction of Aqueous CO₂ by Zero-Valent Iron." *Environ. Sci. Technol.*, 30(1): 57-65.

Interstate Technology and Regulatory Cooperation Working Group. 1997. *Regulatory Guidance for Permeable Barrier Walls Designed to Remediate Dissolved Chlorinated Solvents*. Prepared by ITRC Work Group Permeable Barriers Work Team.

Interstate Technology and Regulatory Cooperation Working Group. 1999. *Regulatory Guidance for Permeable Reactive Barriers Designed to Remediate Inorganic and Radionuclide Contamination*. Draft. Prepared by ITRC Work Group Permeable Barrier Walls Work Team. January 29.

ITRC, see Interstate Technology and Regulatory Cooperation Working Group.

McDonald, M.G. and A.W. Harbaugh. 1988. "A Modular Three-Dimensional Finite-Difference Ground-Water Flow Model." *Techniques of Water Resources Investigations of the United States Geological Survey. Book 6: Modeling Techniques*. U.S. Department of the Interior, Geological Survey.

Naymik, T.G., N.J. Gantos, and G. Yu. 1995. *Reference Manual for Random-Walk Solute Transport Codes, RWLK3D/GUI and RWLK3D*. Version 1.0. Battelle Internal Research and Development.

O'Hannesin, S.F. 1993. A Field Demonstration of a Permeable Reaction Wall for the In Situ Abiotic Degradation of Halogenated Aliphatic Organic Compounds. Unpublished M.S. thesis, University of Waterloo, Ontario, Canada.

Orth, W.S., and R.W. Gillham. 1996. "Dechlorination of Trichloroethene in Aqueous Solution Using Fe(0)." *Environ. Sci. Technol.*, 30(1): 66-71.

Parkhurst, D.L. 1995. *User's Guide to PHREEQC—A Computer Program for Speciation, Reaction-Path, Advective-Transport, and Inverse Geochemical Calculations*. USGS 95-4227. Lakewood, CO.

Reardon, E.J. 1995. "Anaerobic Corrosion of Granular Iron: Measurement and Interpretation of Hydrogen Evolution Rates." *Environ. Sci. Technol.*, 29(12): 2936-2945.

Reynolds, G.W., J.T. Hoff, and R.W. Gillham. 1990. "Sampling Bias Caused by Materials Used to Monitor Halocarbons in Groundwater." *Environ. Sci. Technol.*, 24(1): 135-142.

Senzaki, T. 1988. "Removal of Chlorinated Organic Compounds from Wastewater by Reduction Process: III. Treatment of Tetrachloroethane with Iron Powder II." *Kogyo Yosui*, 391: 29-35 (in Japanese).

Senzaki, T., and Y. Kumangai. 1988a. "Removal of Chlorinated Organic Compounds from Wastewater by Reduction Process: Treatment of 1,1,2,2-Tetrachloroethane with Iron Powder." *Kogyo Yosui*, 357: 2-7 (in Japanese).

Senzaki, T., and Y. Kumangai. 1988b. "Removal of Chlorinated Organic Compounds from Wastewater by Reduction Process: II. Treatment of Tetrachloroethane with Iron Powder." *Kogyo Yosui*, 369: 19-25 (in Japanese).

Sivavec, T. 1997. Personal communication from Tim Sivavec, General Electric Co., NY.

Sivavec, T.M., and D.P. Horney. 1995. "Reductive Dechlorination of Chlorinated Ethenes by Iron Metal." Presented at the 209th ACS National Meeting, Anaheim, CA. April 2-6.

Starr, R.C., and J.A. Cherry. 1994. "In Situ Remediation of Contaminated Ground Water: The Funnel-and-Gate System." *Ground Water*, 32(3): 465-476.

Sweeny, K.H., and J.R. Fischer. 1972. Reductive Degradation of Halogenated Pesticides. U.S. Patent No. 3,640,821.

United States Environmental Protection Agency. 1993. Revisions to OMB Circular A-94 on Guidelines and Discount Rates for Benefit-Cost Analysis. Revised annually at <http://www.whitehouse.gov/OMB/circulars/a094/a094.html#ap-c>.

United States Environmental Protection Agency. 1997. *Selection of Media for the Dover AFB Field Demonstration of Permeable Barriers to Treat Groundwater Contaminated with Chlorinated Solvents*. Preliminary report to U.S. Air Force for SERDP Project 107. August 4.

U.S. EPA, see United States Environmental Protection Agency.

Appendix A
Points of Contact

Appendix A

Points of Contact

AFRL Project Officer

Alison Lightner
Air Force Research Laboratory (AFRL)
139 Barnes Drive, Suite 2
Tyndall AFB, FL 32403
Tel: (850) 283-6303
Fax: (850) 283-6064
E-Mail: alison.lightner@tyndall.af.mil

Technical Information Center

Tel: (850) 283-6285
E-Mail: andrew.poulis@tyndall.af.mil

Battelle Project Manager

Arun R. Gavaskar
Battelle
505 King Avenue
Columbus, OH 43201
Tel: (614) 424-3403
Fax: (614) 424-3667
E-Mail: gavaskar@battelle.org

SERDP Contact

Cathy Vogel
SERDP Program Office
901 North Stuart Street, Suite 303
Arlington, VA 22203
Tel: (703) 696-2118
Fax: (703) 696-2114
E-Mail: VOGELC@acq.osd.mil

Table of Contents

MAIN REPORT	Page
Preface.....	iii
Executive Summary	v
Report.....	1

Appendix A: Points of Contact

APPENDICES B TO H

Appendix B: Supporting Information for Site Characterization and PRB Design
Appendix C: Supporting Information for PRB Construction
Appendix D: Supporting Information for Reactive Performance Evaluation
Appendix E: Supporting Information for Hydraulic Performance Evaluation
Appendix F: Supporting Information for Geochemical Performance Evaluation
Appendix G: Quality Assurance Data
Appendix H: Supporting Information for Cost Evaluation

Appendix B
Supporting Information for Site Characterization
and PRB Design

Table B.1. Half Life Estimates for Various Reactive Media Reported by U.S. EPA Based on On-Site Column Tests

Table B.2. Modeling Scenarios for Area 5 Pilot-Scale PRB Design

Table B.1. Half Life Estimates for Various Reactive Media Reported by U.S. EPA Based on On-Site Column Tests

Time Days	k_{obs} hr^{-1}	r^2	$t_{1/2}$ hr	Avg. $t_{1/2}$ (n=3) hr
COLUMN 1: Connelly Fe				
14	1.2	1.00	0.59	
57	1.0		0.68	
72	2.1		0.33	
85	1.6	1.00	0.44	
98	1.9	0.99	0.37	
112	1.3	1.00	0.52	0.45
COLUMN 2: Cercona Fe				
14	0.17	1.00	4.17	
57	0.62		1.12	
72	1.9		0.37	
85	2.1	1.00	0.33	
98	1.8	0.99	0.38	
112	2.5	1.00	0.28	0.33
COLUMN 3A: Connelly Fe / FeS				
14	0.48	0.92	1.43	
57	0.42	0.96	1.66	
72	0.56		1.23	1.4
COLUMN 3B: Connelly Fe / FeS2				
from Fe/Pyrite interface				
14	2.1		0.32	
27	1.0		0.17	
41	4.5		0.15	0.22
from Pyrite/influent interface				
14	0.86		0.81	
27	1.6		0.43	
41	1.8		0.38	0.54
COLUMN 4: Connelly Fe / Guar Gum				
14	0.78	1.00	1.45	
57	0.88		0.78	
72	0.41	1.00	1.70	
85	1.1	0.91	0.66	
98	1.2	0.92	0.56	
112	1.0	0.99	0.68	0.64

Table B.2. Modeling Scenarios for Area 5 Pilot-Scale PRB Design

Scenario (Design # and Water Level)		Funnel Lengths (ft)	AQ. K (ft/d)	Pea Gravel/Sand	Flux Through Each Gate (cu. ft/d)	Gate Velocity (ft/d)	Pore Vol. Per Month	Total Capture Zone Width At Gate (ft)	Travel Time Through Reactive Cell (Days)
Base Case Dec-93	ND93B1	None	10	NA	1.8	0.067	0.50	NA	60.0
	ND93B3	None	50	NA	8.4	0.323	2.42	NA	12.4
Base Case May-94	NM94B1	None	10	NA	2.1	0.056	0.42	NA	71.0
	NM94B3	None	50	NA	9.9	0.258	1.94	NA	15.5
Base Case Jul-97	NJ97B1	None	10	NA	2.5	0.074	0.55	NA	54.2
	NJ97B3	None	50	NA	11.4	0.345	2.59	NA	11.6
Design 1 Dec-93	ND93D1A	20-20-20	10	Sand	9.3	0.174	1.30	50.4	23.0
	ND93D1B	20-20-20	50	Sand	38.7	0.750	5.63	51.0	5.3
Design 1 May-94	NM94D1A	20-20-20	10	Sand	9.6	0.149	1.12	50.4	26.9
	NM94D1B	20-20-20	50	Sand	39.2	0.625	4.69	49.0	6.4
Design 1 Jul-97	NJ97D1A	20-20-20	10	Sand	11.8	0.198	1.49	50.8	20.2
	NJ97D1B	20-20-20	50	Sand	49.5	0.851	6.38	47.4	4.7
Design 2 Dec-93	ND93D2A	10-40-10	10	Sand	9.8	0.181	1.36	61.6	22.1
	ND93D2B	10-40-10	50	Sand	39.4	0.755	5.66	59.6	5.3
Design 2 May-94	NM94D2A	10-40-10	10	Sand	10.2	0.160	1.20	57.6	25.0
	NM94D2B	10-40-10	50	Sand	40.9	0.645	4.84	57.2	6.2
Design 2 Jul-97	NJ97D2A	10-40-10	10	Sand	12.5	0.207	1.55	59.7	19.3
	NJ97D2B	10-40-10	50	Sand	50.6	0.870	6.52	57.6	4.6
Design 3 Dec-93	ND93D3A	15-30-15	10	Sand	9.6	0.179	1.34	54.0	22.4
	ND93D3B	15-30-15	50	Sand	39.7	0.769	5.77	52.0	5.2
Design 3 May-94	NM94D3A	15-30-15	10	Sand	10.0	0.155	1.16	53.6	25.8
	NM94D3B	15-30-15	50	Sand	40.3	0.645	4.84	53.6	6.2
Design 3 Jul-97	NJ97D3A	15-30-15	10	Sand	12.2	0.203	1.52	53.8	19.7
	NJ97D3B	15-30-15	50	Sand	50.5	0.851	6.38	52.4	4.7
Other Scenarios Design 1 Dec-93	D93D1	20-20-20	10	Pea Gravel	8.7	0.167	1.25	50	24.0
	D93D1A	20-20-20	10	Sand	8.6	0.167	1.25	49.1	24.0
	D93D1B	20-20-20	25	Sand	21	0.400	3.00	49	10.0
Other Scenarios Design 2 Dec-93	D93D2	10-40-10	10	Pea Gravel	9.2	0.177	1.33	60.5	22.6
	D93D2A	10-40-10	10	Sand	9	0.170	1.28	59.2	23.5
	D93D2B	10-40-10	25	Sand	22	0.412	3.09	60.5	9.7

Appendix C

Supporting Information for PRB Construction

- C-1. Granular Iron Analysis Results
- C-2. Pyrite Analysis Results
- C-3. Waterloo Barrier™ Grout Technical Data
- C-4. Monitoring Well Completion Requirements
- C-5. Paved Surface Restoration Requirements
- C-6. In Situ Flow Sensor Probe Information

Appendix C-1

Granular Iron Analysis Results



CONNELLY - GPM, INC.

ESTABLISHED 1875

3154 SOUTH CALIFORNIA AVENUE • CHICAGO, ILLINOIS 60608-5176
PHONE: ~~(312)~~ 247-7231 AREA CODE 773 FAX: ~~(312)~~ 247-7239

July 10, 1997

TYPICAL ANALYSIS OF IRON AGGREGATE

Metallic Iron	89.82
Total Carbon	2.85
Manganese	0.60
Sulphur	0.107
Phosphorous	0.132
Silicon	1.85
Nickel	0.05 - 0.21
Chromium	0.03 - 0.17
Vanadium	Nil
Molybdenum	0.15
Titanium	0.004
Copper	0.15 - 0.20
Aluminum	Trace
Cobalt	0.003

CURTIS A. REVELL
Technical Director

D:\WORD\FORMS\CANALIA.DOC

PLANTS: ELIZABETH, NEW JERSEY • CHICAGO, ILLINOIS



CONNELLY - GPM, INC.

ESTABLISHED 1875

3154 SOUTH CALIFORNIA AVENUE • CHICAGO, ILLINOIS 60608-5176

PHONE: ~~(312)~~ 247-7231

FAX: ~~(312)~~ 247-7239

AREA CODE 773

October 6, 1997

SCREEN SPECIFICATION

ETI CC-1004

U.S. SCREEN NUMBER

4
8
16
30
50
100

100% PASSING
95 - 100% PASSING
75 - 90
25 - 45
0 - 10
0 - 5

MATERIAL WEIGHS APPROXIMATELY 140 - 160 POUNDS PER CUBIC FOOT

Revised 10/97

D:\WORD\FORMS\CRANA.DOC

PLANTS: ELIZABETH, NEW JERSEY • CHICAGO, ILLINOIS

Appendix C-2
Pyrite Analysis Results

HAZEN RESEARCH, INC.

Oxford ED 2000 Qualitative/Semi-Quantitative X-Ray Fluorescence Analysis

September 16, 1997
I188/97-1

002-24R
Pyrite Sample 9/11/97

Battelle

<u>Atomic Number</u>	<u>Analyte</u>	<u>Reported as Element</u>	<u>%</u>	<u>Reported as Oxide</u>	<u>%</u>
13	Aluminum	Al	0.89	Al ₂ O ₃	1.69
14	Silicon	Si	1.40	SiO ₂	2.99
15	Phosphorus	P	0.12	P ₂ O ₅	0.27
16	Sulfur	S	53.80		
17	Chlorine	Cl	0.26	Cl	0.26
19	Potassium	K	<0.01	K ₂ O	<0.01
20	Calcium	Ca	0.06	CaO	0.08
21	Scandium	Sc	<0.01	Sc ₂ O ₃	<0.01
22	Titanium	Ti	<0.01	TiO ₂	<0.01
23	Vanadium	V	<0.01	V ₂ O ₅	<0.01
24	Chromium	Cr	0.03		
25	Manganese	Mn	<0.01		
26	Iron	Fe	44.81		
27	Cobalt	Co	0.15		
28	Nickel	Ni	0.04		
29	Copper	Cu	0.04		
30	Zinc	Zn	<0.01		
31	Gallium	Ga	<0.01		
32	Germanium	Ge	<0.01		
33	Arsenic	As	<0.01		
34	Selenium	Se	<0.01		
35	Bromine	Br	<0.01		
37	Rubidium	Rb	<0.01	Rb ₂ O	<0.01
38	Strontium	Sr	<0.01	SrO	<0.01
39	Yttrium	Y	<0.01	Y ₂ O ₃	<0.01
40	Zirconium	Zr	<0.01	ZrO ₂	<0.01
41	Niobium	Nb	<0.01	Nb ₂ O ₅	<0.01
42	Molybdenum	Mo	<0.01		
74	Tungsten	W	<0.01		
80	Mercury	Hg	<0.01		
81	Thallium	Tl	<0.01		
82	Lead	Pb	<0.01		
83	Bismuth	Bi	<0.01		
47	Silver	Ag	<0.01		
48	Cadmium	Cd	<0.01		
49	Indium	In	<0.01		
50	Tin	Sn	<0.01		
51	Antimony	Sb	<0.01		
52	Tellurium	Te	<0.01		
53	Iodine	I	<0.01		
56	Barium	Ba	<0.01	BaO	<0.01
57	Lanthanum	La	<0.01	La ₂ O ₃	<0.01
58	Cerium	Ce	<0.01	Ce ₂ O ₃	<0.01
90	Thorium	Th	<0.01	ThO ₂	<0.01
92	Uranium	U	<0.01	U ₂ O ₃	<0.01

Appendix C-3

Waterloo Barrier™ Grout Technical Data

WBS 301 - WATERLOO BARRIER GROUT

TECHNICAL DATA SHEET

DESCRIPTION:

Waterloo Barrier Grout - **WBS - 301** - is a prepackaged silica fume modified, cementitious based grout for use as a joint sealant with the Waterloo Barrier™ System.

USES:

This product is used exclusively with the Waterloo Barrier™ Groundwater Containment System as a low hydraulic conductivity joint sealing material.

CHARACTERISTICS:

Contains pre-blended dry superplasticizers providing a low water cement ratio and increased compressive strength.

This sealant offers high compressive strength with a rapid strength gain in the first two days.

Thixotropic nature of the material resists groundwater washout.

The addition of Silica Fume and Fly Ash additives improves the pumpability of the material while reducing the bleeding and permeability of the mix.

Expansion agents in the mix generate a 4-8% volumetric expansion.

Pot life of the mixed material can be varied from 60 to 90 minutes depending upon the installation conditions encountered.

MIXING PROPERTIES:

DESCRIPTION	REQUIREMENTS
SEALANT PACKAGING:	30 kg Bags
MINIMUM WATER VOLUME (per bag):	6.25 L
MAXIMUM WATER VOLUME (per bag):	9.25 L
MIXER TYPE:	Colloidal
MINIMUM MIXING TIME:	2.5 (min.)
MAXIMUM POT LIFE:	180 (min.)

CURING AND SET TIMES:

The initial gel time of the sealant varies from 1.5 to 2.0 hours @ 20°C.
Initial set time of the sealant varies from 1 to 2 days after placement.
Ultimate strength is reached at approximately 28 days.

COMPRESSIVE TESTING	STRENGTH
1 DAY:	31 Mpa
3 DAYS:	49 Mpa
7 DAYS:	56 Mpa
28 DAYS:	67 Mpa

PERMEABILITY TESTING:

Permeability testing was completed by Davroc Testing Laboratories Inc. to confirm a bulk hydraulic conductivity of 3.19×10^{-15} m/s

YIELD:

Each 30 kg (66 lb) bag of WBS 301 sealant produces 0.01 cubic metres of grout.

SAFETY PRECAUTIONS:

Waterloo Barrier Grout - WBS 301 - contains Portland Cement, Fly Ash, Silica Fume and other admixtures. Normal safety wear, such as rubber gloves, dust masks and safety glasses that are used to handle conventional cement based products should be worn. Material Safety Data Sheets available on request.

Appendix C-4

Monitoring Well Completion Requirements

DOVER AFB MONITORING WELLS

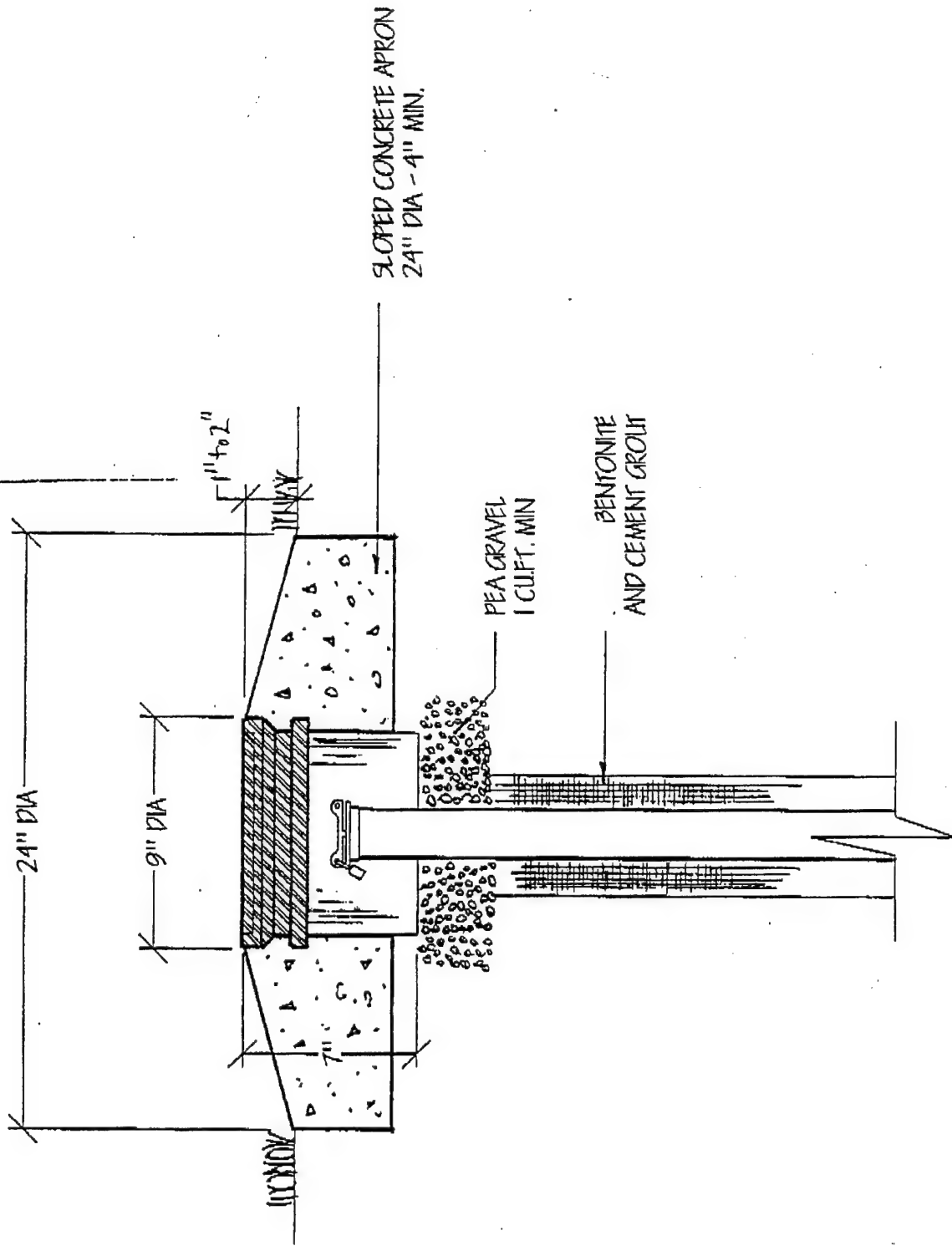
Grass, Dirt or Landscaped Areas

Monitoring wells shall be flush mounted in accordance with the attached detail and shall conform to the following specifications:

1. Pea gravel is to be 1/4" to 1/2" natural washed gravel with rounded edges. Well sand or angular gravel is not an acceptable substitute.
2. The well casing shall be cut to an elevation such that the locking plug is at least 1" beneath the cover, although the casing shall not be more than 4" below the elevation of the rim of the cover.
3. A 5" to 6" section of 24" diameter cardboard form tube shall be used as a form. The form tube shall be cut perpendicular to the axis of the tube such that the top surface shall not be more than 1/2" out of level.
4. The form tube and rim for the cover shall be set level as determined by centering the bubble on a 4' level in 2 directions 90° to one another. The form tube shall be level with the surrounding surface.
5. The rim for the cover shall be placed 1" to 2" above the form tube. The exact slope should be appropriate to conform to surrounding drainage patterns with elevations close to 2" used in swales, low areas or areas receiving sheet flow from parking lots. High, well drained areas should be closer to 1".
6. The form tube shall be placed with compacted soil to shore up the sides to form a circle. The diameter shall not vary by more than 1" out of round when measured in any direction intersecting the center.
7. The rim shall be placed in the center of the form tube. The distance measured from the rim to the form tube along a line intersecting the center shall not vary by more than 1/2".
8. Soil shall be placed and compacted with a suitable tamper in the annular space between the form tube and sleeve for the rim up to an elevation not less than 4" below the top of the form tube.
9. The concrete shall be mixed to the consistency of a proper slump, poured or placed, and worked to remove any air pockets at an even slope to within 1/8" of the rim and form tube at all points.
10. After the concrete takes an initial set an aluminum or stainless steel tag containing a stamped DNREC well permit # and DAFB identification # shall be placed in the pad and the concrete brushed.

11. The cover, rim and tag shall be wiped clean with a wet cloth before the concrete takes a final set.

12. Any concrete outside the form tube shall be removed and the surrounding area topsoiled, graded and seeded if necessary as determined by a DAFB representative.



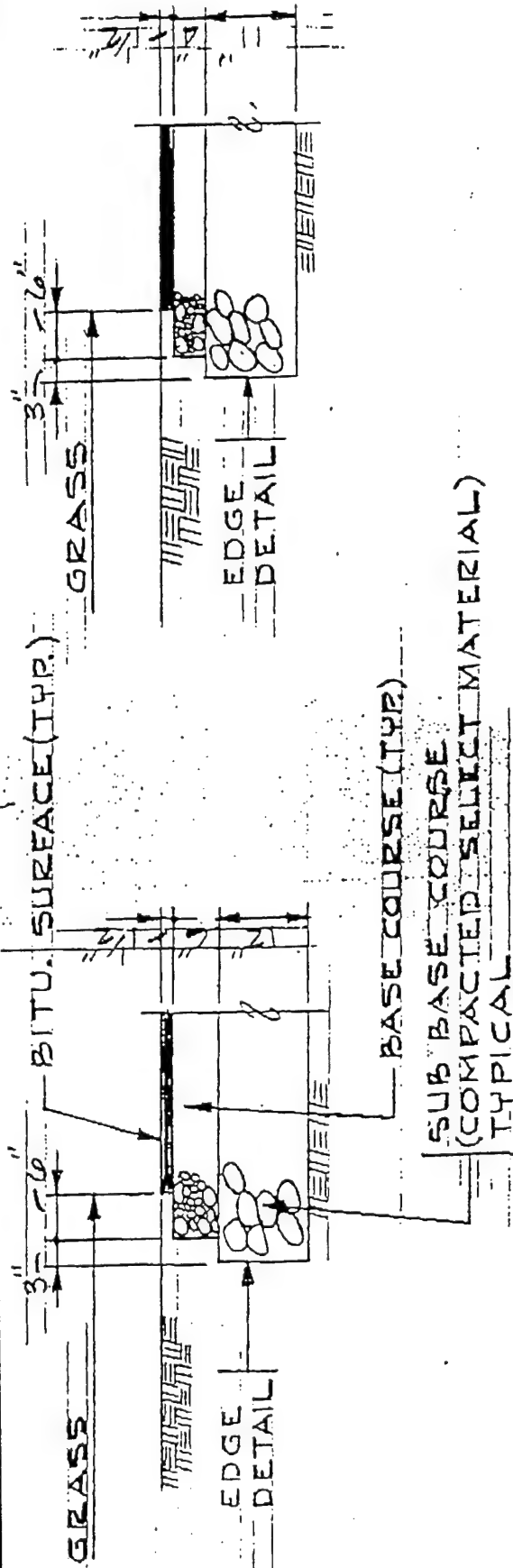
Appendix C-5

Paved Surface Restoration Requirements

DOVER AFB MONITORING WELLS
Paved Areas

Monitoring wells shall be flush mounted conforming to the following specifications:

1. Concrete or asphalt is to be cored. If several wells are to be installed in close proximity to one another saw cutting the area may be permitted provided a plan is submitted for prior approval by a Dover AFB representative. Jackhammering through concrete or augering directly through asphalt will only be permitted if in the opinion of a Dover AFB representative the condition of the pavement doesn't warrant coring or saw cutting.
2. A 9" monitoring well cover and locking plug is to be used to finish the well. Matching material, concrete or asphalt patch, equal to the existing thickness is to be placed in the space between the rim of the cover and existing pavement. The rim of the cover is to be set 1/8" above the existing pavement.
3. A minimum of 1 cubic ft. of pea gravel is to be placed in the soil above the concrete/bentonite grout for drainage. It shall be placed at an elevation such as to contact the soil beneath the pavement and subgrade. Pea gravel is to be 1/4" to 1/2" natural washed gravel with rounded edges. Well sand or angular gravel is not an acceptable substitute.
4. The well casing shall be cut to an elevation such that the locking plug is at least 1" beneath the cover, although the casing shall not be more than 4" below the elevation of the rim of the cover.
5. Concrete shall be mixed to the consistency of a proper slump, poured or placed, and worked to remove any air pockets at an even slope from the existing pavement to the rim of the cover at all points. Asphalt patch shall be tamped to an even slope with a suitable tamper at all points.
6. An aluminum or stainless steel tag containing a stamped DNREC well permit # and DAFB identification # shall be attached to the bottom of the cover.
7. In concrete the concrete shall be brushed after the concrete takes an initial set. The cover and rim shall be wiped clean with a wet cloth before the concrete takes a final set.



TYPE I TYPE II

FLEXIBLE PAVEMENT DETAILS

NOT TO SCALE

This is what exists in the area where the system is proposed.

Appendix C-6

In Situ Flow Sensor Probe Information

The In Situ Permeable Flow Sensor: A Tool for Monitoring 3D Groundwater Flow Velocity

Sandy Ballard
HydroTechnics, Inc.
P. O. Box 92828
Albuquerque, NM 87199
Voice: (505) 797-2421
Fax: (505) 797-0838
ballard@hydrotechnics.com

Table of Contents

- Introduction
- Principle of Operation
- Emplacement
- Application Summaries
 - A Test of the In Situ Permeable Flow Sensors at Savannah River, SC
 - Ground Water - Surface Water Interaction in the Bank of the Columbia River, Hanford, Washington
 - Monitoring the In-Well Vapor Stripping Demonstration at Edwards Air Force Base, California
 - Monitoring the Hydrology of a Sinkhole Over the Strategic Petroleum Reserve Facility at Weeks Island, Louisiana
- References

Introduction

In Situ Permeable Flow Sensors are new instruments which use a thermal perturbation technique to directly measure the three dimensional groundwater flow velocity vector in unconsolidated, saturated, porous media (Ballard, 1996). Since groundwater flow is the most important mechanism for the dispersal of toxic waste once it has been released into the subsurface, accurate information about the groundwater flow field is critical to the characterization and post-closure monitoring of environmental waste sites. In addition, virtually all techniques for remediating contaminated groundwater involve moving the groundwater around in the subsurface to some extent. Understanding the dynamics and zone of influence of these remediation strategies requires accurate monitoring of the groundwater flow field in and around the site during the remediation process. In Situ Permeable Flow Sensors are ideally suited to long term monitoring of groundwater flow fields in these types of situations.

Principle of Operation

The instrument consists of a cylindrical heater 30 inches long by 2 inches in diameter with an array of 30 carefully calibrated temperature sensors on its surface (Figure 1). When the probe is buried in the ground at the point where the measurement is to be made and the heater

activated with approximately 80 watts of continuous power, the sediments and groundwater surrounding the probe are warmed by 20 to 30 °C (Figure 2). In the absence of any flow past the instrument, the temperature distribution on its surface is independent of azimuth and symmetric about the vertical midpoint of the probe. When there is flow past the tool, the surface temperature distribution is perturbed as the heat emanating from the probe is advected around the probe by the moving fluid (Figure 3). Relatively cool temperatures are observed on the upstream side of the tool while relatively warm temperatures are observed on the downstream side. PC-based software is available which converts the measured probe surface temperature distribution into flow velocity (3D magnitude and direction). Darcy velocities in the range of 0.01 to 1 ft/day (3×10^{-6} to 3×10^{-4} cm/s) can be accurately measured with this technology. Measurement resolution is even better (0.001 ft/day or 3×10^{-7} cm/s).

Emplacement Technique

The key to accurately measuring groundwater flow velocity with this technology is to bury the tool in the ground in direct contact with the formation. This avoids all the negative effects on the measured velocity which result from the presence of a borehole, casing, screen and gravel pack. Direct burial is achieved by drilling a hole to the desired depth, installing the probe through the casing and retracting the casing, leaving the probe in the ground. Saturated, unconsolidated sediments will collapse around the tool, leaving it permanently emplaced in the ground. While this deployment strategy means that the relatively inexpensive tool cannot be moved or retrieved after emplacement, flow velocity information as a function of time can be gathered from the probes for extended periods. It is a simple matter to connect a data acquisition system to an array of flow sensors, connect the data acquisition system to a modem and phone line (land line or cellular) and collect the data back in the home office for months to years, in near real time, without routine human intervention on site.

Aside from the substantial data quality benefits realized by permanent emplacement, the deployment strategy often offers cost advantages as well, particularly in a long-term monitoring activity. In an ideal world, whenever any quantity is to be measured at a site, data would be obtained with large spatial and temporal density at minimal cost in terms of personnel time investment. Unfortunately, these objectives are generally mutually exclusive: it is not possible to have the measurement device deployed at a large number of distinct locations, at a large number of distinct points in time, without the involvement of expensive field personnel to move the sensors from point to point. In a characterization activity, when a snapshot of site characteristics at a single point in time is desired, the spatial distribution of the data has precedence over temporal changes and the investigator has no choice but to use a portable device and pay someone to go out and move it around. In a monitoring activity, the key locations where measurements are needed have already been identified during a previous characterization phase and what is required is a deployment strategy which allows data to be acquired with large temporal density and minimal human intervention. In this situation, permanent installation of the instrumentation is generally cost effective since human intervention is not required. Deploy the instrumentation, connect it to a data acquisition system which can be interrogated remotely, and go away.

Application Summaries

The flow sensors were originally tested at the Savannah River Site in South Carolina (Ballard et al., 1996). During this test, it was possible to directly compare the velocity measurements obtained with the flow sensors to measurements obtained using standard hydrological techniques. The technology was subsequently used at the Hanford Site in Washington State in a study of the interaction between the groundwater beneath the site and surface water in the Columbia River (Ballard, 1995). Most recently, the flow sensors were deployed at Edwards Air Force Base, California, to monitor the hydrologic regime at a site where the use of In-Well Vapor Stripping to remediate TCE in groundwater was being demonstrated (Gilmore et al. in press). They have also been used at the Weeks Island Strategic Petroleum Reserve Site to monitor the

hydrologic behavior of a sinkhole which formed over the edge of a former salt mine where the DOE had stored 72 million barrels of crude oil (Neal, 1996). While the highlights of each of these deployments are presented here, please consult the references for complete details. Another application, not described here, includes a study of the hydrology of a field test site adjacent to the Brazos River near College Station, Texas by researchers at Texas A&M University (Alden and Munster, in review). Projects currently underway by HydroTechnics customers include a study of the effects of in situ air sparging/bioremediation on the ground water flow field nearby, a study of the interaction of groundwater and sea water in a coastal environment, monitoring the groundwater flow field around in situ permeable barriers used to remediate VOC's in groundwater, and another study of groundwater-surface water interactions.

A Test of the In Situ Permeable Flow Sensors at Savannah River, SC

The site where the test was conducted is underlain by a 14 m thick, fully saturated, confined aquifer consisting of unconsolidated sandy sediments deposited in a fluvial environment. The aquifer is bounded above and below by relatively impermeable clay layers. For this experiment, a pump was placed in a well which was screened across the entire vertical extent of the aquifer. Two In Situ Permeable Flow Sensors were placed at approximately the vertical midpoint of the aquifer and at distances of 5 and 12 m from the pumping well. The experiment was conducted in two stages. During the first stage, the well was pumped at a rate of 0.98 l/s for about 24 hours and then at 0.57 l/s for about 60 additional hours. During the second stage, which took place about 3 weeks later, the well was pumped at 0.38 l/s for 60 hours and then at 0.17 l/s for 100 hours. The flow velocities measured with the flow sensors were monitored before, during and after the period of time that the well was being pumped.

Figure 4 illustrates the direction and magnitude of the horizontal component of the flow velocity, as a function of time, measured by the flow sensor closest to the pumping well during the second stage of the experiment. Prior to the initiation of pumping, the horizontal component of flow was very low, about 1×10^{-5} cm/s, which is near the lower limit of the velocity that the probes can accurately measure. When the pump was activated at a rate of 0.38 l/s at time 0, the flow velocity changed abruptly, reaching equilibrium after about 1 day of pumping. The horizontal component increased to about $1.75 \times 10^{-4} \pm 3 \times 10^{-5}$ cm/s, oriented in a direction which was toward the pumping well, within the uncertainty in the analysis. When the pumping rate was reduced to 0.17 l/s at time 2.9 days, the magnitude of the horizontal component decreased by about a factor of 2.

The horizontal components of the flow velocities measured by the two probes as a function of pumping rate are plotted in Figure 5. When the pump was operating, both probes measured significant horizontal flow velocities that increased linearly with the pumping rate. The direction of the horizontal component of the flow velocity was directed toward the pumping well, within the uncertainties of the measurements (Figure 5b), with only one exception.

The simplest way of estimating the true Darcy flow velocity toward the pumping well is to assume that there was no flow in the aquifer when the pump was not active, the aquitards above and below the aquifer were perfectly impermeable and that the hydraulic properties of the aquifer were perfectly homogeneous and isotropic. Given these assumptions, the direction of the Darcy velocity vector would be purely horizontal and radially directed toward the pumping well and its magnitude would be

$$v = \frac{Q}{2 \pi R Z} \quad (1)$$

where v is the magnitude of the Darcy velocity, Q is the volume of water pumped from the pumping well per unit time, Z is the thickness of the aquifer and R is the distance from the pumping well to the observation point. Velocities at radial distances from the pumping well corresponding to the positions of the flow sensors and at pumping rates corresponding to those used during the test, calculated according to Equation 1, are compared with the horizontal flow velocities measured with the flow sensors in [Figure 6](#). The theoretical and measured velocities from the far probe differ by only about 11%, which is less than the uncertainties in the measured values. The measured velocities from the near probe exceed the theoretical velocities by about 75%, which is significantly more than the uncertainty in the measured values. The differences between the measured and theoretical velocities are likely due to heterogeneity and anisotropy of the hydraulic properties of the aquifer. Given the linearity of the relationship between the measured flow velocities and the pumping rate, and the excellent correspondence between the measured and expected velocity magnitudes and directions, it can be concluded that the flow sensors worked extremely well.

Ground Water - Surface Water Interaction in the Bank of the Columbia River, Hanford, Washington

To properly characterize the transport of contaminants from the sediments beneath the Hanford Site into the Columbia River, it is important to accurately characterize the hydrologic regime in the banks of the river. The hydrology of the site is significantly impacted by the river stage ([Figure 7](#)), which is controlled by the amount of water released from the Priest Rapids Dam, located approximately 25 miles upstream from the site. Discharge from the dam varies according to the demand for electric power; the higher the demand, the more water is released and the higher the river stage adjacent to the 100H Area. Since demand for power is greatest during the day and decreases at night, the river stage rises and falls with a diurnal frequency. The amplitude of the daily oscillations is about 3 to 5 feet. In addition, demand for power is reduced on the weekends resulting in relatively low river stage on weekends and a significant surge of water being released on Mondays. On longer time scales, there is a seasonal variation in river stage, with relatively high water in June and low water in the fall. The amplitude of the seasonal river stage variations is about 6 to 8 feet.

Flow in the near shore environment (within a few hundred feet of the river) is complicated by the rise and fall of the river level. While the net flow is from the banks into the river when averaged over time periods longer than a few days or months, there are times when the river stage is high and water flows from the river into the banks. Close to the bank of the river, there are three components of the groundwater flow velocity which are superimposed and interact in a complex manner: relatively steady flow from the interior of the Hanford site to the near shore environment, reasonably steady flow downstream, and temporally variable flow in and out of the banks of the river in response to changes in river stage.

Flow velocity data were obtained from two flow sensors ([Figure 8](#)). SFM3 was deployed in the Hanford Formation while SFM5 was de-ployed in the underlying Ringold Formation. The hydraulic conductivity of the Hanford Formation is several orders of magnitude higher than that of the Ringold Formation and the vertical hydraulic gradient at the site is upward resulting in upward flow across the Ringold/Hanford contact.

Flow velocity data were obtained during two time intervals. The first lasted 64 days from May 17 to July 20, 1994 while the second lasted for one week from September 4 to 11, 1994. The first data collection interval coincided with the time of highest river stage while the second measured the flow velocity after the summer high water had subsided ([Figure 7](#)).

In [Figure 9](#), the into-bank component of the flow velocity measured by probe SFM3 during the first data collection period is compared with river stage. The correlation between the velocity data and river stage is excellent. During times of high river stage, water flowed from the river into the bank while during times of low river stage, groundwater flowed toward the river. There appears to be about a 5 hour phase lag between times of maximum river stage and maximum into-bank flow velocity. The into-bank component of the flow velocity measured by probe SFM5, which was located in the deeper Ringold Formation also correlated very well with river stage. The magnitude of the velocity oscillations was

much reduced compared to the oscillations observed by probe SFM3 located in the much more hydraulically conductive Hanford Formation.

Both probes recorded relatively steady vertical and downstream components of flow which were essentially uncorrelated with river stage. The downstream component of flow in the Hanford Formation was substantially higher than that in the Ringold Formation. The vertical component of flow observed in the Hanford Formation was negative, indicating downwardly directed flow, suggesting that the flow sensor was located at a vertical position where the hydraulic conductivity of the sediments was increasing with depth. The vertical flow observed by probe SFM5 in the Ringold Formation was positive, indicating upward flow. The vertical component of flow observed by SFM5 dominated the horizontal components most of the time, which is consistent with the fact that the site is located in a gaining reach of the river.

In Figure 10, the into-bank components of flow measured in the Hanford and Ringold Formations are compared to river stage in two different time intervals. On the left, the data during a one week time interval in June, when the river was at its highest level, is displayed. On the right are illustrated the flow and river stage data during a one week period in September, when the river stage was about 7 feet lower than it was at its peak in June. It should be noted that September 5th, 1994 was Labor Day and relatively little water was released from the dam upriver over the long holiday weekend. There is a marked difference in the flow velocities recorded by the flow sensors in September as compared to June. In June, the nominal flow velocity observed by the two probes was essentially zero, with positive or negative excursions during times of high and low river stage, respectively. In September, when the river stage was low, the flow was predominantly from the bank toward the river, with into-bank flow observed only briefly during times of the very highest river stage.

Overall, the excellent correlation between river stage and the measured flow directions near the river indicates that the flow sensors are capable of providing very useful information about the complex hydrologic regimes found in stream banks.

Monitoring the In-Well Vapor Stripping Demonstration at Edwards Air Force Base, California

In-Well Vapor Stripping is an innovative technology for remediating volatile organic compounds (VOC's) in groundwater which involves injecting air into a dual screen well which penetrates the contaminated plume. As the air bubbles up through the water inside the well casing, the VOC's are volatilized and transferred from the water to the air. The VOC-laden air is then extracted from the well and treated in a surface treatment unit. As the air bubbles up through the water, the water is entrained upward by cavitation, resulting in the upward flow of water inside the well. By this process, contaminated water enters the well through the lower screen, is cleaned up as it flows upward inside the well and then clean water exits the well through the upper screen which is typically located just above the static water table.

This flow pattern creates a toroidal or doughnut shaped groundwater circulation system in the formation outside the well. The groundwater flows away from the well in the upper part of the system adjacent to the upper well screen where water is exiting the well and flows toward the well in the deeper part of the aquifer, adjacent to the lower well screen. The radial distance that the shallow water flows away from the well before sinking and flowing back toward the well is heavily dependent on the anisotropy of the hydraulic conductivity of the formation. If the horizontal conductivity greatly exceeds the vertical conductivity, which is often the case, particularly in situations where clay lenses are interbedded in the coarser aquifer materials, the water will flow very far away from the well before returning. On the other hand, if hydraulic communication between the upper and lower parts of the aquifer are relatively free, then the zone of influence of the system will not be very great since water will not travel very far from the well before sinking and returning to the well.

For the Edwards AFB demonstration, a suite of In Situ Permeable Flow Sensors were deployed to characterize the effect of the In-Well Vapor Stripping System on the groundwater flow field around the well. Three flow sensors were deployed in the lower part of the aquifer, just above the basal aquitard, at radial distances of 17, 35 and 50 feet from the well. The velocity recorded by the flow sensor closest to the well during the

13 months of the demonstration is illustrated in Figure 8. All three flow sensors measured substantial, downwardly directed flow velocity in response to the demonstration, which was likely due to the creation of conduits of disturbed, high conductivity material when the flow sensors were installed. In hindsight, it would have been wise to seal the holes above the flow sensors with grout or bentonite to minimize this effect.

In addition to the downward flow, horizontal flow toward the well was also observed. In Figure 9, the horizontal flow velocity measured by the flow sensors closest and farthest from the well are illustrated. Note that for each flow sensor, the background horizontal flow velocity vector, measured just prior to the start of the demonstration, has been subtracted from the data in order to isolate the effect of the demonstration on the ground water flow field. The data indicate that the In-Well Vapor Stripping system influenced the flow field in the deep part of the aquifer, even as far out as 50 feet from the demonstration well. This information was extremely useful to the principal investigator of the demonstration in attempting to understand the dynamics of this very promising remediation system.

Monitoring the Hydrology of a Sinkhole Over the Strategic Petroleum Reserve Facility at Weeks Island, LA

In 1992, a sinkhole was discovered directly above the edge of the DOE Strategic Petroleum Reserve storage facility at Weeks Island, Louisiana. At the time, 72 million barrels of crude oil (worth ~\$1.5B) were stored at the site in a converted salt mine contained within a salt dome. Extensive investigations (Bauer, 1994), including drilling, revealed that the sinkhole was the surface expression of a sand-filled conduit within the salt which probably formed as a result of the dissolution of salt by partially saturated groundwater flowing down fractures connecting the edge of the mine and the hydrologic regime in the sediments above the salt dome (Figure 13). During the characterization phase of the project, an In Situ Permeable Flow Sensor deployed at the bottom of borehole BH7A, deep within the sand-filled conduit, measured downwardly-directed groundwater flow of approximately 1 ft/day. This observation was a key piece of evidence which convinced the owners of the site to remove the oil and abandon the facility.

To control the situation during the two years required to remove the oil, continuous injection of saturated brine into the sand filled conduit through borehole BH7A was initiated. The brine prevented fresh groundwater from flowing into the conduit, thereby inhibiting further dissolution of the salt and further enlargement of the flow path into the mine. To monitor the hydrologic behavior of the sinkhole, another flowmeter was deployed in borehole BH9. It was located within the sand-filled conduit roughly 10 feet below the normal top of salt. With the data from this meter it was possible to determine the cross sectional area of the conduit at the top of salt and to continuously monitor the amount of brine flowing into the conduit.

The brine injection rate was maintained at a rate higher than the flow rate of fluid down the conduit to the mine, resulting in an upward flow at the location of the flow sensor. By subtracting the brine flux out of the conduit at the top of salt from the brine injection rate into the conduit, the flow rate into the mine could be monitored (Figure 11). It was observed that brine was flowing into the mine at about 190 gallons per hour (gph) and the inflow was increasing, in a non-steady fashion, at a rate of roughly 1 gph/day. After monitoring the situation for several months, a freeze wall was emplaced at the site which imposed a very large thermal gradient on the medium surrounding the flow sensor, rendering it useless. Additional slant boreholes were drilled into the conduit and, since that time, the hydrology has been monitored using piezometers equipped with pressure transducers. The flow sensors, however, provided key data early in the project which were instrumental in the decision to abandon the facility.

References

Alden, A. S. and C. L. Munster, in review, Field Test of the In Situ Permeable Groundwater Flow Sensor, Ground Water Monitoring and

Remediation. Alden, A. S. and C. L. Munster, in review, Assessment of Stream-Aquifer Interaction and Aquifer Characteristics Using the In Situ, 3-D Groundwater Velocity Meter, Ground Water.

Ballard, S., 1996, The In Situ Permeable Flow Sensor: A groundwater flow velocity meter, Ground Water, v. 34, p. 231-240.

Ballard, S., 1995, Ground Water Flow Velocity In the Bank of the Columbia River, Hanford, Washington, SAND95-2187, Internal Report, Sandia National Laboratories.

Ballard, S., G. T. Barker and R. L. Nichols, 1996, A test of the In Situ Permeable Flow Sensor at Savannah River, SC, Ground Water, v. 34, p. 389-396.

Bauer, S. J. (ed.), 1995, Update of assessment of geotechnical risks; Petroleum Reserve Weeks Island Site, Albuquerque, NM, Sandia Report SAND94-2969, 42 p. plus appendices.

Neal, J. T. (ed.), 1996, Summary of events and geotechnical factors leading to decommissioning the Strategic Petroleum Reserve (SPR) Facility at Weeks Island, Louisiana, Albuquerque, NM, Sandia Report SAND96-2263, 38 p.

Gilmore, T. J., M. J. Pinto, M. D. White, S. Ballard, S. M. Gorelick, O. Teban, F. A. Spane, in preparation, Preliminary Performance Assessment In-Well Vapor Stripping, Pacific Northwest National Laboratories Internal Report, Richland, Washington.

different ratios of formation thermal conductivity to total heat flux from the probe. For high K/Q ratios, the temperature of the surface of the probe is relatively low, either because the thermal conductivity of the formation is high, allowing it to dissipate more heat, or because less heat is emanating from the probe. A lower overall temperature of the probe results in smaller temperature variations over the surface of the probe, a lower signal to noise ratio and hence a larger degree of uncertainty in the result. To acquire the most precise flow velocity data with this technology, it is recommended that the heater on the instrument be operated at the highest power possible that does not produce significant natural convection [equation (3)].

Figure 5 indicates that the uncertainties in the magnitude and direction of the flow velocity measurements decrease dramatically with increasing flow velocity. If the lowest flow velocity that can be measured is defined as that velocity for which the uncertainty in the magnitude of the flow velocity is $\pm 100\%$, then the technology can measure flows as low as Peclet number 0.03 which corresponds to approximately 3×10^{-6} to 8×10^{-6} cm/s for typical values of soil thermal conductivity. For Peclet number 0.1 (1×10^{-5} to 2.5×10^{-5} cm/s), uncertainties of $\pm 25\%$ in magnitude and $\pm 15^\circ$ in azimuth are achievable at low K/Q values. At flow velocities in excess of Peclet number 1 the uncertainties in the magnitude and direction of the flow velocity are only a few percent and a few degrees, respectively.

Instrumentation and Deployment

The way in which the probes are fabricated and deployed in the ground is critical to obtaining a valid measurement (Figure 6). The current strategy involves constructing very simple, inexpensive probes that can be permanently buried in saturated, unconsolidated sediments. Each probe consists of a rod of low thermal conductivity, closed cell, polyurethane foam, 75 cm long by 5 cm in diameter, surrounded by a thin film, flex circuit heater, an array of 30 carefully calibrated thermistors and a waterproof jacket. The design seeks to achieve a high degree of uniformity of the heat flux from the surface of the probe and sufficient temperature sensors near the surface of the probe to adequately characterize the temperature distribution on its surface. The thermistors are calibrated such that temperature differences between temperature sensors are accurate to within $\pm 0.01^\circ\text{C}$. The pattern of the temperature sensor distribution on the surface of the probe is illustrated in Figure 7.

At the deployment site, sufficient 2.5 cm diameter PVC pipe is attached to the top of the probe to reach to the ground surface after the probe is deployed in the ground. Marks are made along the PVC pipe so that the horizontal orientation of the probe will be known after the probe is emplaced. While more sophisticated techniques for determining the horizontal orientation of the probes exist, this simple, inexpensive process has worked well in experiments to date (azimuth errors are estimated to be less than about $\pm 10^\circ$ for probes buried less than 50 m below the surface). To emplace the probes, a hollow stem auger, or some other

similar technique that does not involve the use of drilling muds, is used to drill to the depth where the measurement is to be made. The probe is then lowered down the center of the auger and the auger is retracted, leaving the probe in the hole. In saturated, unconsolidated formations, the hole collapses around the probe, leaving it permanently buried in the subsurface, in intimate contact with the formation. Although the probes cannot be recovered or moved after being deployed in this way, they can continue to provide flow measurements until the drift in the temperature sensor calibrations reduces the quality of the temperature measurements to unacceptable levels or the waterproof coatings ultimately leak (about a year or more). The principal advantage of this strategy is that the probe is not deployed in a hole where the flow can be significantly different from the flow in the surrounding formation (Melville et al., 1985; Kerfoot, 1988; Wheatcraft and Winterberg, 1985). It is a simple matter to attach a data acquisition system to a suite of probes at a site and monitor them on a continuous basis via modem and telephone (hard line or cellular) for extended periods of time.

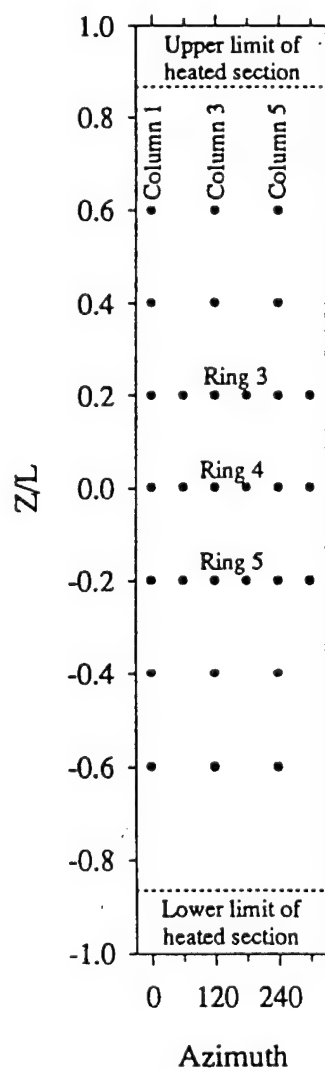


Fig. 7. Distribution pattern of the 30 temperature sensor locations on the surface of the probes.

Appendix D
Supporting Information for Reactive Performance Evaluation

Table D-1. Results of Samplings at Dover Funnel & Gate Site: Target CVOCs (µg/L)

**Table D-1. Results of Samplings at Dover Funnel & Gate Site:
Target CVOCs ($\mu\text{g/L}$)**

Well ID	Dilution Factor	cis -1,2-DCE			TCE			PCE					
		Results Jul 98	Detection Limit	Results Jun 99	Reporting Limit	Results Jul 98	Detection Limit	Results Jun 99	Reporting Limit	Results Jul 98	Detection Limit	Results Jun 99	Reporting Limit
Gate 1 Upgradient Aquifer Wells													
U1S	1	U	5	U	5	U	5	3	3 J	5	3.4 J	3	3
U2S	1	U	5	U	5	U	5	3	3 J	5	1.6 J	3	3
U3S	1	U	5	U	5	U	5	3	3 J	5	1.9 J	3	3
U3D	5	35	5	44	25	16	5	15	273	5	210	15	15
U3D	25	NA	NA	44	125	NA	NA	75	NA	NA	210	75	75
U4S	1	U	5	U	5	U	5	3	2 J	5	U	3	3
U4M	1	62	5	100	5	21	5	3	300	5	470	3	3
U4M	10	NA	NA	130	50	NA	NA	30	NA	NA	470	30	30
U4D	10	69	5	130	50	22	5	30	334	5	520	30	30
U4D-DUP	1	NA	NA	110	5	NA	NA	3	NA	NA	510	3	3
U4D-DUP	10	NA	NA	130	50	NA	NA	30	NA	NA	510	30	30
U5S	1	U	5	U	5	1 J	5	3	2 J	5	1.6 J	3	3
U5D	1	20	5	56	5	11	5	3	155	5	NA	NA	NA
U5D	10	NA	NA	52	50	NA	NA	30	NA	NA	210	30	30
U6S	1	U	5	U	5	U	5	3	2 J	5	1.3 J	3	3
U6S-DUP	1	U	5	NA	NA	U	5	NA	1 J	5	NA	NA	NA
U10S	1	U	5	U	5	U	5	3	4 J	5	7.9	3	3
U10S-DUP	1	NA	NA	U	5	NA	NA	3	NA	NA	9.7	3	3
U11S	1	U	5	U	5	U	5	3	3 J	5	12	3	3
U12S	1	U	5	U	5	U	5	3	3 J	5	2.5 J	3	3
U12S-DUP	1	U	5	NA	NA	U	5	NA	3 J	5	NA	NA	NA
U13S	1	U	5	U	5	U	5	3	3 J	5	2.5 J	3	3
U14S	1	U	5	U	5	U	5	3	2 J	5	U	3	3
U15S	1	U	5	U	5	1 J	5	3	5 J	5	U	3	3
U16S	1	U	5	1.4 J	5	U	5	3	9	5	74	3	3
U17S	1	U	5	U	5	U	5	3	5 J	5	3.3 J	3	3
U18S	1	U	5	U	5	U	5	3	7	5	20	3	3
U19	1	NA	NA	120	5	NA	NA	3	NA	NA	1,400	3	3
U20	1	NA	NA	36	5	NA	NA	3	NA	NA	7,100	3	3
U20	100	NA	NA	U	500	NA	NA	300	NA	NA	7,100	300	300

**Table D-1. Results of Samplings at Dover Funnel & Gate Site:
Target CVOCs ($\mu\text{g/L}$) (Continued)**

Well ID	Dilution Factor	cis-1,2-DCE			TCE			PCE					
		Results Jul 98	Detection Limit	Results Jun 99	Reporting Limit	Results Jul 98	Detection Limit	Results Jun 99	Reporting Limit	Results Jul 98	Detection Limit	Results Jun 99	Reporting Limit
Gate 1 Reactive Cell Wells													
F1S	1	U	5	2.6 J	5	2 J	5	U	3	3 J	5	8.2	3
F1S-DUP	1	NA	NA	1.7 J	5	NA	NA	U	3	NA	NA	6.5	3
F2S	1	U	5	U	5	U	5	U	3	2 J	5	U	3
F2M	1	U	5	U	5	1 J	5	U	3	1 J	5	U	3
F2D	1	2 J	5	4.4 J	5	U	5	1.6 J	3	1 J	5	U	3
F3S	1	U	5	5 U	5	U	5	U	3	U	5	U	3
F3D	1	1 J	5	1.1 J	5	U	5	U	3	1 J	5	U	3
F4S	1	U	5	U	5	1 J	5	U	3	2 J	5	U	3
F4M	1	1 J	5	U	5	4 J	5	U	3	6 J	5	U	3
F4D	1	U	5	U	5	1 J	5	U	3	2 J	5	U	3
F5S	1	U	5	U	5	U	5	U	3	2 J	5	U	3
F5M	1	U	5	U	5	U	5	U	3	U	5	U	3
F5D	1	U	5	U	5	U	5	U	3	U	5	U	3
F5D-DUP	1	NA	NA	U	5	NA	NA	U	3	NA	NA	1.2 J	3
F6S	1	U	5	U	5	1 J	5	U	3	3 J	5	U	3
F6M	1	U	5	U	5	1 J	5	U	3	1 J	5	U	3
F6D	1	U	5	U	5	1 J	5	U	3	3 J	5	U	3
F6D-DUP	1	U	5	NA	NA	2 J	5	NA	NA	4 J	5	NA	NA
F7S	1	U	5	U	5	U	5	U	3	1 J	5	4.4 J	3
F7D	1	5 J	5	U	5	6	5	U	3	7	5	3 J	3
F8S	1	U	5	U	5	U	5	U	3	U	5	3.5 J	3
F8D	1	U	5	U	5	1 J	5	U	3	2 J	5	U	3
F9S	1	U	5	U	5	2 J	5	U	3	2 J	5	3.5 J	3
F9D	1	U	5	U	5	2 J	5	U	3	3 J	5	4.2 J	3
F10	1	U	5	U	5	1 J	5	U	3	2 J	5	U	3
F10-DUP	1	U	5	NA	NA	1 J	5	NA	NA	2 J	5	NA	NA
F11S	1	U	5	U	5	U	5	U	3	1 J	5	3.5 J	3
F11D	1	U	5	U	5	1 J	5	U	3	2 J	5	U	3
F12S	1	U	5	U	5	U	5	U	3	U	5	U	3
F12D	1	U	5	U	5	2 J	5	U	3	U	5	U	3

Table D-1. Results of Samplings at Dover Funnel & Gate Site:
Target CVOCs (µg/L) (Continued)

Well ID	Dilution Factor	cis -1,2-DCE				TCE			PCE				
		Results Jul 98	Detection Limit	Results Jun 99	Reporting Limit	Results Jul 98	Detection Limit	Results Jun 99	Reporting Limit	Results Jul 98	Detection Limit	Results Jun 99	Reporting Limit
F12D-DUP	1	2 J	5	NA	NA	3 J	5	NA	NA	4 J	5	NA	NA
Gate 1 Exit Zone Wells													
F13S	1	U	5	U	5	1 J	5	U	3	3 J	5	U	3
F13D	1	U	5	U	5	1 J	5	U	3	2 J	5	U	3
F14S	1	U	5	U	5	U	5	U	3	U	5	3.6 J	3
F14S-DUP	1	NA	NA	U	5	NA	NA	U	3	NA	NA	3.8 J	3
F14D	1	U	5	U	5	U	5	U	3	2 J	5	1.8 J	3
Gate 1 Downgradient Aquifer Wells													
D1S	1	1 J	5	U	5	2 J	5	U	3	4 J	5	U	3
D2S	1	U	5	U	5	1 J	5	U	3	3 J	5	2.6 J	3
D3S	1	U	5	U	5	1 J	5	U	3	2 J	5	U	3
D4S	1	U	5	U	5	U	5	U	3	3 J	5	U	3
D4S-DUP	1	U	5	NA	NA	1 J	5	NA	NA	5 J	5	NA	NA
D5S	1	U	5	U	5	U	5	U	3	6	5	2.1 J	3
D5D	1	2 J	5	16	5	3 J	5	19	3	110	5	73	3
D6S	1	U	5	U	5	U	5	U	3	2 J	5	U	3
D8S	1	NA	NA	39 J	5	NA	NA	U	120	NA	NA	3,900	3
Gate 2 Upgradient Aquifer Wells													
U7S	1	1 J	5	1.7 J	5	3 J	5	2.6 J	3	3 J	5	5.6	3
U7D	1	6	5	40	5	9	5	15	3	47	5	190 E	3
U8S	1	U	5	U	5	3 J	5	U	3	3 J	5	4.7 J	3
U8M	1	14	5	U	5	15	5	2.5 J	3	150	5	58	3
U8D	1	15	5	17	5	18	5	5.9	3	139	5	118	3
U8D-DUP	1	NA	NA	18	5	NA	NA	6.5	3	NA	NA	120	3
U9S	1	U	5	U	5	45	5	U	3	4 J	5	8	3
U9D	1	52	5	140	5	21	5	42	3	275	5	480 E	3
Gate 2 Reactive Cell Wells													
P1S	1	U	5	U	5	4 J	5	U	3	3 J	5	U	3
P1S-DUP	1	NA	NA	U	5	NA	NA	U	3	NA	NA	U	3
P2S	1	U	5	U	5	1 J	5	U	3	2 J	5	U	3

**Table D-1. Results of Samplings at Dover Funnel & Gate Site:
Target CVOCs ($\mu\text{g/L}$) (Continued)**

Well ID	Dilution Factor	cis-1,2-DCE			TCE			PCE					
		Results Jul 98	Detection Limit	Results Jun 99	Reporting Limit	Results Jul 98	Detection Limit	Results Jun 99	Reporting Limit	Results Jul 98	Detection Limit	Results Jun 99	Reporting Limit
P2M	1	U	5	U	5	2 J	5	1.2 J	3	U	5	U	3
P2D-1	1	U	5	23	5	6	5	35	3	1 J	5	38	3
P2D-2	1	U	5	NA	NA	7	5	NA	NA	2 J	5	NA	NA
P3S	1	U	5	U	5	1 J	5	U	3	2 J	5	U	3
P3S-DUP	1	U	5	NA	NA	U	5	NA	NA	2 J	5	NA	NA
P3D	1	11	5	41	5	24	5	65	3	70	5	71	3
P4S	1	U	5	U	5	1 J	5	U	3	2 J	5	U	3
P4M	1	U	5	U	5	1 J	5	U	3	1 J	5	U	3
P4D	1	U	5	U	5	U	5	U	3	U	5	U	3
P5S	1	U	5	U	5	U	5	U	3	2 J	5	U	3
P5M	1	U	5	U	5	1 J	5	U	3	U	5	U	3
P5D	1	U	5	9.9	5	U	5	7.6	3	1 J	5	11	3
P5D-DUP	1	NA	NA	9	5	NA	NA	7.3	3	NA	NA	10	3
P6S	1	U	5	U	5	1 J	5	U	3	1 J	5	U	3
P6M	1	U	5	U	5	2 J	5	U	3	2 J	5	U	3
P6D	1	U	5	3.4 J	5	1 J	5	5	3	U	5	1.8 J	3
P6D-DUP	1	U	5	NA	NA	1 J	5	NA	NA	U	5	NA	NA
P7S	1	U	5	U	5	U	5	U	3	1 J	5	U	3
P7D	1	U	5	U	5	U	5	U	3	U	5	U	3
P8S	1	U	5	U	5	U	5	U	3	2 J	5	U	3
P8D	1	U	5	U	5	1 J	5	U	3	1 J	5	U	3
P9S	1	U	5	U	5	1 J	5	U	3	1 J	5	U	3
P9D	1	3 J	5	U	5	3 J	5	U	3	4 J	5	U	3
P10S	1	U	5	U	5	1 J	5	U	3	1 J	5	U	3
P11S	1	U	5	U	5	1 J	5	U	3	2 J	5	U	3
P11D	1	U	5	U	5	1 J	5	U	3	U	5	U	3
P12S	1	U	5	U	5	U	5	U	3	1 J	5	U	3
P12D	1	U	5	U	5	1 J	5	U	3	2 J	5	U	3
P12D-DUP	1	U	5	NA	NA	1 J	5	NA	NA	1 J	5	NA	NA
Gate 2 Exit Zone Wells													
P13S	1	U	5	U	5	2 J	5	U	3	3 J	5	U	3

**Table D-1. Results of Samplings at Dover Funnel & Gate Site:
Target CVOCs (µg/L) (Continued)**

Well ID	Dilution Factor	<i>cis</i> -1,2-DCE				TCE				PCE			
		Results Jul 98	Detection Limit	Results Jun 99	Reporting Limit	Results Jul 98	Detection Limit	Results Jun 99	Reporting Limit	Results Jul 98	Detection Limit	Results Jun 99	Reporting Limit
P13D	1	U	5	U	5	U	5	U	3	U	5	U	3
P14S	1	U	5	U	5	1 J	5	U	3	2 J	5	U	3
P14S-DUP	1	NA	NA	U	5	NA	NA	U	3	NA	NA	U	3
P14D	1	3 J	5	U	5	4 J	5	U	3	4 J	5	U	3
Gate 2 Downgradient Aquifer Wells													
D7S	1	U	5	U	5	10	5	U	3	4 J	5	U	3
D7D	1	9	5	U	5	4 J	5	U	3	4 J	5	U	3
D7D-DUP	1	NA	NA	U	5	NA	NA	U	3	NA	NA	U	3
Existing Wells													
214S	1	16	5	NA	NA	17	5	NA	NA	1,923	5	NA	NA
214D	1	95	5	NA	NA	95	5	NA	NA	10	5	NA	NA
Temporary Wells in Upgradient Aquifer													
T31-A	1	NA	NA	7	5	NA	NA	7	3	NA	NA	560 E	3
T31-E	1	NA	NA	72	5	NA	NA	130	3	NA	NA	7.1	3
T32-A	1	NA	NA	65	5	NA	NA	12	3	NA	NA	139	3
T32-E	1	NA	NA	260 E	5	NA	NA	230 E	3	NA	NA	1.2 J	3
T33-A	1	NA	NA	2.2 J	5	NA	NA	2.5 J	3	NA	NA	38	3
T33-B	1	NA	NA	3.7 J	5	NA	NA	3.5 J	3	NA	NA	64	3
T33-E	1	NA	NA	150	5	NA	NA	53	3	NA	NA	2 J	3
T34-A	1	NA	NA	6.4	5	NA	NA	4.2	3	NA	NA	230 E	NA
T34-E	5	NA	NA	210	25	NA	NA	210	15	NA	NA	8.4 J	15
T35-A	1	NA	NA	8.5	5	NA	NA	5	5	NA	NA	200 E	NA
T35-B	1	NA	NA	38	5	NA	NA	18	5	NA	NA	3,900 E	NA
T35-E	1	NA	NA	150	5	NA	NA	84	5	NA	NA	6	3
T36-A	5	NA	NA	20 J	25	NA	NA	9.4 J	15	NA	NA	230	15
T36-B	5	NA	NA	110	25	NA	NA	33	15	NA	NA	380	15
T36-D	1	NA	NA	62	5	NA	NA	69	3	NA	NA	99	3
T36-E	5	NA	NA	100	25	NA	NA	160	15	NA	NA	8.8 J	15
T37-A	1	NA	NA	8.4	5	NA	NA	4.1	5	NA	NA	490 E	NA
T37-B	1	NA	NA	51	5	NA	NA	40	5	NA	NA	8,700 E	NA
T37-C	1	NA	NA	27	5	NA	NA	19	5	NA	NA	6,000 E	NA

**Table D-1. Results of Samplings at Dover Funnel & Gate Site:
Target CVOCs ($\mu\text{g/L}$) (Continued)**

Well ID	Dilution Factor	<i>cis</i> -1,2-DCE			TCE			PCE		
		Results Jul 98	Detection Limit	Results Jun 99	Reporting Limit	Results Jul 98	Detection Limit	Results Jun 99	Detection Limit	Reporting Limit
T37-D	1	NA	NA	14	5	NA	NA	19	NA	5
T37-E	1	NA	NA	260 E	5	NA	NA	210 E	NA	NA
T38-B	1	NA	NA	U	5	NA	NA	U	NA	3
T38-E	5	NA	NA	96	25	NA	NA	25	NA	15
T39-B	5	NA	NA	U	25	NA	NA	3.5 J	NA	15
T39-E	5	NA	NA	84	25	NA	NA	41	NA	15
T40-A	5	NA	NA	56	25	NA	NA	15 J	NA	15
T40-B	5	NA	NA	70	25	NA	NA	20 J	NA	15
T40-D	10	NA	NA	72	50	NA	NA	29 J	NA	30
T40-E	1	NA	NA	120	5	NA	NA	110	NA	3
T41-A	1	NA	NA	U	5	NA	NA	6.8	NA	3
T41-B	10	NA	NA	86	50	NA	NA	26 J	NA	30
T41-D	5	NA	NA	62	25	NA	NA	57	NA	15
T41-E	1	NA	NA	85	5	NA	NA	120	NA	3
T42-A	10	NA	NA	210	50	NA	NA	55	NA	30
T42-B	5	NA	NA	150	25	NA	NA	39	NA	15
T42-D	5	NA	NA	300	25	NA	NA	320	NA	15
T42-E	5	NA	NA	270	25	NA	NA	220	NA	15

NA: Not available.

U: The result is below the reporting limit.

J: The result is less than the sample RL and greater than the MDL.

E: The compound was quantified from a secondary dilution due to analyte abundance in the sample.

Appendix E

Supporting Information for Hydraulic Performance Evaluation

E-1. Slug Test Parameters and Results

E-2. Tables of Water-Level Monitoring Data

E-3. Water-Level Maps for Area 5 (Seven Events Each for Shallow and Deep Wells)

E-4. Plots of Continuous Water-Level Monitoring

Appendix E-1

Slug Test Parameters and Results

August 1998 Dover Permeable Cell Slug Tests

		Sat. Thickness (ft)	Well Radius (ft)	Borehole Radius (ft)	Screen Length (ft)	Sat. Well Depth (ft)	Screen Depth (ft)																
Well	Test	D	rc	R	Le	H		Le/R	A	B	C	LnRe/R	Y0	Yt	t								
Gate 1 Side Upgradient Wells																							
U1S	a	20.0	0.17	0.34	4.0	4.0	20	11.62	1.85	0.50	n/a	1.04	0.15	0.017	4.00							2.99	
U1S	b	20.0	0.17	0.34	4.0	4.0	20	11.62	1.85	0.50	n/a	1.04	0.15	0.017	4.00							2.99	
U2S	a	20.1	0.17	0.34	4.1	4.1	20	12.18	1.85	0.50	n/a	1.08	0.13	0.024	4.00							2.29	
U2S	b	20.1	0.17	0.34	4.1	4.1	20	12.18	1.85	0.50	n/a	1.08	0.12	0.007	6.00							2.57	
U3D	a	20.1	0.17	0.34	5.0	20.1	36	14.71	n/a	n/a	1.70	2.60	2.05	0.740	0.30							36.69	
U3D	b	20.1	0.17	0.34	5.0	20.1	36	14.71	n/a	n/a	1.70	2.60	0.18	0.081	0.30							27.74	
U3S	a	20.1	0.17	0.34	4.1	4.1	20	12.15	1.85	0.50	n/a	1.08	0.19	0.081	0.30							15.42	
U3S	b	20.1	0.17	0.34	4.1	4.1	20	12.15	1.85	0.50	n/a	1.08	0.19	0.081	0.30							15.42	
U4D	a	20.2	0.17	0.34	5.0	20.2	36	14.71	n/a	n/a	1.70	2.60	1.20	0.015	0.80							59.20	
U4D	b	20.2	0.17	0.34	5.0	20.2	36	14.71	n/a	n/a	1.70	2.60	2.20	0.013	0.80							69.32	
U4M	a	20.1	0.17	0.34	5.0	13.1	29	14.71	2.00	0.60	n/a	1.49	2.05	1.050	0.20							20.75	
U4M	b	20.1	0.17	0.34	5.0	13.1	29	14.71	2.00	0.60	n/a	1.49	2.05	0.200	0.70							20.63	
U4S	a	20.1	0.17	0.34	4.1	4.1	20	12.06	1.85	0.50	n/a	1.07	0.08	0.009	5.00							2.35	
U4S	b	20.1	0.17	0.34	4.1	4.1	20	12.06	1.85	0.50	n/a	1.07	0.09	0.007	6.00							2.31	
U5D	a	20.2	0.17	0.34	5.0	20.2	36	14.71	n/a	n/a	1.70	2.60	2.80	0.030	6.00							8.17	
U5D	b	20.2	0.17	0.34	5.0	20.2	36	14.71	n/a	n/a	1.70	2.60	2.75	0.089	5.00							7.42	
U5S	a	20.2	0.17	0.34	4.2	4.2	20	12.41	1.85	0.50	n/a	1.09	0.12	0.013	4.00							2.99	
U5S	b	20.2	0.17	0.34	4.2	4.2	20	12.41	1.85	0.50	n/a	1.09	0.17	0.009	4.00							3.96	
U6S	a	20.4	0.17	0.34	4.4	4.4	20	12.88	1.85	0.50	n/a	1.12	0.31	0.105	0.80							7.22	
U6S	b	20.4	0.17	0.34	4.4	4.4	20	12.88	1.85	0.50	n/a	1.12	0.32	0.105	0.80							7.43	
U10S	a	20.0	0.17	0.34	4.0	4.0	20	11.85	1.85	0.50	n/a	1.06	0.19	0.011	6.00							2.64	
U10S	b	20.0	0.17	0.34	4.0	4.0	20	11.85	1.85	0.50	n/a	1.06	0.15	0.008	8.00							1.98	
U11S	a	20.1	0.17	0.34	4.1	4.1	20	12.00	1.85	0.50	n/a	1.07	0.19	0.002	8.00							3.02	
U11S	b	20.1	0.17	0.34	4.1	4.1	20	12.00	1.85	0.50	n/a	1.07	0.20	0.004	8.00							2.72	
U12S	a	20.2	0.17	0.34	4.2	4.2	20	12.29	1.85	0.50	n/a	1.09	0.16	0.011	8.00							1.81	
U12S	b	20.2	0.17	0.34	4.2	4.2	20	12.29	1.85	0.50	n/a	1.09	0.16	0.012	8.00							1.78	
U13S	a	20.2	0.17	0.34	4.2	4.2	20	12.41	1.85	0.50	n/a	1.09	0.16	0.008	8.00							2.02	
U13S	b	20.2	0.17	0.34	4.2	4.2	20	12.41	1.85	0.50	n/a	1.09	0.18	0.009	8.00							2.04	
U14S	a	20.3	0.17	0.34	4.3	4.3	20	12.59	1.85	0.50	n/a	1.10	0.17	0.004	4.00							4.99	
U14S	b	20.3	0.17	0.34	4.3	4.3	20	12.59	1.85	0.50	n/a	1.10	0.15	0.011	4.00							3.51	
U15S	a	20.4	0.17	0.34	4.4	4.4	20	12.94	1.85	0.50	n/a	1.13	0.20	0.004	4.00							5.21	
U15S	b	20.4	0.17	0.34	4.4	4.4	20	12.94	1.85	0.50	n/a	1.13	0.20	0.004	4.00							5.15	
																Geometric Mean		5.66					
																Standard Deviation		16.32					

Well	Test	Sat. Thickness (ft)	Well Radius (ft)	Borehole Radius (ft)	Screen Length (ft)	Sat. Well Depth (ft)	Screen Depth (ft)	Le/R	A	B	C	LnRe/R	Yo	(ft)	(min)	Permeability (ft/day)
Gate 1 Wells (reactive iron permeable barrier)																
(upgradient pretreatment zone)																
F1S	a	20.1	0.17	0.34	4.1	4.1	20	11.91	1.85	0.50	n/a	1.06	0.27	0.028	0.10	123.66
F1S	b	20.1	0.17	0.34	4.1	4.1	20	11.91	1.85	0.50	n/a	1.06	0.40	0.023	0.10	155.83
(reactive iron treatment zone)																
F10	a	20.1	0.17	0.34	5.0	20.1	36	14.71	n/a	n/a	1.70	2.60	17.00	0.045	0.04	1603.07
F10	b	20.1	0.17	0.34	5.0	20.1	36	14.71	n/a	n/a	1.70	2.60	12.00	0.045	0.04	1508.98
(downgradient reactive iron posttreatment zone)																
F14S	a	20.3	0.17	0.34	4.3	4.3	20	12.50	1.85	0.50	n/a	1.10	0.50	0.005	0.01	2478.49
F14S	b	20.3	0.17	0.34	4.3	4.3	20	12.50	1.85	0.50	n/a	1.10	0.75	0.007	0.01	2485.71
															Geometric Mean	812.25
															Standard Deviation	1055.62
Gate 2 Wells (pyrite permeable barrier)																
(upgradient pyrite pretreatment zone)																
P1	a	20.4	0.17	0.34	4.4	4.4	20	12.79	1.85	0.50	n/a	1.12	3.00	0.010	0.10	307.65
P1	b	20.4	0.17	0.34	4.4	4.4	20	12.79	1.85	0.50	n/a	1.12	1.80	0.011	0.10	272.50
(reactive iron treatment zone)																
P7D	a	20.3	0.17	0.34	5.0	20.3	36	14.71	n/a	n/a	n/a	n/a	n/a	n/a	n/a	n/a
P7D	b	20.3	0.17	0.34	5.0	20.3	36	14.71	n/a	n/a	n/a	n/a	n/a	n/a	n/a	n/a
P7S	a	20.3	0.17	0.34	4.3	4.3	20	12.71	1.85	0.50	n/a	1.11	0.41	0.017	0.10	170.49
P7S	b	20.3	0.17	0.34	4.3	4.3	20	12.71	1.85	0.50	n/a	1.11	0.43	0.014	0.10	183.44
P10	a	20.4	0.17	0.34	5.0	20.4	36	14.71	n/a	n/a	1.70	2.60	0.38	0.005	0.10	468.94
P10	b	20.4	0.17	0.34	5.0	20.4	36	14.71	n/a	n/a	1.70	2.60	0.58	0.010	0.10	442.97
(downgradient pyrite posttreatment zone)																
P14S	a	20.2	0.17	0.34	4.2	4.2	20	12.47	1.85	0.50	n/a	1.10	0.23	0.020	0.10	131.54
P14S	b	20.2	0.17	0.34	4.2	4.2	20	12.47	1.85	0.50	n/a	1.10	0.60	0.060	0.10	124.01
															Geometric Mean	233.66
															Standard Deviation	135.42
Gate 2 Side Upgradient Wells																
U7D	a	20.4	0.17	0.34	5.0	20.4	36	14.71	n/a	n/a	1.70	2.60	2.40	0.820	0.80	14.54
U7D	b	20.4	0.17	0.34	5.0	20.4	36	14.71	n/a	n/a	1.70	2.60	2.45	0.830	0.80	14.65
U7D	c	20.4	0.17	0.34	5.0	20.4	36	14.71	n/a	n/a	1.70	2.60	2.40	0.800	0.80	14.87
U8D	a	20.4	0.17	0.34	5.0	20.4	36	14.71	n/a	n/a	1.70	2.60	0.60	0.009	4.00	11.37
U8D	b	20.4	0.17	0.34	5.0	20.4	36	14.71	n/a	n/a	1.70	2.60	1.35	0.060	2.00	16.85
U8D	c	20.4	0.17	0.34	5.0	20.4	36	14.71	n/a	n/a	1.70	2.60	0.53	0.022	4.00	8.61
U9D	a	20.5	0.17	0.34	5.0	20.5	36	14.71	n/a	n/a	1.70	2.60	1.80	0.110	0.30	100.94
U9D	b	20.5	0.17	0.34	5.0	20.5	36	14.71	n/a	n/a	1.70	2.60	2.00	0.200	0.25	99.79
															Geometric Mean	21.89
															Standard Deviation	40.30

Appendix E-2

Tables of Water-Level Monitoring Data

Table E-2a. Water Level Monitoring Data

Well ID	Northing	Easting	TOC ft MSL	Post-Installation																			
				1/14/98	2/3/98	2/9/98	2/16/98	2/26/98	3/7/98	3/13/98	3/20/98	3/27/98	4/3/98	4/10/98	4/18/98	5/6/98	7/13/98	10/7/98	12/16/98	2/1/99	4/8/99	4/26/99	6/1/99
Gate 1 Far Upgradient Aquifer Wells																							
U16S	411386.11	479618.44	27.31	11.22	12.03	12.35	12.53	12.99	13.39	13.87	14.17	14.60	14.68	14.52	14.32	13.84	12.56	10.80	9.72	9.88	10.76	10.97	10.59
U17S	411396.66	479613.50	27.13	11.22	12.03	12.35	12.54	12.98	13.44	13.88	14.16	14.60	14.69	14.52	14.31	13.85	12.58	10.81	9.72	9.88	10.77	10.97	10.59
U18S	411395.45	479625.52	27.15	11.23	12.03	12.37	12.54	13.01	13.43	13.88	14.18	14.61	14.70	14.53	14.32	13.86	12.60	10.83	9.75	9.90	10.77	10.99	10.61
Average				11.23	12.03	12.36	12.54	13.00	13.42	13.88	14.17	14.61	14.69	14.53	14.32	13.85	12.58	10.82	9.73	9.89	10.77	10.98	10.60
SD				0.01	0.00	0.01	0.01	0.01	0.03	0.01	0.01	0.01	0.01	0.01	0.00	0.01	0.02	0.02	0.02	0.01	0.01	0.01	0.01
Gate 1 Vicinity Upgradient Aquifer Wells																							
U10S	411375.12	479614.43	27.43	11.20	12.03	12.35	12.52	12.98	13.38	13.79	14.08	14.53	14.70	14.55	14.39	13.86	12.58	10.80	9.73	9.88	10.76	10.97	10.59
U11S	411380.13	479611.01	27.38	11.20	12.02	12.36	12.53	12.97	13.42	13.86	14.08	14.53	14.71	14.55	14.36	13.87	12.58	10.82	9.73	9.87	10.76	10.98	10.58
U12S	411385.12	479608.18	27.36	11.21	12.06	12.36	12.54	12.97	13.44	13.81	14.06	14.54	14.71	14.56	14.35	13.87	12.58	10.82	9.74	9.89	10.76	10.96	10.59
U13S	411390.69	479605.32	27.31	11.20	12.01	12.15	12.55	12.99	13.44	13.88	14.16	14.50	14.70	14.55	14.36	13.86	12.57	10.81	9.72	9.88	10.76	10.98	10.59
U14S	411395.42	479602.64	27.25	11.21	12.03	12.66	12.56	13.00	13.43	13.85	14.15	14.58	14.70	14.55	14.34	13.86	12.60	10.82	9.73	9.89	10.76	10.98	10.60
U15S	411400.82	479599.51	27.14	11.23	12.05	12.37	12.25	12.71	13.18	13.86	14.14	14.59	14.69	14.52	14.32	13.85	12.61	10.84	9.75	9.91	11.01	10.98	10.61
Average				11.21	12.03	12.38	12.49	12.94	13.37	13.84	14.11	14.55	14.70	14.55	14.35	13.86	12.59	10.82	9.73	9.89	10.76	10.98	10.59
SD				0.01	0.02	0.16	0.12	0.11	0.11	0.03	0.04	0.03	0.01	0.02	0.02	0.01	0.01	0.01	0.01	0.01	NA	0.02	0.01
Gate 1 Upgradient Aquifer Wells																							
U1S	411368.83	479607.91	27.50	12.20	12.34	12.51	12.98	13.40	13.86	14.13	14.59	14.68	14.50	14.32	13.83	12.55	10.78	9.70	9.85	10.72	10.93	10.97	10.57
U2S	411374.42	479605.39	27.37	11.17	12.02	12.35	12.52	12.99	13.42	13.80	14.07	14.54	14.68	14.49	14.31	13.83	12.57	10.79	9.72	9.87	10.76	10.94	10.59
U3S	411379.04	479602.08	27.52	11.20	12.01	12.35	12.53	12.94	13.43	13.87	14.18	14.61	14.72	14.52	14.32	13.87	12.60	10.81	9.73	9.89	10.76	10.96	10.61
U3D	411379.00	479601.86	27.42	11.18	12.01	12.25	12.52	12.99	13.42	13.88	14.15	14.60	14.71	14.43	14.32	13.86	12.58	10.80	9.74	9.87	10.76	10.95	10.60
U4S	411385.10	479599.96	27.43	11.19	11.92	12.33	12.52	12.91	13.36					14.53	14.33	13.86	12.62	10.88	9.74	9.88	10.83	10.95	10.59
U4M	411385.35	479599.83	27.40	11.18	12.00	12.35	12.53	12.98	13.43			14.58	14.75	14.52	14.32	13.90	12.55	10.81	9.73	9.88	10.94	10.94	10.60
U4D	411385.13	479599.78	27.34	11.17	12.00	12.34	12.52	12.99	13.41			14.61	14.74	14.50	14.32	13.89	12.57	10.79	9.72	9.86	10.67	10.94	10.59
U5S	411389.99	479596.53	27.33	11.22	12.03	12.38	12.56	12.98	13.41	13.84	14.13	14.58	14.78	14.57	14.37	13.93	12.63	10.84	9.75	9.91	10.99	10.99	10.61
U5D	411390.08	479596.34	27.26	11.28	11.98	12.34	12.54	13.00	13.44	13.89	14.20	14.62	14.71	14.53	14.34	13.86	12.58	10.97	9.74	9.90	10.76	10.94	10.60
U6S	411394.94	479594.33	27.17	11.22	12.06	12.38	12.57	12.97	13.42	13.85	14.13	14.59	14.72	14.54	14.34	13.87	12.60	10.83	9.75	9.90	10.78	10.95	10.60
Average				11.20	12.02	12.34	12.53	12.97	13.41	13.86	14.14	14.59	14.72	14.51	14.33	13.87	12.59	10.83	9.73	9.88	10.76	10.95	10.60
SD				0.03	0.07	0.03	0.02	0.03	0.02	0.03	0.04	0.03	0.03	0.04	0.02	0.03	0.03	0.06	0.01	0.02	0.08	0.01	0.01
Gate 1 Pre-Treatment Zone Wells																							
F1S	411383.80	479595.69	27.34	12.00	12.34	12.53	12.99	13.42		13.88	14.25	14.59	14.66	14.51	14.28	13.85	12.49	10.79	9.70	9.86	10.72	10.96	10.56
F2S	411383.56	479595.16	27.26	12.00	12.34	12.52	13.01	13.44		13.86	14.18	14.53	14.63	14.47	14.26	13.83	12.41	10.76	9.69	9.83	10.72	10.94	10.61
F2M	411383.35	479594.95	27.33	11.98	12.32	12.51	12.97	13.42		13.86	14.18	14.53	14.63	14.47	14.26	13.80	12.49	10.90	9.66	9.88	10.92	10.92	10.55
F2D	411383.35	479595.41	27.34	12.00	12.33	12.52	12.98	13.43		13.88	14.20	14.55	14.64	14.49	14.27	13.81	12.49	10.78	9.67	9.82	10.92	10.92	10.56
F3S	411384.24	479594.76	27.37	11.99	12.35	12.52	12.99	13.44		13.91	14.15	14.50	14.65	14.50	14.29	13.82	12.49	10.77	9.68	9.83	10.92	10.92	10.57
F3D	411384.36	479594.97	27.41	12.00	12.34	12.51	12.99	13.43		13.89	14.25	14.60	14.64	14.49	14.27	13.81	12.48	10.77	9.63	9.78	10.92	10.92	10.55
Average				12.00	12.34	12.52	12.99	13.43		13.89	14.21	14.56	14.65	14.49	14.28	13.82	12.48	10.80	9.67	9.83	10.72	10.93	10.57
SD				0.01	0.01	0.01	0.01	0.01		0.02	0.04	0.04	0.01	0.01	0.01	0.02	0.03	0.05	0.02	0.04	NA	0.02	0.02
Gate 1 Reactive Cell Wells																							
F4S	411381.87	479595.19	27.36	11.94	12.29	12.47	12.93	13.36		13.81	14.15	14.51	14.59	14.45	14.22	13.75	12.44	10.72	9.61	9.75	10.72	10.90	10.52
F5S	411382.45	479594.13	27.32	11.99	12.34	12.51	12.98	13.40		13.86	14.20	14.55	14.63	14.50	14.28	13.80	12.49	10.76	9.67	9.79	10.72	10.90	10.55
F6S	411383.48	479593.35	27.36	12.05	12.37	12.55	13.02	13.44		13.88	14.23	14.58	14.67	14.53	14.31	13.82	12.52	10.79	9.70	9.82	10.72	10.93	10.59
F7S	411381.51	479592.76	27.17	11.95	12.29	12.43	12.95	13.37		13.83	14.11	14.51	14.61	14.46	14.24	13.76	12.49	10.72	9.64	9.75	10.68	10.86	10.49
F8S	411380.68	479593.77	27.31	11.99	12.33	12.51	12.98	13.40		13.85	14.19	14.55	14.65	14.49	14.26	13.80	12.49	10.76	9.66	9.78	10.72	10.90	10.55
F9S	411383.09	479592.30	27.38	11.99	12.32	12.51	12.97	13.40		13.85	14.19	14.54	14.63	14.48	14.26	13.79	12.52	10.76	9.66	9.78	10.88	10.88	10.54
F11S	411381.05	479591.87	27.34	11.98	12.30	12.49	12.97	13.37		13.82	14.16	14.53	14.63	14.50	14.27	13.80	12.50	10.76	9.79	9.77	10.89	10.89	10.54

Table E-2a. Water Level Monitoring Data (Continued)

				Post-Installation																			
Well ID	Northing	Easting	TOC ft MSL	1/14/98	2/3/98	2/9/98	2/16/98	2/26/98	3/7/98	3/13/98	3/20/98	3/27/98	4/3/98	4/10/98	4/18/98	5/6/98	7/13/98	10/7/98	12/16/98	2/1/99	4/8/99	4/26/99	6/1/99
F12S	411382.17	479591.39	27.25	11.96	12.30	12.48	12.49	12.97	13.36	13.83	14.15	14.51	14.61	14.45	14.23	13.76	12.41	10.73	9.64	9.78	10.70	10.88	10.52
			Average Shallow Wells	11.98	12.32	12.49	12.97	13.39	13.84	14.17	14.53	14.63	14.48	14.26	13.78	12.48	10.75	9.67	9.78	10.70	10.88	10.52	
			SD	0.03	0.03	0.04	0.03	0.03	0.02	0.04	0.02	0.03	0.03	0.03	0.03	0.03	0.04	0.02	0.06	0.03	0.02	1.07	0.03
				11.96	12.29	12.48	12.94	13.37	13.81	14.16	14.52	14.60	14.45	14.23	13.77	12.45	10.74	9.62	9.73	10.88	10.52		
F4M	411381.74	479595.08	27.33	12.00	12.33	12.50	12.98	13.39	13.85	14.20	14.56	14.64	14.49	14.27	13.81	12.51	10.76	9.67	9.80	10.92	10.56		
F5M	411382.46	479594.56	27.40	11.95	12.28	12.47	12.93	13.36	13.81	14.15	14.49	14.58	14.44	14.22	13.73	12.39	10.70	9.62	9.73	10.84	10.50		
F6M	411383.19	479593.26	27.31	11.97	12.30	12.48	12.95	13.37	13.82	14.17	14.52	14.61	14.46	14.24	13.77	12.45	10.73	9.64	9.75	NA	10.88	10.53	
			Average Mid Wells	0.03	0.03	0.02	0.03	0.02	0.02	0.03	0.04	0.03	0.03	0.03	0.03	0.04	0.06	0.03	0.03	0.04	NA	0.04	0.03
F4D	411381.67	479594.79	27.35	11.98	12.32	12.51	12.98	13.39	13.83	14.19	14.55	14.64	14.48	14.26	13.81	12.46	10.75	9.63	9.76	10.91	10.54		
F5D	411382.73	479594.49	27.33	12.00	12.34	12.52	12.99	13.41	13.86	14.21	14.56	14.64	14.50	14.28	13.79	12.50	10.76	9.65	9.79	10.91	10.56		
F6D	411383.29	479593.56	27.22	11.79	12.12	12.31	12.78	13.19	13.67	13.99	14.35	14.42	14.28	14.05	13.57	12.28	10.55	9.44	9.56	10.68	10.34		
F7D	411381.59	479593.21	27.26	11.97	12.31	12.57	12.97	13.39	13.84	14.18	14.53	14.62	14.46	14.26	13.79	12.48	10.74	9.65	9.77	10.90	10.53		
F8D	411380.71	479593.49	27.38	12.00	12.35	12.53	12.99	13.40	13.86	14.22	14.56	14.65	14.50	14.28	13.82	12.51	10.77	9.68	9.80	10.90	10.56		
F9D	411382.85	479592.46	27.37	11.96	12.31	12.47	12.95	13.38	13.83	14.16	14.51	14.61	14.45	14.22	13.78	12.43	10.74	9.64	9.75	10.86	10.51		
F11D	411380.68	479591.97	27.48	11.99	12.34	12.52	12.98	13.37	13.84	14.19	14.54	14.63	14.49	14.26	13.80	12.53	10.77	9.68	9.79	10.92	10.56		
F12D	411382.03	479591.04	27.43	11.98	12.32	12.50	12.97	13.37	13.84	14.18	14.53	14.62	14.46	14.26	13.79	12.48	10.74	9.65	9.77	10.90	10.53		
			Average Deep Wells	11.96	12.30	12.49	12.95	13.36	13.82	14.16	14.53	14.60	14.46	14.23	13.77	12.46	10.73	9.63	9.75	NA	10.87	10.52	
			SD	0.07	0.07	0.08	0.07	0.07	0.07	0.07	0.08	0.08	0.08	0.08	0.08	0.08	0.07	0.08	0.08	NA	0.08	0.07	
F10	411380.14	479592.34	27.33	11.99	12.32	12.51	12.99	13.40	13.85	14.21	14.62	14.66	14.50	14.26	13.83	12.53	10.78	9.68	9.79	10.91	10.55		
			Average Wells	11.97	12.31	12.49	12.96	13.38	13.83	14.17	14.53	14.62	14.47	14.25	13.78	12.47	10.74	9.65	9.76	10.70	10.73	10.53	
			SD	0.05	0.05	0.05	0.05	0.05	0.05	0.04	0.05	0.06	0.05	0.05	0.05	0.06	0.05	0.05	0.05	0.02	0.68	0.05	
Gate 1 Exit Zone Wells				11.99	12.34	12.50	12.99	13.35	13.85	14.15	14.55	14.64	14.50	14.26	13.79	12.50	10.76	9.65	9.78	10.88	10.55		
F13S	411380.10	479591.62	27.35	11.99	12.34	12.50	12.99	13.35	13.85	14.15	14.55	14.64	14.50	14.26	13.79	12.50	10.76	9.65	9.78	10.88	10.55		
F13D	411379.76	479591.78	27.41	12.00	12.34	12.51	13.00	13.40	13.86	14.25	14.56	14.64	14.50	14.27	13.79	12.51	10.77	9.68	9.79	10.89	10.56		
F14S	411380.88	479591.32	27.20	12.00	12.32	12.52	12.98	13.45	13.91	14.19	14.55	14.63	14.49	14.27	13.78	12.51	10.82	9.68	9.80	10.72	10.91	10.56	
F14D	411380.55	479591.32	27.26	12.00	12.20	12.52	13.04	13.45	13.91	14.19	14.55	14.63	14.49	14.27	13.78	12.51	10.76	9.67	9.78	10.90	10.54		
			Average	12.00	12.30	12.51	13.00	13.40	13.87	14.20	14.55	14.64	14.50	14.26	13.78	12.50	10.78	9.67	9.79	10.72	10.89	10.55	
			SD	0.00	0.07	0.01	0.02	0.05	0.03	0.05	0.05	0.01	0.01	0.01	0.01	0.01	0.03	0.01	0.01	NA	0.01	0.01	
Gate 1 Downgradient Aquifer Wells				11.15	11.98	12.33	12.48	12.97	13.39	13.83	14.12	14.54	14.66	14.48	14.27	13.84	12.48	10.74	9.66	9.84	10.71	10.91	10.52
D1S	411371.55	479597.83	27.42	11.15	11.97	12.32	12.48	12.97	13.38	13.83	14.16	14.57	14.65	14.48	14.28	13.83	12.48	10.57	9.67	9.83	10.92	10.54	
D2S	411376.84	479595.01	27.21	11.14	11.96	12.32	12.47	12.96	13.39	13.84	14.15	14.56	14.64	14.47	14.27	13.82	12.49	10.58	9.66	9.83	10.92	10.53	
D3S	411372.85	479593.71	27.39	11.14	11.95	12.31	12.46	12.96	13.43	13.81	14.15	14.51	14.64	14.46	14.27	13.82	12.47	10.73	9.66	9.82	10.91	10.53	
D4S	411377.21	479590.36	27.55	11.14	11.95	12.31	12.47	12.95	13.38	13.83	14.15	14.57	14.65	14.48	14.27	13.83	12.48	10.73	9.66	9.81	10.70	10.78	
D5S	411379.71	479589.24	27.28	11.14	11.92	12.28	12.44	12.94	13.36	13.82	14.12	14.54	14.62	14.46	14.25	13.78	12.44	10.72	9.63	9.79	10.87	10.50	
D5D	411379.85	479589.14	27.38	11.13	11.94	12.28	12.45	12.91	13.37	13.82	14.07	14.49	14.63	14.47	14.27	13.79	12.46	10.72	9.65	9.81	10.88	10.51	
D6S	411382.15	479587.81	27.19	11.14	11.95	12.31	12.46	12.95	13.39	13.83	14.13	14.54	14.64	14.47	14.27	13.82	12.47	10.68	9.66	9.82	10.71	10.88	
			Average	0.01	0.02	0.02	0.01	0.02	0.02	0.01	0.03	0.03	0.01	0.01	0.01	0.02	0.02	0.08	0.01	0.02	0.00	0.05	0.01
			SD	11.20	12.03	12.32	12.54	13.00	13.43	13.87	14.11	14.48	14.71	14.53	14.32	13.86	12.61	10.82	9.74	9.88	10.76	10.97	10.60
Gate 2 Upgradient Aquifer Wells				11.20	12.03	12.32	12.54	13.00	13.43	13.87	14.11	14.48	14.71	14.53	14.32	13.86	12.61	10.82	9.74	9.88	10.76	10.97	10.60
U7S	411413.20	479583.23	27.21	11.19	12.00	12.33	12.52	12.97	13.43	13.88	14.18	14.60	14.69	14.52	14.33	13.84	12.57	10.81	9.72	9.87	10.95	10.60	
U7D	411413.44	479583.23	27.16	11.20	11.95	12.31	12.52	13.01	13.44	13.87	14.06	14.61	14.72	14.54	14.36	13.87	12.56	10.83	9.73	9.89	10.77	11.04	
U8S	411418.78	479580.33	27.16	11.19	12.02	12.34	12.53	13.00	13.43	13.88	14.14	14.58	14.70	14.53	14.32	13.85	12.60	10.82	9.73	9.86	10.97	10.60	
U8M	411418.69	479580.59	27.22	11.20	12.03	12.34	12.53	13.01	13.44	13.88	14.17	14.60	14.70	14.52	14.32	13.85	12.58	10.81	9.72	9.86	10.97	10.60	
U8D	411418.92	479580.44	27.18	11.21	12.04	12.34	12.53	13.01	13.44	13.88	14.18	14.61	14.72	14.55	14.36	13.87	12.59	10.82	9.73	9.89	10.97	10.60	
U9S	411423.75	479577.68	27.14																				

Table E-2a. Water Level Monitoring Data (Continued)

TOC				Post-Installation																			
Well ID	Northing	Easting	ft MSL	1/14/98	2/3/98	2/9/98	2/16/98	2/26/98	3/7/98	3/13/98	3/20/98	3/27/98	4/3/98	4/10/98	4/18/98	5/6/98	7/13/98	10/7/98	12/16/98	2/1/99	4/8/99	4/26/99	6/1/99
U9D	411423.55	479577.88	27.06	11.19	12.00	12.32	12.51	12.97	13.42	13.87	14.16	14.59	14.69	14.51	14.33	13.85	12.56	10.79	9.69	9.86	10.77	10.96	10.56
Average				11.20	12.01	12.33	12.53	12.99	13.43	13.88	14.14	14.58	14.70	14.53	14.33	13.86	12.58	10.81	9.72	9.87	10.77	10.96	10.59
SD				0.01	0.03	0.01	0.01	0.02	0.01	0.01	0.05	0.05	0.01	0.01	0.02	0.01	0.02	0.01	0.01	0.01	0.00	0.04	0.02
Gate 2 Pre-Treatment Zone Wells																							
P1S	411416.98	479577.54	27.08	11.96	12.32	12.50	12.98	13.38	13.86	14.18	14.54	14.66	14.53	14.38	13.81	12.52	10.80	9.68	9.87	10.73	10.95	10.57	
P2S	411416.84	479576.73	27.16	11.92	12.28	12.47	12.95	13.38	13.83	14.14	14.52	14.62	14.50	14.35	13.78	12.49	10.77	9.65	9.82	10.87	10.87	10.53	
P2M	411417.19	479576.47	27.25	11.98	12.33	12.53	13.00	13.45	13.90	14.20	14.58	14.68	14.56	14.40	13.85	12.53	10.83	9.72	9.89	10.96	10.96	10.59	
P2D	411416.65	479576.50	27.25	11.96	12.34	12.51	12.98	13.41	13.87	14.19	14.56	14.65	14.54	14.38	13.82	12.51	10.80	9.66	9.85	10.91	10.91	10.57	
P3S	411418.29	479575.96	27.17	11.97	12.34	12.52	12.99	13.40	13.87	14.19	14.56	14.69	14.56	14.41	13.86	12.52	10.81	9.79	9.87	10.94	10.94	10.58	
P3D	411417.87	479576.11	27.03	11.95	12.31	12.50	12.98	13.40	13.88	14.16	14.52	14.66	14.52	14.37	13.83	12.53	10.79	9.68	9.82	10.90	10.90	10.55	
Average				11.96	12.32	12.51	12.98	13.40	13.87	14.18	14.55	14.66	14.54	14.38	13.83	12.52	10.80	9.70	9.85	10.73	10.92	10.92	10.57
SD				0.02	0.02	0.02	0.02	0.02	0.02	0.02	0.02	0.02	0.03	0.02	0.02	0.03	0.02	0.02	0.05	0.03	NA	0.03	0.02
Gate 2 Reactive Cell Wells																							
P4S	411415.08	479576.00	27.20	11.94	12.30	12.48	12.99	13.43	13.88	14.15	14.52	14.64	14.52	14.37	13.81	12.55	10.80	9.66	9.82		10.90	10.54	
P5S	411416.59	479575.64	27.16	11.92	12.28	12.47	12.94	13.35	13.79	14.14	14.52	14.60	14.46	14.31	13.77	12.49	10.75	9.66	9.79	10.69	10.88	10.52	
P6S	411417.38	479574.53	27.22	11.99	12.35	12.53	12.98	13.42	13.87	14.20	14.58	14.69	14.56	14.40	13.86	12.54	10.85	9.70	9.85		10.94	10.58	
P7S	411415.78	479574.76	27.18	11.98	12.33	12.52	12.98	13.42	13.85	14.19	14.52	14.63	14.56	14.42	13.80	12.51	10.75	9.70	9.86		10.94	10.57	
P8S	411414.94	479574.94	27.19	11.93	12.30	12.50	12.94	13.36	13.81	14.16	14.51	14.65	14.51	14.37	13.82	12.48	10.81	9.66	9.81		10.90	10.53	
P9S	411416.62	479573.76	27.29	11.94	12.31	12.49	12.95	13.36	13.82	14.17	14.57	14.64	14.51	14.37	13.81	12.47	10.76	9.68	9.81	10.70	10.91	10.53	
P11S	411415.19	479573.23	27.25	11.95	12.30	12.49	12.95	13.36	13.83	14.17	14.55	14.65	14.51	14.39	13.82	12.48	10.86	9.82	9.81		10.91	10.53	
P12S	411416.02	479572.65	27.17	11.96	12.25	12.49	12.96	13.38	13.85	14.17	14.54	14.65	14.51	14.38	13.82	12.52	10.77	9.81	9.81		10.91	10.53	
Average				11.95	12.30	12.50	12.96	13.39	13.84	14.17	14.54	14.64	14.52	14.38	13.81	12.51	10.79	9.71	9.82	10.70	10.91	10.91	10.54
SD				0.02	0.03	0.02	0.02	0.03	0.03	0.02	0.03	0.02	0.02	0.03	0.03	0.02	0.03	0.04	0.07	0.02	0.01	0.02	0.02
P4M	411415.36	479575.82	27.23	11.96	12.31	12.50	12.98	13.44	13.88	14.17	14.55	14.65	14.52	14.37	13.82	12.48	10.77	9.69	9.84		10.92	10.54	
P5M	411416.54	479575.24	27.24	11.95	12.30	12.47	12.96	13.38	13.82	14.16	14.55	14.63	14.50	14.37	13.80	12.47	10.77	9.69	9.83		10.92	10.54	
P6M	411417.54	479574.96	27.13	11.97	12.33	12.52	13.01	13.44	13.89	14.18	14.47	14.68	14.54	14.39	13.85	12.53	10.80	9.72	9.84		10.94	10.57	
Average				11.96	12.32	12.50	12.99	13.42	13.87	14.17	14.53	14.66	14.52	14.38	13.83	12.50	10.78	9.70	9.84	NA	NA	10.93	10.55
SD				0.01	0.01	0.02	0.02	0.03	0.04	0.01	0.05	0.02	0.02	0.01	0.02	0.03	0.02	0.02	0.02	0.00	NA	0.01	0.02
P4D	411415.38	479576.20	27.27	11.94	12.31	12.48	13.02	13.45	13.91	14.15	14.53	14.64	14.51	14.36	13.81	12.52	10.75	9.67	9.82		10.89	10.53	
P5D	411416.24	479575.42	27.25	11.93	12.29	12.51	12.95	13.37	13.83	14.15	14.53	14.62	14.49	14.35	13.79	12.50	10.75	9.67	9.80		10.90	10.52	
P6D	411417.13	479574.79	27.24	11.98	12.34	12.54	12.98	13.43	13.89	14.19	14.67	14.68	14.56	14.39	13.85	12.49	10.79	9.71	9.85		10.93	10.57	
P7D	411415.99	479574.69	27.19	11.98	12.33	12.52	12.99	13.42	13.89	14.19	14.58	14.68	14.56	14.41	13.85	12.51	10.71	9.71	9.86		10.94	10.57	
P8D	411414.62	479575.00	27.25	11.96	12.32	12.51	12.98	13.40	13.85	14.18	14.61	14.66	14.53	14.39	13.83	12.51	10.86	9.70	9.82		10.92	10.53	
P9D	411416.90	479573.88	27.08	11.92	12.29	12.48	12.95	13.37	13.82	14.15	14.53	14.63	14.49	14.36	13.80	12.46	10.76	9.66	9.79		10.89	10.48	
P11D	411414.88	479573.24	27.18	11.98	12.33	12.51	12.98	13.38	13.83	14.19	14.56	14.67	14.53	14.41	13.84	12.50	10.80	9.70	9.85		10.85	10.56	
P12D	411416.32	479572.39	27.26	11.99	12.40	12.52	12.99	13.43	13.88	14.21	14.58	14.69	14.56	14.44	13.86	12.53	10.80	9.71	9.86		10.95	10.57	
Average				11.96	12.33	12.51	12.98	13.41	13.86	14.18	14.57	14.66	14.53	14.39	13.83	12.50	10.78	9.69	9.83	NA	NA	10.91	10.54
SD				0.03	0.04	0.02	0.02	0.03	0.03	0.02	0.05	0.03	0.03	0.03	0.03	0.03	0.02	0.05	0.02	0.03	NA	0.03	0.03
P10	411413.79	479573.96	27.10	11.96	12.31	12.50	12.96	13.39	13.84	14.18	14.57	14.66	14.53	14.41	13.83	12.51	10.79	9.69	9.83		10.92	10.54	
Average				11.96	12.31	12.50	12.97	13.40	13.85	14.17	14.55	14.65	14.52	14.38	13.82	12.50	10.79	9.70	9.83	10.70	10.91	10.91	10.54
SD				0.02	0.03	0.02	0.02	0.03	0.03	0.02	0.04	0.02	0.03	0.03	0.03	0.02	0.03	0.04	0.04	0.02	0.01	0.02	0.02
Gate 2 Exit Zone Wells																							
P13S	411413.83	479572.92	27.15	11.98	12.32	12.51	12.97	13.40	13.86	14.20	14.57	14.67	14.54	14.42	13.84	12.52	10.79	9.70	9.85		10.93	10.55	
P13D	411414.05	479573.11	27.25	11.97	12.33	12.50	12.97	13.40	13.86	14.19	14.56	14.66	14.53	14.40	13.83	12.52	10.79	9.70	9.84		10.91	10.55	
P14S	411414.70	479572.47	27.22	12.00	12.34	12.53	13.02	13.43	13.87	14.21	14.58	14.69	14.56	14.44	13.86	12.51	10.82	9.72	9.86	10.72	10.95	10.56	

Table E-2a. Water Level Monitoring Data (Continued)

Well ID	Northing	Easting	TOC ft MSL	Post-Installation																					
				1/14/98	2/3/98	2/9/98	2/16/98	2/26/98	3/7/98	3/13/98	3/20/98	3/27/98	4/3/98	4/10/98	4/18/98	5/6/98	7/13/98	10/7/98	12/16/98	2/1/99	4/8/99	4/26/99	6/1/99		
P14D	411414.95	479572.26	27.31		11.99	12.32	12.54	13.01	13.42	13.86	14.20	14.56	14.68	14.56	14.43	13.85	12.52	10.78	9.71	9.84	10.93	10.56			
			Average		11.99	12.33	12.52	12.99	13.41	13.86	14.20	14.57	14.68	14.55	14.42	13.85	12.52	10.80	9.71	9.85	10.72	10.93	10.56		
			SD		0.01	0.01	0.02	0.03	0.02	0.00	0.01	0.01	0.01	0.02	0.02	0.01	0.01	0.02	0.01	0.01	0.01	NA	0.02	0.01	
Gate 2 Downgradient Aquifer Wells																									
D7S	411414.02	479570.00	27.32	11.15	11.97	12.32	12.50	12.97	13.42	13.87	14.19	14.58	14.67	14.54	14.40	13.83	12.53	10.81	9.72	9.87	10.75	10.94	10.57		
D7D	411414.03	479570.12	27.22	11.11	11.95	12.30	12.49	12.96	13.41	13.84	14.17	14.55	14.66	14.52	14.37	13.82	12.49	10.78	9.69	9.84	10.91	10.55			
Existing Wells			Average	11.13	11.96	12.31	12.49	12.96	13.41	13.85	14.18	14.56	14.66	14.53	14.38	13.82	12.51	10.79	9.70	9.85	10.75	10.92	10.56		
			SD	0.03	0.02	0.02	0.01	0.01	0.01	0.02	0.02	0.02	0.01	0.02	0.02	0.01	0.03	0.02	0.02	0.02	NA	0.02	0.02		
				12.40	12.74	12.90	13.42	13.80					14.84	14.63	14.18	12.86	11.15						11.26		
214S	411339.0	479621.0	30.84											14.85	14.65	14.18	12.87	11.18	10.08	10.23			11.27	10.96	
214D	411331.0	479631.0	30.67											15.05	14.83	14.35	13.17			10.51			11.59		
332S	411636.0	479760.0	27.37											15.25	14.88	14.42	13.17			10.51			11.60		
332D	411637.0	479758.0	27.5											15.30	14.34	14.14	13.67	12.32	10.56	9.48	9.67			10.78	10.46
333S	411356.0	479340.0	32.32											14.60	14.30	14.11	13.64	12.25	10.54	9.46	9.64			10.76	10.28
333D	411353.0	479342.0	32.22											14.56	13.41	13.26	12.81	11.44	9.76	8.75	8.87			9.98	9.65
223S	NA	NA	34.70												13.39	13.23	12.78	11.44	9.74	8.70	8.86			9.96	9.64
223D	NA	NA	34.64												13.04	12.86	12.40	11.06	9.44	8.33	8.46			9.72	9.27
334S	NA	NA	30.46												13.49	13.30	12.81	11.51	9.85	8.80	8.91			10.18	9.74
334D	NA	NA	30.94												13.82	13.64	13.17	11.80	10.13	9.05	9.15			10.48	10.01
216S	NA	NA	30.05												13.74			11.88	10.22	9.14	9.24			10.57	10.10
216D	NA	NA	30.02												14.83	14.65	14.19	12.60	11.04	9.90	10.18			11.46	10.93
231S	NA	NA	27.63												14.64	14.45	14.01	12.17	10.62	9.47	9.75			11.42	10.49
231D	NA	NA	27.42												15.50	15.29	14.88	14.00	12.34	11.46	11.67			12.93	12.41
234S	NA	NA	27.12												15.32	15.12	14.67	13.78	12.17	11.35	11.54			12.78	12.25
234D	NA	NA	27.37															13.20	11.04	9.88					
329S	NA	NA	27.35															13.19	11.60						
329D	NA	NA	27.41																						
02J	NA	NA	27.56																						
			Average	12.40	12.74	12.90	13.33	13.51	14.17	14.46	14.92	14.95	14.25	14.20	13.74	12.48	10.75	9.61	9.87	9.87	NA	11.08	10.53		
			SD	NA	NA	NA	0.35	0.35	0.35	0.37	0.37	0.35	0.78	0.77	0.78	0.85	0.85	0.92	0.95	NA	NA	0.92	0.95		

SD: Standard deviation.

NA: Not available.

Table E-2b. Water Level Changes over Time

Well ID	Northing	Easting	TOC ft MSL	Change Feb 98 - Jan 98	Change Mar 98 - Feb 98	Change Apr 98 - Mar 98	Change May 98 - Apr 98	Change Jul 98 - May 98	Change Oct 98 - Jul 98	Change Dec 98 - Oct 98	Change Feb 99 - Dec 98	Change Apr 99 - Feb 99	Change Jun 99 - Apr 99
Gate 1 Far Upgradient Aquifer Wells													
U16S	411386.11	479618.44	27.31	1.31	1.34	0.65	-0.68	-1.28	-1.76	-1.08	0.16	1.09	-0.38
U17S	411396.66	479613.50	27.13	1.32	1.34	0.64	-0.67	-1.27	-1.77	-1.09	0.16	1.09	-0.38
U18S	411395.45	479625.52	27.15	1.31	1.34	0.65	-0.67	-1.26	-1.77	-1.08	0.15	1.09	-0.38
Gate 1 Vicinity Upgradient Aquifer Wells													
U10S	411375.12	479614.43	27.43	1.32	1.27	0.76	-0.69	-1.28	-1.78	-1.07	0.15	1.09	-0.38
U11S	411380.13	479611.01	27.38	1.33	1.33	0.69	-0.68	-1.29	-1.76	-1.09	0.14	1.11	-0.4
U12S	411385.12	479608.18	27.36	1.33	1.27	0.75	-0.69	-1.29	-1.76	-1.08	0.15	1.067	-0.367
U13S	411390.69	479605.32	27.31	1.35	1.33	0.67	-0.69	-1.29	-1.76	-1.09	0.16	1.1	-0.39
U14S	411395.42	479602.64	27.25	1.35	1.29	0.7	-0.69	-1.26	-1.78	-1.09	0.16	1.09	-0.38
U15S	411400.82	479599.51	27.14	1.02	1.61	0.66	-0.67	-1.24	-1.77	-1.09	0.16	1.1	-0.4
Gate 1 Upgradient Aquifer Wells													
U1S	411368.83	479607.91	27.50	NA	1.35	0.64	-0.67	-1.28	-1.77	-1.08	0.15	1.08	-0.36
U2S	411374.42	479605.39	27.37	1.35	1.28	0.69	-0.66	-1.26	-1.78	-1.07	0.15	1.07	-0.35
U3S	411379.04	479602.08	27.52	1.33	1.34	0.65	-0.65	-1.27	-1.79	-1.08	0.16	1.07	-0.35
U3D	411379.00	479601.86	27.42	1.34	1.36	0.55	-0.57	-1.28	-1.78	-1.06	0.13	1.08	-0.35
U4S	411385.10	479599.96	27.43	1.33	NA	NA	-0.67	-1.24	-1.74	-1.14	0.14	1.07	-0.36
U4M	411385.35	479599.83	27.40	1.35	NA	NA	-0.62	-1.35	-1.74	-1.08	0.15	1.06	-0.34
U4D	411385.13	479599.78	27.34	1.35	NA	NA	-0.61	-1.32	-1.78	-1.07	0.14	1.08	-0.35
U5S	411389.99	479596.53	27.33	1.34	1.28	0.73	-0.64	-1.3	-1.79	-1.09	0.16	1.08	-0.38
U5D	411390.08	479596.34	27.26	1.26	1.35	0.64	-0.67	-1.28	-1.61	-1.23	0.16	1.04	-0.34
U6S	411394.94	479594.33	27.17	1.35	1.28	0.69	-0.67	-1.27	-1.77	-1.08	0.15	1.05	-0.35
Gate 1 Pre-Treatment Zone Wells													
F1S	411383.80	479595.69	27.34	NA	NA	NA	-0.65	-1.36	-1.7	-1.09	0.16	1.1	-0.4
F2S	411383.56	479595.16	27.26	NA	1.36	0.63	-0.68	-1.42	-1.65	-1.07	0.14	1.11	-0.33
F2M	411383.35	479594.95	27.33	NA	1.35	0.61	-0.67	-1.31	-1.59	-1.24	0.22	1.04	-0.37
F2D	411383.35	479595.41	27.34	NA	1.36	0.61	-0.68	-1.32	-1.71	-1.11	0.15	1.1	-0.36
F3S	411384.24	479594.76	27.37	NA	1.39	0.59	-0.68	-1.33	-1.72	-1.09	0.15	1.09	-0.35
F3D	411384.36	479594.97	27.41	NA	1.38	0.6	-0.68	-1.33	-1.71	-1.14	0.15	1.14	-0.37
Gate 1 Reactive Cell Wells													
F4S	411381.87	479595.19	27.36	NA	1.34	0.64	-0.7	-1.31	-1.72	-1.11	0.14	-1.88	2.65
F5S	411382.45	479594.13	27.32	NA	1.35	0.64	-0.7	-1.31	-1.73	-1.09	0.12	1.11	-0.35
F6S	411383.48	479593.35	27.36	NA	1.33	0.65	-0.71	-1.3	-1.73	-1.09	0.12	1.11	-0.34
F7S	411381.51	479592.76	27.17	NA	1.4	0.63	-0.7	-1.27	-1.77	-1.08	0.11	1.11	-0.37

Table E-2b. Water Level Changes over Time (Continued)

Well ID	Northing	Easting	TOC ft MSL	Change											
				Feb 98 - Jan 98	Mar 98 - Feb 98	Apr 98 - Mar 98	May 98 - Apr 98	Jun 98 - May 98	Jul 98 - Jun 98	Oct 98 - Jul 98	Dec 98 - Oct 98	Feb 99 - Dec 98	Apr 99 - Feb 99	Change	Change
				Jan 98	Feb 98	Mar 98	Apr 98	May 98	Jun 98	Jul 98	Oct 98	Dec 98	Feb 99	Apr 99	Jun 99 - Apr 99
F8S	411380.68	479593.77	27.31	NA	1.34	0.64	-0.69	-1.31	-1.73	-1.1	0.12	0.12	1.12	-0.35	
F9S	411383.09	479592.30	27.38	NA	1.34	0.63	-0.69	-1.27	-1.76	-1.1	0.12	0.12	1.1	-0.34	
F11S	411381.05	479591.87	27.34	NA	1.33	0.68	-0.7	-1.3	-1.74	-0.97	-0.02	1.12	1.12	-0.35	
F12S	411382.17	479591.39	27.25	NA	1.35	0.62	-0.69	-1.35	-1.68	-1.09	NA	NA	NA	-0.36	
F4M	411381.74	479595.08	27.33	NA	1.33	0.64	-0.68	-1.32	-1.71	-1.12	0.11	0.13	1.15	-0.36	
F5M	411382.46	479594.56	27.40	NA	1.35	0.64	-0.68	-1.3	-1.75	-1.09	0.13	0.11	1.12	-0.36	
F6M	411383.19	479593.26	27.31	NA	1.34	0.63	-0.71	-1.34	-1.69	-1.08	0.11	0.11	1.11	-0.34	
F4D	411381.67	479594.79	27.35	NA	1.32	0.65	-0.67	-1.35	-1.71	-1.12	0.13	0.13	1.15	-0.37	
F5D	411382.73	479594.49	27.33	NA	1.34	0.64	-0.71	-1.29	-1.74	-1.11	0.14	0.14	1.12	-0.35	
F6D	411383.29	479593.56	27.22	NA	1.36	0.61	-0.71	-1.29	-1.73	-1.11	0.12	0.12	1.12	-0.34	
F7D	411381.59	479593.21	27.26	NA	NA	NA	-0.65	-1.37	-1.71	-1.1	0.1	0.1	1.13	-0.35	
F8D	411380.71	479593.49	27.38	NA	1.33	0.64	-0.68	-1.31	-1.74	-1.09	0.12	0.12	1.1	-0.34	
F9D	411382.85	479592.46	27.37	NA	1.36	0.62	-0.67	-1.35	-1.69	-1.1	0.11	0.11	1.11	-0.35	
F11D	411380.68	479591.97	27.48	NA	1.32	0.65	-0.69	-1.27	-1.76	-1.09	0.11	0.11	1.13	-0.36	
F12D	411382.03	479591.04	27.43	NA	1.34	0.69	-0.74	-1.31	-1.74	-1.09	0.12	0.12	1.13	-0.37	
F10	411380.14	479592.34	27.33	NA	1.34	0.65	-0.67	-1.3	-1.75	-1.1	0.11	0.11	1.12	-0.36	
Gate 1 Exit Zone Wells															
F13S	411380.10	479591.62	27.35	NA	1.35	0.65	-0.71	-1.29	-1.74	-1.11	0.13	0.13	1.1	-0.33	
F13D	411379.76	479591.78	27.41	NA	1.35	0.64	-0.71	-1.28	-1.74	-1.09	0.11	0.11	1.1	-0.33	
F14S	411380.88	479591.32	27.20	NA	NA	NA	-0.73	-1.28	-1.68	-1.14	0.12	0.12	1.11	-0.35	
F14D	411380.55	479591.32	27.26	NA	1.39	0.58	-0.71	-1.27	-1.75	-1.09	0.11	0.11	1.12	-0.36	
Gate 1 Downgradient Aquifer Wells															
D1S	411371.55	479597.83	27.42	1.33	1.35	0.65	-0.64	-1.36	-1.74	-1.08	0.18	0.18	1.07	-0.39	
D2S	411376.84	479595.01	27.21	1.33	1.35	0.65	-0.65	-1.35	-1.91	-0.9	0.16	0.16	1.09	-0.38	
D3S	411372.85	479593.71	27.39	1.33	1.37	0.63	-0.65	-1.33	-1.91	-0.92	0.17	0.17	1.09	-0.39	
D4S	411377.21	479590.36	27.55	1.32	1.35	0.65	-0.64	-1.35	-1.74	-1.07	0.16	0.16	1.09	-0.38	
D5S	411379.71	479589.24	27.28	1.33	1.36	0.65	-0.65	-1.35	-1.75	-1.07	0.15	0.15	0.97	-0.26	
D5D	411379.85	479589.14	27.38	1.33	1.38	0.64	-0.68	-1.34	-1.72	-1.09	0.16	0.16	1.08	-0.37	
D6S	411382.15	479587.81	27.19	1.32	1.37	0.65	-0.68	-1.33	-1.74	-1.07	0.16	0.16	1.07	-0.37	
Gate 2 Upgradient Aquifer Wells															
U7S	411413.20	479583.23	27.21	1.34	1.33	0.66	-0.67	-1.25	-1.79	-1.08	0.14	0.14	1.09	-0.37	
U7D	411413.44	479583.23	27.16	1.33	1.36	0.64	-0.68	-1.27	-1.76	-1.09	0.15	0.15	1.08	-0.35	
U8S	411418.78	479580.33	27.16	1.32	1.35	0.67	-0.67	-1.31	-1.73	-1.1	0.16	0.16	1.15	-0.43	
U8M	411418.69	479580.59	27.22	1.34	1.35	0.65	-0.68	-1.25	-1.78	-1.09	0.13	0.13	1.11	-0.37	

Table E-2b. Water Level Changes over Time (Continued)

Well ID					Northing		Easting		TOC		Change											
				ft MSL						Change Feb 98 - Jan 98	Change Mar 98 - Feb 98	Change Apr 98 - Mar 98	Change May 98 - Apr 98	Change Jul 98 - May 98	Change Oct 98 - Jul 98	Change Dec 98 - Oct 98	Change Feb 99 - Dec 98	Change Apr 99 - Feb 99	Change Jun 99 - Apr 99			
U8D	411418.92	479580.44	27.18			1.33	1.35	0.64	-0.67	-1.27	-1.77	-1.09	0.14	1.07	-0.35							
U9S	411423.75	479577.68	27.14			1.33	1.35	0.66	-0.68	-1.28	-1.77	-1.09	0.16	1.08	-0.37							
U9D	411423.55	479577.88	27.06			1.32	1.36	0.64	-0.66	-1.29	-1.77	-1.1	0.17	1.04	-0.34							
Gate 2 Pre-Treatment Zone Wells																						
P1S	411416.98	479577.54	27.08			NA	1.36	0.67	-0.72	-1.29	-1.72	-1.12	0.19	1.08	-0.38							
P2S	411416.84	479576.73	27.16			NA	1.36	0.67	-0.72	-1.29	-1.72	-1.12	0.17	1.05	-0.34							
P2M	411417.19	479576.47	27.25			NA	1.37	0.66	-0.71	-1.32	-1.7	-1.11	0.17	1.07	-0.37							
P2D	411416.65	479576.50	27.25			NA	1.36	0.67	-0.72	-1.31	-1.71	-1.14	0.19	1.06	-0.34							
P3S	411418.29	479575.96	27.17			NA	1.35	0.69	-0.7	-1.34	-1.71	-1.02	0.08	1.07	-0.36							
P3D	411417.87	479576.11	27.03			NA	1.38	0.64	-0.69	-1.3	-1.74	-1.11	0.14	1.08	-0.35							
Gate 2 Reactive Cell Wells																						
P4S	411415.08	479576.00	27.20			NA	1.4	0.64	-0.71	-1.26	-1.75	-1.14	0.16	1.08	-0.36							
P5S	411416.59	479575.64	27.16			NA	1.32	0.67	-0.69	-1.28	-1.74	-1.09	0.13	1.09	-0.36							
P6S	411417.38	479574.53	27.22			NA	1.34	0.69	-0.7	-1.32	-1.69	-1.15	0.15	1.09	-0.36							
P7S	411415.78	479574.76	27.18			NA	1.33	0.71	-0.76	-1.29	-1.76	-1.05	0.16	1.08	-0.37							
P8S	411414.94	479574.94	27.19			NA	1.31	0.7	-0.69	-1.34	-1.67	-1.15	0.15	1.09	-0.37							
P9S	411416.62	479573.76	27.29			NA	1.33	0.69	-0.7	-1.34	-1.71	-1.08	0.13	1.08	-0.36							
P11S	411415.19	479573.23	27.25			NA	1.34	0.68	-0.69	-1.34	-1.62	-1.04	-0.01	1.1	-0.38							
P12S	411416.02	479572.65	27.17			NA	1.36	0.66	-0.69	-1.3	-1.75	-0.96	0	1.1	-0.38							
P4M	411415.36	479575.82	27.23			NA	1.38	0.64	-0.7	-1.34	-1.71	-1.08	0.15	1.08	-0.38							
P5M	411416.54	479575.24	27.24			NA	1.35	0.68	-0.7	-1.33	-1.7	-1.08	0.14	1.09	-0.38							
P6M	411417.54	479574.96	27.13			NA	1.37	0.65	-0.69	-1.32	-1.73	-1.08	0.12	1.1	-0.37							
P4D	411415.38	479576.20	27.27			NA	1.43	0.6	-0.7	-1.29	-1.77	-1.08	0.15	1.07	-0.36							
P5D	411416.24	479575.42	27.25			NA	1.32	0.66	-0.7	-1.29	-1.75	-1.08	0.13	1.1	-0.38							
P6D	411417.13	479574.79	27.24			NA	1.35	0.67	-0.71	-1.36	-1.7	-1.08	0.14	1.08	-0.36							
P7D	411415.99	479574.69	27.19			NA	1.37	0.67	-0.71	-1.34	-1.8	-1	0.15	1.08	-0.37							
P8D	411414.62	479575.00	27.25			NA	1.34	0.68	-0.7	-1.32	-1.65	-1.16	0.12	1.1	-0.39							
P9D	411416.90	479573.88	27.08			NA	1.34	0.67	-0.69	-1.34	-1.7	-1.1	0.13	1.1	-0.41							
P11D	411414.88	479573.24	27.18			NA	1.32	0.7	-0.69	-1.34	-1.7	-1.1	0.15	1	-0.29							
P12D	411416.32	479572.39	27.26			NA	1.36	0.68	-0.7	-1.33	-1.73	-1.09	0.15	1.09	-0.38							
P10	411413.79	479573.96	27.10			NA	1.34	0.69	-0.7	-1.32	-1.72	-1.1	0.14	1.09	-0.38							
Gate 2 Exit Zone Wells																						
P13S	411413.83	479572.92	27.15			NA	1.35	0.68	-0.7	-1.32	-1.73	-1.09	0.15	1.08	-0.38							
P13D	411414.05	479573.11	27.25			NA	1.36	0.67	-0.7	-1.31	-1.73	-1.09	0.14	1.07	-0.36							

Table E-2b. Water Level Changes over Time (Continued)

Well ID	Northing	Easting	TOC ft MSL	Change Feb 98 - Jan 98	Change Mar 98 - Feb 98	Change Apr 98 - Mar 98	Change May 98 - Apr 98	Change Jul 98 - May 98	Change Oct 98 - Jul 98	Change Dec 98 - Oct 98	Change Feb 99 - Dec 98	Change Apr 99 - Feb 99	Change Jun 99 - Apr 99
P14S	411414.70	479572.47	27.22	NA	1.34	0.69	-0.7	-1.35	-1.69	-1.1	0.14	1.09	-0.39
P14D	411414.95	479572.26	27.31	NA	1.32	0.7	-0.71	-1.33	-1.74	-1.07	0.13	1.09	-0.37
Gate 2 Downgradient Aquifer Wells													
D7S	411414.02	479570.00	27.32	1.35	1.37	0.67	-0.71	-1.3	-1.72	-1.09	0.15	1.07	-0.37
D7D	411414.03	479570.12	27.22	1.38	1.35	0.68	-0.7	-1.33	-1.71	-1.09	0.15	1.07	-0.36
Existing Wells													
214S	411339.0	479621.0	30.84	NA	NA	NA	-0.66	-1.32	-1.71	NA	NA	NA	NA
214D	411331.0	479631.0	30.67	NA	NA	0.58	-0.67	-1.31	-1.69	-1.1	0.15	1.04	-0.31
332S	411636.0	479760.0	27.37	NA	NA	NA	NA	-1.18	NA	NA	NA	1.08	NA
332D	411637.0	479758.0	27.5	NA	NA	NA	NA	-1.25	NA	NA	NA	1.09	NA
333S	411356.0	479340.0	32.32	NA	NA	0.52	-0.67	-1.35	-1.76	-1.08	0.19	1.11	-0.32
333D	411353.0	479342.0	32.22	NA	NA	0.52	-0.66	-1.39	-1.71	-1.08	0.18	1.12	-0.48
223S			34.70	NA	NA	NA	-0.6	-1.37	-1.68	-1.01	0.12	1.11	-0.33
223D			34.64	NA	NA	NA	-0.61	-1.34	-1.7	-1.04	0.16	1.1	-0.32
334S			30.46	NA	NA	NA	-0.64	-1.34	-1.62	-1.11	0.13	1.26	-0.45
334D			30.94	NA	NA	NA	-0.68	-1.3	-1.66	-1.05	0.11	1.27	-0.44
216S			30.05	NA	NA	NA	-0.65	-1.37	-1.67	-1.08	0.1	1.33	-0.47
216D			30.02	NA	NA	NA	NA	NA	-1.66	-1.08	0.1	1.33	-0.47
231S			27.63	NA	NA	NA	-0.64	-1.59	-1.56	-1.14	0.28	1.28	-0.53
231D			27.42	NA	NA	NA	-0.63	-1.84	-1.55	-1.15	0.28	1.67	-0.93
234S			27.12	NA	NA	NA	-0.62	-0.88	-1.66	-0.88	0.21	1.26	-0.52
234D			27.37	NA	NA	NA	-0.65	-0.89	-1.61	-0.82	0.19	1.24	-0.53
329S			27.35	NA	NA	NA	NA	NA	-2.16	-1.16	NA	NA	NA
329D			27.41	NA	NA	NA	NA	NA	-1.59	NA	NA	NA	NA
02J			27.56	NA	NA	NA	NA	NA	NA	-1.02	0.33	1.03	-0.45

NA: Not available.

Jan 98: 1/14/98 Oct 98: 10/17/98
Feb 98: 2/16/98 Dec 98: 12/16/98
Mar 98: 3/13/98 Feb 99: 2/1/99
Apr 98: 4/10/98 Apr 99: 4/26/99
May 98: 5/6/98 Jun 99: 6/1/99
Jul 98: 7/13/98

Positive water level changes indicate the groundwater level increased.
Negative water level changes indicate the groundwater level decreased.

Table E-2c. Average Water Levels in Various Zones near the Permeable Barriers

		Post-Installation																			
		1/14/98	2/3/98	2/9/98	2/16/98	2/26/98	3/7/98	3/13/98	3/20/98	3/27/98	4/3/98	4/10/98	4/18/98	5/6/98	7/13/98	10/7/98	12/16/98	2/1/99	4/8/99	4/26/99	6/1/99
Gate 1 Far Upgradient Aquifer Wells																					
Average		11.23	12.03	12.36	12.54	13.00	13.42	13.88	14.17	14.61	14.69	14.53	14.32	13.85	12.58	10.82	9.73	9.89	10.77	10.98	10.60
SD		0.01	0.00	0.01	0.01	0.01	0.03	0.01	0.01	0.01	0.01	0.01	0.00	0.01	0.02	0.02	0.02	0.01	0.01	0.01	0.01
Gate 1 Vicinity Upgradient Aquifer Wells																					
Average		11.21	12.03	12.38	12.49	12.94	13.37	13.84	14.11	14.55	14.70	14.55	14.35	13.86	12.59	10.82	9.73	9.89	10.76	10.98	10.59
SD		0.01	0.02	0.16	0.12	0.11	0.11	0.03	0.04	0.03	0.01	0.02	0.02	0.01	0.01	0.01	0.01	0.01	NA	0.02	0.01
Gate 1 Upgradient Aquifer Wells																					
Average		11.20	12.02	12.34	12.53	12.97	13.41	13.86	14.14	14.59	14.72	14.51	14.33	13.87	12.59	10.83	9.73	9.88	10.76	10.95	10.60
SD		0.03	0.07	0.03	0.02	0.03	0.02	0.03	0.04	0.03	0.03	0.04	0.02	0.03	0.03	0.06	0.01	0.02	0.08	0.01	0.01
Gate 1 Pre-Treatment Zone Wells																					
Average		12.00	12.34	12.52	12.99	13.43	13.89	14.21	14.56	14.65	14.49	14.28	13.82	12.48	10.80	9.67	9.83	10.72	10.93	10.57	10.57
SD		0.01	0.01	0.01	0.01	0.01	0.01	0.02	0.04	0.04	0.01	0.01	0.01	0.02	0.03	0.05	0.02	0.04	NA	0.02	0.02
Gate 1 Reactive Cell Wells																					
Average Shallow Wells		11.98	12.32	12.49	12.97	13.39	13.84	14.17	14.53	14.63	14.48	14.26	13.78	12.48	10.75	9.67	9.78	10.70	10.51	10.54	10.54
SD		0.03	0.03	0.04	0.03	0.03	0.02	0.04	0.02	0.03	0.03	0.03	0.03	0.03	0.04	0.02	0.06	0.03	0.02	1.07	0.03
Average Mid Wells		11.97	12.30	12.48	12.95	13.37	13.82	14.17	14.52	14.61	14.46	14.24	13.77	12.45	10.73	9.64	9.75	10.88	10.53	10.53	10.53
SD		0.03	0.03	0.02	0.03	0.02	0.02	0.03	0.04	0.03	0.03	0.03	0.03	0.04	0.06	0.03	0.03	0.04	NA	0.04	0.03
Average Deep Wells		11.96	12.30	12.49	12.95	13.36	13.82	14.16	14.53	14.60	14.46	14.23	13.77	12.46	10.73	9.63	9.75	10.87	10.52	10.52	10.52
SD		0.07	0.07	0.08	0.07	0.07	0.07	0.08	0.08	0.08	0.08	0.08	0.08	0.08	0.08	0.07	0.08	0.08	NA	0.07	0.07
Average Wells		11.97	12.31	12.49	12.96	13.38	13.83	14.17	14.53	14.62	14.47	14.25	13.78	12.47	10.74	9.65	9.76	10.70	10.73	10.53	10.53
SD		0.05	0.05	0.05	0.05	0.05	0.04	0.05	0.06	0.05	0.05	0.05	0.05	0.06	0.06	0.05	0.06	0.05	0.02	0.68	0.05
Gate 1 Exit Zone Wells																					
Average		12.00	12.30	12.51	13.00	13.40	13.87	14.20	14.55	14.64	14.50	14.26	13.78	12.50	10.78	9.67	9.79	10.72	10.89	10.55	10.55
SD		0.00	0.07	0.01	0.02	0.05	0.03	0.05	0.01	0.01	0.01	0.01	0.01	0.01	0.03	0.01	0.01	NA	0.01	0.01	0.01
Gate 1 Downgradient Aquifer Wells																					
Average		11.14	11.95	12.31	12.46	12.95	13.39	13.83	14.13	14.54	14.64	14.47	14.27	13.82	12.47	10.68	9.66	9.82	10.71	10.88	10.52
SD		0.01	0.02	0.02	0.01	0.02	0.02	0.01	0.03	0.03	0.01	0.01	0.01	0.02	0.02	0.08	0.01	0.02	0.00	0.05	0.01
Gate 2 Upgradient Aquifer Wells																					
Average		11.20	12.01	12.33	12.53	12.99	13.43	13.88	14.14	14.58	14.70	14.53	14.33	13.86	12.58	10.81	9.72	9.87	10.77	10.96	10.59
SD		0.01	0.03	0.01	0.01	0.02	0.01	0.01	0.05	0.05	0.01	0.01	0.02	0.01	0.02	0.01	0.01	0.01	0.00	0.04	0.02
Gate 2 Pre-Treatment Zone Wells																					
Average		11.96	12.32	12.51	12.98	13.40	13.87	14.18	14.55	14.66	14.54	14.38	13.83	12.52	10.80	9.70	9.85	10.73	10.92	10.57	10.57
SD		0.02	0.02	0.02	0.02	0.02	0.02	0.02	0.02	0.02	0.03	0.02	0.02	0.03	0.02	0.02	0.05	0.03	NA	0.03	0.02
Gate 2 Reactive Cell Wells																					
Average Shallow Wells		11.95	12.30	12.50	12.96	13.39	13.84	14.17	14.54	14.64	14.52	14.38	13.81	12.51	10.79	9.71	9.82	10.70	10.91	10.54	10.54
SD		0.02	0.03	0.02	0.02	0.03	0.03	0.02	0.03	0.02	0.03	0.03	0.03	0.02	0.03	0.04	0.07	0.02	0.01	0.02	0.02
Average Mid Wells		11.96	12.32	12.50	12.99	13.42	13.87	14.17	14.53	14.66	14.52	14.38	13.83	12.50	10.78	9.70	9.84	NA	10.93	10.55	10.55
SD		0.01	0.01	0.02	0.02	0.03	0.04	0.01	0.05	0.02	0.02	0.01	0.02	0.02	0.03	0.02	0.02	0.00	NA	0.01	0.02
Average Deep Wells		11.96	12.33	12.51	12.98	13.41	13.86	14.18	14.57	14.66	14.53	14.39	13.83	12.50	10.78	9.69	9.83	NA	10.91	10.54	10.54
SD		0.03	0.04	0.02	0.02	0.03	0.03	0.02	0.05	0.03	0.03	0.03	0.03	0.03	0.02	0.05	0.02	0.03	NA	0.03	0.03
Average Wells		11.96	12.31	12.50	12.97	13.40	13.85	14.17	14.55	14.65	14.52	14.38	13.82	12.50	10.79	9.70	9.83	10.70	10.91	10.54	10.54
SD		0.02	0.03	0.02	0.02	0.03	0.03	0.02	0.04	0.02	0.03	0.03	0.02	0.03	0.04	0.04	0.02	0.01	0.02	0.02	0.02

Table E-2c. Average Water Levels in Various Zones near the Permeable Barriers (Continued)

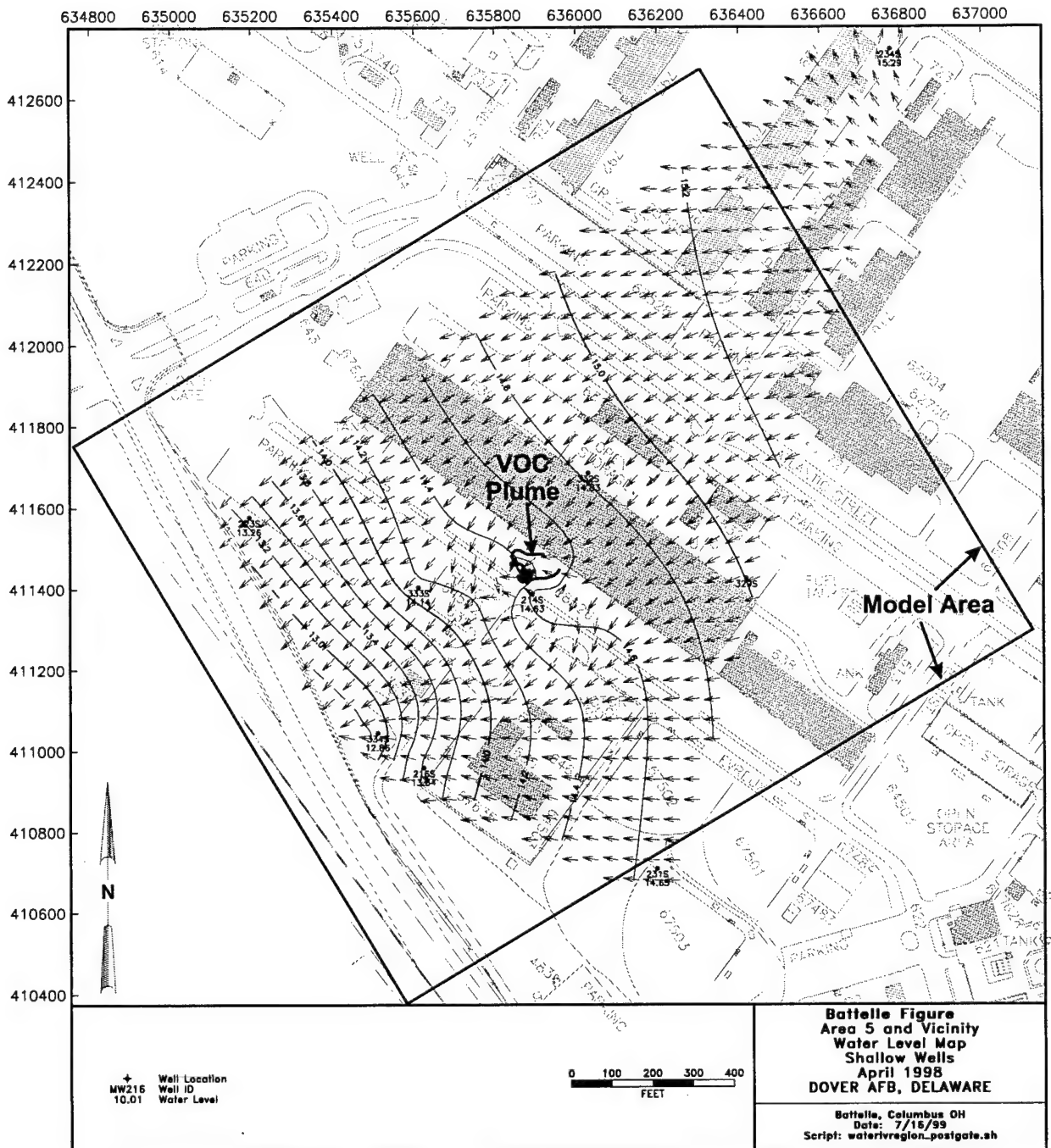
	Post-Installation																			
	1/14/98	2/3/98	2/9/98	2/16/98	2/26/98	3/7/98	3/13/98	3/20/98	3/27/98	4/3/98	4/10/98	4/18/98	5/6/98	7/13/98	10/7/98	12/16/98	2/1/99	4/8/99	4/26/99	6/1/99
Gate 2 Exit Zone Wells																				
Average		11.99	12.33	12.52	12.99	13.41	13.86	14.20	14.57	14.68	14.55	14.42	13.85	12.52	10.80	9.71	9.85	10.72	10.93	10.56
SD		0.01	0.01	0.02	0.03	0.02	0.00	0.01	0.01	0.01	0.02	0.02	0.01	0.01	0.02	0.01	0.01	NA	0.02	0.01
Gate 2 Downgradient Aquifer Wells																				
Average	11.13	11.96	12.31	12.49	12.96	13.41	13.85	14.18	14.56	14.66	14.53	14.38	13.82	12.51	10.79	9.70	9.85	10.75	10.92	10.56
SD	0.03	0.02	0.02	0.01	0.01	0.01	0.02	0.02	0.02	0.01	0.02	0.02	0.01	0.03	0.02	0.02	0.02	NA	0.02	0.02
Existing Wells																				
Average		12.40	12.74	12.90	13.33	13.51	14.17	14.46	14.92	14.95	14.25	14.20	13.74	12.48	10.75	9.61	9.87	NA	11.08	10.53
SD		NA	NA	NA	0.35	0.35	0.35	0.37	0.37	0.35	0.78	0.77	0.78	0.85	0.85	0.92	0.95	NA	0.92	0.95

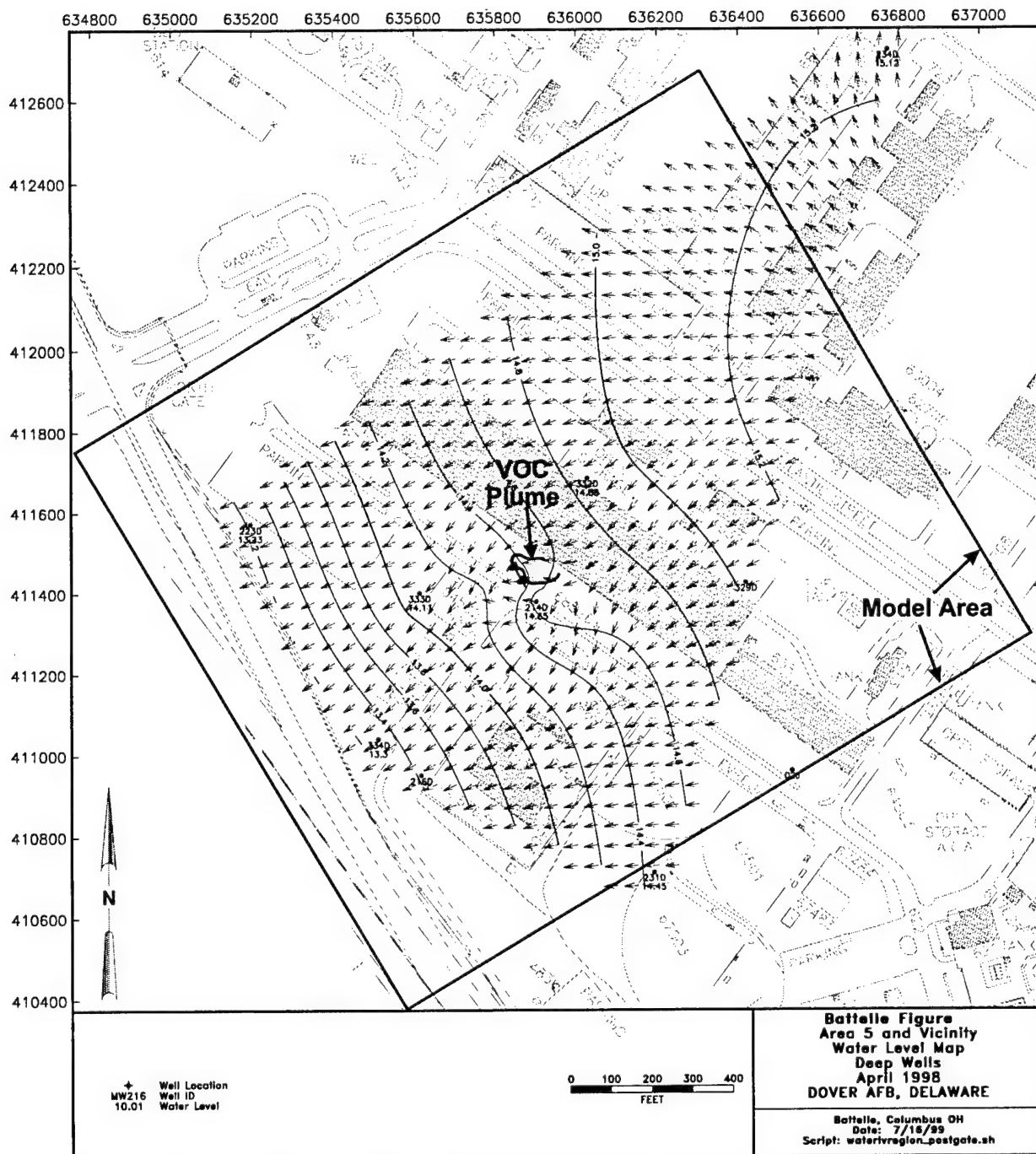
SD: Standard deviation.

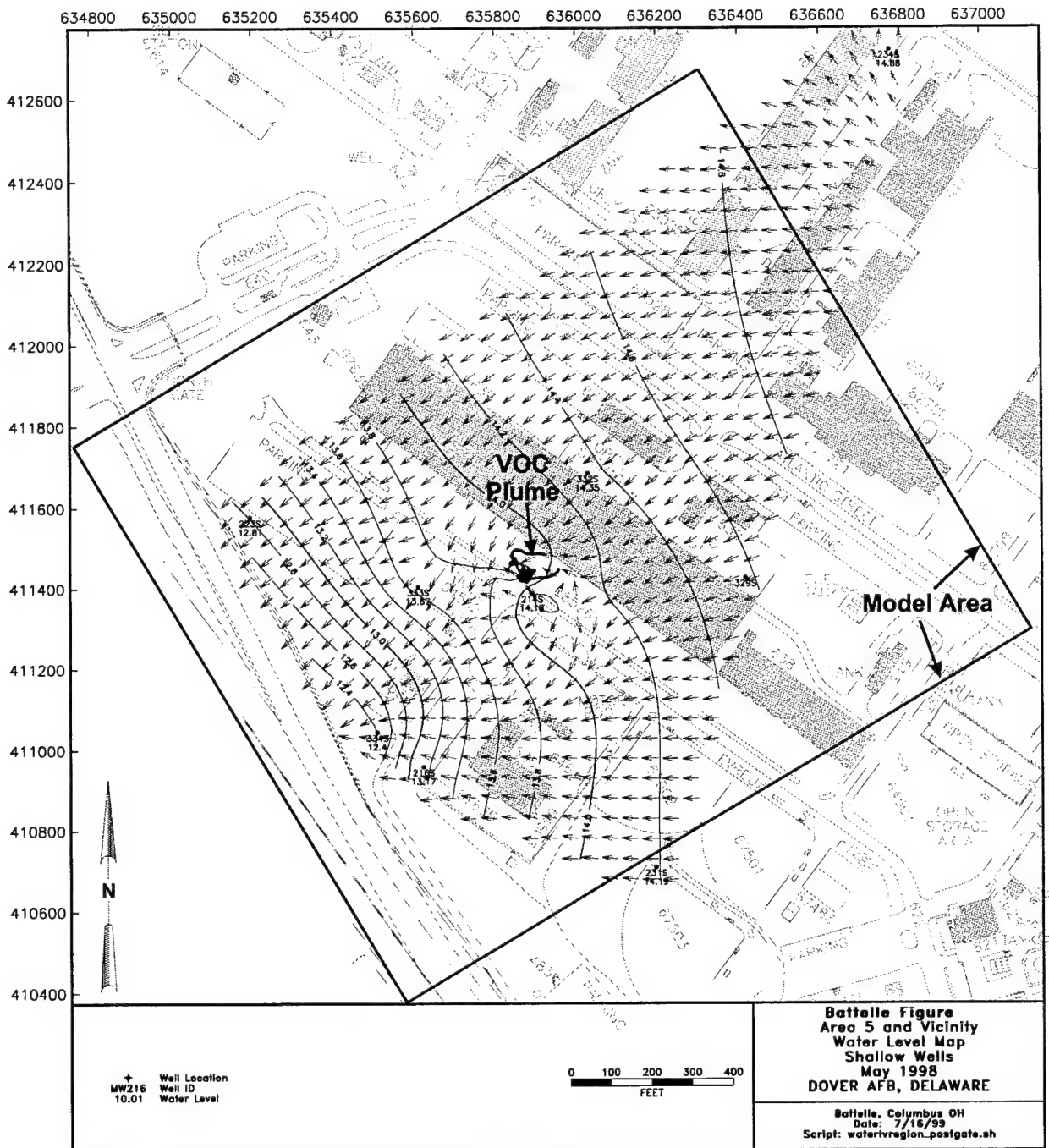
NA: Not available.

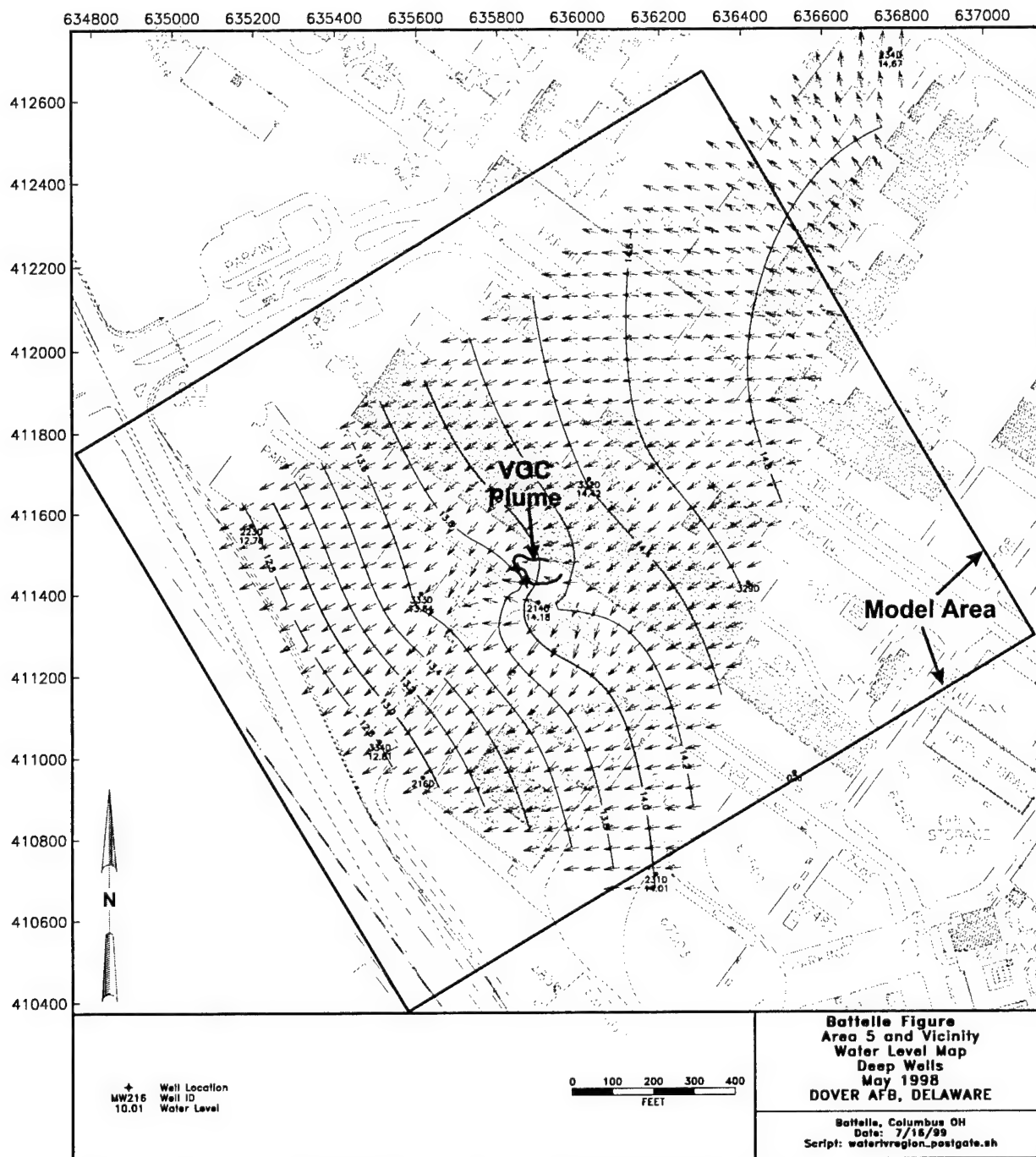
Appendix E-3

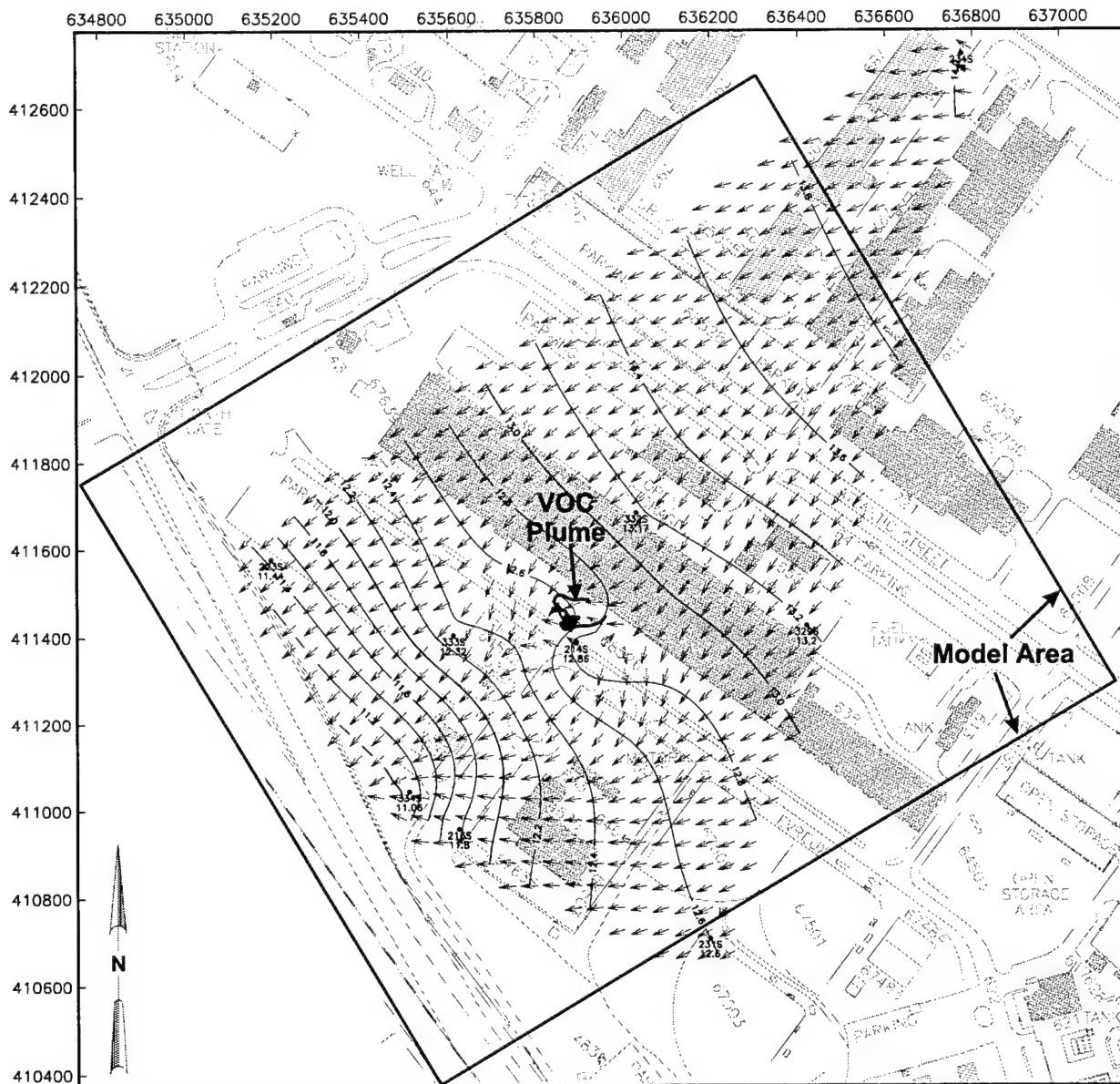
Water-Level Maps for Area 5 (Seven Events Each for Shallow and Deep Wells)









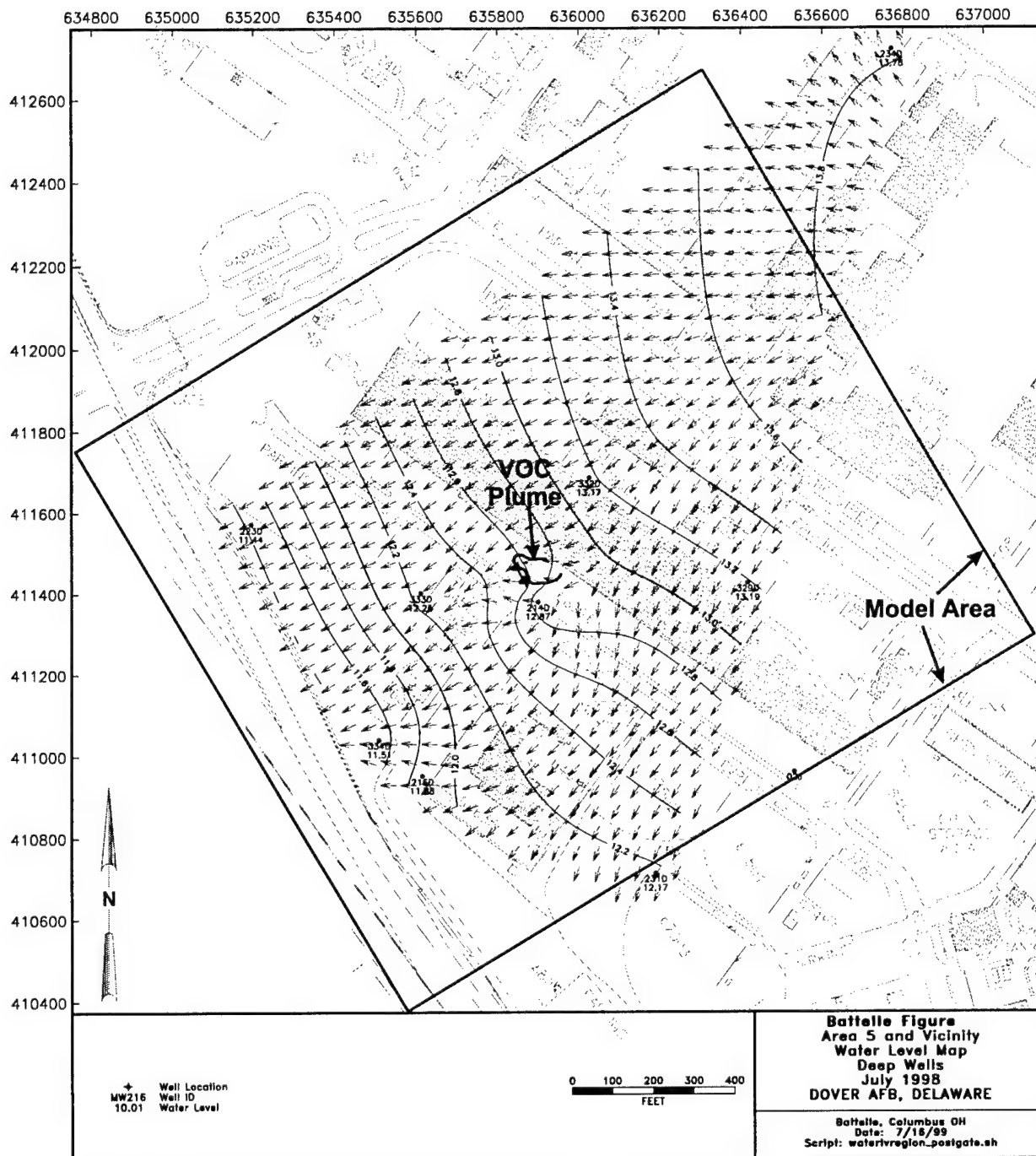


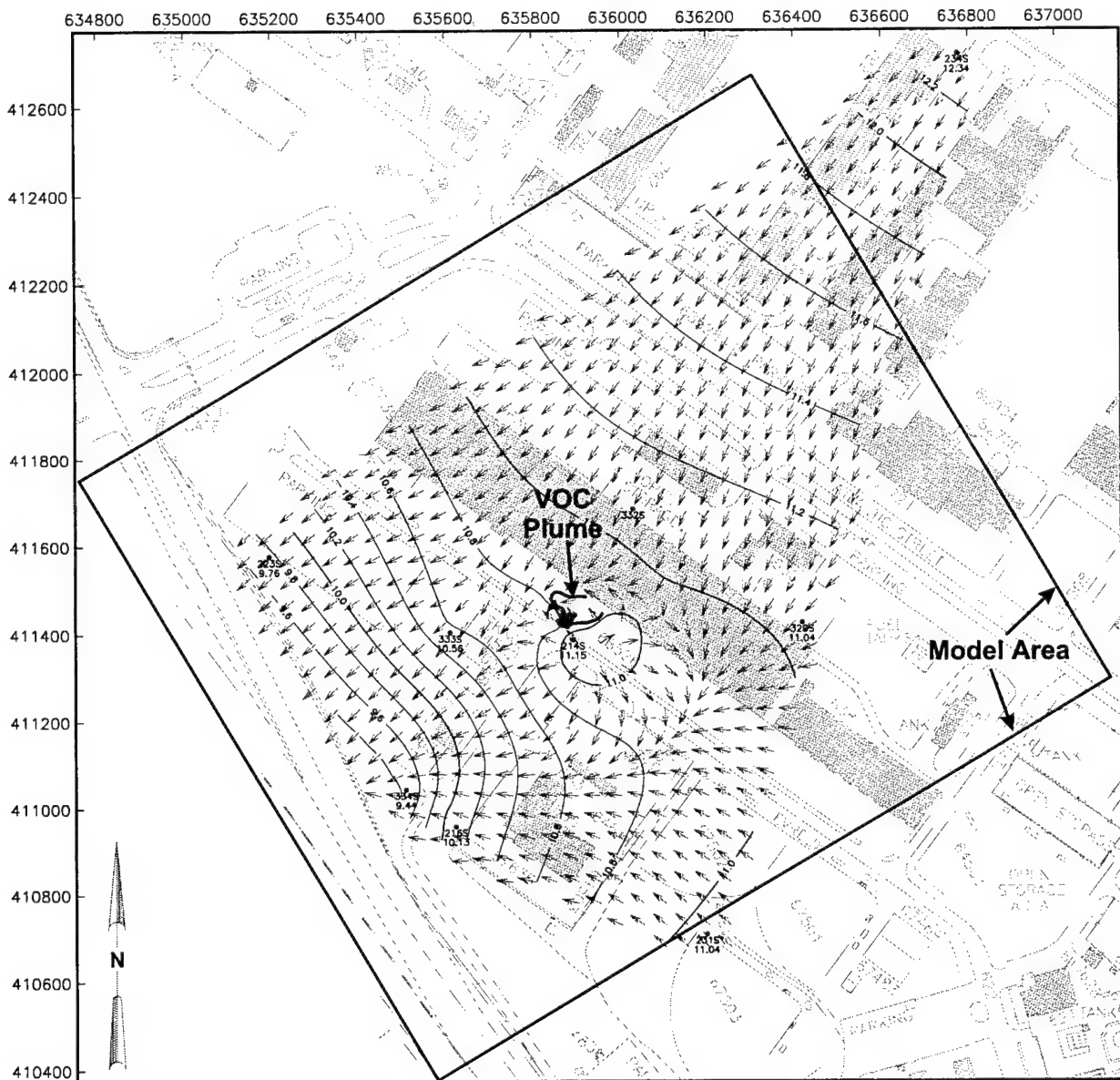
+ Well Location
 MW216 Well ID
 10.01 Water Level

0 100 200 300 400
 FEET

**Battelle Figure
 Area 5 and Vicinity
 Water Level Map
 Shallow Wells
 July 1998
 DOVER AFB, DELAWARE**

Battelle, Columbus OH
 Date: 7/16/99
 Script: waterivregion_postgate.sh



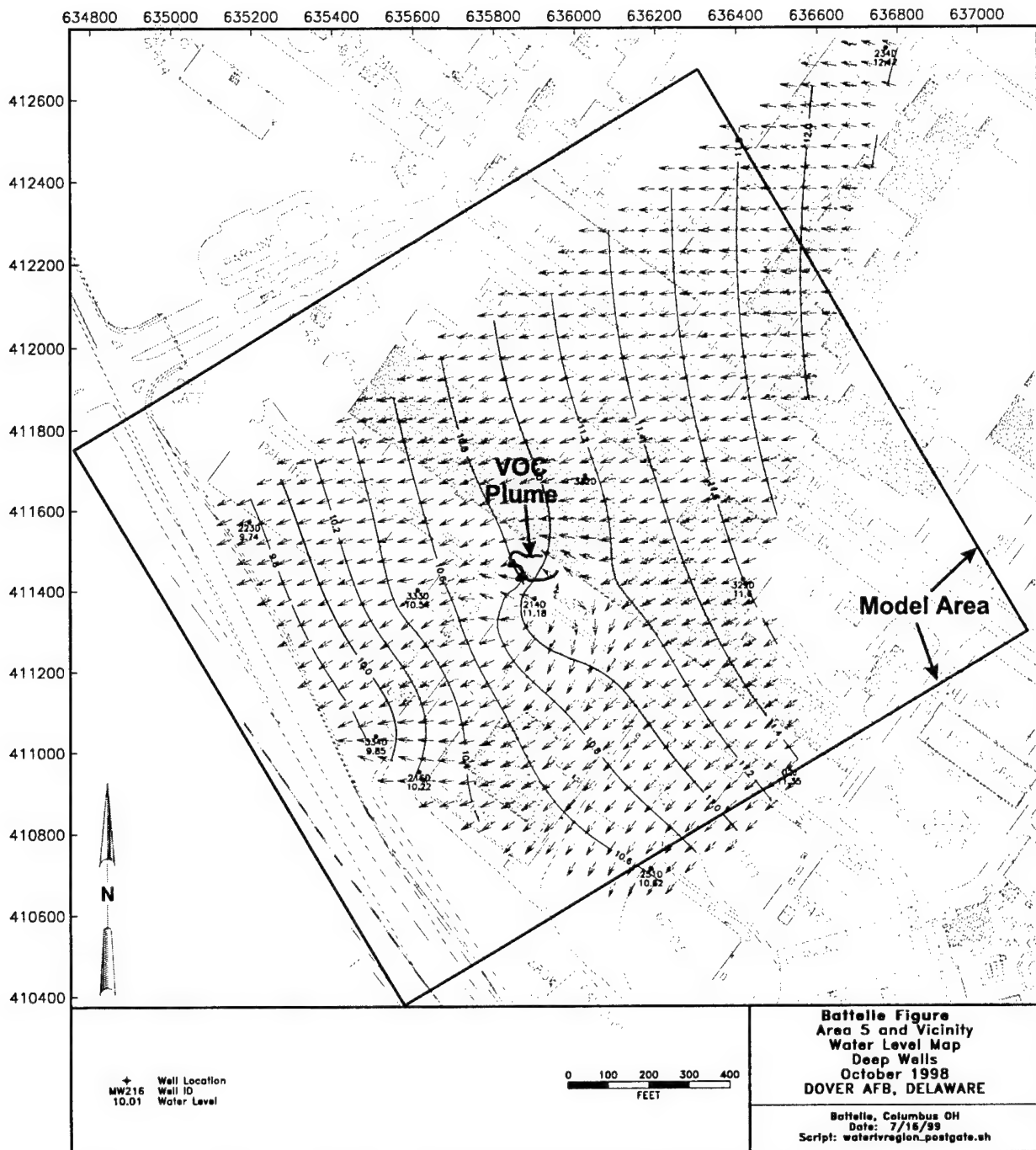


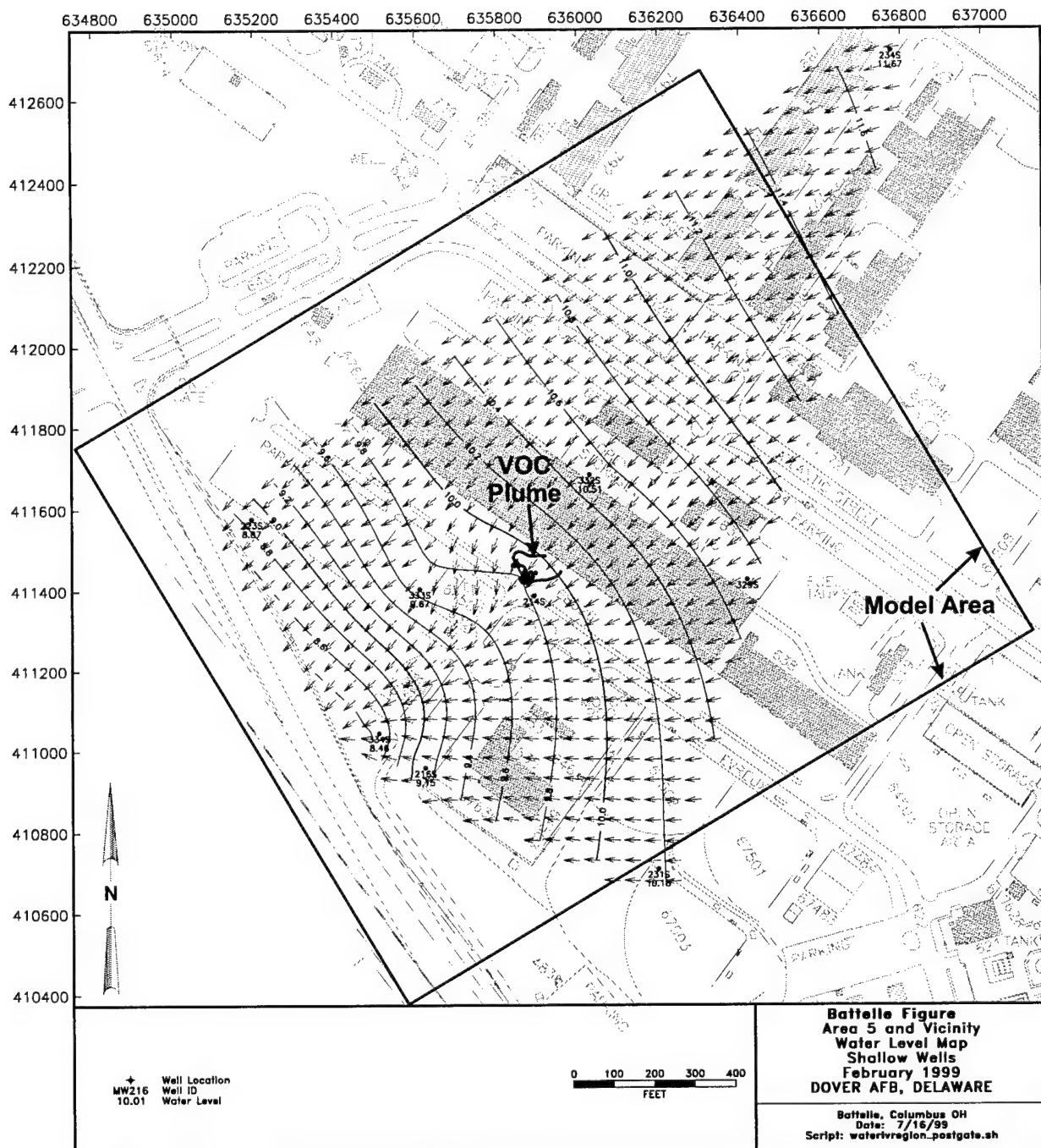
+ Well Location
 MW216 Well ID
 10.01 Water Level

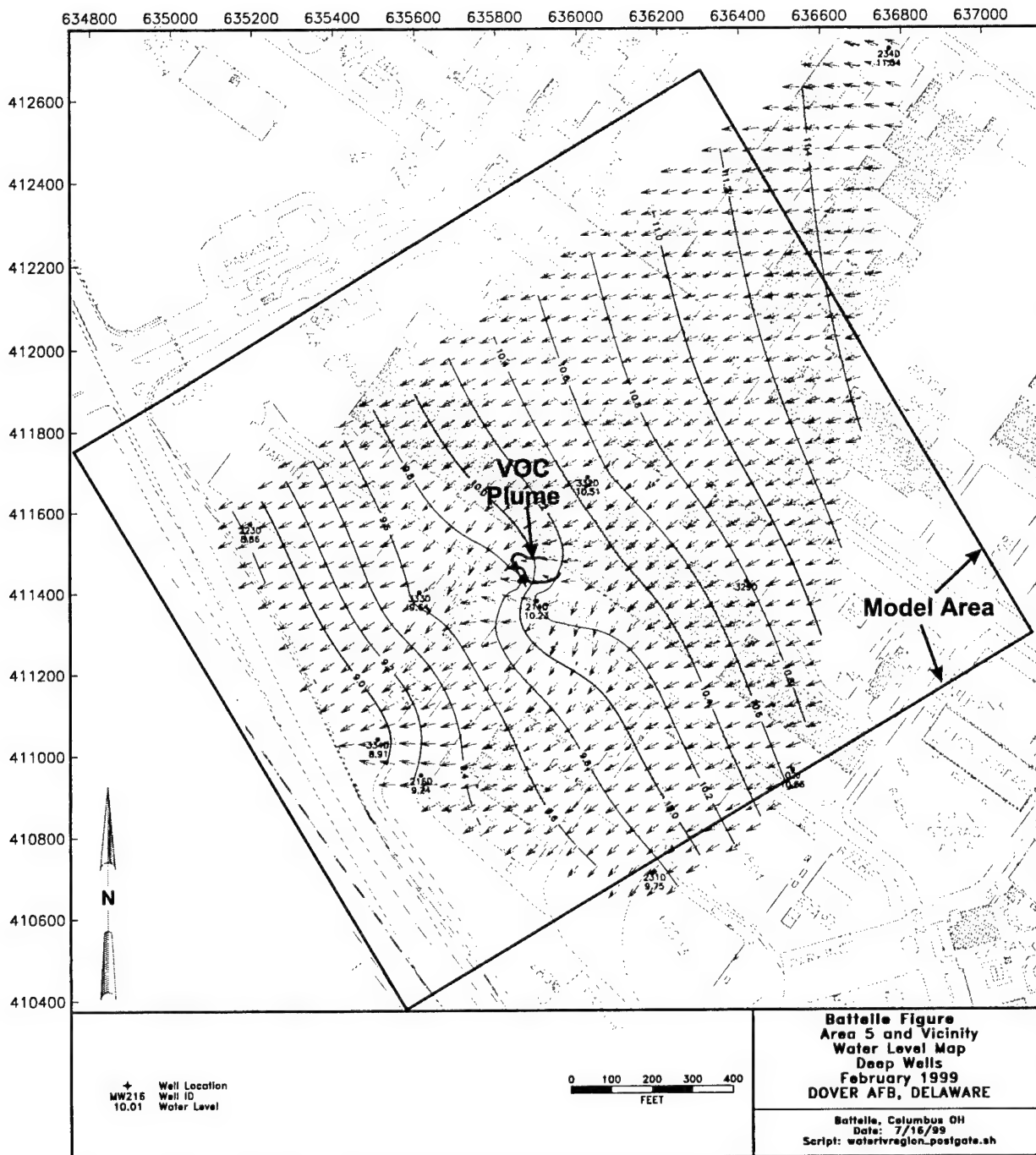
0 100 200 300 400
 FEET

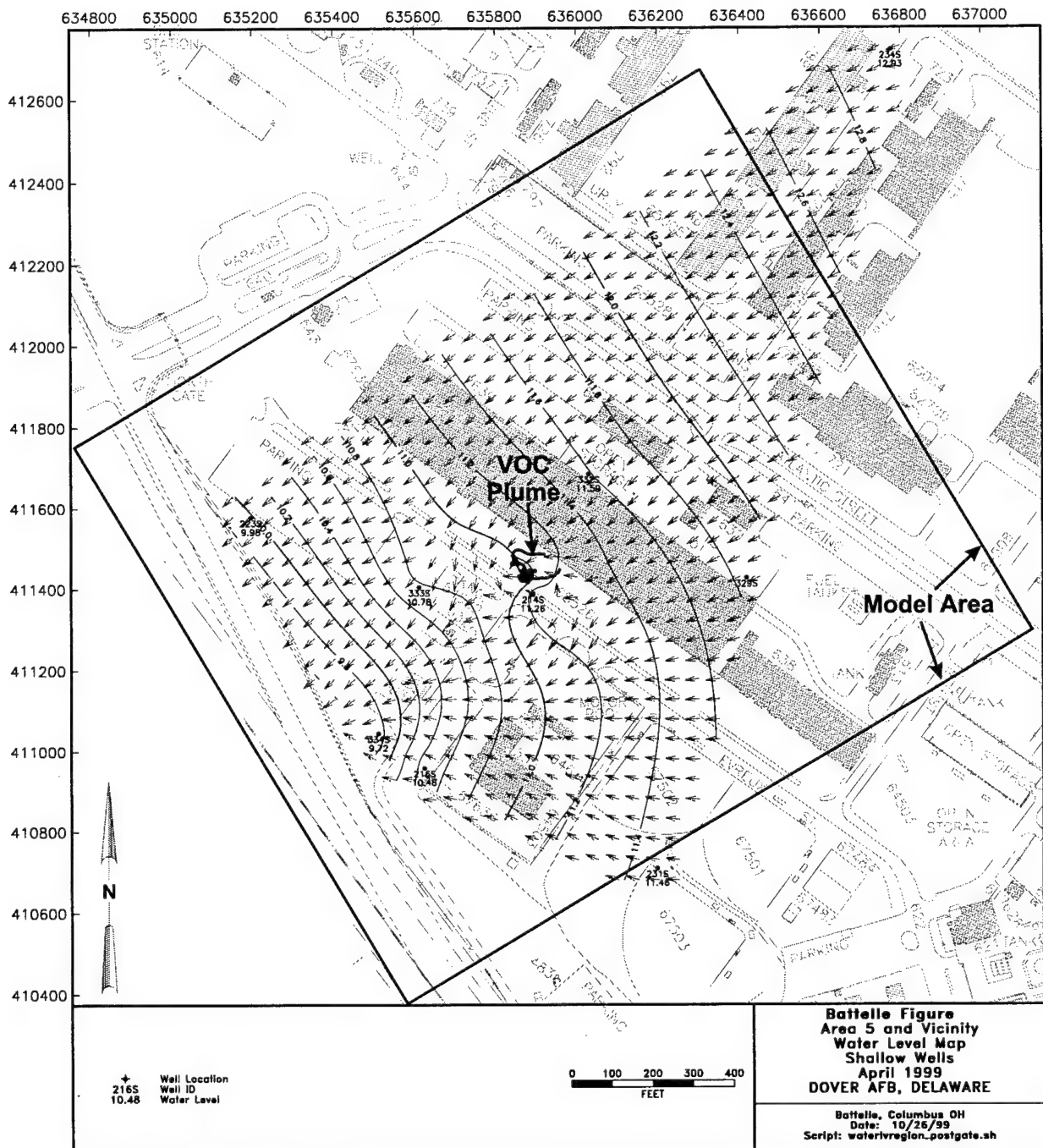
Battelle Figure
Area 5 and Vicinity
Water Level Map
Shallow Wells
October 1998
DOVER AFB, DELAWARE

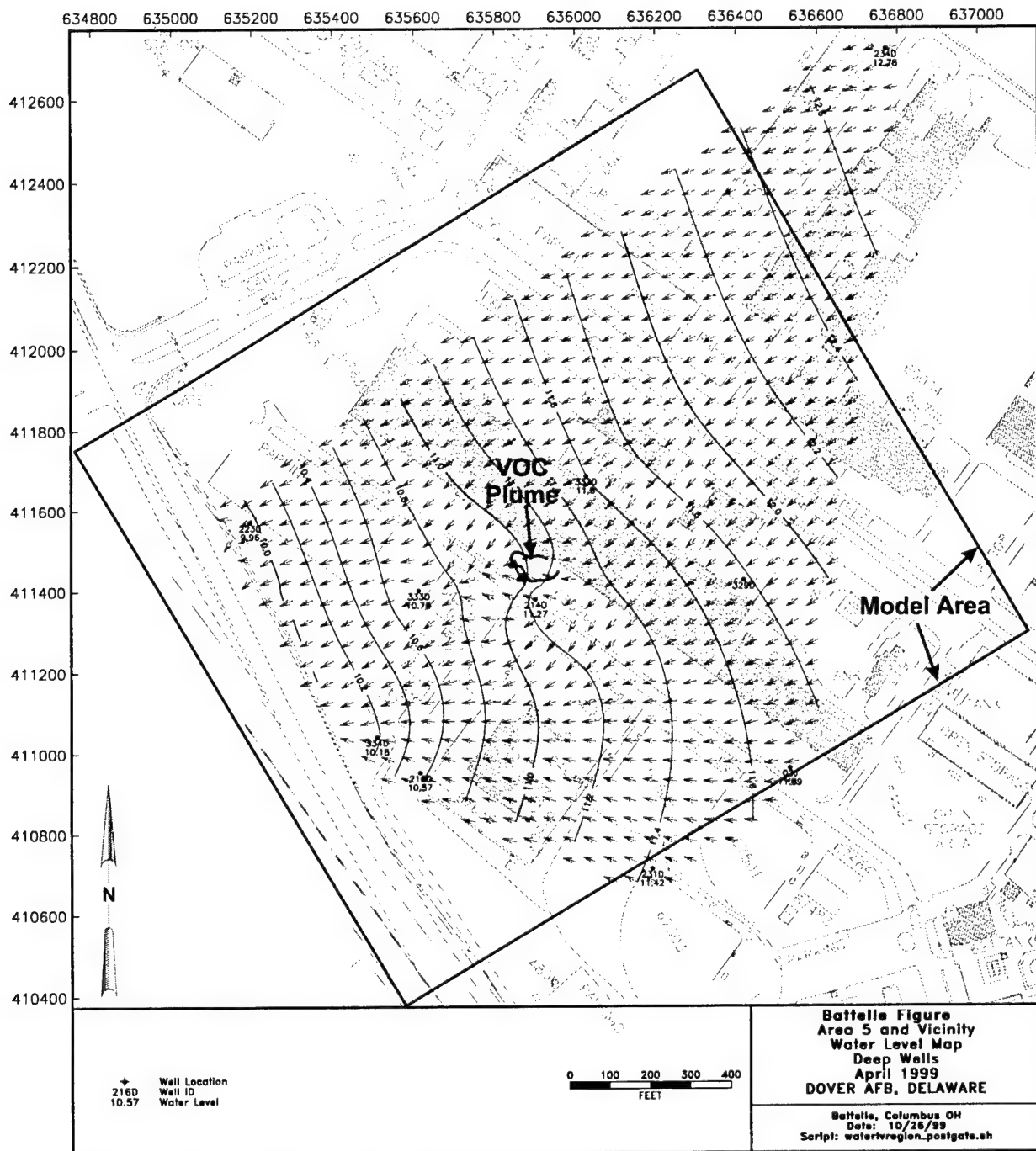
Battelle, Columbus OH
 Date: 7/16/99
 Script: waterivregion_postgate.sh

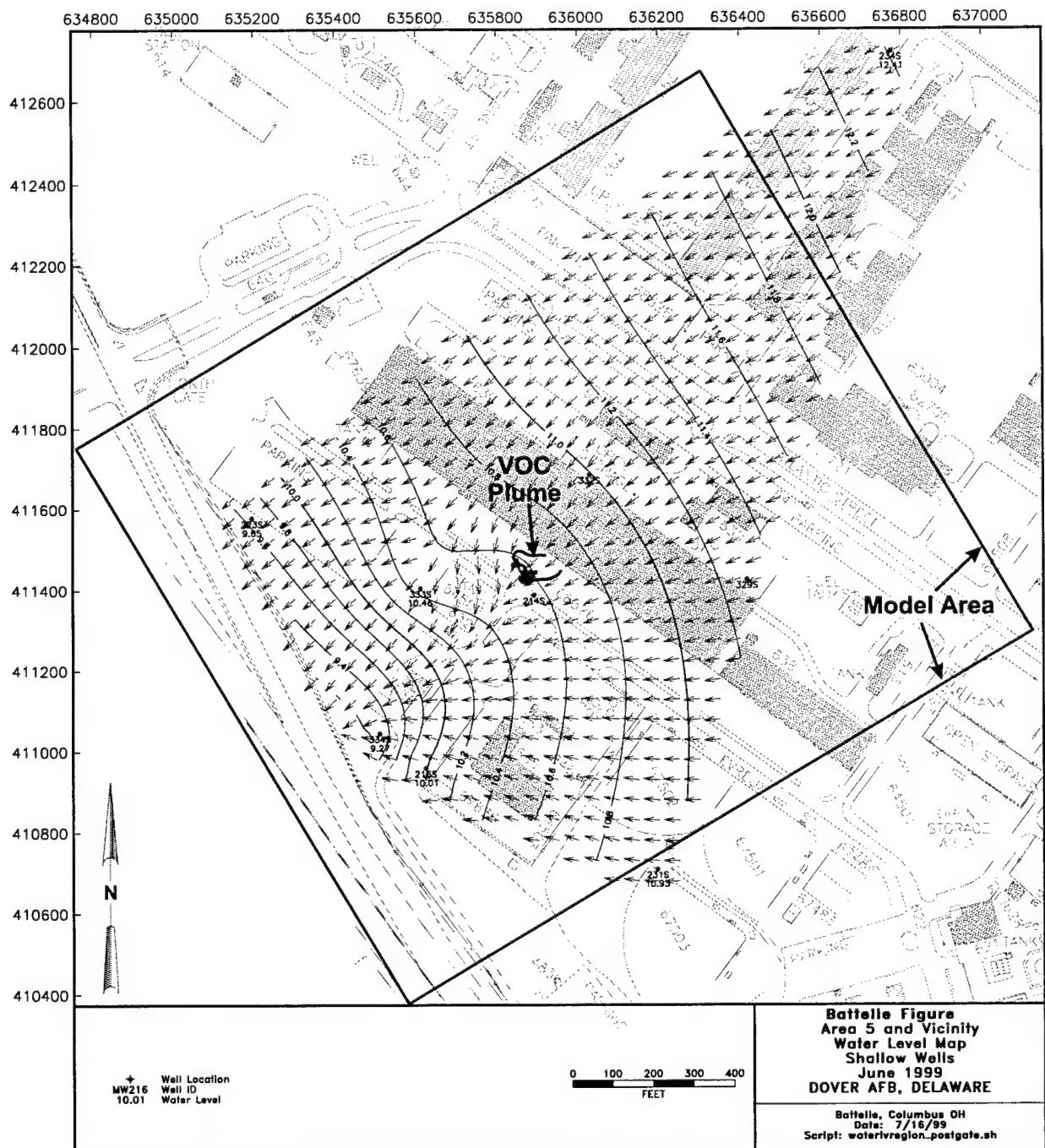


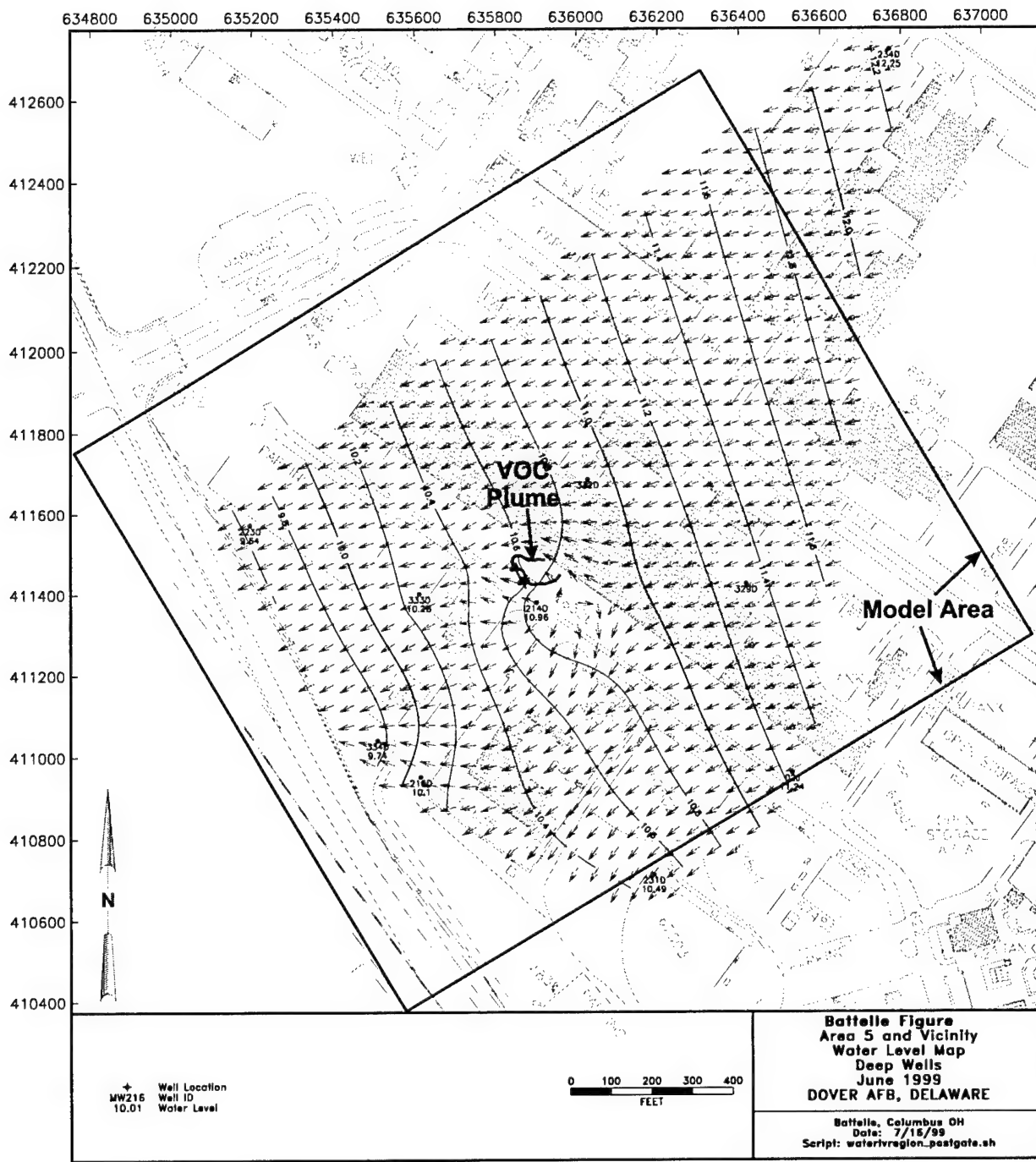








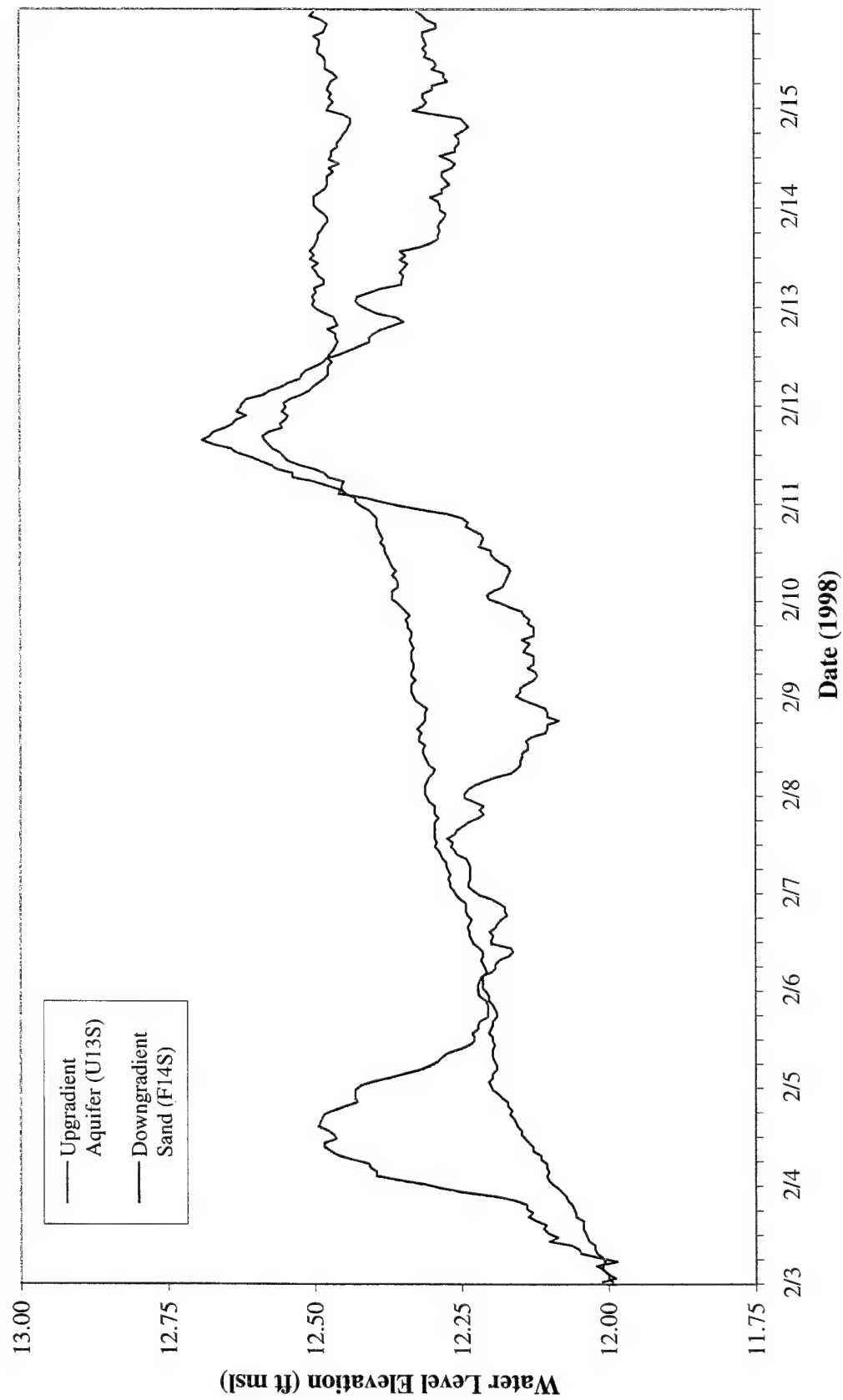




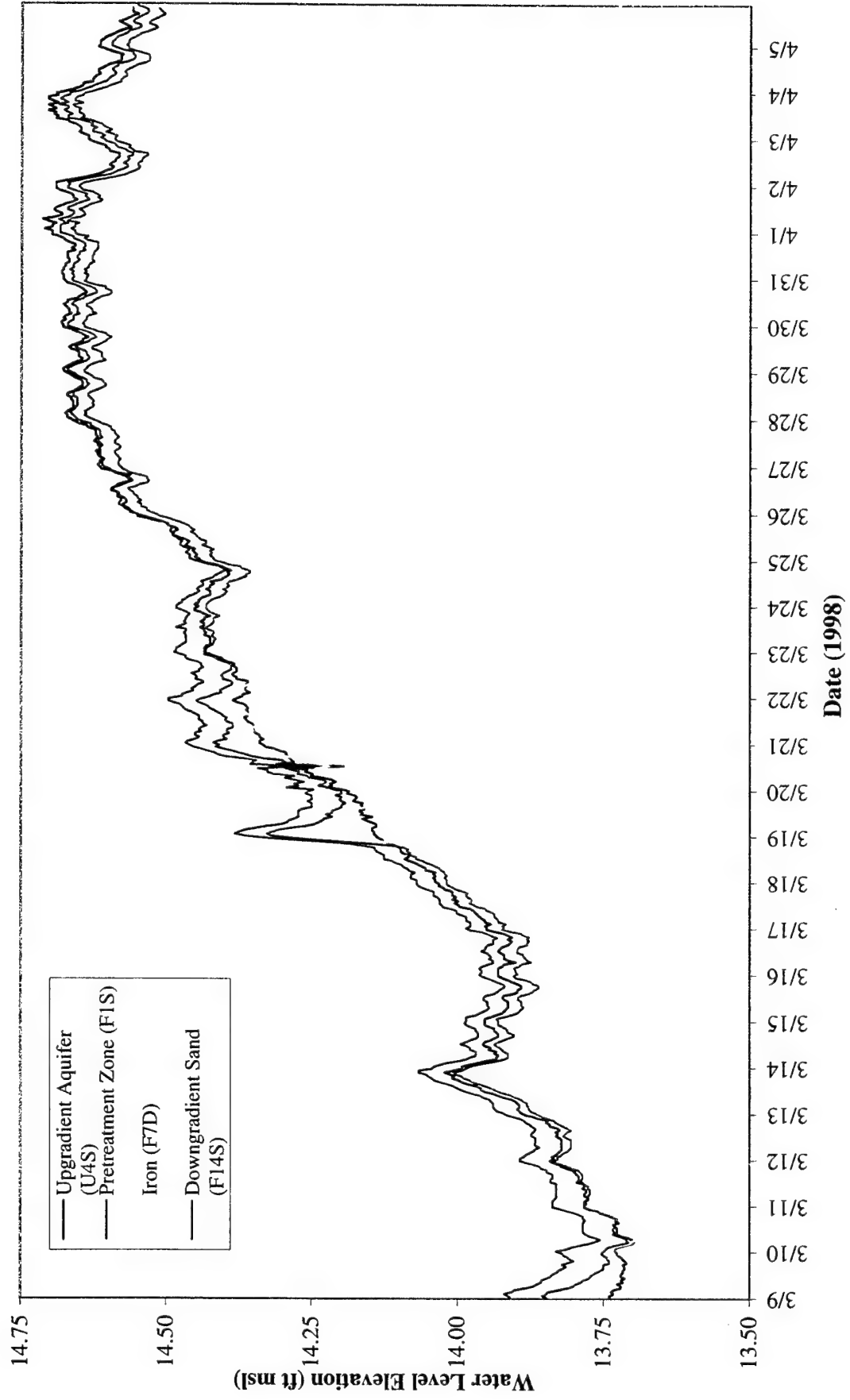
Appendix E-4

Plots of Continuous Water-Level Monitoring

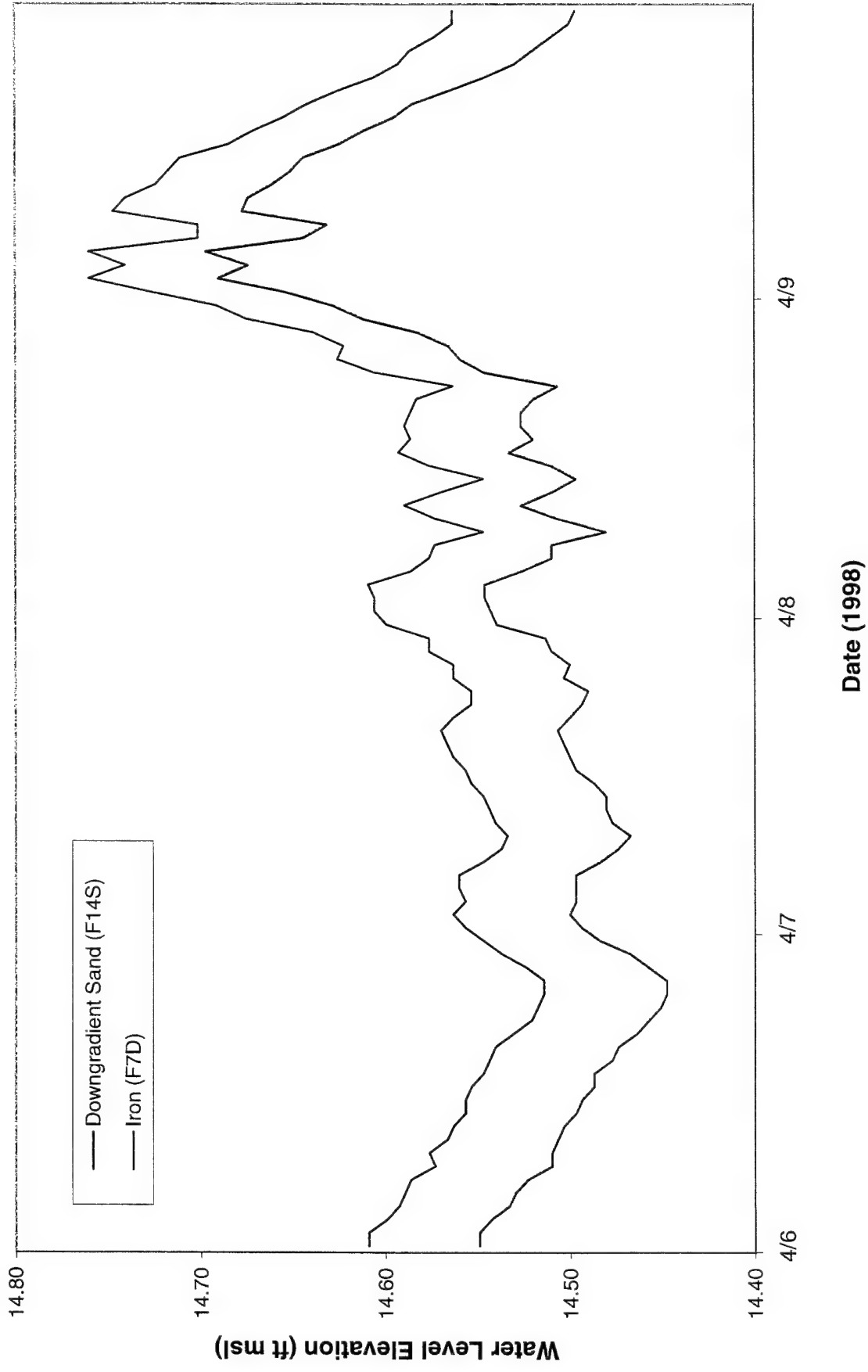
Dover AFB Permeable Barrier Continuous Water Level Elevation - Gate 1



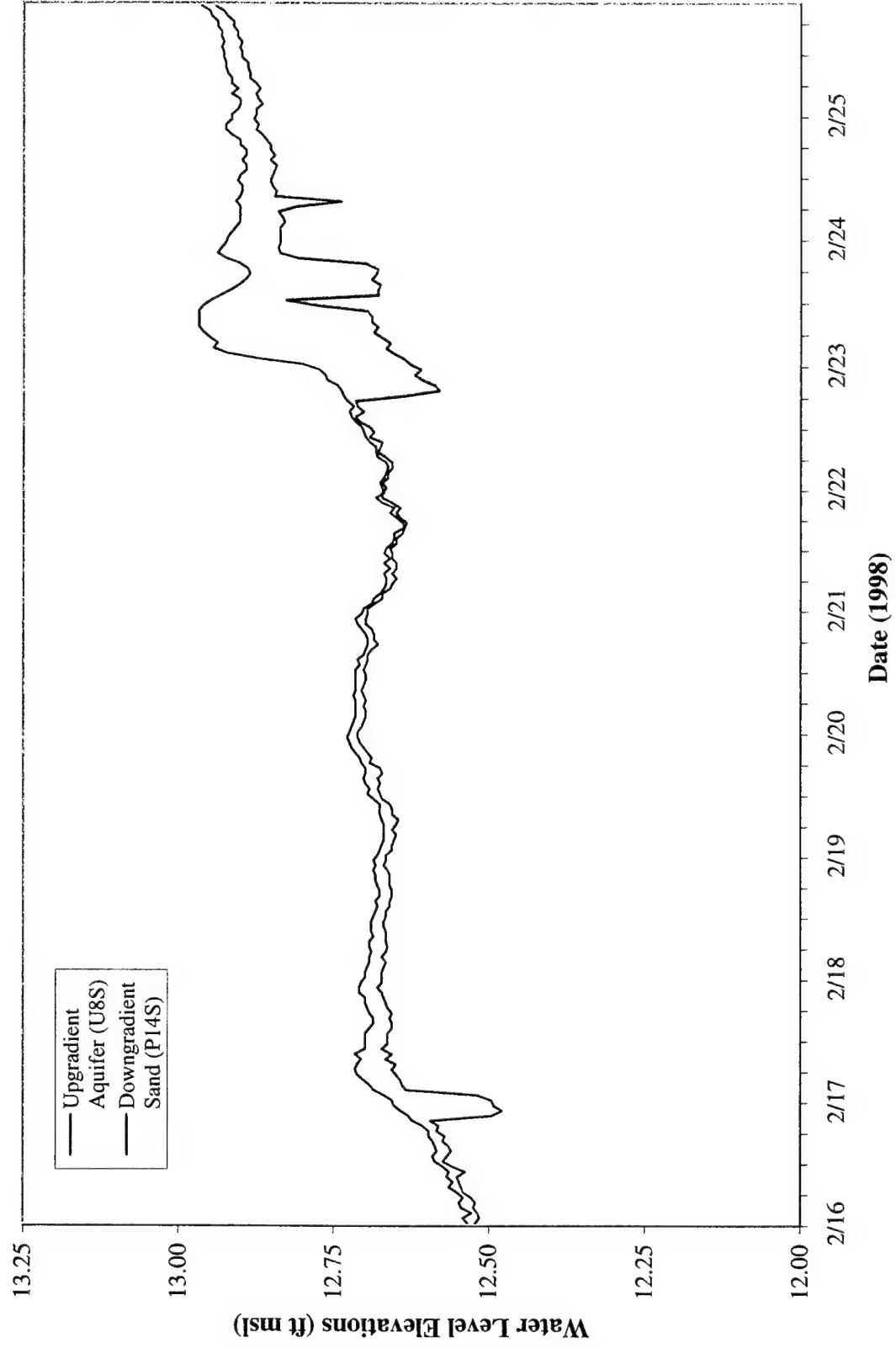
Dover AFB Permeable Barrier Continuous Water Level Elevation - Gate 1



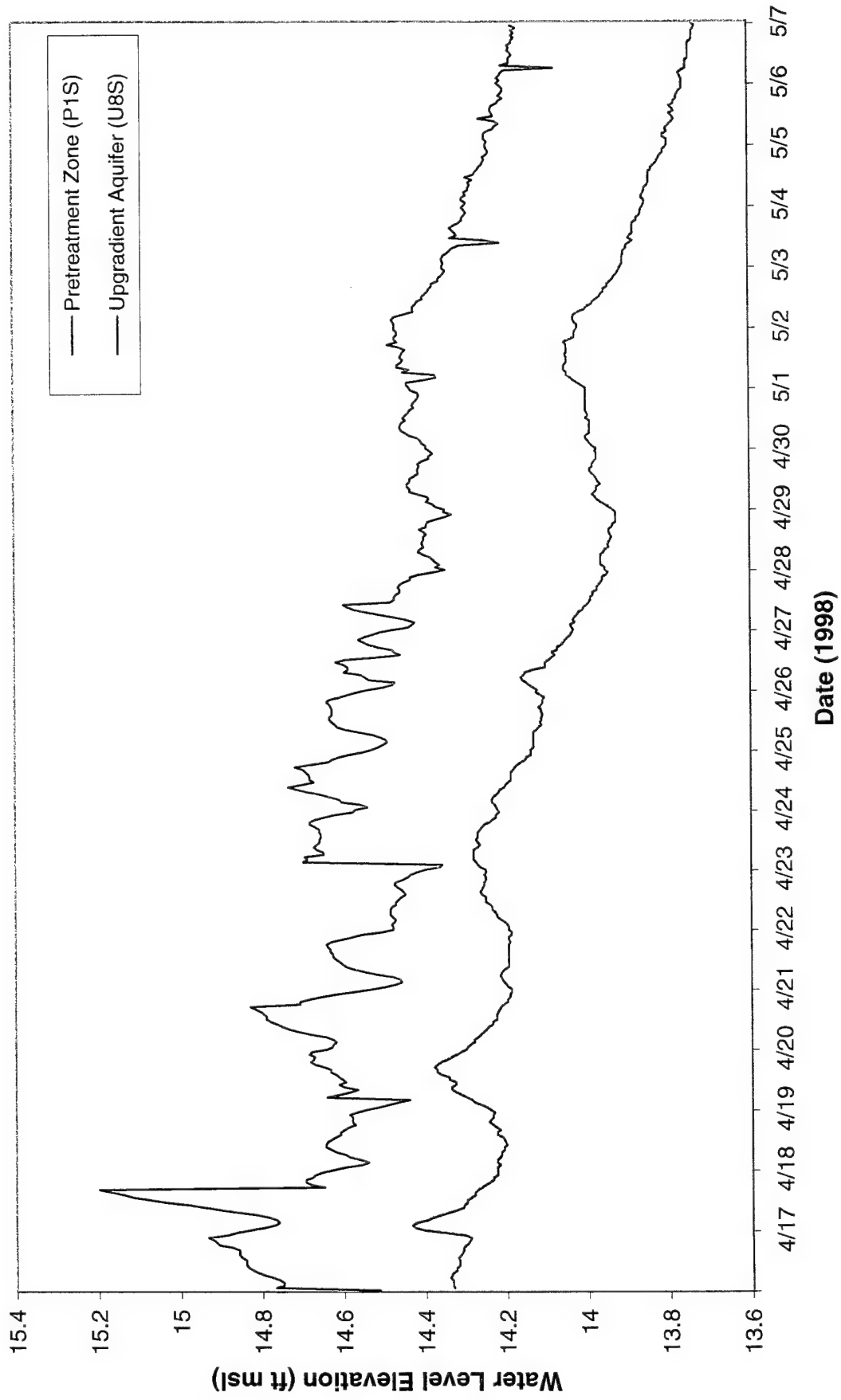
Dover AFB Permeable Barrier Continuous Water Level Elevations - Gate 1



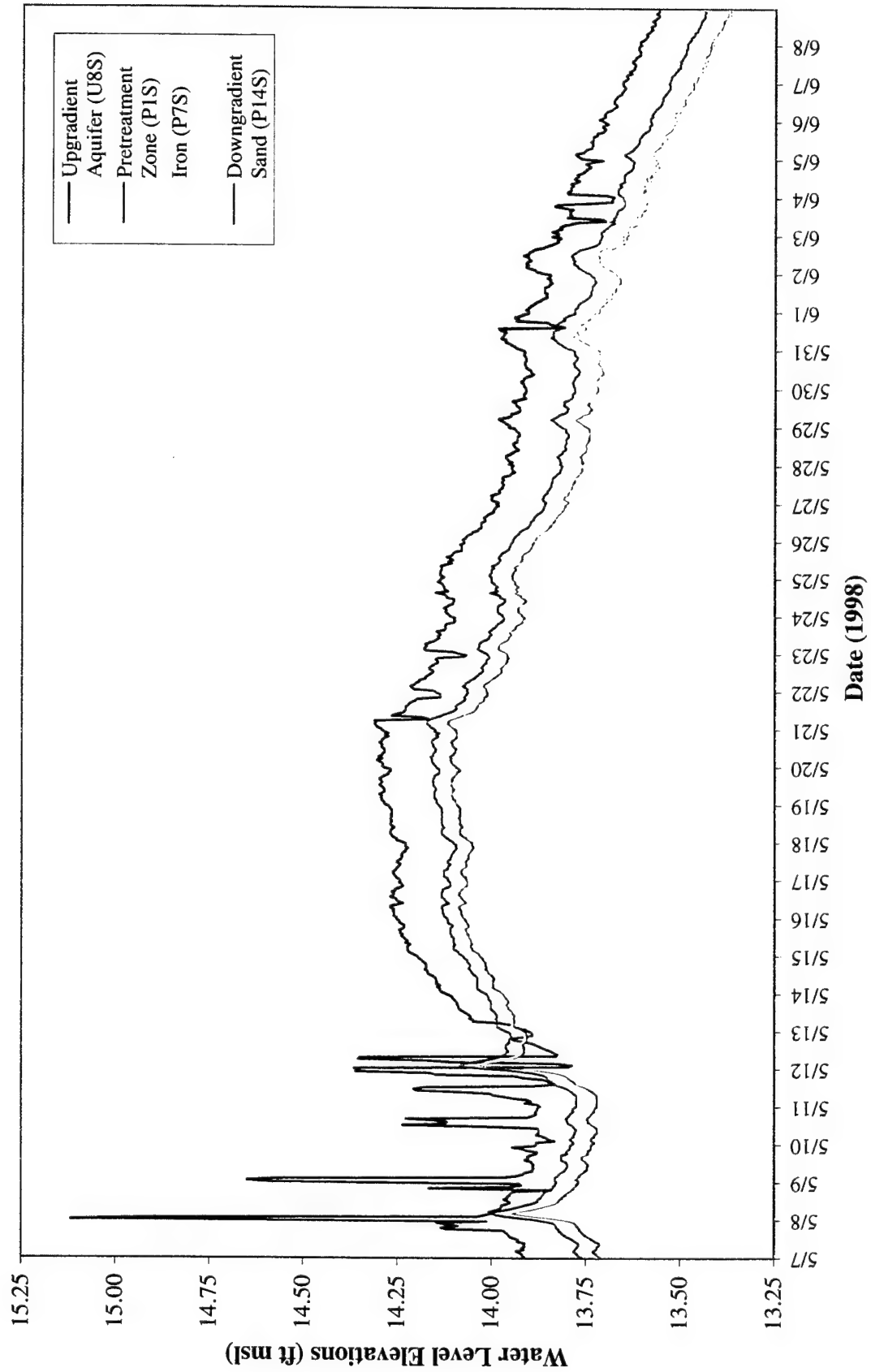
Dover AFB Permeable Barrier Continuous Water Level Elevations - Gate 2



Dover AFB Permeable Barrier Continuous Water Level Elevations - Gate 2



Dover AFB Permeable Barrier Continuous Water Level Elevations - Gate 2



Appendix F

Supporting Information for Geochemical Performance Evaluation

F-1. Data Tables and Figures for Field Parameter and Inorganics Measurements in Groundwater

F-2. XRD Patterns for Iron Core Samples

F-3. FTIR Spectra for Iron Core Samples

F-4. Raman Spectra for Iron Core Samples

Appendix F-1

Data Tables and Figures for Field Parameter and Inorganics Measurements in Groundwater

**Table F-1. Dover Funnel & Gate Area 5 Site:
Field Parameters**

Well ID	pH		ORP (mV)		Eh (mV)		DO (mg/L)		Temp (°C)		
	Jul 98	Jun 99	Jul 98	Jun 99	Jul 98	Jun 99	Jul 98	Apr 99	Jun 99	Jul 98	Jun 99
Gate 1 Upgradient Wells											
U1S	4.81	4.71	78.0	232.7	275.0	530.7	6.16	NA	6.71	26.14	20.67
U2S	4.81	4.61	59.2	275.1	256.2	573.1	4.92	NA	6.04	24.22	21.60
U3S	4.99	5.06	41.9	271.2	238.9	569.2	3.01	NA	4.13	23.95	21.55
U3D	4.63	4.64	32.1	255.0	229.1	553.0	1.38	NA	5.45	23.22	21.74
U4S	5.52	5.07	-40.3	297.8	156.7	595.8	2.14	4.92	4.15	26.91	21.88
U4M	4.62	4.53	67.7	306.0	264.7	604.0	6.09	5.49	6.07	23.71	23.89
U4D	4.69	4.59	72.4	320.4	269.4	618.4	5.32	5.90	6.01	24.88	21.26
U5S	5.19	4.90	72.7	293.3	269.7	591.3	3.99	4.89	5.23	21.89	21.42
U5D	5.47	5.15	71.9	301.7	268.9	599.7	0.86	NA	3.47	21.35	22.00
U6S	5.02	4.88	117.9	299.4	314.9	597.4	6.26	NA	6.21	22.65	21.40
U10S	4.95	4.54	109.5	266.5	306.5	564.5	4.04	NA	6.63	22.17	22.02
U11S	4.83	4.63	117.6	431.1	314.6	729.1	4.47	5.75	6.56	22.70	21.31
U12S	4.67	4.58	123.4	412.6	320.4	710.6	2.69	NA	6.25	23.46	21.88
U13S	4.81	4.74	89.5	406.2	286.5	704.2	4.21	NA	6.53	23.09	21.07
U14S	4.97	4.68	88.6	409.9	285.6	707.9	5.29	NA	7.22	23.71	20.60
U15S	4.80	4.58	77.5	415.7	274.5	713.7	2.64	5.74	6.83	23.18	20.12
U16S	4.76	4.37	81.6	423.0	278.6	721.0	4.07	5.92	6.33	24.19	21.62
U17S	4.74	4.87	84.2	400.1	281.2	698.1	4.61	NA	5.93	23.71	21.99
U18S	4.86	4.35	44.6	416.8	241.6	714.8	1.97	5.49	6.56	23.05	21.56
U19	NA	5.33	NA	393.2	NA	691.2	NA	5.86	6.56	NA	23.53
U20	NA	4.41	NA	415.1	NA	713.1	NA	5.06	6.11	NA	21.76
Gate 1 Pre-Treatment Zone Wells											
F1S	10.33	10.35	-366.1	-316.3	-169.1	-18.3	<0.50	NA	<0.50	26.89	20.13
F2S	10.35	10.44	-443.1	-383.5	-246.1	-85.5	<0.50	NA	<0.50	26.87	20.78
F2M	10.28	10.25	-462.2	-355.9	-265.2	-57.9	<0.50	NA	<0.50	23.76	23.06
F2D	10.18	10.35	-447.4	-337.8	-250.4	-39.8	<0.50	NA	<0.50	23.50	20.60
F3S	10.45	10.46	-449.9	-390.0	-252.9	-92.0	0.50	NA	<0.50	28.89	19.90
F3D	10.42	10.13	-491.9	-361.7	-294.9	-63.7	<0.50	NA	<0.50	24.48	21.19
Gate 1 Reactive Cell Wells											
F4S	10.54	10.88	-492.8	-773.7	-295.8	-475.7	<0.50	NA	<0.50	27.33	20.20

**Table F-1. Dover Funnel & Gate Area 5 Site:
Field Parameters (Continued)**

Well ID	pH		ORP (mV)		Eh (mV)		DO (mg/L)		Temp (°C)	
	Jul 98	Jun 99	Jul 98	Jun 99	Jul 98	Jun 99	Jul 98	Jun 99	Jul 98	Jun 99
F4M	10.51	10.60	-474.5	-356.9	-277.5	-58.9	<0.50	NA	24.78	21.39
F4D	10.75	10.61	-467.2	-729.8	-270.2	-431.8	<0.50	NA	23.12	21.08
F5S	10.49	10.82	-481.3	-383.7	-284.3	-85.7	<0.50	NA	26.84	19.65
F5M	10.63	10.51	-474.3	-749.0	-277.3	-451.0	<0.50	NA	24.49	22.07
F5D	10.69	10.79	-492.8	-388.1	-295.8	-90.1	<0.50	NA	23.47	20.59
F6S	10.64	10.60	-496.6	-751.8	-299.6	-453.8	<0.50	NA	25.36	20.75
F6M	10.64	10.69	-486.4	-374.5	-289.4	-76.5	<0.50	NA	23.89	20.54
F6D	10.79	10.59	-481.0	-560.4	-284.0	-262.4	<0.50	NA	27.09	21.75
F7S	10.45	10.77	-488.3	-777.9	-291.3	-479.9	<0.50	NA	26.31	21.31
F7D	10.71	10.59	-481.8	-686.2	-284.8	-388.2	<0.50	NA	24.69	21.15
F8S	10.59	10.90	-465.3	-742.7	-268.3	-444.7	<0.50	NA	23.81	21.14
F8D	10.66	10.81	-476.2	-746.2	-279.2	-448.2	<0.50	NA	22.93	21.87
F9S	10.57	10.68	-466.6	-628.3	-269.6	-330.3	<0.50	NA	23.83	21.35
F9D	10.63	10.61	-480.1	-717.4	-283.1	-419.4	<0.50	NA	21.74	21.94
F10	10.78	10.87	-462.8	-770.2	-265.8	-472.2	<0.50	NA	22.71	21.56
F11S	10.54	10.88	-448.2	-751.7	-251.2	-453.7	<0.50	NA	26.53	20.33
F11D	10.57	10.80	-468.2	-725.6	-271.2	-427.6	0.50	NA	27.11	21.93
F12S	10.62	10.48	-447.6	-660.4	-250.6	-362.4	<0.50	NA	25.66	21.58
F12D	10.60	10.62	-471.9	-709.8	-274.9	-411.8	0.56	NA	21.73	21.46
Gate 1 Exit Zone Wells										
F13S	10.11	10.37	-206.6	-305.7	-9.6	-7.7	0.59	NA	<0.50	22.46
F13D	10.77	10.70	-451.1	-365.4	-254.1	-67.4	0.70	NA	<0.50	21.54
F14S	10.09	10.62	-295.8	-356.3	-98.8	-58.3	<0.50	NA	<0.50	20.69
F14D	10.48	10.71	-483.9	-375.4	-286.9	-77.4	0.89	NA	<0.50	20.73
Gate 1 Downgradient Aquifer Wells										
D1S	5.02	4.84	71.1	411.2	268.1	709.2	6.44	NA	7.81	24.56
D2S	4.81	4.67	19.1	397.7	216.1	695.7	1.05	NA	4.24	24.32
D3S	4.88	4.64	48.8	412.5	245.8	710.5	3.52	NA	7.02	24.74
D4S	5.41	4.98	50.2	392.0	247.2	690.0	0.74	NA	4.54	24.59
D5S	5.54	5.20	-45.4	351.8	151.6	649.8	1.71	NA	2.99	27.72
D5D	5.87	5.77	-70.3	104.1	126.7	402.1	0.60	NA	1.15	26.23
										21.57

**Table F-1. Dover Funnel & Gate Area 5 Site:
Field Parameters (Continued)**

Well ID	pH		ORP (mV)		Eh (mV)		DO (mg/L)			Temp (°C)	
	Jul 98	Jun 99	Jul 98	Jun 99	Jul 98	Jun 99	Jul 98	Apr 99	Jun 99	Jul 98	Jun 99
D6S	5.80	5.39	35.6	367.5	232.6	665.5	0.65	NA	3.24	23.84	23.23
D8	NA	4.41	NA	411.9	NA	709.9	NA	NA	6.14	NA	24.74
Gate 2 Upgradient Aquifer Wells											
U7S	5.08	4.83	60.5	318.1	257.5	616.1	0.89	NA	3.77	21.73	22.05
U7D	5.17	4.88	73.8	371.4	270.8	669.4	0.73	NA	4.42	20.64	22.02
U8S	6.07	5.67	-44.0	345.1	153.0	643.1	<0.50	0.96	5.00	22.55	21.81
U8M	6.27	5.80	0.9	103.9	197.9	401.9	<0.50	0.42	3.61	22.33	25.22
U8D	6.12	5.74	-28.5	210.8	168.5	508.8	0.92	0.50	4.02	23.92	21.94
U9S	5.45	5.80	1.8	93.0	198.8	391.0	0.50	0.39	2.97	21.04	20.95
U9D	4.72	4.65	95.2	384.4	292.2	682.4	3.62	NA	5.59	21.84	21.16
Gate 2 Pre-Treatment Zone Wells											
P1S	7.98	3.88	-293.5	255.4	-96.5	553.4	<0.50	NA	3.27	28.72	22.43
P1S ¹⁾	8.78	2.43	-228.9	460.0	-31.9	758.0	<0.50	NA	0.66	23.74	27.30
P2S	11.39	11.19	-334.9	-382.6	-137.9	-84.6	<0.50	NA	<0.50	25.84	20.58
P2S ¹⁾	11.52	5.17	-349.3	-461.9	-152.3	-163.9	<0.50	NA	<0.50	23.96	26.32
P2M	10.90	11.26	-420.5	-383.9	-223.5	-85.9	0.50	NA	<0.50	24.63	23.16
P2M ¹⁾	NA	10.81	NA	-542.8	NA	-244.8	NA	NA	<0.50	NA	26.10
P2D	10.72	7.59	-384.6	-504.9	-187.6	-206.9	<0.50	NA	<0.50	23.98	20.48
P2D ¹⁾	10.60	7.38	-375.4	-239.2	-178.4	58.8	0.50	NA	<0.50	22.52	23.63
P3S	11.52	10.65	-394.4	-745.2	-197.4	-447.2	<0.50	NA	<0.50	26.40	19.71
P3S ¹⁾	11.55	10.63	-404.6	-318.0	-207.6	-20.0	<0.50	NA	<0.50	24.14	26.52
P3D	9.92	7.54	-292.2	-236.2	-95.2	61.8	<0.50	NA	<0.50	23.41	20.68
P3D ¹⁾	NA	6.49	NA	-115.0	NA	183.0	NA	NA	<0.50	NA	23.57
Gate 2 Reactive Cell Wells											
P4S	11.76	11.77	-397.8	-369.4	-200.8	-71.4	<0.50	NA	<0.50	24.62	20.38
P4M	11.21	10.92	-408.0	-407.6	-211.0	-109.6	0.51	NA	<0.50	25.04	20.93
P4D	11.07	10.61	-462.4	-673.6	-265.4	-375.6	<0.50	NA	<0.50	22.24	19.70
P5S	11.38	11.63	-401.0	-712.3	-204.0	-414.3	<0.50	NA	<0.50	26.55	19.99
P5M	10.68	10.83	-407.5	-386.5	-210.5	-88.5	0.50	NA	<0.50	24.51	22.21
P5D	10.89	9.09	-450.6	-680.8	-253.6	-382.8	<0.50	NA	<0.50	25.02	20.46
P6S	11.60	11.16	-410.9	-382.4	-213.9	-84.4	<0.50	NA	<0.50	27.97	21.21

**Table F-1. Dover Funnel & Gate Area 5 Site:
Field Parameters (Continued)**

Well ID	pH		ORP (mV)		Eh (mV)		DO (mg/L)		Temp (°C)		
	Jul 98	Jun 99	Jul 98	Jun 99	Jul 98	Jun 99	Jul 98	Apr 99	Jun 99	Jul 98	Jun 99
P6M	10.54	10.89	-403.7	-633.0	-206.7	-335.0	0.53	NA	<0.50	24.98	20.70
P6D	10.72	10.39	-420.9	-323.3	-223.9	-25.3	<0.50	NA	<0.50	22.85	21.20
P7S	11.21	11.38	-401.4	-370.4	-204.4	-72.4	<0.50	NA	<0.50	24.45	20.65
P7D	10.97	10.44	-424.8	-579.6	-227.8	-281.6	<0.50	NA	<0.50	22.45	22.42
P8S	11.44	11.22	-413.2	-356.4	-216.2	-58.4	<0.50	NA	<0.50	24.29	21.65
P8D ²⁾	10.79	10.94	-421.7	-359.0	-224.7	-61.0	<0.50	NA	<0.50	25.80	21.09
P9S	11.17	10.79	-403.0	-629.4	-206.0	-331.4	0.50	NA	<0.50	24.65	21.61
P9D	10.83	10.74	-427.2	-334.1	-230.2	-36.1	0.65	NA	<0.50	22.94	21.48
P10	10.96	10.97	-427.5	-666.2	-230.5	-368.2	<0.50	NA	<0.50	22.99	21.25
P11S	10.69	10.80	-399.5	-691.6	-202.5	-393.6	<0.50	NA	<0.50	25.09	20.82
P11D	11.14	10.93	-425.1	-665.0	-228.1	-367.0	<0.50	NA	0.90	26.26	21.63
P12S	10.88	10.67	-418.4	-624.6	-221.4	-326.6	<0.50	NA	<0.50	23.63	20.60
P12D	10.86	10.95	-434.9	-726.3	-237.9	-428.3	0.58	NA	<0.50	23.17	20.73
Gate 2 Exit Zone Wells											
P13S	11.04	10.77	-399.5	-372.1	-202.5	-74.1	<0.50	NA	<0.50	23.92	20.37
P13D	10.53	10.43	-385.0	-280.8	-188.0	17.2	0.57	NA	<0.50	22.79	20.91
P14S	10.80	10.63	-401.4	-342.1	-204.4	-44.1	<0.50	NA	<0.50	25.06	20.87
P14D	10.56	10.38	-380.3	-206.1	-183.3	91.9	<0.50	NA	<0.50	22.50	21.13
Gate 2 Downgradient Aquifer Wells											
D7S	9.63	10.00	-171.4	-315.8	25.6	-17.8	<0.50	NA	2.96	27.89	21.22
D7D	9.82	9.48	-203.1	-226.5	-6.1	71.5	<0.50	NA	2.99	22.91	21.59
Existing Wells											
214S	4.37	NA	238.1	NA	435.1	NA	4.07	5.55	NA	24.43	NA
214D	4.70	NA	1.8	NA	198.8	NA	1.36	3.12	NA	34.11	NA

NA: Not available.

1) These field parameters were read after a month.

2) P8D field parameters are measured from medium well depth.

**Table F-2. Results of Samplings at Dover Funnel & Gate Site:
Inorganic Analytes (mg/L)**

Well ID	Alkalinity			Calcium			Chloride		
	Results Jul 98	Detection Limit	Results Jun 99	Results Jul 98	Detection Limit	Results Jun 99	Results Jul 98	Detection Limit	Detection Limit
Gate 1 Upgradient Aquifer Wells									
U4S	13	1	6	16.4	0.2	5.5	39	1	37
U4D	4	1	U	4.9	0.2	3.5	20	1	19
U4D-Unf	NA	NA	NA	NA	NA	3.4	NA	NA	NA
Gate 1 Pre-Treatment Zone Wells									
F1S	32	1	26	8.9	0.2	3.1	11	1	4.5
F2S	34	1	27	6	0.2	3.8	18	1	2.4
F2S-Unf	NA	NA	NA	NA	NA	3.8	NA	NA	NA
F2D	46	1	33	3.43	0.2	3.4	21	1	16
F3S	35	1	NA	4.6	0.2	NA	15	1	NA
F3D	46	1	NA	2.42	0.2	NA	20	1	NA
Gate 1 Reactive Cell Wells									
F4S	38	1	NA	7.6	0.2	NA	18	1	NA
F4D	35	1	NA	6.6	0.2	NA	21	1	NA
F5S	37	1	38	12.2	0.2	6.6	19	1	1.6
F5D	29	1	34	5.2	0.2	4.4	24	1	19
F6S	40	1	NA	5.9	0.2	NA	12	1	NA
F6D	39	1	NA	3.83	0.2	NA	18	1	NA
F7S	41	1	44	12.2	0.2	6.9	22	1	3.1
F7D	35	1	36	7.5	0.2	4.1	25	1	18
F10	NA	NA	50	NA	NA	5.9	NA	NA	12
F11S	54	1	52	6	0.2	4	28	1	9.6
F11D	53	1	50	10.3	0.2	4.4	24	1	9.2
F12S	58	1	NA	3.46	0.2	NA	16	1	NA
Gate 1 Exit Zone Wells									
F14S	58	1	41	4.56	0.2	6.4	13	1	8.4
F14D	36	1	47	6	0.2	5.3	26	1	9.6
Gate 1 Downgradient Aquifer Wells									
D5S	13	1	8	47.1	0.2	0.92	30	1	8.9
D5D	28	1	22	6.2	0.2	4.6	43	1	19
Gate 2 Upgradient Aquifer Wells									
U8S	30	1	8	21.3	2	21	59	1	61
U8D	54	1	38	9.2	2	6.8	26	1	24

**Table F-2. Results of Samplings at Dover Funnel & Gate Site:
Inorganic Analytes (mg/L) (Continued)**

Well ID	Alkalinity			Calcium			Chloride		
	Results Jul 98	Detection Limit	Results Jun 99	Results Jul 98	Detection Limit	Results Jun 99	Detection Limit	Results Jul 98	Detection Limit
Gate 2 Reactive Cell Wells									
P1S	59	1	U	31.1	0.2	40	0.5	41	1
P2S	180	1	96	44.3	2	48	0.5	27	1
P2D	42	1	32	8.9	0.2	40	0.5	18	1
P3S	185	1	NA	66	2	NA	NA	20	1
P3D	94	1	NA	13.2	0.2	NA	NA	19	1
P4S	265	1	NA	63	0.2	NA	NA	21	1
P4D	87	1	NA	2.84	0.2	NA	NA	20	1
P5S	150	1	140	50	2	54	0.5	24	1
P5D	79	1	28	3.37	0.2	28	0.5	23	1
P6S	134	1	NA	45.7	0.2	NA	NA	31	1
P6D	79	1	NA	7.2	2	NA	NA	30	1
P7S	133	1	82	14.8	0.2	24	0.5	14	1
P7D	81	1	26	4.25	0.2	42	0.5	24	1
P10	NA	NA	62	NA	NA	13	0.5	NA	NA
P11S	73	1	70	97	2	3.7	0.5	37	1
P11D	75	1	70	45.7	0.2	12	0.5	29	1
P12S	66	1	NA	12	0.2	NA	NA	27	1
P12S-DUP	66	1	NA	10.8	0.2	NA	NA	32	1
Gate 2 Exit Zone Wells									
P14S	82	1	66	5.3	2	2.5	0.5	26	1
P14D	92	1	102	4.65	0.2	6.3	0.5	22	1
Gate 2 Downgradient Aquifer Wells									
D7S	137	1	NA	16.3	2	NA	NA	20	1
D7S-DUP	134	1	NA	10.6	0.2	NA	NA	12	1
D7D	112	1	NA	5.3	2	NA	NA	23	1
Existing Wells									
214S	2	1	NA	3.18	0.2	NA	NA	16	1
214D	7	1	NA	3.13	0.2	NA	NA	22	1

**Table F-2. Results of Samplings at Dover Funnel & Gate Site:
Inorganic Analytes (mg/L) (Continued)**

Well ID	Iron			Magnesium			Manganese		TOC	
	Results Jul 98	Detection Limit	Results Jun 99	Detection Limit	Results Jul 98	Detection Limit	Results Jul 98	Detection Limit	Results Jun 99	Detection Limit
Gate 1 Upgradient Aquifer Wells										
U4S	U	0.03	U	0.05	14.5	0.2	0.5	0.03	0.02	1.7
U4D	U	0.03	U	0.05	4.8	0.2	0.5	0.12	0.02	1.1
U4D-Unf	NA	NA	0.081	0.05	NA	NA	0.5	NA	NA	NA
Gate 1 Pre-Treatment Zone Wells										
F1S	0.04	0.03	U	0.05	U	0.2	0.5	U	0.02	3.3
F2S	U	0.03	U	0.05	U	0.2	0.5	U	0.02	NA
F2S-Unf	NA	NA	U	0.05	NA	NA	0.5	NA	NA	NA
F2D	0.05	0.03	0.078	0.05	0.48	0.2	0.5	U	0.02	NA
F3S	0.05	0.03	NA	NA	U	0.2	NA	U	0.02	NA
F3D	0.04	0.03	NA	NA	U	0.2	NA	U	0.02	NA
Gate 1 Reactive Cell Wells										
F4S	0.08	0.03	NA	NA	U	0.2	NA	U	0.02	NA
F4D	0.05	0.03	NA	NA	U	0.2	NA	U	0.02	NA
F5S	0.04	0.03	U	0.05	U	0.2	0.5	U	0.02	NA
F5D	U	0.03	U	0.05	U	0.2	0.5	U	0.02	NA
F6S	U	0.03	NA	NA	U	0.2	NA	U	0.02	NA
F6D	U	0.03	NA	NA	U	0.2	NA	U	0.02	NA
F7S	0.06	0.03	U	0.05	U	0.2	0.5	U	0.02	4.2
F7D	0.07	0.03	U	0.05	U	0.2	0.5	U	0.02	4.9
F10	NA	NA	U	0.05	NA	NA	0.5	NA	NA	7.7
F11S	0.07	0.03	U	0.05	U	0.2	0.5	U	0.02	7.4
F11D	U	0.03	U	0.05	U	0.2	0.5	U	0.02	6.5
F12S	0.06	0.03	NA	NA	U	0.2	NA	U	0.02	NA
Gate 1 Exit Zone Wells										
F14S	0.11	0.03	U	0.05	U	0.2	0.5	U	0.02	NA
F14D	U	0.03	U	0.05	U	0.2	0.5	U	0.02	NA
Gate 1 Downgradient Aquifer Wells										
D5S	0.04	0.03	0.3	0.05	20.3	0.2	0.5	0.06	0.02	1.3
D5D	0.22	0.03	U	0.05	1.16	0.2	0.5	0.35	0.02	1.8
Gate 2 Upgradient Aquifer Wells										
U8S	0.05	0.03	0.082	0.05	8.7	2	0.5	0.31	0.02	1.5
U8D	0.04	0.03	U	0.05	4.99	0.2	0.5	0.65	0.02	U

**Table F-2. Results of Samplings at Dover Funnel & Gate Site:
Inorganic Analytes (mg/L) (Continued)**

Well ID	Iron			Magnesium			Manganese		TOC	
	Results Jul 98	Detection Limit	Results Jun 99	Detection Limit	Results Jul 98	Detection Limit	Results Jul 98	Detection Limit	Results Jun 99	Detection Limit
Gate 2 Reactive Cell Wells										
P1S	0.49	0.03	32	0.05	4.61	0.2	0.15	0.02	4.5	1
P2S	0.18	0.03	U	0.05	U	0.2	U	0.02	NA	NA
P2D	U	0.03	16	0.05	U	0.2	U	0.02	NA	NA
P3S	0.05	0.03	NA	NA	U	0.2	U	0.02	NA	NA
P3D	0.07	0.03	NA	NA	1.12	0.2	0.08	0.02	NA	NA
P4S	0.07	0.03	NA	NA	U	0.2	U	0.02	NA	NA
P4D	0.07	0.03	NA	NA	U	0.2	U	0.02	NA	NA
P5S	0.04	0.03	U	0.05	U	0.2	U	0.02	NA	NA
P5D	U	0.03	0.34	0.05	U	0.2	U	0.02	NA	NA
P6S	U	0.03	NA	NA	U	0.2	U	0.02	NA	NA
P6D	0.04	0.03	NA	NA	U	0.2	U	0.02	NA	NA
P7S	U	0.03	U	0.05	1.5	0.2	U	0.02	10	1
P7D	U	0.03	U	0.05	U	0.2	U	0.02	3	1
P10	NA	NA	U	0.05	NA	NA	NA	NA	9.2	1
P11S	U	0.03	U	0.05	U	0.2	U	0.02	6.4	1
P11D	U	0.03	U	0.05	U	0.2	U	0.02	6.2	1
P12S	U	0.03	NA	NA	U	0.2	U	0.02	NA	NA
P12S-DUP	U	0.03	NA	NA	U	0.2	U	0.02	NA	NA
Gate 2 Exit Zone Wells										
P14S	U	0.03	U	0.05	U	0.2	U	0.02	NA	NA
P14D	0.18	0.03	U	0.05	U	0.2	U	0.02	NA	NA
Gate 2 Downgradient Aquifer Wells										
D7S	0.11	0.03	NA	NA	U	0.2	U	0.02	NA	NA
D7S-DUP	NA	NA	NA	NA	1.52	0.2	U	0.02	NA	NA
D7D	0.11	0.03	NA	NA	U	0.2	U	0.02	NA	NA
Existing Wells										
214S	U	0.03	NA	NA	3.75	0.2	0.08	0.02	NA	NA
214D	U	0.03	NA	NA	2.75	0.2	0.05	0.02	NA	NA

**Table F-2. Results of Samplings at Dover Funnel & Gate Site:
Inorganic Analytes (mg/L) (Continued)**

Well ID	Nitrate			Silica			Sodium		
	Results Jul 98	Detection Limit	Results Jun 99	Detection Limit	Results Jul 98	Detection Limit	Results Jul 98	Detection Limit	Detection Limit
Gate 1 Upgradient Aquifer Wells									
U4S	6.84	1	8	0.5	4.67	2	10	14.5	0.2
U4D	11	1	7.1	0.5	10.2	2	15	16.6	0.2
U4D-Unf	NA	NA	NA	NA	NA	NA	NA	NA	0.5
Gate 1 Reactive Cell Wells									
F1S	0.03	0.02	U	0.1	U	2	1.3	23.2	0.2
F2S	U	0.02	NA	NA	U	2	1.7	27	0.2
F2S-Unf	NA	NA	NA	NA	NA	NA	NA	NA	0.5
F2D	0.08	0.02	NA	NA	U	2	2.5	23.3	0.2
F3S	U	0.02	NA	NA	U	2	NA	26.5	0.2
F3D	U	0.02	NA	NA	U	2	NA	25.9	0.2
Gate 1 Reactive Cell Wells									
F4S	U	0.02	NA	NA	U	2	NA	31	0.2
F4D	U	0.02	NA	NA	U	2	NA	19	0.2
F5S	U	0.02	NA	NA	U	2	0.25 J	30	0.2
F5D	U	0.02	NA	NA	U	2	0.59	24.5	0.2
F6S	U	0.02	NA	NA	U	2	NA	25.4	0.2
F6D	0.08	0.02	NA	NA	U	2	NA	27.3	0.2
F7S	U	0.02	U	0.1	U	2	0.55	25.1	0.2
F7D	U	0.02	U	0.1	U	2	1	24	0.2
F10	NA	NA	U	0.1	NA	NA	0.85	NA	0.2
F11S	U	0.02	U	0.1	U	2	1.8	38.5	0.2
F11D	U	0.02	U	0.1	U	2	1.2	35.5	0.2
F12S	U	0.02	NA	NA	2.39	2	NA	40.4	0.2
Gate 1 Exit Zone Wells									
F14S	U	0.02	NA	NA	5.27	2	5.5	37.5	0.2
F14D	U	0.02	NA	NA	3.01	2	5.4	31	0.2
Gate 1 Downgradient Aquifer Wells									
D5S	23.1	2	6.1	NA	4.69	2	10	13.9	0.2
D5D	0.16	0.02	0.31	NA	9.95	2	8.8	38.9	0.2
Gate 2 Upgradient Aquifer Wells									
U8S	2.75	0.2	2.8	NA	11.7	2	11	47.9	2
U8D	2.89	0.2	2.3	NA	9.42	2	13	44.9	2

**Table F-2. Results of Samplings at Dover Funnel & Gate Site:
Inorganic Analytes (mg/L) (Continued)**

Well ID	Nitrate			Silica			Sodium		
	Results Jul 98	Detection Limit	Results Jun 99	Detection Limit	Results Jul 98	Detection Limit	Results Jun 99	Detection Limit	Detection Limit
Gate 2 Reactive Cell Wells									
P1S	U	0.02	U	0.1	8.78	2	13	0.2	0.5
P2S	0.05	0.02	NA	NA	8.26	2	5.8	2	0.5
P2D	U	0.02	NA	NA	U	2	4.4	0.2	0.5
P3S	0.02	0.02	NA	NA	6.14	2	NA	2	NA
P3D	U	0.02	NA	NA	4.65	100	NA	0.2	NA
P4S	0.02	0.02	NA	NA	3.77	2	NA	0.2	NA
P4D	U	0.02	NA	NA	U	2	NA	2	NA
P5S	0.02	0.02	NA	NA	3.87	2	3.7	2	0.5
P5D	0.03	0.02	NA	NA	U	2	1.3	2	0.5
P6S	U	0.02	NA	NA	3.11	2	NA	0.2	NA
P6D	U	0.02	NA	NA	U	2	NA	2	NA
P7S	0.06	0.02	U	0.1	4.74	2	2.6	0.2	0.5
P7D	U	0.02	U	0.1	U	2	0.46 J	0.2	0.5
P10	NA	NA	U	0.1	NA	NA	1.4	NA	0.5
P11S	U	0.02	U	0.1	U	2	1.8	2	0.5
P11D	U	0.02	U	0.1	U	2	0.71	0.2	0.5
P12S	0.02	0.02	NA	NA	U	2	NA	0.2	NA
P12S-DUP	U	0.02	NA	NA	U	2	NA	0.2	NA
Gate 2 Exit Zone Wells									
P14S	U	0.02	NA	NA	3.38	2	3.4	2	0.5
P14D	U	0.02	NA	NA	5.19	2	5.3	0.2	0.5
Gate 2 Downgradient Aquifer Wells									
D7S	U	0.02	NA	NA	U	2	NA	2	NA
D7S-DUP	0.06	0.02	NA	NA	4.82	2	NA	0.2	NA
D7D	U	0.02	NA	NA	8	2	NA	2	NA
Existing Wells									
214S	4.54	1	NA	NA	10.8	100	NA	0.2	NA
214D	3.57	0.5	NA	NA	10.8	100	NA	0.2	NA

**Table F-2. Results of Samplings at Dover Funnel & Gate Site:
Inorganic Analytes (mg/L) (Continued)**

Well ID	Sulfate			TDS			BOD		COD	
	Results Jul 98	Detection Limit	Results Jun 99	Detection Limit	Results Jul 98	Detection Limit	Results Jul 98	Detection Limit	Results Jun 99	Detection Limit
Gate 1 Upgradient Aquifer Wells										
U4S	53	5	9.3	1	244	10	280	5	NA	NA
U4D	12	5	4	1	142	10	120	5	NA	NA
U4D-Unf	NA	NA	NA	NA	NA	NA	NA	NA	NA	NA
Gate 1 Reactive Cell Wells										
F1S	28	5	U	1	128	10	50	5	NA	NA
F2S	31	5	2.4	5	128	10	8	5	NA	NA
F2S-Unf	NA	NA	NA	NA	NA	NA	NA	NA	NA	NA
F2D	U	5	2.5	5	94	10	78	5	NA	NA
F3S	32	5	NA	NA	112	10	NA	NA	NA	NA
F3D	U	5	NA	NA	100	10	NA	NA	NA	NA
Gate 1 Reactive Cell Wells										
F4S	39	5	NA	NA	138	10	NA	NA	NA	NA
F4D	U	5	NA	NA	82	10	NA	NA	NA	NA
F5S	44	5	2.9	5	160	10	26	5	NA	NA
F5D	15	5	2.4	5	94	10	8	5	NA	NA
F6S	35	5	NA	NA	126	10	NA	NA	NA	NA
F6D	18	5	NA	NA	116	10	NA	NA	NA	NA
F7S	35	5	U	1	136	10	8	5	2.7	20
F7D	24	5	U	1	118	10	18	5	6.2	20
F10	NA	NA	U	1	NA	NA	24	5	7.8	20
F11S	22	5	U	1	154	10	50	5	12	20
F11D	19	5	U	1	148	10	U	5	5.1	20
F12S	31	5	NA	NA	142	10	NA	NA	NA	NA
Gate 1 Exit Zone Wells										
F14S	22	5	15	5	154	10	32	5	NA	NA
F14D	22	5	5.6	5	156	10	86	5	NA	NA
Gate 1 Downgradient Aquifer Wells										
D5S	94	10	28	5	418	10	120	5	U	20
D5D	24	5	5.1	5	154	10	80	5	U	20
Gate 2 Upgradient Aquifer Wells										
U8S	71	5	140	25	278	10	340	5	U	20
U8D	61	5	23	5	210	10	130	5	U	20

**Table F-2. Results of Samplings at Dover Funnel & Gate Site:
Inorganic Analytes (mg/L) (Continued)**

Well ID	Sulfate			TDS			BOD		COD	
	Results Jul 98	Detection Limit	Results Jun 99	Detection Limit	Results Jul 98	Detection Limit	Results Jul 98	Detection Limit	Results Jun 99	Detection Limit
Gate 2 Reactive Cell Wells										
P1S	84	10	210	25	282	10	100	5	NA	NA
P2S	41	5	60	5	324	10	180	5	NA	NA
P2D	53	5	98	10	186	10	160	5	NA	NA
P3S	53	5	NA	NA	350	10	NA	NA	NA	NA
P3D	26	5	NA	NA	188	10	NA	NA	NA	NA
P4S	35	5	NA	NA	400	10	NA	NA	NA	NA
P4D	15	5	NA	NA	228	10	NA	NA	NA	NA
P5S	35	5	27	5	288	10	170	5	NA	NA
P5D	21	5	81	5	254	10	120	5	NA	NA
P6S	52	5	NA	NA	268	10	NA	NA	NA	NA
P6D	18	5	NA	NA	240	10	NA	NA	NA	NA
P7S	46	5	31	5	288	10	110	5	7.7	2
P7D	29	5	110	25	228	30	140	5	U	2
P10	NA	NA	39	5	NA	NA	58	5	8	6
P11S	71	5	20	5	336	10	36	5	U	6
P11D	37	5	76	5	234	10	94	5	13	2
P12S	62	5	NA	5	248	10	NA	NA	NA	NA
P12S-DUP	66	5	NA	NA	256	10	NA	NA	NA	NA
Gate 2 Exit Zone Wells										
P14S	61	5	14	5	300	10	82	5	NA	NA
P14D	23	5	67	5	256	10	180	5	NA	NA
Gate 2 Downgradient Aquifer Wells										
D7S	23	5	NA	NA	266	10	NA	NA	NA	NA
D7S-DUP	45	5	NA	NA	290	10	NA	NA	NA	NA
D7D	8	5	NA	NA	266	10	NA	NA	NA	NA
Existing Wells										
214S	U	5	NA	NA	90	10	NA	NA	NA	NA
214D	U	5	NA	NA	102	10	NA	NA	NA	NA

NA: Not available.

U: The result is below the reporting limit.

J: The result is less than the sample RL and greater than the MDL.

**Table F-3. Results of July 1998 Sampling at Dover Funnel & Gate Site:
Inorganic Analytes (mmol/L)**

Well ID	Na	Ca	Mg	NO ₃	SO ₄	Cl	Alkalinity	meq of Cations	meq of Anions	Charge Balance ^(a)
Gate 1 Upgradient Aquifer Wells										
U4S	0.631	0.409	0.597	0.110	0.552	1.100	0.130	2.642	2.574	1.32%
U4D	0.722	0.122	0.198	0.177	0.125	0.564	0.040	1.362	1.071	11.94%
Gate 1 Pre-Treatment Zone Wells										
F1S	1.009	0.222	0.000	0.000	0.291	0.310	0.320	1.453	1.533	-2.68%
F2S	1.174	0.150	0.000	0.000	0.323	0.508	0.340	1.474	1.833	-10.85%
F2D	1.013	0.086	0.020	0.001	0.000	0.592	0.460	1.224	1.513	-10.55%
F3S	1.153	0.115	0.000	0.000	0.333	0.423	0.350	1.382	1.789	-12.82%
F3D	1.127	0.060	0.000	0.000	0.000	0.564	0.460	1.247	1.483	-8.64%
Gate 1 Reactive Cell Wells										
F4S	1.348	0.190	0.000	0.000	0.406	0.508	0.380	1.728	2.079	-9.23%
F4D	0.826	0.165	0.000	0.000	0.000	0.592	0.350	1.156	1.292	-5.55%
F5S	1.305	0.304	0.000	0.000	0.458	0.536	0.370	1.914	2.191	-6.77%
F5D	1.066	0.130	0.000	0.000	0.156	0.677	0.290	1.325	1.569	-8.42%
F6S	1.105	0.147	0.000	0.000	0.364	0.339	0.400	1.399	1.867	-14.31%
F6D	1.187	0.096	0.000	0.001	0.187	0.508	0.390	1.379	1.663	-9.35%
F7S	1.092	0.304	0.000	0.000	0.364	0.621	0.410	1.701	2.169	-12.10%
F7D	1.044	0.187	0.000	0.000	0.250	0.705	0.350	1.418	1.904	-14.63%
F11S	1.675	0.150	0.000	0.000	0.229	0.790	0.540	1.974	2.327	-8.20%
F11D	1.544	0.257	0.000	0.000	0.198	0.677	0.530	2.058	2.132	-1.75%
F12S	1.757	0.086	0.000	0.000	0.323	0.451	0.579	1.930	2.256	-7.78%
Gate 1 Exit Zone Wells										
F14S	1.631	0.114	0.000	0.000	0.229	0.367	0.579	1.859	1.984	-3.25%
F14D	1.348	0.150	0.000	0.000	0.229	0.733	0.360	1.648	1.911	-7.39%
Gate 1 Downgradient Aquifer Wells										
D5S	0.605	1.175	0.835	0.372	0.979	0.846	0.130	4.626	3.435	14.77%
D5D	1.692	0.155	0.048	0.003	0.250	1.213	0.280	2.097	2.275	-4.07%
Gate 2 Upgradient Aquifer Wells										
U8S	2.084	0.531	0.358	0.044	0.739	1.664	0.300	3.862	3.786	0.99%
U8D	1.953	0.230	0.205	0.047	0.635	0.733	0.540	2.823	3.129	-5.15%
Gate 1 Pre-Treatment Zone Wells										
P1S	1.749	0.776	0.190	0.000	0.874	1.157	0.589	3.680	4.084	-5.21%
P2S	1.196	1.105	0.000	0.001	0.427	0.762	1.798	3.407	5.213	-20.95%
P2D	1.505	0.222	0.000	0.000	0.552	0.508	0.420	1.949	2.451	-11.40%
P3S	1.013	1.647	0.000	0.000	0.552	0.564	1.848	4.307	5.365	-10.94%
P3D	1.509	0.329	0.046	0.000	0.271	0.536	0.939	2.260	2.956	-13.33%
Gate 2 Reactive Cell Wells										
P4S	0.966	1.572	0.000	0.000	0.364	0.592	2.648	4.109	6.617	-23.38%
P4D	1.975	0.071	0.000	0.000	0.156	0.564	0.869	2.117	2.615	-10.53%
P5S	1.157	1.248	0.000	0.000	0.364	0.677	1.499	3.652	4.403	-9.33%
P5D	1.840	0.084	0.000	0.000	0.219	0.649	0.789	2.008	2.665	-14.06%
P6S	0.953	1.140	0.000	0.000	0.541	0.874	1.339	3.233	4.635	-17.82%
P6D	1.918	0.180	0.000	0.000	0.187	0.846	0.789	2.278	2.800	-10.28%
P7S	2.075	0.369	0.062	0.001	0.479	0.395	1.329	2.937	4.011	-15.46%
P7D	1.779	0.106	0.000	0.000	0.302	0.677	0.809	1.991	2.899	-18.57%
P11S	2.118	2.420	0.000	0.000	0.739	1.044	0.729	6.959	3.981	27.22%

**Table F-3. Results of July 1998 Sampling at Dover Funnel & Gate Site:
Inorganic Analytes (mmol/L) (Continued)**

Well ID	Na	Ca	Mg	NO ₃	SO ₄	Cl	Alkalinity	meq of Cations	meq of Anions	Charge Balance ^(a)
P11D	1.705	1.140	0.000	0.000	0.385	0.818	0.749	3.986	3.087	12.70%
P12S	1.701	0.299	0.000	0.000	0.645	0.762	0.659	2.300	3.372	-18.90%
P12S-DUP	1.723	0.269	0.000	0.000	0.687	0.903	0.659	2.261	3.596	-22.78%
Gate 2 Exit Zone Wells										
P14S	2.088	0.132	0.000	0.000	0.635	0.733	0.819	2.352	3.642	-21.51%
P14D	1.949	0.116	0.000	0.000	0.239	0.621	0.919	2.181	2.938	-14.79%
Gate 2 Downgradient Aquifer Wells										
D7S	1.292	0.407	0.000	0.000	0.239	0.564	1.369	2.105	3.781	-28.46%
D7S-DUP	2.053	0.264	0.063	0.001	0.468	0.339	1.339	2.707	3.954	-18.72%
D7D	2.101	0.132	0.000	0.000	0.083	0.649	1.119	2.365	3.053	-12.70%
Existing Wells										
214S	0.378	0.079	0.154	0.073	0.000	0.451	0.020	0.846	0.564	19.95%
214D	0.535	0.078	0.113	0.058	0.000	0.621	0.070	0.918	0.818	5.74%

(a) Charge Balance = (meq of Cations - meq of Anions) / (meq of Cations + meq of Anions)

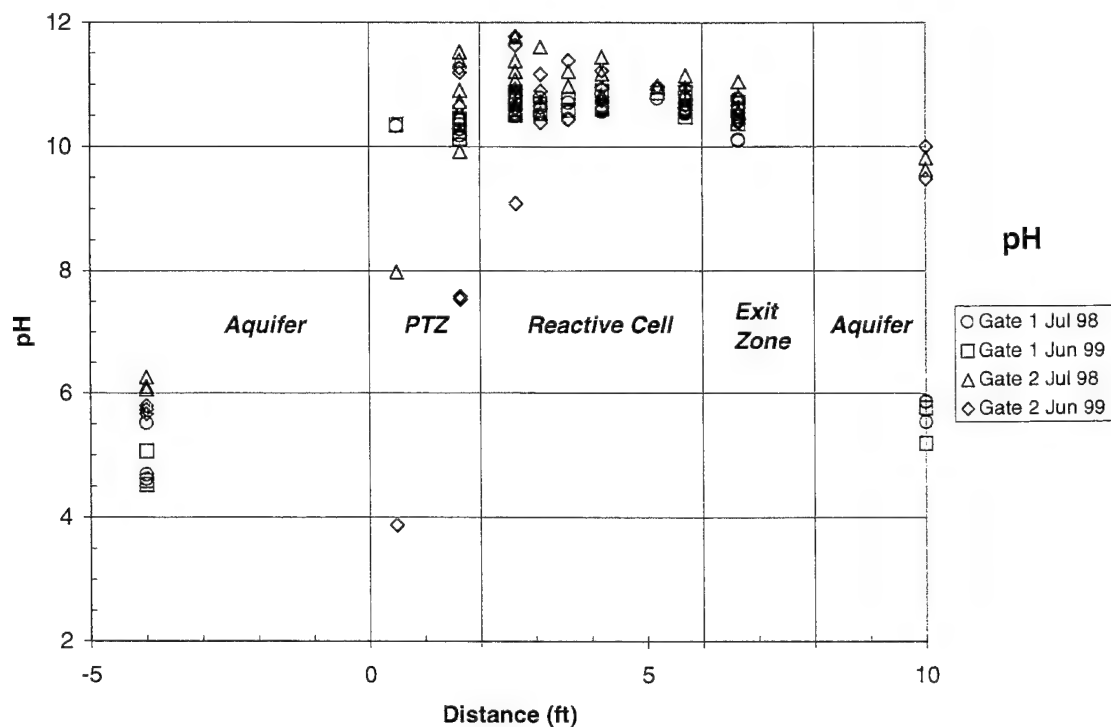


Figure F-1. pH Distribution in PRB.

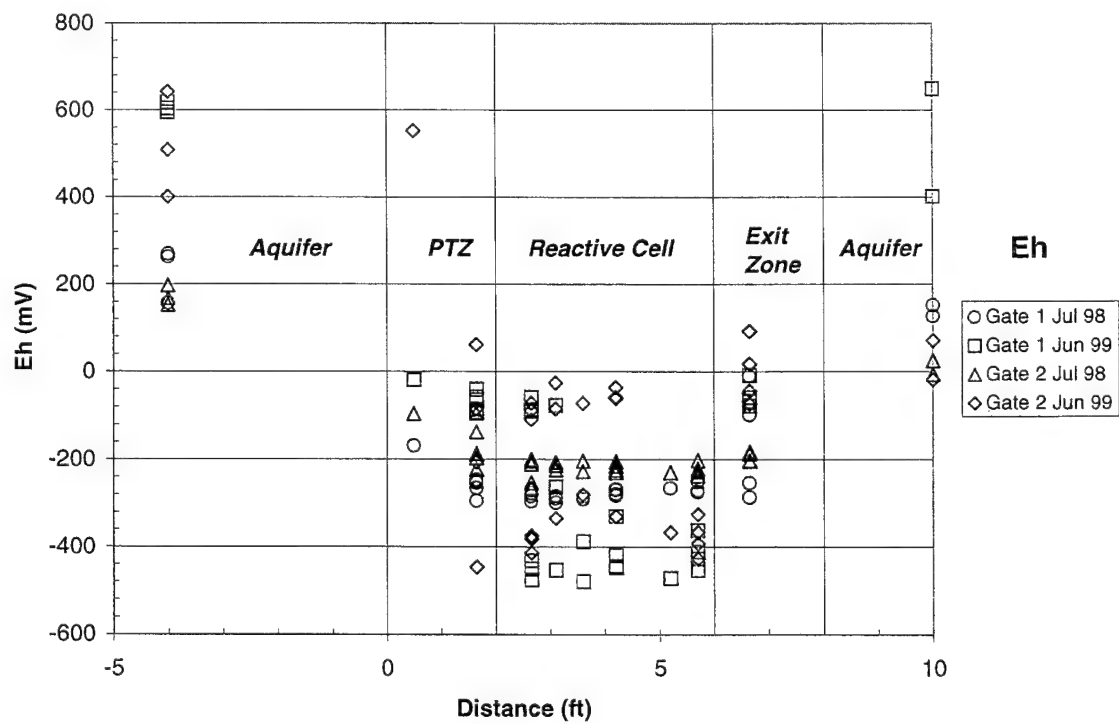


Figure F-2. Eh Distribution in PRB.

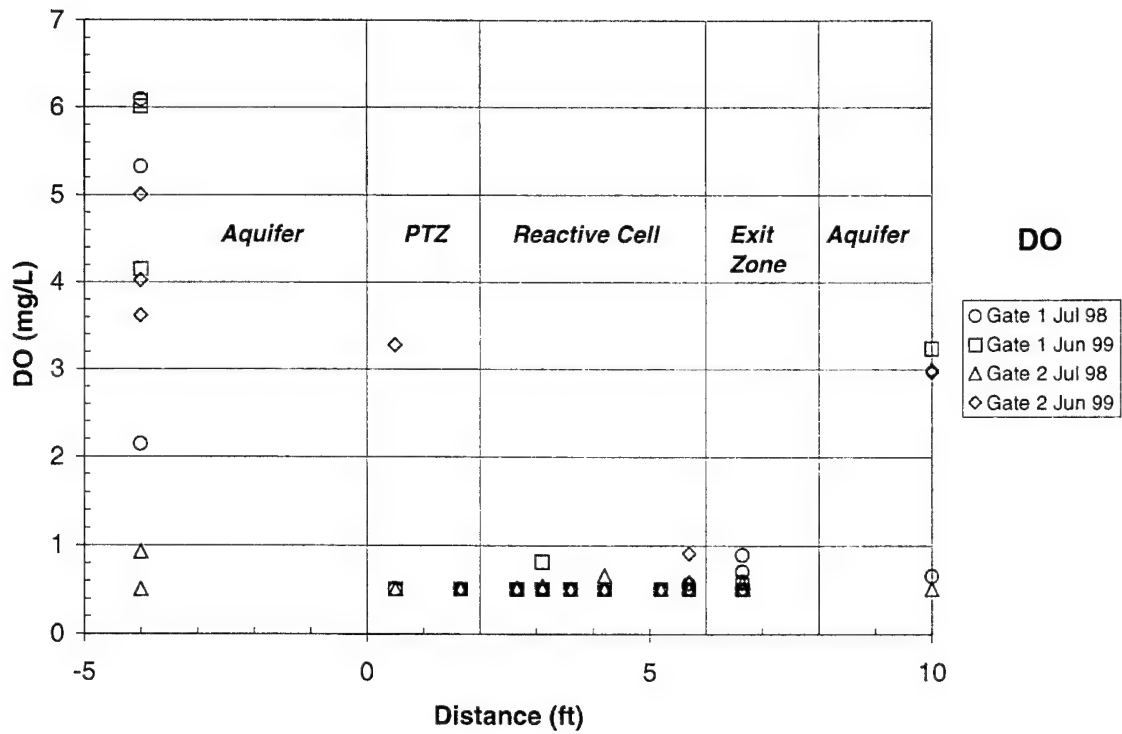


Figure F-3. Dissolved Oxygen Distribution in PRB.

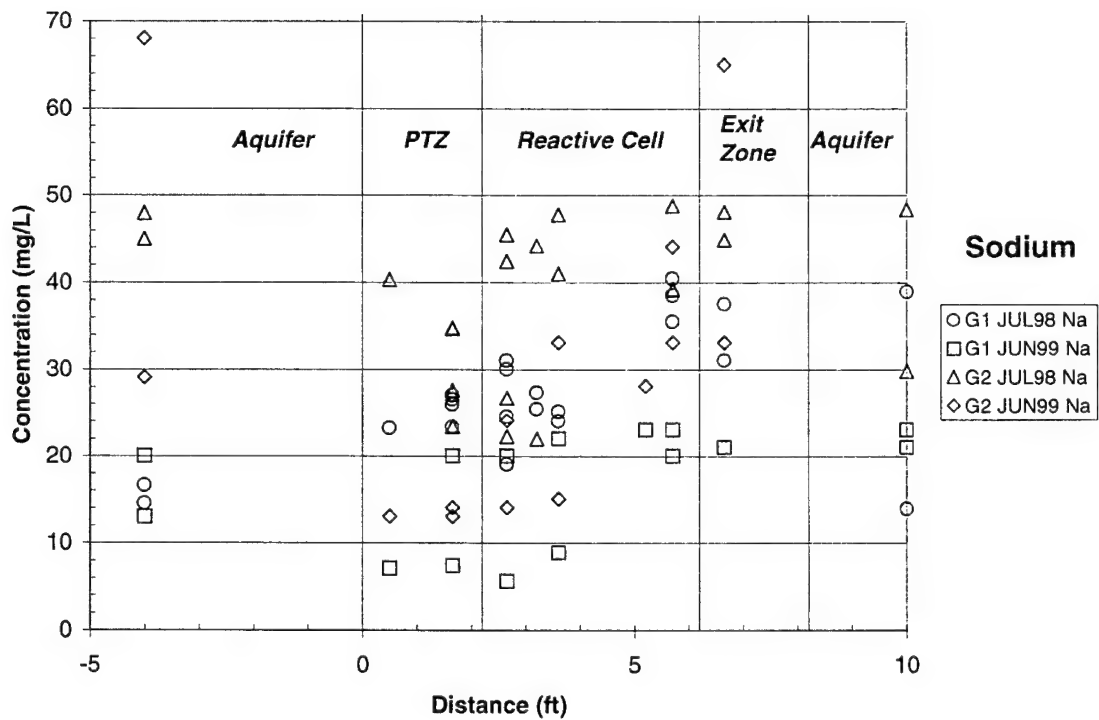


Figure F-4. Sodium Distribution in PRB.

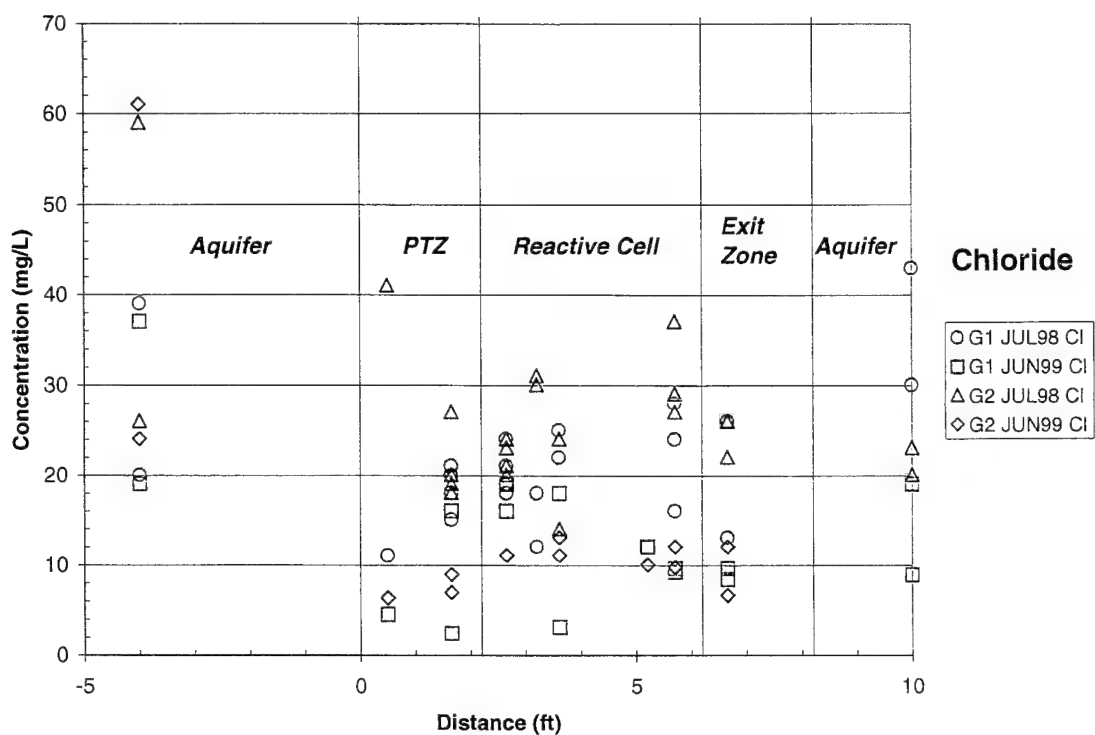


Figure F-5. Chloride Distribution in PRB.

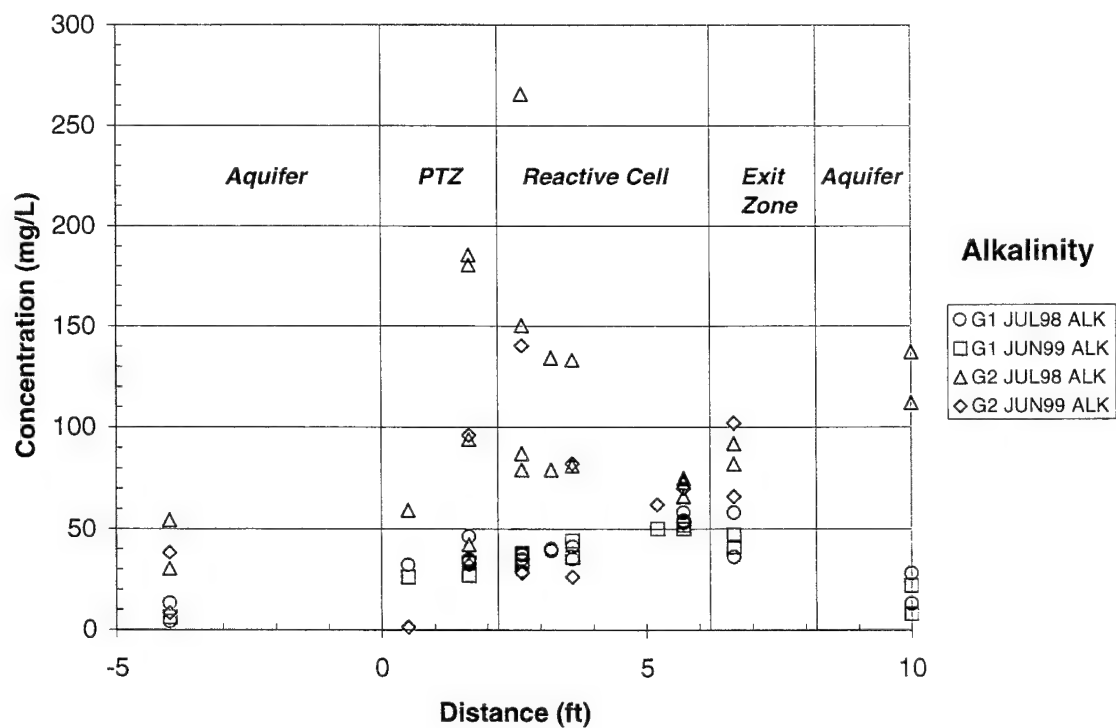


Figure F-6. Alkalinity Distribution in PRB.

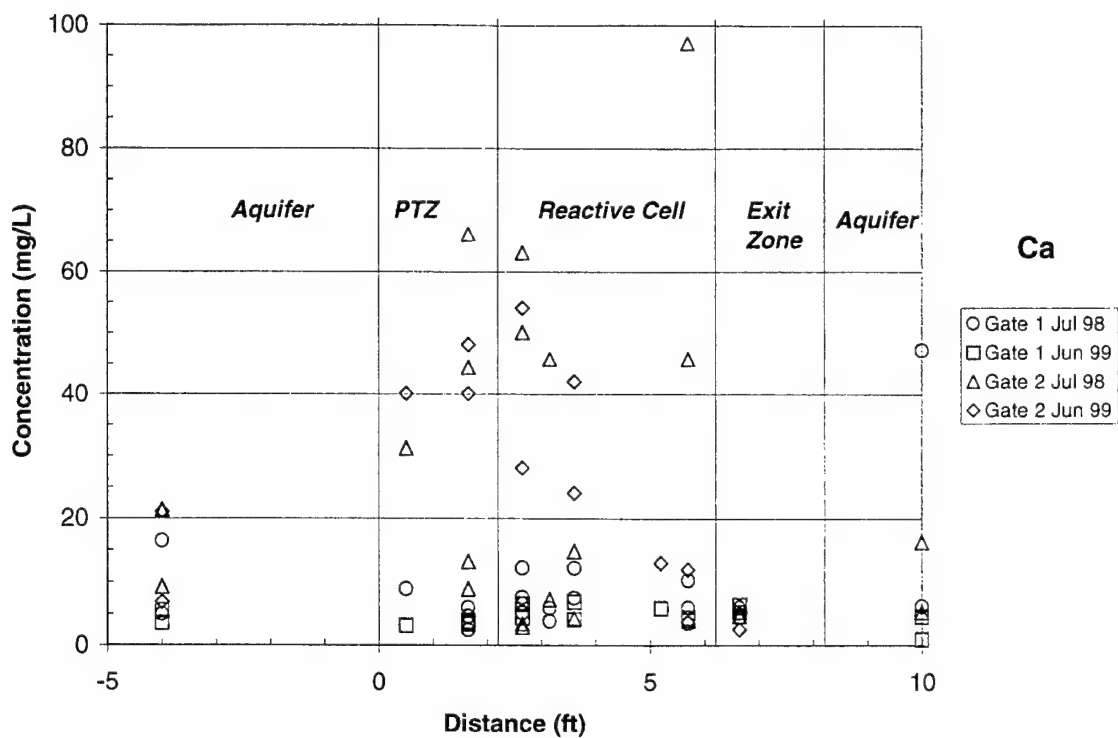


Figure F-7. Calcium Distribution in PRB.

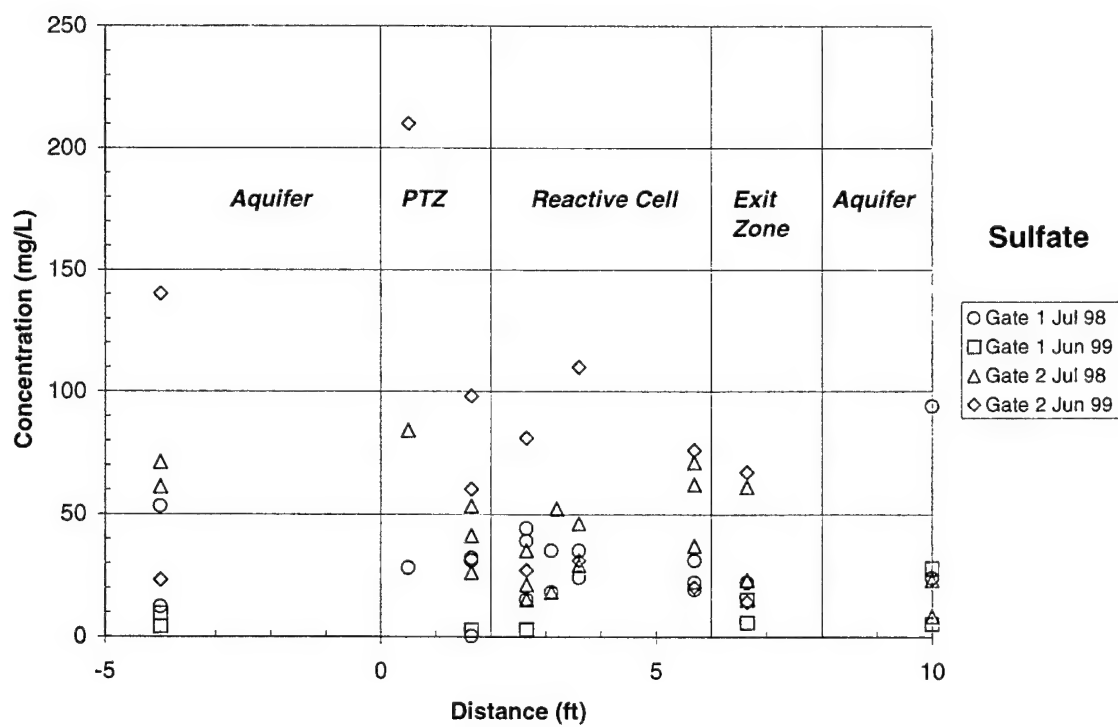


Figure F-8. Sulfate Distribution in PRB.

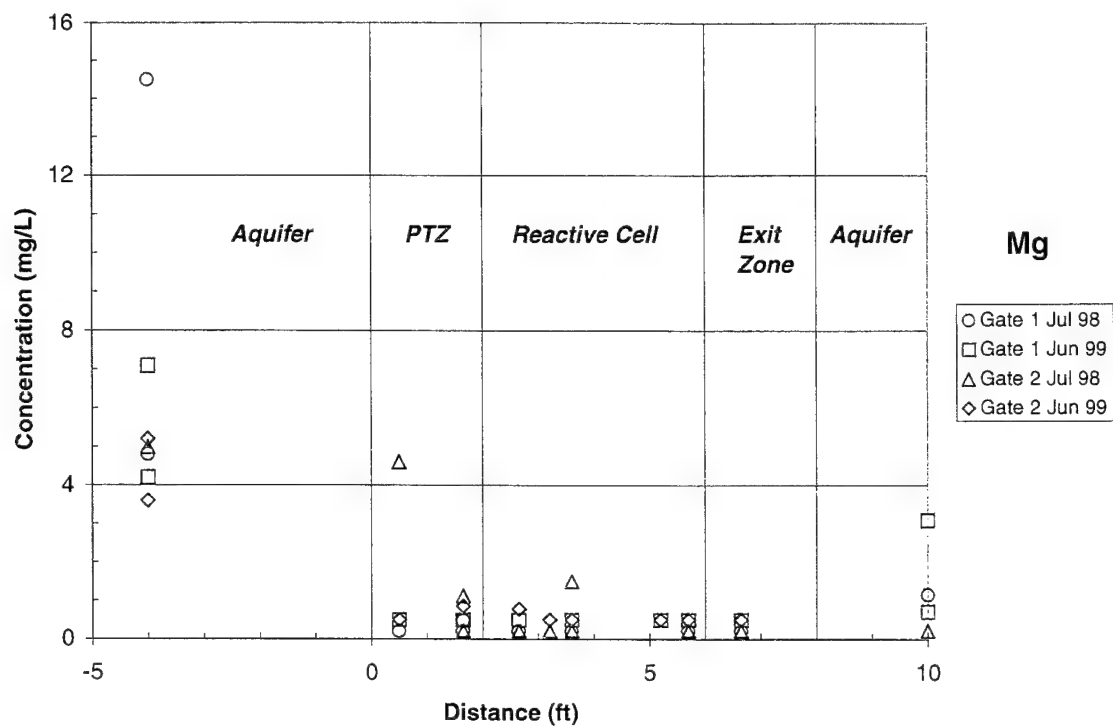


Figure F-9. Magnesium Distribution in PRB.

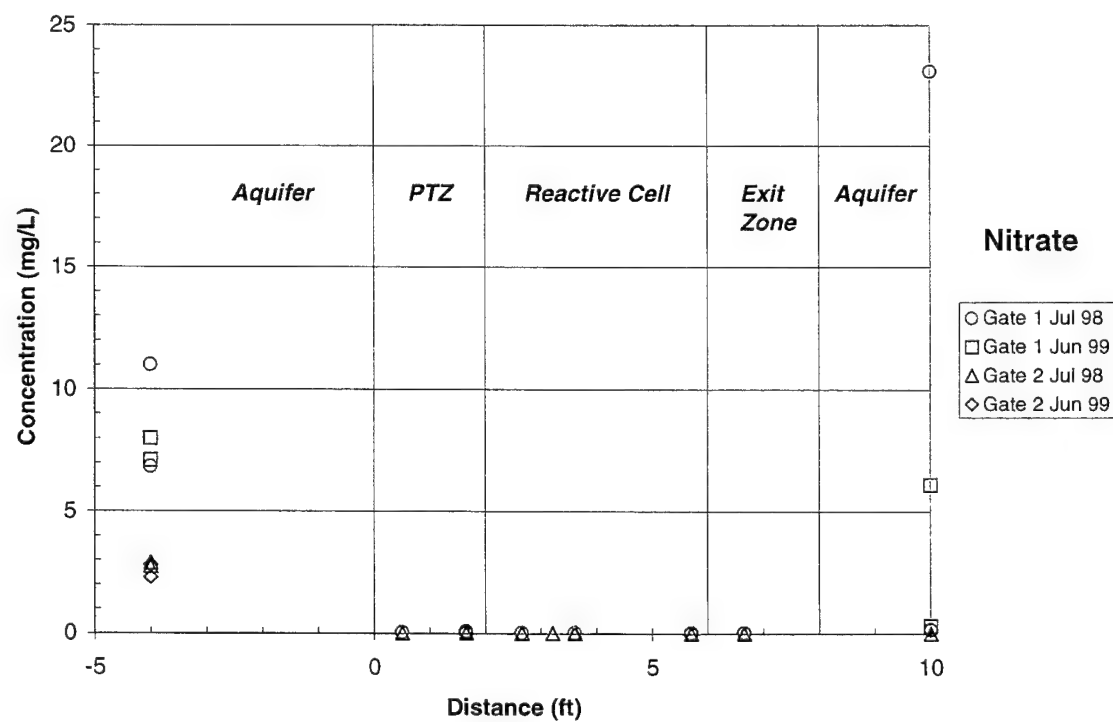


Figure F-10. Nitrate Distribution in PRB.

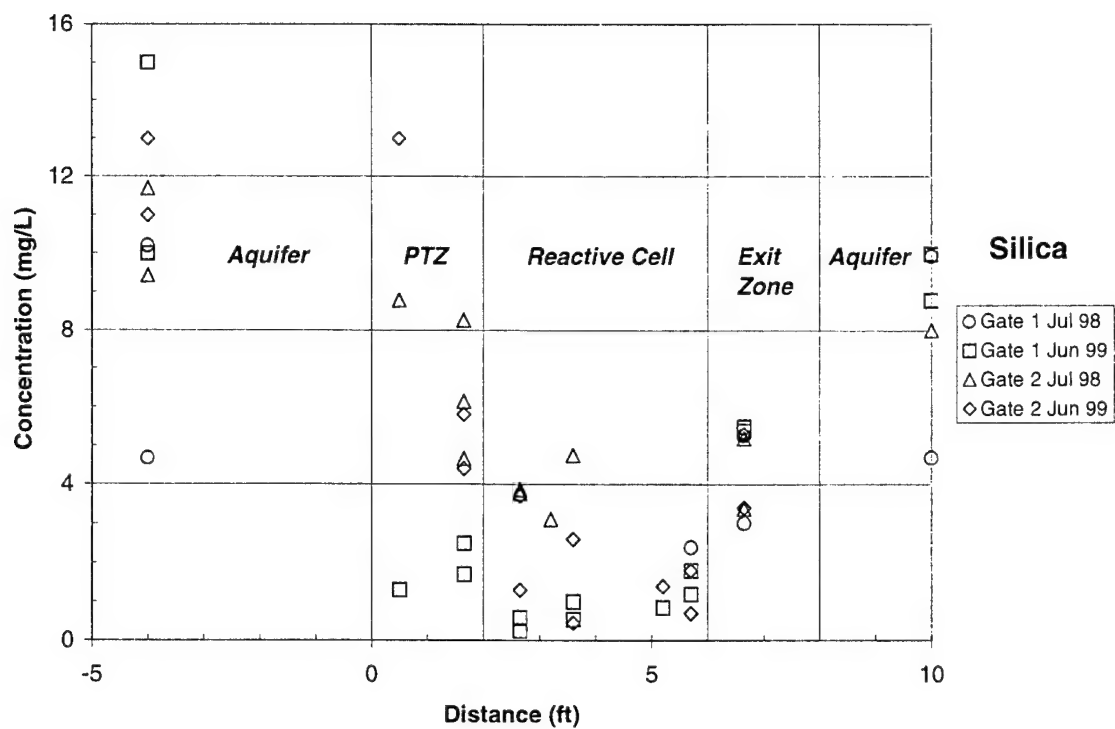
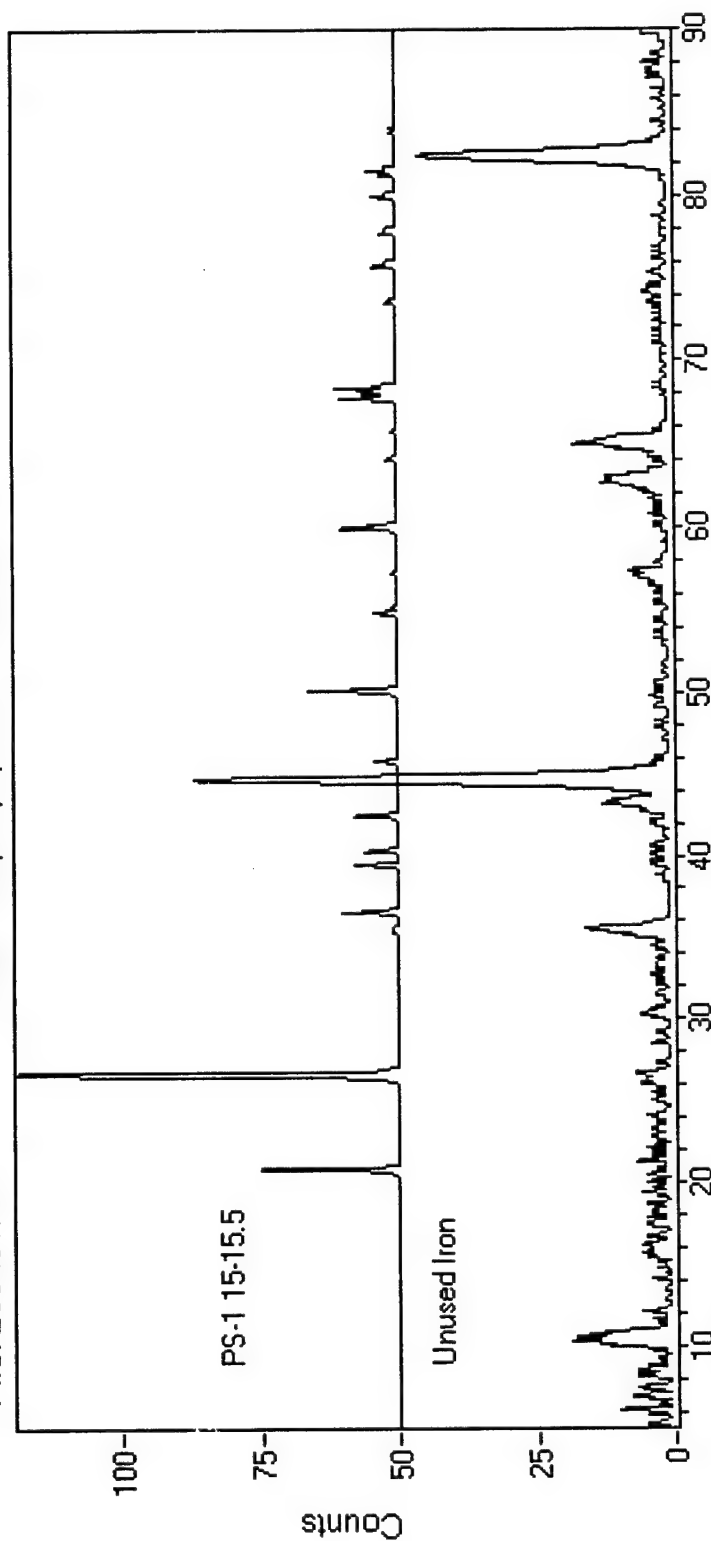


Figure F-11. Dissolved Silica Distribution in PRB.

Appendix F-2

XRD Patterns for Iron Core Samples

ID: UNUSED IRON, 20-JUL-98@08:30
File: Z00491.DIF Scan: 5-90/.02/1/#4251, Anode: CU



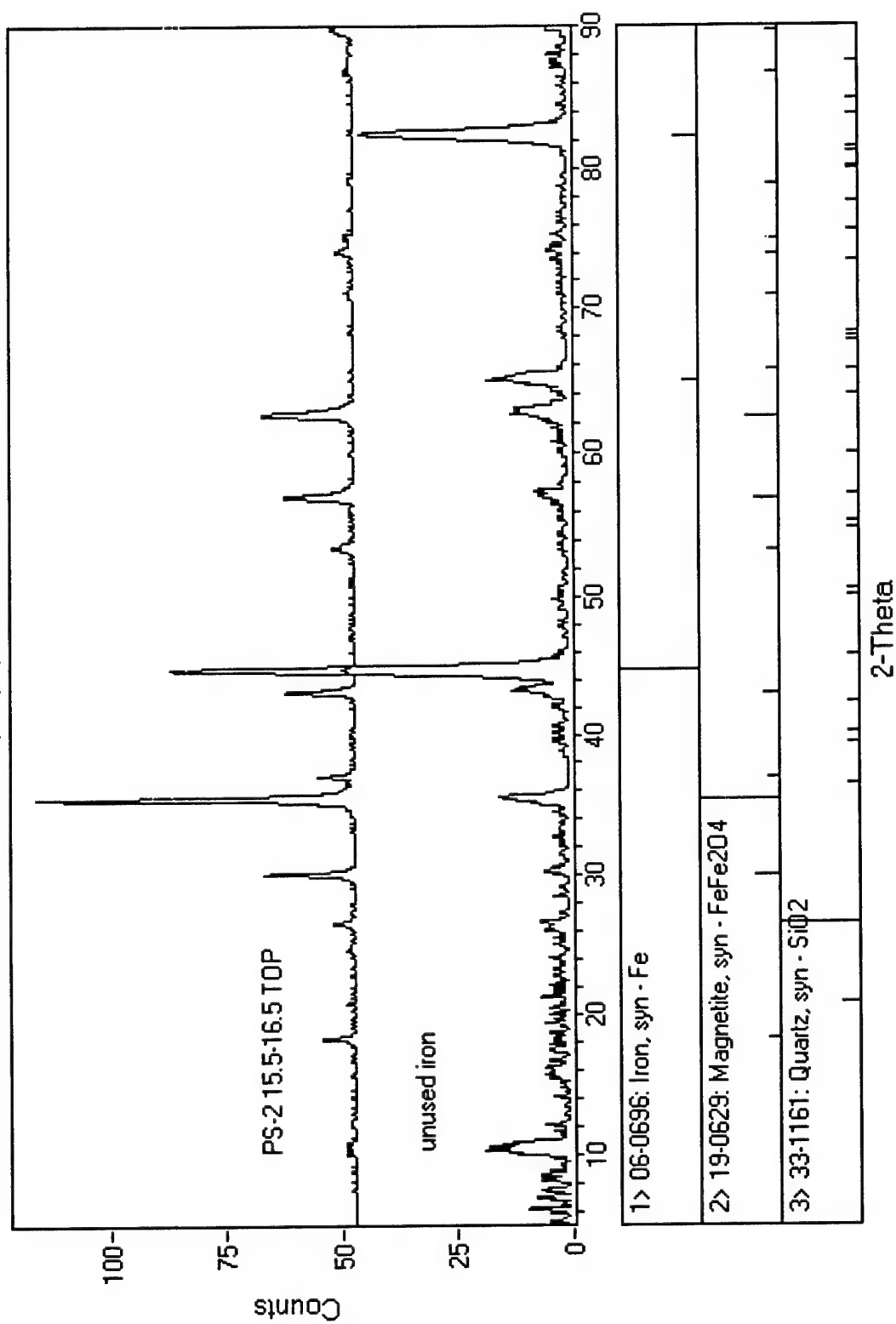
1> 06-0696: Iron, syn - Fe

2> 19-0629: Magnetite, syn - FeFe2O4

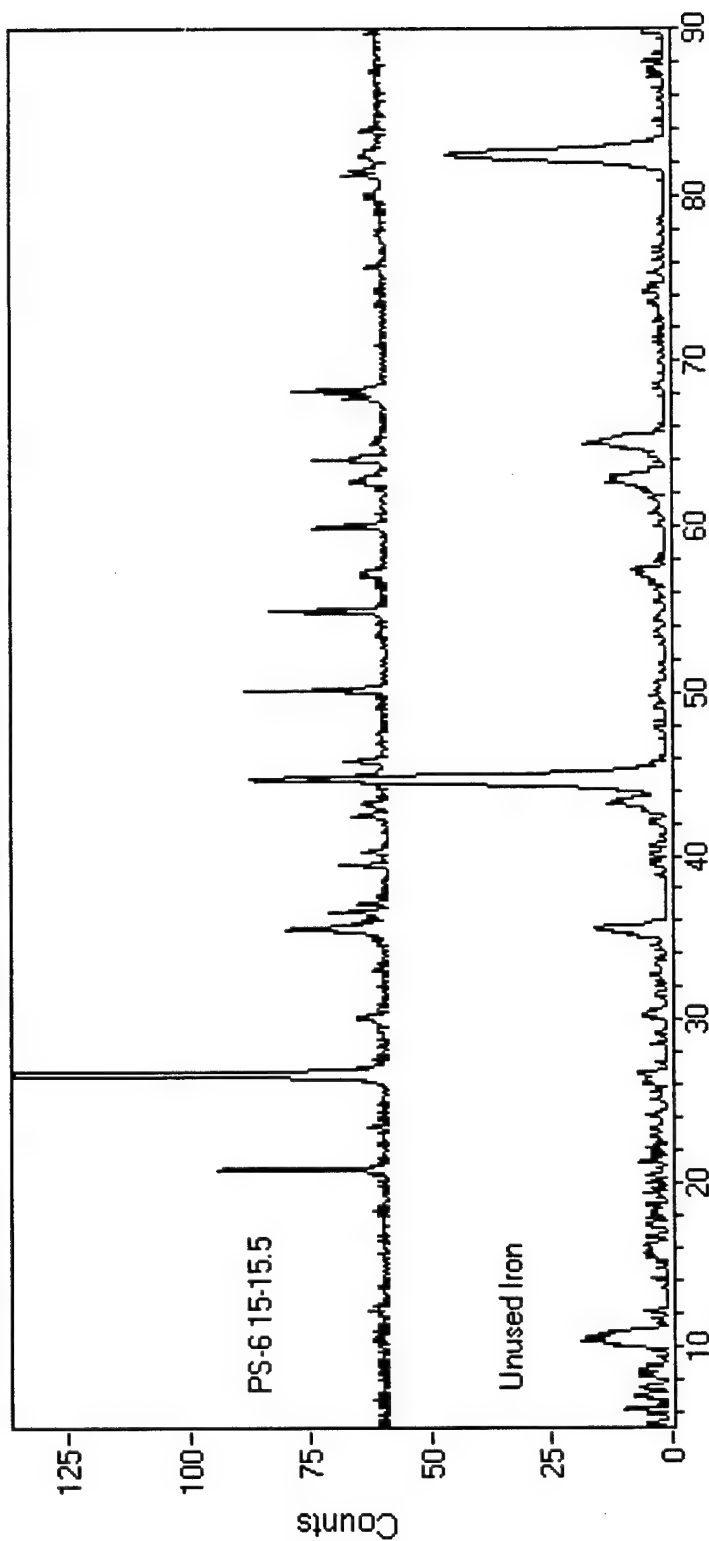
3> 33-1161: Quartz, syn - SiO2

2-Theta

ID: UNUSED IRON, 20-JUL-98@08:30
File: Z00491.DIF Scan: 5-90/02/1/#4251, Anode: CU



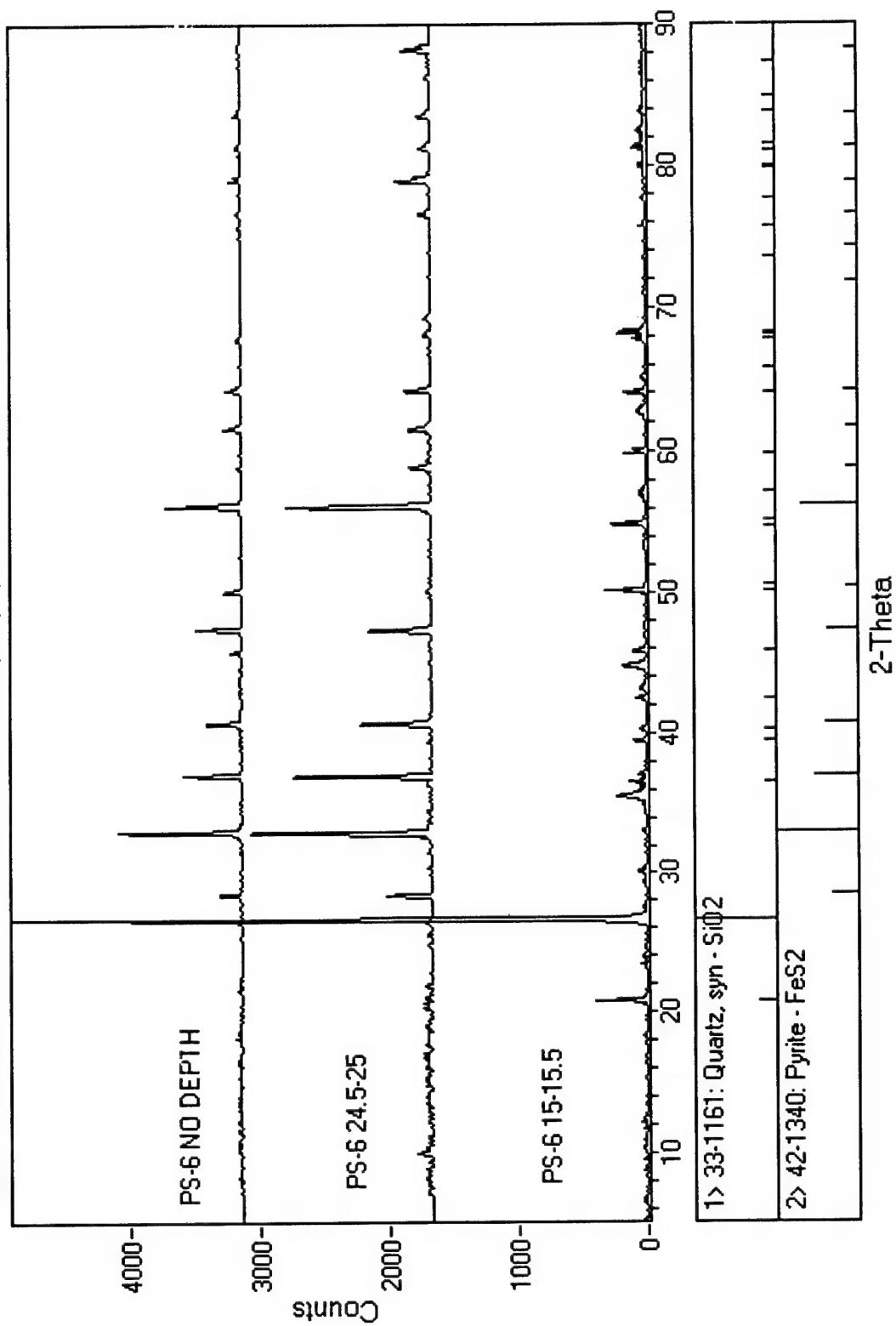
ID: UNUSED IRON, 20-JUL-98@08:30
 File: Z00491.DIF Scan: 5-90/.02/1/#4251, Anode: CU



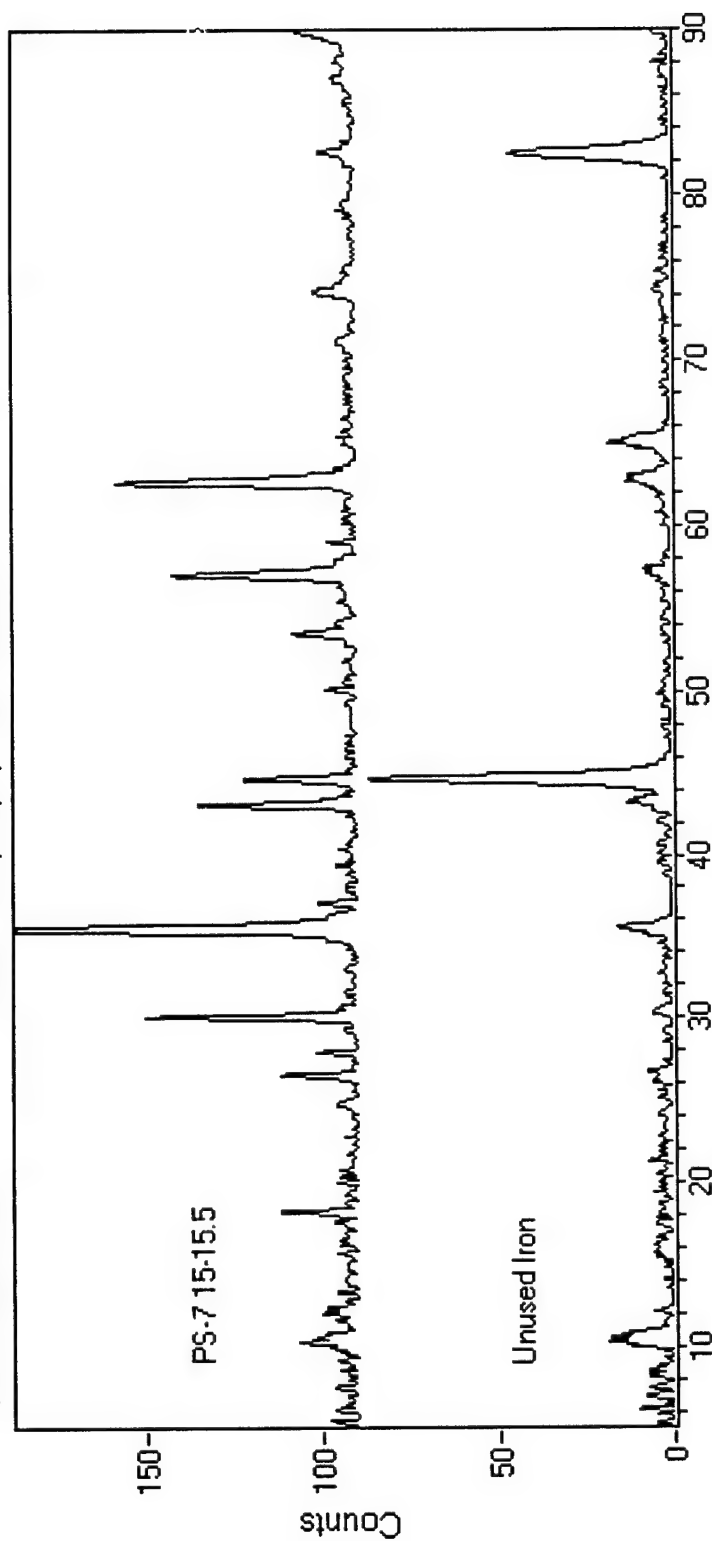
1> 06-0696: Iron, syn - Fe	
2> 42-1340: Pyrite - FeS2	
3> 19-0629: Magnetite, syn - FeFe2O4	

2-Theta

ID: (#13) PS-6 15-15.5, 19-JUL-98@08:55
File: Z00490.DIF Scan: 5.04-90.04/.02/1/#4251, Anode: CU



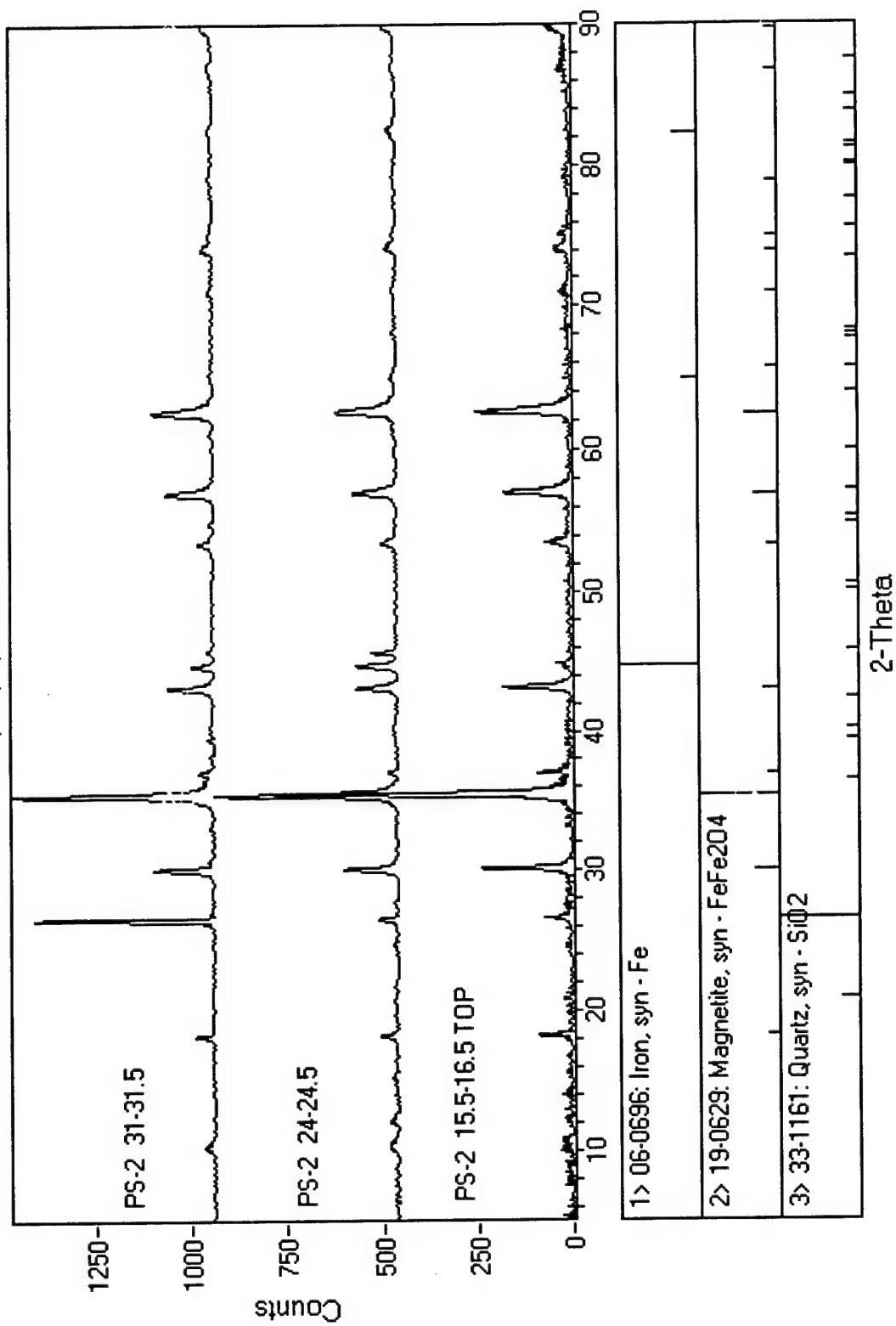
ID: UNUSED IRON, 20-JUL-98@08:30
File: Z00491.DIF Scan: 5-90/.02/1/#4251, Anode: CU



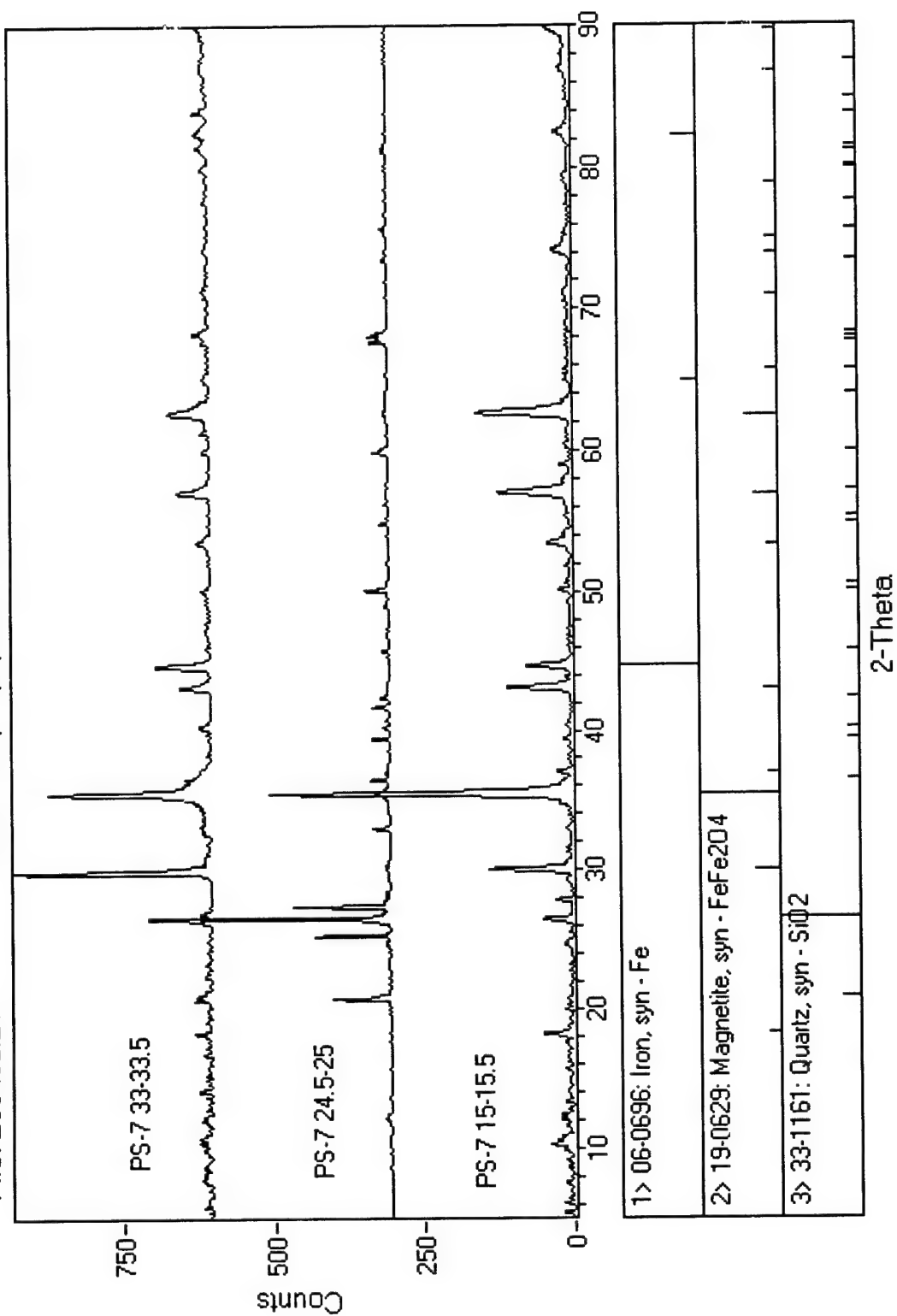
1> 06-0696: Iron, syn - Fe	
2> 19-0629: Magnetite, syn - FeFe2O4	
3> 33-1161: Quartz, syn - SiO2	

2-Theta

ID: (#1) PS-2 15.5-16.5 TOP, 15-JUL-98@11:23
File: Z00479.DIF Scan: 5-90/02/1/#4251, Anode: CU

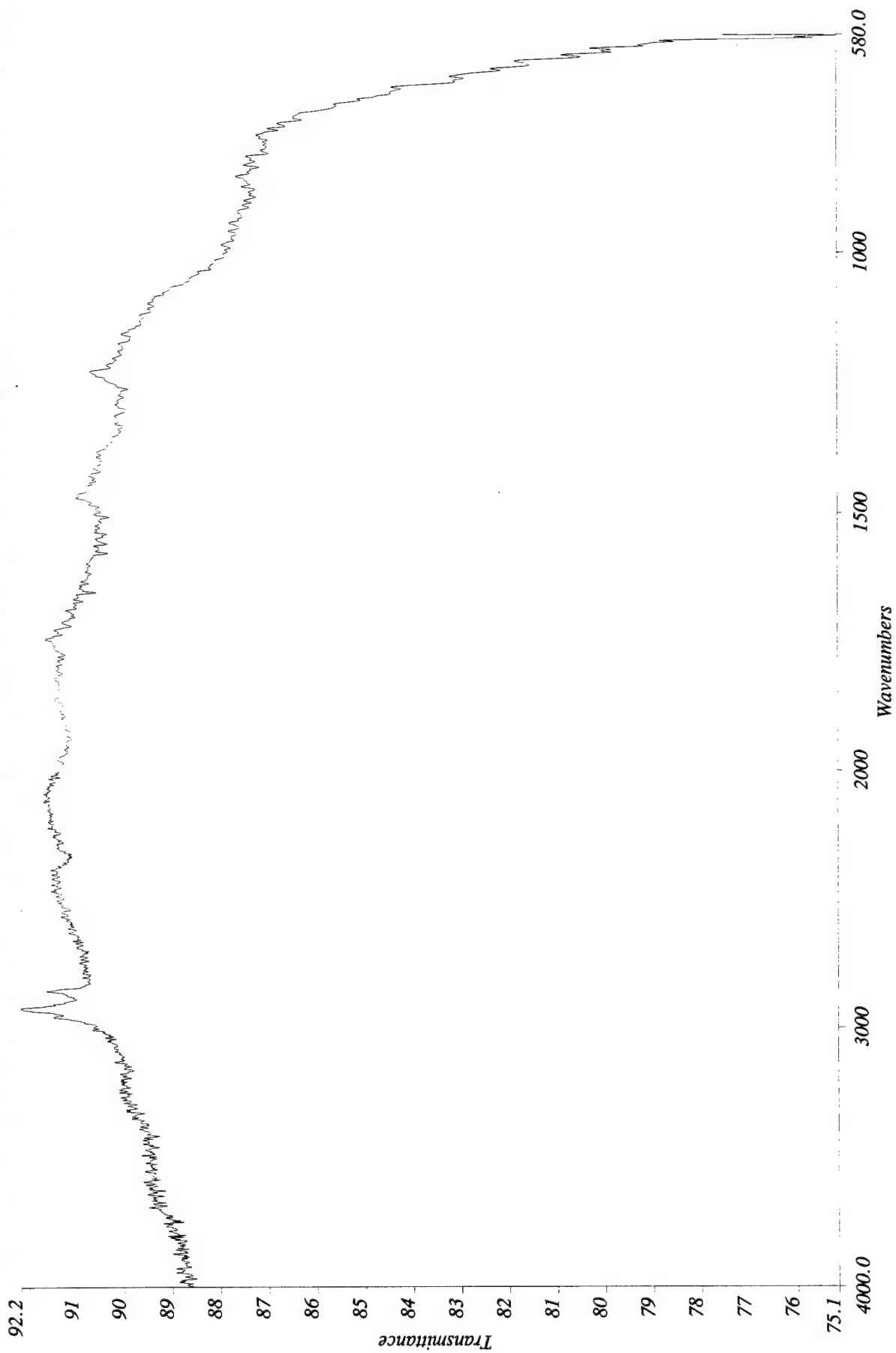


ID: (#4) PS-7 15-15.5, 16-JUL-98@14:35
File: Z00482.DIF Scan: 5-90/.02/1/#4251, Anode: CU



Appendix F-3

FTIR Spectra for Iron Core Samples



Spectrum Name: a:\bat285.sp

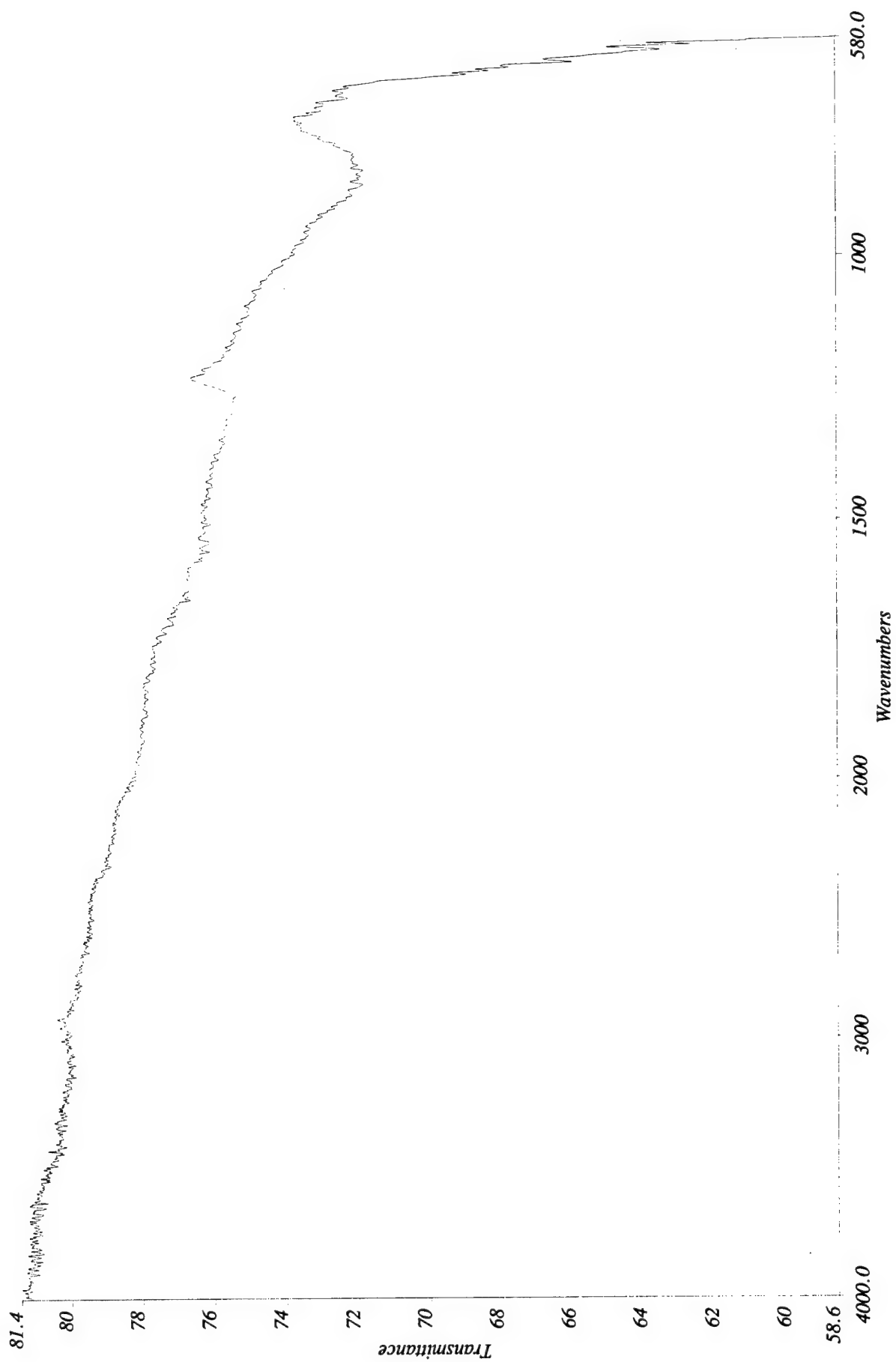
Description: Unused iron

Date Created: Sat Oct 02 11:23:17 1999

Resolution: 4 cm-1

Accumulations: 64

Molecular Microspectroscopy Laboratory



Spectrum Name: a:\bat286.sp

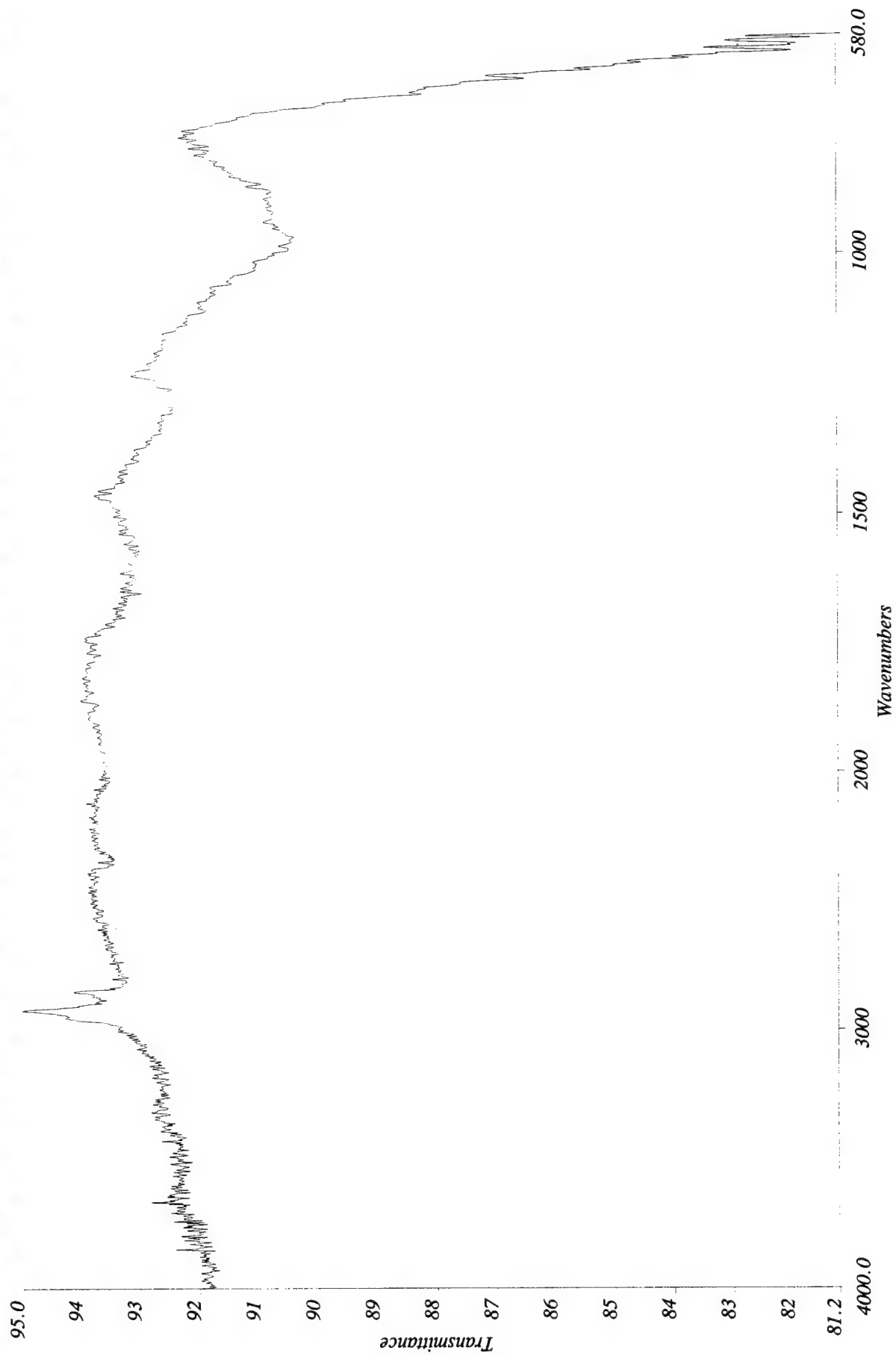
Resolution: 4 cm-1

Description: Unused iron

Accumulations: 64

Date Created: Sat Oct 02 11:21:14 1999

Molecular Microspectroscopy Laboratory



Spectrum Name: A:\BAT284.SP

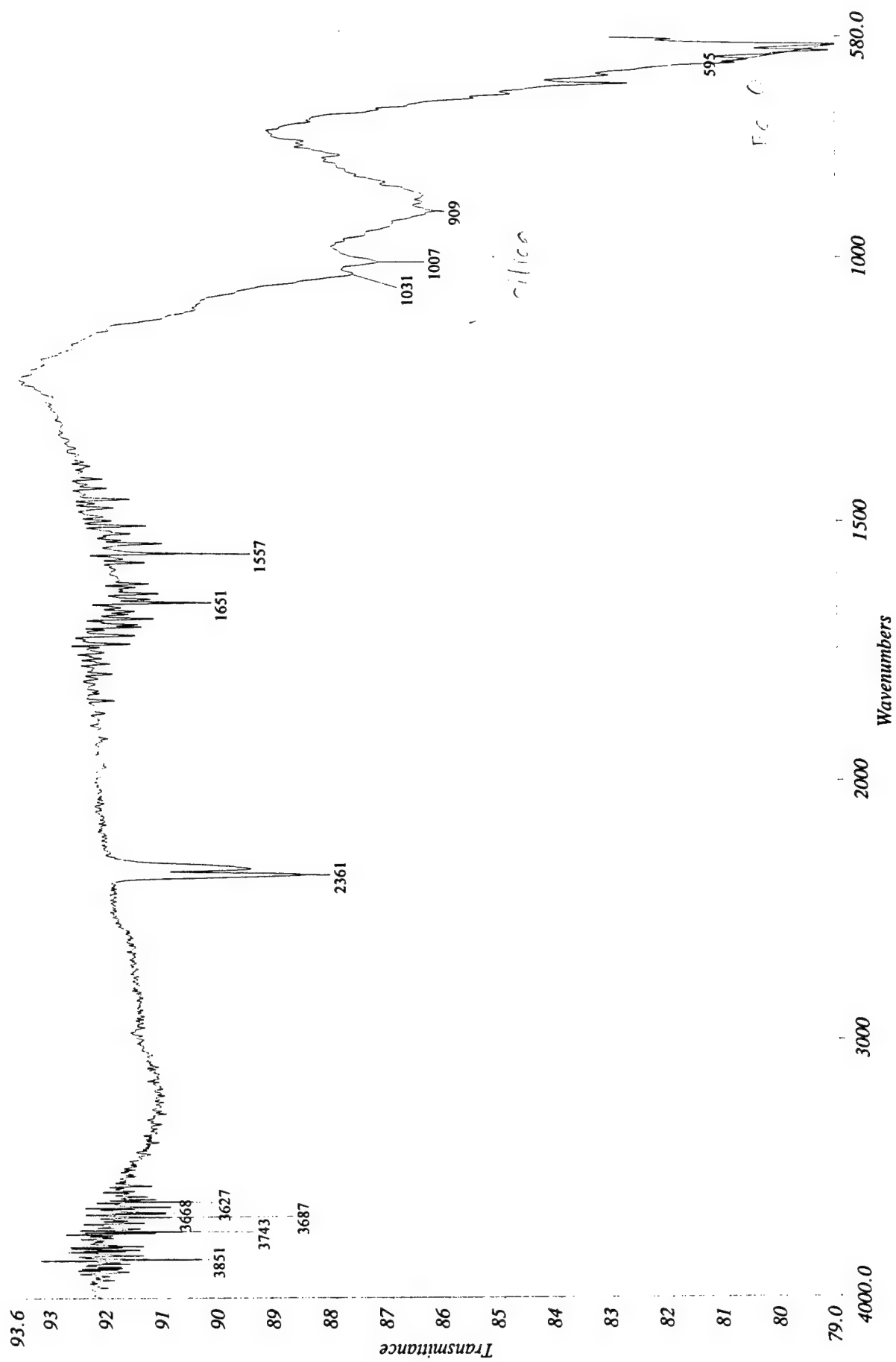
Resolution: 4 cm-1

Description: Unused iron

Accumulations: 64

Date Created: Sat Oct 02 11:26:42 1999

Molecular Microspectroscopy Laboratory



Spectrum Name: A:\BAT251.SP

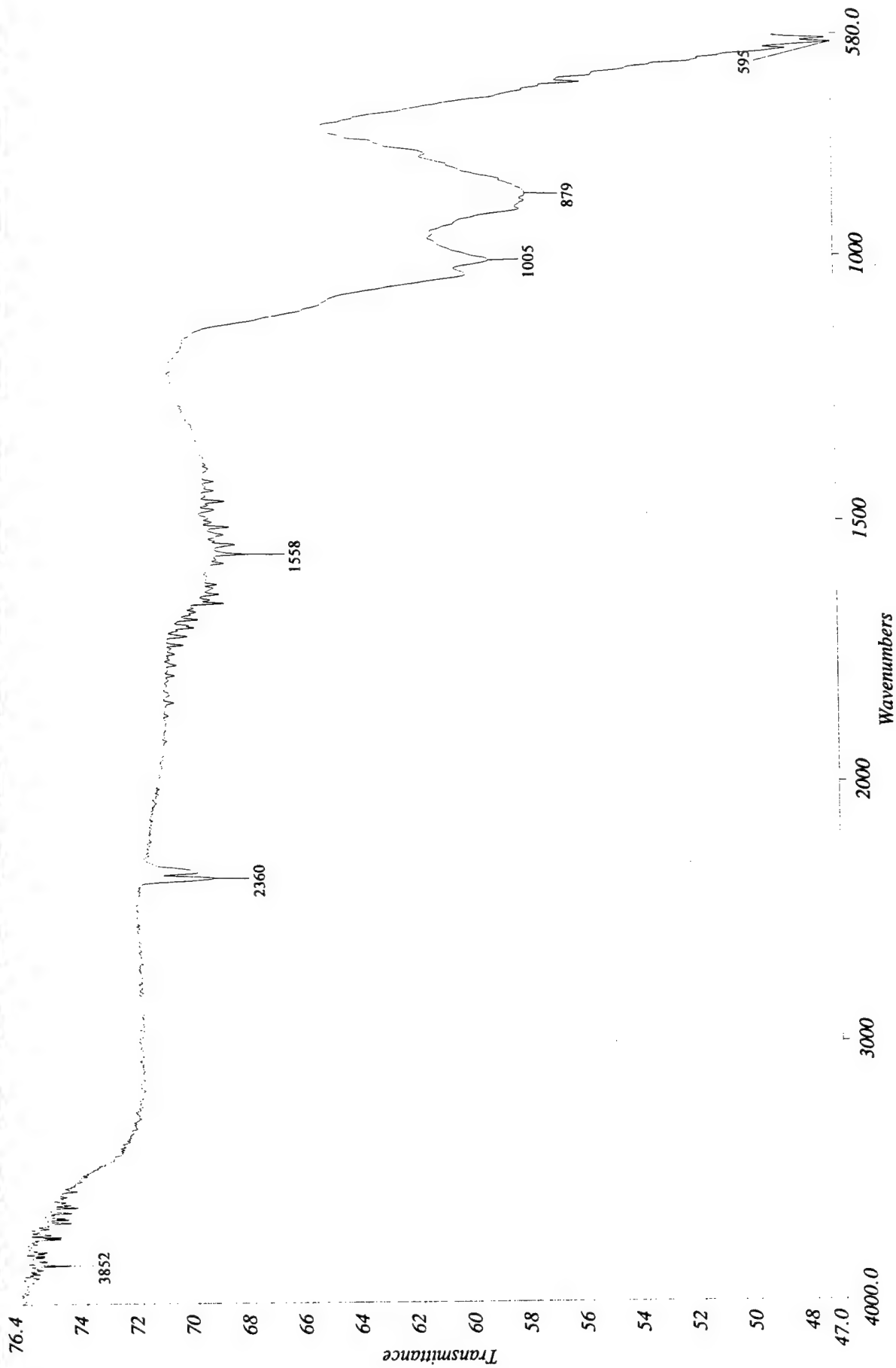
Description: Spectrum At 2588,1157,1252 Micrometers Aperture: 100,100

Resolution: 4 cm-1

Accumulations: 32

Date Created: Sat Sep 11 09:53:54 1999

Molecular Microspectroscopy Laboratory



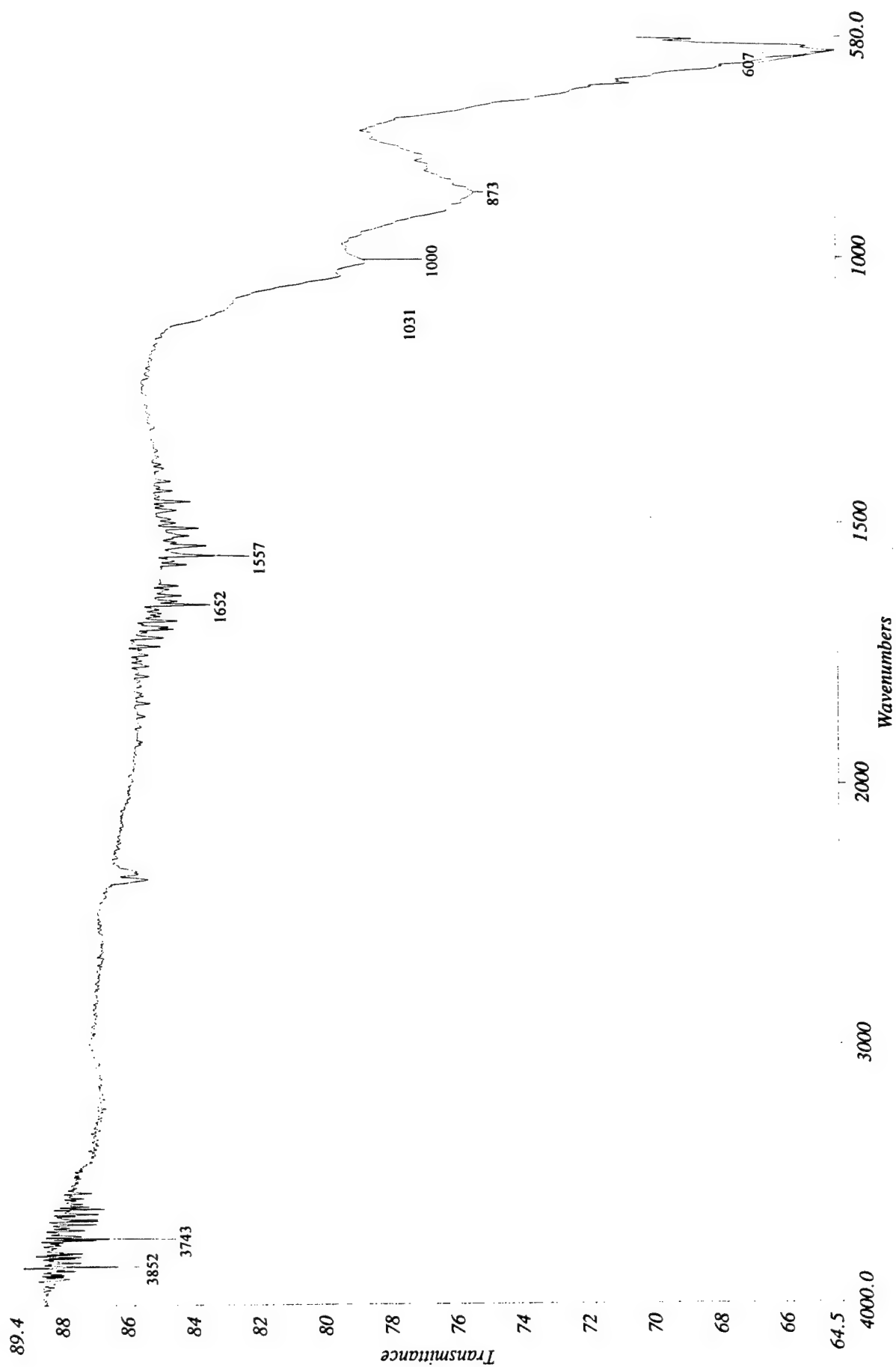
Resolution: 4 cm-1

Accumulations: 32

Spectrum Name: A:\BAT252.SP
Description: Spectrum At 8494,972,1196 Micrometers Aperture: 100,100

Molecular Microspectroscopy Laboratory

Date Created: Sat Sep 11 09:55:15 1999



Spectrum Name: A:\BAT253.SP

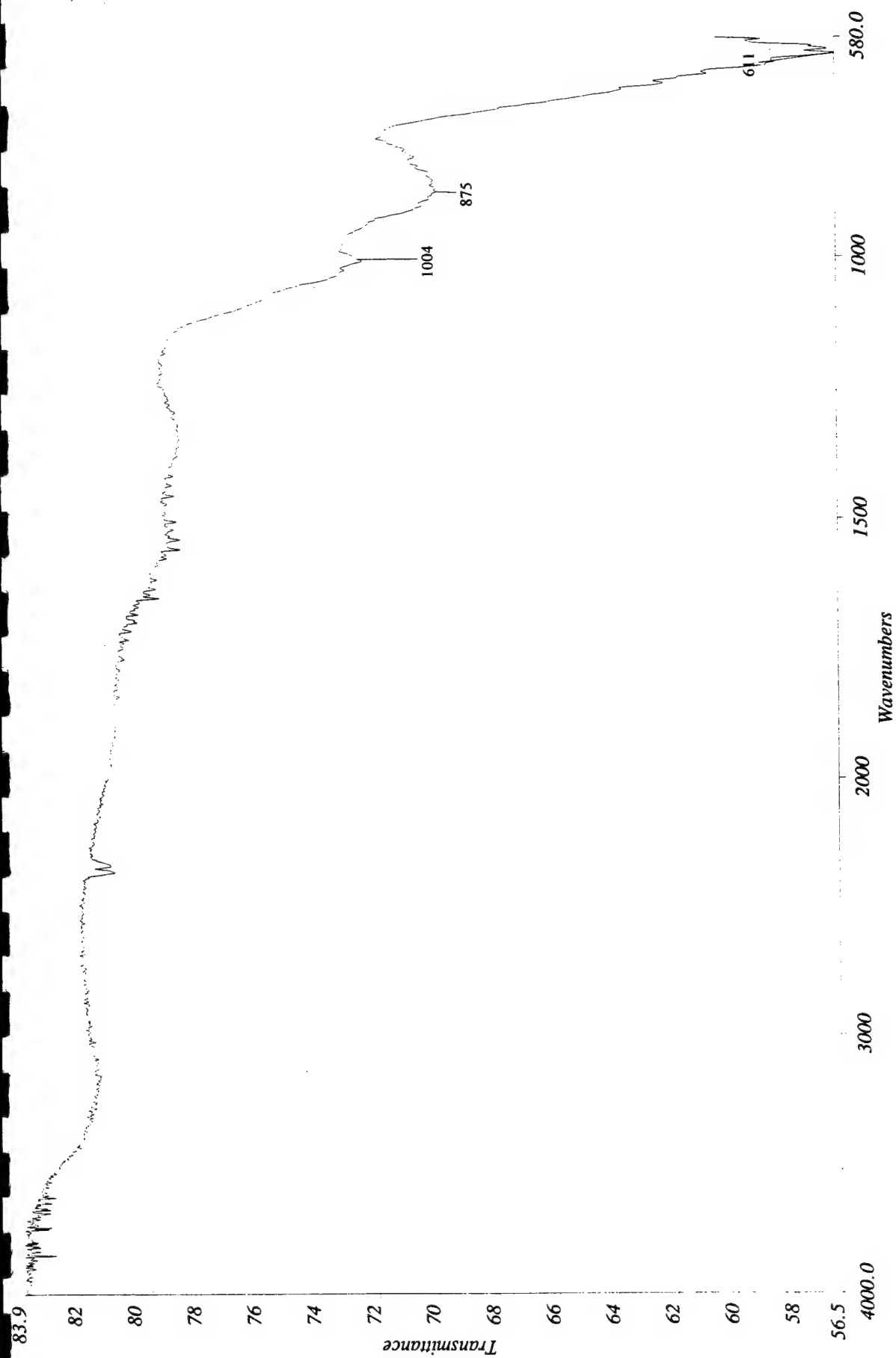
Description: Spectrum At 8747,406,1111 Micrometers Aperture: 100,100

Resolution: 4 cm-1

Accumulations: 32

Date Created: Sat Sep 11 09:56:28 1999

Molecular Microspectroscopy Laboratory



Spectrum Name: A:\BAT254.SP

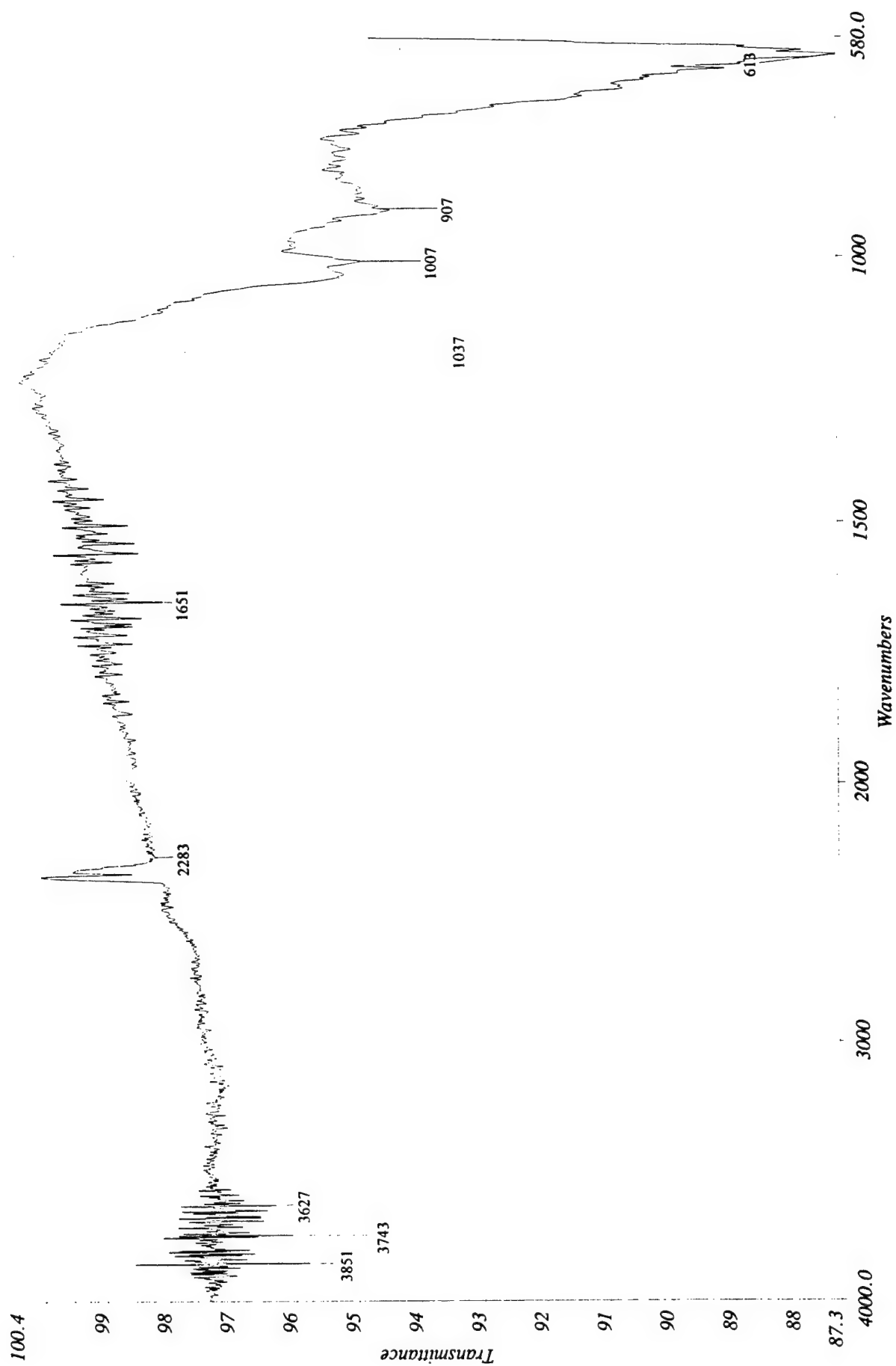
Description: Spectrum At 4900,1973,1448 Micrometers □ Aperture: 100,100

Resolution: 4 cm-1

Accumulations: 32

Date Created: Sat Sep 11 10:06:48 1999

Molecular Microspectroscopy Laboratory



Spectrum Name: A:\BAT255.SP

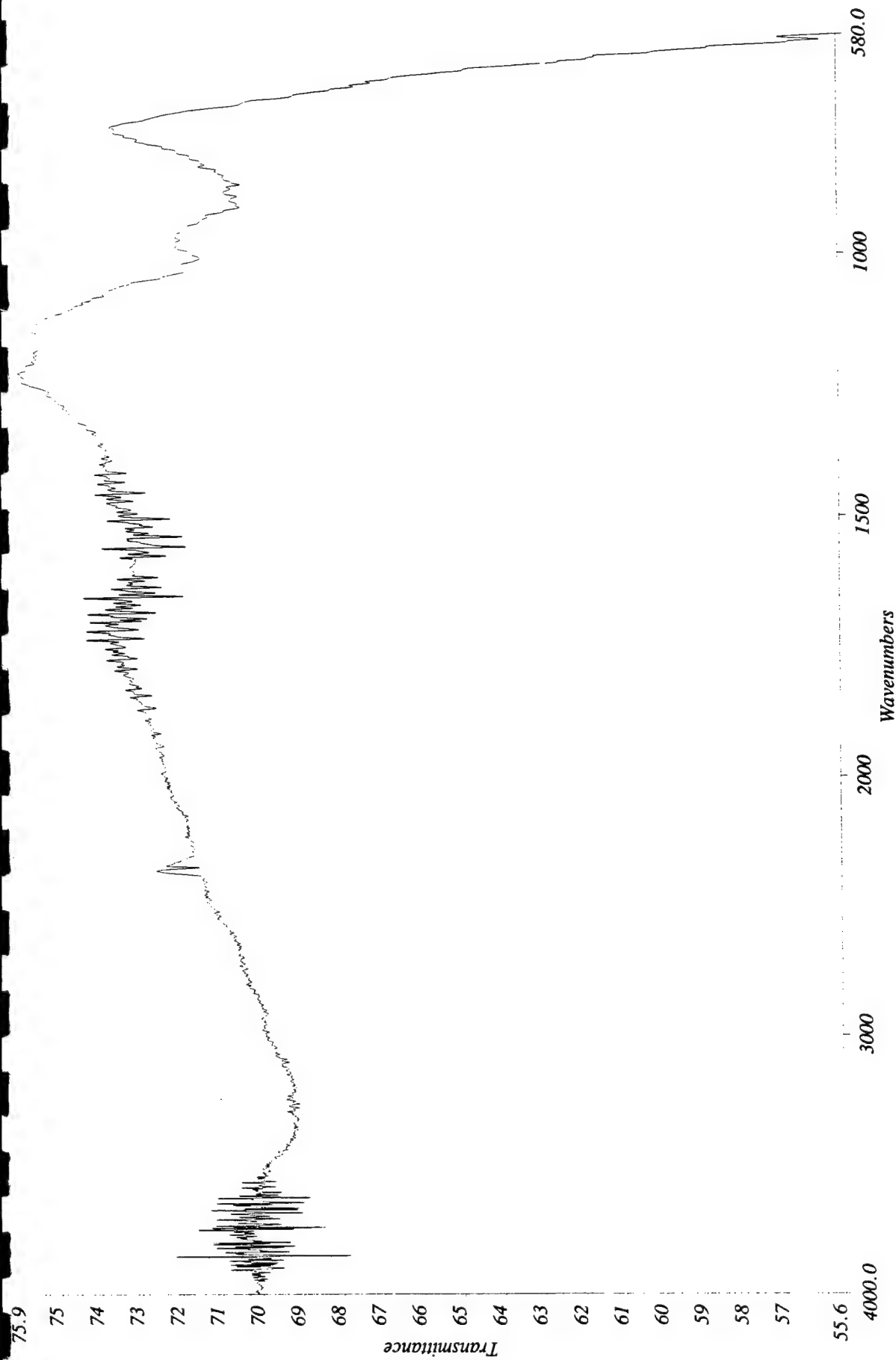
Description: Spectrum At 930,1187,1426 Micrometers Aperture: 100,100

Resolution: 4 cm⁻¹

Accumulations: 32

Date Created: Sat Sep 11 10:03:41 1999

Molecular Microspectroscopy Laboratory

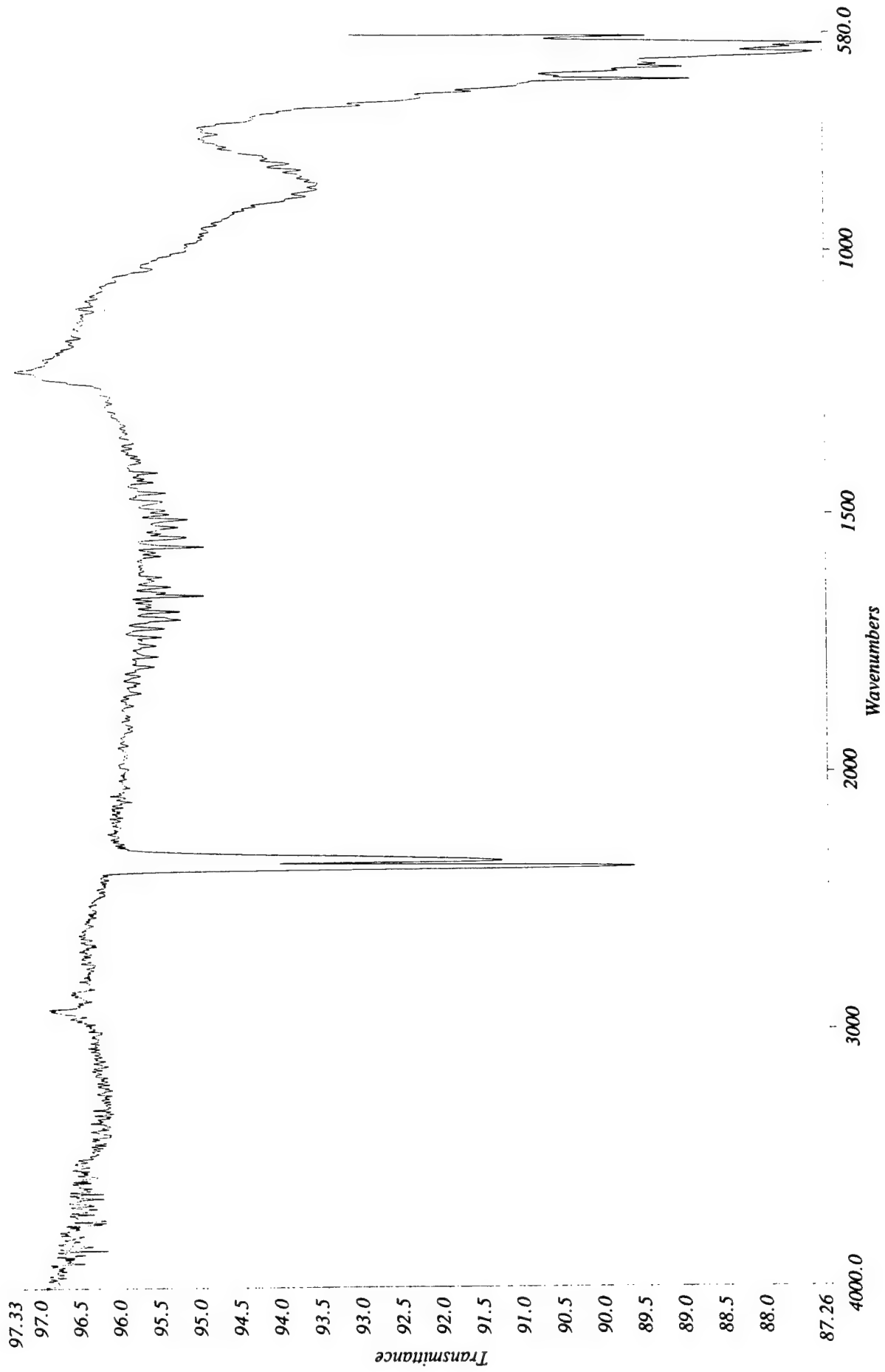


Resolution: 4 cm-1
Accumulations: 32

Spectrum Name: A:\BAT256.SP
Description: Spectrum At 9633,1778,1424 Micrometers□Aperture: 100,100

Molecular Microspectroscopy Laboratory

Date Created: Sat Sep 11 10:05:21 1999



Spectrum Name: A:\BAT257.SP

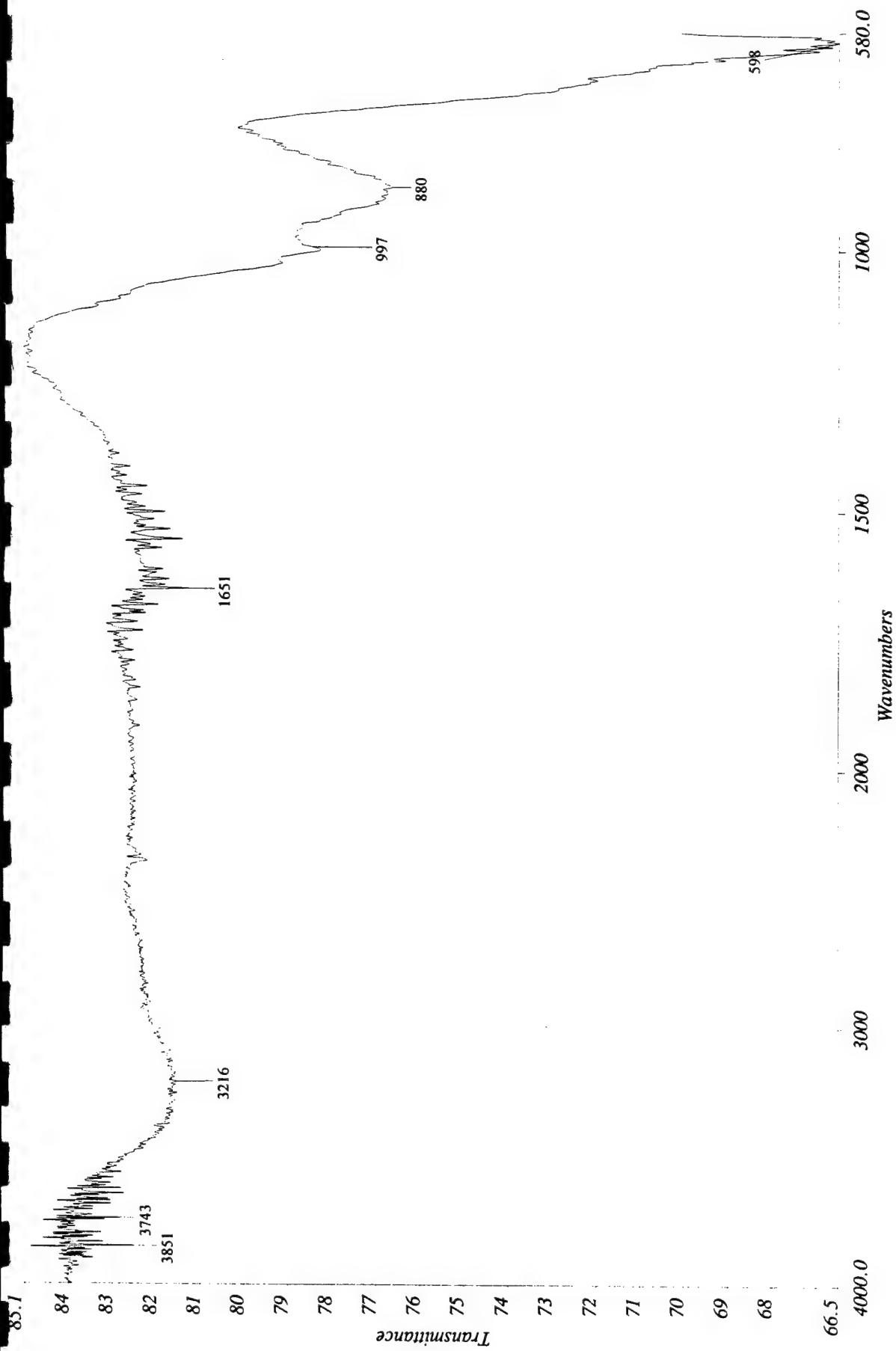
Resolution: 4 cm-1

Description: Spectrum At 9153,2416,1414 Micrometers □ Aperture: 100,100

Accumulations: 32

Date Created: Sat Sep 11 10:22:03 1999

Molecular Microspectroscopy Laboratory



Spectrum Name: A:\BAT258.SP

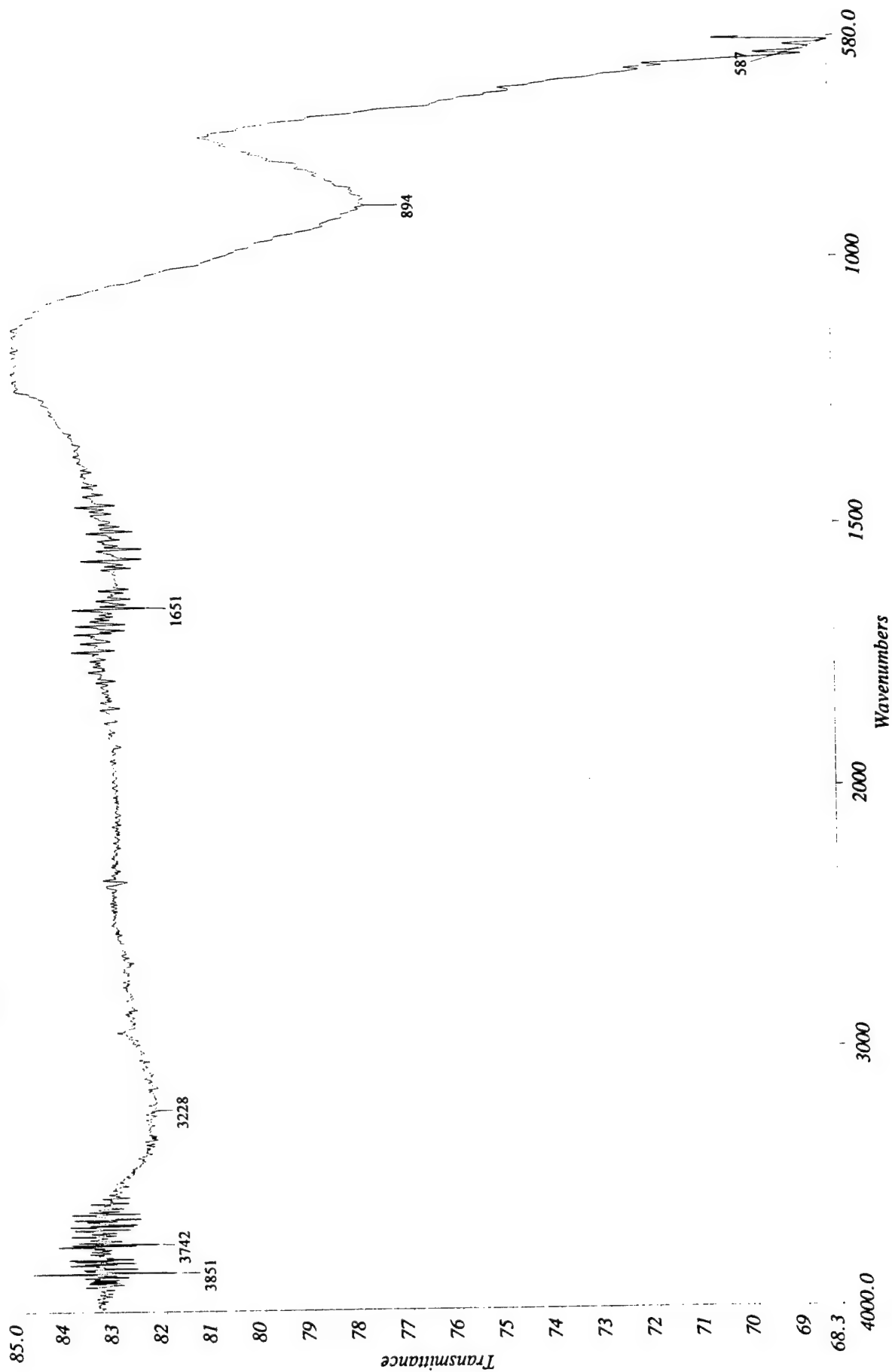
Resolution: 4 cm-1

Description: Spectrum At 10359,2102,1281 MicrometersAperture: 100,100

Accumulations: 32

Date Created: Sat Sep 11 10:20:17 1999

Molecular Microspectroscopy Laboratory



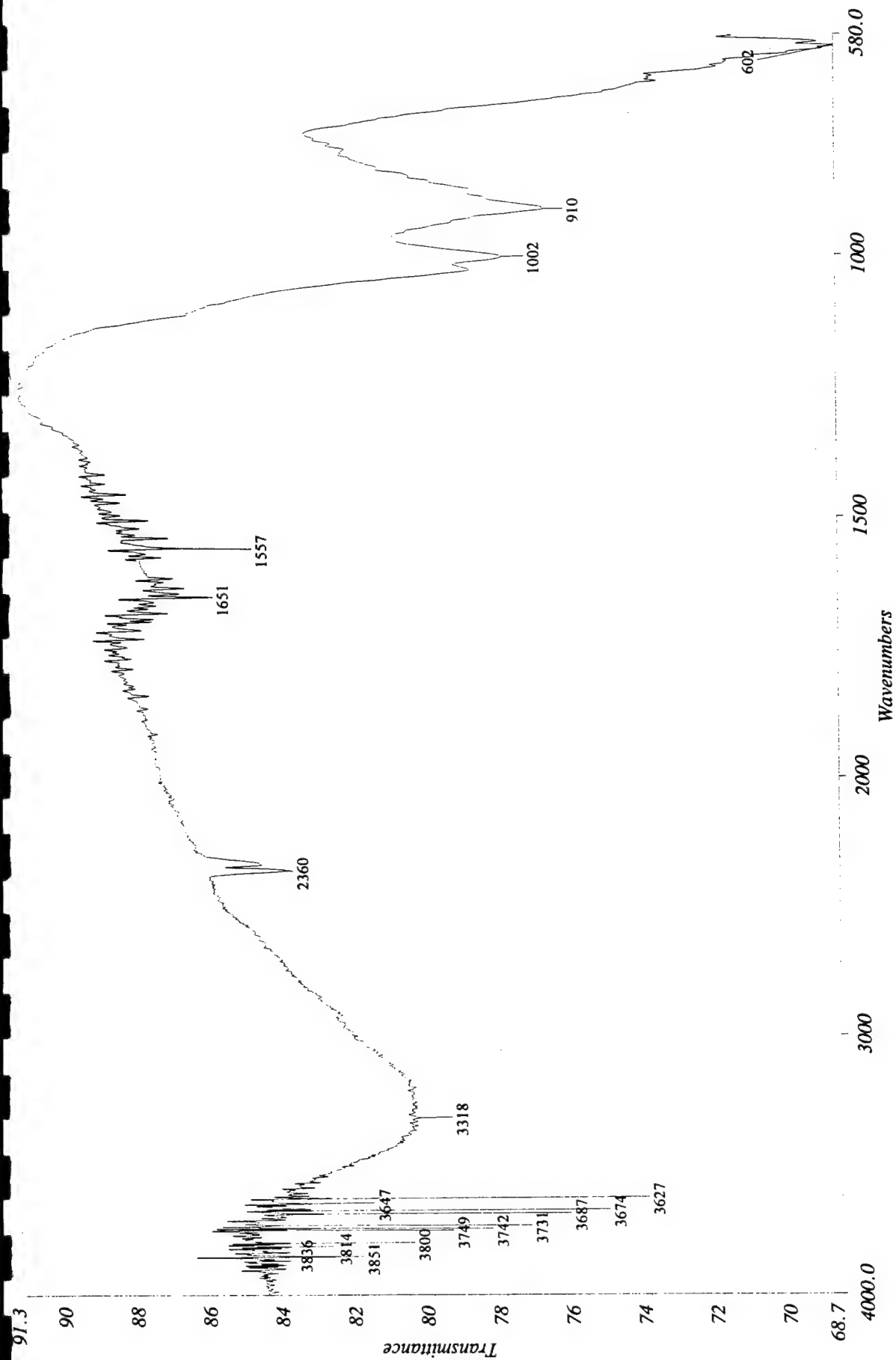
Resolution: 4 cm-1

Accumulations: 32

Spectrum Name: A:\BAT259.SP
Description: Spectrum At -1750,2327,1492 Micrometers □ Aperture: 100,100

Molecular Microspectroscopy Laboratory

Date Created: Sat Sep 11 10:16:33 1999



Spectrum Name: A:\BAT260.SP

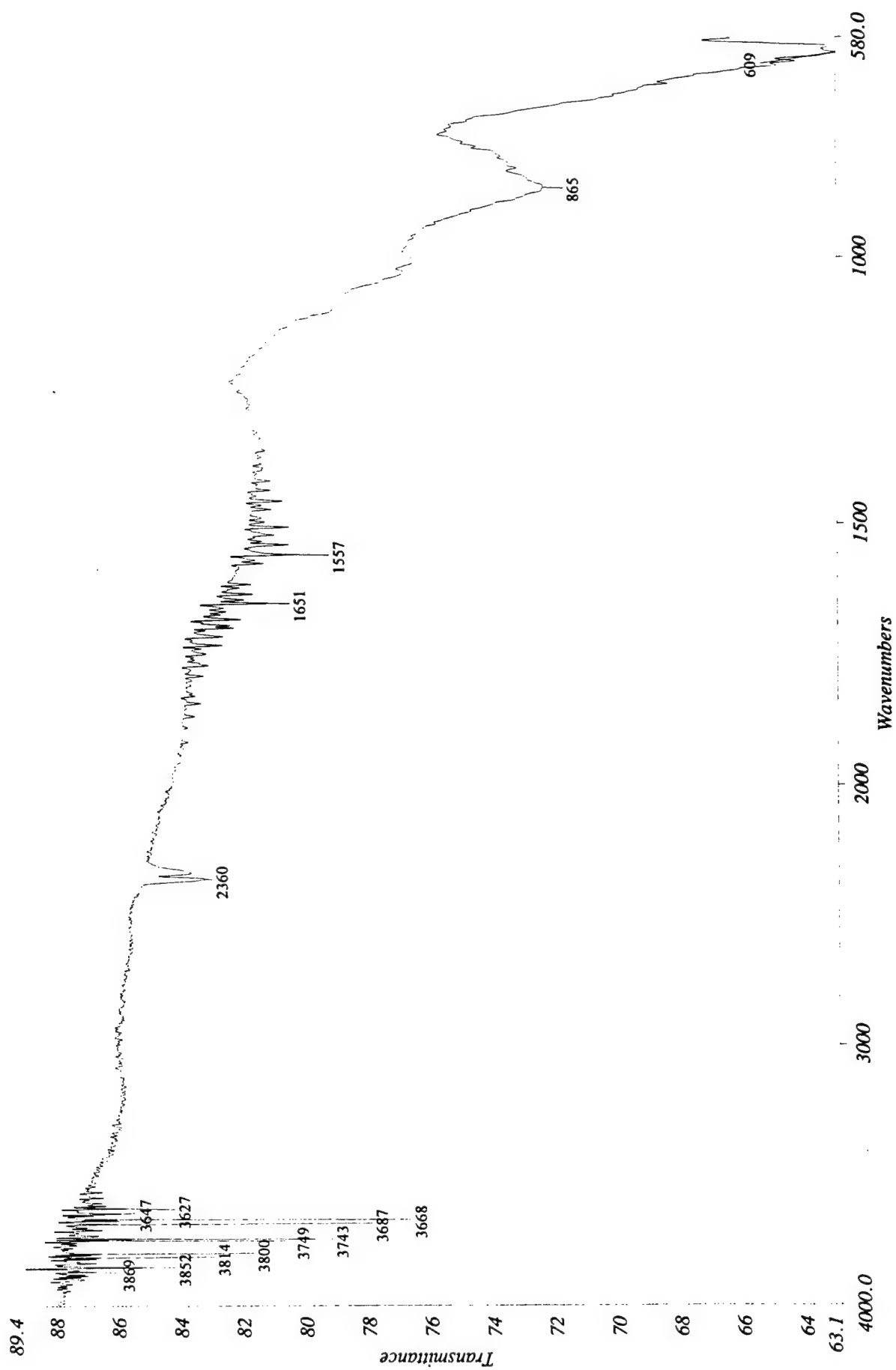
Description: Spectrum At 8442,1668,1223 MicrometersAperture: 100,100

Resolution: 4 cm-1

Accumulations: 32

Date Created: Sat Sep 11 09:38:07 1999

Molecular Microspectroscopy Laboratory



Spectrum Name: A:\BAT261.SP

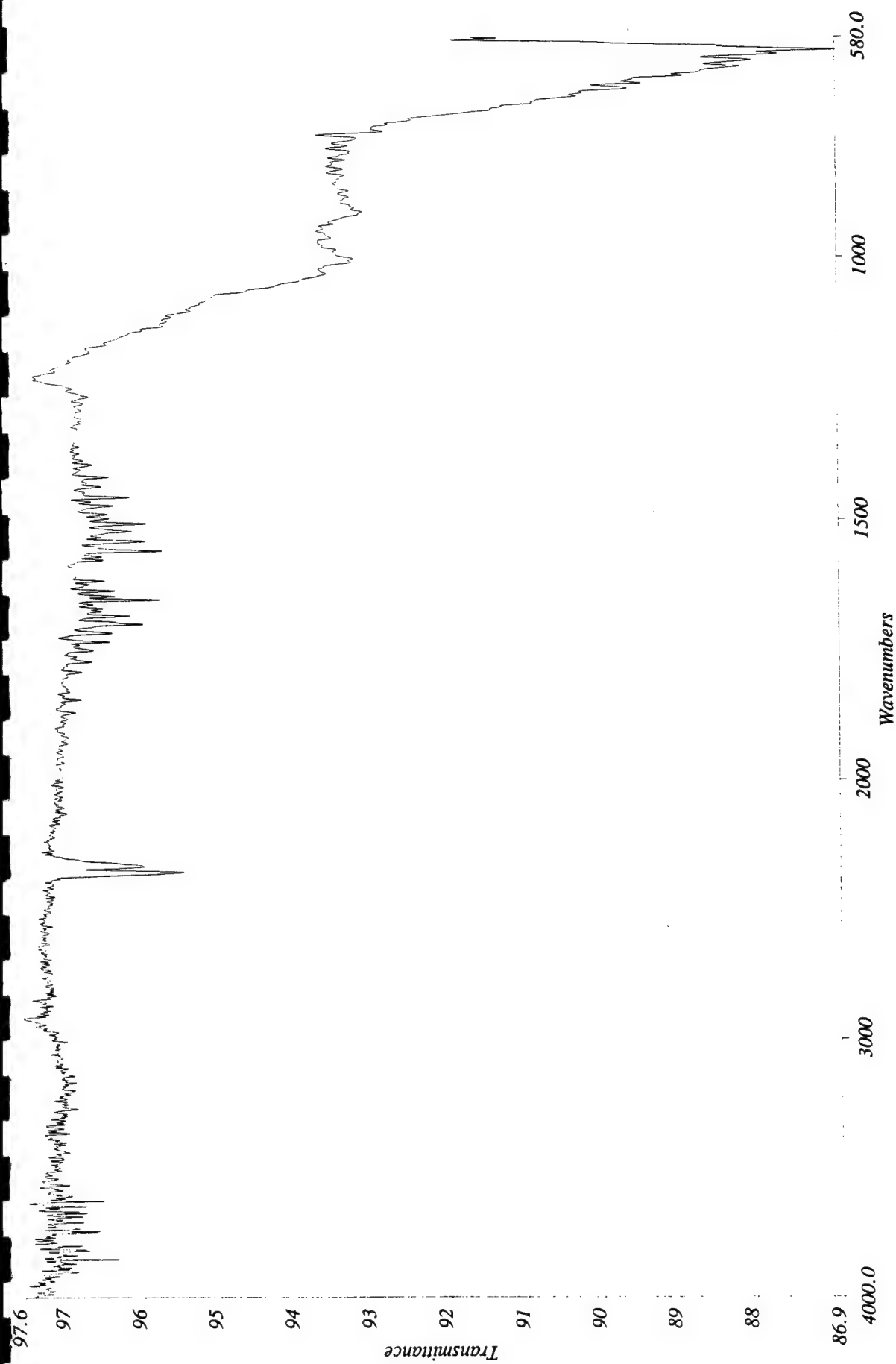
Resolution: 4 cm-1

Description: Spectrum At 1931,1241,1440 Micrometers Aperture: 100,100

Accumulations: 32

Date Created: Sat Sep 11 09:34:44 1999

Molecular Microspectroscopy Laboratory



Spectrum Name: A:\BAT262.SP

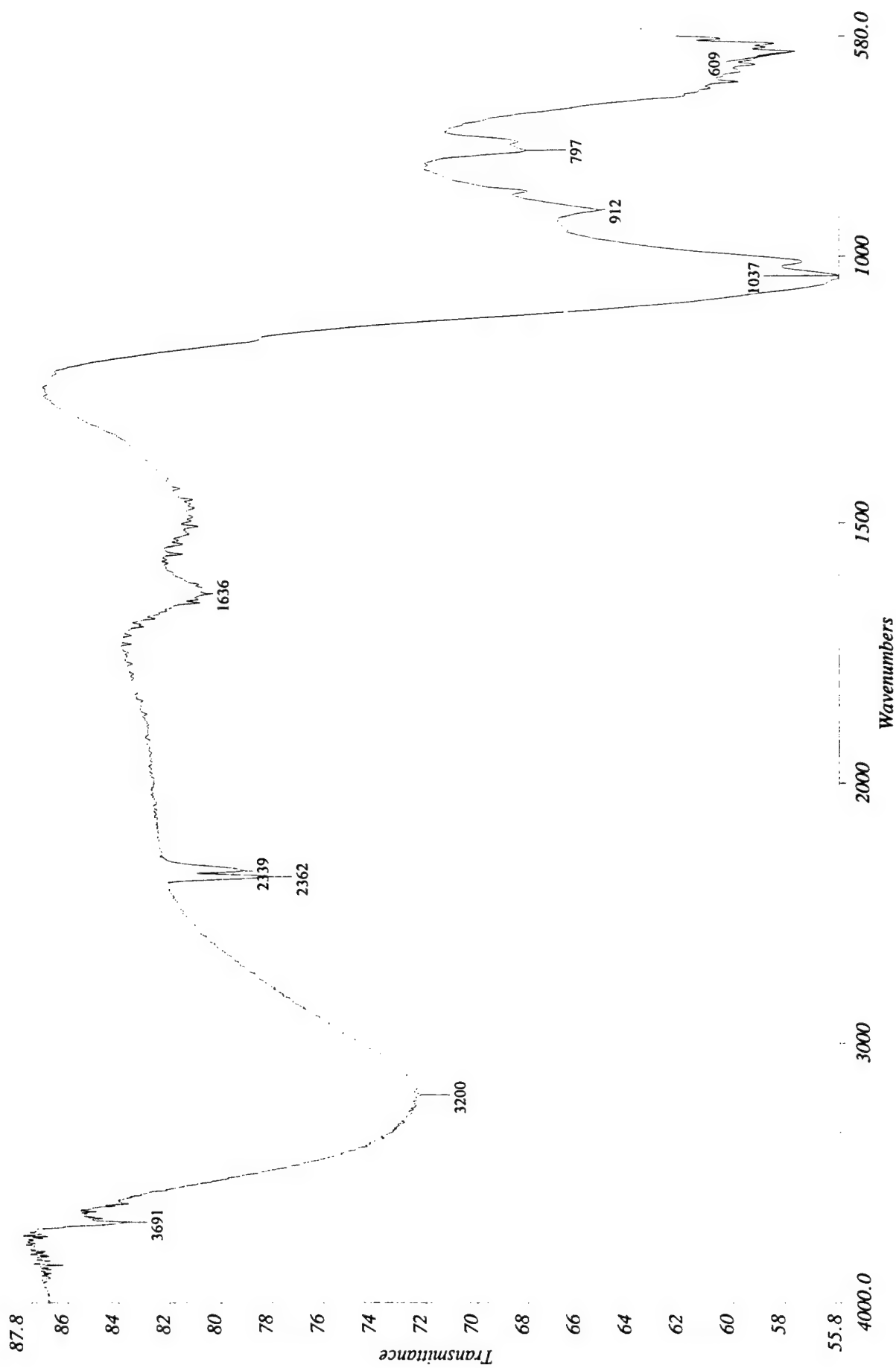
Description: Spectrum At 8577,1549,1302 Micrometers Aperture: 100,100

Resolution: 4 cm-1

Accumulations: 32

Date Created: Sat Sep 11 09:36:13 1999

Molecular Microspectroscopy Laboratory



Spectrum Name: A:\BAT263.SP

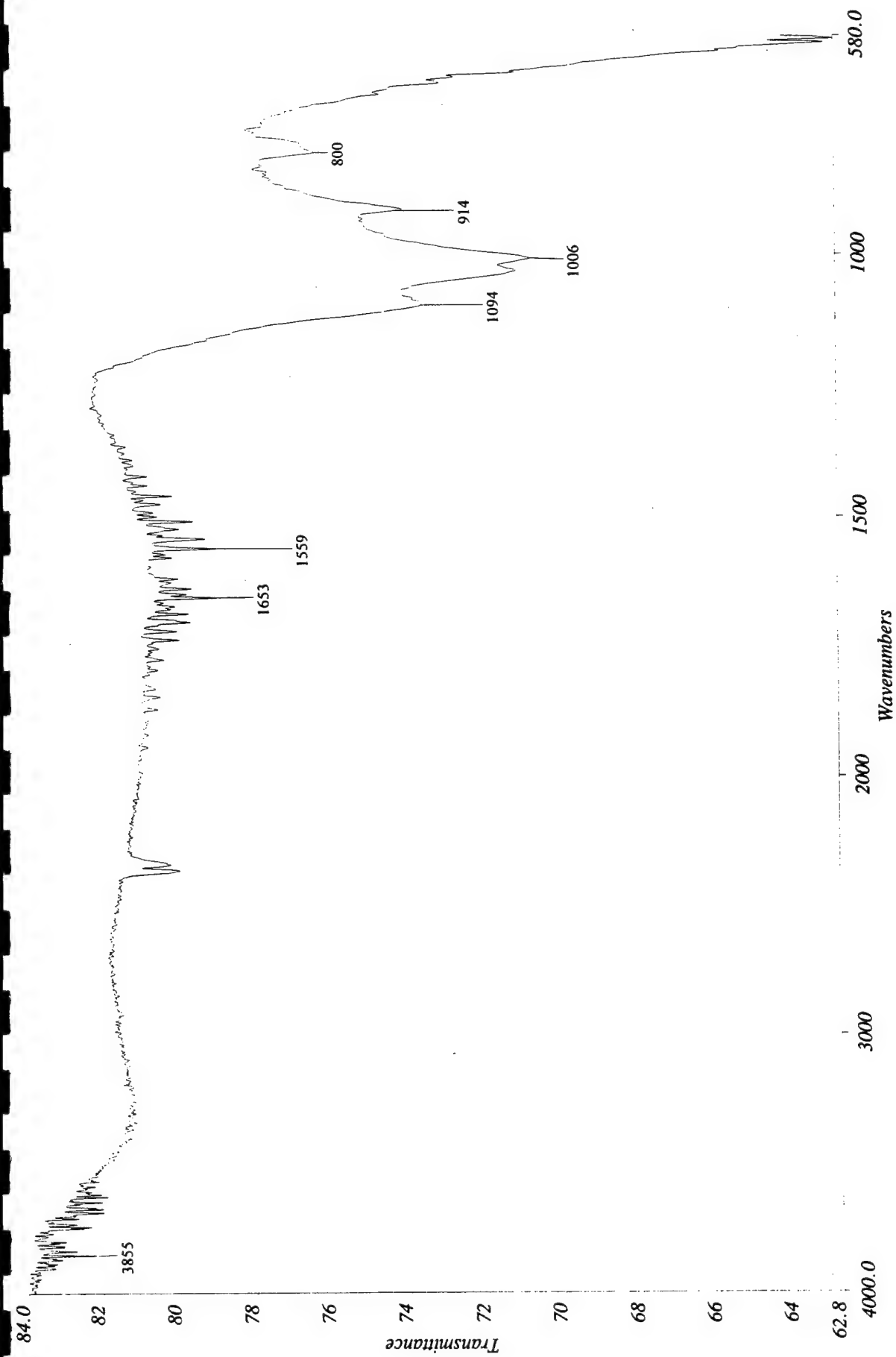
Description: Spectrum At 6810,1237,1585 Micrometers □ Aperture: 100,100

Resolution: 4 cm⁻¹

Accumulations: 32

Date Created: Sat Sep 11 10:32:50 1999

Molecular Microspectroscopy Laboratory



Spectrum Name: A:\BAT264.SP

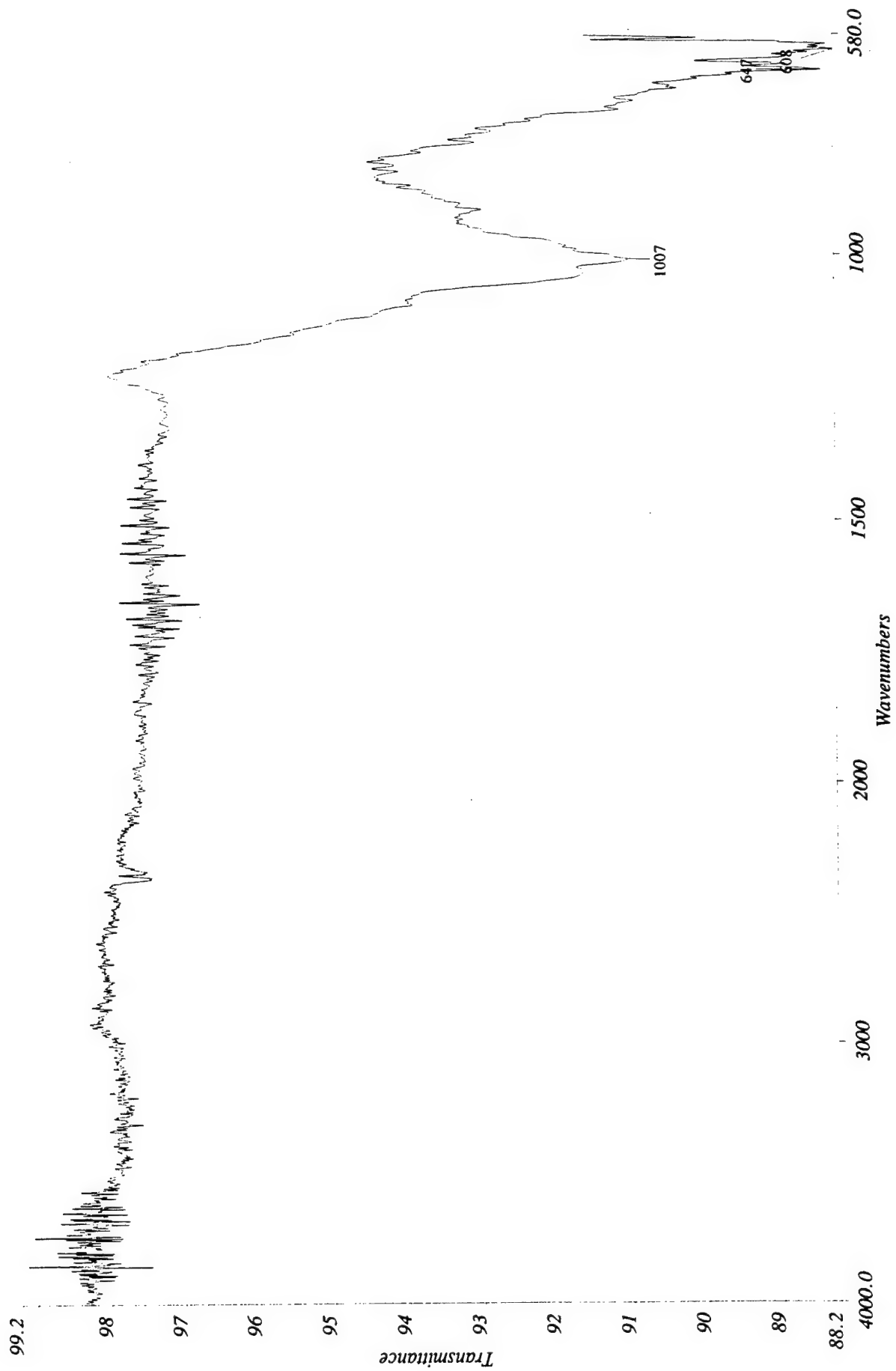
Description: Spectrum At 11731,1675,1335 Micrometers Aperture: 100,100

Resolution: 4 cm-1

Accumulations: 32

Date Created: Sat Sep 11 10:35:21 1999

Molecular Microspectroscopy Laboratory



Spectrum Name: A:\BAT265.SP

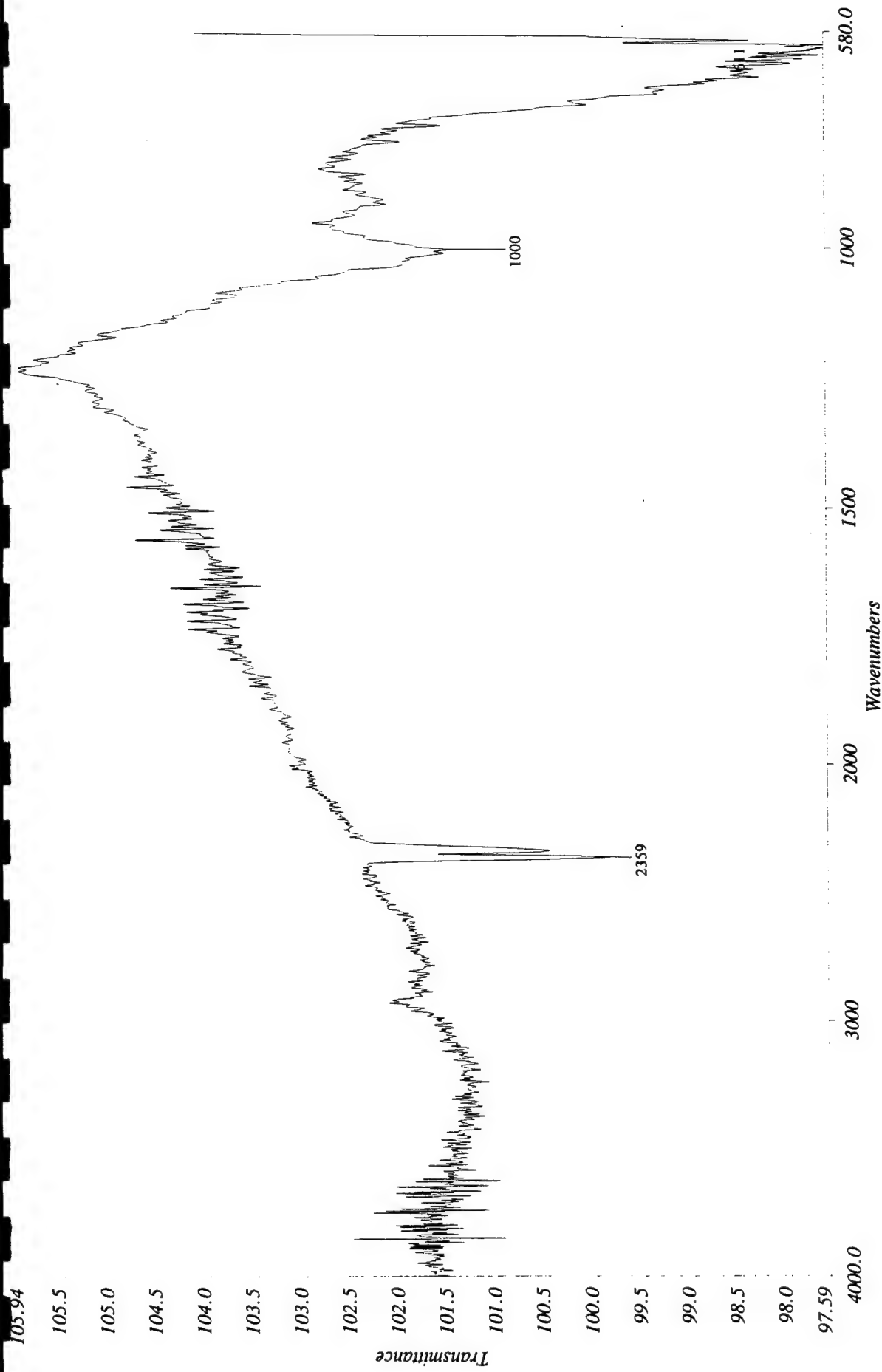
Resolution: 4 cm-1

Description: Spectrum At 6635,1344,1597 Micrometers □ Aperture: 100,100

Accumulations: 32

Date Created: Sat Sep 11 10:30:24 1999

Molecular Microspectroscopy Laboratory



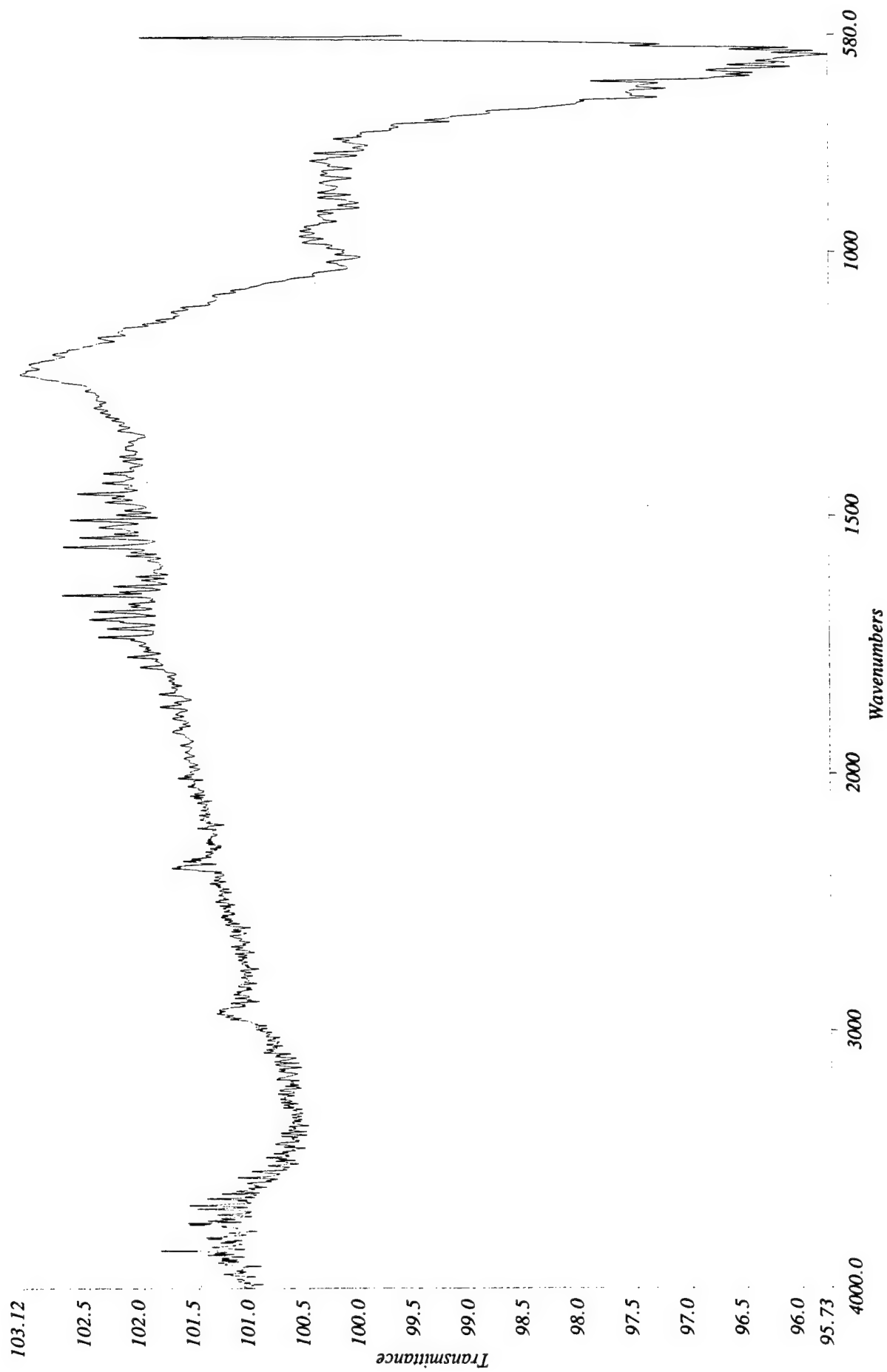
Resolution: 4 cm-1

Accumulations: 32

Molecular Microspectroscopy Laboratory

Spectrum Name: A:\BAT266.SP
Description: Spectrum At 286,32,1425 Micrometers Aperture: 100,100

Date Created: Sat Sep 11 10:50:32 1999



Spectrum Name: A:\BAT267.SP

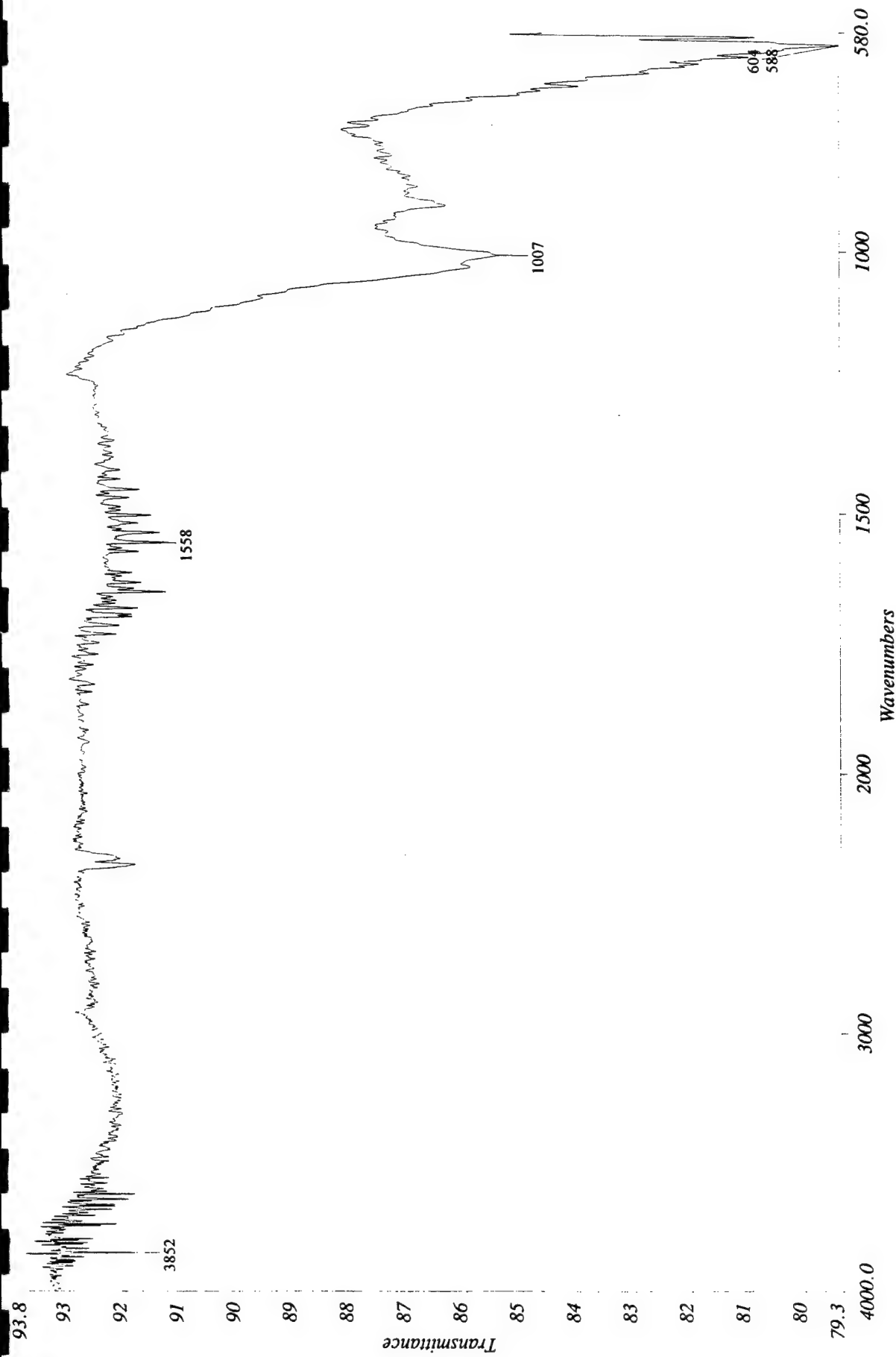
Description: Spectrum At 628,224,1457 Micrometers □ Aperture: 100,100

Resolution: 4 cm-1

Accumulations: 32

Date Created: Sat Sep 11 10:49:02 1999

Molecular Microspectroscopy Laboratory



Spectrum Name: A:\BAT268.SP

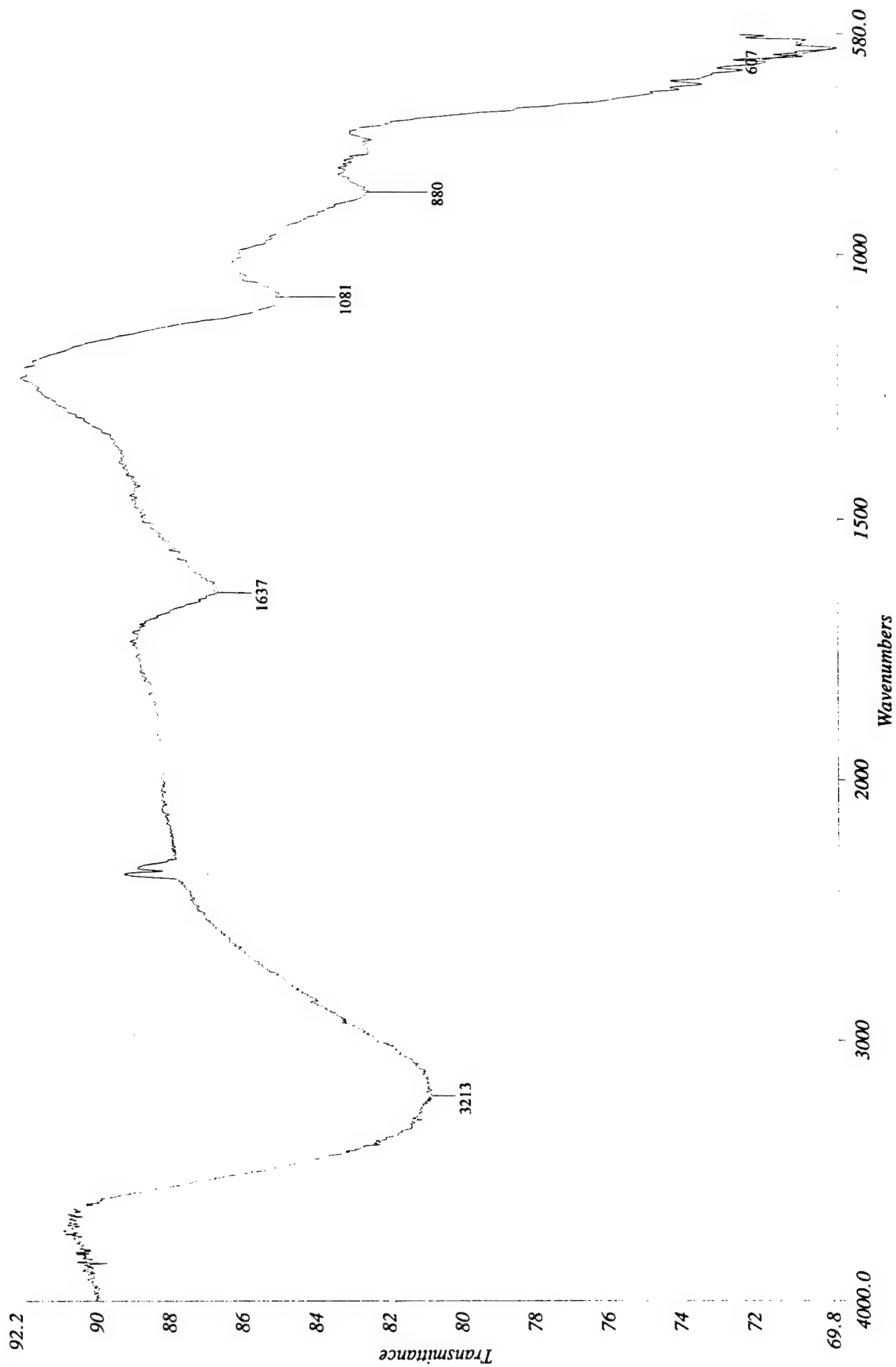
Description: Spectrum At -73,410,1338 Micrometers Aperture: 100,100

Resolution: 4 cm-1

Accumulations: 32

Date Created: Sat Sep 11 10:43:43 1999

Molecular Microspectroscopy Laboratory



Spectrum Name: A:\BAT269.SP

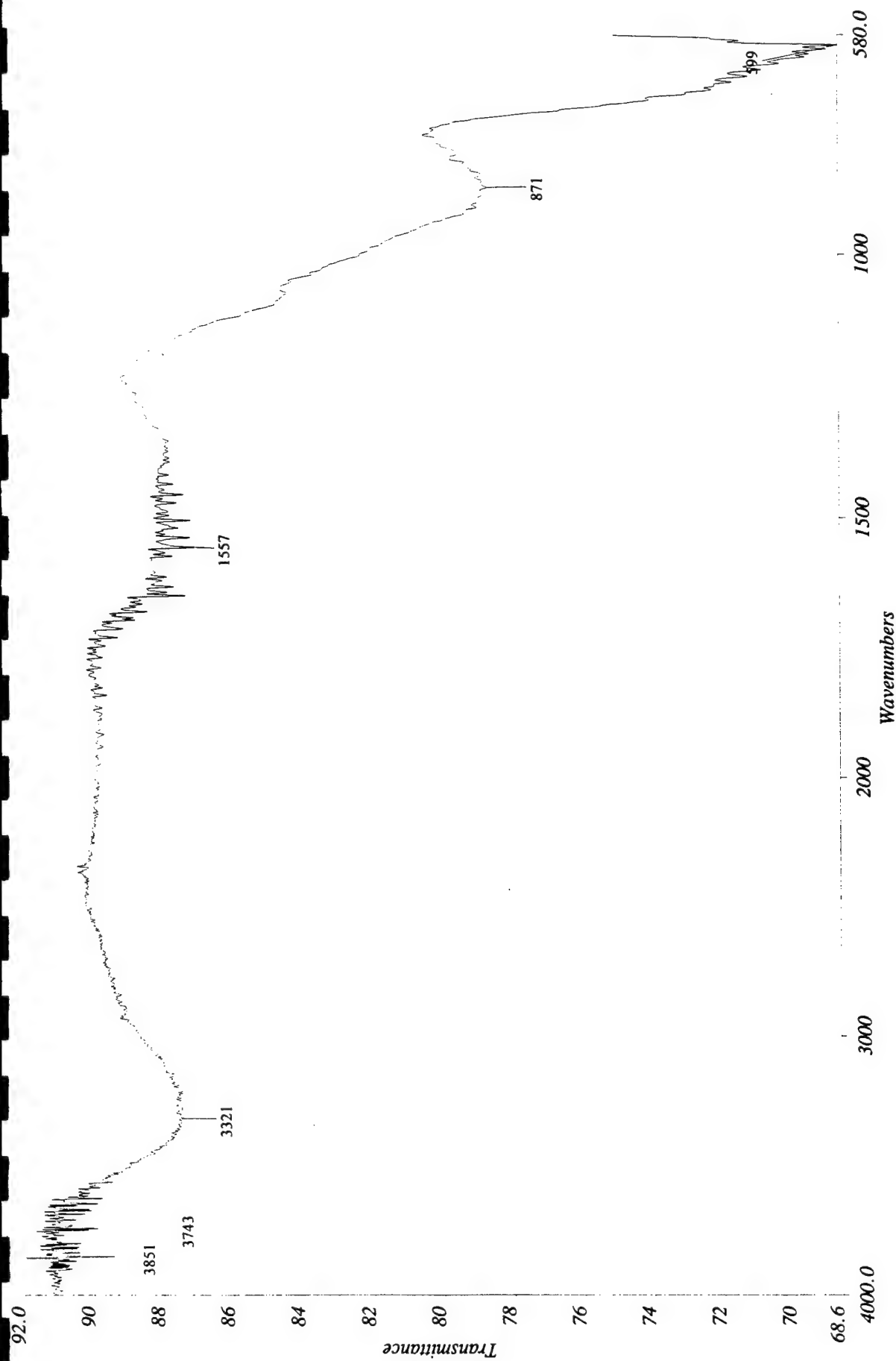
Description: Spectrum At 10298,2583,1551 Micrometers □ Aperture: 100,100

Resolution: 4 cm-1

Accumulations: 32

Date Created: Sat Sep 11 11:05:52 1999

Molecular Microspectroscopy Laboratory



Spectrum Name: A:\BAT270.SP

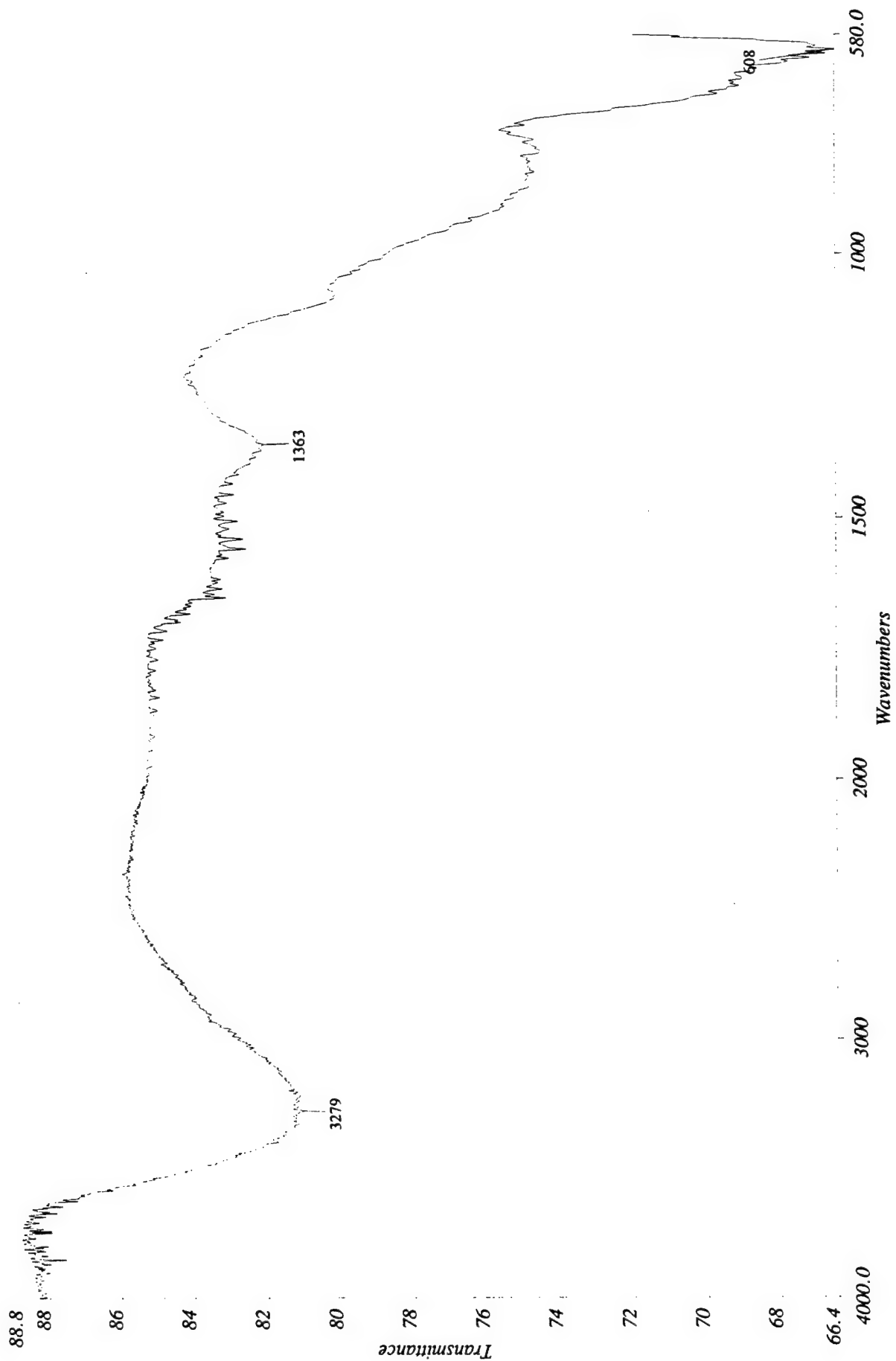
Description: Spectrum At 5338,2669,1429 Micrometers Aperture: 100,100

Resolution: 4 cm-1

Accumulations: 32

Date Created: Sat Sep 11 11:04:27 1999

Molecular Microspectroscopy Laboratory



Spectrum Name: A:\BAT271.SP

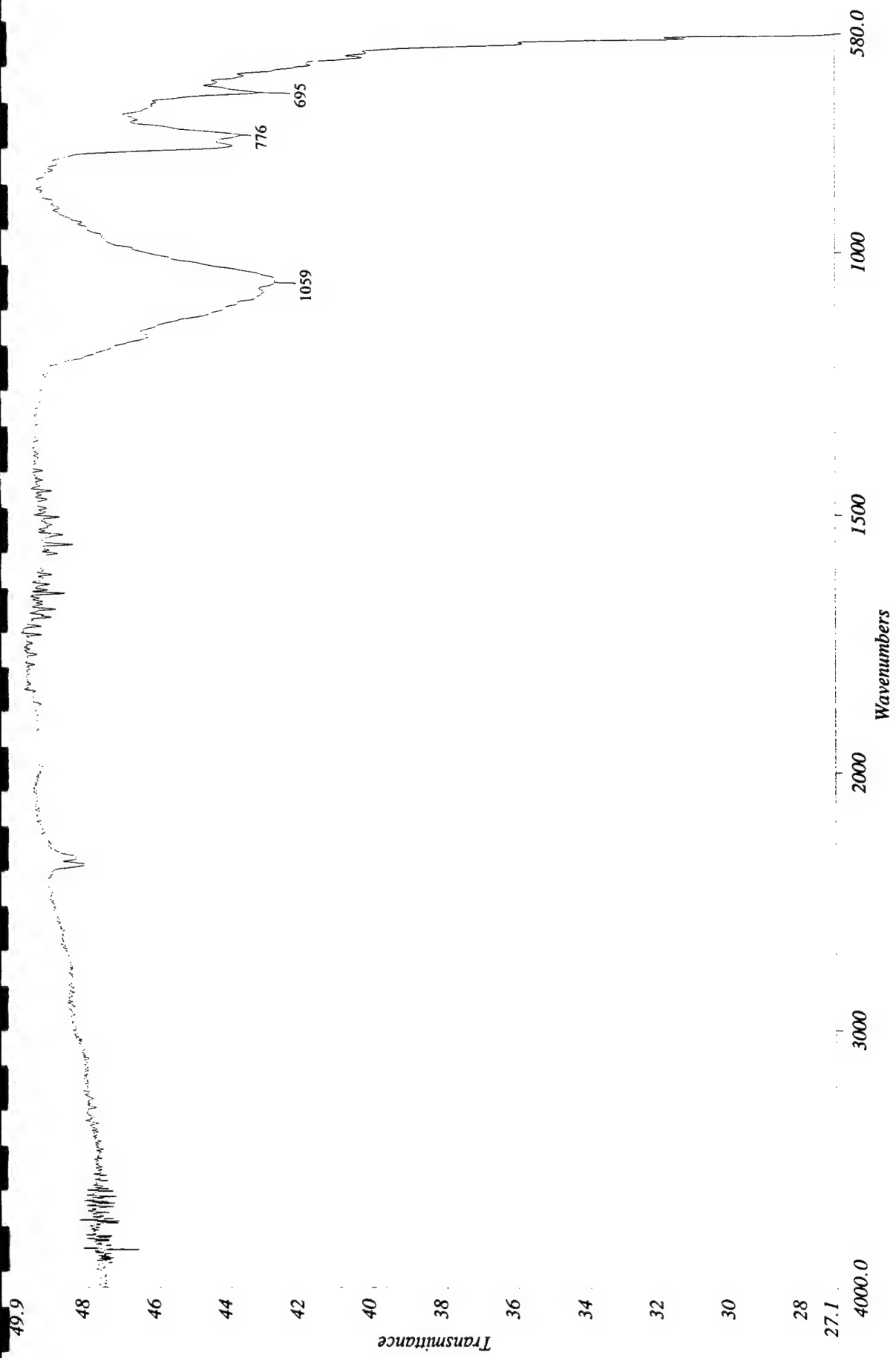
Description: Spectrum At 10841,2014,1534 Micrometers Aperture: 100,100

Resolution: 4 cm-1

Accumulations: 32

Date Created: Sat Sep 11 11:07:32 1999

Molecular Microspectroscopy Laboratory

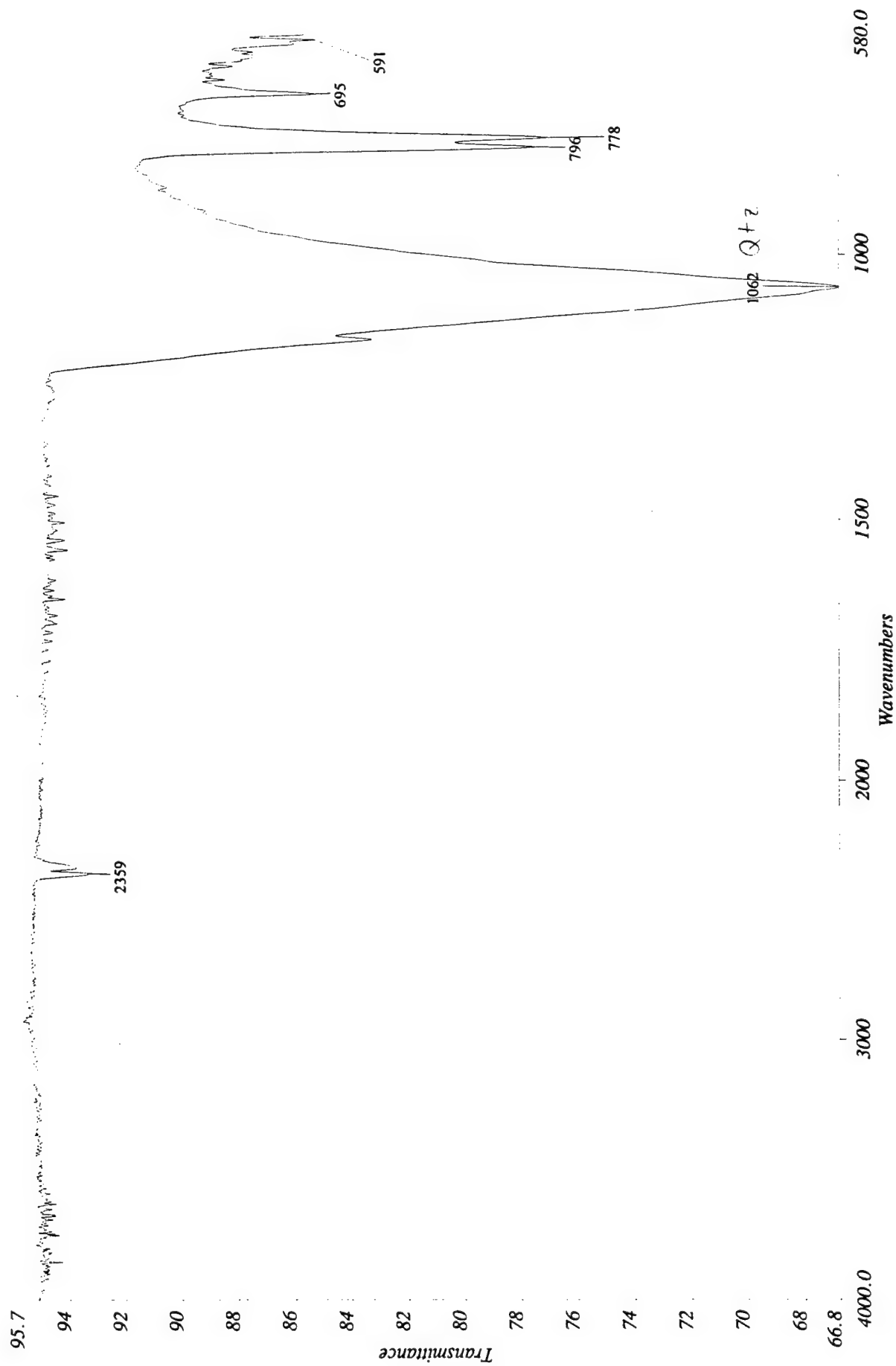


Resolution: 4 cm-1
Accumulations: 32

Spectrum Name: A:\BAT272.SP
Description: Spectrum At 23539,1625,1436 Micrometers □ Aperture: 100,100

Molecular Microspectroscopy Laboratory

Date Created: Sat Sep 11 11:17:26 1999



Spectrum Name: A:\BAT273.SP

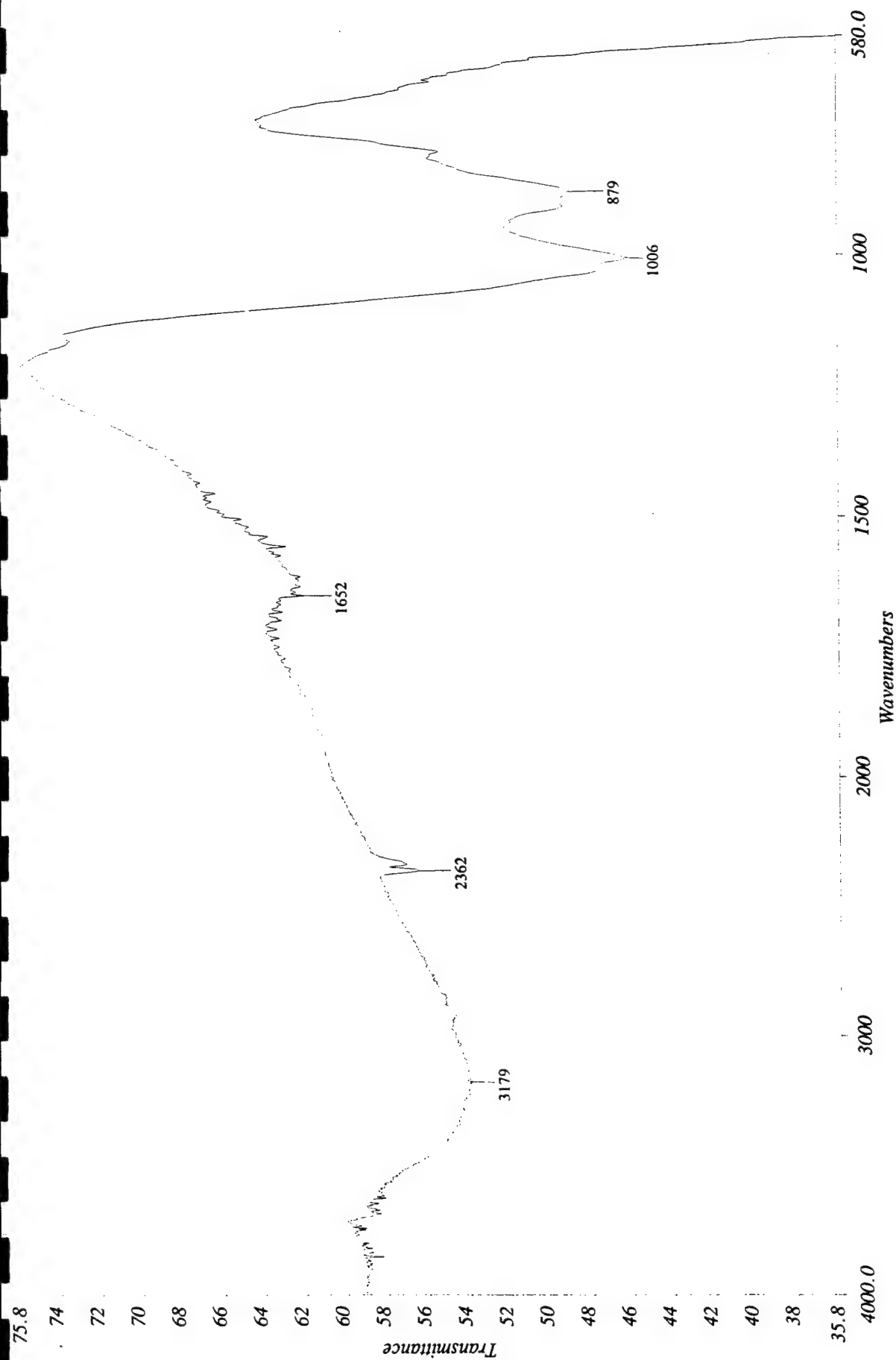
Description: Spectrum At 20148,1608,1468 Micrometers Aperture: 100,100

Resolution: 4 cm-1

Accumulations: 32

Date Created: Sat Sep 11 11:15:41 1999

Molecular Microspectroscopy Laboratory



Spectrum Name: A:\BAT274.SP

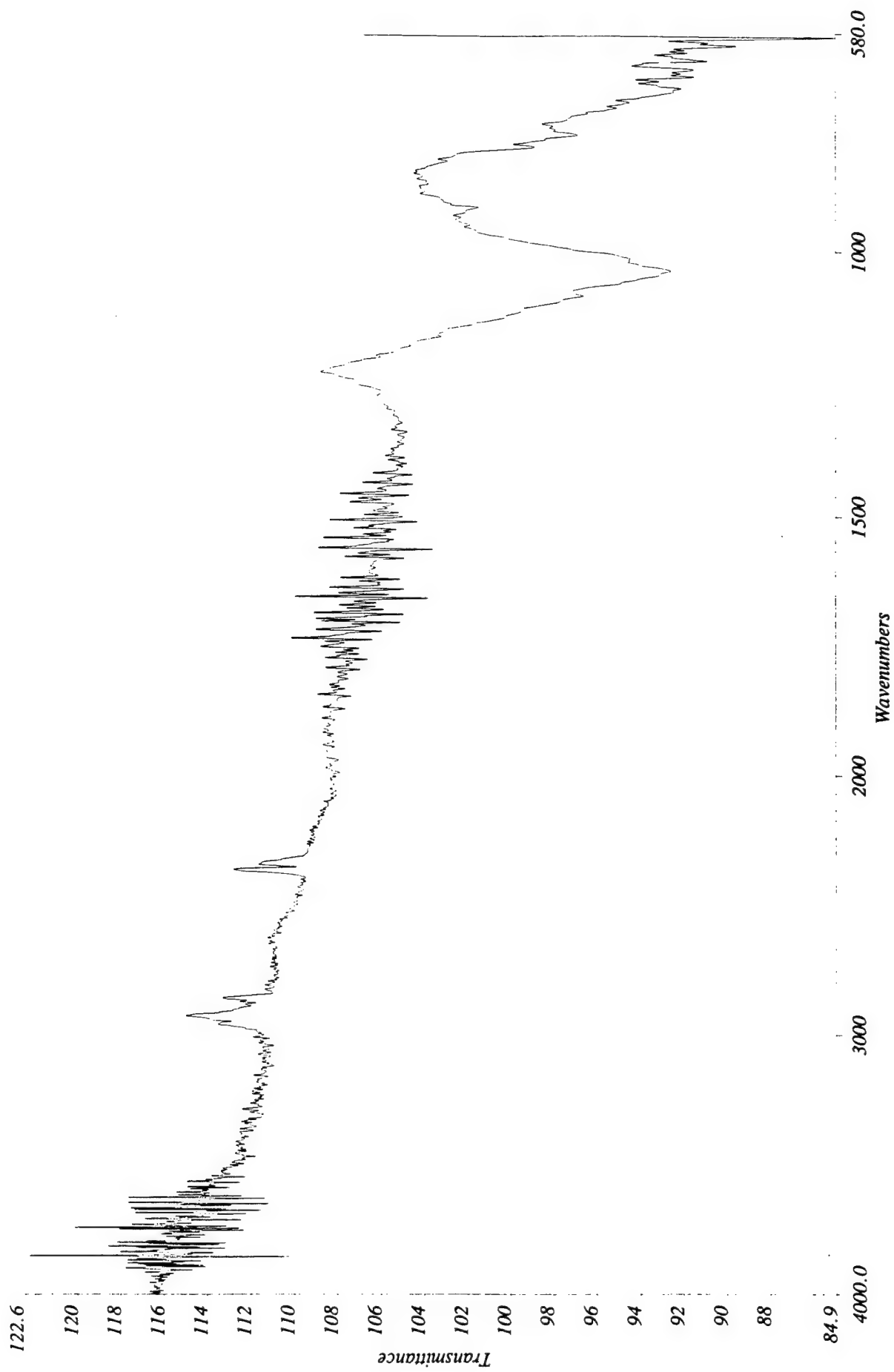
Description: Spectrum At 14598,893,1420 Micrometers Aperture: 100,100

Resolution: 4 cm⁻¹

Accumulations: 32

Date Created: Sat Sep 11 11:14:08 1999

Molecular Microspectroscopy Laboratory



Spectrum Name: A:\BAT275.SP

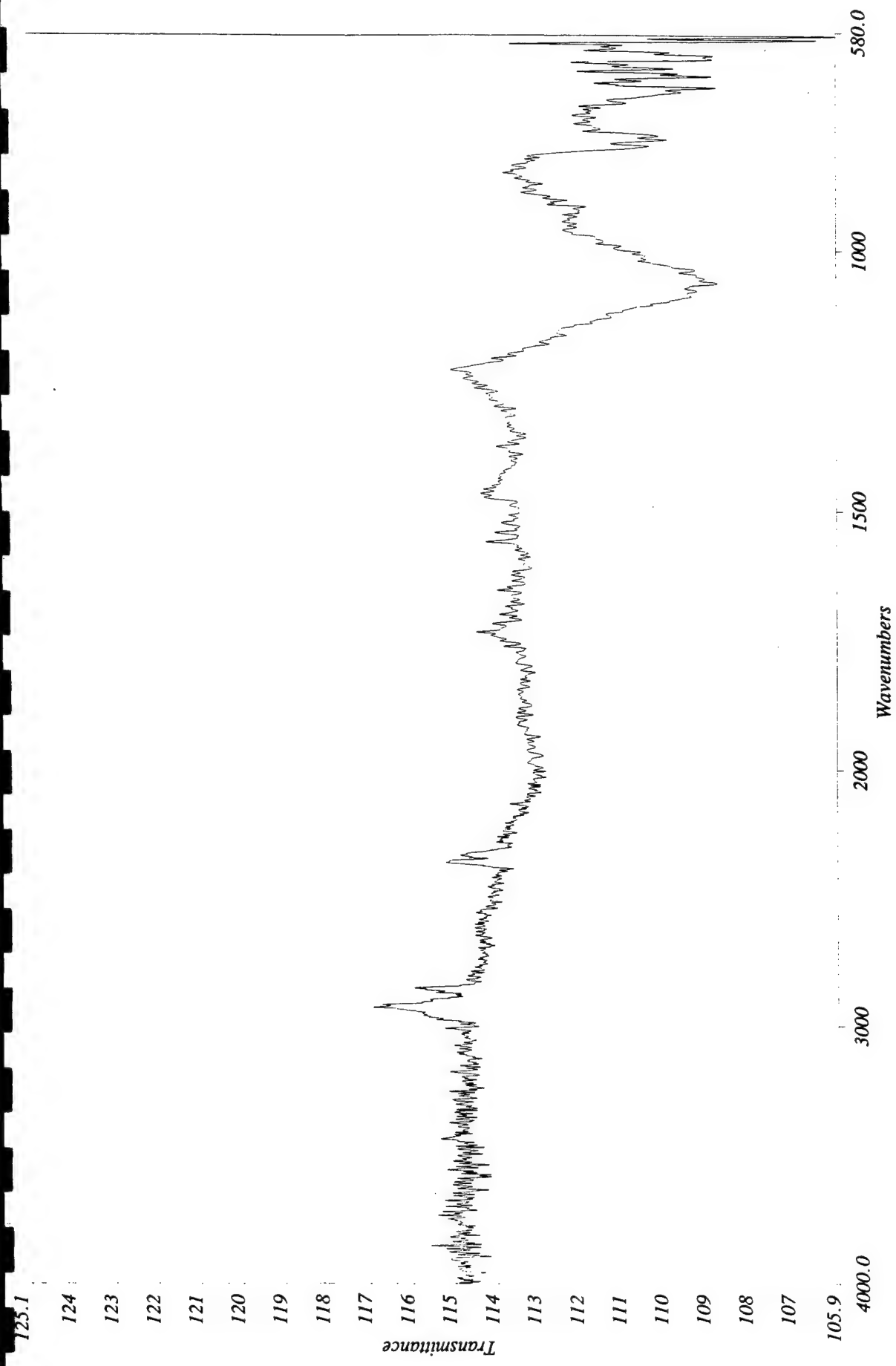
Resolution: 4 cm-1

Description: Spectrum At 19103,1585,1505 Micrometers □ Aperture: 100,100

Accumulations: 32

Date Created: Sat Sep 11 11:31:28 1999

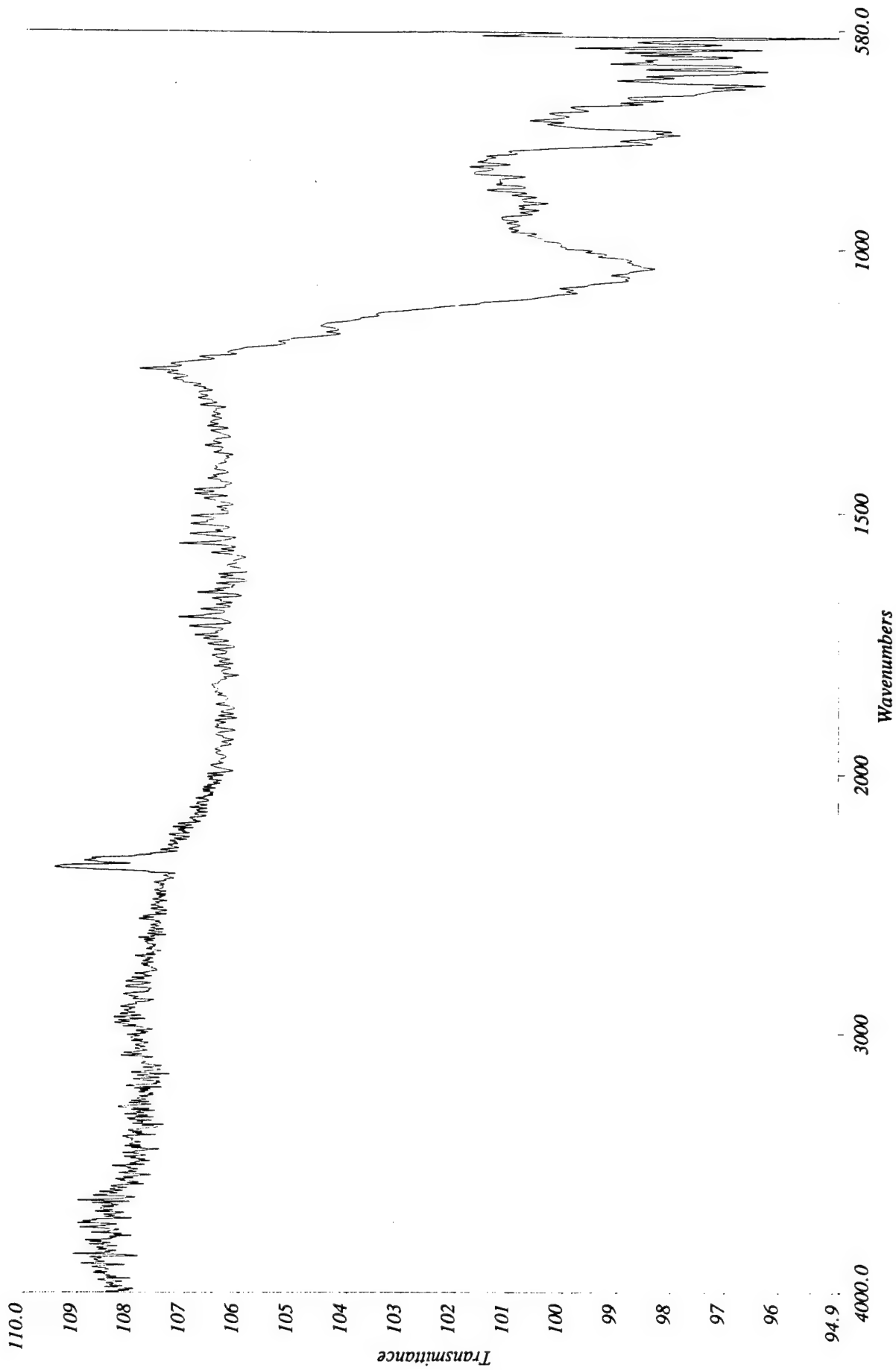
Molecular Microspectroscopy Laboratory



Spectrum Name: A:\BAT276.SP
Description: Spectrum At 14900,1024,1506 MicrometersAperture: 100,100
Resolution: 4 cm-1
Accumulations: 32

Molecular Microspectroscopy Laboratory

Date Created: Sat Sep 11 11:30:09 1999



Spectrum Name: A:\BAT277.SP

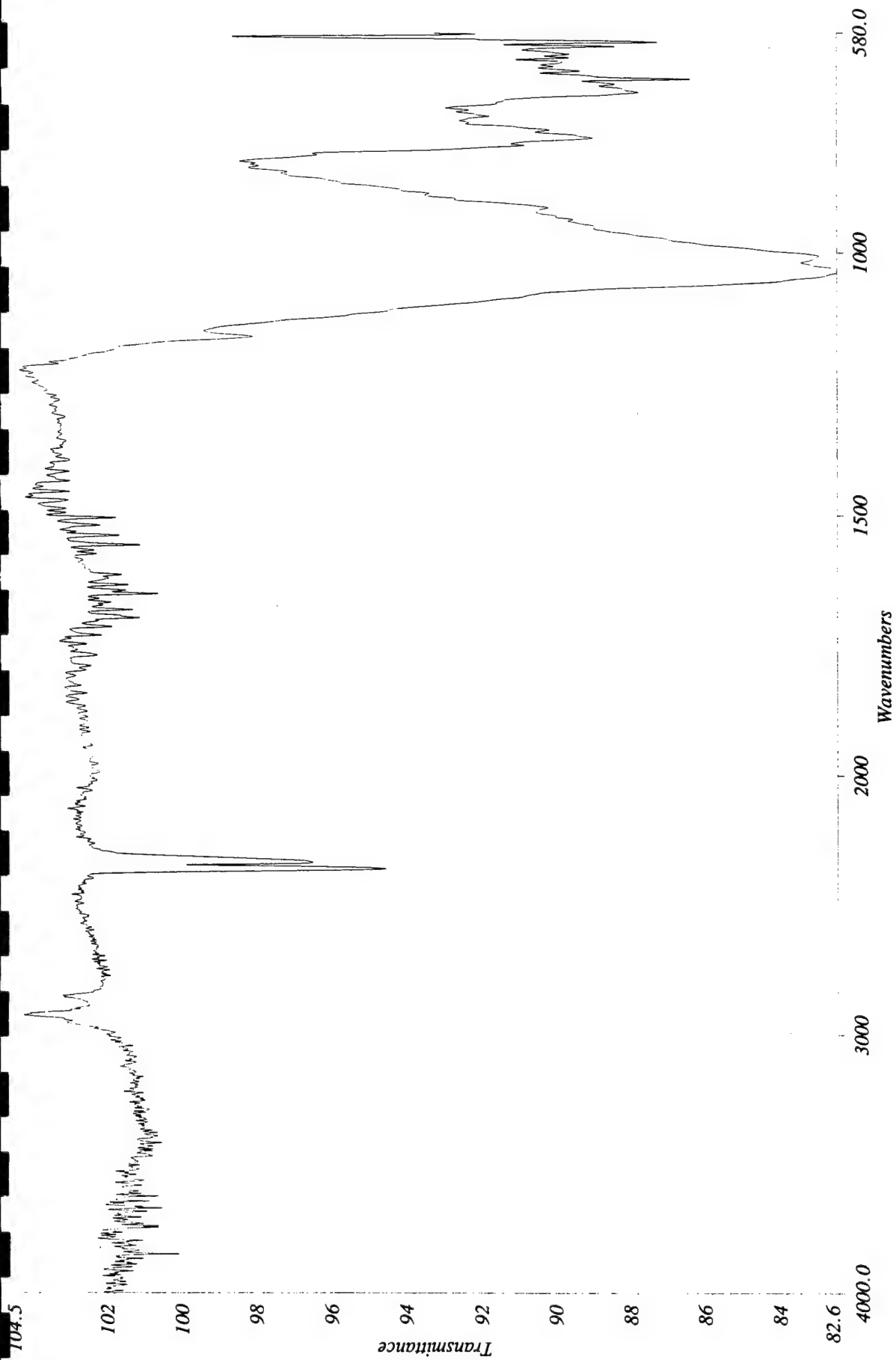
Description: Spectrum At 10443,1766,1391 Micrometers Aperture: 100,100

Resolution: 4 cm-1

Accumulations: 32

Date Created: Sat Sep 11 11:28:00 1999

Molecular Microspectroscopy Laboratory



Spectrum Name: A:\BAT278.SP

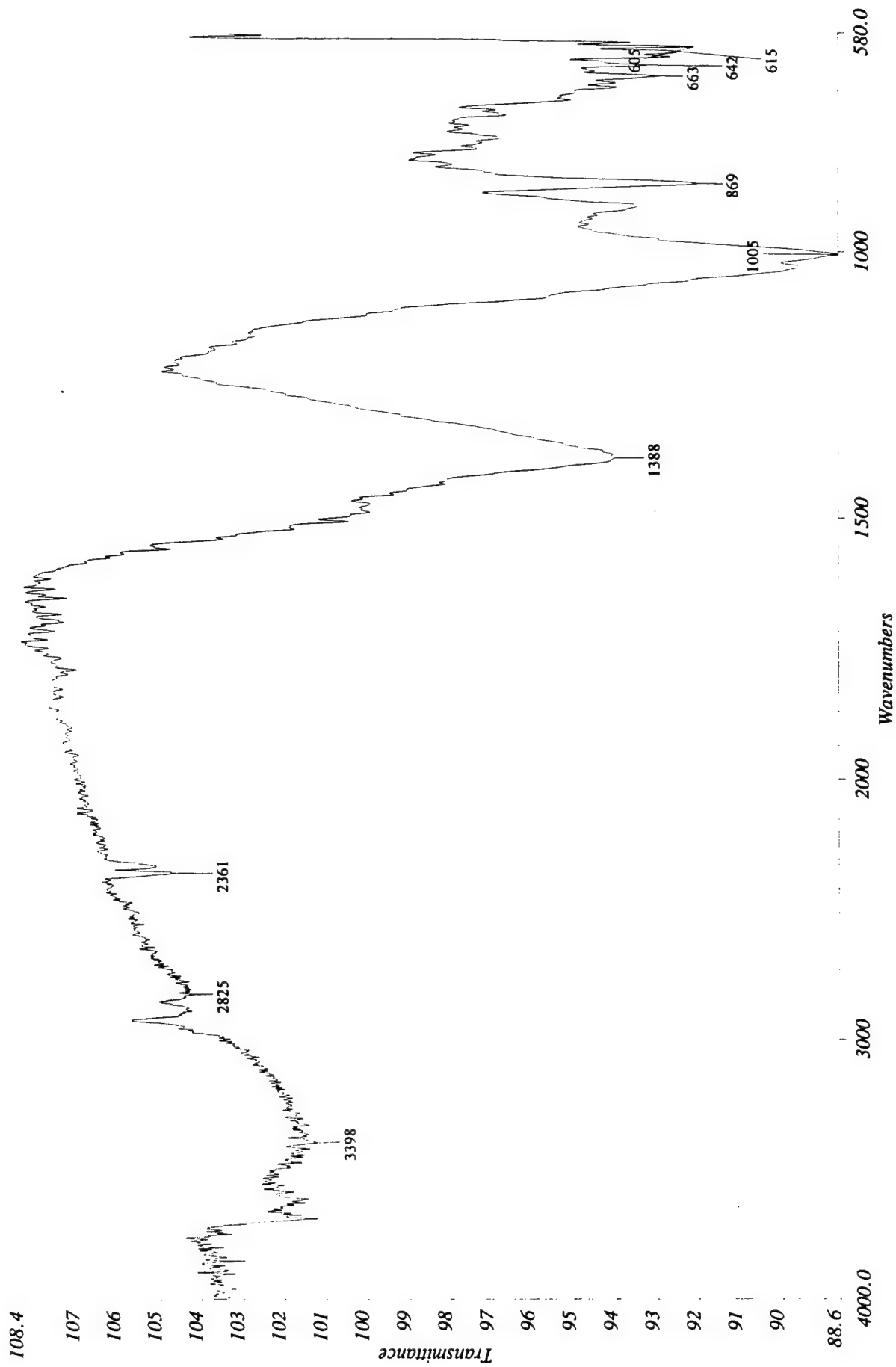
Description: Spectrum At 14389,1235,1402 Micrometers □ Aperture: 100,100

Resolution: 4 cm-1

Accumulations: 32

Date Created: Sat Sep 11 11:44:12 1999

Molecular Microspectroscopy Laboratory



Spectrum Name: A:\BAT279.SP

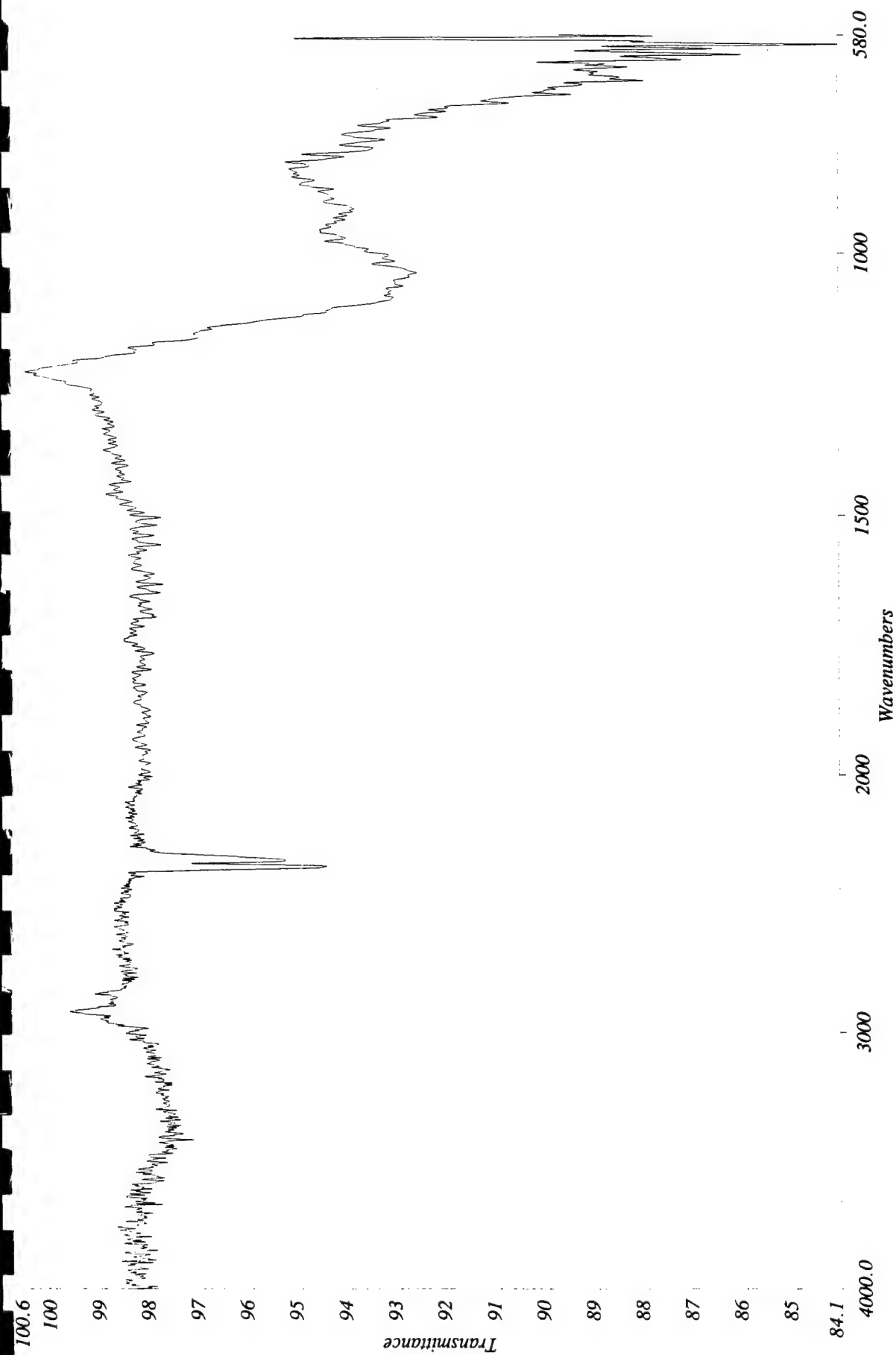
Description: Spectrum At 14282,1079,1364 Micrometers Aperture: 100,100

Resolution: 4 cm-1

Accumulations: 32

Date Created: Sat Sep 11 11:40:58 1999

Molecular Microspectroscopy Laboratory



Spectrum Name: A:\BAT280.SP

Description: Spectrum At 9055,1736,1341 Micrometers □ Aperture: 100,100

Resolution: 4 cm-1

Accumulations: 32

Date Created: Sat Sep 11 11:39:23 1999

Molecular Microspectroscopy Laboratory

Appendix F-4

Raman Spectra for Iron Core Samples

Battelle - Infrared and Raman Microanalysis

Investigator: Dr. Andre' J. Sommer

September 10, 1999

The samples submitted for analysis included a number of solid materials containing either iron chips, pyrite particles or quartz particles mixed in various combinations. These materials had been employed as reactive media for underground purification tests. In an effort to determine their effectiveness, the chemical nature of their surfaces was being investigated. Raman and infrared microanalyses were therefore employed to identify the surface components of these materials. Tables 1 and 2 provide a summary of the analysis.

Experimental

Raman microanalysis was conducted with a Renishaw Raman S2000 confocal Raman microprobe. A HeNe laser was employed as the excitation using 8 milliwatts of power at the sample. In an effort to obtain better sampling statistics a cylindrical lens was placed in the optical path of the system prior to the sample. In conjunction with the 50X (0.80 N.A.) objective, this lens produced a line image on the sample 2 micrometers in width and approximately 200 micrometers long. Spectra were collected at 4 cm^{-1} resolution using a 300 second per point integration time. Three spectra were collected for each sample to obtain an average composition.

Infrared spectra were collected with a Perkin Elmer Spectrum 2000 FTIR coupled with an Auto image microscope. Attenuated total internal reflection (ATR) spectra were collected with this system using a germanium internal reflection element. This device probes the surface of the sample to a depth of approximately 2 micrometers. Spectra were collected at 4 cm^{-1} resolution and each spectrum is the result of 32 individual scans. Once again three spectra were collected to obtain an average composition for each sample.

Results and Discussion

In general, those samples having an iron or iron and sand medium yielded Raman spectra characteristic for a composition containing magnetite (Fe_3O_4) and carbon. The main transition observed for magnetite is located at 670 cm^{-1} shift and those for carbon at 1350 and 1600 cm^{-1} shift. Samples having a pyrite and sand medium produced spectra, which were characteristic for pyrite and small amounts of either quartz or carbon. Transitions characteristic of pyrite are located at 345 , 381 and 433 cm^{-1} shift and that for quartz is located at 466 cm^{-1} shift.

Infrared analysis of the samples whose medium was iron or iron and sand yielded spectra characteristic of a silicate and iron oxide materials. The absorption located near 590 cm^{-1} is characteristic for most of the iron oxides, however, it is not very specific with regard to the polymorph present. Absorptions observed at 900 , 1002 and 1031 cm^{-1} are characteristic

for a silicate material but not quartz. An infrared spectrum that closely resembles that of quartz is labeled BAT273.

Table 1. Raman Analysis Summary

Spectra	Sample Description	Medium	Sample Composition
BAT200 - BAT202	PS-2, 15.5-16.5 top	Iron	Magnetite and carbon + am. $\text{FeO}(\text{H})$;
BAT203 - BAT205	PS-2, 24-24.5	Iron	Magnetite and carbon
BAT206 - BAT208	PS-2, 31-31.5	Iron	Magnetite and carbon
BAT209 - BAT211	PS-7, 15-15.5	Iron	Magnetite and carbon
BAT212 - BAT214	PS-7, 24.5-25	Iron	alpha- FeOOH , magnetite, quartz and carbon
BAT215 - BAT217	PS-7, 28-28.5	Iron	alpha- FeOOH , magnetite and carbon
BAT218 - BAT220	PS-7, 33-33.5	Iron	Magnetite and carbon
BAT221 - BAT223	PS-7, 37-37.5	Iron	Pyrite
BAT224 - BAT226	PS-1, 15-15.5	Iron & sand	Quartz, magnetite and carbon
BAT227 - BAT229	PS-1, 19-19.5	Iron & sand	Magnetite and carbon + Am $\text{Fe}(\text{OH})_2$
BAT230 - BAT232	PS-1, 24-24.5	Iron & sand	Quartz, magnetite and carbon
BAT233 - BAT235	PS-1, 26-28.5(1)	Iron & sand	Magnetite and carbon
BAT236 - BAT238	PS-6, 15-15.5	Pyrite & sand	Magnetite and carbon
BAT239 - BAT241	PS-6, 22-22.5	Pyrite & sand	Rutile, magnetite and carbon

BAT242 - BAT244	PS-6, 24.5-25	Pyrite & sand	Pyrite, quartz and carbon
BAT245 - BAT247	PS-6, 27.5-28	Pyrite & sand	Pyrite, quartz and carbon
BAT248 - BAT250	PS-6, no depth	Pyrite and sand	Pyrite, quartz and carbon

Table 2. Infrared Analysis Summary

Spectra	Sample Description	Medium	Sample Composition
BAT251 - BAT253	PS-2, 15.5-16.5 top	Iron	Silicate and iron oxide
BAT254 BAT256	PS-2, 24-24.5	Iron	Silicate and iron oxide
BAT257 - BAT259	PS-2, 31-31.5	Iron	Silicate and iron oxide
BAT260 - BAT262	PS-7, 15-15.5	Iron	Silicate and iron oxide
BAT263 - BAT265	PS-7, 24.5-25	Iron	Silicate and iron oxide
BAT266 - BAT268	PS-7, 28-28.5	Iron	Silicate and iron oxide
BAT269 - BAT271	PS-7, 33-33.5	Iron	Silicate and iron oxide
BAT272- BAT274	PS-1, 15-15.5	Iron & sand	Silicate (quartz) and iron oxide 1062
BAT275 - BAT277	PS-1, 19-19.5	Iron & sand	Silicate
BAT278 - BAT280	PS-1, 26-28.5(1)	Iron & sand	Silicate, carbonate and iron oxide + qtz

Strong

S

to S

Battelle - Infrared and Raman Microanalysis

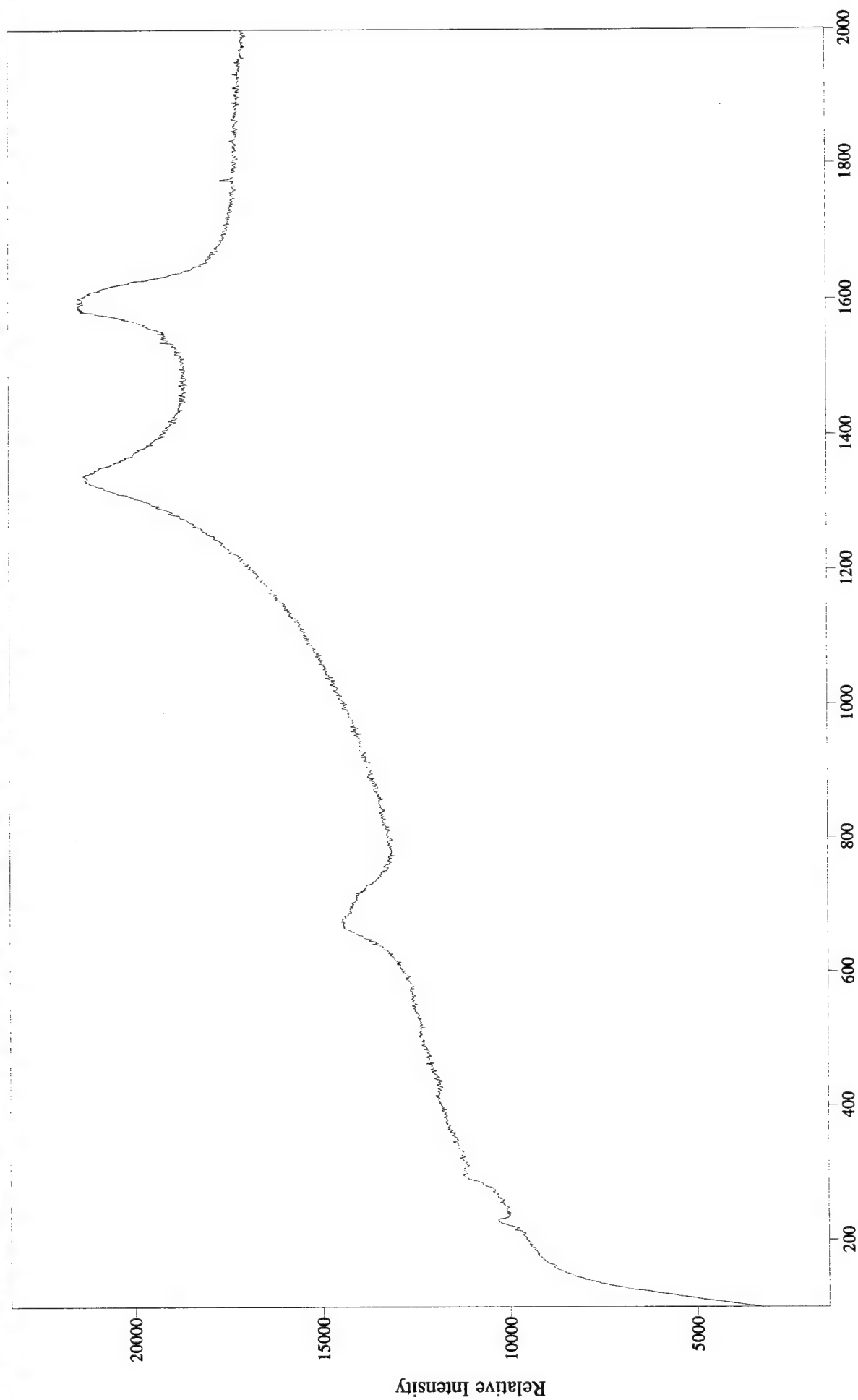
Investigator: Dr. Andre' J. Sommer

October 7, 1999

The sample analyzed in this report was labeled unused iron. Analysis of this sample was conducted to obtain baseline information on the material. This information was needed to determine the extent of chemical changes on similar samples buried in contaminated soil. Analysis conditions were identical to those detailed in a report dated September 10, 1999.

Raman spectra obtained on the sample are labeled BAT281 through BAT283. Transitions observed in the spectra are characteristic for a mixture containing amorphous carbon (1350 and 1600 cm^{-1} shift), magnetite (670 cm^{-1} shift) and hematite (227, 297, and 412 cm^{-1} shift).

Infrared spectra obtained on the samples are labeled BAT284 through BAT286. Features observed in these spectra are very weak owing to the fact that the oxide layer on the surface of the sample is extremely thin. The only feature that can be assigned to iron oxides is the trailing absorption located near 580 cm^{-1} . The negative bands located in the C-H stretch region (2900 cm^{-1}) indicate that the ATR crystal had slightly more hydrocarbon present on it during the collection of the background spectrum. However, this contaminant has no effect on the analysis.

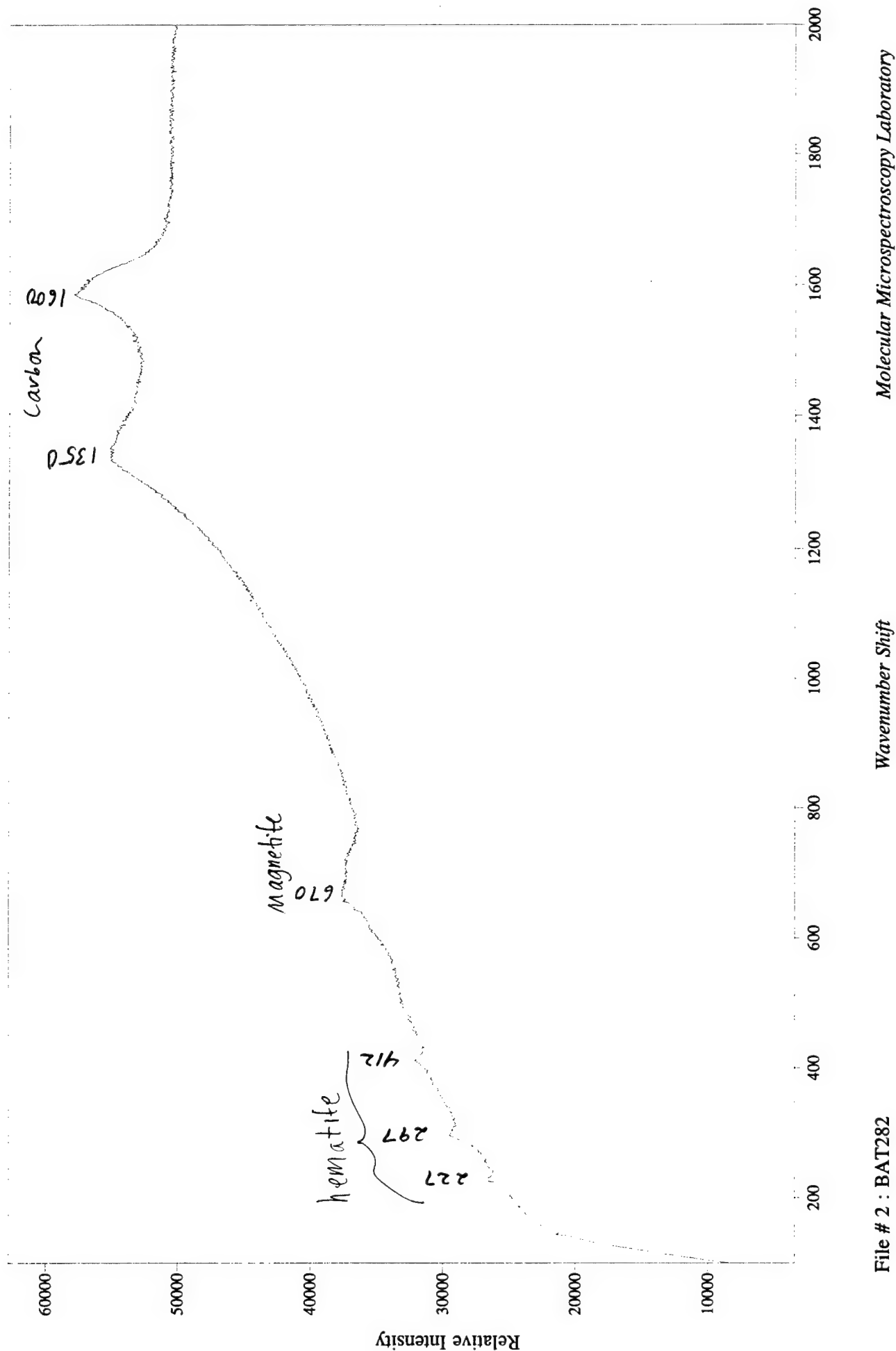


Molecular Microspectroscopy Laboratory

Wavenumber Shift

File # 1 : BAT281

Unused iron

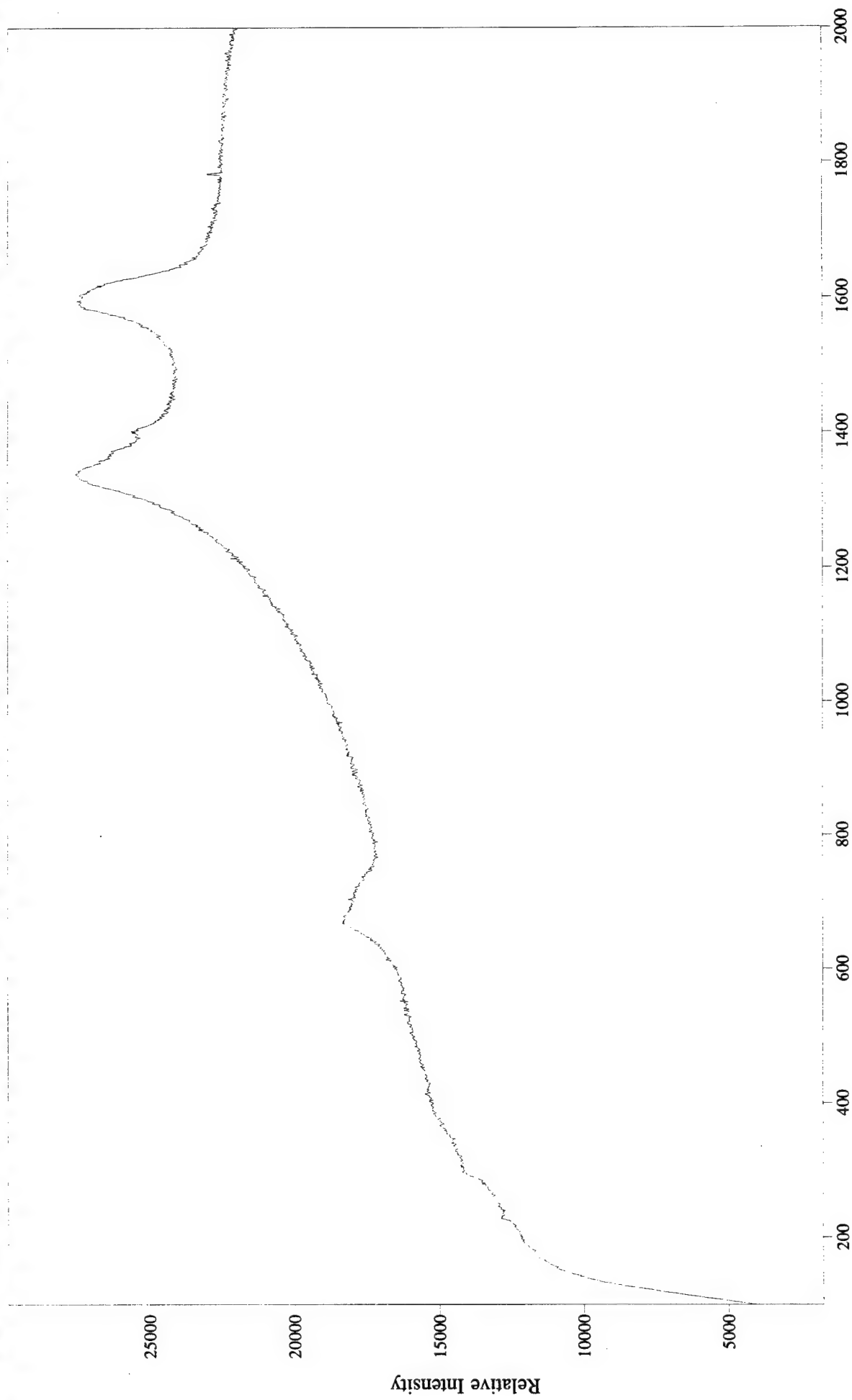


Molecular Microspectroscopy Laboratory

Wavenumber Shift

File # 2 : BAT282

Unused iron

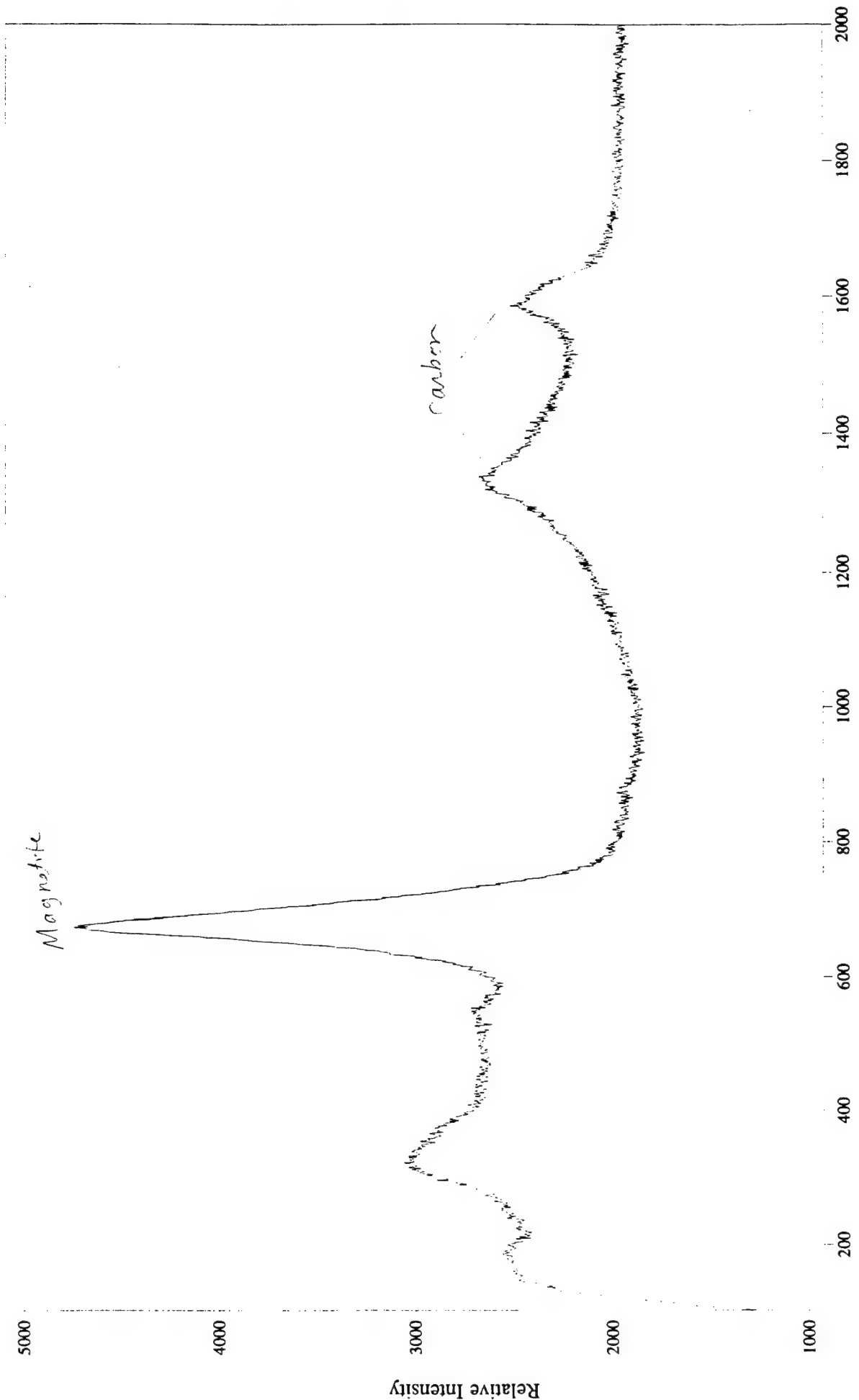


Molecular Microspectroscopy Laboratory

Wavenumber Shift

File # 3 : BAT283

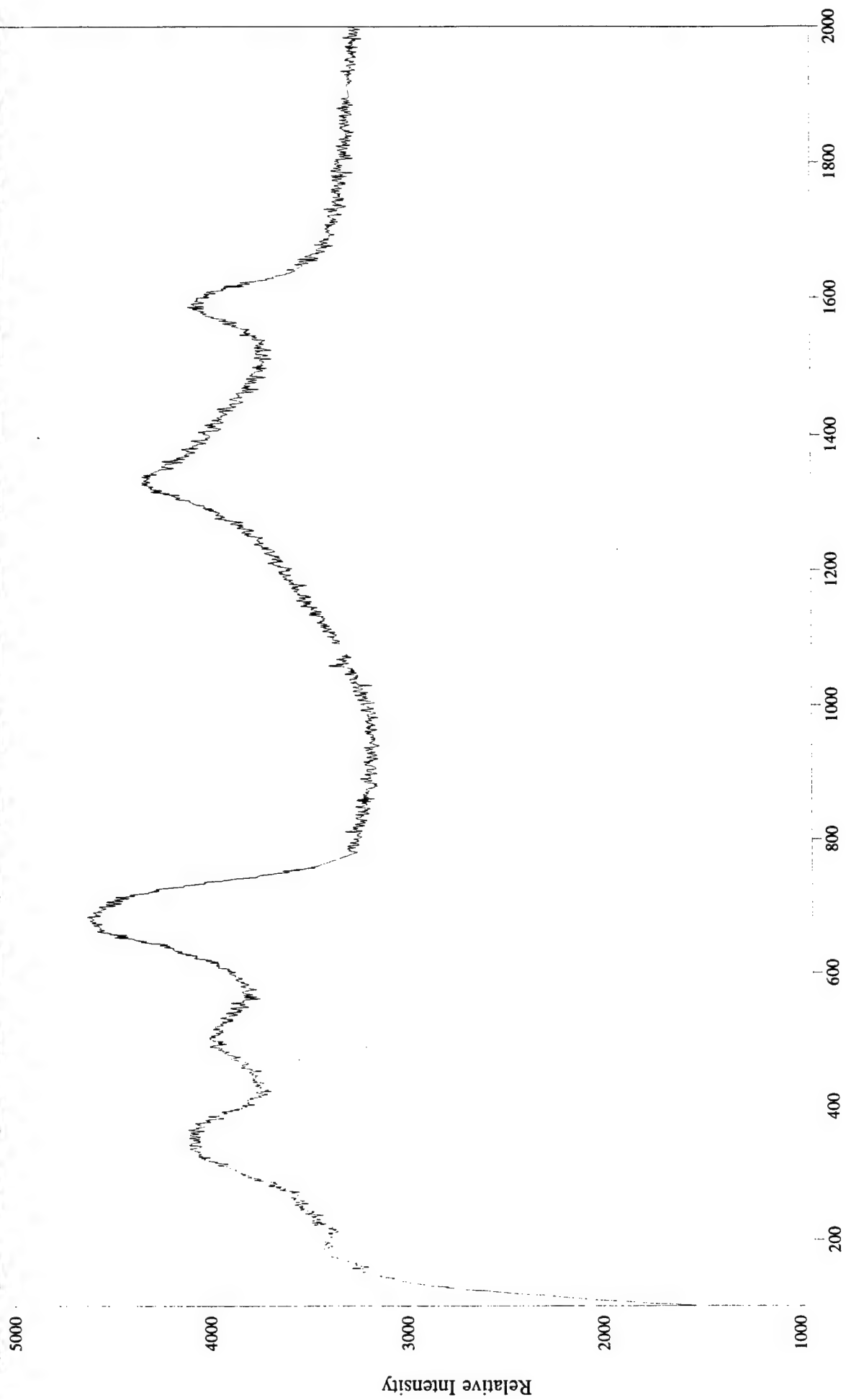
Unused iron



File # 1 : BAT200

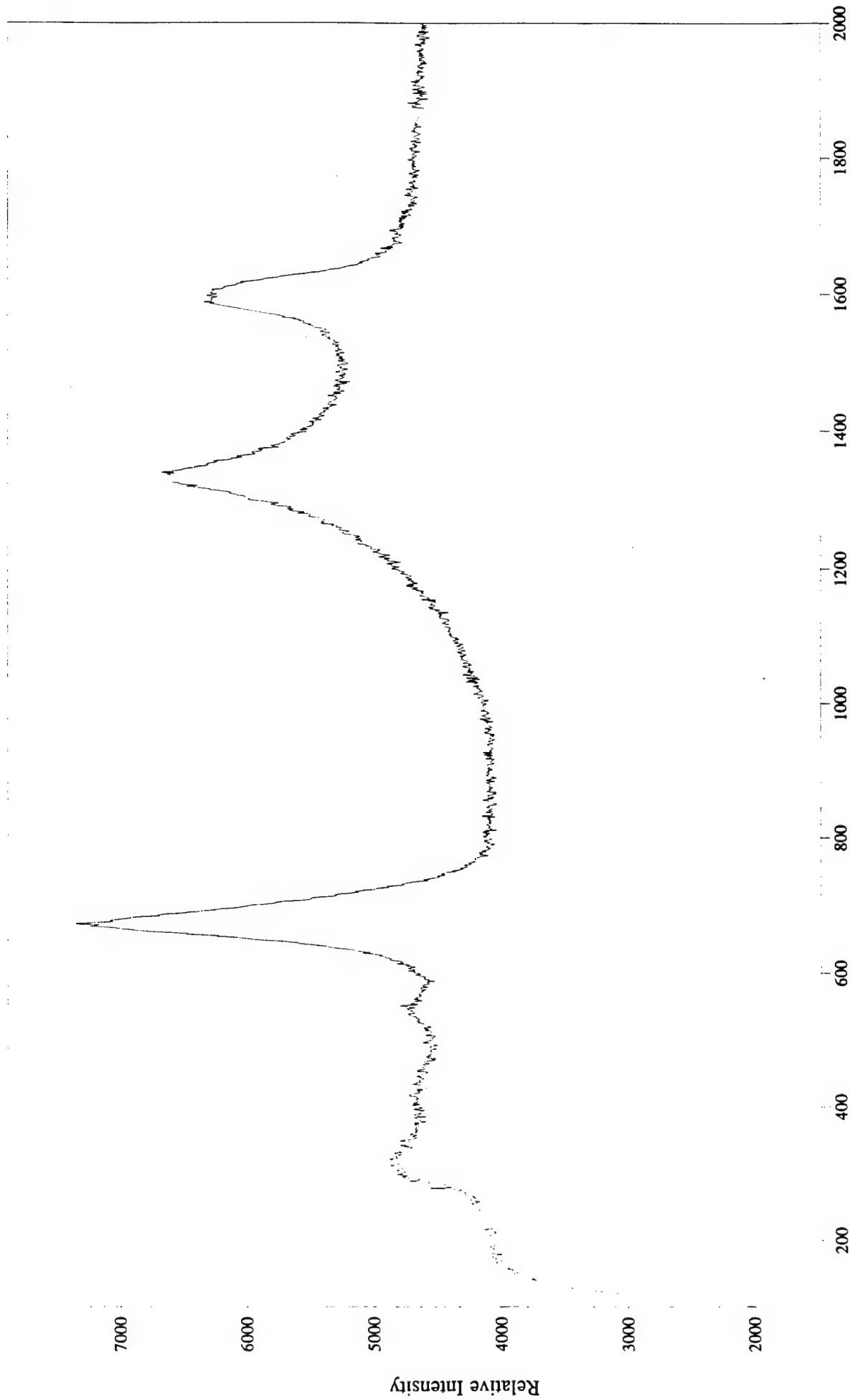
Wavenumber Shift

Molecular Microspectroscopy Laboratory



File # 1 : BAT201

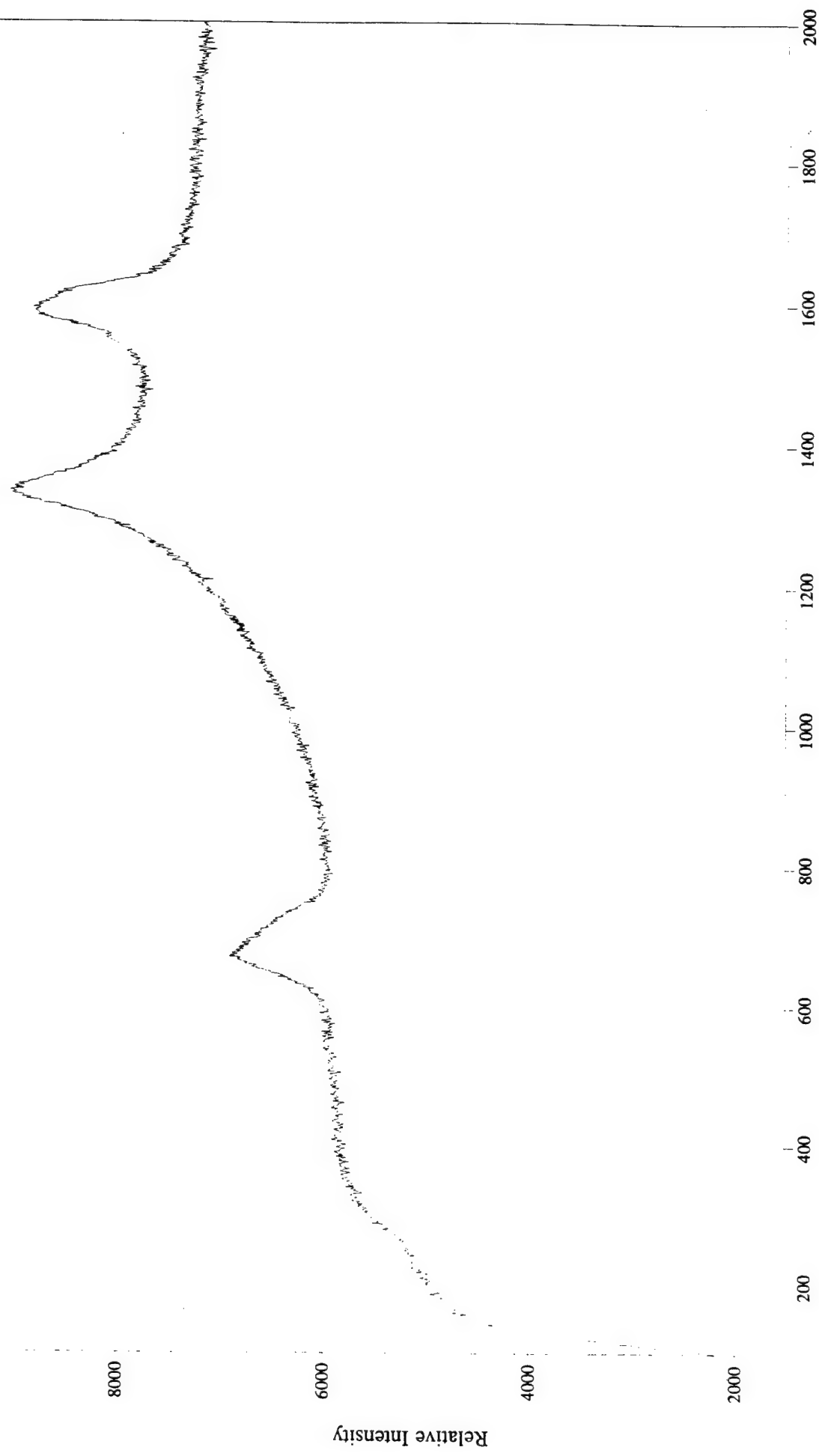
Molecular Microspectroscopy Laboratory



File # 1 : BAT202

Wavenumber Shift

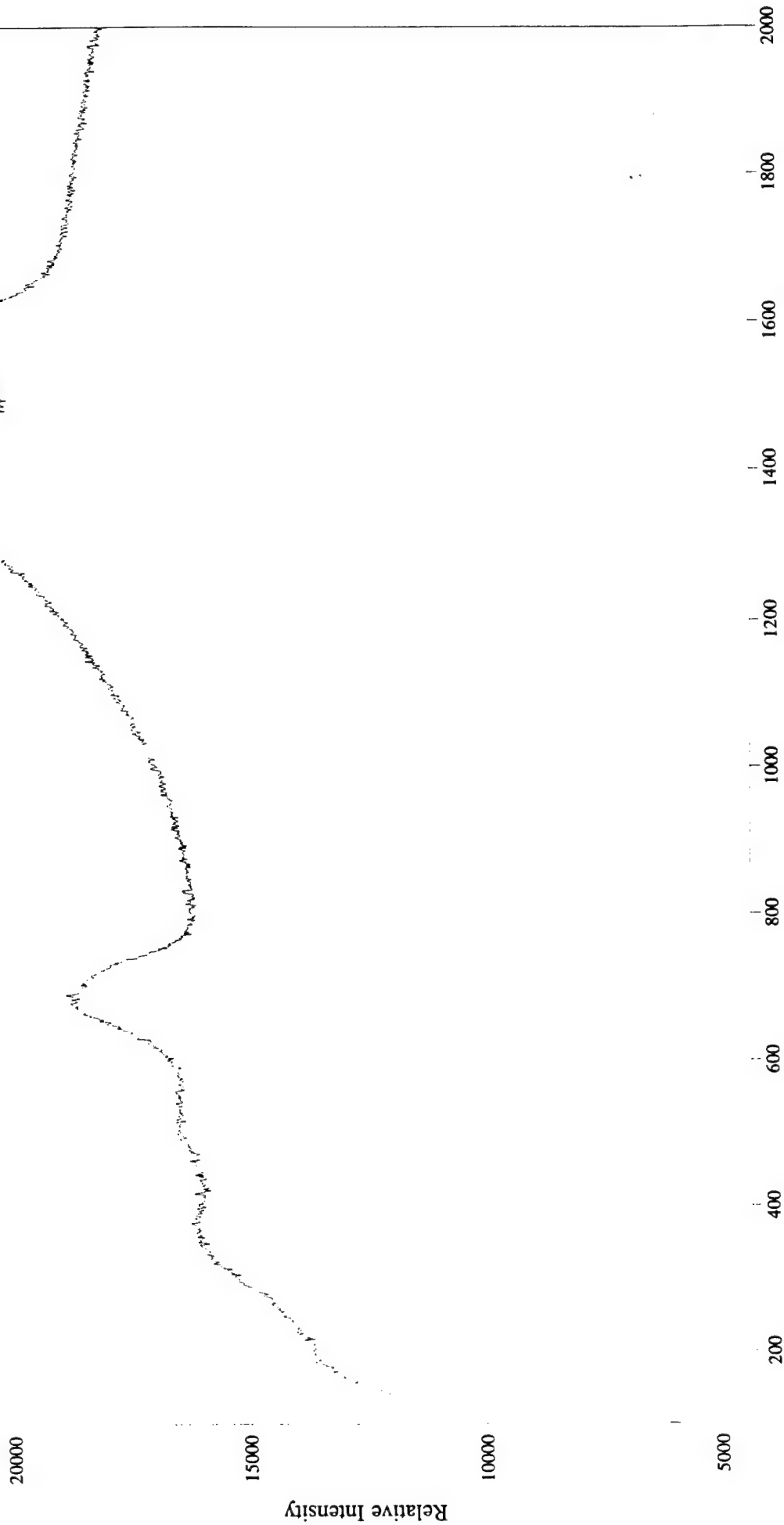
Molecular Microspectroscopy Laboratory



File # 1 : BAT203

Wavenumber Shift

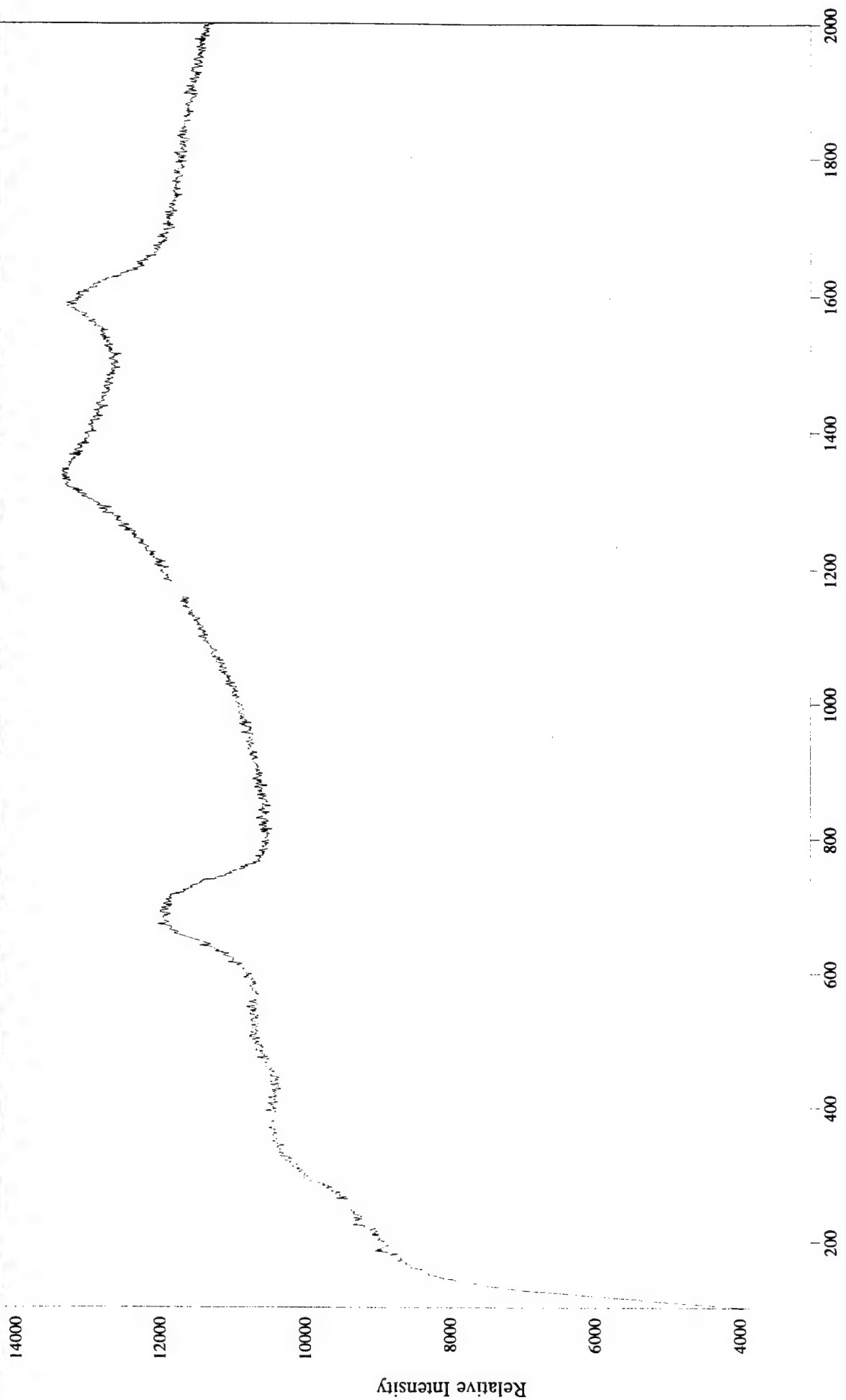
Molecular Microspectroscopy Laboratory



File # 1 : BAT204

Wavenumber Shift

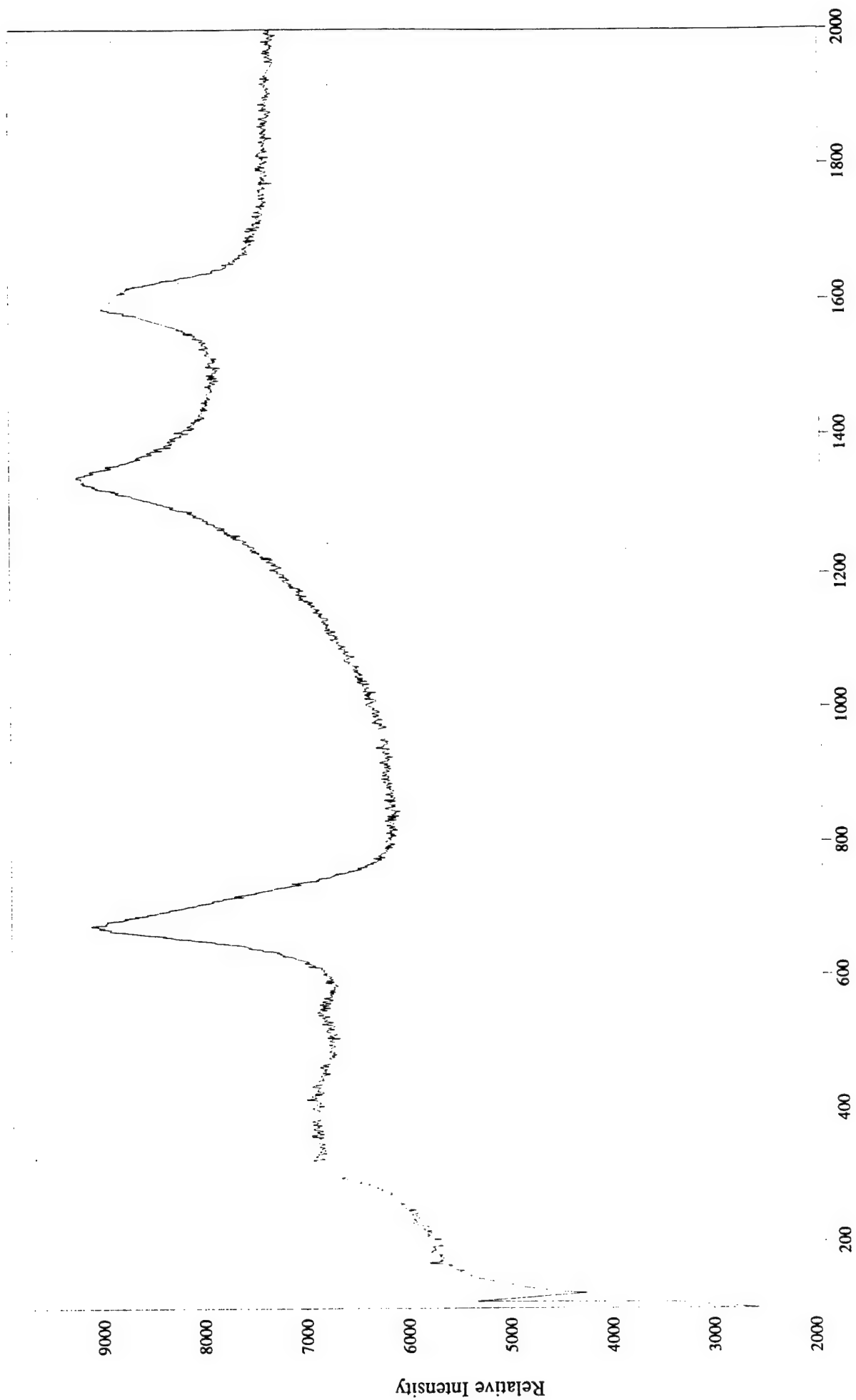
Molecular Microspectroscopy Laboratory



File # 2 : BAT205

Wavenumber Shift

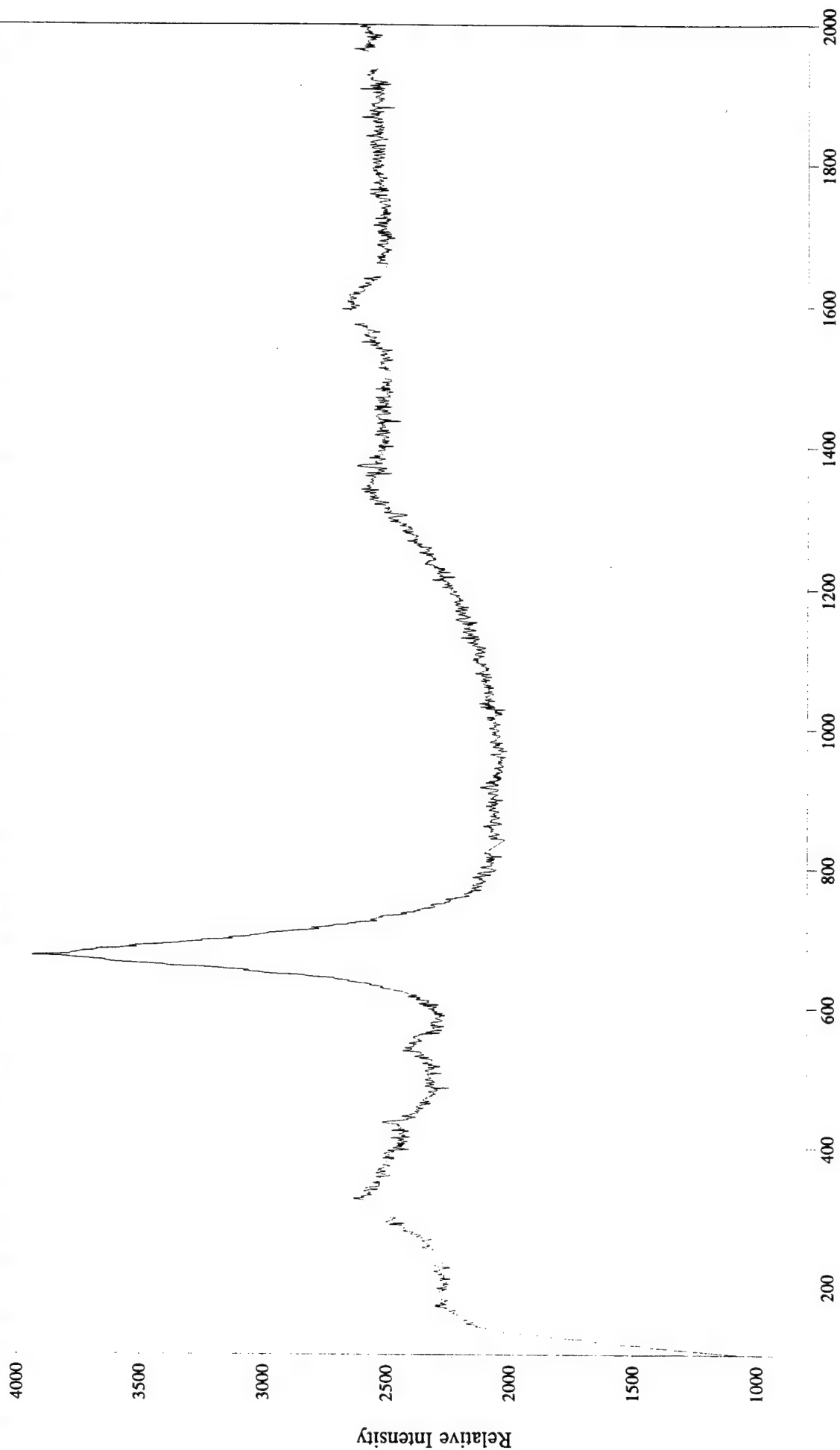
Molecular Microspectroscopy Laboratory



Molecular Microspectroscopy Laboratory

Wavenumber Shift

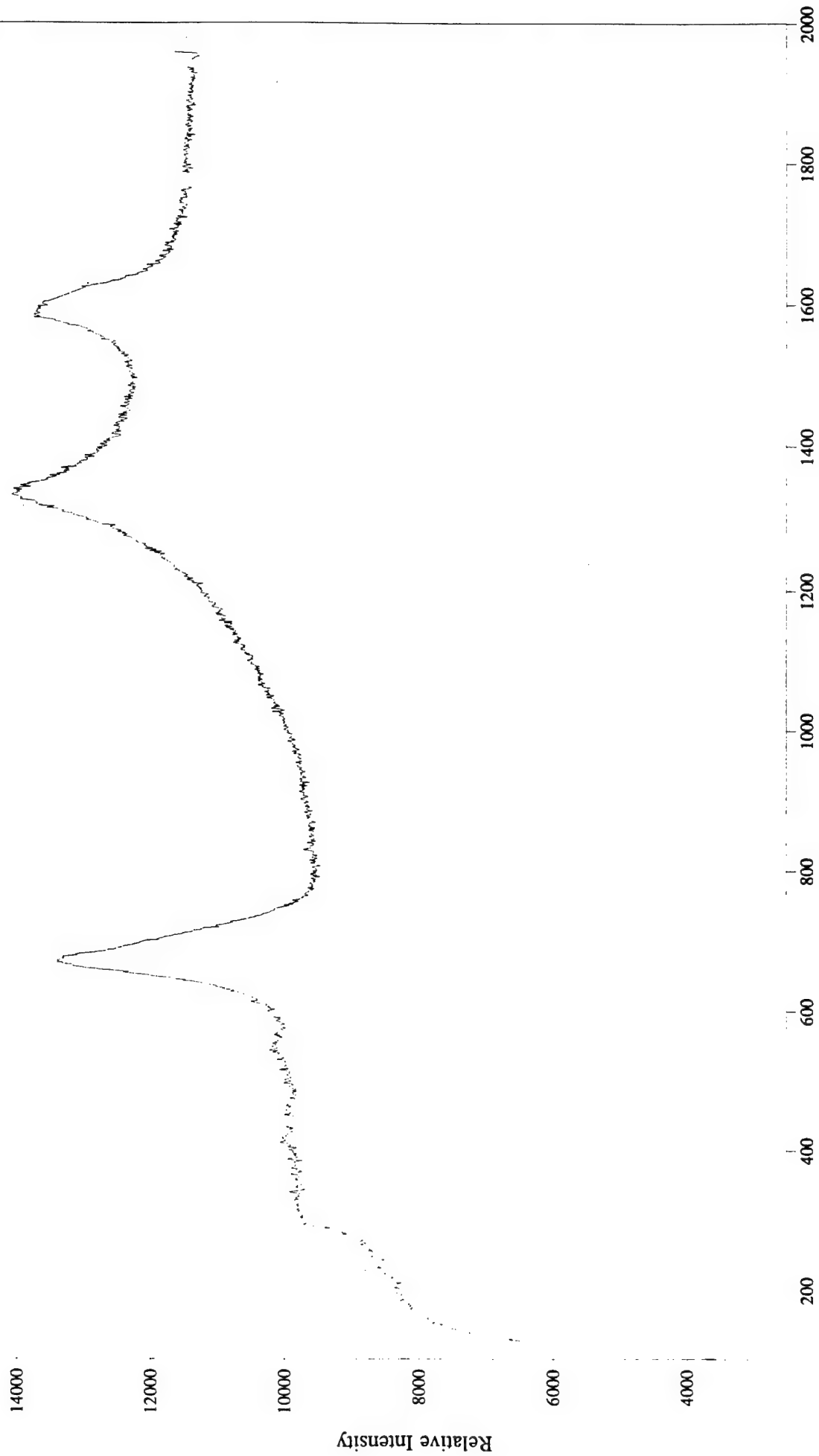
File # 1 : BAT206



File # 1 : BAT207

Wavenumber Shift

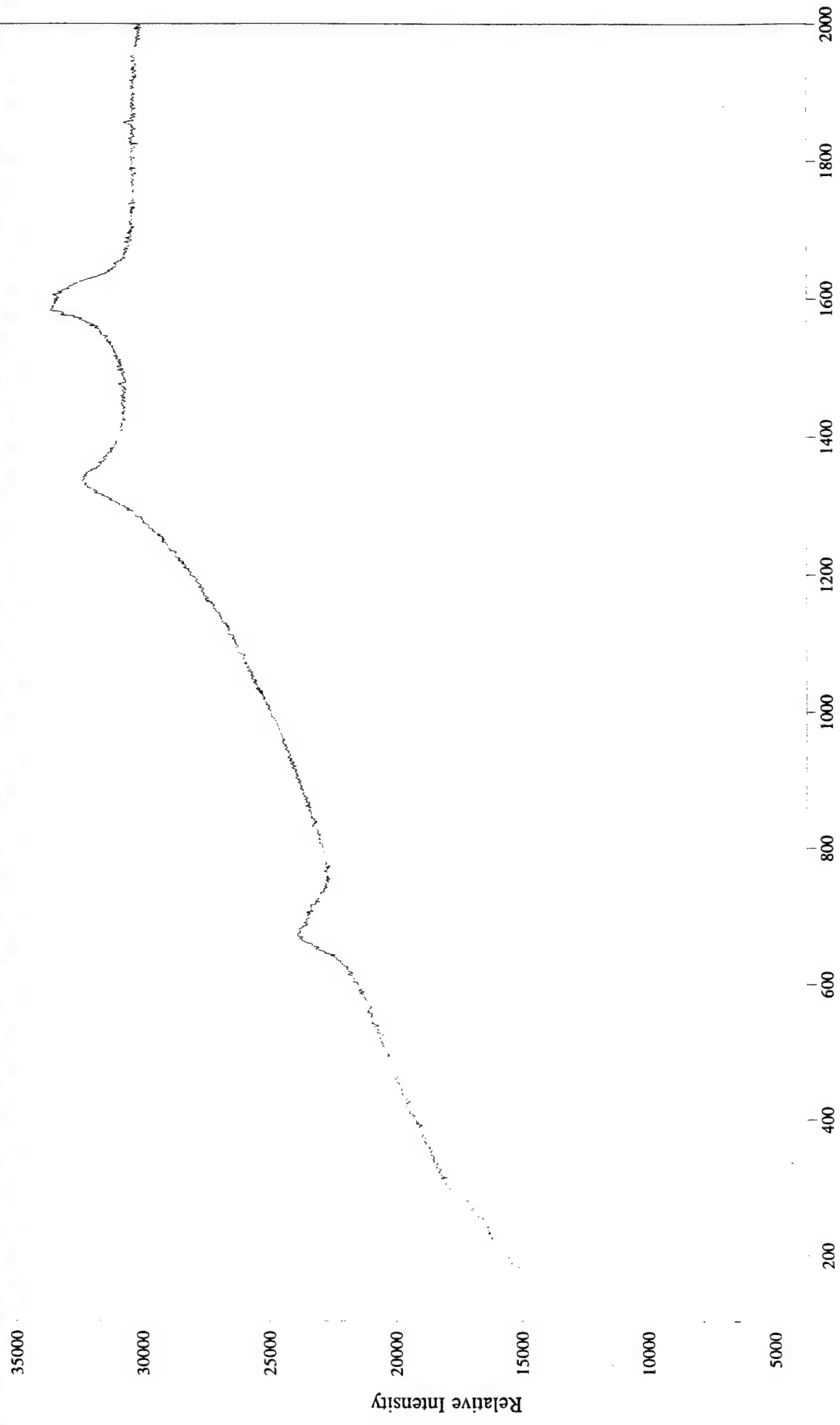
Molecular Microspectroscopy Laboratory



Molecular Microspectroscopy Laboratory

Wavenumber Shift

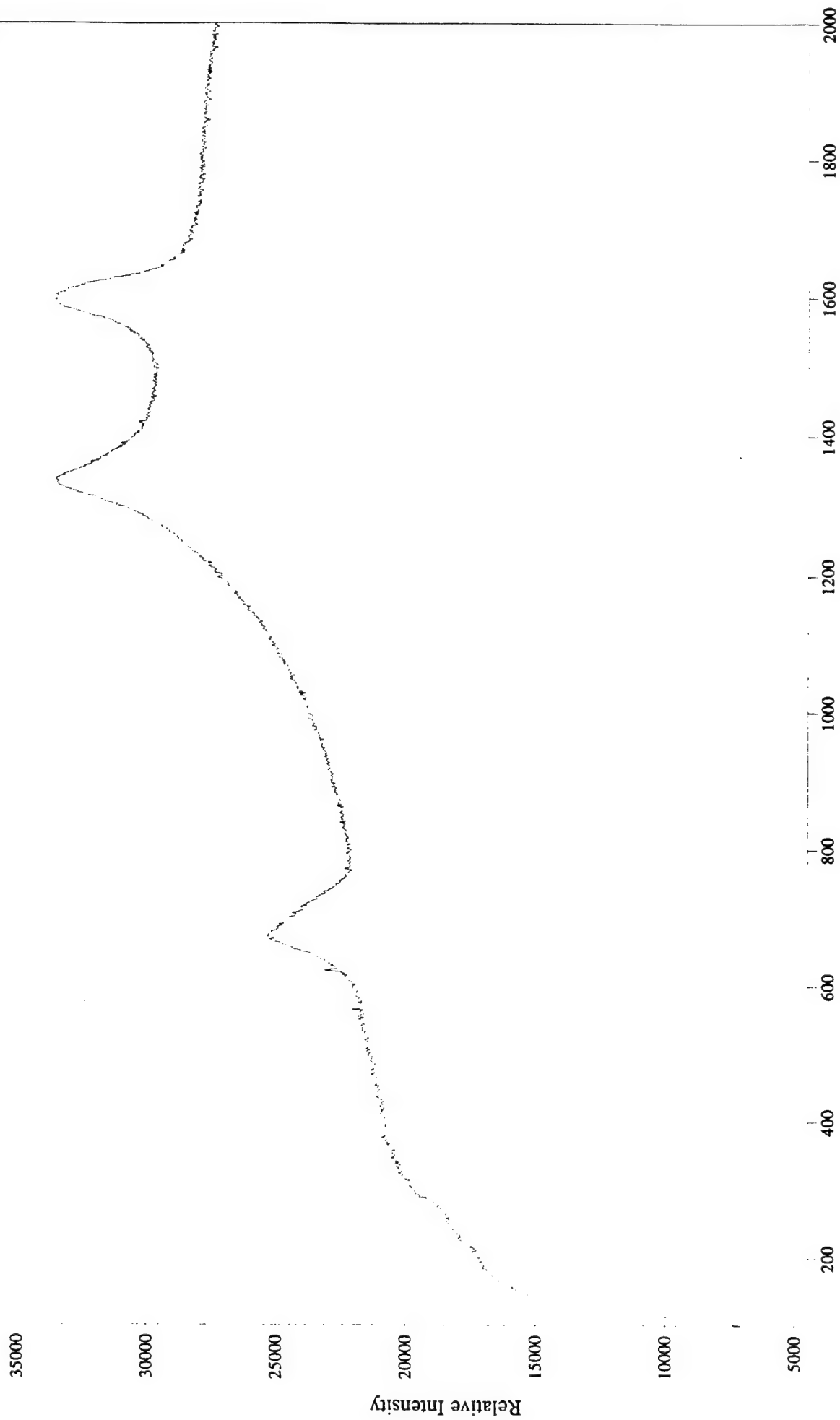
File # 1 : BAT208



File # 1 : BAT209

Wavenumber Shift

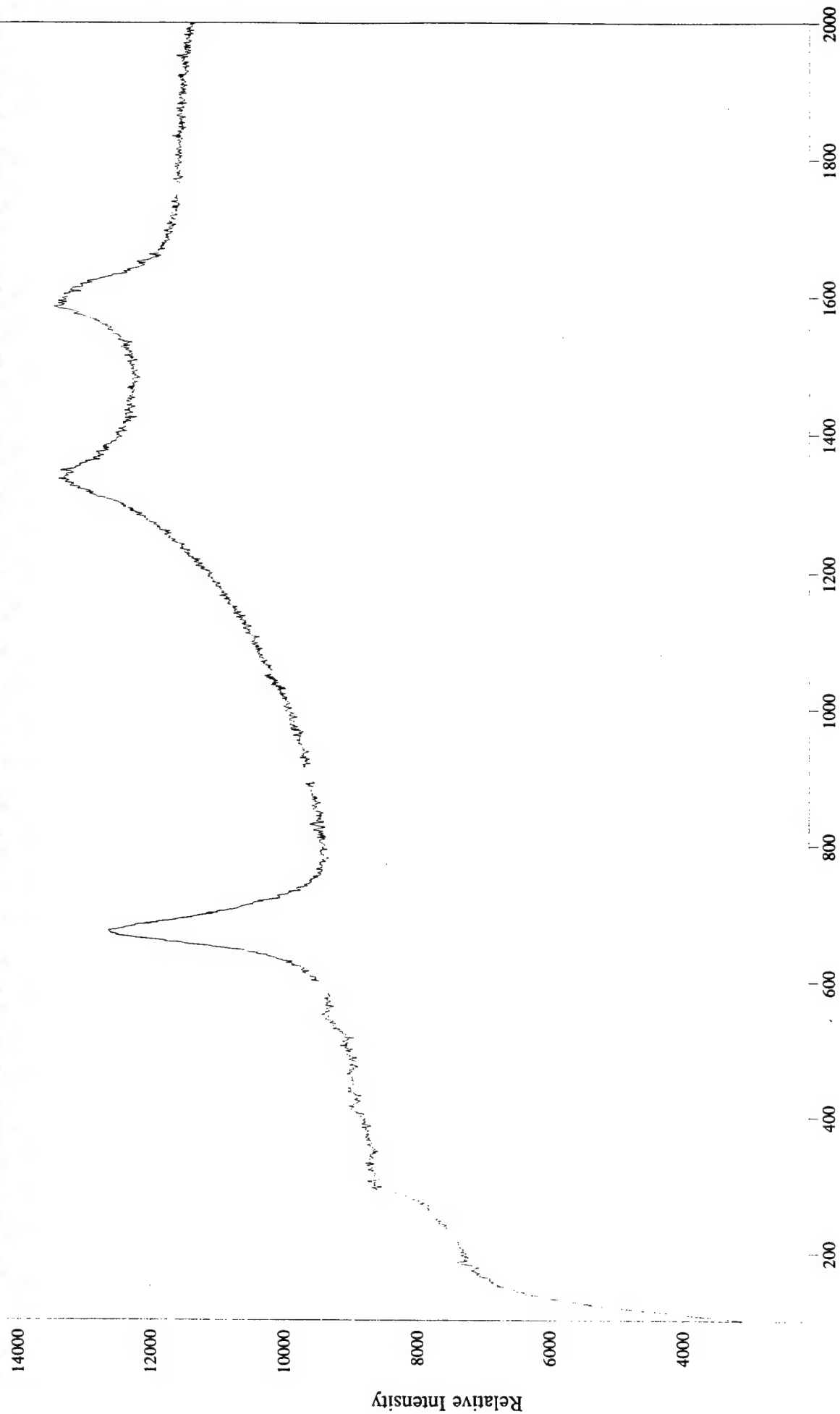
Molecular Microspectroscopy Laboratory



File # 1 : BAT210

Wavenumber Shift

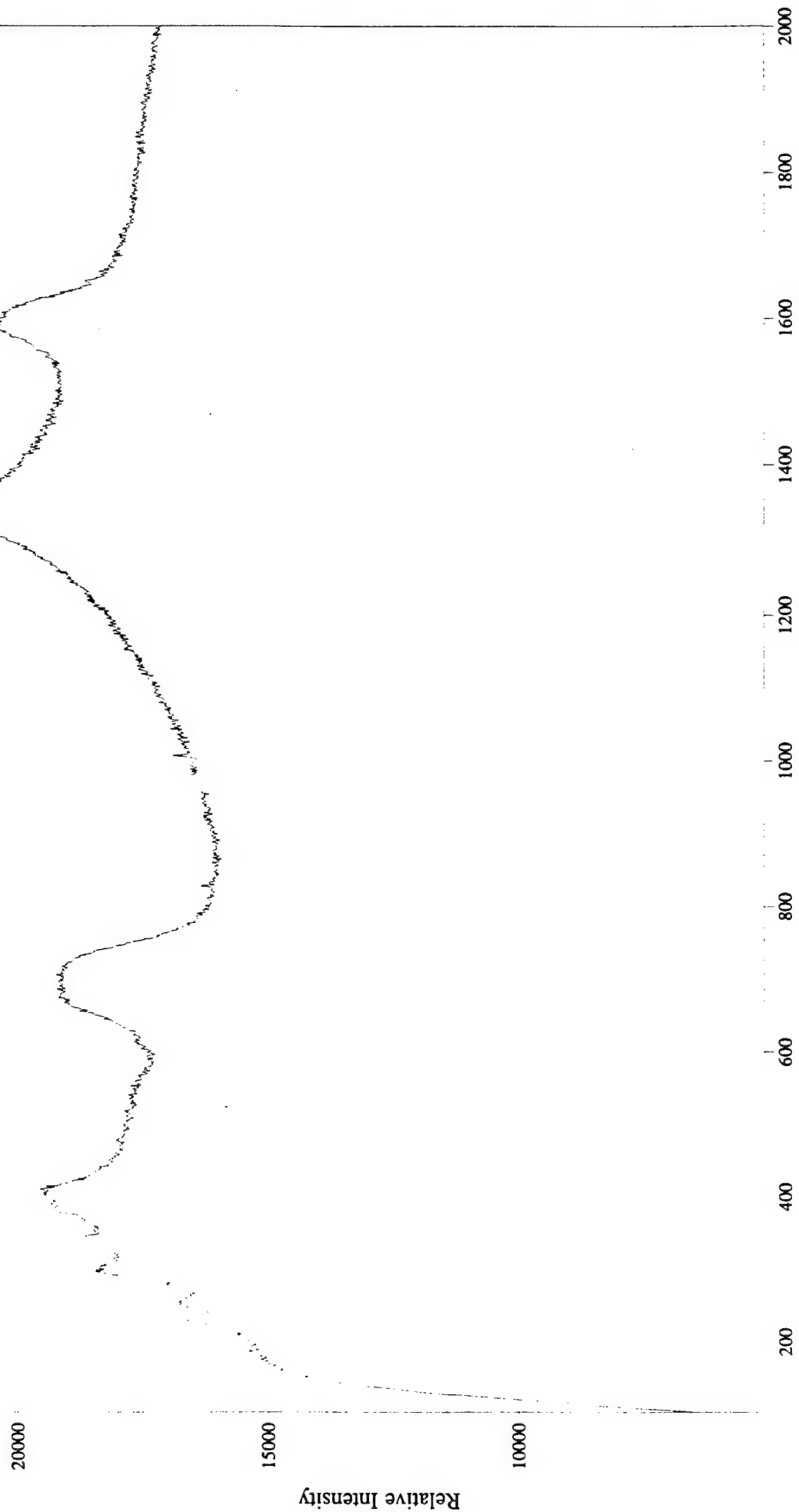
Molecular Microspectroscopy Laboratory



File # 1 : BAT211

Wavenumber Shift

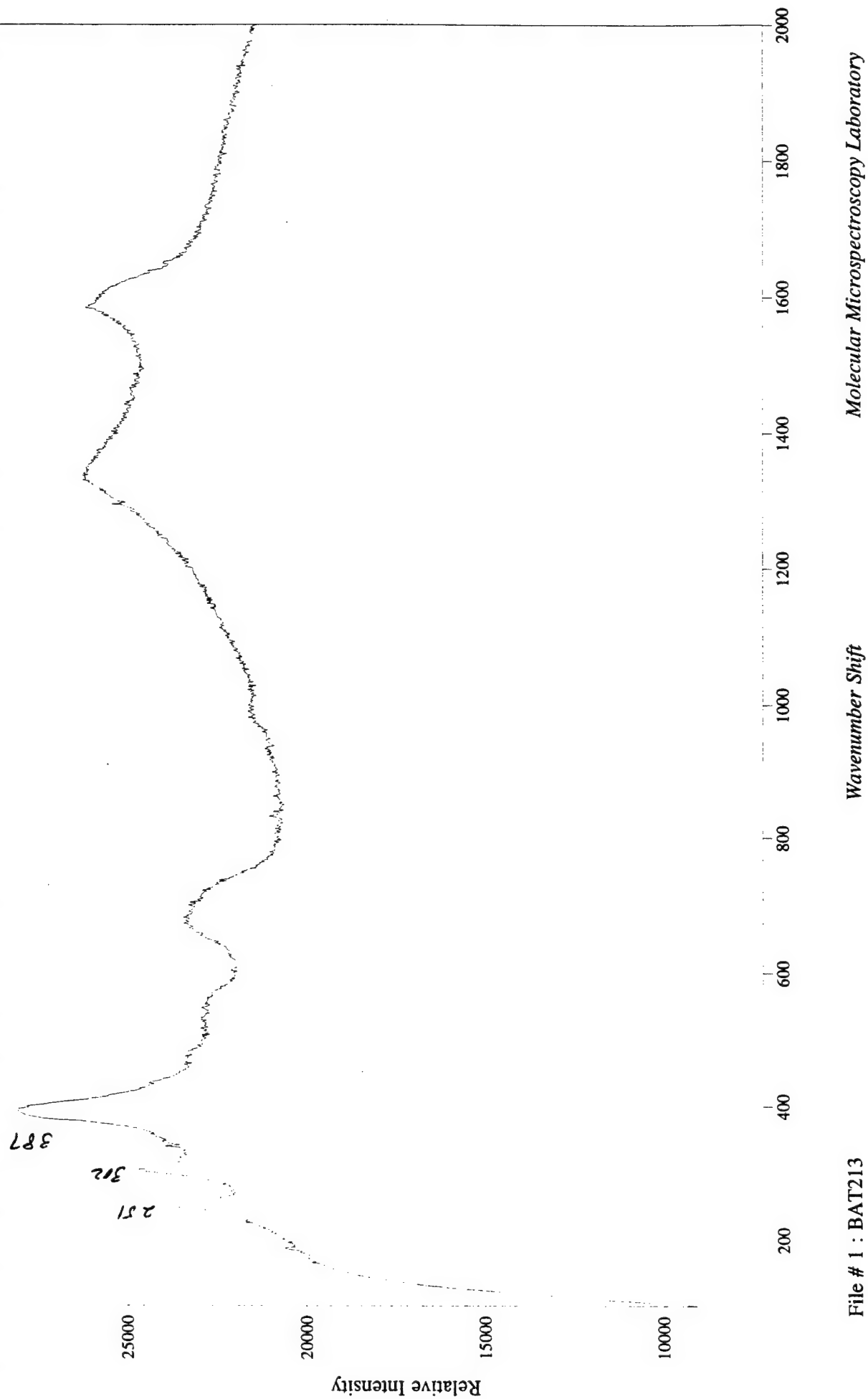
Molecular Microspectroscopy Laboratory



File # 1 : BAT212

Wavenumber Shift

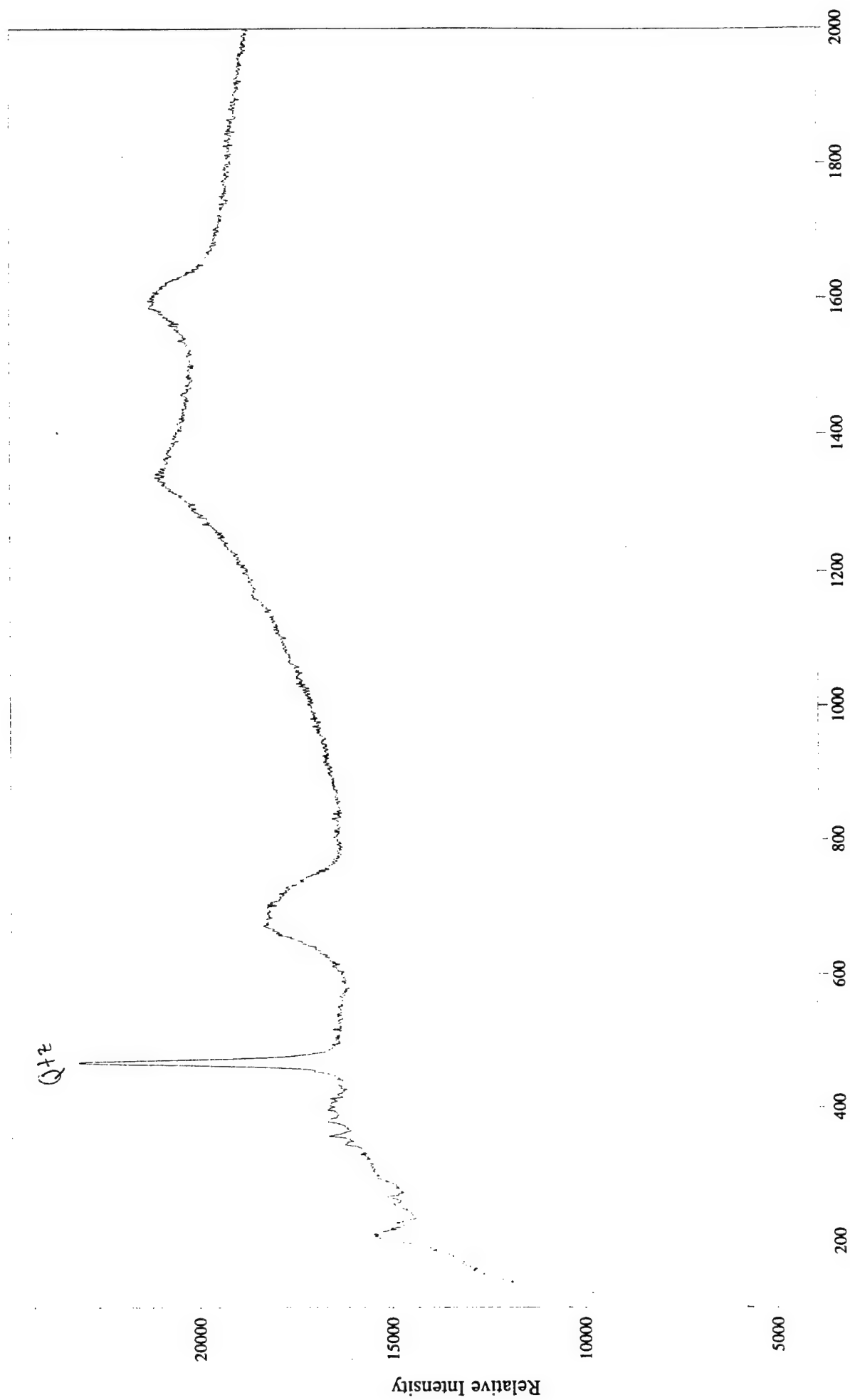
Molecular Microspectroscopy Laboratory



File # 1 : BAT213

Wavenumber Shift

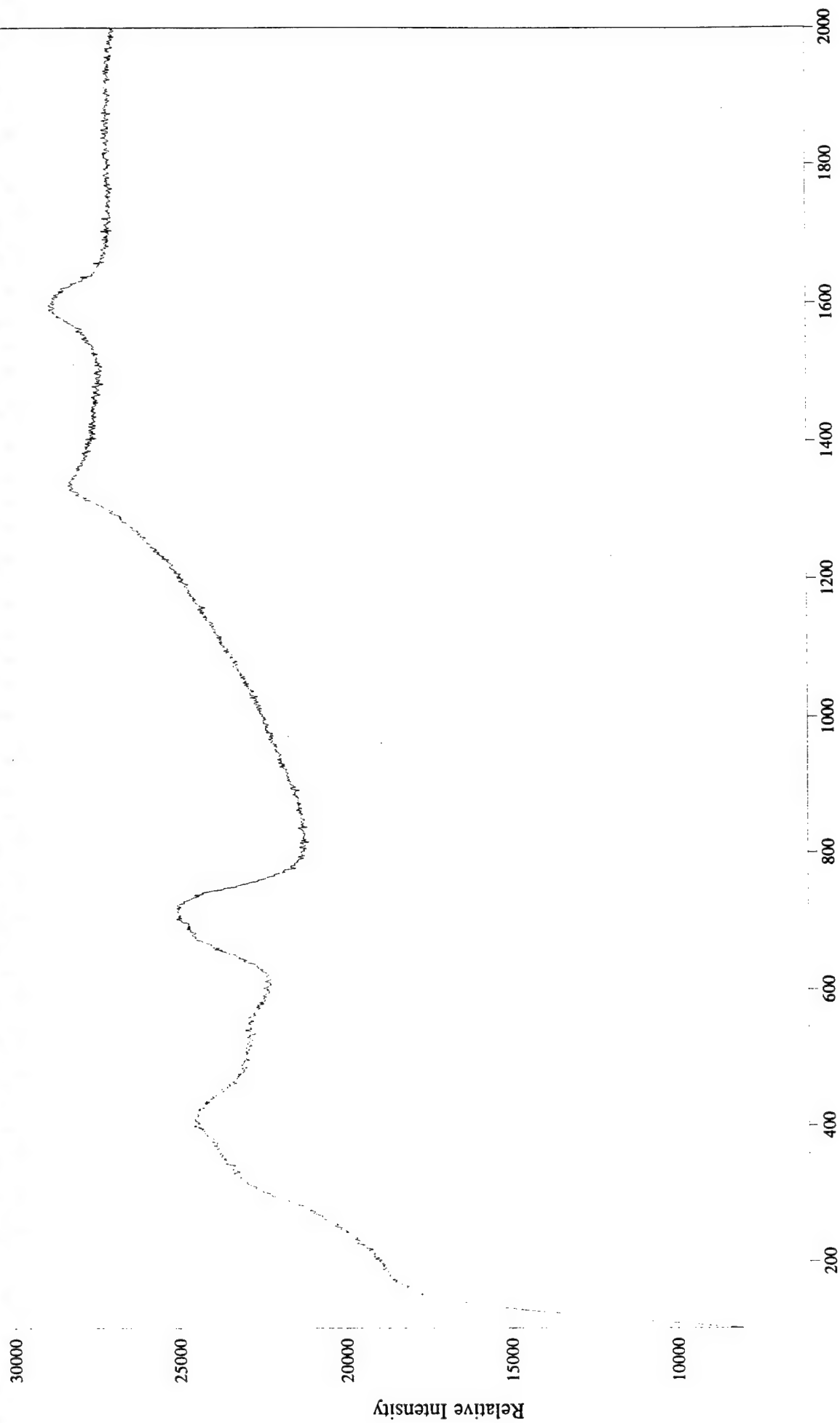
Molecular Microspectroscopy Laboratory



File # 1 : BAT214

Wavenumber Shift

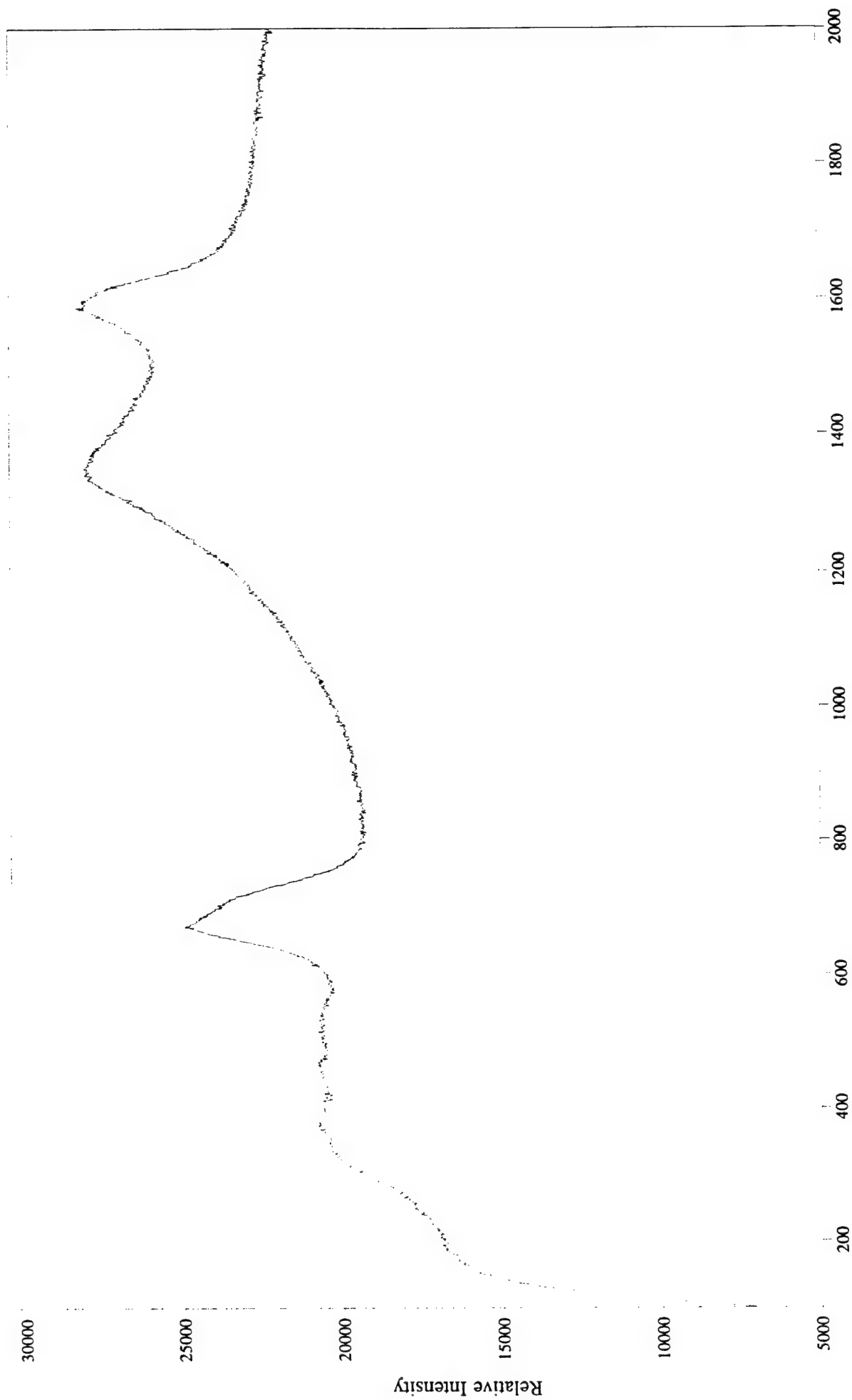
Molecular Microspectroscopy Laboratory



File # 1 : BAT215

Wavenumber Shift

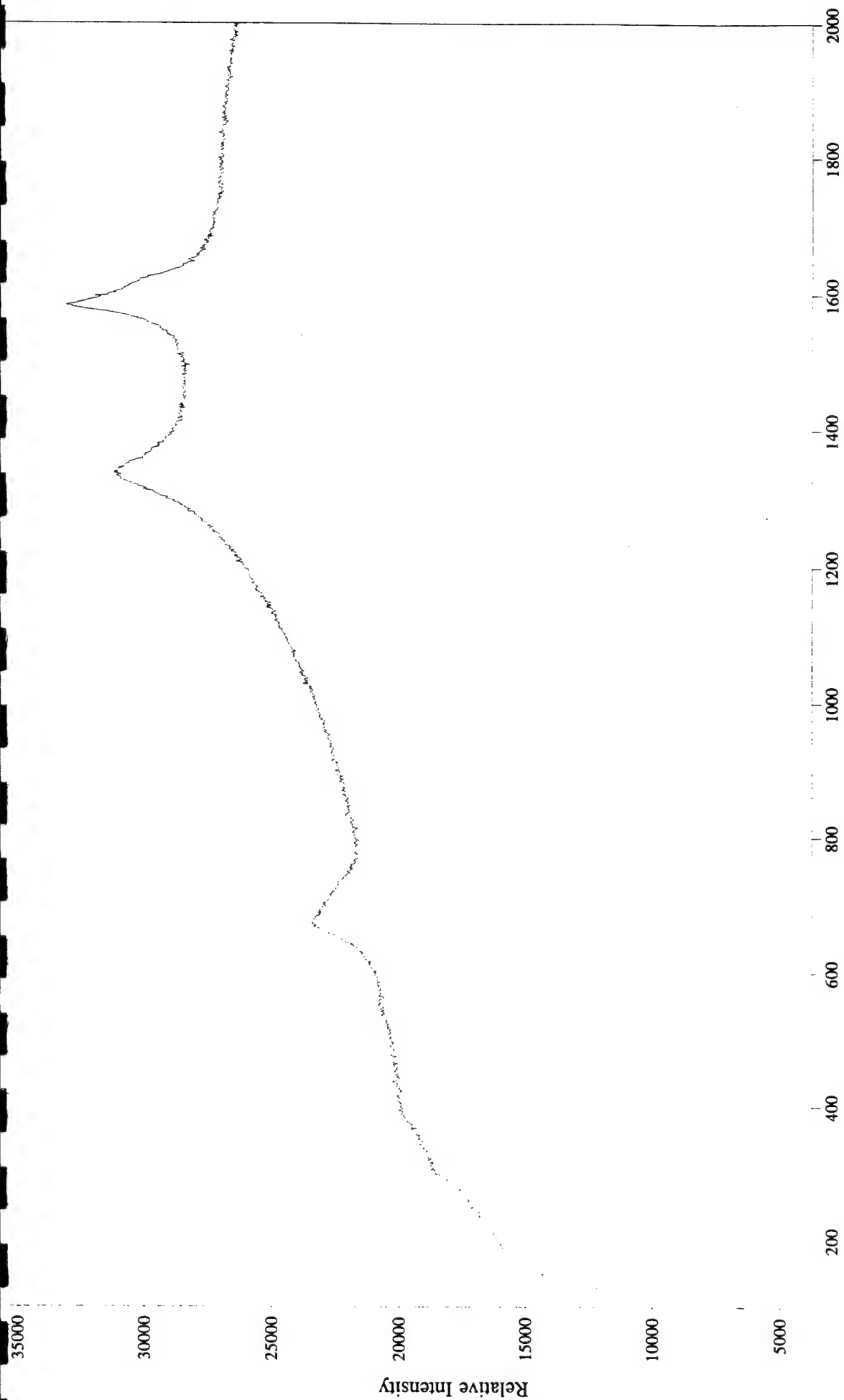
Molecular Microspectroscopy Laboratory



File # 1 : BAT216

Wavenumber Shift

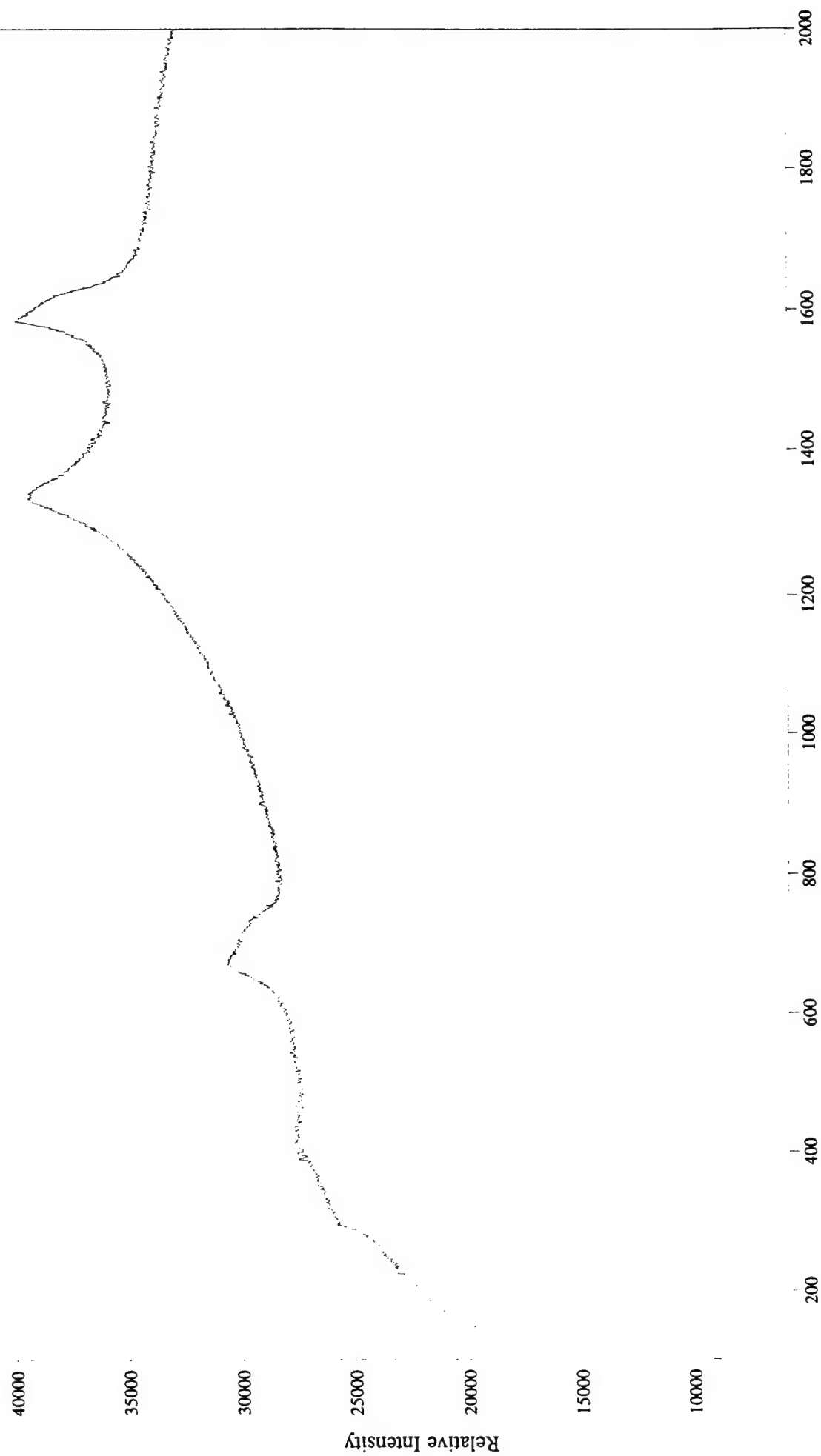
Molecular Microspectroscopy Laboratory



File # 1 : BAT217

Wavenumber Shift

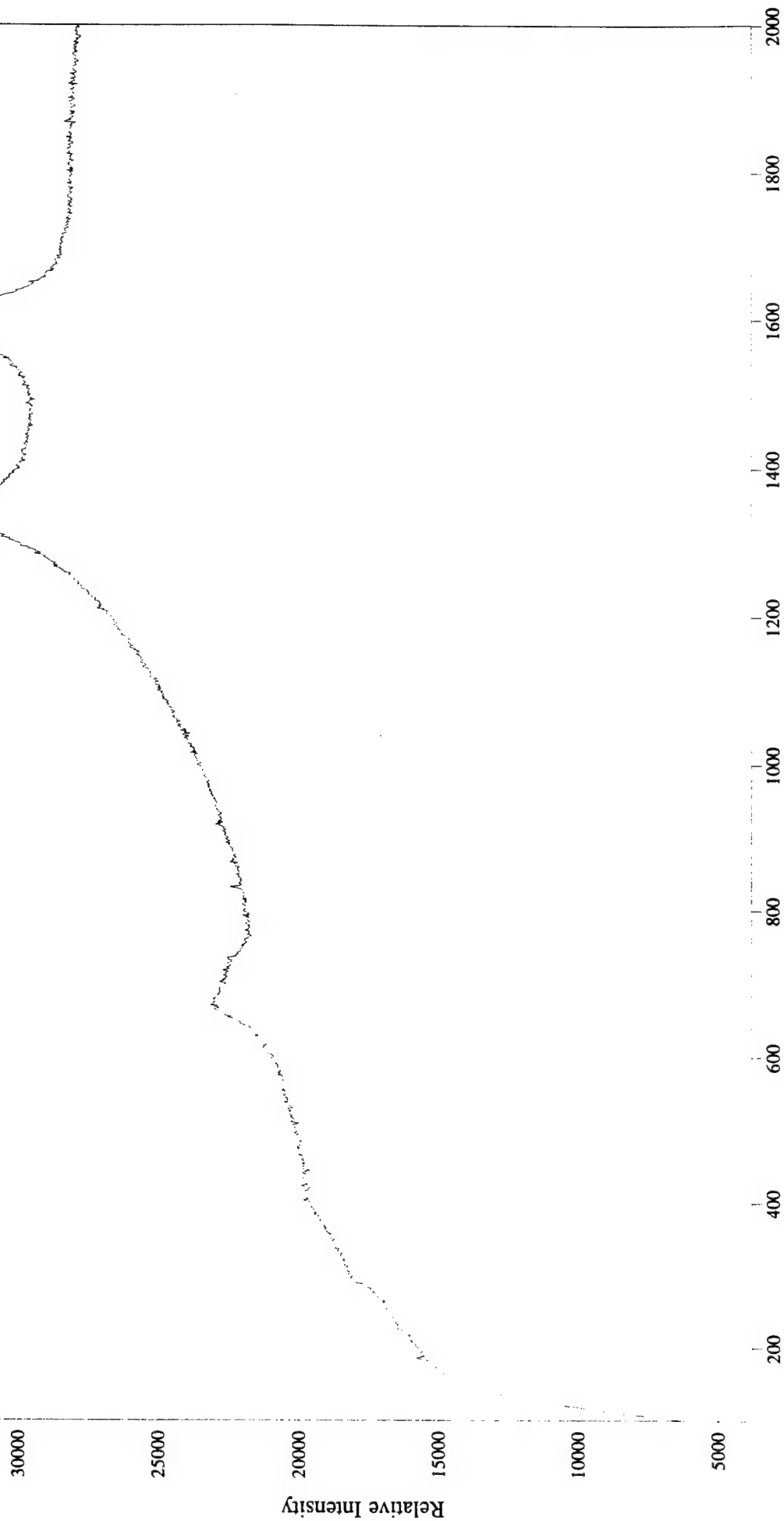
Molecular Microspectroscopy Laboratory



File # 1 : BAT218

Wavenumber Shift

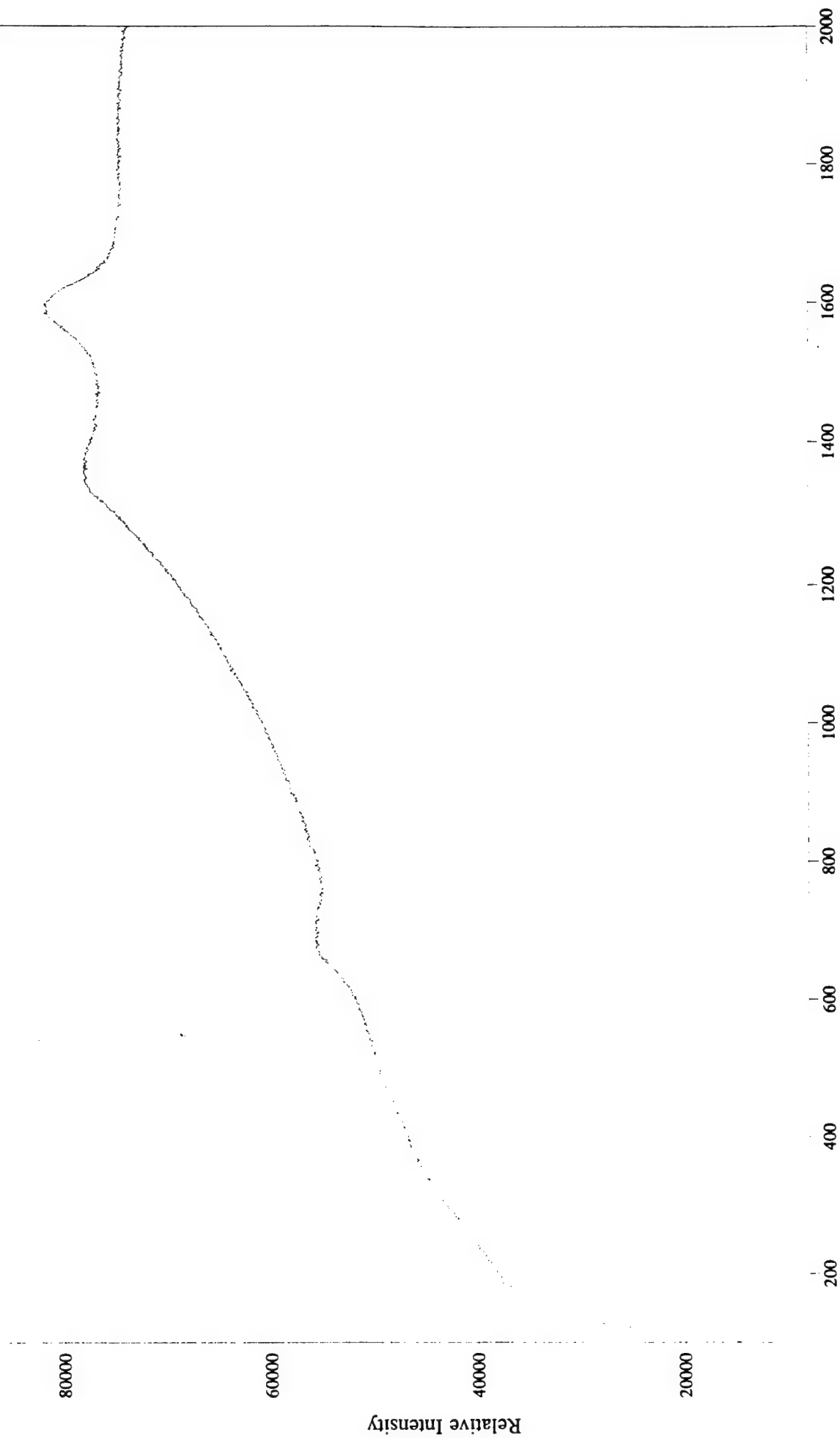
Molecular Microspectroscopy Laboratory



File # 1 : BAT219

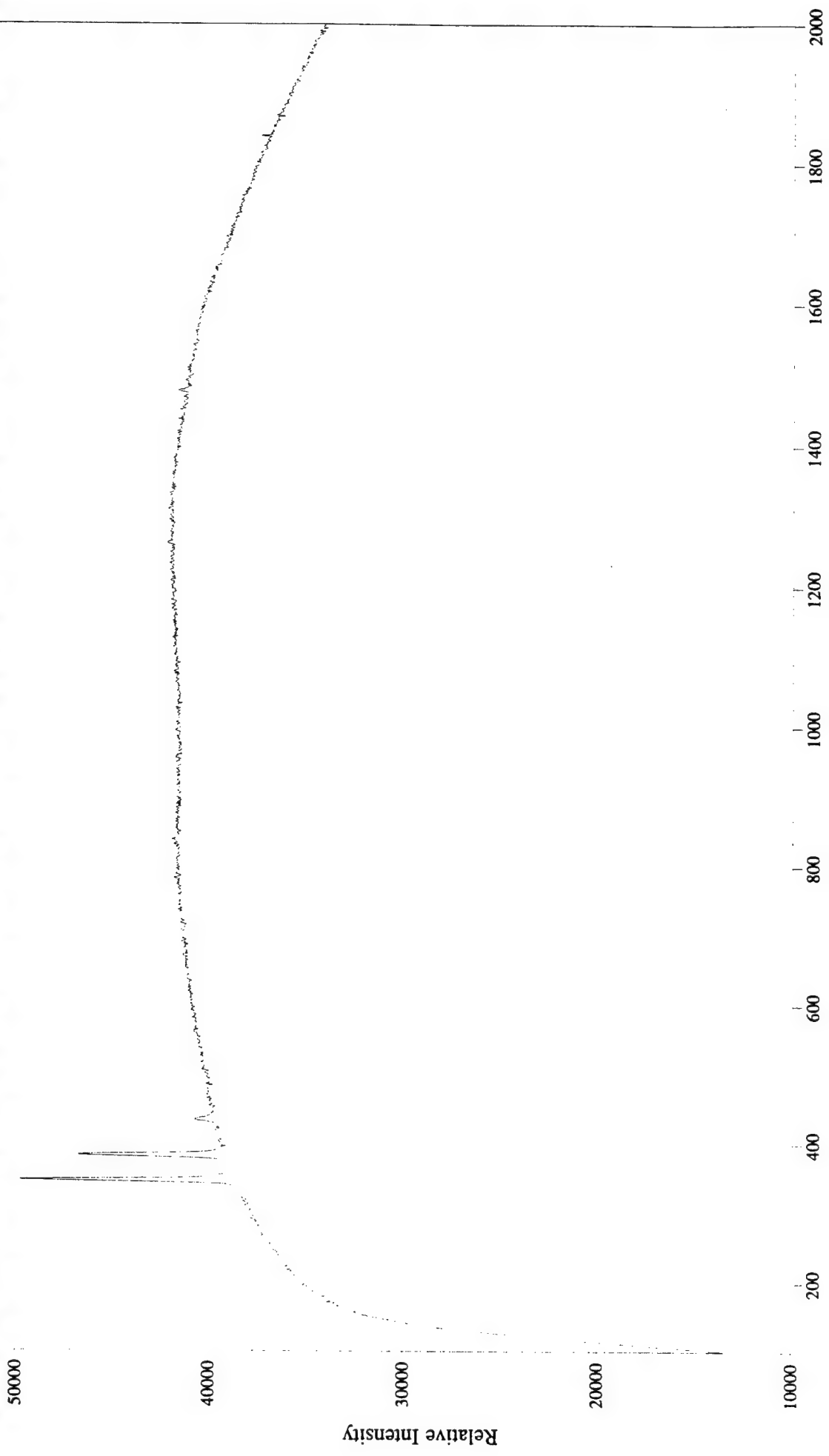
Wavenumber Shift

Molecular Microspectroscopy Laboratory



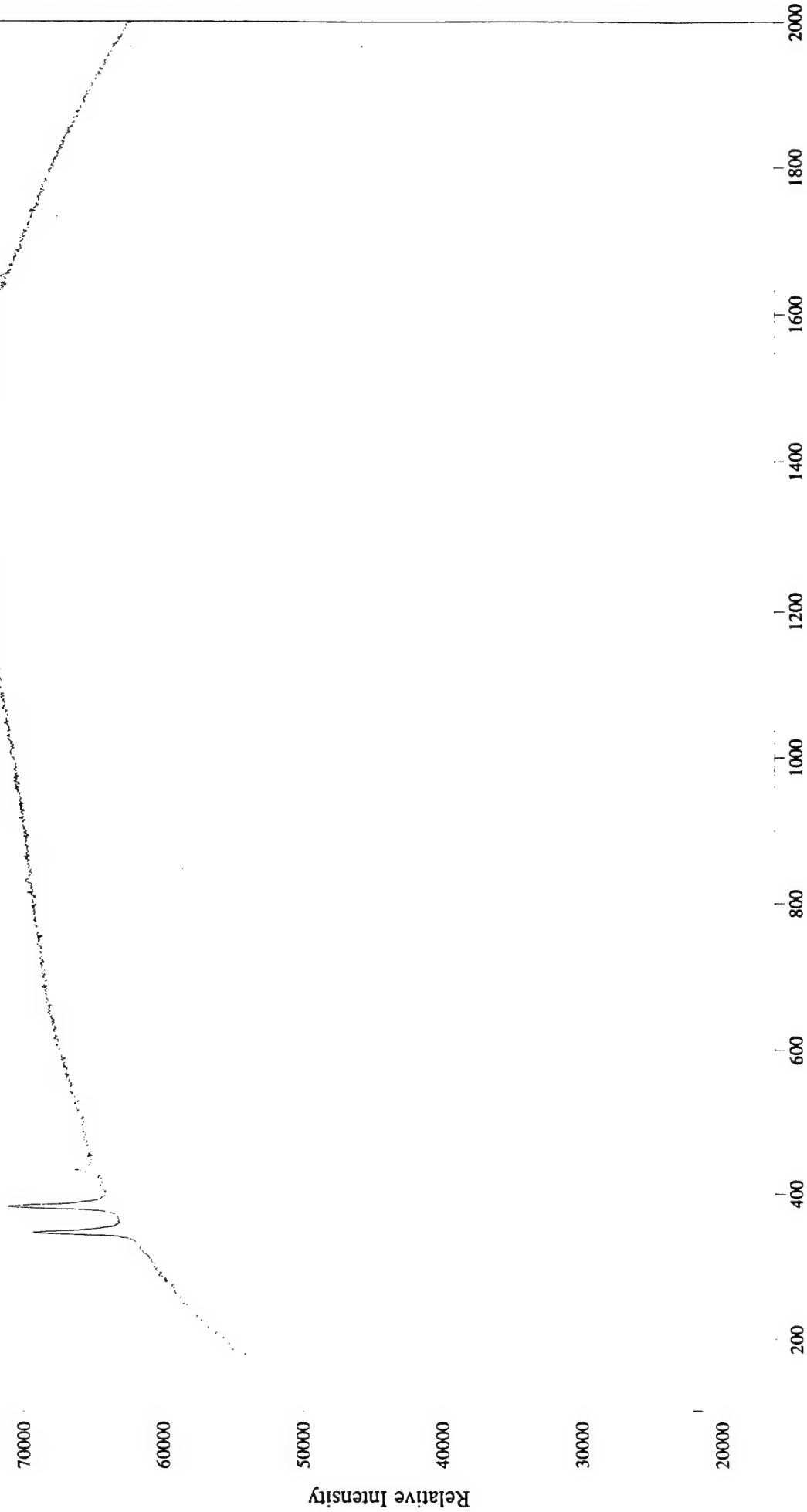
File # 1 : BAT220

Molecular Microspectroscopy Laboratory



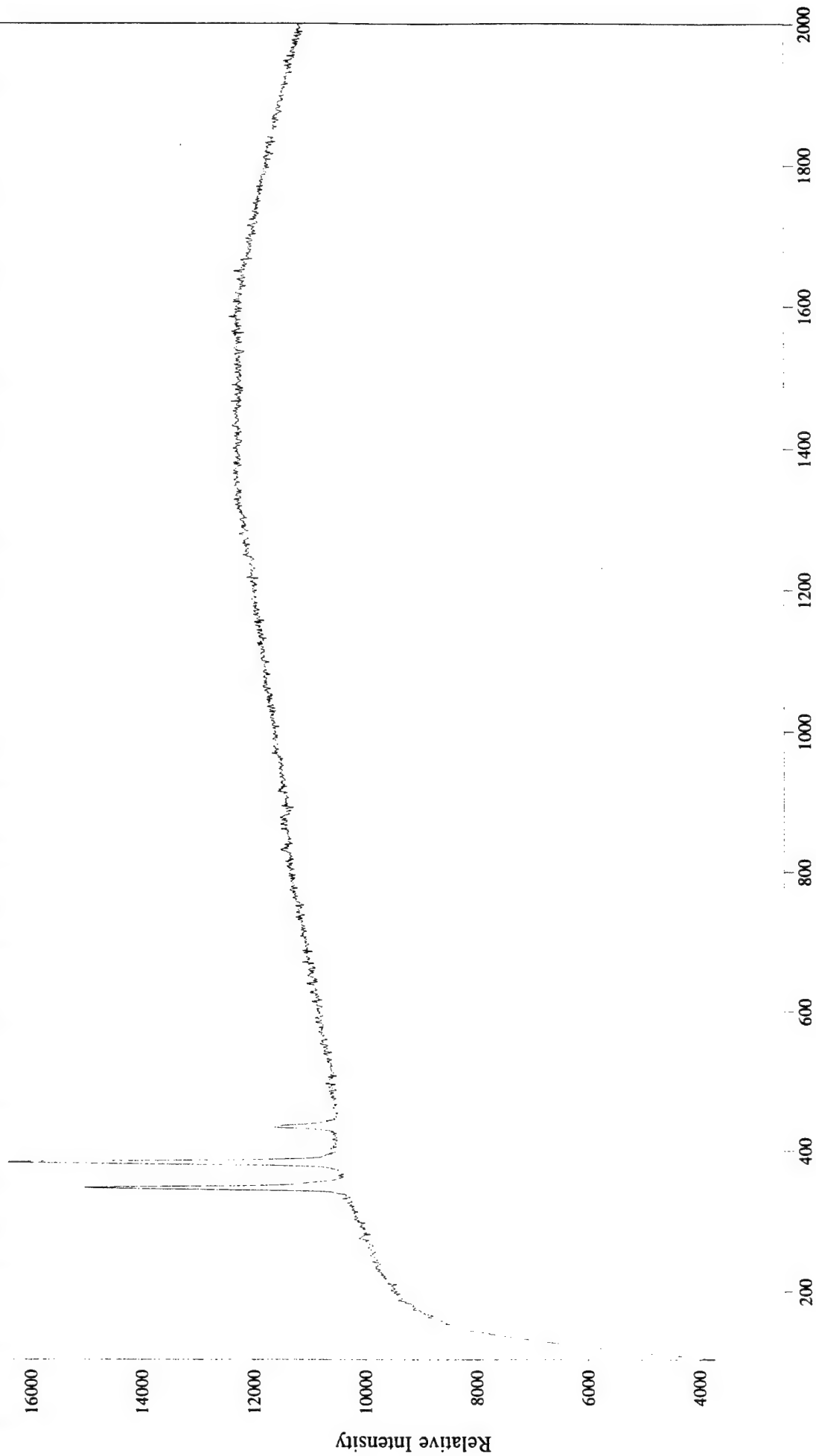
File # 1 : BAT221

Molecular Microspectroscopy Laboratory



File # 1 : BAT222

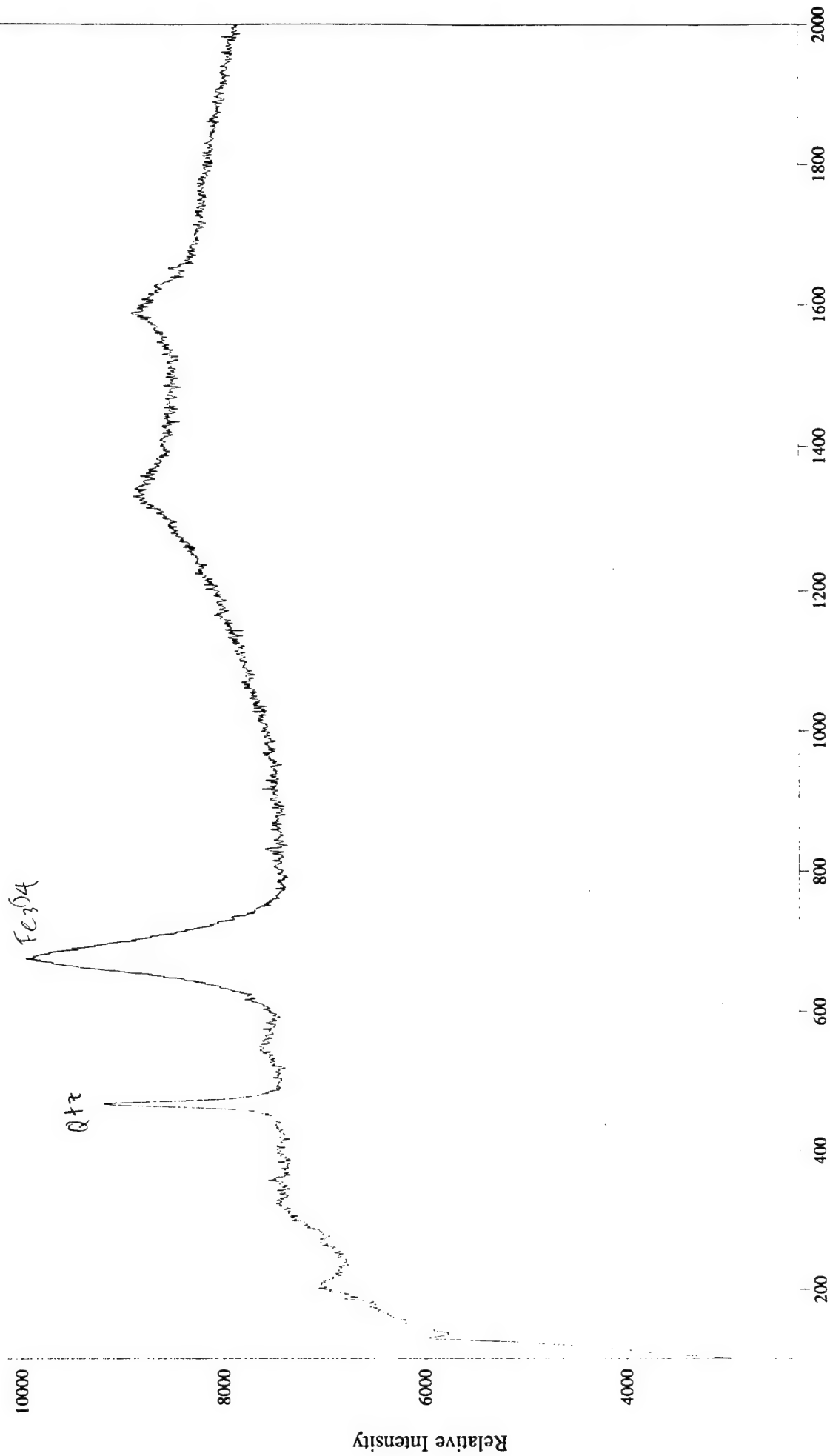
Molecular Microspectroscopy Laboratory



File # 1 : BAT223

Wavenumber Shift

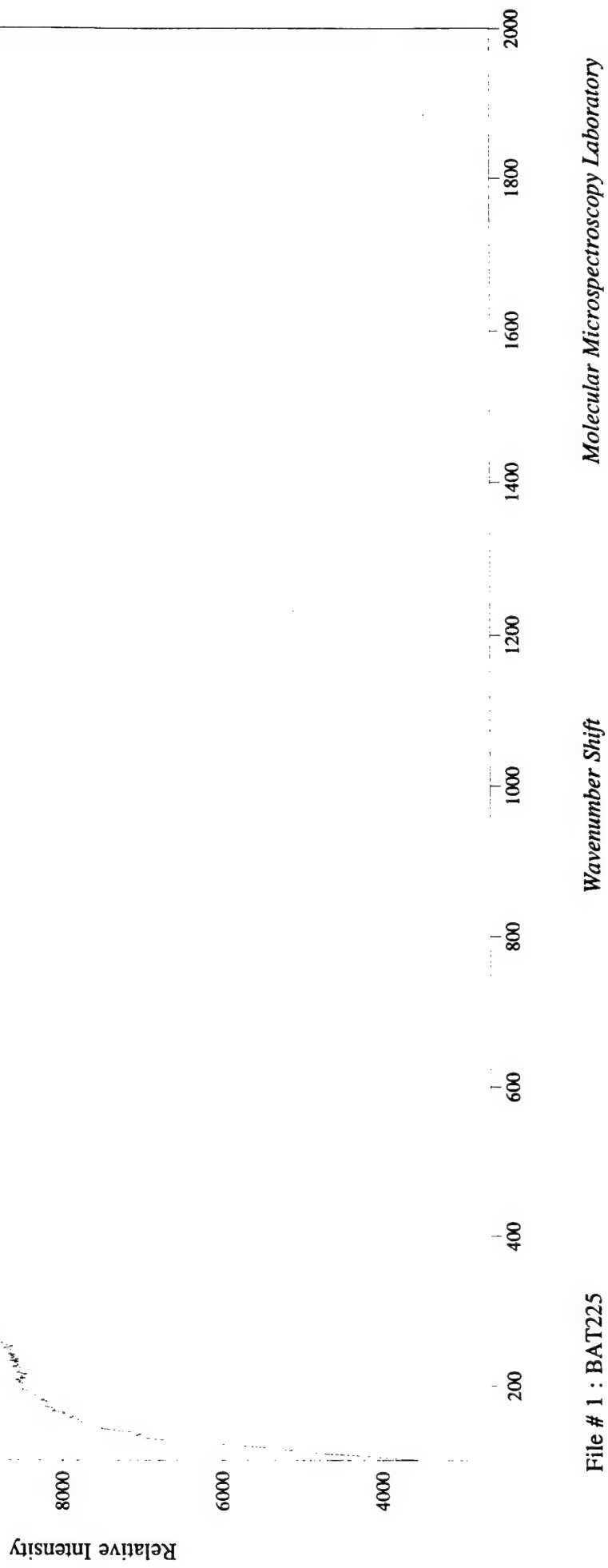
Molecular Microspectroscopy Laboratory

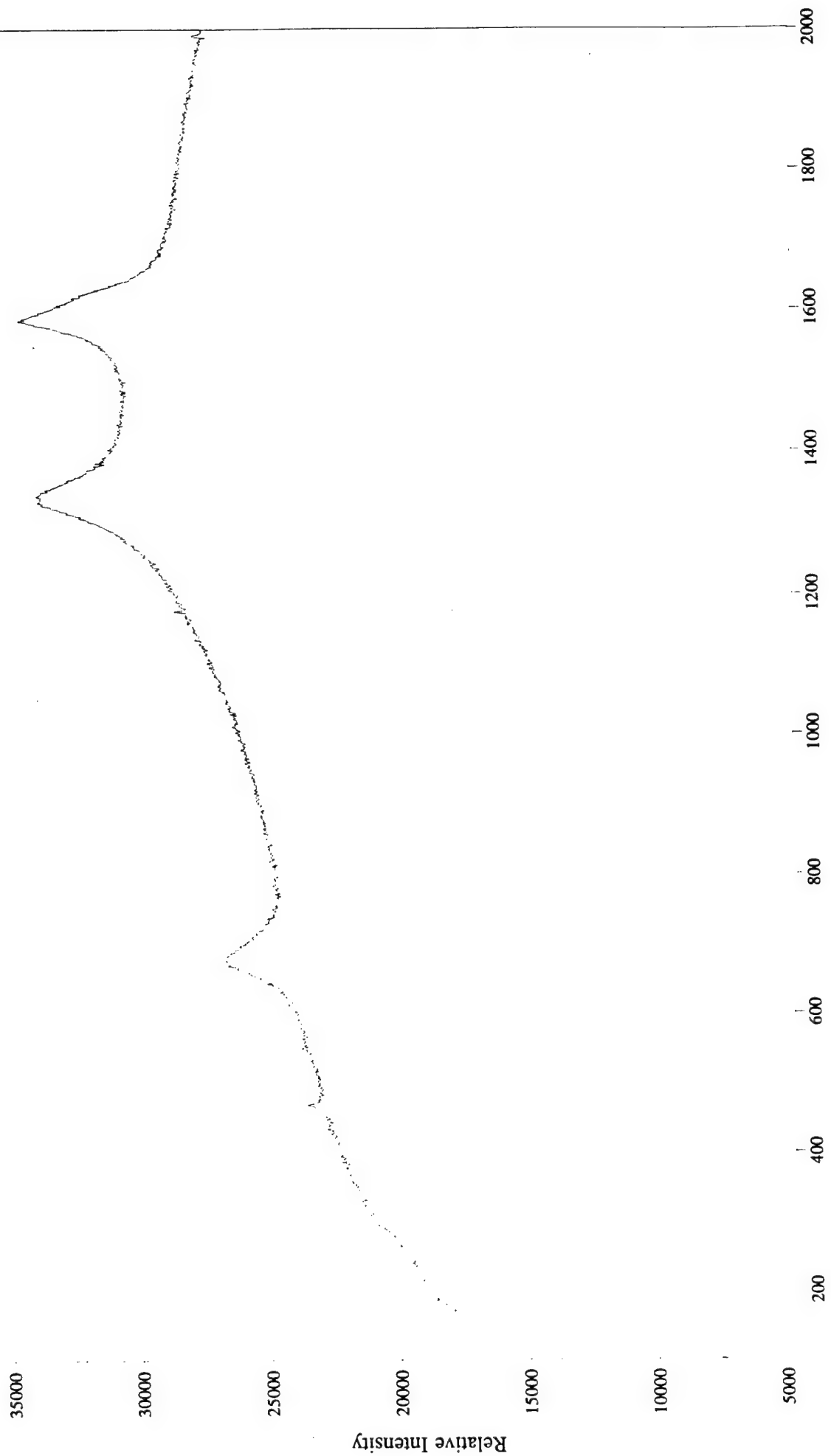


File # 1 : BAT224

Wavenumber Shift

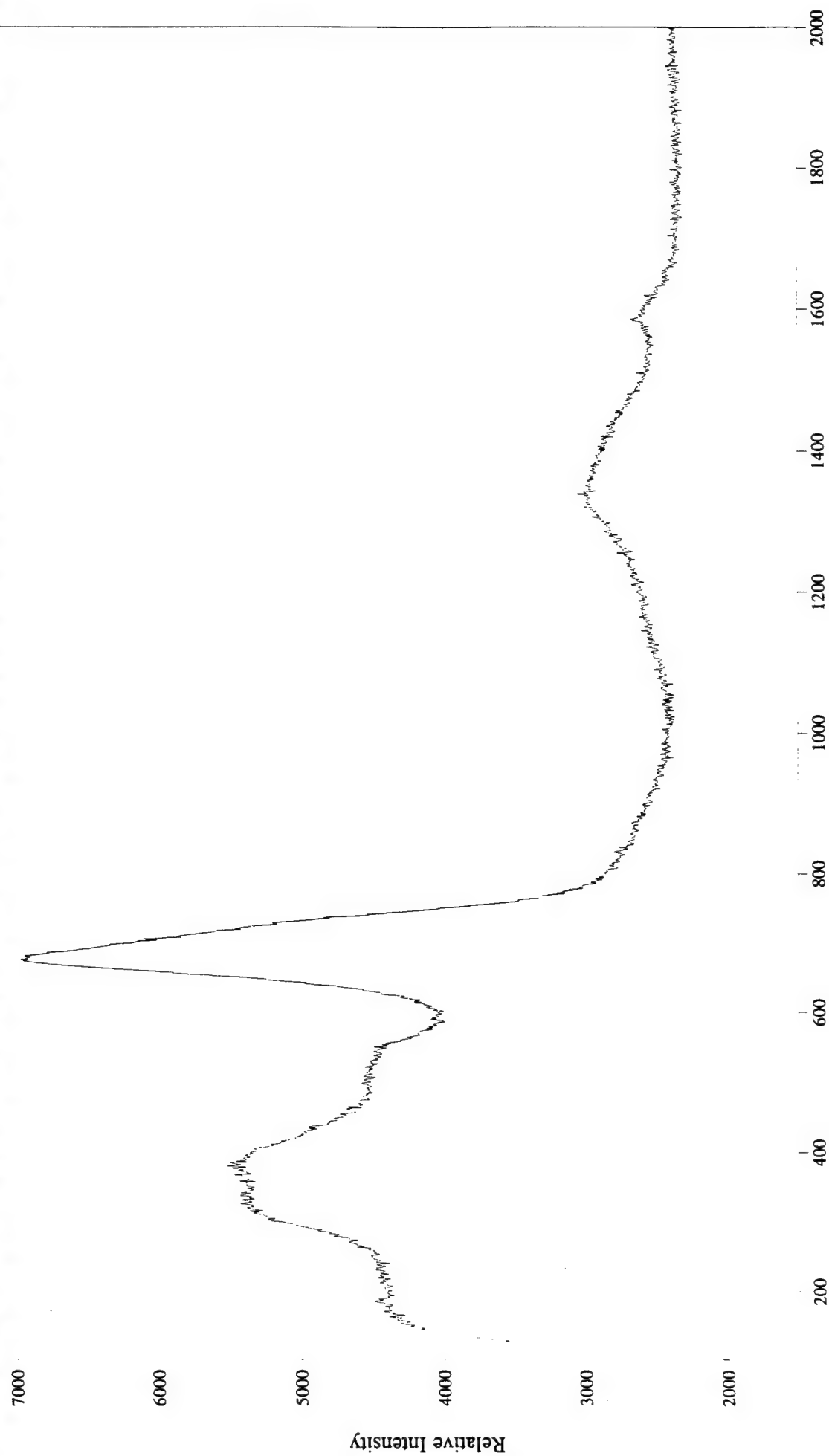
Molecular Microspectroscopy Laboratory





File # 1 : BAT226

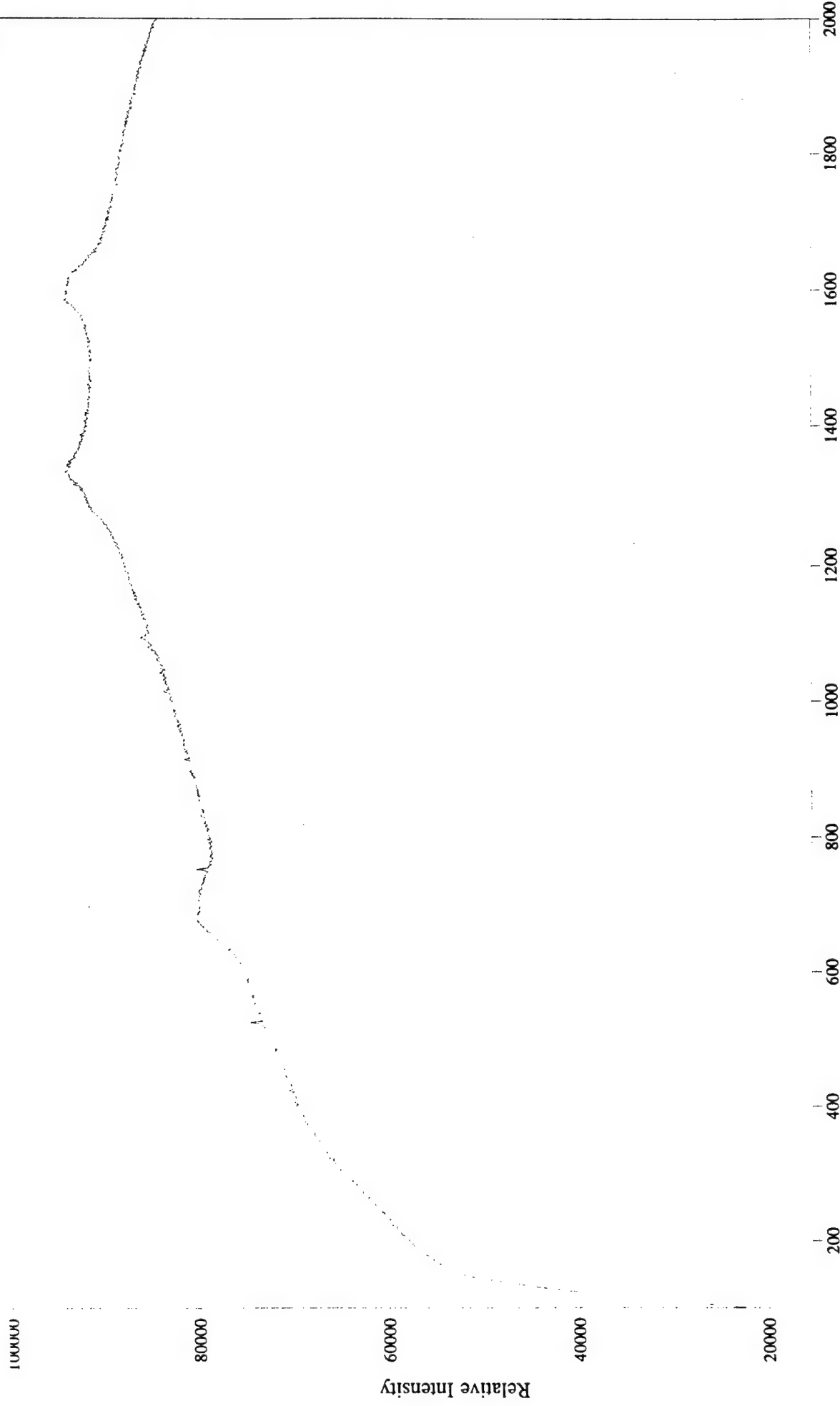
Molecular Microspectroscopy Laboratory



File # 1 : BAT227

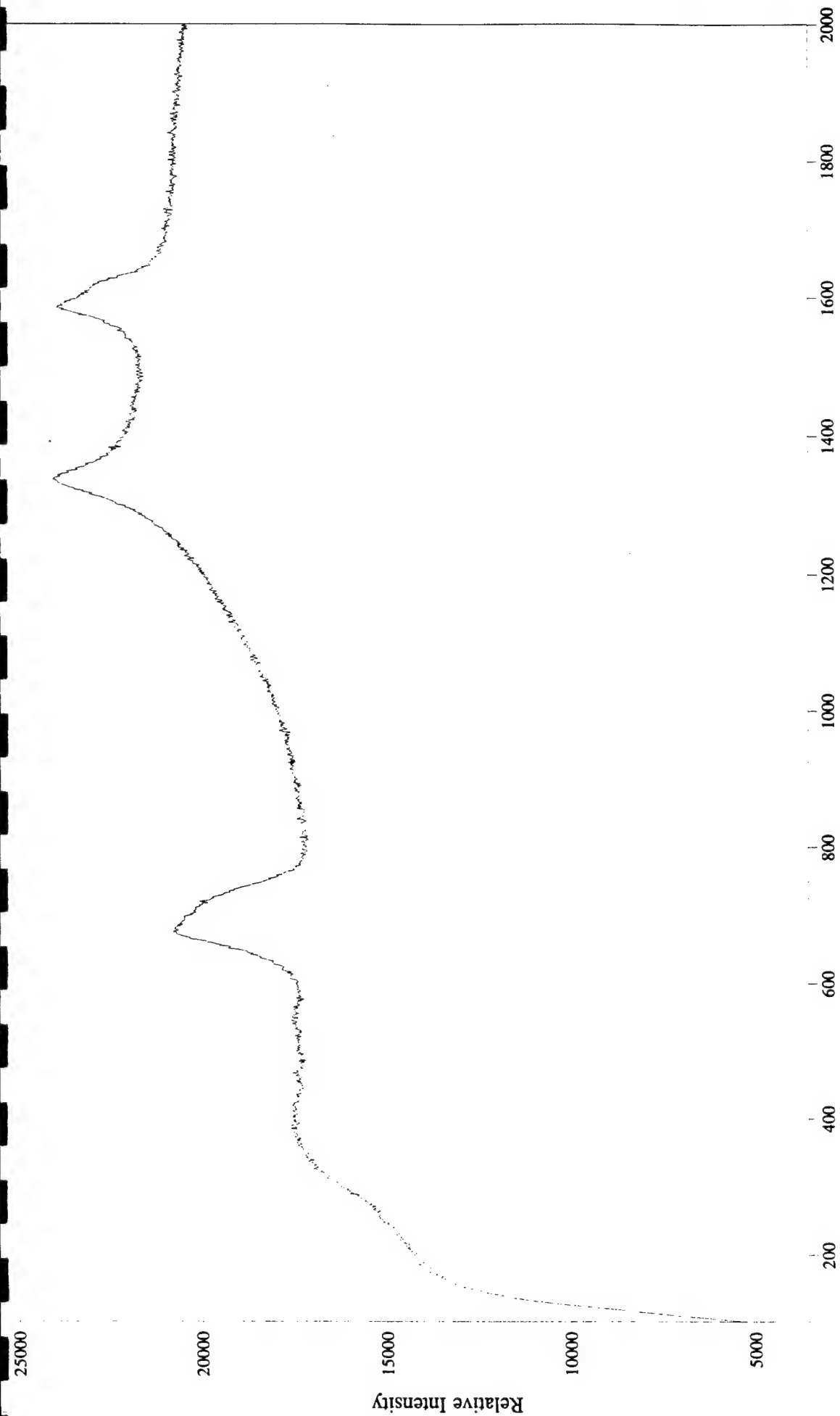
Wavenumber Shift

Molecular Microspectroscopy Laboratory



File # 1 : BAT228

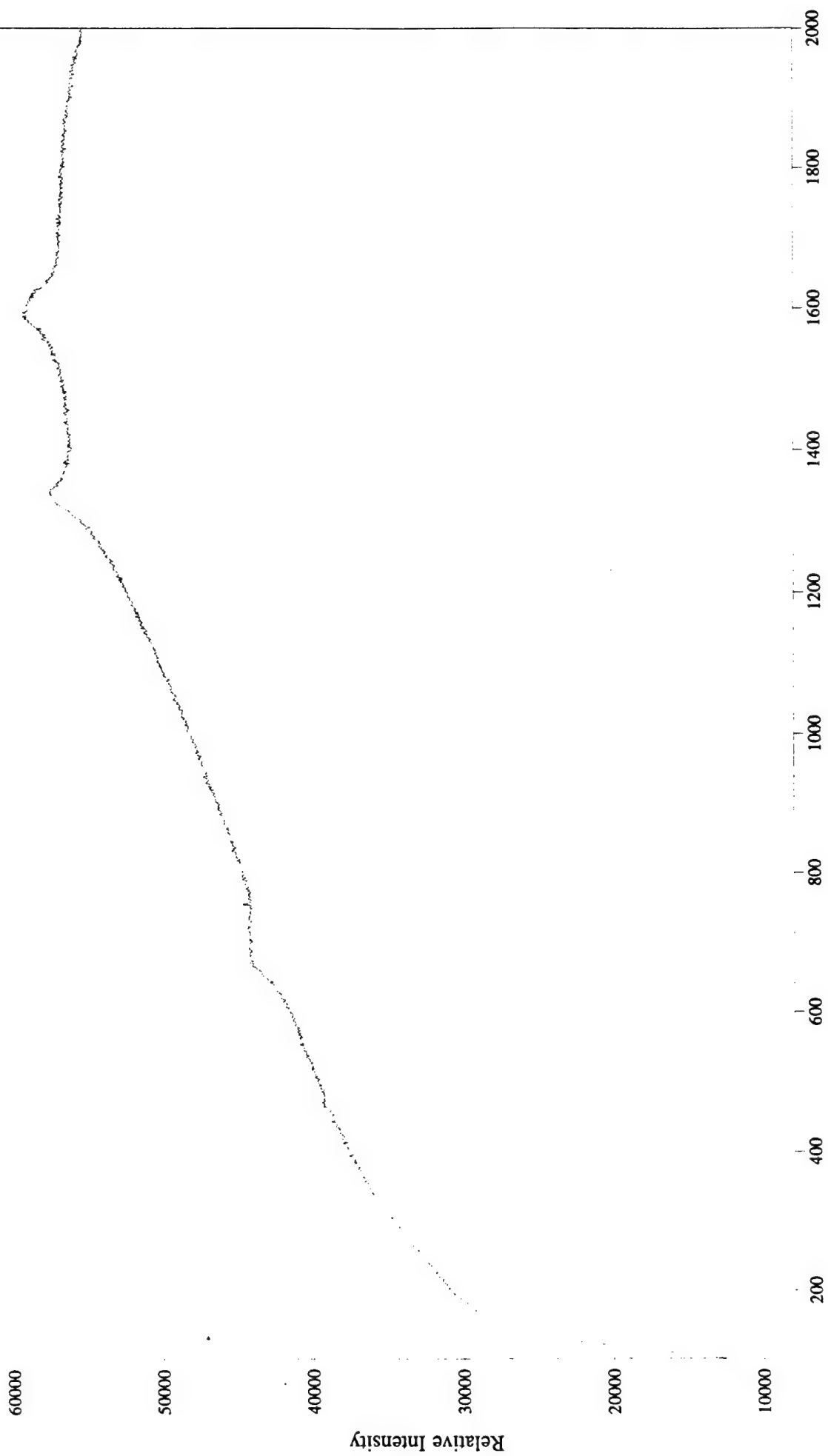
Molecular Microspectroscopy Laboratory



File # 1 : BAT229

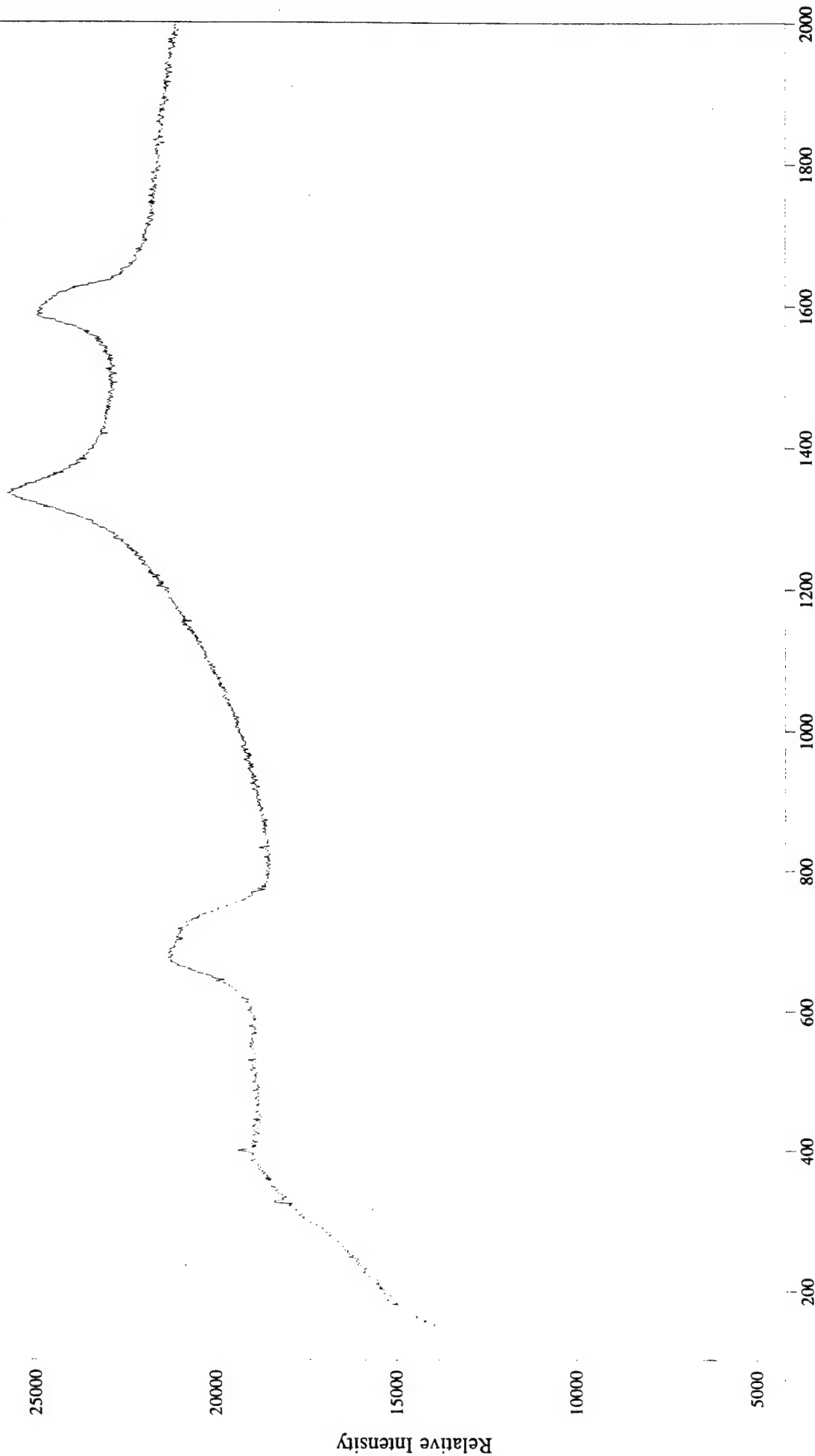
Wavenumber Shift

Molecular Microspectroscopy Laboratory



File # 1 : BAT230

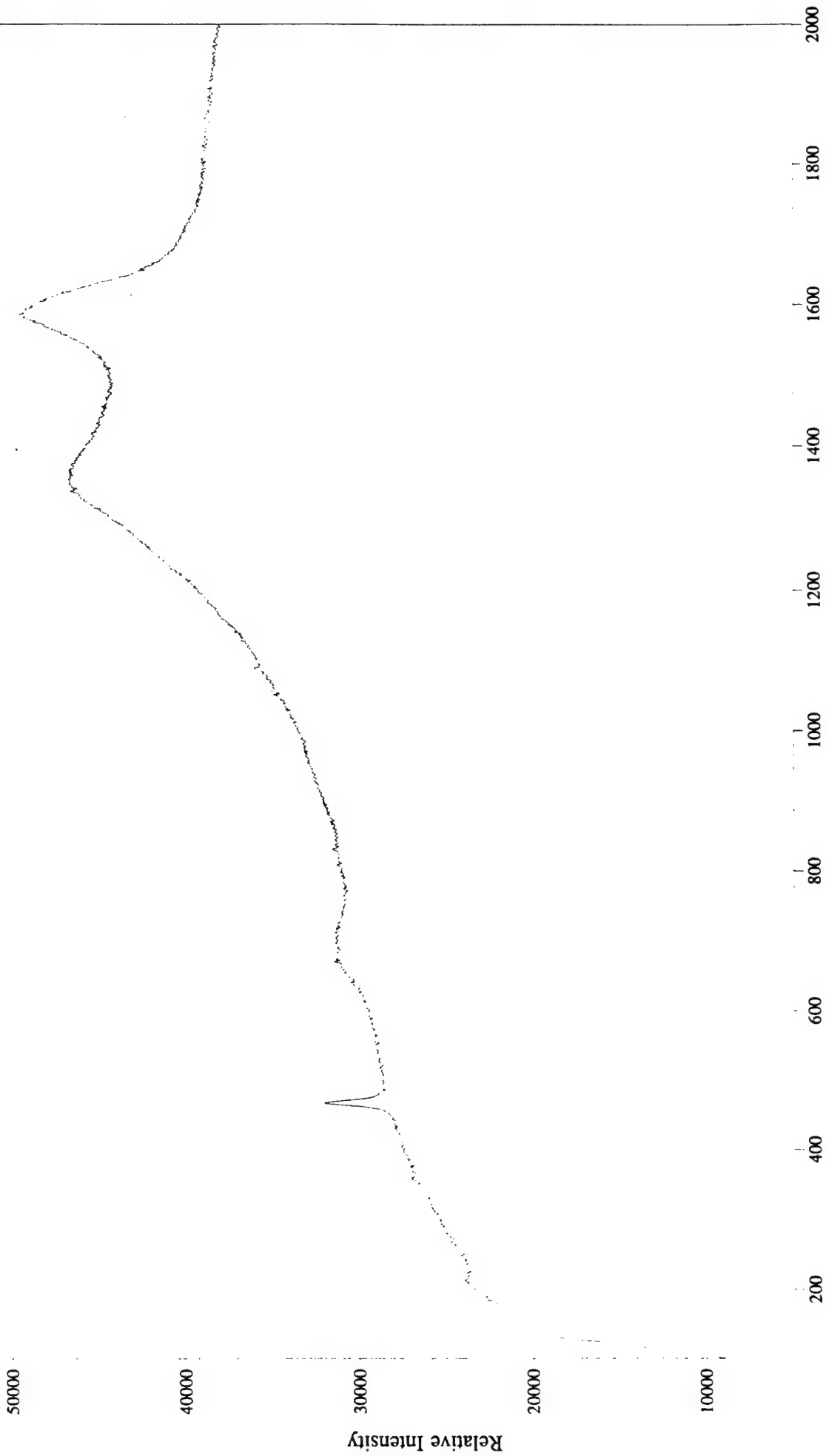
Molecular Microspectroscopy Laboratory



File # 1 : BAT231

Wavenumber Shift

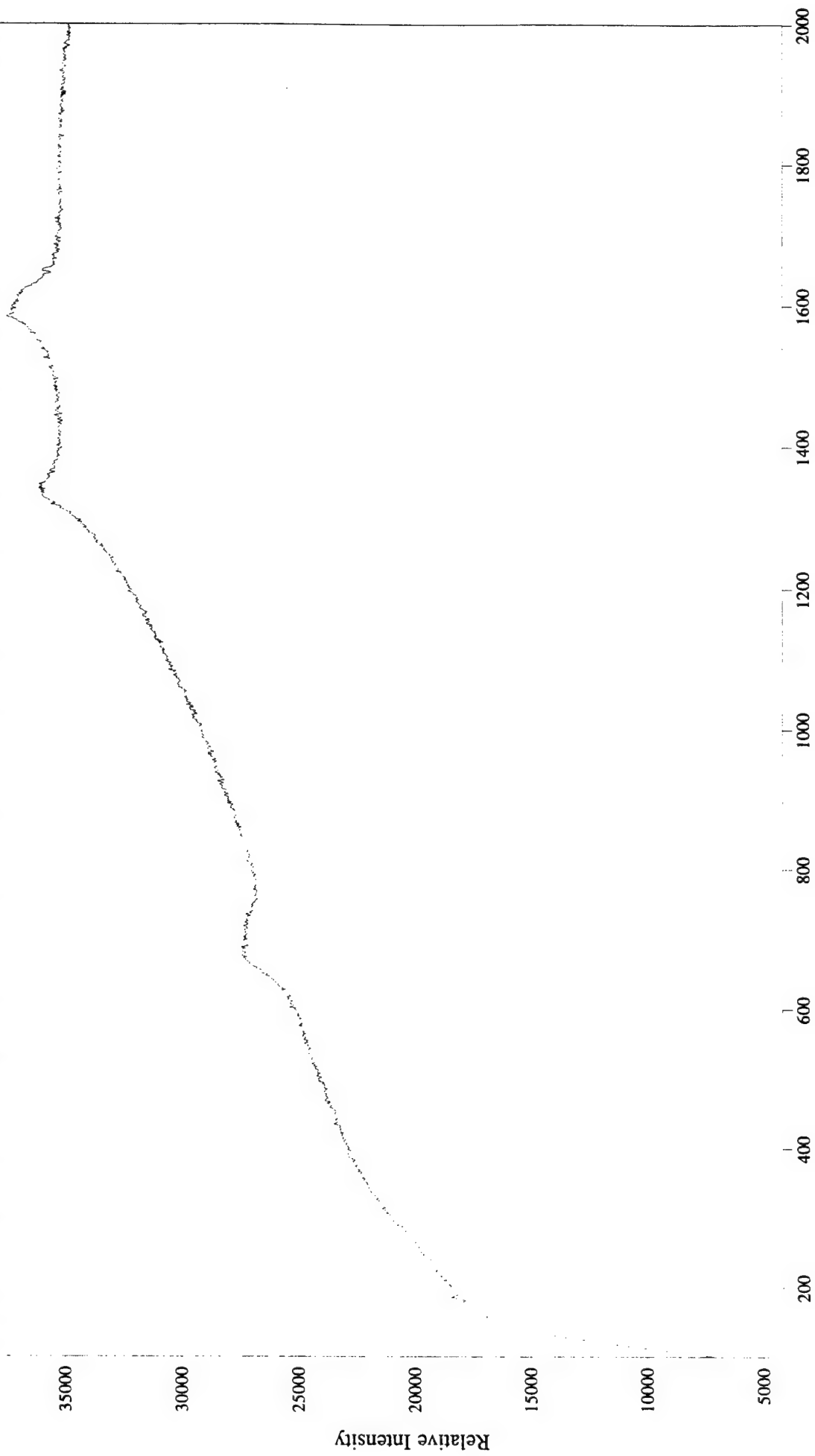
Molecular Microspectroscopy Laboratory



File # 1 : BAT232

Wavenumber Shift

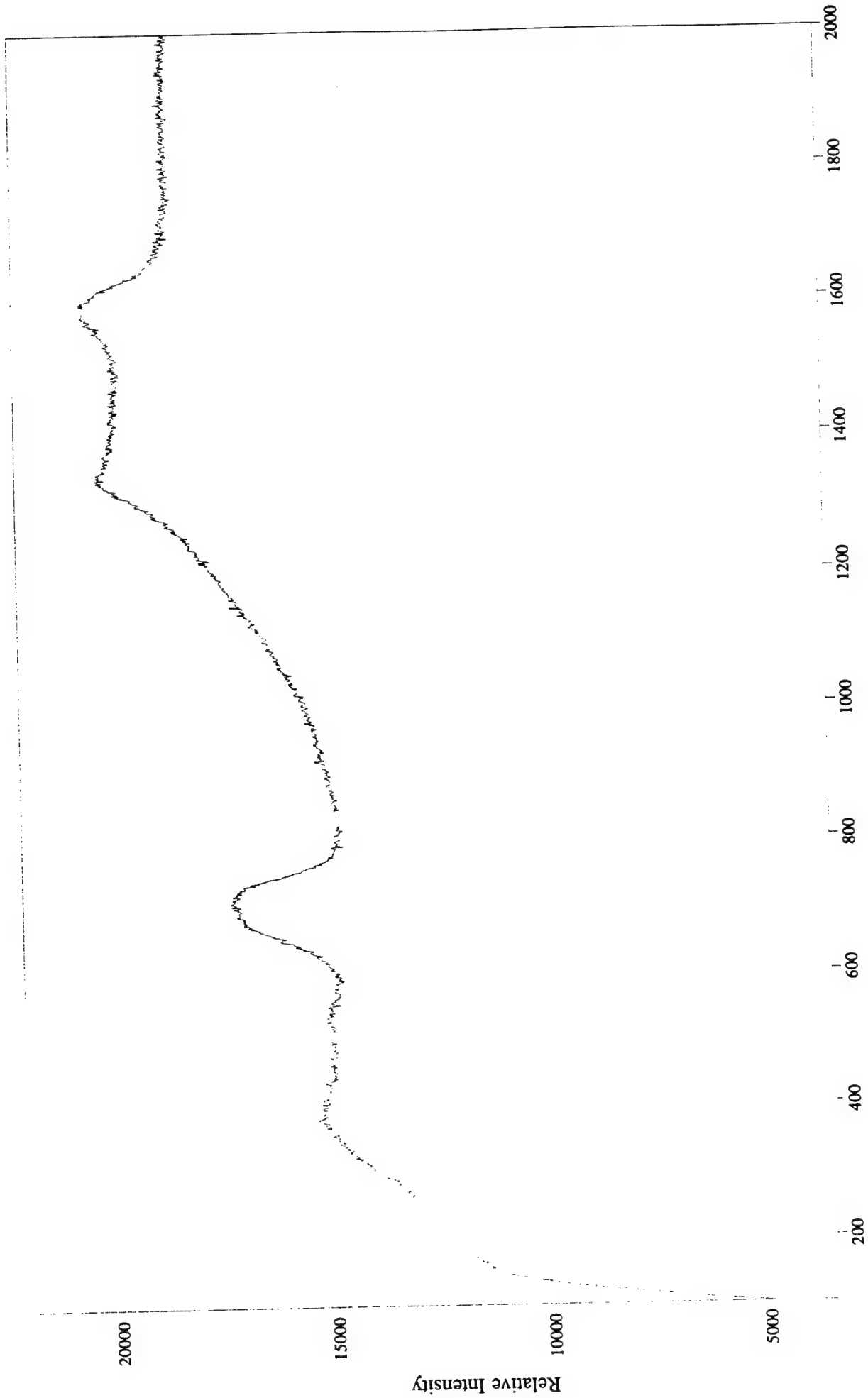
Molecular Microspectroscopy Laboratory



File # 1 : BAT233

Wavenumber Shift

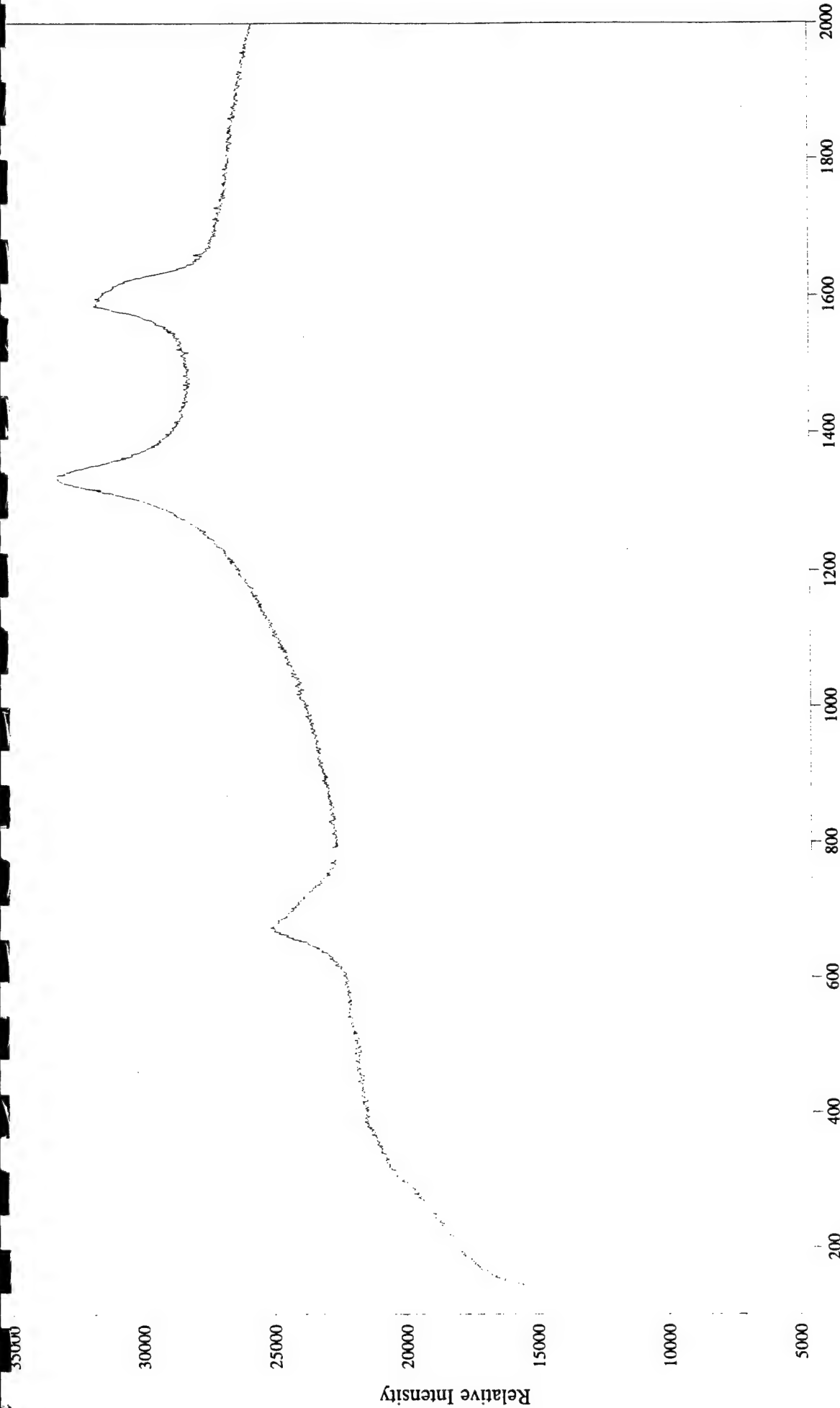
Molecular Microspectroscopy Laboratory



Molecular Microspectroscopy Laboratory

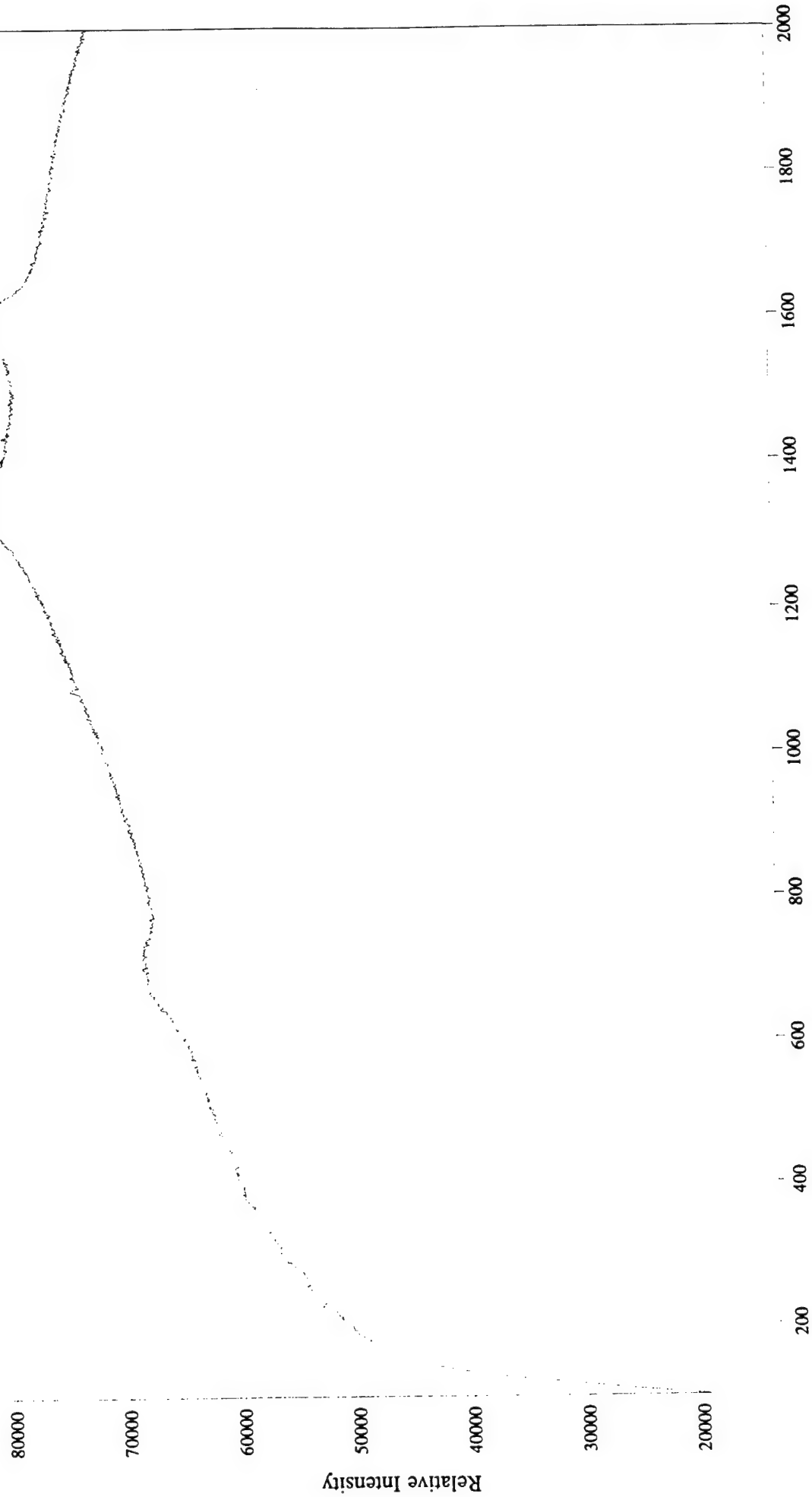
Wavenumber Shift

File # 1 : BAT234



File # 1 : BAT235

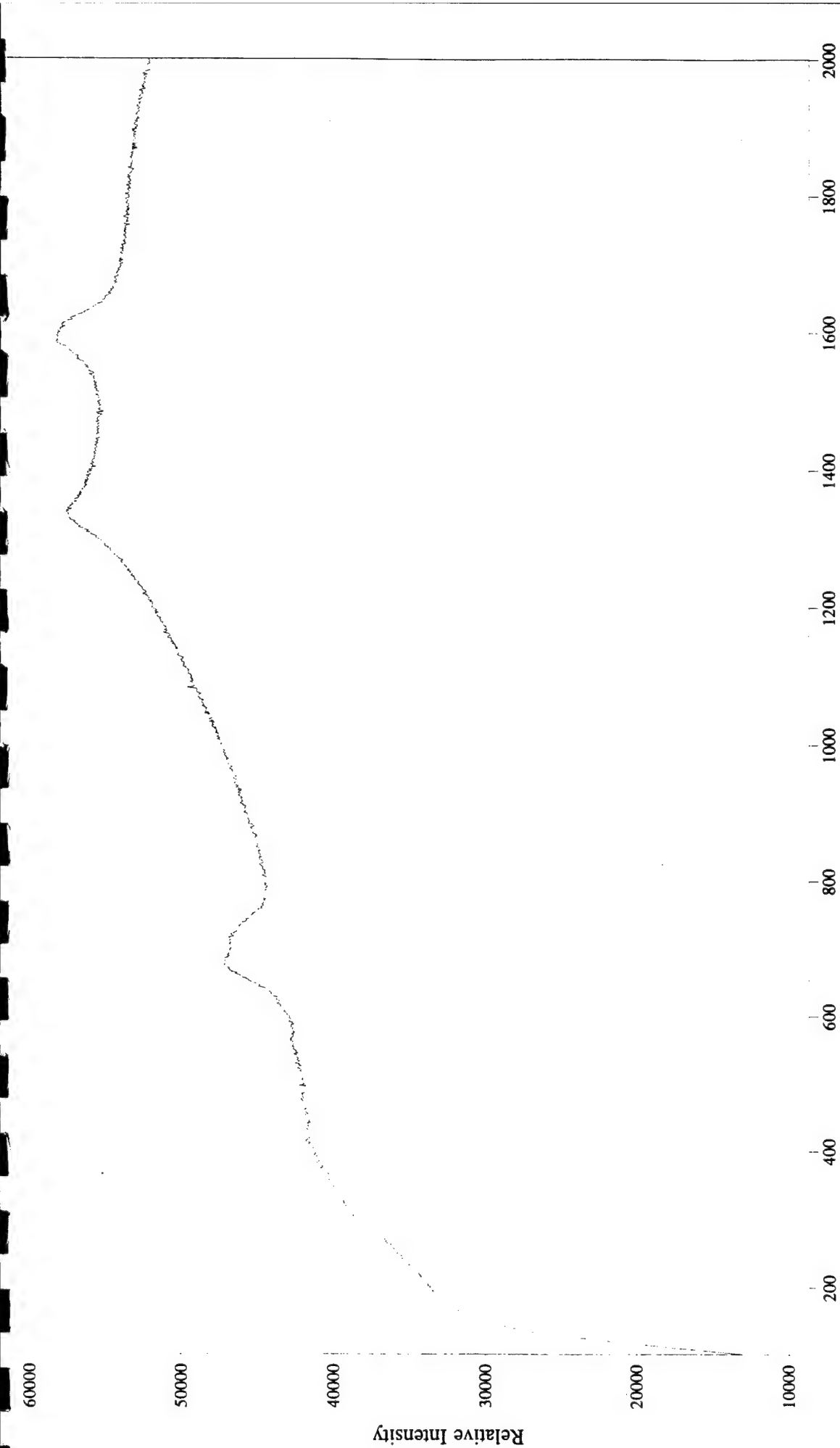
Molecular Microspectroscopy Laboratory



Molecular Microspectroscopy Laboratory

Wavenumber Shift

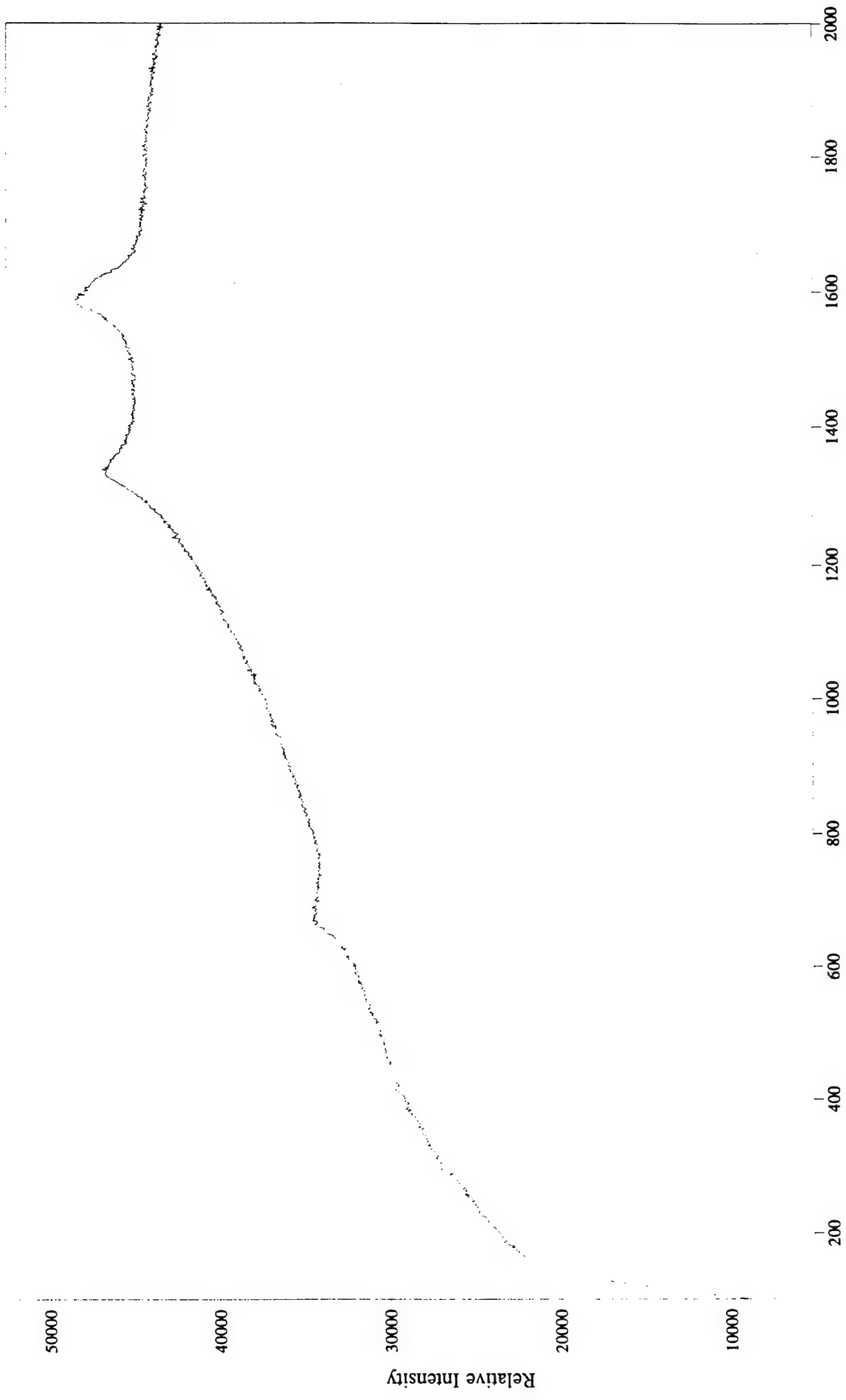
File # 1 : BAT236



File # 1 : BAT237

Wavenumber Shift

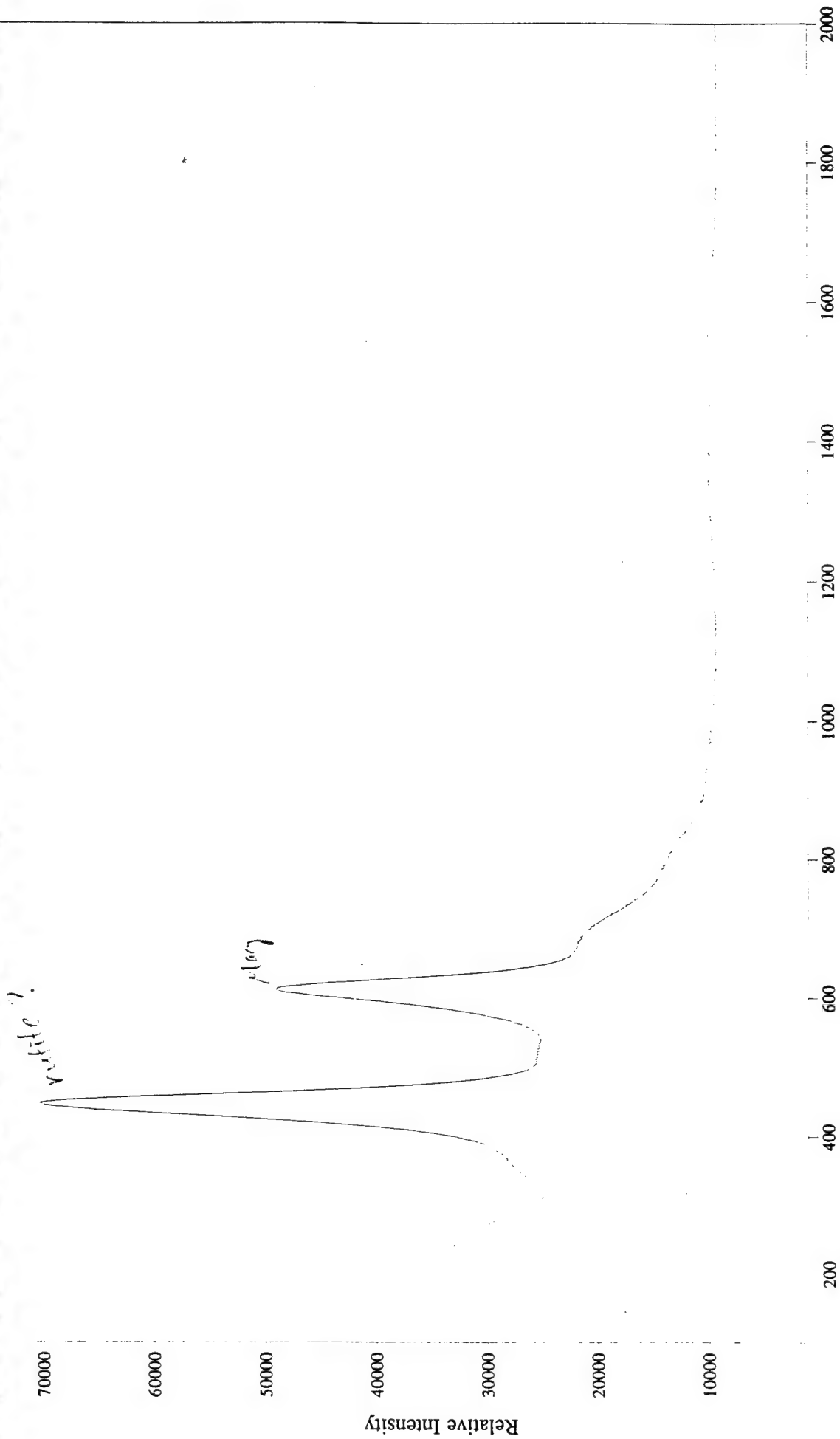
Molecular Microspectroscopy Laboratory



File # 1 : GP238

Wavenumber Shift

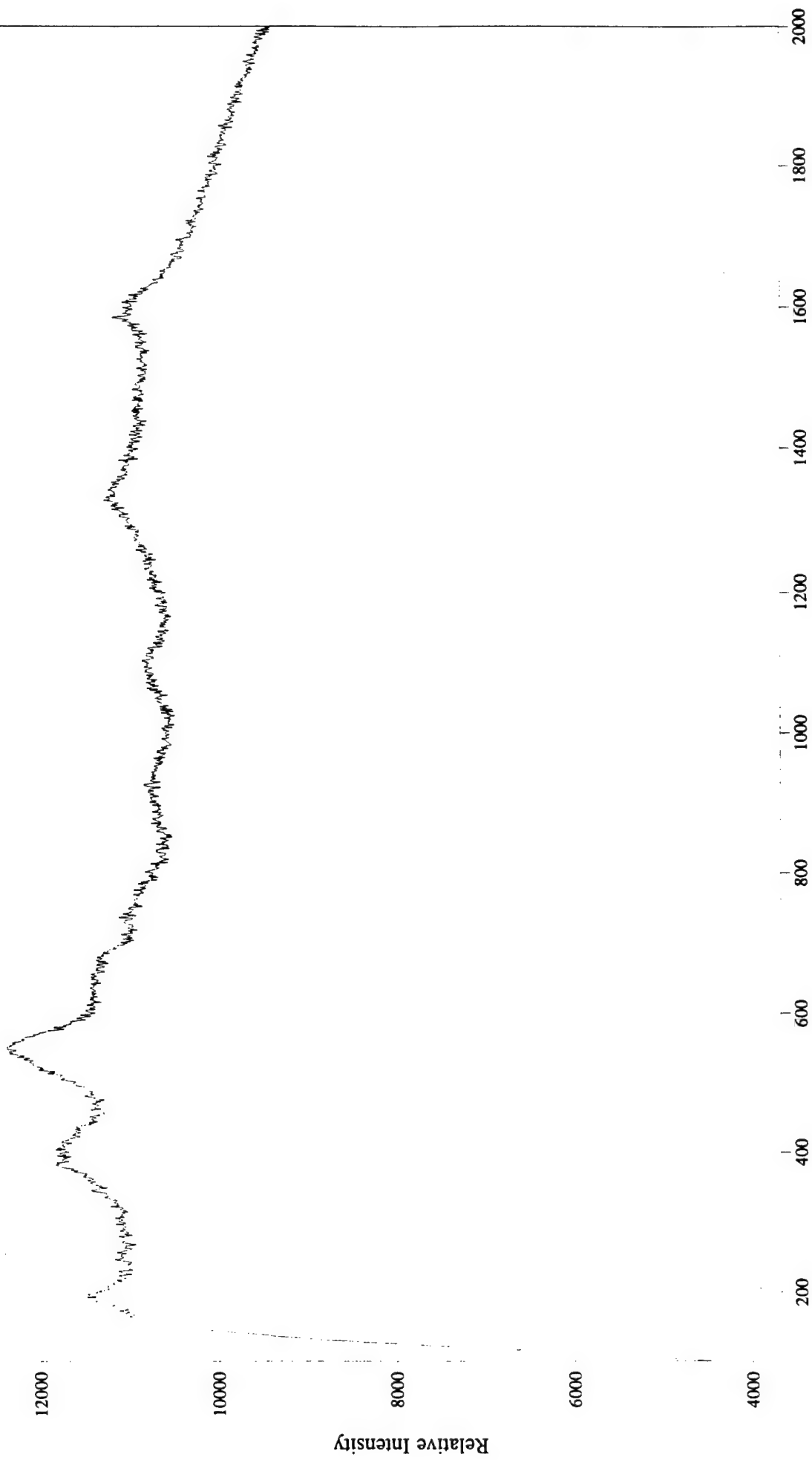
Molecular Microspectroscopy Laboratory



File # 1 : BAT239

Wavenumber Shift

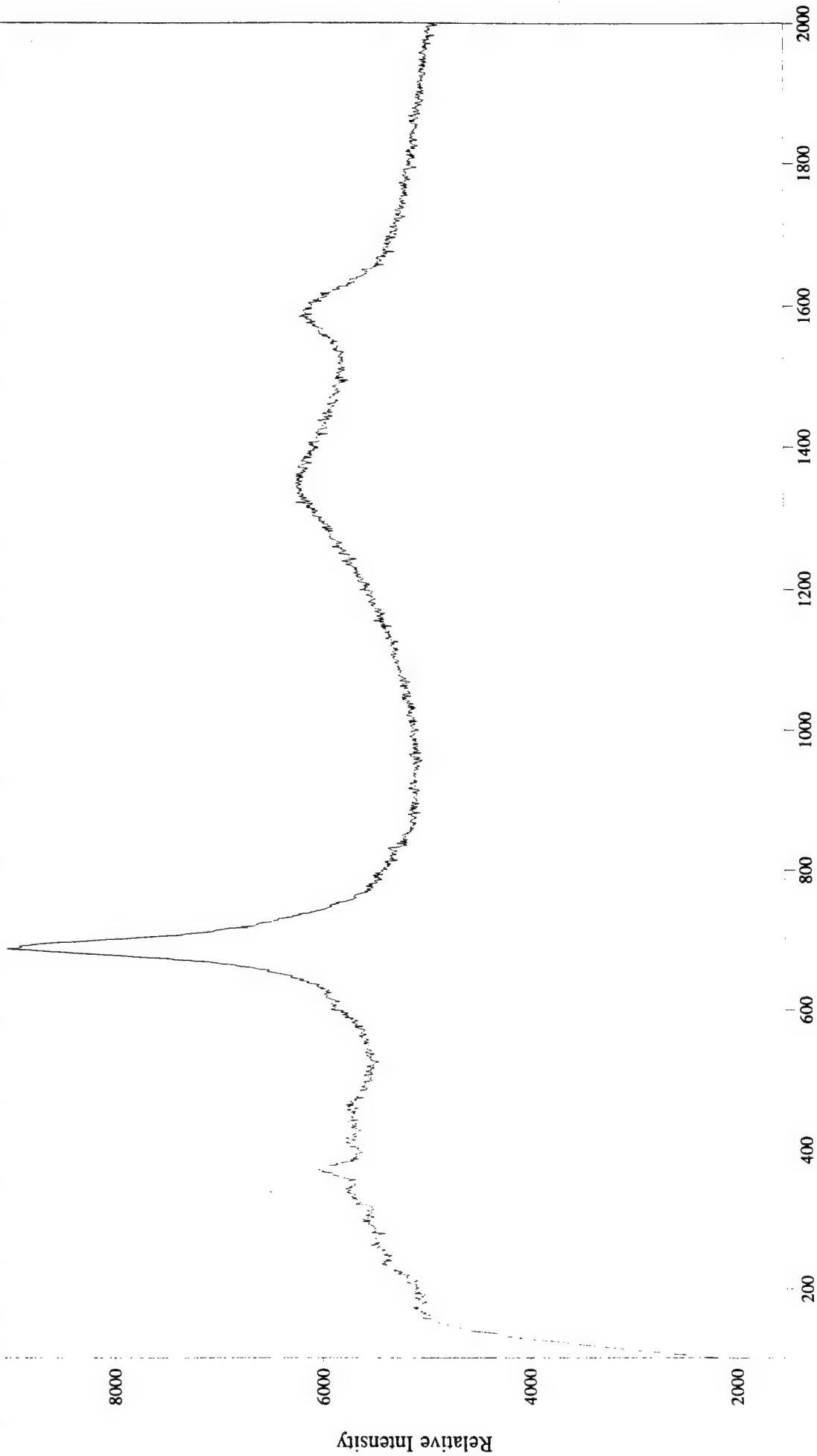
Molecular Microspectroscopy Laboratory



File # 1 : BAT240

Wavenumber Shift

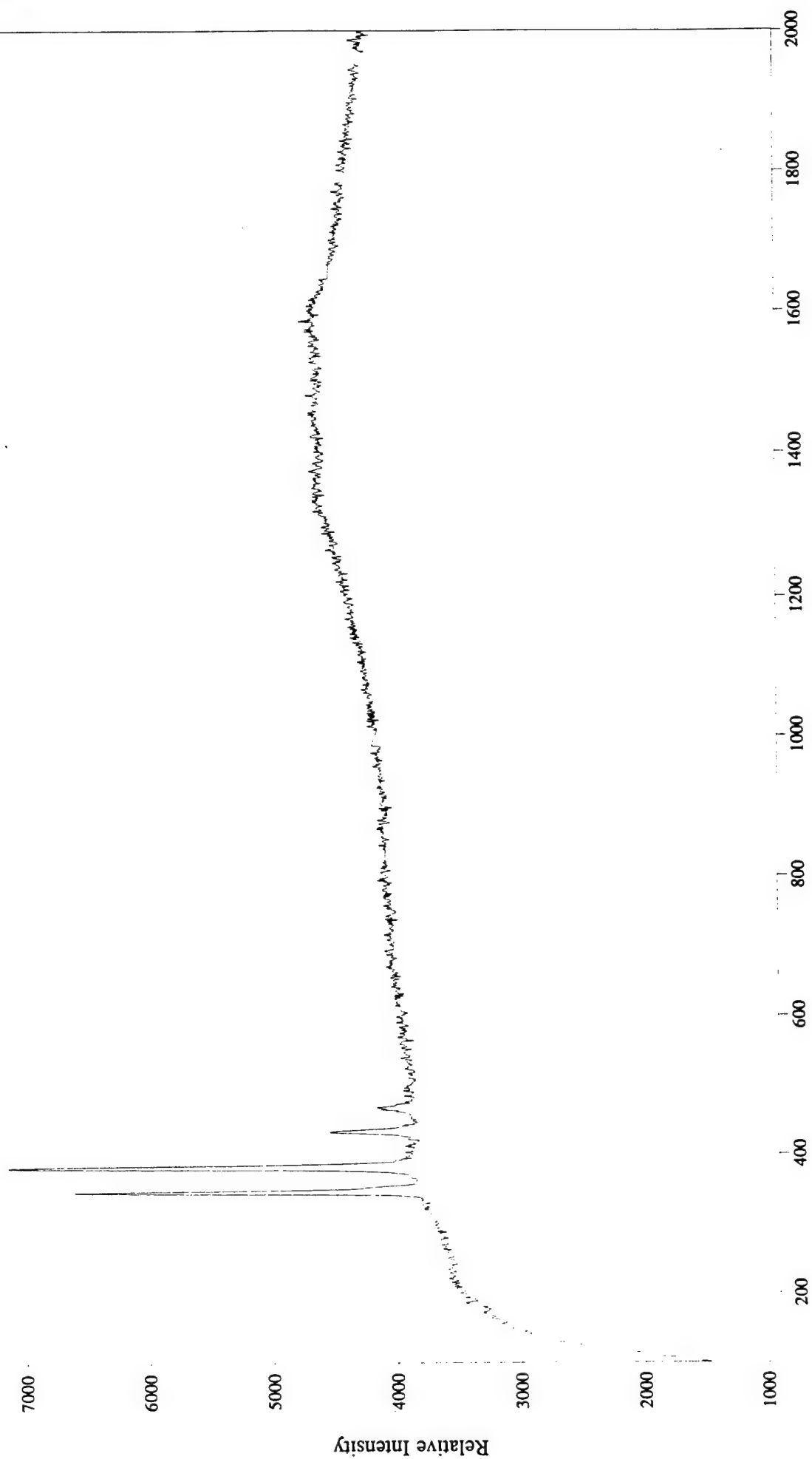
Molecular Microspectroscopy Laboratory



File # 1 : BAT241

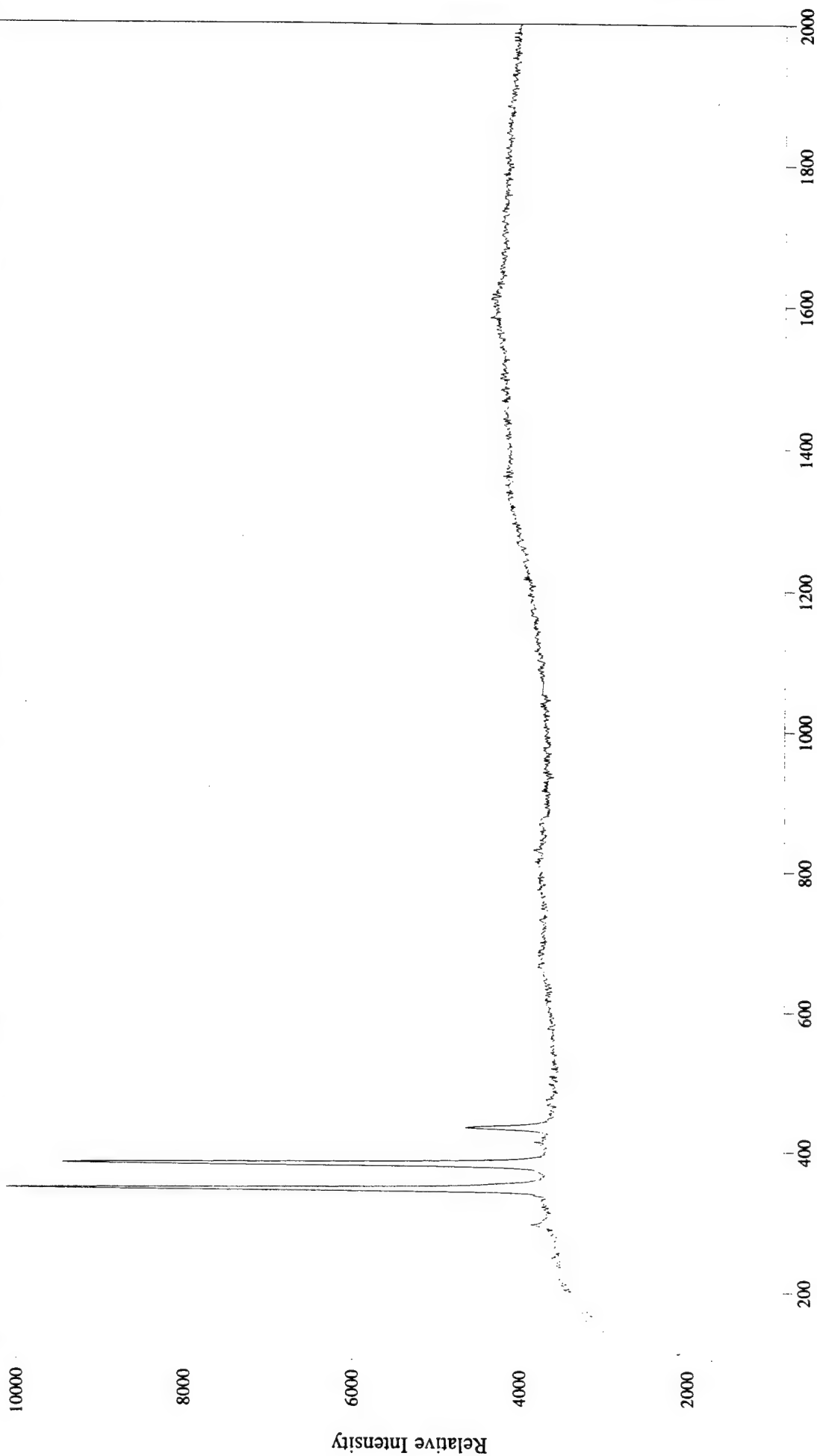
Wavenumber Shift

Molecular Microspectroscopy Laboratory



File # 1 : BAT242

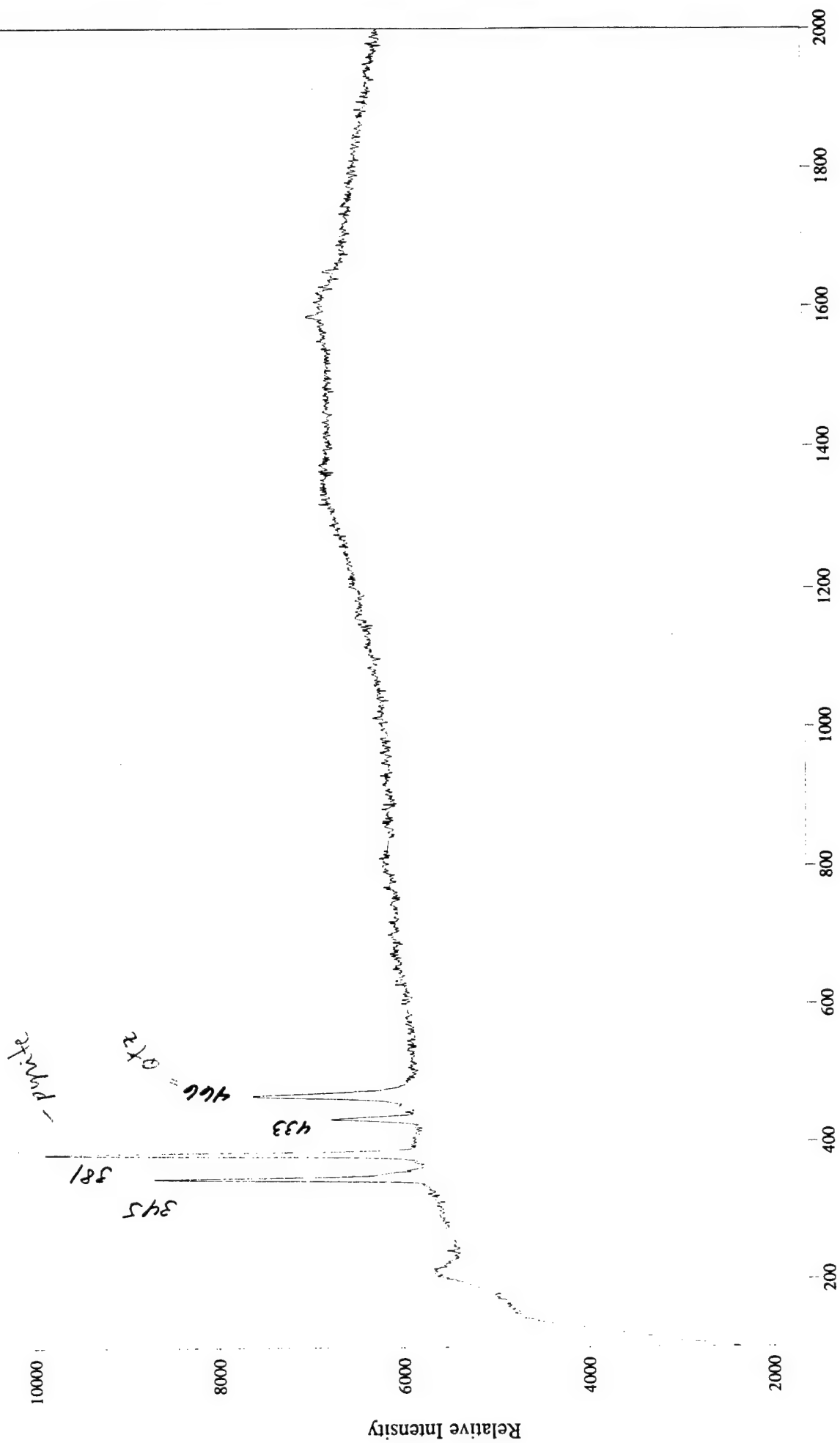
Molecular Microspectroscopy Laboratory



File # 1 : BAT243

Wavenumber Shift

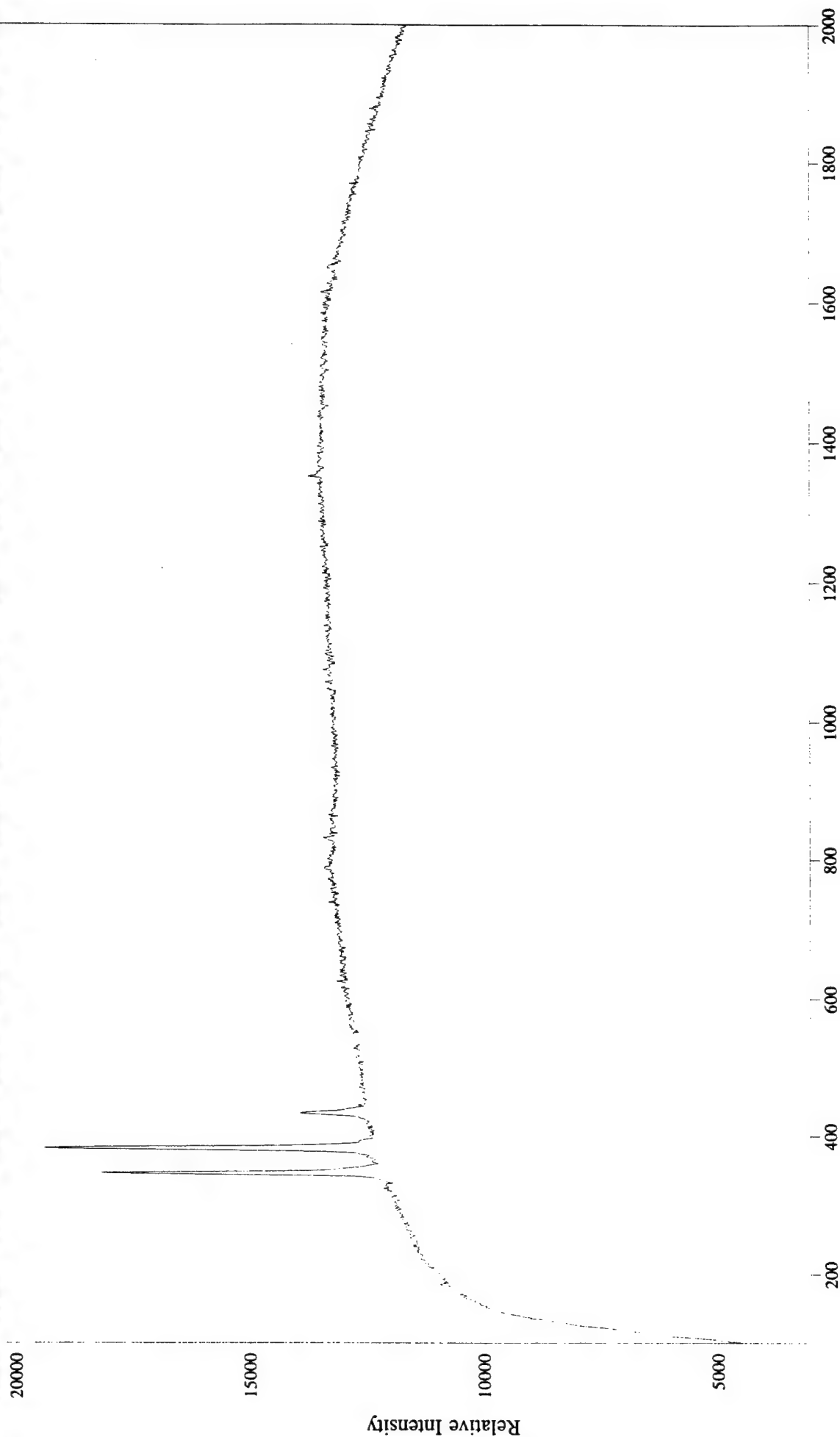
Molecular Microspectroscopy Laboratory



Molecular Microspectroscopy Laboratory

Wavenumber Shift

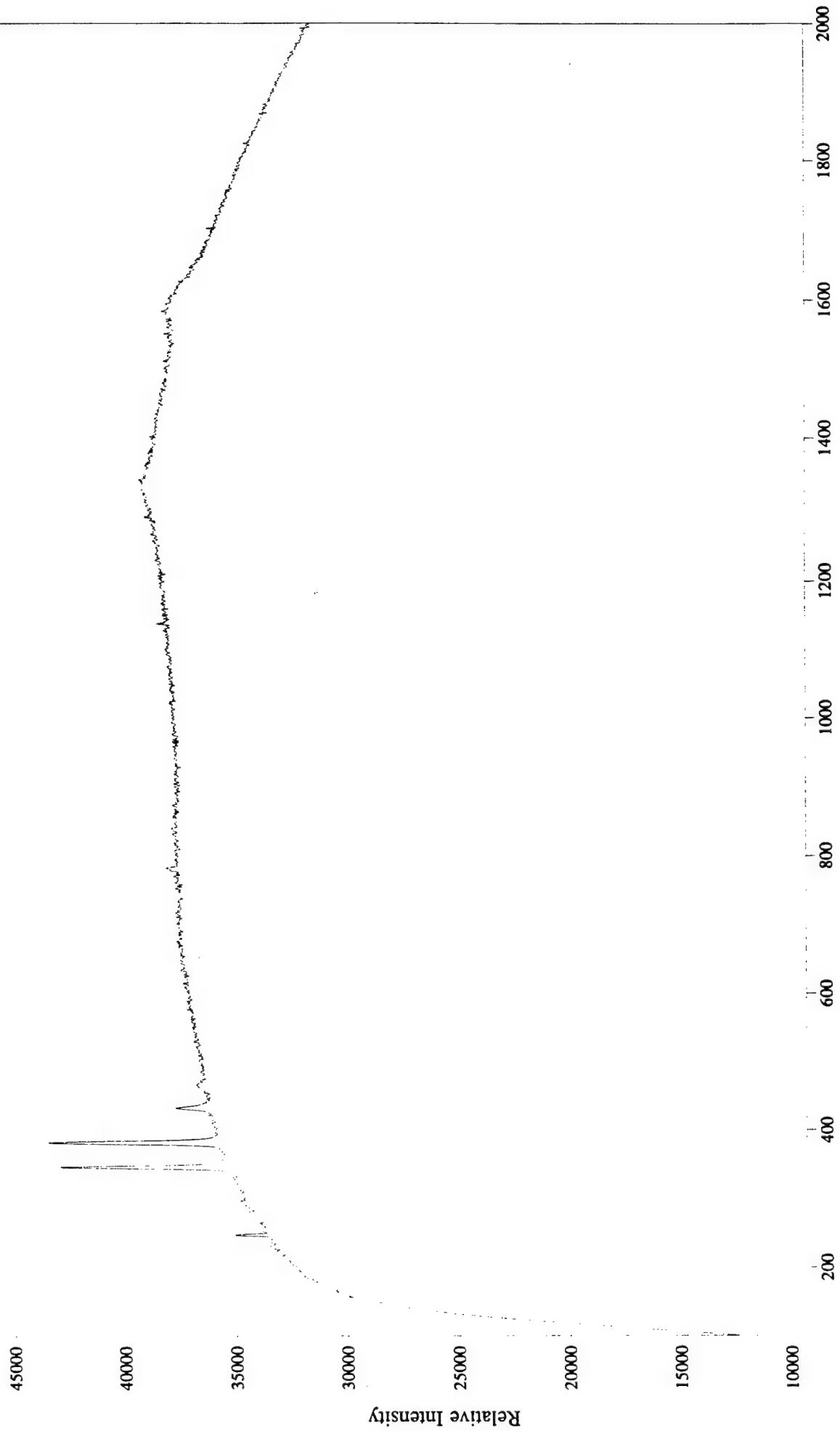
File # 1 : BAT244



File # 1 : BAT245

Wavenumber Shift

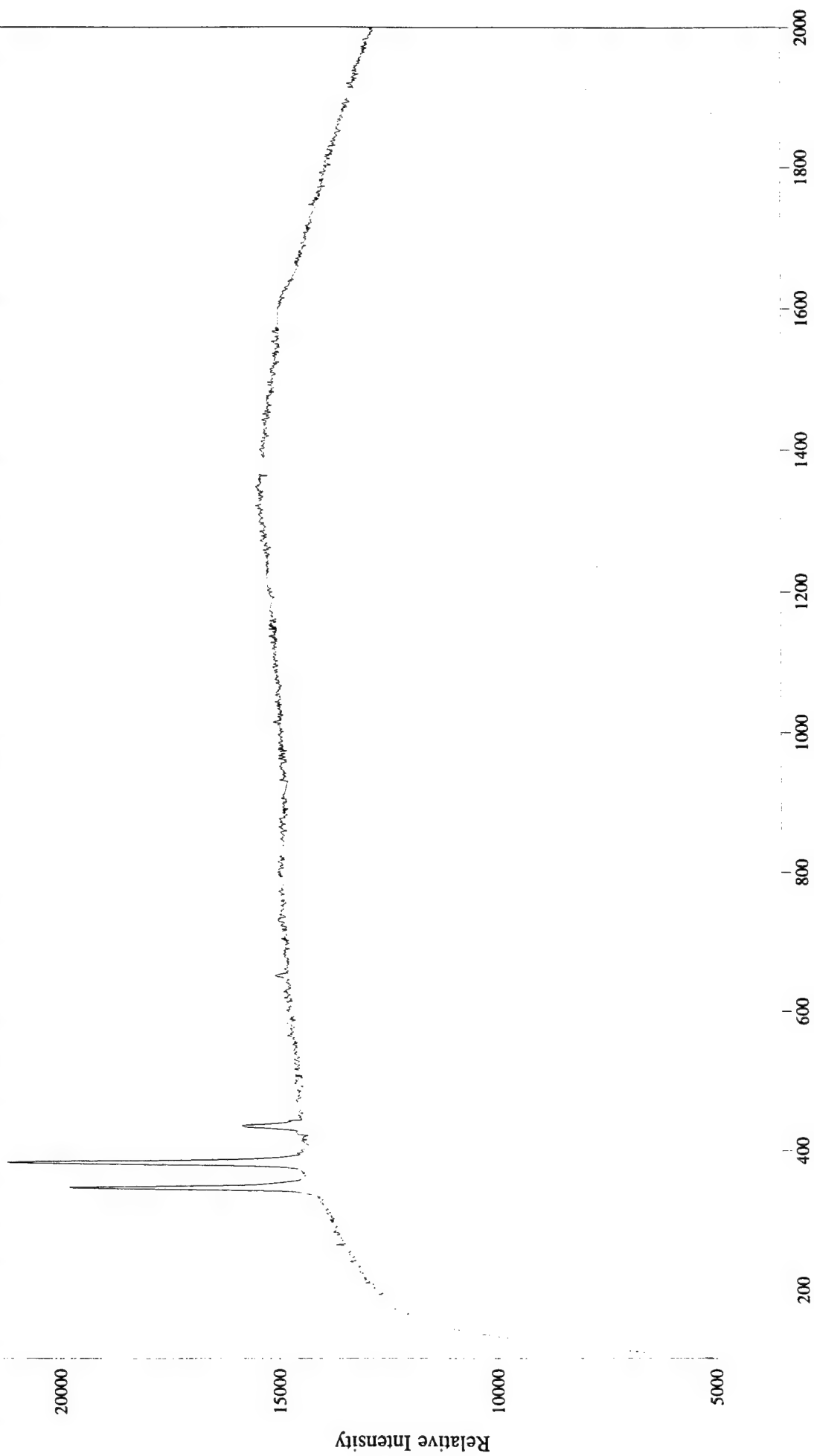
Molecular Microspectroscopy Laboratory



File # 1 : BAT246

Wavenumber Shift

Molecular Microspectroscopy Laboratory



File # 1 : BAT247

Wavenumber Shift

Molecular Microspectroscopy Laboratory

2500

2000

1500

1000

500

0

Relative Intensity

200

400

600

800

1000

1200

1400

1600

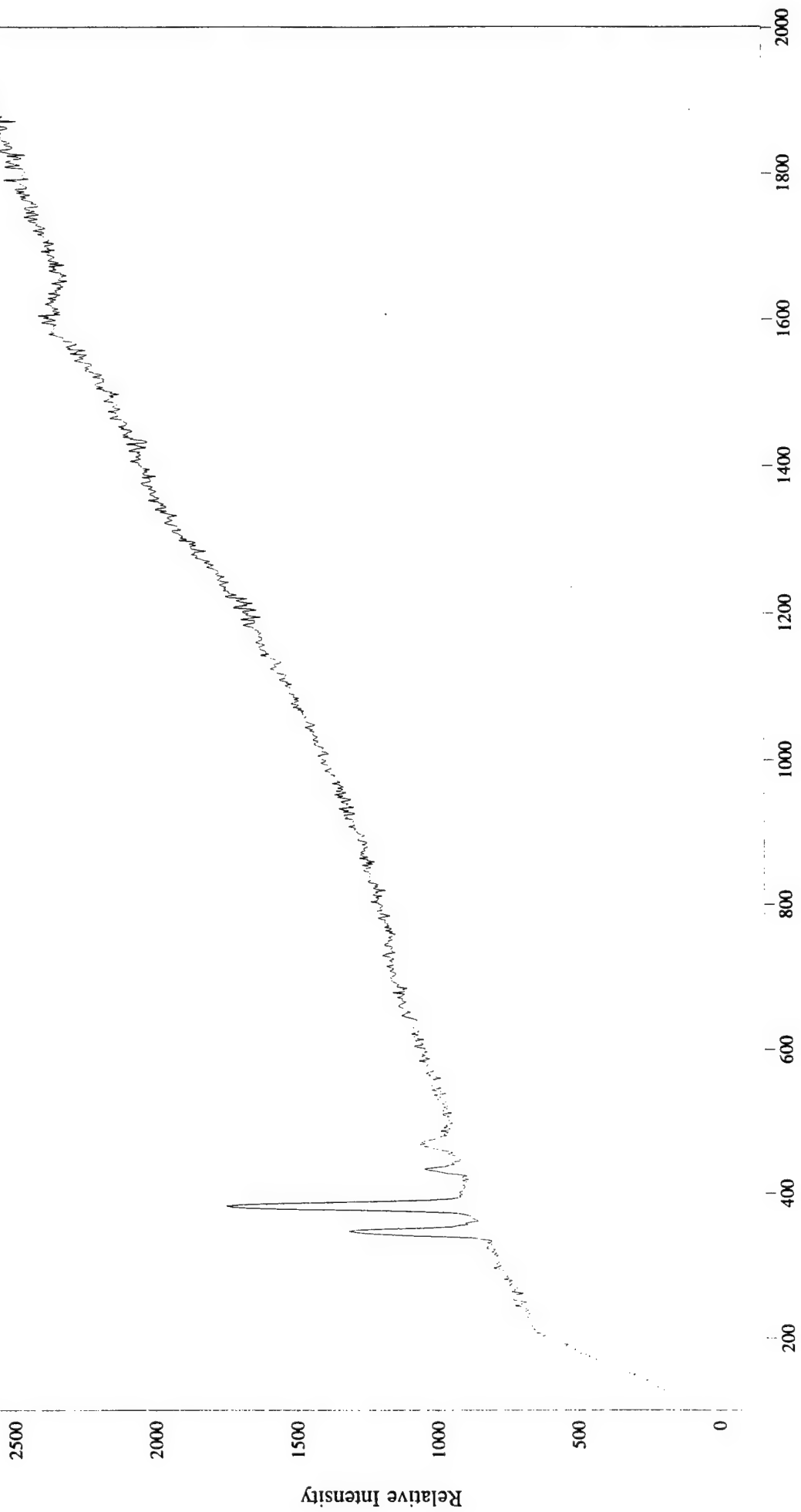
1800

2000

File # 1 : BAT248

Wavenumber Shift

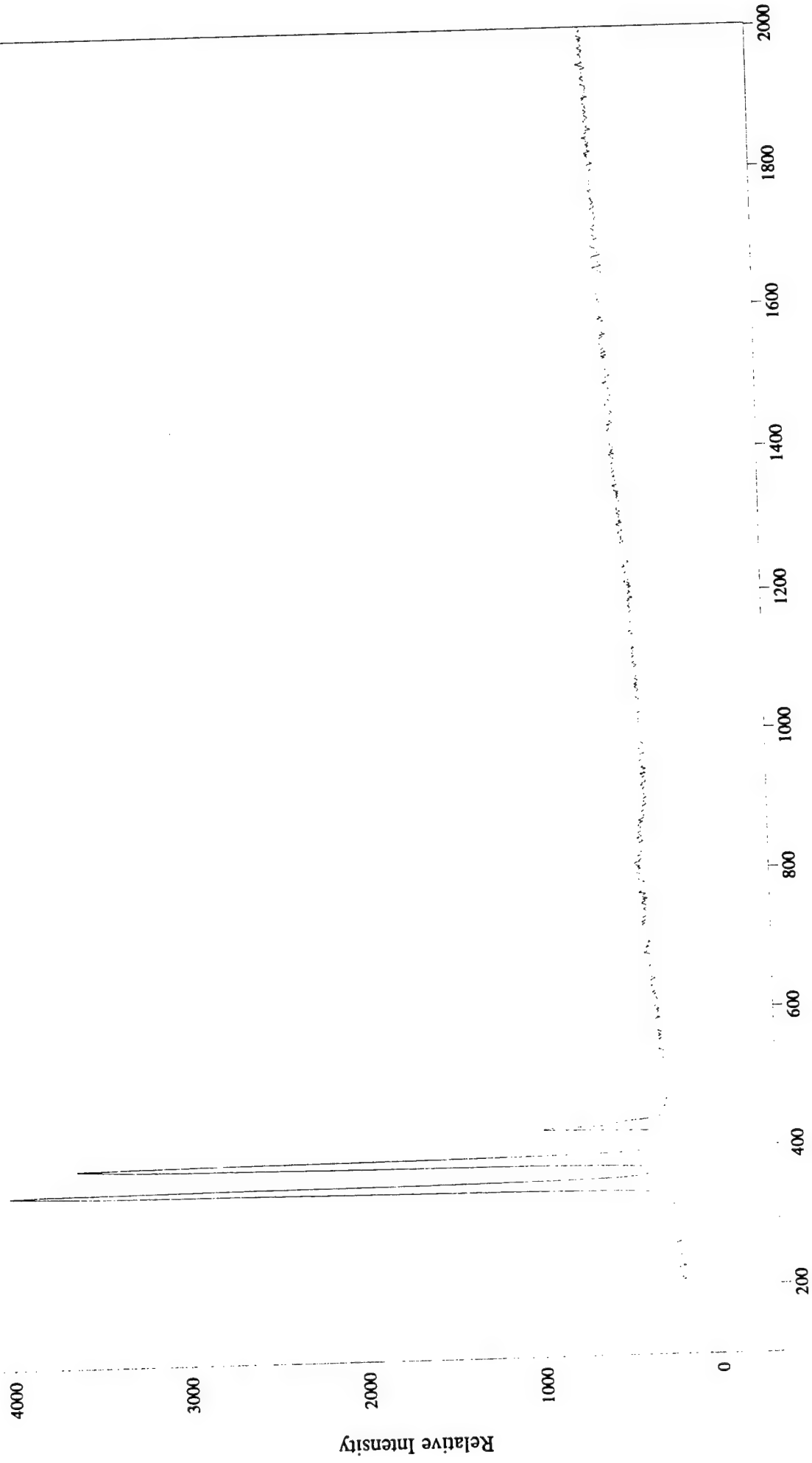
Molecular Microspectroscopy Laboratory



Molecular Microspectroscopy Laboratory

Wavenumber Shift

File # 1 : BAT249



Molecular Microspectroscopy Laboratory

Wavenumber Shift

File # 1 : BAT250

Appendix G

Quality Assurance Data

G-1. Construction Quality Control

G-2. C³ Environmental, Inc.'s CQC Report on Sheet Pile Installation

G-3. Field and Laboratory QA

Appendix G-1
Construction Quality Control

Appendix G.1 Construction Quality Control (CQC)

CQC was exercised during gates installation, funnel installation, and monitoring system installation. The project engineer for C3 Environmental, Inc. performed the on-site CQC unction, and was overseen by the Battelle field coordinator.

G.1.1 Gates Construction

During the driving of the caisson, the penetration rate was monitored and recorded by the project engineer. After the interior of the caisson was excavated with a auger, the project engineer conducted a visual inspection to ensure that the sides of the caisson were free of soil and that the desired depth (2 ft below the clay aquitard) had been reached. The monitoring wells inside the gate were attached to the cross-bracing on two permanent dividers and lowered in to the excavation. To ensure a good seal between the funnel and the gate, a section of sheet pile with a female joint was welded onto the permanent dividers. The first sheet pile on either side of the gate was then inserted into this joint and sealed with grout. The reactive media were placed in the excavation with a tremie tube for better packing.

G.1.2 Funnel Construction

The sheet pile installation QA inspection was conducted in three stages – visual inspection, pile driving monitoring, and sealable cavity inspection. Appendix G.2 contains the C3 Environmental, Inc. project engineer's report outlining the CQC procedures during the sheet pile funnel installation.

Appendix G-2

C³ Environmental, Inc.'s CQC Report on Sheet Pile Installation

3.5 WATERLOO BARRIER® INSTALLATION PROCEDURES

In the initial stage, George & Lynch set the sheet piling to a depth so that sufficient strength of the soil was obtained to support the weight of the piling. Frequently, they used an I-beam frame as a guide to assist in this initial driving. This method helped the pile driver to maintain the vertical axis and to follow the desired line of the cutoff wall. After the initial installation, the piles were driven to full depth in the order they were set. The purpose of this procedure was to ensure that the enlarged joint, with the footplate, was driven onto the smaller interlock thus minimizing the entry of debris in the cavity.

3.5.1 General

The sheet pile quality assurance inspection was performed in three stages, visual inspection, pile driving monitoring, and sealable cavity inspection.

3.5.2 Visual Inspection

A visual survey of the Waterloo Barrier® sheet piles was performed to confirm the general condition of each sheet pile. The visual inspection was conducted by a Quality Assurance Engineer/Technician at the construction site prior to installation. The following is a brief outline of the inspection points:

- 1) **Pile Thickness** - A hand micrometer was used to measure the thickness of the sheet piling prior to driving.
- 2) **Linearity Inspection** - A visual inspection was conducted on each of the piles to ensure that the piles had not been bent or bowed during transportation.
- 3) **Surface Condition** - The surface of the piles were inspected for defects and/or deformations.
- 4) **Sheet Pile Length** - Each sheet pile was measured to confirm the specified length.
- 5) **Foot Plate Inspection** - A visual inspection of each foot plate was conducted to ensure proper installation.
- 6) **Pile Marking** - One foot graduations were marked on the sheet piles to assist in the measurement of driving rates during installation.

3.5.3 Monitoring of Sheet Pile Driving

Records were collected for each of the installed sheet piles. A Quality Assurance Engineer was present on site during the entire driving process. The following is a brief description of the documented inspection items:

- 1) **Sheet Pile Identification** - Each sheet pile was numbered for reference purposes.
- 2) **Driving Records** - Driving records were collected for each sheet pile installed in the Waterloo Barrier[®] System. These records documented the driving rates and any notes regarding the installation (Photo 3 with C³ Quality Assurance Engineer in foreground).

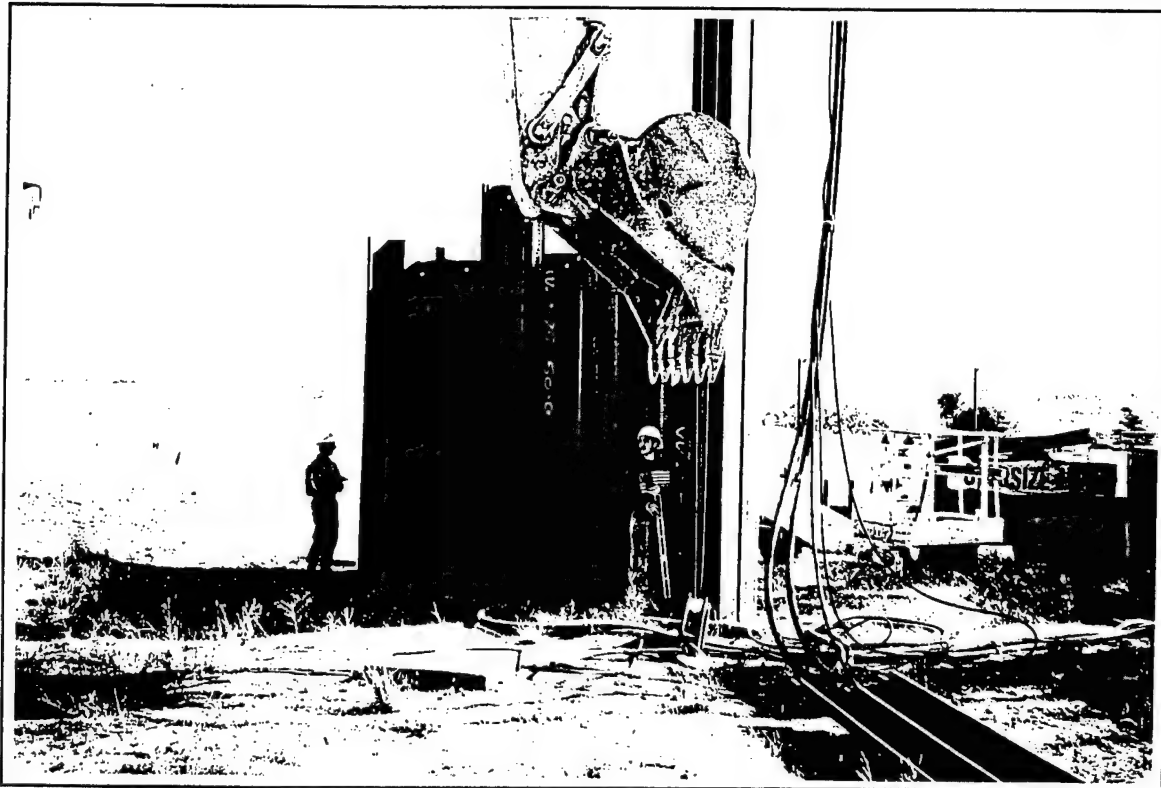


Photo 3. Typical Driving Record Collection

- 3) **Driving Depth** - A Quality Assurance Engineer measured and documented the installed depth of each sheet pile.
- 4) **Sheet Pile Alignment** - After the installation of the sheet piles, the final alignment of each pile was recorded using a digital inclinometer (See Figure 4 for Axis Definitions).

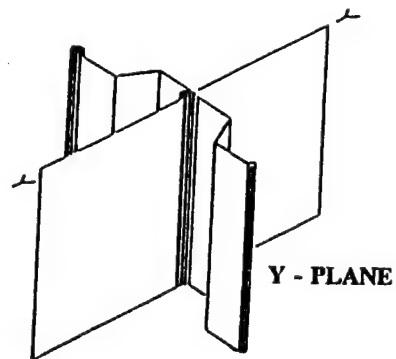
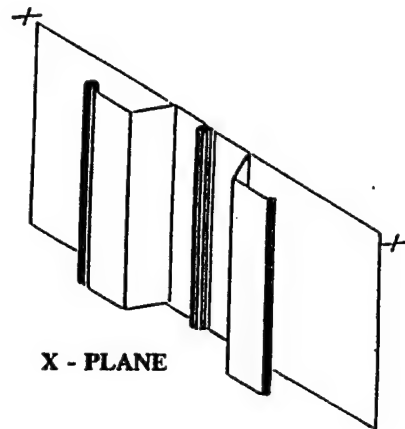
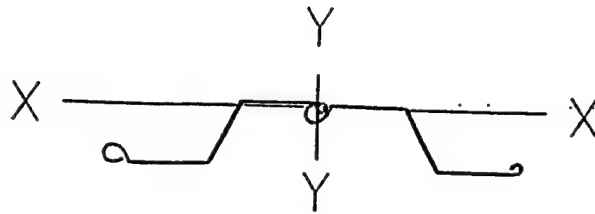


Figure 4. Waterloo Barrier® Sheet Pile Axes

3.5.4 Sealable Cavity Inspection

Inspection of the sealable cavities was the final stage of the Sheet Pile Installation QA/QC Program. The inspection was completed using a high pressure water pump, water tank and rigid hose to probe each sealable cavity (Photo 4). Joint probing was conducted to inspect the integrity of each of the WZ75 sealable cavities and to determine if:

- The WZ75 sheet piles were installed so that a sound sealable cavity existed.
- The sheet piling was installed to the minimum design depth.
- The sealable cavity was free of obstructions.

The following is a description of the documented inspection items:

- 1) **Depth Measurement** - The depth of penetration of the inspection probe was recorded for each joint.
- 2) **Condition of Sealable Cavity** - Any unusual conditions encountered during the inspection of the sealable cavities were recorded. Documented conditions included the following:
 - Damage to the top of joint (due to driving).
 - Debris present at the base of the sealable cavity.
 - Obstructions/Restrictions present in the sealable cavity.

3.6 SEALANT INSTALLATION PROCEDURES

3.6.1 Secondary Flushing

Prior to commencing grouting operations all joints to be grouted were checked for obstruction and, if necessary, reflushed.

3.6.2 Sealant Mixing

The following is a point-form description of the sealant mixing:

- 1) **Water/Grout Ratio** - Approximately 5 U.S. gallons of clean, potable water was added to the mixer.
- 2) **Sealant Addition** - The sealant materials were provided in pre-measured (30 lbs) bags and two bags were slowly added to the mixing tank to allow for uniform mixing.



Photo 4. Joint Flushing



Photo 5. Typical Sealant Injection

- 3) **Mixing Time** - Upon addition of the sealant, mixing was carried out for approximately 2 minutes.
- 4) **Material Testing** - Random Marsh Cone tests were conducted to ensure that mixed sealant met viscosity requirements.

3.6.3 Joint Grouting

The following is a brief description of the sealant installation:

- 1) **Initial Volume Measurement** - The sealant level in the holding tank of the grout plant was measured and recorded prior to the start of injection.
- 2) **Sealant Injection** - The grout line was inserted to the base of the clean joint and the sealant was tremie into the cavity.
- 3) **Grout Line Withdrawal** - Once sealant was observed to be flowing out the top of the sealable cavity (Photo 5), the injection line was slowly withdrawn.
- 4) **Final Volume Measurement** - Once the grout line had been removed from the joint the sealant level in the holding tank was measured and recorded.
- 5) **Joint Grouting** - Steps 1 - 4 were repeated for each joint to be sealed.

3.7 WATERLOO BARRIER® SHEET PILING LAYOUT

The Waterloo Barrier® cutoff wall was installed at the location specified by Battelle. The sheet pile and joint identification numbers used in this report are indicated in Figure 5.

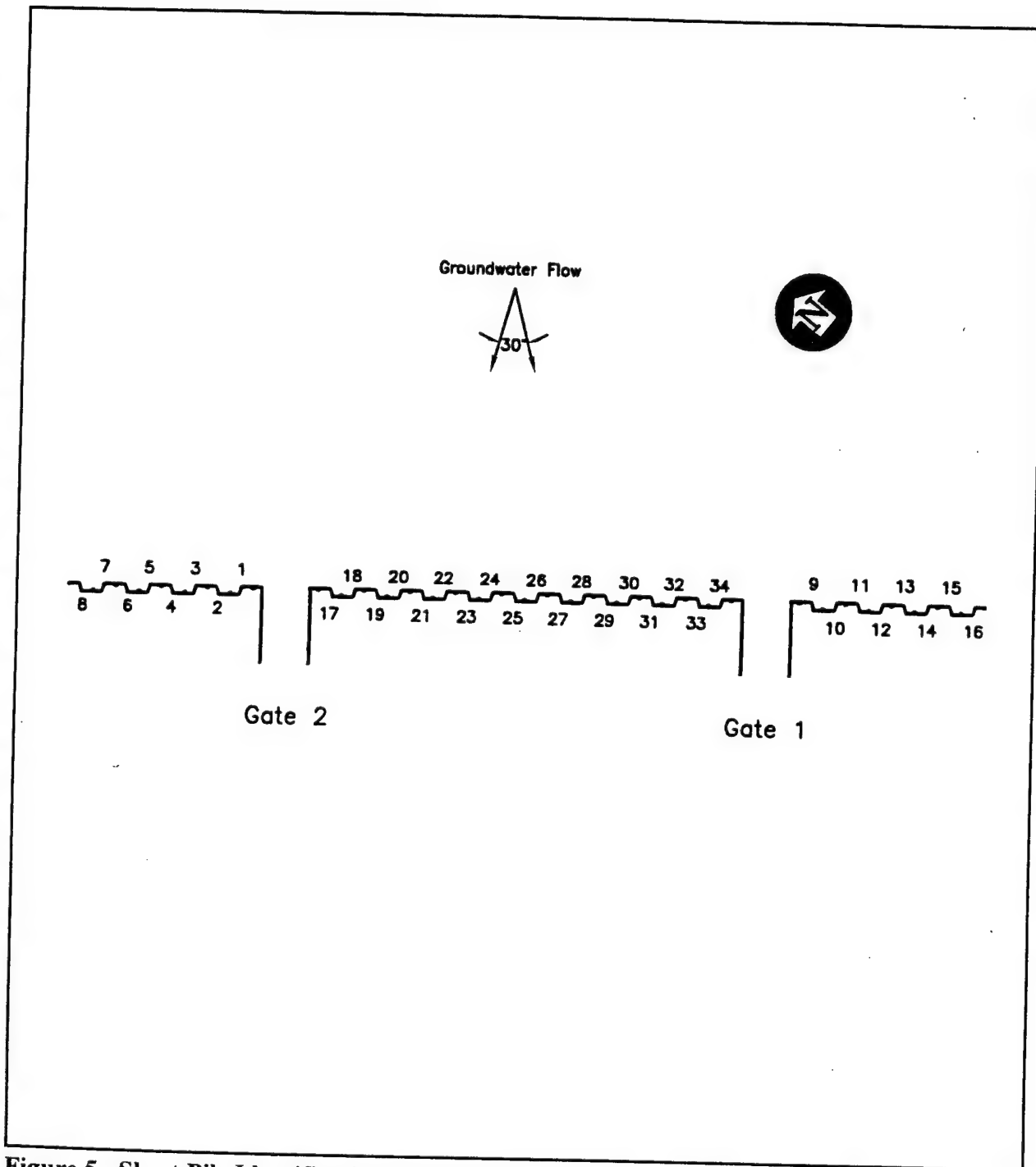


Figure 5. Sheet Pile Identification Numbers

3.8 SEALANT QUANTITIES

Figure 6 illustrate a cross-section of the sealable cavity of the Waterloo Barrier® WZ75 section. The typical cross-section area of this section is approximately 1.22×10^{-2} square feet. Based on this, the minimum theoretical sealant volume required for the sheet piles would be 0.488 cubic feet.

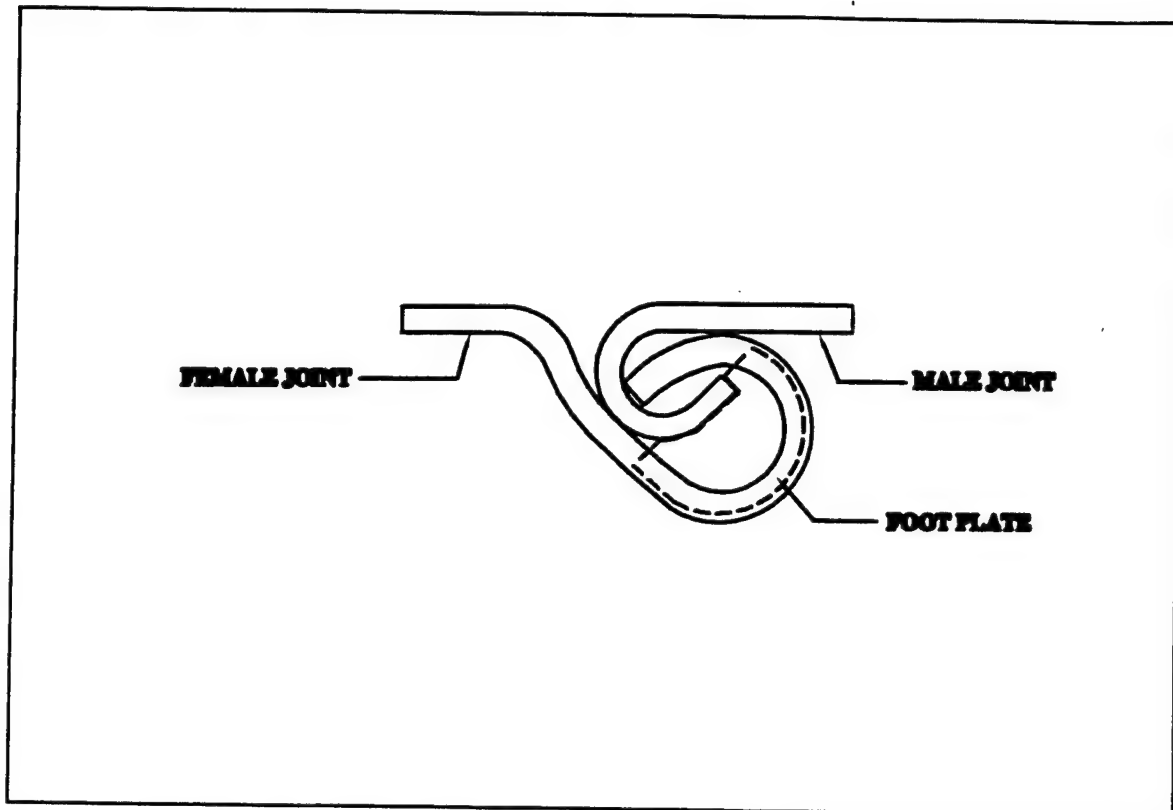


Figure 6. Waterloo Barrier® Sealable Cavity Cross Section

A number of factors affect the actual volume of grout required to seal the joint cavities. They include:

- Porosity of the surrounding media.
- Contact area of the interlocking joints.
- The presence of subsurface voids adjacent to the interlocking joints.
- Consolidation of the native materials during sheet installation.
- Preferential flow paths along the sheet piling to adjacent sealable cavities.

As indicated in the sealant installation logs, the actual grout volumes required were greater than the theoretical amount. This was due to leakage of the grout into the surrounding soil during the primary grouting operation. Thus, a secondary grouting process was required in some instances to seal the cavities for their entire length.

APPENDIX A: VISUAL INSPECTION REPORT

The results of the visual inspection are contained in Table 4. This table documents the following information:

- ◆ Pile Identification Number.
- ◆ Surface Condition.
- ◆ Sheet Pile Length.
- ◆ Sheet Pile Linearity.
- ◆ Foot Plate Condition.
- ◆ Sheet Pile Thickness.

VISUAL INSPECTION SUMMARY
DOVER AIR FORCE BASE, DOVER, DELAWARE
PERMEABLE BARRIER

Pile ID #	Surface Condition	Length (ft.)	Linearity	Foot Plate	Pile Thickness (mm)
1	Acceptable	40	Acceptable	Acceptable	7.5
2	Acceptable	40	Acceptable	Acceptable	7.5
3	Acceptable	40	Acceptable	Acceptable	7.5
4	Acceptable	40	Acceptable	Acceptable	7.5
5	Acceptable	40	Acceptable	Acceptable	7.5
6	Acceptable	40	Acceptable	Acceptable	7.5
7	Acceptable	40	Acceptable	Acceptable	7.5
8	Acceptable	40	Acceptable	Acceptable	7.5
9	Acceptable	40	Acceptable	Acceptable	7.5
10	Acceptable	40	Acceptable	Acceptable	7.5
11	Acceptable	40	Acceptable	Acceptable	7.5
12	Acceptable	40	Acceptable	Acceptable	7.5
13	Acceptable	40	Acceptable	Acceptable	7.5
14	Acceptable	40	Acceptable	Acceptable	7.5
15	Acceptable	40	Acceptable	Acceptable	7.5
16	Acceptable	40	Acceptable	Acceptable	7.5
17	Acceptable	40	Acceptable	Acceptable	7.5
18	Acceptable	40	Acceptable	Acceptable	7.5
19	Acceptable	40	Acceptable	Acceptable	7.5
20	Acceptable	40	Acceptable	Acceptable	7.5
21	Acceptable	40	Acceptable	Acceptable	7.5
22	Acceptable	40	Acceptable	Acceptable	7.5
23	Acceptable	40	Acceptable	Acceptable	7.5
24	Acceptable	40	Acceptable	Acceptable	7.5
25	Acceptable	40	Acceptable	Acceptable	7.5
26	Acceptable	40	Acceptable	Acceptable	7.5
27	Acceptable	40	Acceptable	Acceptable	7.5
28	Acceptable	40	Acceptable	Acceptable	7.5
29	Acceptable	40	Acceptable	Acceptable	7.5
30	Acceptable	40	Acceptable	Acceptable	7.5
31	Acceptable	40	Acceptable	Acceptable	7.5
32	Acceptable	40	Acceptable	Acceptable	7.5
33	Acceptable	40	Acceptable	Acceptable	7.5
34	Acceptable	40	Acceptable	Acceptable	7.5

APPENDIX B: SHEET PILE DRIVING SUMMARY

The results of the sheet pile driving inspection are contained in Table 5. This table documents the following information:

- ◆ Pile Identification Number.
- ◆ Pile Length.
- ◆ Length Installed.
- ◆ X-Axis Alignment.
- ◆ Y-Axis Alignment.
- ◆ Comments.

DOVER AIR FORCE BASE, DOVER, DE PERMEABLE BARRIER SYSTEM

C3 Environmental

APPENDIX C: JOINT INSPECTION SUMMARY

The results of the sealable cavity inspection following the installation of the WZ75 sheet piles are contained in Table 6. This table documents the following information:

- ◆ Joint Identification Number.
- ◆ Sheet Pile Joint Length.
- ◆ Probe Penetration Depth.
- ◆ Observations.

DOVER AIR FORCE BASE, DOVER, DE PERMEABLE BARRIER SYSTEM

SEALABLE CAVITY INSPECTION FORM

APPENDIX D: SEALANT INSTALLATION LOGS

The results of the sealant installation are contained in Table 7. This table documents the following information:

- ◆ Date of Sealant Installation.
- ◆ Start Time of Joint Sealant Installation.
- ◆ Volume of Sealant Injected During Primary.
- ◆ Depth of Grout Line Insertion During Injection.
- ◆ Date of Secondary Sealant Injection.
- ◆ Secondary Sealant Volume.

SEALANT INSTALLATION LOGS

DOVER AIR FORCE BASE, DOVER, DELAWARE
PERMEABLE BARRIER SYSTEM

JOINT I.D. #	SHEET PILE DATA		PRIMARY SEALANT DATA					SECONDARY DATA	
	SHEET LENGHT (ft)	PROBE DEPTH (ft)	DATE	GROUT TIME		GROUT (C.F.)	LINE PRES.	DATE	GROUT (Litres)
				START	STOP				
1	40.00	42.00	12-Dec-97	2:01 PM	2:02 PM	0.8	100.0	13-Dec-97	5.00
2	40.00	42.00	12-Dec-97	2:03 PM	2:04 PM	1.1	100.0	13-Dec-97	6.00
3	40.00	42.00	12-Dec-97	2:05 PM	2:06 PM	0.8	100.0	13-Dec-97	8.00
4	40.00	42.00	12-Dec-97	2:06 PM	2:09 PM	1.1	100.0	13-Dec-97	8.00
5	40.00	42.00	12-Dec-97	2:09 PM	2:11 PM	1.1	100.0	13-Dec-97	4.00
6	40.00	42.00	12-Dec-97	2:12 PM	2:13 PM	0.8	100.0	13-Dec-97	5.00
7	40.00	42.00	12-Dec-97	2:14 PM	2:17 PM	1.1	100.0	13-Dec-97	7.00
8	40.00	42.00	12-Dec-97	2:17 PM	2:23 PM	1.1	100.0	13-Dec-97	8.00
9	40.00	42.00	12-Dec-97	2:26 PM	2:28 PM	1.1	100.0	13-Dec-97	5.00
10	40.00	42.00	12-Dec-97	2:29 PM	2:31 PM	0.8	100.0	13-Dec-97	8.00
11	40.00	42.00	12-Dec-97	2:31 PM	2:33 PM	0.8	100.0	13-Dec-97	8.00
12	40.00	42.00	12-Dec-97	2:34 PM	2:36 PM	1.9	100.0	13-Dec-97	8.00
13	40.00	42.00	12-Dec-97	2:37 PM	2:41 PM	2.7	100.0	13-Dec-97	8.00
14	40.00	42.00	12-Dec-97	2:41 PM	2:44 PM	0.8	100.0	13-Dec-97	8.00
15	40.00	42.00	12-Dec-97	2:45 PM	2:47 PM	1.9	100.0	13-Dec-97	4.00
16	40.00	42.00	12-Dec-97	2:51 PM	2:53 PM	0.8	100.0	13-Dec-97	5.00
17	40.00	42.00	12-Dec-97	4:16 PM	4:20 PM	0.8	100.0	13-Dec-97	6.00
18	40.00	42.00	12-Dec-97	4:14 PM	4:15 PM	0.8	100.0	13-Dec-97	8.00
19	40.00	42.00	12-Dec-97	4:10 PM	4:12 PM	0.8	100.0	13-Dec-97	3.00
20	40.00	42.00	12-Dec-97	4:07 PM	4:09 PM	1.5	100.0	13-Dec-97	7.00
21	40.00	42.00	12-Dec-97	4:03 PM	4:06 PM	0.8	100.0	13-Dec-97	3.00
22	40.00	42.00	12-Dec-97	3:58 PM	4:01 PM	0.8	100.0	13-Dec-97	8.00
23	40.00	42.00	12-Dec-97	3:54 PM	3:57 PM	1.5	100.0	13-Dec-97	4.00
24	40.00	42.00	12-Dec-97	3:49 PM	3:51 PM	1.1	100.0	13-Dec-97	3.00
25	39.00	41.00	12-Dec-97	3:47 PM	3:49 PM	0.8	100.0	13-Dec-97	5.00
26	39.00	41.00	12-Dec-97	3:44 PM	3:46 PM	1.1	100.0	13-Dec-97	7.00
27	40.00	42.00	12-Dec-97	3:42 PM	3:44 PM	0.8	100.0	13-Dec-97	6.00
28	40.00	42.00	12-Dec-97	3:31 PM	3:33 PM	1.5	100.0	13-Dec-97	6.00
29	40.00	42.00	12-Dec-97	3:28 PM	3:30 PM	1.5	100.0	13-Dec-97	6.00
30	40.00	42.00	12-Dec-97	3:25 PM	3:28 PM	1.5	100.0	13-Dec-97	4.00
31	40.00	42.00	12-Dec-97	3:22 PM	3:25 PM	1.5	100.0	13-Dec-97	6.00
32	37.00	39.00	12-Dec-97	3:10 PM	3:21 PM	1.5	100.0	13-Dec-97	6.00

C3 ENVIRONMENTAL

SEALANT INSTALLATION FORM

C3 ENVIRONMENTAL

SEALANT INSTALLATION FORM

APPENDIX E: SHEET PILE ELEVATION

Table 8 contains the elevation of the top of the installed sheet piles. This table documents the following information:

- ◆ Pile Identification Number.
- ◆ Initial Length of the Sheet Pile.
- ◆ Final Length of the Sheet Pile.
- ◆ The Elevation of the Top of the Sheet Pile.

**DOVER AIR FORCE BASE, DOVER, DELAWARE
PERMEABLE BARRIER**

[illegible]

Appendix G-3

Field and Laboratory QA

Appendix G.3 Field and Laboratory QA

The field QA consisted of measures taken during each of the two comprehensive monitoring events (July 1998 and June 1999) to assure the quality of the sampling.

To obtain a representative assessment of the PRB performance, the monitoring strategy outlined in Section 4 of this document and detailed in the Design/Test Plan (Battelle, 1997) was designed and followed from the outset of the project. Representative groundwater samples were obtained by using the micropurging technique described in Section 4 and validated by Kearn et al. (1994). In this technique, at least one well volume of water is withdrawn from a well by gentle pumping with a peristaltic pump, before a sample is collected. For representative field parameter measurement, a flow through cell was used to circulate the water around the pH, DO, and ORP probes. Sample bottles were preserved and analyzed by standard EPA methods within the recommended holding times.

Rinsate blanks, trip blanks, and field duplicate precision were the two measures used to ensure that groundwater samples were collected in a consistent fashion and without cross contamination. Tables G-1 and G-2 show the analysis of the rinsate blanks for the July 1998 and June 1999 sampling events, respectively. All field rinsate and trip blanks had either undetected or low (less than 10% of the corresponding sample results) levels of the target organic and inorganic analytes. The field duplicate precision was within $\pm 25\%$ acceptable range for all samples as shown in Tables G-3 and G-4 for the two events. Field parameter measurements were conducted with a YSI meter (with a flow through cell) that was calibrated daily. The instrument was within acceptable calibration limits on each day.

Laboratory QA included the use of method blanks, matrix spikes (MS), and matrix spike duplicates (MSD). Tables G-5 and G-6 list the results of the MS and MSD, respectively. Method blanks were below detection in all cases. MS recoveries were within the 70-130% acceptable range for all target CVOC and inorganic analytes. The precision between MS and MSDs was within the acceptable $\pm 25\%$ range. Method blanks showed undetectable levels of the target analytes.

The QA evaluation described in this Appendix indicates that valid data were obtained during construction and monitoring.

**Table G-1. Results of July 1998 Sampling at Dover Funnel & Gate Site
Equipment Rinsate Blank (µg/L)**

Compound	F10-RINS	F10	F12D-RINS	F12D	U12S-RINS	U12S
<i>cis</i> -12-DCE	<5	<5	<5	<5	<5	<5
TCE	1J	1J	2J	2J	2J	<5
PCE	1J	2J	1J	<5	<5	3J
Compound	U6S-RINS	U6S	P12D-RINS	P12D	P6D-RINS	P6D
<i>cis</i> -12-DCE	<5	<5	<5	<5	<5	<5
TCE	1J	<5	2J	1J	1J	1J
PCE	1J	2J	2J	2J	<5	<5
Compound	P3S-RINS	P3S	F6D-RINS	F6D	P4S-RINS	P4S
<i>cis</i> -12-DCE	<5	<5	<5	<5	<5	<5
TCE	3J	1J	2J	1J	<5	1J
PCE	2J	2J	2J	3J	1J	2J

J: The compound was analyzed but not detected at or above the specified reporting limit.

**Table G-2. Results of June 1999 Sampling at Dover AFB Area 5 Funnel & Gate Site
Equipment Rinsate Blank ($\mu\text{g/L}$)**

Compound	Rinsate 1	P10	Rinsate 2	F12D
<i>cis</i> -12-DCE	<5	<5	<5	<5
TCE	<3	5	<3	<3
PCE	<3	<3	<3	<3
Compound	Rinsate 3	P3S	Rinsate 4	F1S
<i>cis</i> -12-DCE	<5	<5	<5	2.6J
TCE	<3	<3	<3	<3
PCE	<3	<3	<3	8.2
Compound	Rinsate 5	D5S	Rinsate 6	T31-A
<i>cis</i> -12-DCE	<5	<5	1.3J	7
TCE	<3	<3	2.3J	7
PCE	<3	2.1J	9	560

J: The compound was analyzed but not detected at or above the specified reporting limit.

Table G-3. Results of July 1998 Sampling at Dover Funnel Gate Site
Field Precision ($\mu\text{g/L}$)

Compound	U6S				U12S				F6D			
	Primary	Duplicate	Mean	RPD	Primary	Duplicate	Mean	RPD	Primary	Duplicate	Mean	RPD
<i>cis</i> -1,2-DCE	<5	<5	NA	NA	<5	<5	NA	NA	<5	<5	NA	NA
TCE	<5	<5	NA	NA	<5	<5	NA	NA	1J	2J	1.5	67%
PCE	2J	1J	1.5	67%	3J	3J	3	0%	3J	4J	3.5	29%
Compound	F10				F12D				D4S			
	Primary	Duplicate	Mean	RPD	Primary	Duplicate	Mean	RPD	Primary	Duplicate	Mean	RPD
<i>cis</i> -1,2-DCE	<5	<5	NA	NA	<5	2J	NA	NA	<5	<5	NA	NA
TCE	1J	1J	1	0%	2J	3J	2.5	40%	<5	1J	NA	NA
PCE	2J	2J	2	0%	<5	4J	NA	NA	3J	5J	4	50%
Compound	P3S				P6D				P12D			
	Primary	Duplicate	Mean	RPD	Primary	Duplicate	Mean	RPD	Primary	Duplicate	Mean	RPD
<i>cis</i> -1,2-DCE	<5	<5	NA	NA	<5	<5	NA	NA	<5	<5	NA	NA
TCE	1J	<5	NA	NA	1J	1J	1	0%	1J	1J	1	0%
PCE	2J	2J	2	0%	<5	<5	NA	NA	2J	1J	1.5	67%

RPD: $\left[\frac{|MS-MSD|}{\frac{1}{2}(MS+MSD)} \right] \times 100$.

NA: Not available.

J: Estimated value.

Table G-4. Results of June 1999 Sampling at Dover AFB Area 5 Funnel & Gate Site
Field Precision ($\mu\text{g/L}$)

Compound	U4D				U8D			
	Primary	Duplicate	Mean	RPD	Primary	Duplicate	Mean	RPD
<i>cis</i> -1,2-DCE	130	130	130	0%	17	18	17.5	6%
TCE	44 J	44	44	0%	5.9	6.5	6.2	10%
PCE	520	510	515	2%	118	120	119	2%
Compound	U10S				F1S			
	Primary	Duplicate	Mean	RPD	Primary	Duplicate	Mean	RPD
<i>cis</i> -1,2-DCE	<5	<5	NA	NA	2.6 J	1.7 J	2.15	42%
TCE	<3	<3	NA	NA	<3	<3	NA	NA
PCE	7.9	9.7	8.8	20%	8.2	6.5	7.35	23%
Compound	F5D				F14S			
	Primary	Duplicate	Mean	RPD	Primary	Duplicate	Mean	RPD
<i>cis</i> -1,2-DCE	<5	<5	NA	NA	<5	<5	NA	NA
TCE	<3	<3	NA	NA	<3	<3	NA	NA
PCE	<3	1.2 J	NA	NA	3.6 J	3.8 J	3.7	5%
Compound	P1S				P5D			
	Primary	Duplicate	Mean	RPD	Primary	Duplicate	Mean	RPD
<i>cis</i> -1,2-DCE	<5	<5	NA	NA	9.9	9	9.45	10%
TCE	<3	<3	NA	NA	7.6	7.3	7.45	4%
PCE	<3	<3	NA	NA	11	10	10.5	10%
Compound	P14S				D7D			
	Primary	Duplicate	Mean	RPD	Primary	Duplicate	Mean	RPD
<i>cis</i> -1,2-DCE	<5	<5	NA	NA	<5	<5	NA	NA
TCE	<3	<3	NA	NA	<3	<3	NA	NA
PCE	<3	<3	NA	NA	<3	<3	NA	NA

RPD: $[(\text{MS}-\text{MSD})/(\frac{1}{2}(\text{MS}+\text{MSD}))] \times 100$.

NA: Not available.

J: Estimated value.

Table G-5. Results of July 1998 Sampling at Dover Funnel & Gate Site
Lab Recovery (µg/L)

	214S			214S			D4S		
Compound	MS	MSD	% RPD	MS	MSD	% RPD	MS	MSD	% RPD
cis-1,2-DCE	515	541	5%	476	542	13%	479	454	5%
TCE	728	766	5%	678	765	12%	680	649	5%
PCE	2379	2278	4%	2113	2439	14%	634	605	5%
	F12D			F4M			F6S		
Compound	MS	MSD	% RPD	MS	MSD	% RPD	MS	MSD	% RPD
cis-1,2-DCE	525	379	32%	447	540	19%	460	458	0%
TCE	742	541	31%	633	749	17%	657	648	1%
PCE	697	515	30%	592	690	15%	620	608	2%
	P13S			P2D			U3D		
Compound	MS	MSD	% RPD	MS	MSD	% RPD	MS	MSD	% RPD
cis-1,2-DCE	534	515	4%	459	505	10%	453	433	5%
TCE	733	736	0%	661	731	10%	599	566	6%
PCE	622	664	7%	614	682	10%	798	746	7%
	U4D			U5S			U8D		
Compound	U4D MS	U4D MSD	% RPD	U5S MS	U5S MSD	% RPD	U8D MS	U8D MSD	% RPD
cis-1,2-DCE	588	612	4%	482	435	10%	539	530	2%
TCE	766	812	6%	669	605	10%	771	739	4%
PCE	1015	1044	3%	586	538	9%	838	789	6%

RPD: $[(MS-MSD)/\frac{1}{2}(MS+MSD)] \times 100$.

QC limits for RPD are $\pm 25\%$ and recoveries are within limits.

Table G-6. Results of June 1999 Sampling at Dover AFB Area 5 Funnel & Gate Site
Lab Precision (µg/L)

Batch ID	0607S		0609S		0610S	
Compound	MS	% RPD	MS	% RPD	MS	% RPD
Benzene	100%	4.00%	101%	4.60%	116%	6.40%
Chlorobenzene	109%	0.13%	104%	4.90%	111%	3.40%
1,1-DCE	94%	3.70%	99%	3.20%	108%	2.80%
Toluene	108%	0.89%	102%	2.70%	111%	1.80%
TCE	117%	9.40%	102%	4.80%	108%	3.90%
Batch ID	0611P		0612S		0612S-2	
Compound	MS	% RPD	MS	% RPD	MS	% RPD
Benzene	100%	7.70%	89%	2.40%	89%	2.40%
Chlorobenzene	69%	9.70%	105%	4.70%	100%	4.70%
1,1-DCE	100%	8.70%	88%	0.71%	90%	0.71%
Toluene	78%	5.10%	98%	4.10%	96%	4.10%
TCE	89%	3.30%	105%	4.50%	102%	4.50%
Batch ID	0615P		0617S		0620S	
Compound	MS	% RPD	MS	% RPD	MS	% RPD
Benzene	114%	8.40%	106%	0.72%	116%	3.40%
Chlorobenzene	101%	8.50%	107%	2.30%	104%	2.30%
1,1-DCE	120%	8.70%	100%	0.14%	107%	3.70%
Toluene	100%	2.90%	101%	0.04%	100%	2.10%
TCE	112%	0.21%	109%	1.60%	109%	3.30%
Batch ID	0622S		0625S		0630S	
Compound	MS	% RPD	MS	% RPD	MS	% RPD
Benzene	105%	1.80%	119%	7.10%	95%	2.20%
Chlorobenzene	109%	0.92%	116%	3.10%	93%	4.30%
1,1-DCE	104%	3.60%	112%	9.70%	94%	1.80%
Toluene	108%	0.50%	119%	4.40%	89%	0.56%
TCE	114%	3.50%	117%	4.80%	88%	8.70%
Batch ID	0826S		0827S		Listed % RPD are reported on analytical lab reports.	
Compound	MS	% RPD	MS	% RPD		
Benzene	110%	3.20%	114%	2.30%		
Chlorobenzene	108%	2.30%	108%	3.20%		
1,1-DCE	114%	3.20%	117%	2.70%		
Toluene	109%	2.70%	110%	2.40%		
TCE	108%	2.60%	117%	4.30%		

RPD: $[(MS-MSD)/\frac{1}{2}(MS+MSD)] \times 100$.

QC limits for RPD are $\pm 25\%$ and recoveries are within limits.

Appendix H
Supporting Information for Cost Evaluation

Appendix H Supporting Information for Cost Evaluation

H.1 Capital Investment and O&M Cost of a P&T System for Area 5

A pump-and-treat (P&T) system equivalent to the full-scale PRB at Area 5 would capture the same volume of groundwater as the PRB. The full-scale PRB has four 4-foot wide gates and a 120-foot wide funnel. The thickness of the aquifer is about 30 ft. Based on the maximum estimated groundwater velocity through the gates of 4.1 ft/day, approximately 10 gpm of water flows through the gates. Because extraction wells need to be oversized to ensure the capture of the entire plume, a system that extracts 20 gpm of water would be needed. Table H-1 describes the capital investment for a 20-gpm P&T system for Area 5 that includes the following elements:

- Three 4-inch diameter PVC wells for extraction of 20 gpm of water.
- Three submersible pumps for pumping a total of 20 gpm of water from a dept of about 20 ft bgs.
- A low-profile air stripper to effect mass transfer of up to 15 mg/L of CVOCs from water to air.
- Two activated carbon drums to polish off any residual CVOCs in the water effluent from the stripper down to MCLs.
- A catalytic oxidizer to destroy the CVOCs in the air stream.
- A concrete pad and shelter to house the equipment.
- Associated piping and instruments.
- Site preparation, including permitting and arrangements for power supply.
- Preliminary site assessment, site characterization, and design costs similar to those for a PRB.

The O&M costs associated with the P&T system are described in Table H-2 and fall into two categories, annual operating/monitoring costs and periodic maintenance costs. Annual costs include the labor and energy requirements for operating the P&T system. Energy requirements include electricity for the pumps and fuel for the catalytic oxidizer. Periodic maintenance includes replacement of the catalyst in the oxidizer every 5 years and replacement of one polishing carbon drum every 10 years.

H.2 Present Value Analysis Background

Typically, present value (PV) or discounted cash flow analysis is used to determine the life cycle cost of a technology. PV cost represents the amount of money (dollars) that would have to be set aside today to cover all the installed and O&M costs occurring in the present and future.

$$PV_{\text{technology}} = \text{Capital Investment} + PV_{\text{annual O\&M costs over life of the new unit}} \quad (\text{H-1})$$

In the above equation, $PV_{\text{annual O\&M costs over life of the new unit}}$ represents the annual O&M costs (and savings realized, if any) adjusted for opportunity costs. This adjustment is done by dividing each year's O&M costs by a factor that incorporates a discount rate (r), which is a rate of return that includes the combined effect of inflation, productivity, and risk.

$$PV_{\text{annual O\&M costs}} = \frac{\sum \text{O\&M cost in Year } t}{(1 + r)^t} \quad (\text{H-2})$$

$$PV_{\text{annual O\&M costs}} = \frac{\text{O\&M cost in Year 1}}{(1 + r)^1} + \frac{\text{O\&M cost in Year 2}}{(1 + r)^2} + \dots + \frac{\text{O\&M cost in Year } n}{(1 + r)^n} \quad (\text{H-3})$$

One implication of Equation H-3 is that because O&M costs are incurred gradually over the next several years, a smaller amount of money can be set aside today (say in a bank deposit that provides a rate of return, r) to cover future O&M costs. The further into the future, or greater the t , greater is the denominator for the relevant t , and lesser is the present value of that year's O&M cost. That is, fewer dollars have to be set aside today (in a separate investment that provides a rate of return, r) to cover the O&M costs of the future. Installed cost is typically not affected by the time factor because it is incurred more or less immediately (at $t = 0$).

A total time period of 30 years ($n = 30$) is used in this report for the long-term evaluation of PRB and P&T system costs.

H.3 PV Calculations for PRB and P&T System

Tables H-3 to H-5 contain PV costs for a PRB and a P&T system for 10-, 20-, and 30-year life expectancies, respectively, of the iron in the gates. At the end of the life cycle of the iron, it is assumed that the used iron is excavated and fresh iron is filled into the four gates. Alternatively, an all new PRB could be build upgradient or downgradient of the current PRB. However, replacing just the iron in the gates eliminates the necessity to have a new funnel. The shaded cells in the tables indicate the break-even point, or the time period when the total (cumulative) long-term cost of the PRB becomes equal to or less than the cost of the P&T system. Note that the PRB requires a higher initial capital, but the long-term savings resulting from reduced O&M costs more than offset the higher capital investment. Table H-6 contains PV costs for an extended 50-year period of application, with PRB maintenance after the first 30 years. Because the CVOC plume may last for several decades or centuries, longer periods of application under passive operation are increasingly more cost-effective than a P&T system.

Table H-1. Capital Investment for Pump and Treat System at Area 5 with 20 gpm Total Flow

Item	Description	Units	No of Units	Unit Price	Item Cost
Phase 1: Pre-Construction Activities					
	Preliminary site assessment	RI/FS, other reports; site meeting			\$15,000
	Site Characterization (CPT, temporary wells; analysis of samples; slug tests)				\$200,000
	Design (characterization data evaluation; modeling; engineering; report)				\$100,000
	Total Pre-Construction Cost				\$315,000
Phase 2. Construction Activities					
	Site preparation		1	\$10,000	\$10,000
33 23 1101	Auger 8" well	LF	120	\$44	\$5,239
33 23 0202	4" PVC well pipe	LF	120	\$21	\$2,531
33 23 1402	Filter pack	LF	30	\$16	\$491
33 23 1813	Grout	LF	90	\$8	\$702
33 23 2103	Surface finish well	EA	3	\$137	\$412
33 23 0501	Well pump	EA	3	\$1,340	\$4,020
18 02 0321	6" Structural slab on grade	SF	400	\$4	\$1,792
151 551 1910	2" PVC surface piping	LF	200	\$15	\$2,900
151 558 0860	2" PVC misc fittings	EA	15	\$44	\$653
151 975 1260	2" PVC misc valves	EA	5	\$97	\$485
	Instruments	EA	10	\$500	\$5,000
	Construction labor	HRS	800	\$50	\$40,000
	Contractor Fee				\$10,000
33 13 0802	Low profile air stripper	EA	1	\$7,424	\$7,424
33 31 0150	1 HP blower	EA	1	\$754	\$754
33 29 0103	3 HP Centrifugal pump	EA	1	\$2,279	\$2,279
33 13 1907	400 lb liquid phase GAC drum	EA	2	\$1,764	\$3,528
est	Shed	EA	1	\$2,000	\$2,000
	Catalytic oxidation unit	EA	1	\$50,000	\$50,000
	Shipping				\$5,000
	Monitoring system construction	Wells	30		\$32,000
	Total construction cost				\$187,210
	TOTAL CAPITAL INVESTMENT				\$502,210

Table H-2. Operating and Maintenance (O&M) Cost of Pump & Treat System at Area 5

Description		Units	No. of Units/yr	Unit Price	Item Cost/yr
System Operating cost					
H2O flow (gpm)	Organic load (mg/L)	Carbon load (lbs carbon/lb organic)			
20	0.015	30			
	Water flow (L/month)	2982459			
	Organic load (lbs VOC/month)	0.09863			
	Operating labor - 40 hrs/month	hr/yr	480	\$50	\$24,000
	General maintenance parts				\$28,081.44
Total power use (HP)					
5					
	Electricity	kw/yr	29395.49	\$0	\$2,058
	Fuel - Catalytic oxidation unit	Btu/hr	2.0E+05	\$0	\$12,264
	Total annual system operating cost				\$66,403
Annual Monitoring Activities					
	Groundwater sampling	40 wells x 4 quarters			\$80,000
	CVOC analysis	44 smpls @ \$120 ea x 4 quarters			\$20,000
	Inorganic analysis	22 smpls @ \$200/sample			\$4,400
	Water level survey	40 wells x 4 quarters			\$4,000
	Data analysis, report	Labor x 4 quarters			\$40,000
	Total annual monitoring cost				\$148,400
Maintenance (every 10 yrs)					
	Carbon use (lbs/yr)	35.5055			
est	GAC removal and disposal	lbs/ 10 yrs	355.0546	\$3	\$1,065
	Maintenance labor	hrs	40	\$50	\$2,000
33 13 1907	400 lb liquid phase GAC drum	EA	2	\$1,764	\$3,528
	Total maintenance every 10 yrs				\$6,593
Maintenance (every 5 yrs)					
	New catalyst	bed	1	\$15,000	\$15,000
	Old catalyst disposal	bed	1	\$2,000	\$2,000
	Maintenance labor	hrs	80	\$50	\$4,000
	Total maintenance every 5 yrs				\$21,000

Table H-3. PV Analysis of PRB and P&T Systems for Area 5 Assuming 10-Year Life of PRB

Year	PRB			P&T System		
	Annual Cost	PV of Annual Cost	Cumulative PV of Annual Cost	Annual Cost	PV of Annual Cost	Cumulative PV of Annual Cost
0	\$947,000	\$947,000	\$947,000	\$502,000	\$502,000	\$502,000
1	\$148,000	\$143,829	\$1,090,829	\$214,000	\$207,969	\$709,969
2	\$148,000	\$139,775	\$1,230,604	\$214,000	\$202,108	\$912,077
3	\$148,000	\$135,836	\$1,366,441	\$214,000	\$196,412	\$1,108,489
4	\$148,000	\$132,008	\$1,498,449	\$214,000	\$190,876	\$1,299,365
5	\$148,000	\$128,288	\$1,626,736	\$235,000	\$203,700	\$1,503,065
6	\$148,000	\$124,672	\$1,751,408	\$214,000	\$180,269	\$1,683,334
7	\$148,000	\$121,159	\$1,872,567	\$214,000	\$175,189	\$1,858,523
8	\$148,000	\$117,744	\$1,990,311	\$214,000	\$170,251	\$2,028,774
9	\$148,000	\$114,426	\$2,104,737	\$214,000	\$165,453	\$2,194,228
10	\$569,000	\$427,522	\$2,532,259	\$242,000	\$181,828	\$2,376,056
11	\$148,000	\$108,067	\$2,640,326	\$214,000	\$156,259	\$2,532,315
12	\$148,000	\$105,021	\$2,745,347	\$214,000	\$151,855	\$2,684,170
13	\$148,000	\$102,061	\$2,847,408	\$214,000	\$147,575	\$2,831,745
14	\$148,000	\$99,185	\$2,946,593	\$214,000	\$143,416	\$2,975,162
15	\$148,000	\$96,390	\$3,042,983	\$235,000	\$153,051	\$3,128,213
16	\$148,000	\$93,673	\$3,136,656	\$214,000	\$135,446	\$3,263,659
17	\$148,000	\$91,033	\$3,227,690	\$214,000	\$131,629	\$3,395,289
18	\$148,000	\$88,468	\$3,316,158	\$214,000	\$127,920	\$3,523,208
19	\$148,000	\$85,974	\$3,402,132	\$214,000	\$124,314	\$3,647,523
20	\$569,000	\$321,222	\$3,723,354	\$242,000	\$136,618	\$3,784,141
21	\$148,000	\$81,197	\$3,804,550	\$242,000	\$132,768	\$3,916,908
22	\$148,000	\$78,908	\$3,883,459	\$214,000	\$114,097	\$4,031,006
23	\$148,000	\$76,685	\$3,960,143	\$214,000	\$110,882	\$4,141,887
24	\$148,000	\$74,523	\$4,034,667	\$214,000	\$107,757	\$4,249,644
25	\$148,000	\$72,423	\$4,107,090	\$235,000	\$114,996	\$4,364,641
26	\$148,000	\$70,382	\$4,177,472	\$214,000	\$101,769	\$4,466,409
27	\$148,000	\$68,399	\$4,245,871	\$214,000	\$98,901	\$4,565,310
28	\$148,000	\$66,471	\$4,312,341	\$214,000	\$96,113	\$4,661,423
29	\$148,000	\$64,598	\$4,376,939	\$214,000	\$93,405	\$4,754,827
30	\$569,000	\$241,352	\$4,618,291	\$242,000	\$102,649	\$4,857,476

Table H-4. PV Analysis of PRB and P&T Systems for Area 5 Assuming 20-Year Life of PRB

Year	PRB			P&T System		
	Annual Cost	PV of Annual Cost	Cumulative PV of Annual Cost	Annual Cost	PV of Annual Cost	Cumulative PV of Annual Cost
0	\$947,000	\$947,000	\$947,000	\$502,000	\$502,000	\$502,000
1	\$148,000	\$143,829	\$1,090,829	\$214,000	\$207,969	\$709,969
2	\$148,000	\$139,775	\$1,230,604	\$214,000	\$202,108	\$912,077
3	\$148,000	\$135,836	\$1,366,441	\$214,000	\$196,412	\$1,108,489
4	\$148,000	\$132,008	\$1,498,449	\$214,000	\$190,876	\$1,299,365
5	\$148,000	\$128,288	\$1,626,736	\$235,000	\$203,700	\$1,503,065
6	\$148,000	\$124,672	\$1,751,408	\$214,000	\$180,269	\$1,683,334
7	\$148,000	\$121,159	\$1,872,567	\$214,000	\$175,189	\$1,858,523
8	\$148,000	\$117,744	\$1,990,311	\$214,000	\$170,251	\$2,028,774
9	\$148,000	\$114,426	\$2,104,737	\$214,000	\$165,453	\$2,194,228
10	\$148,000	\$111,201	\$2,215,937	\$242,000	\$181,828	\$2,376,056
11	\$148,000	\$108,067	\$2,324,004	\$214,000	\$156,259	\$2,532,315
12	\$148,000	\$105,021	\$2,429,026	\$214,000	\$151,855	\$2,684,170
13	\$148,000	\$102,061	\$2,531,087	\$214,000	\$147,575	\$2,831,745
14	\$148,000	\$99,185	\$2,630,272	\$214,000	\$143,416	\$2,975,162
15	\$148,000	\$96,390	\$2,726,662	\$235,000	\$153,051	\$3,128,213
16	\$148,000	\$93,673	\$2,820,335	\$214,000	\$135,446	\$3,263,659
17	\$148,000	\$91,033	\$2,911,369	\$214,000	\$131,629	\$3,395,289
18	\$148,000	\$88,468	\$2,999,836	\$214,000	\$127,920	\$3,523,208
19	\$148,000	\$85,974	\$3,085,811	\$214,000	\$124,314	\$3,647,523
20	\$569,000	\$321,222	\$3,407,032	\$242,000	\$136,618	\$3,784,141
21	\$148,000	\$81,197	\$3,488,229	\$242,000	\$132,768	\$3,916,908
22	\$148,000	\$78,908	\$3,567,138	\$214,000	\$114,097	\$4,031,006
23	\$148,000	\$76,685	\$3,643,822	\$214,000	\$110,882	\$4,141,887
24	\$148,000	\$74,523	\$3,718,346	\$214,000	\$107,757	\$4,249,644
25	\$148,000	\$72,423	\$3,790,769	\$235,000	\$114,996	\$4,364,641
26	\$148,000	\$70,382	\$3,861,151	\$214,000	\$101,769	\$4,466,409
27	\$148,000	\$68,399	\$3,929,549	\$214,000	\$98,901	\$4,565,310
28	\$148,000	\$66,471	\$3,996,020	\$214,000	\$96,113	\$4,661,423
29	\$148,000	\$64,598	\$4,060,618	\$214,000	\$93,405	\$4,754,827
30	\$148,000	\$62,777	\$4,123,395	\$242,000	\$102,649	\$4,857,476

Table H-5. PV Analysis of PRB and P&T Systems for Area 5 Assuming 30-Year Life of PRB

Year	PRB			P&T System		
	Annual Cost	PV of Annual Cost	Cumulative PV of Annual Cost	Annual Cost	PV of Annual Cost	Cumulative PV of Annual Cost
0	\$947,000	\$947,000	\$947,000	\$502,000	\$502,000	\$502,000
1	\$148,000	\$143,829	\$1,090,829	\$214,000	\$207,969	\$709,969
2	\$148,000	\$139,775	\$1,230,604	\$214,000	\$202,108	\$912,077
3	\$148,000	\$135,836	\$1,366,441	\$214,000	\$196,412	\$1,108,489
4	\$148,000	\$132,008	\$1,498,449	\$214,000	\$190,876	\$1,299,365
5	\$148,000	\$128,288	\$1,626,736	\$235,000	\$203,700	\$1,503,065
6	\$148,000	\$124,672	\$1,751,408	\$214,000	\$180,269	\$1,683,334
7	\$148,000	\$121,159	\$1,872,567	\$214,000	\$175,189	\$1,858,523
8	\$148,000	\$117,744	\$1,990,311	\$214,000	\$170,251	\$2,028,774
9	\$148,000	\$114,426	\$2,104,737	\$214,000	\$165,453	\$2,194,228
10	\$148,000	\$111,201	\$2,215,937	\$242,000	\$181,828	\$2,376,056
11	\$148,000	\$108,067	\$2,324,004	\$214,000	\$156,259	\$2,532,315
12	\$148,000	\$105,021	\$2,429,026	\$214,000	\$151,855	\$2,684,170
13	\$148,000	\$102,061	\$2,531,087	\$214,000	\$147,575	\$2,831,745
14	\$148,000	\$99,185	\$2,630,272	\$214,000	\$143,416	\$2,975,162
15	\$148,000	\$96,390	\$2,726,662	\$235,000	\$153,051	\$3,128,213
16	\$148,000	\$93,673	\$2,820,335	\$214,000	\$135,446	\$3,263,659
17	\$148,000	\$91,033	\$2,911,369	\$214,000	\$131,629	\$3,395,289
18	\$148,000	\$88,468	\$2,999,836	\$214,000	\$127,920	\$3,523,208
19	\$148,000	\$85,974	\$3,085,811	\$214,000	\$124,314	\$3,647,523
20	\$148,000	\$83,551	\$3,169,362	\$242,000	\$136,618	\$3,784,141
21	\$148,000	\$81,197	\$3,250,559	\$242,000	\$132,768	\$3,916,908
22	\$148,000	\$78,908	\$3,329,468	\$214,000	\$114,097	\$4,031,006
23	\$148,000	\$76,685	\$3,406,152	\$214,000	\$110,882	\$4,141,887
24	\$148,000	\$74,523	\$3,480,676	\$214,000	\$107,757	\$4,249,644
25	\$148,000	\$72,423	\$3,553,099	\$235,000	\$114,996	\$4,364,641
26	\$148,000	\$70,382	\$3,623,481	\$214,000	\$101,769	\$4,466,409
27	\$148,000	\$68,399	\$3,691,879	\$214,000	\$98,901	\$4,565,310
28	\$148,000	\$66,471	\$3,758,350	\$214,000	\$96,113	\$4,661,423
29	\$148,000	\$64,598	\$3,822,948	\$214,000	\$93,405	\$4,754,827
30	\$569,000	\$241,352	\$4,064,300	\$242,000	\$102,649	\$4,857,476

Table H-6. PV Analysis of PRB and P&T systems for Area 5 assuming 30-year life of PRB (Longer Duration of 50 years)

Year	PRB			P&T System		
	Annual Cost	PV of Annual Cost	Cumulative PV of Annual Cost	Annual Cost	PV of Annual Cost	Cumulative PV of Annual Cost
0	\$947,000	\$947,000	\$947,000	\$502,000	\$502,000	\$502,000
1	\$148,000	\$143,829	\$1,090,829	\$214,000	\$207,969	\$709,969
2	\$148,000	\$139,775	\$1,230,604	\$214,000	\$202,108	\$912,077
3	\$148,000	\$135,836	\$1,366,441	\$214,000	\$196,412	\$1,108,489
4	\$148,000	\$132,008	\$1,498,449	\$214,000	\$190,876	\$1,299,365
5	\$148,000	\$128,288	\$1,626,736	\$235,000	\$203,700	\$1,503,065
6	\$148,000	\$124,672	\$1,751,408	\$214,000	\$180,269	\$1,683,334
7	\$148,000	\$121,159	\$1,872,567	\$214,000	\$175,189	\$1,858,523
8	\$148,000	\$117,744	\$1,990,311	\$214,000	\$170,251	\$2,028,774
9	\$148,000	\$114,426	\$2,104,737	\$214,000	\$165,453	\$2,194,228
10	\$148,000	\$111,201	\$2,215,937	\$242,000	\$181,828	\$2,376,056
11	\$148,000	\$108,067	\$2,324,004	\$214,000	\$156,259	\$2,532,315
12	\$148,000	\$105,021	\$2,429,026	\$214,000	\$151,855	\$2,684,170
13	\$148,000	\$102,061	\$2,531,087	\$214,000	\$147,575	\$2,831,745
14	\$148,000	\$99,185	\$2,630,272	\$214,000	\$143,416	\$2,975,162
15	\$148,000	\$96,390	\$2,726,662	\$235,000	\$153,051	\$3,128,213
16	\$148,000	\$93,673	\$2,820,335	\$214,000	\$135,446	\$3,263,659
17	\$148,000	\$91,033	\$2,911,369	\$214,000	\$131,629	\$3,395,289
18	\$148,000	\$88,468	\$2,999,836	\$214,000	\$127,920	\$3,523,208
19	\$148,000	\$85,974	\$3,085,811	\$214,000	\$124,314	\$3,647,523
20	\$148,000	\$83,551	\$3,169,362	\$242,000	\$136,618	\$3,784,141
21	\$148,000	\$81,197	\$3,250,559	\$242,000	\$132,768	\$3,916,908
22	\$148,000	\$78,908	\$3,329,468	\$214,000	\$114,097	\$4,031,006
23	\$148,000	\$76,685	\$3,406,152	\$214,000	\$110,882	\$4,141,887
24	\$148,000	\$74,523	\$3,480,676	\$214,000	\$107,757	\$4,249,644
25	\$148,000	\$72,423	\$3,553,099	\$235,000	\$114,996	\$4,364,641
26	\$148,000	\$70,382	\$3,623,481	\$214,000	\$101,769	\$4,466,409
27	\$148,000	\$68,399	\$3,691,879	\$214,000	\$98,901	\$4,565,310
28	\$148,000	\$66,471	\$3,758,350	\$214,000	\$96,113	\$4,661,423
29	\$148,000	\$64,598	\$3,822,948	\$214,000	\$93,405	\$4,754,827
30	\$569,000	\$241,352	\$4,064,300	\$242,000	\$102,649	\$4,857,476
31	\$148,000	\$61,008	\$4,125,307	\$214,000	\$88,214	\$4,945,690
32	\$148,000	\$59,288	\$4,184,596	\$214,000	\$85,728	\$5,031,418
33	\$148,000	\$57,617	\$4,242,213	\$214,000	\$83,312	\$5,114,730
34	\$148,000	\$55,994	\$4,298,207	\$214,000	\$80,964	\$5,195,694
35	\$148,000	\$54,416	\$4,352,623	\$235,000	\$86,403	\$5,282,097
36	\$148,000	\$52,882	\$4,405,505	\$214,000	\$76,465	\$5,358,561
37	\$148,000	\$51,392	\$4,456,896	\$214,000	\$74,310	\$5,432,871
38	\$148,000	\$49,943	\$4,506,840	\$214,000	\$72,215	\$5,505,086
39	\$148,000	\$48,536	\$4,555,375	\$214,000	\$70,180	\$5,575,267
40	\$148,000	\$47,168	\$4,602,543	\$242,000	\$77,126	\$5,652,392
41	\$148,000	\$45,839	\$4,648,382	\$242,000	\$74,952	\$5,727,345
42	\$148,000	\$44,547	\$4,692,929	\$214,000	\$64,412	\$5,791,757
43	\$148,000	\$43,291	\$4,736,220	\$214,000	\$62,597	\$5,854,354
44	\$148,000	\$42,071	\$4,778,291	\$214,000	\$60,833	\$5,915,187
45	\$148,000	\$40,886	\$4,819,177	\$235,000	\$64,920	\$5,980,106
46	\$148,000	\$39,733	\$4,858,910	\$214,000	\$57,452	\$6,037,558
47	\$148,000	\$38,613	\$4,897,524	\$214,000	\$55,833	\$6,093,391
48	\$148,000	\$37,525	\$4,935,049	\$214,000	\$54,259	\$6,147,651
49	\$148,000	\$36,468	\$4,971,517	\$214,000	\$52,730	\$6,200,381
50	\$148,000	\$35,440	\$5,006,956	\$242,000	\$57,949	\$6,258,330